

PALACKÝ UNIVERSITY OLMOUC
FACULTY OF MEDICINE AND DENTISTRY
DEPARTMENT OF NEUROLOGY



Faculty of Medicine
and Dentistry

**MODULATION AND PLASTICITY OF SENSORIMOTOR BRAIN
NETWORKS DURING AFFERENT STIMULATION**

Dissertation thesis in the field of Neurology

MUDr. Pavel Hok

Olomouc 2020

This page is intentionally left blank

MODULATION AND PLASTICITY OF THE SENSORIMOTOR BRAIN NETWORKS DURING AFFERENT STIMULATION

MUDr. Pavel Hok

Supervisor: prof. MUDr. Ing. Petr Hlušík, Ph.D.

Institution: Department of Neurology
Faculty of Medicine and Dentistry
Palacký University Olomouc
University Hospital Olomouc

E-mail: pavel.hok@upol.cz

DECLARATION OF AUTHORSHIP

I hereby declare that I am the sole author of this dissertation thesis and that I have not used any sources other than those listed in the bibliography and identified as references.

I also certify that the experimental work submitted is my own, except where work which has formed part of jointly-authored publications has been included. My contribution and those of the other authors to this work have been explicitly indicated below. I confirm that appropriate credit has been given within this thesis where reference has been made to the work of others.

This thesis has not been submitted for any other degree or professional qualification.

.....

Place and date

.....

Signature of the author

ACKNOWLEDGEMENTS

First and foremost, I would like to express my deepest gratitude to my supervisor, prof. MUDr. Ing. Petr Hlušík, Ph.D., for his continuous support, guidance and valuable advice throughout my study. Over the years, he has become one of my closest friends as he has been to me not only an example of a brilliant scientist, but above all, an example of personal integrity and kindness.

I also wish to appreciate the motivation and support, as well as methodological inspiration provided by prof. MUDr. Petr Kaňovský, CSc., head of the Department of Neurology, University Hospital Olomouc and Palacký University Olomouc.

My sincere thanks belong also to Priv.-Doz. Dr. med. Christian A. Kell, co-chair of the Brain Imaging Center of Goethe University Frankfurt am Main, Germany, for his repeated kind reception during my research fellowships at his institution. His enthusiasm and continuous positive attitude have been encouraging me even at times of unsuccess. I also thank the European Union, German Academic Exchange Service (DAAD) and University Hospital Olomouc for the financial support allowing me to fully experience the work at international team of excellent and open-minded researchers.

Furthermore, I thank all my collaborators and co-authors, including those from Olomouc and Frankfurt, for their collegial support, selfless help, and critical intellectual input. Without them, none of the works could be published in their final form.

Last, but not least, I would like to thank my beloved wife Radka and family for their unconditional support, patience and great deal of understanding.

FUNDING

The experimental part of this work was supported by the grant of the Czech Science Foundation (GACR) [grant number 14-22572S] and by Ministry of Health, the Czech Republic – conceptual development of research organisation (University Hospital Olomouc – FNOL, 00098892).

The international scholarships during the doctoral study were supported by European Union (LLP Erasmus), German Academic Exchange Service (DAAD), and jointly by Pierre Fabre Medicament and the French Republic.

Contents

I. Introduction	10
II. Anatomy and physiology of the sensorimotor system	12
1. Somatosensation: Cutaneous mechanoreceptors.....	12
2. Somatosensation: Proprioceptors of the musculoskeletal system.....	13
3. Somatosensory afferent pathways.....	14
4. Motor system structures and sensorimotor integration.....	16
5. Cortical plasticity.....	17
III. Methods for mapping the sensorimotor system and its plasticity	20
1. Transcranial magnetic stimulation (TMS).....	20
1.1. Paired-pulse protocols.....	21
1.2. TMS as an intervention.....	21
2. Positron emission tomography (PET).....	22
3. Functional magnetic resonance imaging (fMRI).....	22
3.1. Magnetic resonance imaging principles.....	22
3.2. Blood oxygenation level-dependent (BOLD) contrast.....	24
3.3. Other functional MRI techniques.....	27
IV. Enhancing the afferent input: Modalities of peripheral stimulation	28
1. Vibratory stimulation.....	28
1.1. Sensory structures responding to vibration.....	28
1.2. Behavioural effects of vibratory stimulation.....	29
1.2.1. Cutaneous vibratory stimulation.....	29
1.2.2. Vibratory muscle stimulation.....	31
1.2.3. Vibration in motor system disorders.....	34
1.3. Electrophysiological evidence for central effects of vibration.....	36
1.3.1. Immediate effects of vibration.....	36
1.3.2. Effect of kinaesthetic illusions.....	37
1.3.3. Sustained effects of vibration.....	38

1.3.4. Cortical reorganisation due to vibration.....	39
1.3.5. Effects of vibration during voluntary contraction.....	40
1.3.6. Lower limb vibration.....	41
1.3.7. Vibration in motor system disorders.....	41
1.3.8. Summary of evidence from electrophysiological studies.....	43
1.4. Neuroimaging evidence for central effects of vibration.....	43
1.4.1. Kinaesthetic illusions.....	44
1.4.2. Postural effects of vibration.....	45
1.4.3. Sustained effects of vibration.....	46
1.4.4. Vibrotactile stimulation: combined effects of muscle and skin vibration?....	46
1.4.5. Are there motor effects of pure cutaneous vibration?.....	48
1.4.6. Vibration in motor system disorders.....	50
1.5. Summary of sensorimotor interactions during vibratory stimulation.....	50
2. Mechanical pressure stimulation.....	52
2.1. Sensory structures responding to innocuous pressure.....	52
2.2. Behavioural effects of peripheral pressure stimulation.....	52
2.2.1. Involuntary motor responses to pressure stimulation.....	53
2.3. Electrophysiological evidence for central effects of pressure stimulation.....	55
2.4. Neuroimaging evidence for central effects of pressure stimulation.....	56
V. Reducing the afferent input: Means of plasticity facilitation	59
1. Reduction of cutaneous and mixed-nerve input.....	59
2. Selective muscle denervation: botulinum neurotoxin (BoNT-A).....	60
2.1. Electrophysiological evidence for central effects of BoNT-A.....	60
2.1.1. Healthy subjects.....	60
2.1.2. Dystonia.....	61
2.1.3. Spasticity.....	62
2.2. Neuroimaging evidence for central effects of BoNT-A.....	63
2.2.1. Dystonia.....	63
2.2.2. Spasticity.....	71

2.2.3. Summary of central effects of BoNT-A.....	74
VI. Premises and theoretical background of the experimental studies	76
1. Hypothesis I.....	78
2. Hypothesis II.....	78
3. Hypothesis III.....	79
4. Hypothesis IV.....	79
VII. Aims of the thesis	80
VIII. Materials and methods	81
1. Study design.....	81
2. Participants.....	81
2.1. Study I and II (fMRI).....	81
2.2. Study III (TMS).....	81
2.3. Study IV (HRV).....	81
3. Tasks and procedures.....	82
3.1. Visit schedule.....	82
3.2. Pressure stimulation.....	82
3.3. Pressure-related behavioural measures.....	84
3.4. Motor task in Study II (fMRI of stimulation after-effects).....	84
4. Data acquisition.....	85
4.1. Study I and II (fMRI).....	85
4.2. Study III (TMS).....	86
4.2.1. Motor evoked potentials (MEP).....	86
4.2.2. Paired-pulse TMS protocol.....	87
4.3. Study IV (HRV).....	87
4.3.1. Spectral analysis of heart rate variability (SAHRV).....	87
4.3.2. Respiratory rate assessment.....	89
5. Data analysis.....	89
5.1. Analysis of behavioural data.....	89
5.2. Study I (fMRI during stimulation).....	89

5.2.1. Data pre-processing.....	89
5.2.2. Statistical analysis.....	90
5.2.3. <i>Post-hoc</i> ROI analysis: Mean condition effects.....	91
5.2.4. <i>Post-hoc</i> ROI analysis: Within-subject differences.....	92
5.3. Study II (fMRI of stimulation after-effects).....	93
5.3.1. Data pre-processing.....	93
5.3.2. Statistical analysis.....	93
5.4. Study III (TMS).....	95
5.5. Study IV (HRV).....	95
IX. Results	96
1. Study I and II (fMRI): Behavioural data.....	96
2. Study I (fMRI during stimulation): Imaging results.....	96
2.1. Heel and Ankle: Mean activation maps and their conjunction.....	96
2.2. Characterising temporal dynamics: <i>Post-hoc</i> ROI analysis.....	99
2.3. Heel versus Ankle: Within-subject differences between conditions.....	104
3. Study II (fMRI of stimulation after-effects): Imaging results.....	107
3.1. Mean fMRI activation during sequential finger opposition (SFO).....	107
3.2. Differences between baseline conditions.....	108
3.3. Repetition effects: Mean activation difference before and after the stimulation	108
3.4. Heel versus Ankle: Interaction between stimulation site and task repetition....	110
3.5. Decomposing the interaction: <i>Post-hoc</i> ROI analysis.....	112
4. Study III (TMS).....	114
4.1. Behavioural data.....	114
4.2. Electrophysiology.....	114
4.2.1. Heel versus Ankle: pTMS results.....	115
5. Study IV (HRV).....	117
5.1. Heel versus Ankle: SAHRV.....	117
5.2. Respiratory rate.....	118
5.3. Stimulation discomfort.....	119

5.4. Behavioural and motor responses to stimulation.....	119
X. Discussion	120
1. Patterns of activation associated with pressure stimulation.....	120
1.1. Temporal features of the BOLD responses.....	120
1.2. Deactivations associated with pressure stimulation.....	121
1.3. Differences between the stimulation sites.....	122
1.3.1. Characterising temporal dynamics: Group-wise activation patterns.....	122
1.3.2. Heel versus Ankle: Voxel-wise within-subject comparison.....	123
2. After-effects of pressure stimulation on brain activation.....	125
2.1. Average activation during SFO.....	126
2.2. Repetition effects: Activation decrease post-stimulation.....	126
2.3. Heel versus Ankle: Site-specific effects on motor-related activation.....	127
3. After-effects of pressure stimulation on cortical excitability.....	128
3.1. Short-interval intracortical inhibition (SICI).....	128
3.2. Intracortical facilitation (ICF).....	130
4. Autonomic after-effects of pressure stimulation.....	130
5. Brain structures involved in site-specific pressure stimulation processing.....	131
5.1. Primary motor and premotor cortex (M1/PMC).....	132
5.2. Brainstem.....	133
5.3. Cerebellum.....	134
6. Brain structures associated with discomfort/pain processing.....	135
7. Implications for physiotherapeutic techniques.....	136
8. Limitations.....	139
8.1. General limitations.....	139
8.2. Study I and II (fMRI).....	141
8.3. Study III (TMS).....	142
8.4. Study IV (HRV).....	143
9. Summary of effects of pressure stimulation and future directions.....	143
XI. References	147

XII. List of abbreviations	191
XIII. List of figures	195
XIV. List of tables	196
XV. List of publications	197
1. Published research papers directly related to the topic of the thesis.....	197
2. Research papers directly related to the topic of the thesis submitted and in preparation.....	198
3. Published research papers from broader area of sensorimotor plasticity research...	199
4. Other published original research papers.....	200
5. Author record.....	201
XVI. Abstract	202
XVII. List of annexes	204
XVIII. Annexes	205
1. Annex 1.....	205
2. Annex 2.....	219
3. Annex 3.....	231
4. Annex 4.....	254
5. Annex 5.....	260
6. Annex 6.....	279
7. Annex 7.....	287
8. Annex 8.....	294
9. Annex 9.....	305

I. INTRODUCTION

Peripheral afferent input provides a critical drive for primate motor control and its complete removal can lead to paralysis (Mott and Sherrington, 1895), while partial sensory deficits result in loss of coordination (Bard et al., 1995; Ghez and Sainburg, 1995; Gordon et al., 1995). Deafferentation in the absence of specific intervention also suppresses motor plasticity and learning (Bard et al., 1995; Ghez and Sainburg, 1995; Pavlides et al., 1993; Taub and Berman, 1968). Conversely, long term potentiation-like (LTP-like) facilitation of neuronal discharge can be demonstrated in the primary motor cortex (M1) of the mammalian brain following direct stimulation of the primary somatosensory cortex (S1; Kaneko et al., 1994a; Sakamoto et al., 1987). Hence, peripheral afferent stimulation has been used to induce experimental plasticity of the human motor system (e.g., Charlton et al., 2003; Hamdy et al., 1998; Ridding et al., 2001) and has become an important component of techniques to improve or restore motor function (e.g., Conforto et al., 2002; Fraser et al., 2002; Powell et al., 1999). Beyond short-term facilitation of motor responses known since Sherrington (1906, pp. 36–37), longer duration of peripheral stimulation can induce facilitatory changes that persist for minutes and hours (Chipchase et al., 2011). Most commonly studied peripheral stimulation modalities include nerve stimulation by electrical current or vibration, which are easy to control and administer (Chipchase et al., 2011; Proske and Gandevia, 2018, 2012; Taylor et al., 2017). Natural modalities of peripheral stimulation, such as tactile, pressure or proprioceptive, have been explored less extensively (Rosenkranz and Rothwell, 2003), even though they represent essential elements of clinical rehabilitation techniques and procedures.

Among the modalities of the peripheral mechanical stimulation, vibration has been more thoroughly studied especially due to its ability to almost selectively entrain the signal from muscle spindle afferents (Burke et al., 1976). It has thus become an invaluable tool to investigate the proprioception, kinaesthesia and motor control (Proske and Gandevia, 2018, 2012; Taylor et al., 2017).

In contrast, non-vibratory sustained pressure stimulation has been investigated only infrequently (Chung et al., 2015, 2014). Furthermore, processing of the proprioceptive inputs has been shown to integrate not only muscle or tendon afferents, but also skin receptors (Aimonetti et al., 2007; Edin and Abbs, 1991; Kavounoudias et al., 2001, 1998; Roll et al., 2002), further highlighting the need for research that would span multiple modalities.

In the first part of the thesis, an overview is provided of how the sensorimotor system is affected by manipulation of peripheral input using vibration, sustained pressure, and reduction of the afferent input by reversible deafferentation, including intramuscular application of botulinum neurotoxin type A (BoNT-A). The three modalities of peripheral interventions are included for the following reasons: First, a selection of basic research on vibratory stimulation is presented to demonstrate possible applications of peripheral mechanical stimulation in general, being an inspiration for less thoroughly studied stimulation modalities, such as mechanical pressure. Second, current evidence for central effects of mechanical pressure stimulation is summarised to provide background for the original research described in this thesis. Third, evidence for central effects of BoNT-A is presented as an effort to provide a broader perspective on the role of afferentation in motor control and for its prominent clinical applications and rich evidence in neurological disorders, including number of studies from our lab on which the author of this thesis collaborated. Since a full overview of each of the modalities would be far beyond the scope of a thesis, the literature review is focused on the central effects of prolonged manipulation, both in sense of increase and decrease of afferent input. For the same reasons, primarily the evidence from transcranial magnetic stimulation (TMS) and functional magnetic resonance imaging (fMRI) studies is considered, although other selected approaches are discussed where required to provide a sufficient background.

II. ANATOMY AND PHYSIOLOGY OF THE SENSORIMOTOR SYSTEM

1. Somatosensation: Cutaneous mechanoreceptors

Several somatosensory afferent systems can be distinguished in the human central nervous system (CNS). Although defined anatomically and physiologically, they roughly correspond to the sensory modalities they convey (Abraira and Ginty, 2013). The perception of innocuous mechanical skin stimulation, which is the main focus of this thesis, is mediated by the so-called low-threshold mechanoreceptors (LTMR; Abraira and Ginty, 2013). These involve four types of afferents defined based on their discharge pattern and receptive fields (Vallbo and Johansson, 1984), including slow-adapting type I afferents (SA-I, Merkel endings or disks) for low-frequency (static) stimuli such as mechanical pressure; slow-adapting type II (SA-II) for skin stretching; fast-adapting type I (FA-I, Meissner endings) for flutter up to 40–50 Hz, and fast-adapting type II (FA-II, Pacinian corpuscles) for high-frequency (vibratory) stimuli up to 400 Hz (Delmas et al., 2011; Johansson and Flanagan, 2009; Johansson and Vallbo, 1983; Vallbo and Johansson, 1984). The signals from LTMR are conducted by relatively fast class A β myelinated fibres (McGlone and Reilly, 2010).

The receptive field of FA-I and SA-I afferents is small and circumscribed, whereas FA-II and SA-II afferents respond to stimuli from much broader and overlapping areas (Johansson and Flanagan, 2009; McGlone and Reilly, 2010). The SA-I afferents are very sensitive to the slightest skin displacements and have high spatial resolution (down to 0.5 mm), providing detailed image of the tactile stimuli (Abraira and Ginty, 2013). They also respond to static pressure and their discharge rate scales with the depth of indentation (Abraira and Ginty, 2013; McGlone and Reilly, 2010). The SA-II receptors are likely to participate in proprioception as they detect limb shape and conformation (Abraira and Ginty, 2013), particularly at fingers where muscle proprioceptors yield ambiguous signals (Collins et al., 2000). Another role of the SA-II afferents lies probably in detection of object motion that is associated with skin stretch (Abraira and Ginty, 2013). FA-I mechanoreceptors are suggested to have a function complementary to SA-I afferents. As they are quite ignorant of static forces, they might be tuned to detection of sudden object or surface motion. FA-II afferents, with their large receptive fields and deep location, are less suited to discriminate spatial characteristics of the stimuli. On the other hand, they are extremely sensitive to high frequency stimuli, thus, particularly capable of resolving

temporal structure of stimulation, similar to our auditory system (Abraira and Ginty, 2013; Formby et al., 1992).

As opposed to LTMR, the high-threshold mechanoreceptors (HTMR) respond to noxious touch and can be divided into fast A δ afferents that are implicated in mediating fast mechanical pain or noxious thermic stimuli, and C afferents that are responsible for slow mechanical pain sensation. Neither A δ nor C afferents form any specialised skin organs, but rather branch into free nerve endings (Abraira and Ginty, 2013).

Much more detailed description of functional and molecular characteristics of skin afferents has been provided elsewhere (Abraira and Ginty, 2013; Johansson and Flanagan, 2009; McGlone et al., 2014; McGlone and Reilly, 2010; Strzalkowski et al., 2018).

2. Somatosensation: Proprioceptors of the musculoskeletal system

Another group of afferents consists of sensory endings enclosed within specialised sensory organs in joints, skeletal muscles, and their tendons. In general, they provide information about relative body position and movement, and contribute to the sensation of body ownership and self agency (Koch et al., 2018; Proske and Gandevia, 2018, 2012). The main proprioceptors are the muscle spindles, which are stretch receptors of the skeletal muscles (Proske and Gandevia, 2012; Windhorst, 2007). They are innervated by two types of afferents: the primary endings with the group Ia afferents and the secondary endings with the group II afferents (Windhorst, 2007). The primary endings are sensitive to dynamic stretch (they are length- and velocity-dependent), whereas the response of secondary endings is proportional mainly to the stretch size (Proske and Gandevia, 2012).

Another important type of proprioceptor, the Golgi organs, can be found in tendons at the musculotendinous junction (Windhorst, 2007). They are innervated by the type Ib afferents and are sensitive to tendon stretch, especially during muscle contraction (Proske and Gandevia, 2012). Therefore, Golgi tendon organs are considered as muscle force receptors rather than passive muscle stretch detectors (Windhorst, 2007).

Further afferent input comes from joint receptors, including Ruffini-like endings detecting tissue stretch and Paciniform corpuscles sensitive to compression. The joint receptors discharge mostly in positions near the limits of the joint movement range and produce ambiguous signals in intermediate joint positions. Therefore, their contribution to coding of joint position and movement is rather limited, and they have been suggested to serve as “limit detectors” of movement (Proske and Gandevia, 2012).

3. Somatosensory afferent pathways

Somatosensory and proprioceptive input from the trunk and limbs enters the spinal cord via dorsal roots of the spinal nerves. The axons of the pseudounipolar dorsal root ganglion cells either enter ipsilateral dorsal column or synapse on neurons in the ipsilateral dorsal horn (Abraira and Ginty, 2013; McGlone and Reilly, 2010). It has been suggested that major processing of sensory stimuli occurs already at the spinal level and only a minority of fibres continue directly as the first-order neurons to the brainstem (Abraira and Ginty, 2013; Koch et al., 2018). Spinal grey matter is responsible for the low-level sensorimotor integration as it contains anatomical substrates of monosynaptic and complex polysynaptic spinal reflexes (for review, see Windhorst, 2007).

Several distinct afferent pathways can be recognised in the spinal white matter, partly reflecting the variety of peripheral receptors. Axons responsible for thermic sensation, pain, but also non-discriminative touch and pressure decussate soon in the spinal cord to continue within the anterolateral system to the reticular formation, periaqueductal grey, hypothalamus and thalamic nuclei (Abraira and Ginty, 2013; Kayalioglu, 2009). Neurons of the spinothalamic tract send also collaterals to several structures other than thalamus, such as the medullary reticular formation (Kevetter and Willis, 1983), the parabrachial area (Hylden et al., 1989), the periaqueductal grey (Harmann et al., 1988), and the nucleus accumbens (Kayalioglu, 2009; Kayalioglu et al., 1996). On the other hand, direct branches of the pseudounipolar neurons as well as many post-synaptic dorsal horn projection neurons conveying tactile and proprioceptive information ascend in the gracile (for the lower body) and cuneate fasciculi (for the upper body) to reach two nuclei in the dorsal medulla bearing the same names (Abraira and Ginty, 2013; McGlone and Reilly, 2010). Another proprioceptive pathway, the dorsal spinocerebellar tract (DSCT), consists of post-synaptic muscle afferents from the ipsilateral lower limb synapsing either in the dorsal horns or in the Clarke's column (Proske and Gandevia, 2012; Stecina et al., 2013). The post-synaptic DSCT neurites ascend to the anterior cerebellum, although animal data also indicate another termination in the nucleus Z of the medulla (Mackel and Miyashita, 1993; Proske and Gandevia, 2012). Similar to DSCT, the ventral spinocerebellar tract also terminates in the cerebellum. However, it conveys mostly reafferentation from the ventral horns and spinal central pattern generators (CPG; Stecina et al., 2013). For a detailed review of spinal circuits involved in somatosensory processing, see (Abraira and Ginty, 2013; Koch et al., 2018).

After the dorsal column pathway is relayed in the medulla (in the gracile and cuneate nuclei, as well as the nucleus Z), its post-synaptic neurons cross the midline and continue

as the medial lemniscus to the thalamus (Proske and Gandevia, 2012). In the thalamus, inputs from the face area originating from the trigeminal nerve and trigeminal nuclei synapse at the ventral posteromedial (VPM) nucleus, whereas the medial lemniscus pathway carrying information from the rest of the body terminates in the ventral posterolateral (VPL) nucleus (Hooks, 2017). In contrast, the nucleus Z neurons project to the ventral lateral (VL) nucleus and to the oral part of the ventral posterolateral (VPLo) nucleus, i.e., motor thalamic nuclei that also receive cerebellar inputs (Mackel and Miyashita, 1993).

Thalamic neurons send their axons via the internal capsule to a number of cortical areas (McGlone and Reilly, 2010). The initial somatosensory processing occurs in the S1 located in the postcentral gyrus. It consists of four distinct cytoarchitectonic areas designated as Brodmann area (BA) 3a, 3b, 1, and 2 in rostro-caudal order (Kaas et al., 1979; McGlone and Reilly, 2010). The S1 is somatotopically organised mainly in the mediolateral and superior-inferior direction. Its dorsomedial apex holds the primary somatosensory representation of the lower limb, whereas the ventrolateral part contains the representation of the face. The upper limb representation is found between these two on the dorsolateral convexity of the hemisphere. This topographical organisation has been classically depicted as a somatosensory homunculus (Foerster, 1936; McGlone and Reilly, 2010; Penfield and Boldrey, 1937). In fact, it has been suggested that each of the cytoarchitectonic areas within the S1 contains its own representation of the body surface, thus creating four parallel body maps (Kaas et al., 1979; Sanchez-Panchuelo et al., 2012). Area 3a was shown to receive mainly proprioceptive input including afferents from muscle spindles (Delhaye et al., 2018; Hore et al., 1976; Iwamura et al., 1993; Kaas et al., 2018; Naito, 2004), whereas areas 3b and 1 process chiefly tactile input (Delhaye et al., 2018; Iwamura et al., 1993; Kaas et al., 2018). Area 2 receives both tactile and proprioceptive input (Delhaye et al., 2018; Iwamura, 2000; Iwamura et al., 1993; Kaas et al., 2018). Additionally, it has been shown to receive bilateral input (Iwamura, 2000; Iwamura et al., 1994), integrate multiple afferent signals and perform higher-order processing, such as shape recognition (Delhaye et al., 2018; Ehrsson et al., 2005; Iwamura et al., 1993; Naito et al., 2005). Furthermore, according to the current concept of cortical somatosensory processing, only area 3b can be truly viewed as the proper S1, whereas areas 1 and 2 are already considered as higher-order areas (for review, see Delhaye et al., 2018).

Besides the S1, sensory input is additionally processed in another cortical somatosensory area located in the parietal opercular cortex, i.e., the secondary somatosensory cortex (SII or S2; Adrian, 1940; Bretas et al., 2020; Delhaye et al., 2018; Eickhoff et al., 2006; McGlone

and Reilly, 2010). In a narrow sense, the S2 corresponds to the OP1 area defined by Eickhoff et al. (2006), whereas in a broader sense, it also contains the more anterior parietal ventral area (PV or OP4) and both OP1 and OP4 have separate body representation maps (Bretas et al., 2020; Delhaye et al., 2018; Eickhoff et al., 2006). Processing of sensory information in the S1 and S2 was suggested to occur in both parallel and serial fashion (i.e., from S1 to S2; Chung et al., 2014). The S2 is a higher-order area: it receives bilateral input, its responses to somatosensory stimulation are context-dependent, and it hosts complex processing and multimodal sensory integration (Bretas et al., 2020; Delhaye et al., 2018). Further higher-order cortical areas involved in somatosensory processing are the insular cortex and the posterior parietal cortex, areas 5 and 7b, but detailed discussion of their properties is beyond the scope of this thesis (Delhaye et al., 2018; McGlone and Reilly, 2010).

4. Motor system structures and sensorimotor integration

The classical motor system consists of several hierarchically organised cortical areas and cortico-subcortical loops. The control of low-level dynamic characteristics of movement, especially in distal limb muscles, has been attributed to the M1 (Chouinard and Paus, 2006; Omrani et al., 2017), which is located in the precentral gyrus and corresponds to two cytoarchitectonic areas, the area 4a and 4p (Roland and Zilles, 1996). Both areas seem to contain separate body map representations and distinct functions, e.g., area 4p is modulated by attention, whereas area 4a is not (Binkofski et al., 2002; Geyer et al., 1996). The M1 follows similar somatotopic organisation as the S1 (Roland and Zilles, 1996), together being also referred to as the sensorimotor cortex (SMC; e.g., Tempel and Perlmutter, 1990). Within the motor system, M1 receives cortical input from the dorsal premotor cortex (BA 6, dorsal PMC or PMd) located just rostral to the M1 (Picard and Strick, 2001). The PMd is implicated in motor planing and movement generation (Picard and Strick, 2001), as well as in selecting movements based on arbitrary or spatial cues and motor learning (Chouinard and Paus, 2006). In contrast, ventral premotor cortex (PMv), also densely connected with the M1, participates in object-related hand movements (Chouinard and Paus, 2006) and has been associated with object and action observation, containing the so-called “mirror neurons” (di Pellegrino et al., 1992; Gallese et al., 1996). Further input into the M1 comes from the mesial part of the area 6, which has a distinct function and has been named supplementary motor area (SMA; Picard and Strick, 2001, 1996; Tanji and Shima, 1996). The caudal part of the SMA adjacent to the M1 (the SMA proper) can be differentiated from the more anterior pre-SMA, which does not receive

significant somatosensory input and lacks reciprocal connections with the M1 (Picard and Strick, 1996; Tanji and Shima, 1996). The SMA proper (further referred to as SMA) has been associated with initiation of internally driven movements, connecting conditional rules with actions (choosing a movement appropriate for the context), and possibly movement sequencing or motor learning (Hoffstaedter et al., 2013; Nachev et al., 2008). Another area involved in motor control has been identified in the cingulate cortex. In primates, it has been termed cingulate motor area (CMA), corresponding to the anterior midcingulate cortex in humans. It was suggested to participate in conflict monitoring, response selection and/or transforming intentions into motor actions (Hoffstaedter et al., 2014, 2013; Picard and Strick, 2001).

Cortical sensorimotor integration takes place at several levels. Somatosensory (mainly proprioceptive) thalamic projections from the VL or VPLo are long known to reach PMd and SMA (Omrani et al., 2017), which are in turn connected to the M1 (Chouinard and Paus, 2006). Direct projections from the thalamus to the M1 were also documented (for reviews, see Naito, 2004; Omrani et al., 2017). Namely, cortical responses in the primate M1 have been observed following both natural and artificial muscle spindle stimulation (e.g., Colebatch et al., 1990; Fourment et al., 1996; Hore et al., 1976; Lucier et al., 1975; Rosén and Asanuma, 1972). Similar to PMd and SMA, the M1 is also likely to receive direct afferentation from the muscle spindles via the thalamocortical pathway from the VPLo (e.g., Asanuma et al., 1980; Darian-Smith and Darian-Smith, 1993; Hore et al., 1976; Jones and Porter, 1980; Lemon and van der Burg, 1979; Wong et al., 1978) or VL nuclei (Fang et al., 2006; Huffman and Krubitzer, 2001). Simultaneously, M1 receives indirect input from areas 3a (e.g., Ghosh et al., 1987; Huerta and Pons, 1990; Stepniewska et al., 1993), 2 (e.g., Darian-Smith et al., 1993; Ghosh et al., 1987; Jones et al., 1978; Stepniewska et al., 1993), 1 (e.g., Ghosh et al., 1987; Stepniewska et al., 1993), and 5 (e.g., Darian-Smith et al., 1993; Strick and Kim, 1978; Zarzecki et al., 1978). Somatosensory cortices are also densely connected with SMA and PMd (Jones et al., 1978). Further convergence of somatosensory influences and motor commands occurs via the cortico-subcortical loops involving the basal ganglia, cerebellum, and thalamus (for reviews, see Nachev et al., 2008; Omrani et al., 2017). Thus, considerable amount of anatomical and physiological evidence supports close interactions between the somatosensory and motor systems.

5. Cortical plasticity

The capacity to adapt cortical representations is a hallmark of a developing brain (Ismail et al., 2017; Krägeloh-Mann et al., 2017). Even adult cortical motor representations may be

subject to change in the process of neuroplasticity (for reviews, see Buonomano and Merzenich, 1998; Donoghue, 1995; Froemke, 2015; Roelfsema and Holtmaat, 2018; Sammons and Keck, 2015). Cortical reorganisation has been shown both during motor learning (Classen et al., 1998; Hund-Georgiadis and von Cramon, 1999; Karni et al., 1998, 1995; Pascual-Leone et al., 1994, 1993) and in response to a focal brain damage (Cicinelli et al., 1997; Liepert et al., 2000; Traversa et al., 1997; for review, see Ward and Cohen, 2004) or spinal cord injury (SCI; Ding et al., 2005; Levy et al., 1990; for review, see Topka et al., 1991) and limb amputation (Chen et al., 1998; Cohen et al., 1991; Fuhr et al., 1992). Reversible though sustained plasticity has also been experimentally induced in healthy subjects (Classen et al., 1998; Stefan et al., 2000).

Several cellular mechanisms have been proposed as neurobiological substrates of cortical plasticity (Bütefisch, 2006; Feldman, 2009). One mechanism, first discovered in the mammalian hippocampus, involves modification of the post-synaptic membrane that can be experimentally induced by short tetanic stimulation. After such stimulation, a long-term potentiation (LTP) of synaptic transmission can be observed (Bliss and Lomo, 1973). The phenomenon is first involves activation of the post-synaptic voltage-dependent N-methyl-D-aspartate (NMDA) glutamate receptors, and is then maintained by accumulation of the α -amino-3-hydroxy-5-methyl-4-isoxazolepropionic acid (AMPA) receptors on the post-synaptic membrane and enlargement of dendritic spines (for reviews, see Malinow and Malenka, 2002; Nicoll, 2017). Pre-synaptic mechanisms, e.g., involving retrograde nitric oxide (NO) signalling, were also documented (Feldman, 2009). The resulting strengthening of synaptic transmission underlies use-dependent learning and memory (Bliss and Lomo, 1973; Nicoll, 2017; Rioult-Pedotti et al., 2000). Besides the hippocampus, similar LTP-like facilitation was also demonstrated in the mammalian M1 following direct stimulation of the S1 (Iriki et al., 1989; Kaneko et al., 1994a; Sakamoto et al., 1987). Somatosensory inputs were thus shown to directly participate in acquiring new motor skills (Iriki et al., 1989; Sakamoto et al., 1989). Simultaneous associative stimulation of cortico-cortical and thalamocortical pathways can also induce LTP in interneurons receiving thalamic input (Iriki et al., 1989). This thalamocortical pathway was also suggested to mediate indirect somatosensory influence relayed by the interposed nucleus of the cerebellum (Luft et al., 2005; Manto et al., 2006).

In contrast to LTP, sustained low-frequency stimulation can induce long-term depression (LTD) of synaptic transmission (Hess and Donoghue, 1996a; Linden, 1994). Several mechanisms underlying LTD have been proposed including NMDA receptor-dependent LTD, LTD mediated by metabotropic glutamate receptor, and LTD related to cannabinoid

type 1 receptor (Feldman, 2009). Unlike LTP, the LTD is implicated in use-dependent response weakening possibly associated with stimulus deprivation (Feldman, 2009). LTP and LTD thus illustrate how sensory input may have bi-directional influence on connection strength depending on stimulus parameters (Feldman, 2000; Hess and Donoghue, 1996b; Linden, 1994).

Another mechanism has been proposed to underlie rapid adaptive reorganisation of cortical motor output zones by unmasking latent horizontal projections (Bütefisch, 2006; Donoghue, 1995; Jacobs and Donoghue, 1991; Rosenkranz and Rothwell, 2006a). The mechanism was suggested to involve modification of γ -aminobutyric acid A (GABA_A)-ergic inhibitory intracortical circuits (Jacobs and Donoghue, 1991), leading to changes in intracortical inhibition that may be assessed non-invasively using paired-pulse TMS (pTMS) protocols (Chen et al., 1999; Ilić et al., 2002; Kujirai et al., 1993; Ziemann et al., 1996a).

Besides microstructural changes at the level of receptors, plasticity may involve experience-dependent structural changes in dendritic spines and synaptogenesis that occur within hours and days (Bütefisch, 2006; Feldman, 2009). Slower structural changes in thalamocortical and horizontal projections are also possible over several days or weeks (Feldman, 2009), but a detailed account of structural plasticity is not within the scope of this work.

In summary, this section has provided an overview of anatomical structures and physiological mechanisms universally participating in modulation and reorganisation of the motor cortex. The next section introduces some commonly used electrophysiological and imaging methods allowing non-invasive assessment of the resulting macroscopic neuroplastic changes in humans. Despite recent advances in neuroimaging techniques, direct translation of animal neurophysiological data into human research is not straightforward. Since multiple neuroplastic processes commonly coincide, it is likely that effects of natural stimulation involve a combination of several mechanisms, such as strengthening or weakening of excitatory connections (LTP/LTD), modification of inhibitory GABA-ergic circuits, and subsequent structural changes (Bütefisch, 2006; Feldman, 2009). It is therefore challenging to link the neuronal processes identified on the microscale with human data from behavioural, electrophysiological, or neuroimaging studies. Though being mostly based on indirect evidence, such conceptual relationships are pointed out on several occasions when discussing specific effects of stimulation or deafferentation in the sections “IV. Enhancing the afferent input: Modalities of peripheral stimulation” and “V. Reducing the afferent input: Means of plasticity facilitation”.

III. METHODS FOR MAPPING THE SENSORIMOTOR SYSTEM AND ITS PLASTICITY

Human research of experimentally induced plasticity is essentially limited to non-invasive or semi-invasive methods. Electrophysiology and magnetoencephalography (MEG) can provide superb temporal resolution down to milliseconds. However, except for a few direct invasive applications reserved for patients with structural brain lesions or epilepsy, standard non-invasive electrophysiological approaches available in healthy subjects lack the spatial resolution necessary to unambiguously relate their findings to a specific cytoarchitectonic area (Lotze et al., 2003).

In contrast, modern neuroimaging methods, including ultra-high field magnetic resonance imaging (MRI), can provide outstanding spatial resolution at sub-millimetre dimensions that allows visualisation of individual cortical columns and laminae (Petridou and Siero, 2019). Yet despite technological advances, current neuroimaging methods cannot get even close to the time scale of individual neuronal events, which are obscured not only due to technological constraints, but also due to physiological delay caused by neurovascular coupling (Ogawa et al., 1993).

Some limitations can be addressed by combining the evidence from both approaches. While there have been studies combining imaging and electrophysiology recordings (e.g., Lotze et al., 2003), most of the available evidence originates from unimodal studies with different protocols and study populations, which limits translation of results from one method to another. In this section, three methodological approaches widely used in mapping of the sensorimotor system function and plasticity are briefly introduced as they are frequently referred to in the following sections.

1. Transcranial magnetic stimulation (TMS)

TMS is an electrophysiological method commonly used for assessment of corticomotor excitability. The procedure involves electromyographic (EMG) recordings following cortical stimulation delivered by a magnetic stimulator typically equipped with a figure-of-eight coil. When the coil is positioned over the scalp approximately above the M1, a suprathreshold stimulus elicits the so-called motor evoked potential (MEP) in a target muscle. Due to inherent MEP variability, recordings require substantial averaging. Parameters of the MEP that reflect cortical excitability include the amplitude, resting motor threshold (rMT), active motor threshold (aMT), and MEP area (total MEP amplitude time integral). Whereas the amplitude reflects the transsynaptic cortical excitability

(Devanne et al., 1997), the rMT is more associated with membrane excitability (Christova et al., 2010; Ziemann et al., 1996b). MEP are commonly used clinically to assess the integrity of the corticospinal system, sensitive to detect its lesions in the brain or spinal cord. Additional, more elaborate, TMS protocols are used in research.

1.1. Paired-pulse protocols

Paired-pulse protocols can provide additional information about intracortical circuitry unbiased by spinal motoneuron excitability. One of frequently used paradigms utilises a sub-threshold conditioning stimulus (optimally 80% of rMT) followed by a supra-threshold test stimulus (usually 120% rMT; Kujirai et al., 1993). Stimulation protocols with short (2–4 ms) inter-stimulus intervals (ISI) between the test and the conditioning stimuli (Rosenkranz and Rothwell, 2003) reflect the so-called short-interval (or short-latency) intracortical inhibition (SICI), which depends on the function of the GABA_A-ergic inhibitory intracortical circuits (Chen et al., 1999; Ilić et al., 2002; Kujirai et al., 1993; Ziemann et al., 1996a). Decrease in SICI presumably reflects rapid plasticity involving unmasking of latent horizontal connections (Christova et al., 2010; Jacobs and Donoghue, 1991). Conversely, administration of GABA_A agonists increases SICI and prevents plastic changes (Ziemann et al., 2001). Longer ISIs (10–15 ms) (Rosenkranz and Rothwell, 2003) reflect the so-called intracortical facilitation (ICF). The physiological background of the ICF is less understood, but it is likely to rely on glutamatergic NMDA synapses (Liepert et al., 1997; Nakamura et al., 1997). Changes in ICF have been suggested to reflect LTP-like mechanisms (Christova et al., 2011; Kaneko et al., 1994a; Sakamoto et al., 1987).

Another pTMS protocol utilises a suprathreshold conditioning stimulus delivered 100 ms (range 50–200 ms) before the test stimulus to evoke so-called long-interval (or long-latency) intracortical inhibition (LICI), which reflects the function of the GABA_B-ergic inhibitory interneurons interacting with GABA_A-ergic neurons (Rosenkranz and Rothwell, 2003; Swayne et al., 2008). Further parameters that could be obtained from paired-pulse protocols include contralateral and ipsilateral cortical silent period (CSP), short-latency afferent inhibition (SAI), long-latency afferent inhibition (LAI), and interhemispheric inhibition (IHI; for review, see Di Pino et al., 2014).

1.2. TMS as an intervention

Several TMS protocols have been introduced as means of direct inhibitory or facilitatory intervention, often combined with manipulations of afferent input to study their central effects (e.g., Rollnik et al., 2001; Rosenkranz and Rothwell, 2006a; Ziemann et al., 1998a).

A repeated delivery of a peripheral stimulus followed by a single-pulse TMS (so-called paired associative stimulation or PAS) may lead to outlasting increases or decreases of MEP amplitude, depending on the ISI. Repetitive TMS (rTMS) alone may also produce short-term changes in cortical excitability. Low-frequency (< 1 Hz) continuous rTMS applied over a cortical area has inhibitory effect on MEP, whereas high-frequency stimulation increases MEP. For more details on rTMS alone, see a comprehensive review by Jacobs et al. (2012).

2. Positron emission tomography (PET)

Before the era of fMRI, positron emission tomography (PET) has been one of the most widely used methods for non-invasive imaging of brain function. The technique exploits the ionising radiation (β^+ particles) emitted by radiotracer injected or inhaled by the subject. There is a constantly growing number of clinical applications of PET in neurology, e.g., in diagnostics of brain tumours or neurodegenerative disorders such as Alzheimer's disease, in which a radionuclide (usually ^{18}F , but also ^{11}C , ^{15}O , ^3H , ^{125}I , or ^{64}Cu) is attached to a specific metabolite or ligand (Drake et al., 2020; Uzuegbunam et al., 2020). In functional neuroimaging, use of radiotracers such as ^{18}F -fluoro-deoxy-glucose (^{18}F -FDG or FDG), ^{15}O -labelled water (H_2^{15}O), and ^{15}O -butanol has allowed quantitative measurement of regional cerebral blood flow (rCBF) and regional cerebral blood volume (rCBV; Raichle, 1986). The rCBF correlates well with neuronal activity (Raichle, 2011). With the advances in stereotactic localisation (Fox et al., 1985), it has therefore become an important tool to investigate human brain function (Bodegård et al., 2003; Naito et al., 1999; Raichle, 1986; Tempel and Perlmutter, 1990). Even after the development of fMRI (see the next section), it still retains its advantages, e.g., a great spectrum of specifically binding radioligands for certain brain research applications.

3. Functional magnetic resonance imaging (fMRI)

3.1. Magnetic resonance imaging principles

Before discussing specific fMRI applications, some fundamental principles of nuclear magnetic resonance imaging (NMRI or shorter MRI) have to be introduced. MRI utilises interaction of nuclei that possess spin magnetic moment (such as ^1H , ^{13}C , ^{31}P) with an external magnetic field. By far, ^1H is the most frequently used element in neuroimaging and is, therefore, implicitly considered in this thesis (Jezzard and Clare, 2001).

Typical clinical and research MRI scanners consist of several electromagnets. In a strong background magnetic field (B_0), usually between 1.5 and 3.0 T, magnetic moments of the hydrogen nuclei in tissues become aligned parallel or anti-parallel to the external field. A small surplus of parallelly aligned moments results in net magnetisation in the direction of the external magnetic field. From a simplified point of view, the image is acquired when a radio-frequency (RF) magnetic field pulse selectively excites the hydrogen nuclei, which subsequently emit energy as they gradually return to their original state. From a more detailed perspective, when exposed to a transverse radio-frequency (RF) magnetic field (B_1) pulse at a certain frequency, the so-called Larmor frequency, proportion of magnetic moments absorbs the energy and enters a higher energy state. The Larmor frequency is determined by the strength of B_0 and local shielding of the electron shell depending on electron distribution in the given compound, which are important considerations for the selective excitation of a tissue sample. As a result of the excitation, the longitudinal component of net magnetisation decreases, while instead, a transverse component appears and starts to precess with the Larmor frequency, causing oscillatory signal that can be detected by a receiver coil. As magnetic moments return to the original state, net longitudinal magnetisation recovers with T_1 time constant (longitudinal relaxation time), while transverse magnetisation decays with T_2 time constant (transverse relaxation time). Whereas T_1 reflects spin-lattice interactions (i.e., return into a thermodynamic equilibrium state, which is slowed down by random molecular movements), T_2 decay is mostly dependent on energy exchange between nuclei due to small shifts in local (molecular-level) magnetic fields resulting in loss of precession coherence (dephasing or spin-spin interactions; Jezzard and Clare, 2001; Matthews, 2001).

The tissue-specific relaxation time constants depend on multiple intrinsic properties, such as water content, the degree of myelination, or the content of iron (Gracien et al., 2019). By adjusting the spacing between consecutive excitation RF pulses (repetition time, TR) and between the excitation pulses and their respective readouts (echo time, TE) in the so-called MRI sequences, the MRI scanner can be tuned to record signal that is more affected either by T_1 (T_1 -weighted contrast) or T_2 relaxation (T_2 -weighted contrast). A sequence with negligible T_1 and T_2 -weighting reflects the density of hydrogen nuclei in the tissue (proton density contrast, PD). These three parameters govern most of the image properties in routine anatomical (morphological) imaging. By applying additional magnetic fields (gradient fields) that linearly modify the background B_0 field during the MRI sequence, spatial distribution of the signal sources and, therefore, a two-dimensional or three-dimensional image of the scanned object can be reconstructed (Jezzard and Clare, 2001).

The T_1 and T_2 -weighted brain images are included in most protocols for standard clinical applications. An example of a common T_1 -weighted MRI sequence is magnetisation-prepared rapid acquisition with gradient echo (MPRAGE), whereas an example of a routinely T_2 -weighted sequence with an additional water-suppression module is fluid-attenuated inversion recovery (FLAIR). Note that the aforementioned sequences as well as their names are vendor-specific. Though they are mainly used in the clinical routine, these or similar sequences are also included in research protocols to provide anatomical reference for functional imaging. For advanced research purposes, special quantitative techniques measuring exact relaxation time constants or PD have also been developed (for more details, see our recent works Gracien et al., 2019, 2017; Nürnberger et al., 2017).

3.2. Blood oxygenation level-dependent (BOLD) contrast

T_1 , T_2 , and PD are not the only parameters affecting the image signal. In some cases, transversal magnetisation decay is much faster than it would be just due to local molecular tissue properties. A principle similar to that underlying T_2 relaxation also applies when the homogeneity of the static B_0 field is compromised, e.g., at the borders of areas with different magnetic susceptibility, such as air/tissue interfaces. The transverse relaxation decay that includes these larger-scale field inhomogeneities is called T_2^* relaxation. Due to usually static nature of the inhomogeneities, their effects can be largely reversed by a 180° refocusing RF pulse positioned exactly at $\frac{1}{2}$ TE. The refocusing pulse is a key element of a simple spin echo (SE) sequence and many more complex imaging techniques. Hence, an almost pure T_2 image contrast is attainable (Jezzard and Clare, 2001).

However, the T_2^* relaxation is not always undesired. Effects resembling artefacts at air/tissue boundaries can be observed around the blood vessels where magnetic field is affected by the level of deoxyhaemoglobin, which is paramagnetic (increasing magnetic flux) as opposed to diamagnetic (slightly reducing magnetic flux) oxyhaemoglobin (Jezzard and Clare, 2001; Matthews, 2001). It was therefore shown that increased content of deoxyhaemoglobin reduces the signal around the blood vessels, whereas increased oxygenation does the opposite. This phenomenon, first described by Ogawa et al. (1993, 1990), was termed blood oxygenation level-dependent (BOLD) effect.

The blood flow in the smallest cerebral arteries is, to a large degree, regulated by local mechanisms. The continuously changing energy demands and oxygen consumption of local neuronal populations result in corresponding fluctuations of rCBF. The exact processes leading to changes in regional perfusion are still largely unknown (Gauthier and Fan, 2019; Nuriya and Hirase, 2016). Put in a very simplified way, increased rate of

synaptic activity (possibly predominantly involving transmission at glutamatergic synapses) initiates an inter-cellular signalling cascade via astrocytes that eventually leads to vasodilatation, increased rCBF and rCBV. Since the blood inflow exceeds the metabolic demands (at least by a factor of 2), the process results in a local net increase in haemoglobin oxygenation and, hence, increased BOLD signal. This reproducible response of the cerebral vascular tree to neuronal activity has been called neurovascular coupling (Gauthier and Fan, 2019; Gjedde, 2001; Matthews, 2001).

Some features of neurovascular coupling have critical impact on functional neuroimaging. The signalling cascade delays the vascular response by a few seconds relative to the neuronal activity. A response to a short stimulus appears 2–3 s later and peaks at about 6 s post-stimulus. This delay can be modelled by a haemodynamic response function (HRF; Donaldson and Buckner, 2001; Worsley, 2001). When exposed to a longer steady-state stimulus, the classical (canonical) HRF predicts an initial overshoot, followed by a plateau phase, and a post-stimulus undershoot (Glover, 1999). However, the neurovascular coupling may differ in various brain areas (Gauthier and Fan, 2019), as well as under various clinical conditions and during healthy ageing (Chen, 2019).

Typically, BOLD signal is measured using a gradient echo (GE) sequence that basically consists of a single excitation pulse and gradient fields. In fact, any applied gradient field is detrimental for the transverse magnetisation and the overall signal. In contrast to SE sequences, GE sequences have no refocusing pulse. Instead, the gradient field is reversed at a certain point to nullify the dephasing caused by the gradient field itself. However, as the T_2^* effects are not removed, the resulting image still suffers from signal loss and geometrical distortions especially around air/tissue boundaries, and for the same reason, it also contains BOLD weighting.

Neuronal activity and the resulting BOLD signal fluctuations are fast dynamic processes. Conventional anatomical images take up to several minutes to acquire. To allow reasonably fast imaging (~2–3 s for the whole-brain volume), reduced resolution and fast imaging techniques such as echo planar imaging (EPI) are required (Jones et al., 2001). Recently, advances in acceleration techniques, such simultaneous multislice or multiband imaging sequences, allowed for considerable improvements in temporal and/or spatial resolution of the functional images, with special protocols achieving even < 1 mm in-plane resolution or ~300 ms TR (i.e., time between two consecutive volumes; Demetriou et al., 2018; Setsompop et al., 2016).

In conventional fMRI, the relatively slow acquisition (2–3 s TR) may result in overlapping with respiratory movements and aliasing of high-frequency cardiac artefacts (Smith, 2001). Furthermore, head motion may occur at the same time scale as the neuronal activations (Brammer, 2001). All these artefacts may lead to signal changes of similar amplitude or even exceeding the BOLD signal change of neuronal origin (Jones et al., 2001; Smith, 2001). For this reason, several pre-processing steps are necessary to reduce the random and physiological artefacts and correct for head motion (Brammer, 2001; Smith, 2001). More recently, data driven approaches based on decomposition into independent components have been introduced that further improve data de-noising (Pruim et al., 2015b, 2015a; S. M. Smith et al., 2013). Most of these procedures are implemented in specialised software tools dedicated to analysis of fMRI data, such as FSL (FMRIB's Software Library, developed by Analysis Group, The Wellcome Centre for Integrative Neuroimaging [formerly FMRIB], Oxford, UK, <https://fsl.fmrib.ox.ac.uk/fsl/fslwiki>; Jenkinson et al., 2012) or SPM (Statistical Parametric Mapping, developed by The Wellcome Centre for Human Neuroimaging, UCL Queen Square Institute of Neurology, London, UK, <https://www.fil.ion.ucl.ac.uk/spm/>).

Even though artefact removal strategies are constantly improving, MRI signal is a dimensionless quantity reflecting many tissue-related and hardware-specific factors. This means that although we can quite accurately measure the relative percent signal change (%SC) of the BOLD signal, the signal baseline remains unknown. Consequently, the neuronal activity under investigation needs to be compared to an adequate baseline condition in which there is reduced or no neuronal activity in question (Bandettini, 2001). Given the low relative %SC (0.5–5%) of the signal of interest and the abundance of noise, repeated testing of the same condition and a subsequent statistical analysis is paramount to achieve reasonable confidence that the observed signal change is actually related to a relevant neuronal process (Smith, 2001; Worsley, 2001). The two basic experiment designs for repeated stimulation include block paradigms, in which sustained stimuli or longer active tasks (with typical duration between 15–30 s) alternate with rest or different baseline condition, and event-related paradigms, in which single stimuli or short tasks (< 2 s) are usually (pseudo-)randomly dispersed throughout the acquisition. The former approach offers superior robustness in terms of statistical power and is easier to set up, whereas the latter provides, at least for some psychophysiological processes, a more natural mode of interaction and is less prone to habituation (Donaldson and Buckner, 2001). In both cases, the acquired and pre-processed functional data are usually analysed in the same way. The externally imposed stimulation or tasks are modelled by box-car or

impulse functions and convolved with the HRF. Next, a general linear model (GLM) is established as a combination of individual regressors (one for each condition) with an additional error term. The resulting GLM is fit to the data by estimating individual model parameters (β) and minimising the residual error (ε). The existence of an effect (difference between two β parameters or difference of a single parameter from zero) is then usually evaluated using parametric statistical tests, such as t -test or F -test (Worsley, 2001).

Last but not least, signal of interest can be extracted using data-driven approaches, such as independent component analysis (ICA; Beckmann and Smith, 2004), and subsequent statistical inference can be performed using non-parametric tests, including permutation testing (Winkler et al., 2014). Such model-free techniques also allow analysis of randomly fluctuating data, such as those from resting-state imaging acquisitions (Beckmann et al., 2005). These methods are capable of establishing the strength of intrinsic signal correlations among distant brain regions (i.e., functional connectivity, FC), identifying so-called resting state networks. However, a detailed description of resting-state fMRI acquisition and analysis techniques is beyond the scope of this thesis.

To summarise, BOLD fMRI offers superior spatial and temporal resolution compared to PET. Furthermore, it does not involve any ionising radiation, and so far no long-term health risks of repeated exposure to MRI have been identified. With the development of BOLD technique (Ogawa et al., 1993), fMRI has thus become the primary tool for functional human brain mapping (Matthews, 2001). With recent advances, it continues to be the leading state-of-the-art method to evaluate human brain function *in vivo* (Demetriou et al., 2018; Setsompop et al., 2016).

3.3. Other functional MRI techniques

Besides BOLD imaging, there are alternative MRI methods that allow mapping of human brain function *in vivo*. A technique called arterial spin labelling (ASL) employs an RF tagging pulse that labels the blood entering the brain. ASL allows obtaining quantitative data on brain perfusion, but is considerably slower, more complicated, and offers lower functional activation contrast than BOLD imaging, therefore, it is much less frequently used (Bandettini, 2001).

IV. ENHANCING THE AFFERENT INPUT: MODALITIES OF PERIPHERAL STIMULATION

1. Vibratory stimulation

Though being typically non-natural, vibration is perhaps the most extensively studied modality of mechanical peripheral stimulation. In particular, studies of vibratory muscle stimulation deeply influenced our understanding of proprioception and kinaesthesia (for reviews, see Proske and Gandevia, 2018, 2012; Windhorst, 2007). However, vibration is a complex mechanical stimulus affecting simultaneously number of sensory structures in different tissues. Many of those receptors respond readily to other stimulation modalities as well, including innocuous pressure. Therefore, even though vibration has not been used in the design of experiments included in this thesis, many of the phenomena and observations are relevant for the related but less developed research area of mechanical pressure stimulation, which will be the topic of the next section. Out of the rich and extensive evidence about locally applied vibration, only a small selection most closely related to the topic of this thesis is presented here.

1.1. Sensory structures responding to vibration

Mechanical vibration applied over the body surface stimulates several classes of cutaneous receptors. At the site of action, vibration mainly excites Meissner (FA-I) and Pacinian corpuscles (FA-II), but also the Merkel endings (SA-I). The FA-I afferents respond the most to stimulation from ~5 Hz up to 40–50 Hz (so-called flutter), while the Pacinian corpuscles are sensitive to vibration of higher frequency between 40 and 400 Hz (Johansson and Flanagan, 2009; Johansson and Vallbo, 1983; Vallbo and Johansson, 1984). Finally, the SA-I afferents, which otherwise register low-frequency dynamic skin deformations and static pressure, respond to low frequency vibration usually below 5 Hz, though they could be stimulated by vibration up to ~30 Hz (Johansson et al., 1982).

As the mechanical waves propagate into deeper tissues, they stimulate mechanoreceptors in tendons or muscles (Gizewski et al., 2005), namely the primary and secondary muscle spindle endings (type Ia and type II afferents, respectively) and Golgi tendon corpuscles (type Ib afferents), especially when applied over the muscle tendon or belly (Burke et al., 1976). Most primary muscle spindle endings discharge in a one-to-one manner to the vibratory stimulation at frequencies up to 80–100 Hz, though some are capable to reach frequencies 180–220 Hz (Roll et al., 1989a). In a relaxed muscle, vibration with amplitude

below 0.5 mm is almost a selective stimulus for the Ia afferents (Roll et al., 1989a; Roll and Vedel, 1982), while some effects of vibration were observed with amplitude as low as 0.005–0.05 mm (Fattorini et al., 2006; Marconi et al., 2008). As opposed to Ia afferents, the secondary muscle spindle endings are entrained by vibration at much lower frequencies up to 20–40 Hz (Cordo et al., 1993), whereas Golgi tendon organs generally do not respond to vibration in a relaxed muscle, but their sensitivity increases during contraction (Roll et al., 1989a). The maximum discharge rate of the Ia afferents depends on the actual muscle length, it also increases during muscle stretching and decreases or even diminishes during muscle shortening, while the firing rate of the secondary endings is less affected by movements (Burke et al., 1976). This illustrates the complexity of vibratory stimulus and some of its dependence on multiple static and dynamic factors.

Since various mechanoreceptors differ in their sensitivity to vibration, the involved afferent pathways and their central projections, it is obvious that they exert different influence on perception, cognition, and motor behaviour, while their interaction can cause complex effects difficult to seize. Therefore, in this section, a special emphasis is put on disentangling the individual contributions of cutaneous and muscle mechanoreceptors.

1.2. Behavioural effects of vibratory stimulation

1.2.1. Cutaneous vibratory stimulation

The central correlates of vibratory skin stimulation have been studied since the dawn of neuroimaging, mostly as a means of mapping the somatotopic representations in the S1 and S2 (e.g., Fox et al., 1987; Gelnar et al., 1998; Sanchez-Panchuelo et al., 2016). Although these studies involved short stimulation restricted to a superficial skin area rather than a particular muscle or tendon, there have been several reports of stimulus-related activation in classical motor areas, such as the M1 and SMA. This was first observed in early PET studies (Burton et al., 1993; Seitz and Roland, 1992) and was later confirmed in some fMRI studies (Francis et al., 2000; Gelnar et al., 1998), indicating the potential of cutaneous afferentation to influence motor control. Despite the relatively large amount of neuroimaging research on cutaneous vibration with some compelling reports of prominent sensorimotor integration, the evidence for interaction between cutaneous vibration and motor control from behavioural and neurophysiological studies is surprisingly scarce compared to a vast body of such literature for muscle vibration.

One of the stimulation sites that attracted wider attention is the foot sole, which is in almost constant tactile contact with the ground, thus providing somatosensory cues

during stance and gait. In a series of studies, Kavounoudias et al. (2001, 1998) demonstrated that vibratory stimulation of the tactile afferents at the foot sole produces body sway away from the stimulation site: backwards in the forefoot area, forwards in the heel area, and laterally during unilateral stimulation. Similar body sways have been elicited by low-intensity transcutaneous electrical foot stimulation (Kavounoudias et al., 2001), muscle tendon vibration (e.g., Eklund, 1972; Lund, 1980), and manipulation of visual and vestibular input (e.g., Karnath et al., 1994). Moreover, cutaneous foot sole vibration was demonstrated to evoke a sensation of illusory body tilt (Roll et al., 2002) similar to illusions caused by muscle vibration (Lackner and Levine, 1979; Wierzbicka et al., 1998). These postural effects of cutaneous vibration are likely of central origin since they follow vector addition laws when interacting with the responses to muscle vibration (Diener et al., 1984; Kavounoudias et al., 2001, 1998; Roll et al., 1989b). Furthermore, cutaneous vibration of the foot sole was recently shown to affect joint position sense at the ankle (Mildren and Bent, 2016). This is in line with microneurographic evidence that ankle joint position is coded by the surrounding SA-II and FA-II afferents (Aimonetti et al., 2007). The role of foot cutaneous afferents in the maintenance of upright posture and their modulation by peripheral stimulation has therefore been well established (for reviews, see Rasman et al., 2018; Strzalkowski et al., 2018).

Another line of research has shown that random mechanical vibrations (i.e., white noise vibration low-pass filtered to 100 Hz) applied to the foot soles may improve postural sway in both healthy subjects (e.g., Priplata et al., 2003) and patients with diabetes or after stroke (Priplata et al., 2006). Similar positive effects of added noise were also observed during visuomotor tracking hand movements (e.g., Mendez-Balbuena et al., 2012). It was suggested that random vibration acts by introducing so-called stochastic resonance to the sensorimotor control loops and by improving transmission of weak signals (Priplata et al., 2006). Clinical efficacy of stochastic resonance has been mostly assessed using whole-body vibration applied via a standing platform (for review, see Dincher et al., 2019). However, application of such diffuse stimulation implicates that both cutaneous and non-cutaneous receptors are simultaneously excited, possibly masking the underlying mechanisms by introduction of complex somatosensory interactions. The effects of whole-body vibration therapy are therefore not reviewed in this thesis.

In general, the presented evidence illustrates two distinct mechanisms responsible for central effects of cutaneous vibration: (1) deterministic stimulation of specific afferents participating in motor feedback loops, possibly mimicking their normal firing rate; and (2) random stimulation introducing stochastic resonance into the sensorimotor control

loops. However, despite the promising behavioural data, follow-up research on cutaneous vibration using neurophysiological and neuroimaging methods is still lacking. In contrast, far more evidence for sensorimotor integration is available from studies using muscle vibration, which is therefore discussed to a greater extent in the next section.

1.2.2. Vibratory muscle stimulation

In comparison to cutaneous vibration, stimulation of muscle afferents has attracted much wider interest in physiological research. Careful observations of behavioural effects of muscle vibration led to discovery of several phenomena that can be generally described as alterations of conscious perceptions, implicit motor behaviour, or both. Although the extensive literature on muscle vibration has already been covered elsewhere (Proske and Gandevia, 2018, 2012; Souron et al., 2017b), some physiological background is still discussed here, as it is crucial for understanding the rationale and correct interpretation of the recent imaging studies.

Notably, the vast majority of human research was conducted at elbow or wrist flexors and extensors, whereas more complex joints or lower limbs were investigated less frequently. Therefore, unless otherwise stated, the discussed evidence is based on data from the arm and/or the forearm.

Immediate effects of vibration

It has been long known that muscle vibration can interfere with proprioception. If the visual feedback is obscured (regardless whether the eyes are open or closed), muscle vibration is accompanied by erroneous judgement of the corresponding joint position (Goodwin et al., 1972). By observing the vibration-evoked position sense errors, researchers came to believe that muscle spindle afferents significantly contribute to kinaesthesia and motor control, and distinguished two independent pathways for static (II afferents) and dynamic (Ia afferents) position sense (McCloskey, 1973). Static position information prevails in the slow movement control, whereas the (dynamic) velocity information dominates in the control of faster movements (Sittig et al., 1987). These two systems respond differentially to vibration. Performance in slow position matching tasks reflecting static position sense is consistently disturbed by vibration irrespective of the tested movement direction (Sittig et al., 1985). In contrast, velocity matching (Sittig et al., 1985) or dynamic position matching (e.g., Capaday and Cooke, 1981) is only affected when the stimulated muscle is lengthening, usually causing target undershooting (i.e., velocity overestimation). Both systems also show different dependence on vibration frequency (Cordo et al., 1995; Sittig et al., 1987). However, motor control does not always rely on

proprioception. For instance, very fast movements seem to be pre-programmed and completely unaffected by vibration (Sittig et al., 1987). Moreover, the interaction with motor planning is context-specific, depending on the frame of reference imposed by the task (Tsay et al., 2016). Further specific situations in which muscle vibration interferes with motor control are discussed below.

Selective excitation of the primary endings (Ia afferents) by sustained muscle vibration entraining elicits so-called tonic vibration reflex (TVR) characterised by tonic contraction of the stimulated muscle and relaxation of its antagonist (e.g., Hagbarth and Eklund, 1968). Furthermore, if the visual feedback is removed and the stimulated muscle is fully relaxed or restrained to isometric conditions (i.e., not allowed to shorten under the influence of the TVR or not moved voluntarily), an illusory kinaesthetic (proprioceptive) sensation of limb movement usually arises (Calvin-Figuière et al., 1999; Goodwin et al., 1972). The illusory movement sensation is often accompanied by gradually developing tonic contraction of the antagonist muscle, the so-called antagonist vibratory response (AVR; Roll et al., 1980), or inverted TVR (Calvin-Figuière et al., 1999).

When in freestanding upright position, vibration of specific muscles (usually at the neck or lower limb) can elicit an overt involuntary postural response called vibration-induced falling (VIF; Eklund, 1972). If the body movement is prevented or if the subject is deprived of visual cues, an illusory body tilt or rotation is perceived (Wierzbicka et al., 1998). Besides the effects on static posture, leg vibration may also affect locomotion (for review, see Layne et al., 2019). For instance, hamstring vibration was shown to increase forward gait velocity, whereas quadriceps vibration increased backward gait velocity (Ivanenko et al., 2000). Furthermore, vibration of an air-suspended thigh, shank, or foot can evoke complex gait-like phasic movements of the entire lower limb. The observed air-stepping is similar to voluntary movements, both in terms of kinematics and EMG patterns, and is even accompanied by alternating movement of the contralateral limb (Gurfinkel et al., 1998).

Different illusory movements and overt motor responses share many fundamental characteristics. During vibration-evoked illusion of static limb displacement, the apparent stretch of the vibrated muscle is constantly overestimated, i.e., the muscle stimulated is perceived longer than it actually is (Goodwin et al., 1972). These illusions are not bound by physical limitations. If the muscle is vibrated when extended close to its anatomical limit, subjects may feel the joint in a position beyond its maximum operating range or even experience multiple forearms (Craske, 1977). Congruent with the apparent static displacement, the direction of the dynamic illusion of movement or body tilt is opposite to

the stimulated muscle action (i.e., opposite to the effect of TVR) and is therefore perceived as if the vibrated muscle was lengthening (Calvin-Figuière et al., 1999; Goodwin et al., 1972). The motor response associated with AVR is consistent with the kinaesthetic illusion, as it is evoked in the muscle group that would cause the corresponding movement if it were to be carried out voluntarily (Calvin-Figuière et al., 1999). In contrast, the overt whole-body tilts, compensate for the perceived lengthening of the vibrated muscle by leaning in the opposite direction (Eklund, 1972; Kavounoudias et al., 2001). A hallmark of all vibration-evoked involuntary responses is their vulnerability to attentional shifts, sensorial preference, and dependence on the current task and postural context (e.g., Calvin-Figuière et al., 1999; Wierzbicka et al., 1998), reflecting the cortical integrative processes maintaining internal body representation. Notably, these responses emphasise the context-dependence of central mechanisms that are constantly weighting the continuous multimodal afferent inflow into the brain, and highlight the need for careful control of the experimental conditions, such as body posture, when assessing motor sequelae of peripheral stimulation.

Vibration after-effects

In addition to phenomena that accompany the vibration, such as kinaesthetic illusions, TVR, and AVR, there have been reports of sensory and motor effects emerging after the stimulation cessation (Gilhodes et al., 1992; Rogers et al., 1985; Wierzbicka et al., 1998). For instance, kinaesthetic illusions accompanying the muscle vibration are usually followed by a short (up to several s) movement sensation in the opposite direction (i.e., as if the muscle were shortening) when the stimulation is stopped (Kito et al., 2006; Roll et al., 1980; Seizova-Cajic et al., 2007). This effect was suggested to be due to cortical sensory processing of post-vibratory decline of muscle spindle activity (Kito et al., 2006).

Besides these brief post-vibratory effects, a more enduring disruption of the position sense was observed up to 4 min after vibration applied for 30–60 s, producing position matching errors in an opposite direction than during the vibration (Cordo et al., 1995; Rogers et al., 1985), disruption of gait trajectory (Bove et al., 2001), or unidirectional sway in the upright stance (Wierzbicka et al., 1998). Some of these effects could still be observed 3 hours post-stimulation (Wierzbicka et al., 1998).

Vibration applied for at least 30 s may also elicit sustained involuntary contractions of the stimulated muscle after the cessation of vibration (Gilhodes et al., 1992). These motor after-effects develop in the muscle previously vibrated, have low amplitude and last up to several minutes, but can repeatedly switch to the antagonist muscle after change of visual

input. Similar characteristics and EMG patterns were observed in muscular responses after a strong voluntary contraction, i.e., the 'Kohnstamm's phenomenon', thus a common possibly supraspinal origin was suggested, such as LTP (Gilhodes et al., 1992).

Regardless of the central mechanisms involved, numerous studies assessed the effect of muscle vibration on force-generation capacity as a training modality (for review, see Souron et al., 2017b). Maximal voluntary contraction (MVC) was shown to decrease immediately following prolonged vibration (e.g., Bongiovanni et al., 1990), possibly due to fatigue and depression of spinal loop excitability (Farabet et al., 2016; Souron et al., 2017b). Repeated muscle vibration was shown to increase MVC, although this was consistently observed only when combined with simultaneous muscle contraction (Souron et al., 2017b). A detailed account of research on vibration effects on force-generation is, however, beyond the scope of this thesis.

Vibration was also shown to positively influence the control of fine skilled hand movements: Increased movement speed and decreased reaction times were observed in healthy subjects following wrist vibration at 80 Hz applied for 30 s (Macerollo et al., 2018). It was suggested that additional noise from proprioceptors increases the internal estimate of afferent input uncertainty, thus, lowering the gain of the afferent input, which facilitates initiation of movements (Tan et al., 2016).

Interventions using extended periods of vibration were also tested in pre-clinical stages of research on possible therapeutical applications of vibration. In one of repeatedly employed protocols, stimulation was typically delivered for 3 consecutive days. Each day, vibration was applied for 30 min in total, either as a single train or split into 3 blocks of 10 min duration (e.g., Fattorini et al., 2006). For instance, such vibration protocol applied to deltoid, biceps, and pectoralis muscles in healthy subjects was shown to improve performance of phasic movements 10 days post-treatment (Aprile et al., 2016). The effects of muscle vibration in various patient cohorts are discussed separately below.

1.2.3. Vibration in motor system disorders

Possible therapeutical applications of vibratory muscle stimulation have been extensively explored since the first studies of muscle vibration in healthy subjects (for review, see Cochrane, 2011; Murillo et al., 2014). Besides focal muscle vibration described here, an indirect or whole-body vibratory stimulation has also been frequently investigated, but the physiological effects of indirect vibration are not yet fully understood (Cochrane, 2011) and therefore are not covered in this thesis.

Focal muscle vibration was shown to either briefly facilitate or depress the voluntary contraction (and range of movement) in hemi- or paraparetic patients or in experimentally partially anaesthetised muscles, depending on whether the contraction was tested in the vibrated muscle (facilitation), or in its antagonist (attenuation; e.g., Hagbarth and Eklund, 1968). Interestingly, a marked transient motor improvement was observed when the vibration was applied to an antagonist of a spastic muscle, possibly by alleviating the spasticity (Hagbarth and Eklund, 1968). Since then, several studies confirmed positive effect of muscle vibration on spasticity after SCI or stroke (e.g., Marconi et al., 2011; Murillo et al., 2011).

Beneficial effects of vibration are not limited to alleviation of spasticity. In a study by Conrad et al. (2011), wrist vibration in patients after stroke caused improvement of arm target tracking outlasting the stimulation. Positive effect on balance parameters in various patient groups was observed as well (e.g., Pazzaglia et al., 2016). Complex behaviour such as gait can also be improved by prolonged and repeated muscle vibration, as demonstrated in patients after stroke (Paoloni et al., 2010) or incomplete SCI (Cotey et al., 2009). More elaborate patterns of multifocal vibration were also shown to improve qualitative gait parameters in cases of incomplete SCI (Barthélémy et al., 2016) or patients with idiopathic Parkinson's disease (IPD; De Nunzio et al., 2010).

Vibration can also have more specific influence on some disorders. In patients with IPD, improved movement speed and reaction times were demonstrated following brief wrist vibration (Macerollo et al., 2018). It was suggested that the failure to attenuate the sensory input underlies the symptoms of bradykinesia in IPD, and that increased sensory noise lowered the gain of sensory information (Macerollo et al., 2018). Muscle vibration has also become a frequent tool to investigate the neurobiological basis of dystonia since the suspected mechanisms involve abnormal proprioceptive processing (Rosales and Dressler, 2010). In patients with focal dystonia, the perception of kinaesthetic illusions is reduced in comparison to healthy controls or patients with IPD, even though perception of passive movements is unimpaired (Rome and Grünewald, 1999). Likewise, the VIF response from neck muscles is absent in patients with cervical dystonia despite intact VIF response to soleus vibration (Lekhél et al., 1997). The abnormal perception of illusion in patients with dystonia improves with muscle fatigue, suggesting that central motor programs could be adapted to the fatigued state, which is inappropriate for relaxed muscles (Frima et al., 2003). Furthermore, transient positive effect of vibratory stimulation applied at certain anatomical areas was observed in some patients with cervical dystonia, possibly as an analogy to the sensory tricks (Leis et al., 1992). However, other studies showed worsening

of dystonic signs in response to vibration (Kaji et al., 1995; Tempel and Perlmutter, 1990). More in-depth evidence from TMS and imaging studies is discussed in separate sections below.

1.3. Electrophysiological evidence for central effects of vibration

1.3.1. Immediate effects of vibration

Number of studies indicate that muscle vibration at frequency up to 120 Hz is associated with a concomitant augmentation of the MEP amplitude in a stimulated muscle at the hand (Claus et al., 1988; Rosenkranz et al., 2005; Rosenkranz and Rothwell, 2003) or forearm (Kossev et al., 2001, 1999; Rosenkranz et al., 2003, 2000; Steyvers et al., 2003b), which is accompanied by MEP depression in the non-vibrated antagonist (Kossev et al., 2001; Rosenkranz et al., 2003; Siggelkow et al., 1999). Similar inhibition was observed in the adjacent non-vibrated muscles at the hand (Rosenkranz et al., 2005; Rosenkranz and Rothwell, 2003). The effects in the vibrated muscle have been termed “homotopic”, whereas the typically opposite effects on other muscles have been named “heterotopic” (Rosenkranz and Rothwell, 2004). Distant muscles, such as *abductor pollicis brevis* (APB) or first dorsal *interosseus* (FDI) when vibrating the *flexor carpi radialis* muscle (FCR), are usually not affected by vibration (Rosenkranz et al., 2003). However, contralateral inhibition in the homologous antagonist (Kossev et al., 2001) or even homologous agonist was observed (Swayne et al., 2006).

Changes in paired stimulation protocols were also observed during vibration, reflecting, among others, modulation of the GABA_A-ergic inhibitory intracortical circuits (Kujirai et al., 1993; Ziemann et al., 1996a). In the vibrated muscle, increased ICF (Rosenkranz et al., 2003) as well as decreased SICI (Rosenkranz et al., 2005, 2003; Rosenkranz and Rothwell, 2003) and increased LICI (Rosenkranz and Rothwell, 2003) were demonstrated. An opposite effect was observed in the non-vibrated, yet adjacent hand muscles (Rosenkranz et al., 2005; Rosenkranz and Rothwell, 2003). As an exception, a recent study showed that random frequency wrist vibration also reduced SICI for the non-vibrated though adjacent APB muscle (Seo et al., 2019), suggesting that vibrating across a range of frequencies may induce less focal effects in the vibrated limb. In contralateral hand muscles, SICI and IHI also increase non-selectively, affecting both agonist and antagonist muscles likely via transcallosal commissural pathways (Swayne et al., 2006).

The mechanisms underlying the vibration-induced changes in cortical excitability are thought to be mediated by Ia afferents as the effects depend on optimal vibration

frequency of primary muscle spindle endings around 75–80 Hz, whereas frequencies below 20 Hz or above 160 Hz elicit no changes (Siggelkow et al., 1999; Steyvers et al., 2003b). The role of muscle afferents is further supported by analogous consequences of voluntary contraction (Rosenkranz et al., 2003), and lack of similar effects during electrical cutaneous stimulation (Rosenkranz and Rothwell, 2003). Although spinal mechanisms were originally suggested (Claus et al., 1988), prevailing evidence indicates that the effects involve a supraspinal mechanism rather than a spinal one (Kossev et al., 1999; Rosenkranz and Rothwell, 2003; Smith and Brouwer, 2005). First, the MEP augmentation during muscle vibration was demonstrated using TMS but not using transcranial electrical stimulation. Since the TMS activates cortical cells transsynaptically, whereas transcranial electrical stimulation activates corticomotoneurons at the axon hillock, the vibration-induced augmentation of MEPs elicited by TMS indicates a cortical rather than subcortical origin of the phenomenon (Kossev et al., 1999). Second, the augmentation/suppression of the SICI and LICI is unlikely to be caused by spinal mechanisms (Rosenkranz and Rothwell, 2003). Third, muscle vibration at 80 Hz was shown to evoke cortical responses in the contralateral perirolandic cortex, confirming that afferentation from primary endings reaches the sensorimotor cortex (Münste et al., 1996). It was suggested that intracortical interactions between S1 and M1, possibly similar to the LTP-like mechanisms observed in the feline brain (Sakamoto et al., 1987) mediated by cortico-cortical pathways between BA 3a and 4 (Ghosh et al., 1987), might be responsible for the homotopic effects (Marconi et al., 2008), though direct effect of proprioceptive afferentation on area 4 is also possible (e.g., Hore et al., 1976). Different mechanisms were suggested for the MEP depression in the non-vibrated muscles (Kossev et al., 2001; Siggelkow et al., 1999). A spinal reciprocal inhibition or inhibition of the corticospinal output to antagonist muscles was proposed as a possible underlying mechanism ipsilaterally, whereas an involvement of IHI was suggested contralaterally (Kossev et al., 2001).

Taken together, the available evidence supports the idea that afferent input from muscle spindles is involved in supraspinal motor control (for reviews, see Cochrane, 2011; Souron et al., 2017b) and that muscle vibration can be used to selectively manipulate motor cortical representations, an effect possibly unique for muscle vibration (Rosenkranz and Rothwell, 2004).

1.3.2. Effect of kinaesthetic illusions

There is growing evidence for changes in cortical excitability associated with kinaesthetic illusions and AVR (for review, see Dilena et al., 2019). Kito et al. (2006) evaluated MEP

amplitude during AVR in forearm muscles and showed increased cortical excitability in the non-vibrated antagonist muscle representation during vibration, but decreased excitability after vibration. However, there were no changes in excitability in the vibrated muscle (Kito et al., 2006). The imbalance between cortical excitability in M1 representations of the vibrated and non-vibrated muscle correlated with the degree of the kinaesthetic illusion (Kito et al., 2006). The MEP facilitation in the antagonist muscles can also be observed in the contralateral limb, following the so-called transfer of the illusion that takes place when both limbs are in contact (Naito et al., 2002). Mancheva et al. (2017) demonstrated that the effects of kinaesthetic illusions interact with the visual input, as the antagonist responses were only augmented in no-feedback eyes-open condition, but not in the eyes-closed condition. The eyes-closed condition was suggested to increase the gain of proprioceptive input, reinforcing the heterotopic antagonist suppression possibly of spinal origin (Mancheva et al., 2017). Finally, Suzuki et al. (2019) observed interaction with complex visual stimuli as well: whereas a visual stimulus congruent with the kinaesthetic illusion (video of flexing wrist) increased MEP in the non-vibrated antagonist muscle (FCR), conflicting (static) visual stimulus increased MEP in the vibrated agonist (*extensor carpi radialis*, ECR), i.e., in line with homotopic vibration effect.

To summarise, effects of kinaesthetic illusions demonstrate that sensorimotor integration strongly depends on multi-sensory interactions and possibly higher-order processing.

1.3.3. Sustained effects of vibration

Short vibration of a relaxed muscle seems to be ineffective in producing sustained effects detectable using TMS as no post-vibratory effects on MEP amplitude following up to 30 s of stimulation could be demonstrated (Siggelkow et al., 1999; Steyvers et al., 2003b). In contrast, periods of stimulation longer than 15 min were associated with changes outlasting the stimulation itself (Forner-Cordero et al., 2008; Marconi et al., 2008; Rosenkranz and Rothwell, 2006b, 2004; Smith and Brouwer, 2005; Steyvers et al., 2003a). In comparison, robust changes of cortical excitability require 1.5 h of much less specific electrical nerve stimulation (Ridding et al., 2000).

Smith and Brouwer (2005) showed that muscle vibratory stimulation applied for 15 min to a relaxed ECR increased both the MEP size and the cortical representation area of the target muscle and the effect was maintained for at least 5 min. Nevertheless, 30 min of vibration did not lead to any significant changes compared to baseline. The fact, that longer stimulation produced no changes was speculated due to mutual cancellation of effects due to SICI and LICI (Smith and Brouwer, 2005). Similarly, the existence of optimal

stimulus duration with lower effect of both shorter and longer stimuli was observed following electrical stimulation (Fraser et al., 2002). The effects of sustained vibration also suggest high inter-subject variability, as seen in study by Lapole and Tindel (2015). Whereas no significant group effect on SAI and LAI was observed immediately following 15 min of APB vibration, a proportion of subjects showed profound increase in cortical excitability (Lapole and Tindel, 2015).

However, some of those studies (Lapole and Tindel, 2015; Smith and Brouwer, 2005) might have missed the effects of longer stimulation simply by not measuring long enough post-vibration. Steyvers et al. (2003a) observed that the increase in cortical excitability following a 30-min stimulation of the FCR had gradual onset and reached significance only 25–30 min post vibration. In the same study, a more robust facilitation was found in the antagonist muscle (ECR), which became significant already 10 min after vibration and could be still detected 40–45 min later. The fact that amplitudes in the antagonist muscle were increased could be due to the AVR reported consistently by the subjects (Steyvers et al., 2003a). A corresponding delayed effect of AVR on MEP amplitude was also reported following 60-min stimulation of FCR (Forner-Cordero et al., 2008). Sustained effects with decreased SICI and increased ICF were also documented after less specific low frequency (25 Hz) whole-hand vibration (Christova et al., 2011). Since analogous delayed and prolonged effects were reported also following electrical stimulation (Fraser et al., 2002), the vibration after-effect were likewise speculated to involve synaptic plasticity, such as LTP or LTD (Forner-Cordero et al., 2008; Fraser et al., 2002).

1.3.4. Cortical reorganisation due to vibration

Prolonged vibration below the threshold of sensory illusions is associated with less obvious effect on motor cortex excitability since unconditioned MEP remain unchanged (Rosenkranz and Rothwell, 2006a, 2004). Nevertheless, vibration was shown to influence the highly organised patterns of immediate cortical responses to short-term vibration, affecting both homotopic and heterotopic effects up to 30 min post-intervention (Rosenkranz and Rothwell, 2006a, 2004). Following 15 min of intermittent vibration simultaneously applied to two hand muscles (APB and FDI), the heterotopic effects (on MEP amplitude, SICI, and LICI) were replaced by homotopic effects when tested in one of the two previously co-vibrated muscles. Thus, the vibration resulted in facilitation rather than inhibition, possibly due to an overlap or fusion of cortical representations without changing the overall cortical excitability (Rosenkranz and Rothwell, 2004). A follow-up study with single muscle vibration reported a similar switch of the homotopic and

heterotopic effects in the non-vibrated FDI, suggesting that the nearby representation of vibrated APB governed the responses in FDI (Rosenkranz and Rothwell, 2006a). Overall, these focal effects are in sharp contrast with sequelae of rather non-specific electric cutaneous stimulation (Ridding et al., 2001; Rosenkranz and Rothwell, 2006a) and motor training (Rosenkranz and Rothwell, 2006a), which are likely mediated by a different, possibly LTP-like mechanism. As there were no changes in unconditioned cortical excitability following focal vibration, it was suggested that its effects were confined to the input side of the motor cortex circuitry, possibly acting by unmasking latent horizontal connections (Jacobs and Donoghue, 1991; Rosenkranz and Rothwell, 2006a).

Furthermore, it was demonstrated that the cortical reorganisation following muscle vibration is only apparent when subject's attention is focused on the vibration frequency during the intervention. When the attention is directed elsewhere (e.g., to a cognitive task or a different body part), both heterotopic and homotopic effects in the vibrated muscles are reduced or completely abolished, possibly by a general mechanism suppressing unattended stimuli. In contrast, the heterotopic inhibition remains unaffected in a non-vibrated muscle (Rosenkranz and Rothwell, 2006b, 2004). The results of Rosenkranz and Rothwell (2006b, 2004) are not surprising considering how different vibration-induced phenomena switch depending on the attention level and multisensory feedback (Calvin-Figuère et al., 1999; Goodwin et al., 1972). This suggests that cortical circuits subserving sensorimotor integration and plasticity are also subject to dynamic context-dependent adjustments and it might explain some counter-intuitive findings from other studies (cf. Smith and Brouwer, 2005).

1.3.5. Effects of vibration during voluntary contraction

Opposite effects on cortical organisation were observed when vibration was applied during voluntary contraction (Marconi et al., 2008). Using longer stimulus duration (90 min daily for 3 consecutive days), vibration applied at FCR during contraction led to reduction of the corresponding cortical map and increased SICI, whereas an enlargement of cortical map and decreased SICI was detected for the antagonistic *extensor digitorum communis* (EDC) muscle. Notably, these effects lasted for up to 2 weeks after last session and no changes were observed after vibration or contraction alone, either in cortical maps or in SICI (Marconi et al., 2008). In contrast, Christova et al. (2010) observed increased cortical excitability in the FDI following a single session of 10-min tonic index finger abduction with concomitant 60-Hz vibration. The enhanced MEP amplitude in the FDI was accompanied by reduced SICI and later by augmented ICF. The effects of vibration

were maintained up to 30 min post-intervention, whereas tonic contraction alone produced no post-effects (Christova et al., 2010). The conflicting results of the two studies might be due to different duration of the applied protocols: With longer repeated stimulation, different plastic mechanisms including microstructural changes may take place.

1.3.6. Lower limb vibration

In comparison to upper limbs, cortical excitability changes during local vibration of the lower limb muscles were evaluated much less frequently (Farabet et al., 2016; Lapole et al., 2015, 2012; Mileva et al., 2009; Souron et al., 2018, 2017a, 2017b, 2017c). Mileva et al. (2009) were first to show increased MEP amplitude in the tibialis anterior muscle but not in the soleus during lower limb vibration. However, since the stimulation was delivered via a standing platform, it is difficult to characterise what mechanisms contributed to this effect. In fact, Lapole et al. (2015) reported the opposite, i.e., increased cortical excitability in the soleus muscle during Achilles tendon vibration. Surprisingly, this finding was accompanied by decreased ICF and unchanged SICI, implicating that different mechanisms than those previously demonstrated in upper limbs were involved. Regarding the vibration after-effects, neither Farabet et al. (2016) nor Souron et al. (2017a) found any convincing change in cortical excitability immediately following 30 min of tibialis anterior or quadriceps vibration. Indeed, in an earlier study assessing sustained effects of Achilles tendon vibration, initially, no change in cortical excitability was observed immediately following 1 hour of stimulation, but the MEP amplitude significantly increased both in the soleus and in the antagonistic tibialis anterior after 1 hour of subsequent resting (Lapole et al., 2012). Such delayed and non-specific effects are similar to those observed in the upper limbs (Steyvers et al., 2003a). However, a series of follow-up studies (Souron et al., 2018, 2017c) assessed chronic post-vibration effects, but found no change in cortical excitability despite increased maximal voluntary contraction following repeated sessions of tibialis anterior or quadriceps vibration (Souron et al., 2017c). The observed changes in MVC were thus hypothesised to be of spinal or muscular origin. Therefore, the persistence of cortical excitability changes in lower limbs remains unconfirmed.

1.3.7. Vibration in motor system disorders

In line with the large amount of evidence at the behavioural level (e.g., Lekhel et al., 1997; Rome and Grünewald, 1999; Rosales and Dressler, 2010), frequent vibration-associated abnormalities of the corticospinal excitability were identified in patients with focal

dystonia, although different patterns were observed in various forms (Rosenkranz et al., 2005; Urban and Rolke, 2004). Whereas in non-professional patients with writer's cramp, the vibration-induced reorganisation of cortical representations of hand muscles was completely abolished, professional musicians with musician's dystonia showed an opposite change since the effects of vibration were rather exaggerated in comparison to healthy controls (Rosenkranz et al., 2005). More specifically, in healthy controls, SICI increased in all non-vibrated muscles and decreased in the vibrated muscle only (see homotopic and heterotopic effects in the section "IV.1.3.4. Cortical reorganisation due to vibration"), whereas in musicians with musician's dystonia, SICI decreased in all muscles. However, yet another control group consisting of healthy professional musicians exhibited coupling (i.e., reciprocal facilitation) between FDI and APB muscles with preserved reciprocal inhibition of the *abductor digiti minimi*. This sensorimotor cortical organisation pattern resembled the effect of prolonged attended vibration and was interposed between those in non-professional healthy controls and in patients with musician's dystonia (Rosenkranz et al., 2005; Rosenkranz and Rothwell, 2004). It was therefore suggested that normal practice-evoked changes that support sensorimotor integration during skilled performance may become excessive in musician's dystonia (Rosenkranz et al., 2005). In contrast, the findings in writer's cramp indicated that sensory feedback had less influence on the motor control, hence different pathophysiological mechanisms were proposed. Patients with writer's cramp either fail to focus sensory afferentation on the intended movement representation, or simply filter it as excessive or useless signal (Rosenkranz et al., 2005). Indeed, the abnormal cortical organisation pattern could be reversed by a proprioceptive training involving 15 min of attended hand muscle vibration in patients with musician's dystonia, but not in patients with writer's cramp (Rosenkranz et al., 2009, 2008).

In cervical dystonia, the vibration-induced MEP facilitation is also attenuated in the affected sternocleidomastoid muscle (SCM; Urban and Rolke, 2004). This again resembles the pattern previously described in writer's cramp (Rosenkranz et al., 2005) and suggests decreased sensory input from the affected muscle. However, it could not be ruled out that this was a carry-over effect of previous BoNT-A treatment as the facilitation further decreased after the next BoNT-A injection and returned partially to baseline after the effect wore off (Urban and Rolke, 2004).

Vibration was also shown to affect cortical excitability in stroke patients. In a TMS study in hemiparetic patients, Marconi et al. (2011) demonstrated positive effects of an add-on repeated muscle vibration (FCR and biceps brachii, 30 min daily for 3 days) on spasticity

and motor function as compared to physiotherapy alone. The improvement was associated with lowered rMT, as well as increased motor map areas in the vibrated muscle. Motor map volumes (sum of MEP amplitudes of excitable scalp sites) increased in all muscles, including the non-vibrated EDC, whereas SICI increased in the flexors, but decreased in the extensors, paralleling the effect on flexor spasticity. The affects were maintained for 2 weeks following the intervention (Marconi et al., 2011).

1.3.8. Summary of evidence from electrophysiological studies

TMS research has unveiled complex intracortical processes following vibratory stimulation occurring at multiple time scales, both immediate and substantially delayed. In normal brain, the observed experimentally evoked sustained cortical reorganisation likely reflects the plasticity driven by ever-changing proprioceptive input. These fundamental mechanisms have been shown to be significantly altered in some neurological conditions, especially in focal forms of dystonia. The putative plasticity-inducing capability of vibration has already attracted attention of clinical research in various forms of physiotherapy. We discuss in the next section how are these conclusions from neurophysiological research mirrored in neuroimaging studies.

1.4. Neuroimaging evidence for central effects of vibration

The evidence from TMS studies discussed in the previous section implicates that stimulation of muscle spindle afferents affects the primary motor regions associated with the muscle vibrated (Kossev et al., 2001, 1999; Rosenkranz et al., 2005, 2003, 2000; Rosenkranz and Rothwell, 2003; Smith and Brouwer, 2005; Steyvers et al., 2003b), but also with other muscles on the ipsilateral limb (Kossev et al., 2001; Rosenkranz et al., 2003; Siggelkow et al., 1999) or even contralaterally (Swayne et al., 2006). Sustained post-vibratory changes in cortical excitability (Forner-Cordero et al., 2008; Marconi et al., 2008; Rosenkranz and Rothwell, 2004; Smith and Brouwer, 2005; Steyvers et al., 2003a) and cortical sensorimotor organisation (Rosenkranz and Rothwell, 2006a, 2004) were documented. Considering the available data from animal preparations showing intracortical sensorimotor interactions (Sakamoto et al., 1987) and direct involvement of the M1 in processing of the muscle spindle input (Hore et al., 1976), as well as human data on cortical evoked responses (Münte et al., 1996), the task for imaging studies was not to tell whether the vibration-generated afferentation is processed in the motor cortex, but to define the spatial boundaries and temporal scales at which these processes take place.

Several PET and fMRI studies indicated that high-amplitude cutaneous vibration, which is likely to stimulate also nearby muscles and tendons, is associated with motor cortex activation (Burton et al., 1993; Gelnar et al., 1998; Golaszewski et al., 2002a; Seitz and Roland, 1992). However, in these papers, no specific muscle was vibrated, possibly obscuring differential effects of vibration applied at various sites as described in TMS research (e.g., Rosenkranz et al., 2005; Rosenkranz and Rothwell, 2003). More specific evidence of motor cortex activation during muscle vibration was provided by later PET studies (e.g., Naito et al., 1999) and was subsequently extended in fMRI research (e.g., Gizewski et al., 2005; Kavounoudias et al., 2008; Naito et al., 2007, 2005; Romaguère et al., 2003). However, since the central effects of muscle vibratory stimulation have been shown to depend on multiple variables, e.g., site, duration, amplitude and frequency of the stimulation (Cignetti et al., 2014; Gizewski et al., 2005; Naito et al., 2007; Roll and Vedel, 1982; Romaguère et al., 2003), an overall summary of results from different studies is not possible. Considering the vast behavioural and neurophysiological evidence of manifold context-dependent interactions between the sensory and motor systems, the central correlates of vibratory stimulation are best grasped from the point of view of the vibration-related behavioural phenomena. Here, we first discuss the muscle vibration as it is better behaviourally and physiologically characterised, followed by physiologically less grounded sensorimotor effects of vibrotactile stimulation.

1.4.1. Kinaesthetic illusions

Number of studies employing muscle vibration focused on the central correlates of vibration-evoked kinaesthetic illusions (e.g., Amemiya and Naito, 2016; Cignetti et al., 2014; Naito et al., 2007, 2005, 1999; Romaguère et al., 2003). As these studies focused on sensory processing rather than interaction of vibration with motor control, we provide only a brief and condensed overview of the main results. For detailed reviews, see (Naito, 2004; Naito et al., 2016).

Imaging of vibration-induced illusory kinaesthetic perceptions demonstrated that cortical processing of proprioceptive afferentation involves both higher-order somatosensory, including BA 2, BA 5, and inferior parietal lobule (IPL; e.g., Naito et al., 2005; Romaguère et al., 2003), and proper motor areas implicated in the corresponding real movement (M1, PMd, SMA, CMA; e.g., Naito et al., 2007, 1999). The activation of motor areas reflects their somatotopic organisation, with hierarchical integration from multiple limbs occurring in the rostral parts of the SMA and CMA (Naito et al., 2007), thus, motor cortices are thought to process and transform afferent information from the skeletal muscles (Naito et al., 2016).

Parietal cortices (BA 2 and 5), as well as the insula and cerebellum participate in multisensory integration (e.g., Hagura et al., 2009; Naito et al., 2008). On top of this, a shared right-sided frontoparietal network (including BA 44 and IPL) subserves the actual awareness of the kinaesthetic perception and it is possibly the substrate the internal body representation (self-awareness; e.g., Amemiya and Naito, 2016; Cignetti et al., 2014), whereas left-sided IPL participates in somatosensory integration information required during external object manipulation (Naito et al., 2008; Naito and Ehrsson, 2006). In summary, imaging of kinaesthetic illusions has demonstrated an indeed revolutionary notion that motor cortices are involved in sensory processing even in situations when there is no intention to move. This implicates that motor cortices are inherently under continuous proprioceptive sensory influence (not just on demand) and integrate motor programs into the constant sensory inflow rather than the opposite. Such idea is compatible with the active inference theory proposing that sensorimotor system is fine-tuned to create predictions of sensory consequences of actions which are then updated by the actual sensory feedback (Friston, 2011).

1.4.2. Postural effects of vibration

The maintenance of balance requires central processing of proprioceptive and multisensory input to continuously update the internal model of the body geometry (Kavounoudias et al., 2001; Roll et al., 1989b). The central representation of body posture can be perturbed using vibration of antigravitational muscles (Eklund, 1972; Lackner and Levine, 1979; Lekhel et al., 1997; Wierzbicka et al., 1998).

In fMRI studies by Goble et al. (2012, 2011) in young and elderly healthy individuals, vibration of toe extensors associated with an illusion of plantar flexion elicited limb-specific activations in the contralateral primary sensorimotor cortices and bilateral activations in the secondary/associative areas (IPL, BA 2, 44, 45, SMA, anterior insula) and thalamus. Right-sided activations in the PMv, orbitofrontal cortex (BA 47), dorsolateral prefrontal cortex (DLPFC, BA 46) and dorsal anterior cingulate cortex (BA 32) were detected, in line with studies by Naito et al. (2007, 2005). In the elderly, activation decreased in the right putamen regardless of the vibrated side. Activity in the putamen was positively correlated with the accuracy of lower limb position sense and was higher in elderly with higher fractional anisotropy in the putamen, possibly reflecting its role as a “sensory analyser” with respect to proprioceptive feedback (Goble et al., 2012). Moreover, activation in the right-sided basal ganglia (pallidum and putamen), parietal (BA 2 and IPL), frontal (PMv, pre-SMA, anterior cingulate, BA 44, 45, 46 and 47), and

bilateral insular and opercular cortex (S2) was positively correlated with balance performance, regardless of age and vibrated side. It was proposed that, in part, these areas correspond to the right-sided salience network, possibly monitoring the changes in body sway (Goble et al., 2011).

1.4.3. Sustained effects of vibration

Only a few imaging studies evaluated the correlates of prolonged vibration and the motor after-effects. Gizewski et al. (2005) observed that activation in contralateral sensory (S1, S2) and motor (M1, SMA, PMv) areas during biceps vibration associated with illusory movement followed an exponential decay over 34 s, which is in line with behavioural observations of gradually degrading movement illusion (Seizova-Cajic et al., 2007). Interestingly, the motor areas briefly engaged bilaterally after the stimulation was stopped (Gizewski et al., 2005), coinciding with a kinaesthetic after-sensation reported by the subjects (Cordo et al., 1995, 2005; Kito et al., 2006; Roll and Vedel, 1982; Seizova-Cajic et al., 2007).

On a larger time-scale, it was shown that extended vibration associated with kinaesthetic illusion may replace the missing proprioceptive input from an immobilised limb. Repeated complex neuromimetic vibratory stimulation applied for 30 min daily was shown to prevent neuroplastic changes of cortical motor hand representations following 5 days of experimental hand immobilisation (Roll et al., 2012). However, despite extensive evidence for sustained after-effects of vibration in neurophysiological studies, to our knowledge (Forner-Cordero et al., 2008; Marconi et al., 2008; Rosenkranz and Rothwell, 2006a, 2004; Smith and Brouwer, 2005; Steyvers et al., 2003a), the corresponding data from fMRI or other imaging methods are still limited.

1.4.4. Vibrotactile stimulation: combined effects of muscle and skin vibration?

The effects of muscle vibration are always mixed with afferentation from cutaneous receptors. Whereas in the previously discussed studies, the skin vibration was kept minimal or the effects were separated by specific contrasts (i.e., tendon vs. bone vibration), a number of studies tested vibration protocols, in which skin mechanoreceptors were significantly stimulated along with the muscle endings, either on purpose or as a consequence of non-specific stimulation.

Several PET studies assessed brain activation during vibrotactile stimulation applied to fingers (Fox et al., 1987; Meyer et al., 1991), palm (Burton et al., 1993; Seitz and Roland,

1992), forearm (Coghill et al., 1994), or toes (Burton et al., 1993; Fox et al., 1987). The stimulation amplitude (2 mm) and frequency (110–130 Hz) were similar across the paradigms. High amplitude vibration implicated that besides the skin mechanoreceptors, deeper afferents in muscles and joints were also likely stimulated by the propagating mechanical waves (Burton et al., 1993; Gizewski et al., 2005). Activation was consistently reported in the contralateral S1, bilateral S2, and contralateral SMA (Burton et al., 1993; Coghill et al., 1994; Fox et al., 1987; Seitz and Roland, 1992). An involvement of the contralateral M1 (or SMC) was reported less frequently (Burton et al., 1993; Seitz and Roland, 1992), though it was probably not directly evaluated by others (Coghill et al., 1994; Fox et al., 1987). Additional activations were observed in the IPL (Seitz and Roland, 1992), bilateral posterior insular cortices (Burton et al., 1993; Coghill et al., 1994), and ipsilateral cerebellum (Fox et al., 1987). Besides activations, deactivations in multiple frontal, parietal, and temporal associative areas were demonstrated as well (Coghill et al., 1994; Seitz and Roland, 1992). However, the spatial uncertainty of PET data and lack of reliable anatomical reference decreases the capability to draw definite conclusions regarding the anatomo-functional relationships (i.e., preventing any reliable distinction between the M1 and S1). Furthermore, the relative contribution of cutaneous and muscle afferents was neither controlled nor evaluated in these studies, making the interpretation of the findings even more challenging. In some cases, activations reported in the M1 might have been biased by the reflex movements, such as TVR, as reported by Seitz and Roland (1992).

It can be assumed that some fMRI studies of vibrotactile stimulation also unintentionally evaluated effects of mixed rather than pure skin vibration. Possible reasons include high amplitude stimulation (Burton et al., 1993; Gizewski et al., 2005) and/or frequencies within the range of muscle spindle afferents (Roll et al., 1989a). For example, Gelnar et al. (1998) reported that 50 Hz vibration of a fingertip with 2 mm amplitude elicited activation of contralateral somatosensory cortices (S1, S2, posterior parietal cortex, posterior insula), but also of the M1. Contralateral sensorimotor activation was also observed in response to relatively high-amplitude (1 mm) bursts of vibrotactile finger pad stimulation despite low stimulus frequency within flutter range at 25 Hz (Brouwer et al., 2015). The inconsistent appearance of motor activation compelled the authors to consider them as potentially spurious and refrain from inspecting them in greater detail (Brouwer et al., 2015; Gelnar et al., 1998).

Combined skin and muscle stimulation is even more likely to occur when broad body surface areas are stimulated. In an fMRI study by Golaszewski et al. (2002a), a 50-Hz high-amplitude (2 mm) vibratory stimulation of hand palm over the flexor tendons (roughly

36 cm²) was compared to a finger tapping task. Both paradigms elicited similar activation pattern mainly in the contralateral precentral and postcentral gyrus (M1, S1), medial frontal gyrus (SMA/pre-SMA), cingulate cortex, and bilaterally in the superior and inferior parietal lobule. The brain activation pattern during vibrotactile stimulation of the palm has been deemed similar to the activation during voluntary motor task. The vibratory cutaneous and muscle stimulation has been therefore proposed as a surrogate task in subjects unable to perform voluntary movements (Golaszewski et al., 2002b, 2002a). Two follow-up studies evaluated vibrotactile stimulation applied to a foot sole over approx. 20 cm² (Golaszewski et al., 2006; Siedentopf et al., 2008). Using 50-Hz stimulation with 1 mm displacement, most significant activations were found in the contralateral primary sensorimotor cortex, posterior insula, bilateral S2, cingulate cortex, thalami, basal ganglia and cerebellum (Golaszewski et al., 2006). When applying 100-Hz stimulation either with 0.4-mm or 1.6-mm displacement, activations were observed in bilateral S2, posterior insulae and contralateral sensorimotor cortex. On direct comparison, higher amplitude was associated with increased activation in the contralateral S2, whereas lower amplitude vibration evoked higher activation in the dorsolateral sensorimotor cortices (S1, M1, PMd; Siedentopf et al., 2008).

1.4.5. Are there motor effects of pure cutaneous vibration?

Studies of mixed cutaneous and muscle vibration cannot provide definite answers regarding the influence of cutaneous receptors on motor control. Fortunately, some of the discussed limitations have been better addressed by studies on somatotopic organisation of the somatosensory cortex that utilised low-amplitude cutaneous vibration (< 0.5 mm) and higher magnetic field strength (> 1.5 T). Using very low-amplitude (< 0.15 mm) 80-Hz fingertip vibration, Francis et al. (2000) observed motor activations in predominantly contralateral precentral gyrus (BA 4 and 6) in addition to contralateral activations in S1, BA 5, posterior insula and bilateral S2 (Francis et al., 2000; McGlone et al., 2002). A series of follow-up studies at ultra-high magnetic field (7 T) (e.g., Sanchez-Panchuelo et al., 2018, 2016, 2012) also reported simultaneous activation of the M1 and S1 during low-amplitude (0.1 mm) 150-Hz fingertip stimulation (Sanchez-Panchuelo et al., 2012), as well as during high-amplitude (1 mm) 30-Hz (Sanchez-Panchuelo et al., 2016). The unilateral stimulation evoked bilateral activations in the primary sensorimotor cortices, S2, PMd, and contralateral activation in posterior insula (Sanchez-Panchuelo et al., 2016). Notably, using a microneurographic technique capable of stimulating a single cutaneous afferent, it was also demonstrated that the contralateral primary motor cortical projections of the SA-I and FA-I units overlapped with activations evoked by vibrotactile stimulation applied over

their receptive fields (Sanchez-Panchuelo et al., 2016). Yet despite their superb spatial resolution (1.5 mm in-plane), authors did not rule out the possibility that M1 activations were due to small finger movements or the haemodynamic response extending from the nearby postcentral gyrus (Sanchez-Panchuelo et al., 2016). Therefore, though clearly depicted in the published figures, activations in the M1 were completely ignored in the most recent studies (e.g., Puckett et al., 2020; Sanchez-Panchuelo et al., 2018).

Another research area frequently investigated using pure cutaneous vibrotactile stimulation is somatosensory working memory (e.g., Schmidt et al., 2017; Sörös et al., 2007; Wu et al., 2018). Although, a detailed account of this function is beyond the focus of this review, one study is worth noting. Using multivoxel pattern analysis, Schmidt et al. (2017) identified structures encoding memory of vibration frequency in the SMA, anterior cingulate cortex, bilateral PMd, and right inferior frontal gyrus. Though the finding was not replicated by Wu et al. (2018), who rather observed involvement of bilateral parietal and associative frontal cortices, it may still point to a more universal role of motor areas in somatosensory processing, analogous to processing of proprioceptive afferentation (Naito et al., 2016).

In spite of the numerous evidence for motor cortex activation during pure cutaneous vibration, just as many imaging studies found no reliable responses beyond the somatosensory network, either using low-frequency vibration (15–40 Hz; e.g., Maldjian et al., 1999; Nelson et al., 2004; Vidyasagar and Parkes, 2011) or even stimulation across wide range of frequencies between 20 and 200 Hz (e.g., Chung et al., 2013; Harrington et al., 2000; Kim et al., 2014). Out of these, only two studies (Kim et al., 2014; Nelson et al., 2004) reported activity in the SMA in addition to parietal cortices. However, direct comparison among the studies is only possible to a limited extent as the exact vibration amplitude was not reported by the authors (Chung et al., 2013; Harrington et al., 2000; Maldjian et al., 1999; Nelson et al., 2004; Vidyasagar and Parkes, 2011). Furthermore, sensorimotor activations due to finger pad vibration were shown to be strongly modulated by the attention shifts and the task context (e.g., Albanese et al., 2009).

Regarding the effects of mechanically evoked stochastic resonance, only one study evaluated the effects of random noise vibration applied to the whole body via a standing platform. The study found increased activation in the left caudate nucleus during a simple motor task, however, only after small-volume statistical correction (Kaut et al., 2016).

Hence, despite some compelling evidence, it is yet to be confirmed whether (and/or under what conditions) the M1 and other motor areas responds to pure cutaneous vibratory

stimulation as they do to muscle afferentation. Future studies with carefully controlled vibration parameters (such as frequency, amplitude, stimulation site, or subject's attention) and control conditions are warranted to elucidate this outstanding issue.

1.4.6. Vibration in motor system disorders

In an early PET study, patients with idiopathic dystonia, including writer's cramp, showed abnormally reduced rCBF in the bilateral sensorimotor cortex during high-amplitude 130 Hz finger pad vibration (Tempel and Perlmutter, 1990). Similarly, patients with focal hand or arm dystonia showed later also reduced separation of S1 digit separation and reduced activation in S2 and posterior parietal cortex as assessed using 80 Hz digit tip vibratory stimulation in fMRI (Butterworth et al., 2003). In patients with blepharospasm, PET revealed that sensorimotor responses to perioral vibratory stimulation were also decreased bilaterally, whereas finger vibration was associated with a non-significant decrease of the contralateral sensorimotor rCBF (Feiwell et al., 1999).

Similar high-frequency (150 Hz) vibrotactile stimulation applied to the right index finger was also evaluated in a PET study in IPD and Huntington's disease patients compared to healthy controls (Boecker et al., 1999). In IPD patients, rCBF was lower in the contralateral M1/S1, PMd, S2, posterior cingulate, basal ganglia, and bilateral prefrontal cortex, whereas in Huntington's disease, decreased activation was found mostly in contralateral sensory areas (S2, posterior parietal cortex), basal ganglia and bilateral prefrontal cortex. Both IPD and Huntington's disease were associated with increased activation of the ipsilateral S1, S2, and insular cortex. It has been suggested that the altered sensory processing contributes to the motor deficits in both conditions (Boecker et al., 1999).

1.5. Summary of sensorimotor interactions during vibratory stimulation

In this section, it was demonstrated that vibratory stimulation is a powerful tool capable of evoking robust and replicable behavioural and cognitive effects that interact with one's internal body representation and control of voluntary movements. Especially, the effects of local muscle vibration have been extensively studied using electrophysiological and functional neuroimaging methods and are becoming increasingly well understood. Besides providing detailed descriptions of normal sensorimotor integration, vibration proved to be a valuable tool to investigate pathophysiological mechanisms in motor system disorders, such as idiopathic focal dystonia. Moreover, there is increasing evidence supporting potential therapeutical application of muscle vibration in various neurological conditions. In contrast, the relative contribution of cutaneous mechanoreceptors to these

phenomena remains largely unknown as the available data has not yet converged to answer some fundamental questions, such as the integration of cutaneous vibratory stimuli in proper motor cortical areas. It can be argued that, whereas during muscle vibration, the afferentation simulates natural stimuli likely occurring during normal limb movements, skin vibration does not produce any commonly occurring percept. We suggest that different modes of mechanical stimulation that are closer to natural interaction with the environment, such as mechanical pressure stimulation, could provide complementary data on the role of other types of tissue mechanoreceptors.

2. Mechanical pressure stimulation

Whereas innocuous peripheral mechanical pressure stimulation has been repeatedly employed in studies focusing on somatosensory processing (e.g., Chung et al., 2015, 2014; Hao et al., 2013; Miura et al., 2013) and noxious mechanical pressure stimulation has been utilised to study central pain processing (for review, see Baliki and Apkarian, 2015), there has been little interest in the interaction of pressure stimulation with the “classical” motor system. Following chapter provides therefore a new perspective on integration of mechanical pressure sensation into motor control.

Parts of the following section have been submitted as a review paper: **Hok, P.**, and Hlušík, P., in submission. *Modulation of the sensorimotor system by manipulation of afferent somatosensory input: evidence from mechanical pressure stimulation*. Biomed Pap-Olomouc.

2.1. Sensory structures responding to innocuous pressure

Mechanical pressure stimulation excites mainly SA-I afferents which, in addition to static pressure, respond to low frequency (usually below 5 Hz) mechanical stimulation and skin deformation (Johansson et al., 1982; for review, see Johansson and Flanagan, 2009; Ribot-Ciscar et al., 1989; Vedel and Roll, 1982). Therefore, unlike FA-I and FA-II afferents, the SA-I afferents (Merkel endings) are not particularly entrained by vibration and probably do not participate in kinaesthetic sensations during muscle vibratory stimulation (Roll and Vedel, 1982; Vedel and Roll, 1982). Still, some SA-I endings were shown to participate in coding joint positions in microneurographic studies (Aimonetti et al., 2007; Edin, 1992; Edin and Abbs, 1991), suggesting their participation in mediating proprioceptive information about relative limb positions (for review, see Proske and Gandevia, 2012).

2.2. Behavioural effects of peripheral pressure stimulation

Central effects of peripheral pressure stimulation on motor control are best demonstrated by taking a closer look at the phenomena that alter motor behaviour and performance. A rather thorough physiological background is introduced here, as it is crucial for describing the observed behavioural effects as well as understanding the rationale and correct interpretation of the electrophysiology and imaging studies.

Peripheral mechanical stimulation modalities, such as vibration, have been long known to elicit muscle contraction, overt involuntary tonic and phasic movements, postural sways, and modification of voluntary motor actions during and after the stimulation (Proske and

Gandevia, 2012; Souron et al., 2017b). Similar modulation of motor behaviour, including involuntary motor responses and outlasting motor after-effects, has also been demonstrated after mechanical pressure stimulation (Bauer, 1926; Vojta, 1970, 1968). It is therefore no surprise that pressure stimulation has been incorporated into a number of physiotherapeutic techniques, such as clinical massage, acupuncture (Wong et al., 2016), reflexology, or myofascial trigger point therapy (Smith et al., 2018). Another example of mechanical pressure stimulation in clinical use is stimulation according to Vojta, i.e., a component of physiotherapeutic technique also known as reflex locomotion therapy (RLT) or Vojta method (Bauer et al., 1992; Vojta, 1984, 1973a, 1970, 1968, 1966; Vojta and Peters, 2007) which is clinically employed in several European (Gajewska et al., 2018; Giannantonio et al., 2010; Juárez-Albuixech et al., 2020; Jung et al., 2017; Kiebzak et al., 2012; Laufens et al., 2004; Meholjić-Fetahović, 2007; Pavlikova et al., 2020) and Asian countries (Kanda et al., 2004; Lim and Kim, 2013). Given the lack of comprehensive literature on RLT and its relevance to some published imaging research, we provide here a broader historical perspective on this topic.

2.2.1. Involuntary motor responses to pressure stimulation

Inspired by the published neurophysiological and clinical studies (Bauer, 1926; Bobath, 1959; Fay, 1954a, 1954b; Kabat, 1958; Magnus and de Kleijn, 1912; Peiper, 1956) and his own clinical observations (Vojta, 1968, 1964), Vojta noted that, in several body configurations, sustained manual pressure stimulation of specific points on the skin surface (“stimulus points” or “stimulation/reflex/trigger zones”) gradually evokes a widespread motor response (asymmetrical muscle contraction in both sides of the neck, trunk, and limbs) which has been called “reflex locomotion” and involves two basic patterns, “reflex creeping” (also called crawling) – first observed by Bauer (Bauer, 1926; Vojta, 1968) – and “reflex turning” (also called rotation or rolling; Vojta, 1973a, 1970, 1968, 1966). These tonic motor responses share some similarities with other automatisms described in neonates, pre-term infants, human fetuses, and under certain conditions in healthy adults (Hellebrandt et al., 1962; Hooker, 1938; Vojta, 1973a, p. 269, 1972a, p. 468, 1966, p. 235; Zafeiriou, 2004). Reflex locomotion is likewise easiest to observe in healthy newborns up to 6 weeks of age (Vojta, 1973a, p. 275), but can also be elicited in children with cerebral palsy, adults with nervous system injury, as well as in healthy humans upon longer sustained peripheral stimulation of multiple trigger zones (temporal and spatial summation; Bauer et al., 1988; Vojta, 1973a, p. 276; Vojta and Peters, 2007, pp. 21-22,34,108).

Besides evoked (involuntary) muscle contraction, further effects of reflex locomotion have been described as well: voluntary movement facilitation, improvement of neurological abnormalities, and autonomic changes (Bauer and Vojta, 1979; Juárez-Albuixech et al., 2020; Jung et al., 2017; Laufens et al., 1995; Tomi, 1985; Vojta, 1973a, p. 269, 1973b, 1972a, p. 475; Vojta and Peters, 2007, pp. 18-19,96-98,108,155). The effects have been observed to persist for at least 30 min (Vojta and Peters, 2007, p. 35). It has been originally speculated that these sequelae of stimulation are mediated by massive, mainly proprioceptive afferentation which accompanies the reflex locomotion (Vojta, 1973a, pp. 257–276, 1972a, p. 475; Vojta and Peters, 2007, p. 20). Supported by the published works (Fulton, 1949, p. 161; Rushworth, 1959; Windle, 1966) and his own observations (Vojta, 1965, 1964), Vojta emphasised the central role of proprioception also in the development of spasticity, as opposed to a mere loss of inhibitory control from higher-order motor centres (Vojta, 1972a, p. 467,476, 1966, p. 235, 1964, p. 336).

Despite the decades of clinical use of RLT, there has been limited knowledge of its neurobiological basis, as the available evidence mostly consisted of kinesiology and observation studies (Vojta and Peters, 2007, p. 19). Originally, proprioception has been suggested to dominate the sensory afferentation triggering the motor response (Vojta, 1973a, p. 275,281; Vojta and Peters, 2007, p. 105). Indeed, pressure sensation from the foot soles contributes to maintenance of upright stance (Kavounoudias et al., 2001; Rasman et al., 2018). It was further emphasised that, in certain cases, the initial body configuration is essential to elicit the complete motor response (Vojta, 1973a, p. 278). Such posture-dependent involuntary responses were also demonstrated using cutaneous and muscle vibration (Gurfinkel et al., 1998; Smetanin et al., 1993). The efferent pathways mediating reflex locomotion have been speculated to involve extrapyramidal or parapyramidal system (i.e., bypassing the corticospinal tract), since reflex locomotion is best observed in neonates whose motor cortex is not yet mature (Vojta, 1973a, pp. 276–277). Due to its complex nature involving all extremities and truncal muscles at the same time, a common coordination centre has been suggested (Vojta, 1973a, p. 280). The horizontal gaze deviation observed during the motor response indicates that its neural substrate involves supraspinal, at least upper brainstem structure, including the midbrain reticular formation (Vojta, 1973a, p. 276,283, 1972b, p. 466, 1968, p. 329, 1964, p. 330; Vojta and Peters, 2007, p. 98). In fact, the evidence for CPG from animal experimental research suggests an existence of similar structures also in humans, possibly located to the midbrain or neighbouring structures (Grillner, 1975; Grillner and Wallén, 1985; Laufens et al., 1991). However, a frequent observation of partial motor responses limited to one or more extremities

additionally suggests an existence of multiple lower-level independent sources of the motor responses (Vojta and Peters, 2007, p. 4,20). This is again in line with the animal research evidence showing that lower-order generators of simple locomotion patterns independent for each extremity reside on the spinal level and are under top-down control of higher-order areas (Laufens et al., 1991). Reflex locomotion has been also contrasted with other primitive reflexes, e.g., “tonic neck reflexes” (Magnus and de Kleijn, 1912; Vojta, 1973a, 1970, p. 446, 1968), which have could be suppressed by reflex locomotion (Vojta, 1973a, p. 277,291). The structures responsible for the tonic neck reflexes have been therefore suggested to lie hierarchically lower than those implicated in reflex locomotion, namely in the lower brainstem (Vojta, 1973a, p. 279). However, at the time of methodological development of RLT, there were no non-invasive human methods available to test these hypotheses.

2.3. Electrophysiological evidence for central effects of pressure stimulation

Several studies using EMG recordings in both animals and humans evaluated the reflex muscle activity during pressure stimulation. In cats, complex tonic reflexes were elicited by short as well as longer maintained pressure applied at the pads (Hongo et al., 1990), whereas pressure stimulation of the chest modulated posture-dependent muscle activity (D’Ascanio et al., 1986). In humans, EMG studies demonstrated gradual and rhythmical motor response during RLT (Bauer et al., 1988) and confirmed the spatial and temporal summation of these responses (Laufens et al., 1994). Despite slight inter-individual differences, the order of muscle engagement seems to be relatively constant across subjects (Čemusová et al., 2011; Gajewska et al., 2018). Gajewska et al. (2018) suggested that the stereotypic and crossed nature of the observed muscle activations reflected excitation via long propriospinal pathways, but an influence of supraspinal motor centres could not be ruled out.

Currently, there are no non-invasive methods available to directly investigate electrophysiological activity in the brainstem sensorimotor nuclei. However, non-invasive assessment of cortical excitability may still provide some indications of changes occurring in cortico-subcortical loops, beyond the cortex itself. Studies employing pTMS (Kujirai et al., 1993) have evaluated corticomotor excitability changes due to extended peripheral electrical (Chipchase et al., 2011) and mechanical stimulation (Christova et al., 2011) and revealed that longer periods of sustained or repetitive stimulation (up to 2 hours) lead to an increase of motor cortical excitability outlasting the stimulation period (on the order of

several hours). It is likely that sustained pressure stimulation involving the same cutaneous afferents would evoke similar changes of cortical excitability. The underlying mechanisms within intracortical circuits potentially involve changes in intracortical inhibition (SICI) and/or ICF as seen in a number of studies using different modalities of peripheral stimulation (Christova et al., 2011; Golaszewski et al., 2012, 2010; Ridding and Rothwell, 1999; Rosenkranz and Rothwell, 2006a). However, to our knowledge, there are currently no published studies regarding such changes following mechanical pressure.

2.4. Neuroimaging evidence for central effects of pressure stimulation

The lack of neurophysiological evidence for the central motor effects of peripheral pressure stimulation has been compensated for by an increasing body of neuroimaging research. However, in most of these studies, the relationship between sensory stimulation and motor control has not been purposefully investigated. In this section, we therefore present mostly indirect evidence for sensorimotor integration based on the reported motor cortex co-activations.

A pioneering PET study assessed activation during discrimination task of slow-onset yet short pressure stimuli applied to the distal phalanx of the right index finger (Bodegård et al., 2003). Compared to a rest condition, subjects activated the contralateral S1 (BA 3b, 1 and 2), M1 (BA 4a), PMd, posterior insula and S2, and ipsilateral supramarginal gyrus (SMG). The study thus demonstrated immediate involvement of motor cortices during steady pressure stimulation.

Two fMRI studies evaluated static pressure stimulation applied over the right index fingertip using an air-cuff (Chung et al., 2015, 2014). Stimulation evoked an extensive activation pattern including bilateral postcentral gyrus (S1), S2, paracentral lobuli, insulae, ipsilateral dorsolateral precentral gyrus (M1), and contralateral midcingulate gyrus (Chung et al., 2014). Subsequent dynamic connectivity modelling revealed that the intrahemispheric processing of the pressure stimuli employed both serial (from S1 to S2) and parallel processing in the S1 and S2 (Chung et al., 2014). In the follow-up study, Chung et al. (2015) evaluated temporal evolution of the cortical activation during static sustained pressure stimulation of the index finger tip applied over 3 to 15 s. On overall, they found most consistent activations in the contralateral postcentral gyrus (S1), ipsilateral precentral gyrus (M1), bilateral S2, insulae, cingulate cortices, thalami and cerebellum. Notably, they observed that activations differed substantially depending on duration of stimulus and the time-window chosen and provided evidence for gradual adaptation of the activated areas to stimulation.

However, several studies of sustained pressure finger stimulation reported much less extensive activations restricted to somatosensory areas. Contralateral S1 and SMG activations were observed in a small group of 8 subjects in response to air-cuff sustained 30-s pressure applied to one of the four fingers: index, middle, ring, and little finger. A multivariate analysis found that activation in the contralateral SMG encoded the stimulated finger locations (proximal vs. distal; Kim et al., 2016a). Another study evaluated the effect of sustained pressure applied via a plastic piston to a thumb in 24 subjects during a working memory n-back task. No effect on task performance was observed and imaging data revealed pressure-related activation (contrast n-back with pressure vs. n-back without pressure) again only in the contralateral S1 and S2, but motor activations could be masked by the required button responses (Dehghan Nayyeri et al., 2019).

Several studies also evaluated pressure stimulation applied to lower limbs. In the first yet still preliminary fMRI study, only limited activation in the primary sensorimotor cortex and bilateral S2 was observed during sustained 1-Hz sinusoidal pressure stimulation applied for 30 s to the foot sole (Hao et al., 2013). In a follow-up fMRI study with twice as many participants (16), sustained right foot sole stimulation evoked more widespread activations in the bilateral precentral, postcentral, middle and superior frontal cortices, CMA, and IPL, as well as in the contralateral insula, temporal cortex, superior parietal lobule (SPL; Wang et al., 2015). In an even bigger sample (30 subjects), Miura et al. (2013) reported more circumscribed activation in the contralateral S1, S2, M1, SMA, and ipsilateral cerebellum in response to considerably shorter 5-s manual pressure stimuli applied over the base of the toes of either foot.

Further fMRI studies (Boendermaker et al., 2014; Meier et al., 2014) investigated central correlates of manual pressure applied over the lumbar vertebrae in the prone position. Besides bilateral activation in the medial S1 and S2, insular and cingulate cortices as well as cerebellum were significantly activated (Meier et al., 2014). Nevertheless, the roles of cutaneous afferents from the limbs and trunk in motor control may be essentially different.

To summarise, non-therapeutic pressure stimulation of the fingers, foot sole, or lower back were mostly associated with somatosensory cortical activity in the S1 and S2, and in sufficiently powered studies, also with widespread sensorimotor activations including M1, SMA, posterior parietal cortices, insulae and cerebellum. The differences among studies may be related not only to various sample sizes, but also to different stimulus intensities, duration, tactile stimulus properties, attention level, or differences in statistical analysis. The analytic approach seems to be especially important since Chung et al. (2015)

demonstrated that canonical haemodynamic response function may be insensitive to adapting cortical activations. An intriguing picture emerges when we contrast these results with different stimulation modalities, such as mechanical vibration. The widespread activation pattern observed in sufficiently powered focal pressure stimulation studies is consistent with studies using rather broad-area vibrotactile stimulation (Golaszewski et al., 2006; Siedentopf et al., 2008) or muscle stimulation (e.g., Naito et al., 2007, 2005) and far exceeds cortical maps of relatively circumscribed finger vibrotactile stimulation in other studies (e.g., Francis et al., 2000; Gelnar et al., 1998; Kim et al., 2016b). Though qualitatively different stimuli are not directly comparable, this illustrates that pressure stimulation can be associated with robust motor activations that provide the neuroanatomical substrate for sensorimotor interactions and motor after-effects of mechanical pressure stimulation.

However, as shown in vibration studies, sensorimotor activations are sensitive to modulation by higher-order processes, such as attention and cognitive task demands (Albanese et al., 2009; Goltz et al., 2015; Loayza et al., 2011). This necessitates an adequate control condition, e.g., a comparison between similar kinds of stimulation with or without known motor consequences. Therefore, the specific effects of some types of pressure stimulation, such as stimulation according to Vojta (1970, 1968), were contrasted with non-specific control (sham) stimulation. Besides the project reported in this thesis, there was only one previous neuroimaging study of RLT, which utilised pressure stimulus applied to an active site at the anterior thorax (Vojta, 1970) and reported the main effect of stimulation site (active versus control) in the ipsilateral putamen (Sanz-Esteban et al., 2018). However, due to unbalanced group sizes, a control stimulation site in a distant body part, and uncorrected statistical thresholds, the conclusions that can be drawn are substantially limited and further evidence for specific effects of pressure stimulation are still warranted.

V. REDUCING THE AFFERENT INPUT: MEANS OF PLASTICITY FACILITATION

1. Reduction of cutaneous and mixed-nerve input

Cortical motor representations are not only subject to change in response to enhanced afferentation or practice, but also due to sensory loss. Cortical reorganisation with increased cortical excitability and decreased intracortical inhibition was observed in upper- and lower-limb amputees (Chen et al., 1998; Cohen et al., 1991; Fuhr et al., 1992; Ridding and Rothwell, 1997), i.e., changes similar to effects of some plasticity-inducing peripheral stimulation protocols such as PAS (Rosenkranz and Rothwell, 2006a). Similar changes have been observed following reversible means of deafferentation. During ischaemic nerve block (INB), the intracortical GABA-ergic inhibitory influence decreases proximal to the block, thus, cortical excitability and the readiness for plastic changes are increased (Brasil-Neto et al., 1993; Ridding and Rothwell, 1997; Ziemann et al., 1998b, 1998a). The same was observed during pharmacologically induced regional anaesthesia (Brasil-Neto et al., 1992). The effects of INB can be further facilitated by muscle practice (Ziemann et al., 2001) or rTMS (Ziemann et al., 1998b, 1998a). Similar effect could be elicited also in distal hand muscles with improvement of skilled performance when the experiment was inverted and anaesthetic drug was applied to induce upper arm anaesthesia in chronic stroke patients (Muellbacher et al., 2002). Analogous effects have also been demonstrated in homotopic cortical regions of the limb contralateral to the deafferented extremity, which was associated with decreased IHI (Werhahn et al., 2002). Furthermore, anaesthesia of the healthy arm was shown to improve skilled motor performance of the paretic arm in patients after stroke (Floel et al., 2004).

However, opposite changes can be observed in the limb parts deprived of somatosensation. Cortical representation of hand muscles is reduced during pure cutaneous sensory loss around the particular muscle due to nerve anaesthesia even though the muscle afferentation is spared (Rossini et al., 1996). Reduction of sensory input with concomitant decrease of muscle use due to immobilisation also diminishes the cortical representation of the muscle (Liepert et al., 1995).

In general, sensory deprivation increases cortical excitability and promotes plasticity of nearby non-deprived muscles, as well as in contralateral limbs. In contrast, muscles in the deafferented segment show reduced cortical excitability. These effects thus resemble inverted sequelae of peripheral stimulation (cf. Christova et al., 2011; Fraser et al., 2002).

2. Selective muscle denervation: botulinum neurotoxin (BoNT-A)

Besides rather non-selective deafferentation using INB or anaesthetic drugs, afferentation can be selectively reduced from muscles using BoNT-A. Primary action of BoNT-A occurs at the neuromuscular junction: Following an intramuscular application, BoNT-A enters presynaptic terminals and acts as a metalloproteinase by cleaving soluble *N*-ethylmaleimide-sensitive factor attachment protein receptor (SNARE) complex, effectively blocking acetylcholine release and neuromuscular transmission. This peripheral effect is transient though long-lasting; it has gradual onset as maximum changes at the synapses can be observed at approx. 4 weeks after application, and it slowly wears off as the neuromuscular junction recovers within 12 weeks (Caleo and Restani, 2018; Weise et al., 2019).

Thanks to the long-lasting effect and good safety profile, intramuscular injections of BoNT-A have become a first-line treatment in therapy of focal spasticity (Dressler et al., 2017; Rosales et al., 2011; Simpson et al., 2016) and dystonia (Albanese et al., 2015; Kaňovský and Rosales, 2011). Although, in general, clinical improvement usually follows the timecourse of the peripheral changes, there are many reports of discrepancies between the clinical symptoms and the duration or degree of neuromuscular junction blockade (Weise et al., 2019). Since BoNT-A hampers neuromuscular transmission not only in extrafusal, but also in intrafusal muscle fibres, it inevitably alters also the afferentation from muscle spindles. It was therefore suggested that some of the BoNT-A effects could be mediated (indirectly) by central structures, including supraspinal motor control centres (Currà et al., 2004; Giladi, 1997; Kaňovský and Rosales, 2011). These central effects of intramuscular BoNT-A have been summarised in a recent comprehensive review by Weise et al. (2019). However, due to the relevance to the research related to this thesis, some evidence is discussed here in greater detail as well.

2.1. Electrophysiological evidence for central effects of BoNT-A

2.1.1. Healthy subjects

The electrophysiological evidence in healthy subjects is scarce (Palomar and Mir, 2012). The only study using TMS by Kim et al. (2006) evaluated cortical excitability in 10 healthy subjects following BoNT-A application into the *extensor digitorum brevis* muscle. Authors reported increased SICI and decreased ICF, and significant shortening of CSP. Notably, these changes were present 1 month after injection and were maintained at least for 3 months (Kim et al., 2006). However, much more data on central effects of BoNT-A is available from clinical studies in patient cohorts, in which BoNT-A is a recommended

treatment, such as dystonia and spasticity.

2.1.2. Dystonia

As indicated in “IV.1.2.3 Vibration in motor system disorders”, patients with dystonia show abnormal sensory processing of muscle spindle afferentation (Grünewald et al., 1997; Rome and Grünewald, 1999). There is some evidence that BoNT-A injections may normalise some of those findings. For instance, abnormal sensorimotor integration in cervical dystonia was demonstrated in the precentral P22/N30 component of the median nerve somatosensory evoked potentials (SEP). Namely, patients exhibited higher P22/N30 amplitude in the side contralateral to the involuntary head rotation, as compared both to the ipsilateral side and to healthy controls (Kaňovský et al., 1998, 1997). Following BoNT-A treatment, the amplitude of P22/N30 was reduced to normal levels (Kaňovský et al., 1998). However, neither baseline SEP abnormalities nor treatment-related changes were later observed in patients with focal hand dystonia, suggesting that various forms of dystonia may involve distinct pathophysiological mechanisms and responses to therapy (Contarino et al., 2007).

Further studies indicated that dystonia might be associated with other electrophysiological abnormalities confined to the motor cortex, including changes affecting inhibitory circuits. In fact, the previously reported abnormal augmentation of P22/N30 was associated with decreased SICI in the same hemisphere (Kaňovský et al., 2003) that also improved after BoNT-A (Kaňovský et al., 2004). Decreased SICI was also demonstrated in 15 patients with focal hand dystonia (Ridding et al., 1995) and in a mixed cohort of 12 patients with the majority of generalised forms of dystonia (Gilio et al., 2000). Although Ridding et al. (1995) did not assess the treatment effect, Gilio et al. (2000) observed that SICI transiently normalised after BoNT-A. However, a later study in a smaller group of 6 patients with focal hand dystonia found no evidence of changes in MEP amplitude or intracortical inhibition and failed to observe any treatment-related changes (Borojerdi et al., 2003). Similarly, no such changes were reported in a group of 10 patients with blepharospasm (Allam et al., 2005). The absence of effects in some of the studies might be related either to differences among the phenotypes of dystonia or to relatively low sample sizes. Nevertheless, even when the overall MEP amplitude remains unchanged, there can still be treatment-related changes in cortical organisation, as shown by a series of studies demonstrating shifts and distortions of cortical motor maps in patients with cervical or focal hand dystonia and their temporary normalisation after BoNT-A (Byrnes et al., 2005, 1998; Thickbroom et al., 2003).

Additional evidence for central effects of BoNT-A originates from studies that evaluated how the treatment interfered with processing of muscle vibration. A study by Trompetto et al. (2006) demonstrated that BoNT-A treatment in writer's cramp patients reduced otherwise normal TVR and decreased peripheral response (maximal M-wave) from the injected muscle. Longitudinal evaluation in 2 patients revealed that persisting clinical effects were still associated with decreased TVR despite normalised M-wave. The outlasting BoNT-A effect might have thus affected the supraspinal component of the TVR (Romaiguère et al., 1991). In cervical dystonia patients, BoNT-A injection into the affected SCM muscle prevented MEP facilitation during muscle vibration, which is considered to be of cortical origin (see "IV.1.3 Electrophysiological evidence for central effects of vibration"). The effect returned partially to baseline after the expiration of the BoNT-A blockade. However, in comparison to healthy control subjects, vibration-induced MEP facilitation in patients was somewhat attenuated at baseline, possibly as a carry-over effect from previous injections in pre-treated patients (Urban and Rolke, 2004).

Besides affecting the immediate responses to peripheral stimulation, BoNT-A was also shown to prevent abnormal plasticity triggered by peripheral stimulation in patients with focal dystonia. In untreated patients with dystonia, both facilitatory and inhibitory protocols of PAS cause changes in cortical excitability that spread beyond the somatotopic representations of the stimulated sites and are more diffuse than in healthy controls. These changes were observed in various forms of focal dystonia, including cervical dystonia, blepharospasm, and writer's cramp, suggesting more global abnormalities in the processes mediating the LTP-like and LTD-like plasticity (Weise et al., 2011, 2006). Following application of BoNT-A in cervical dystonia patients, the facilitatory effect of PAS was completely abolished after 1 month and was partially restored after a 3-month follow-up (Kojovic et al., 2011).

2.1.3. Spasticity

The available literature on central effects of BoNT-A in spasticity is more limited than in dystonia (Weise et al., 2019). Still, several studies reported that, apart from alleviation of spasticity, BoNT-A also improved abnormal SEP (Basaran et al., 2012; Frascarelli et al., 2011; Park et al., 2002). In general, spasticity was associated with decreased SEP amplitude that increased after treatment, which is quite opposite to the effect reported in dystonia (Kaňovský et al., 1998). However, recent data from our lab in a large cohort of 30 patients show that, despite confirming decreased SEP at baseline, BoNT-A did not lead to any changes in SEP amplitude throughout a 3-month follow-up (Veverka et al., in submission).

Although SEPs seem to be affected differently in spasticity and dystonia, the processing of vibratory stimuli in patients with spasticity was similarly altered by BoNT-A, i.e., with decreased TVR amplitude outlasting the peripheral effects of BoNT-A (Trompetto et al., 2008).

Among the few TMS studies evaluating motor cortical excitability following BoNT-A treatment in spasticity disorders, one has evaluated BoNT-A in lower limb and one in upper limb spasticity. Pauri et al. (2000) observed increased MEP latency and central conduction time following BoNT-A application into shank muscles in patients with paraparesis, however, there was no change in MEP amplitude that would suggest supraspinal effect. On the other hand, Redman et al. (2008) evaluated the shift in cortical representation of FDI in children with cerebral palsy following BoNT-A, but found no statistical difference in comparison to controls. This illustrates the paucity of direct evidence of motor cortex involvement in the therapeutic effects of BoNT-A (for review, see Phadke et al., 2012).

In summary, electrophysiological data available to date provide strong indications that BoNT-A affects cortical motor representations and somatosensory processing, similar to experimental procedures reducing the afferentation in a more diffuse way or to protocols enhancing the afferent input. However, the literature is still too scarce at least for some applications, and several controversies are yet to be resolved.

2.2. Neuroimaging evidence for central effects of BoNT-A

Similar to electrophysiology research, imaging studies of central effects of BoNT-A in healthy subjects are virtually non-existent. However, numerous studies investigated effects of BoNT-A in multiple forms of dystonia and spasticity. As shown below, the spectrum of findings is quite broad, which probably reflects distinct aetiologies of dystonic and spastic movement disorders, differences among patient cohorts, as well as the diversity of imaging protocols. The studies in the following section are therefore discussed with special emphasis on factors that potentially account for those inconsistencies.

2.2.1. Dystonia

Since BoNT-A is the recommended first-line treatment for focal dystonia, many imaging studies on dystonia involve patients receiving regular BoNT-A injections. However, most of them assessed brain activation at a single time point (e.g., Burciu et al., 2017; de Vries et al., 2008; Obermann et al., 2010, 2008), either in the middle (Feiwell et al., 1999; Obermann et al., 2010) or at the end of the 3-month treatment cycle (Burciu et al., 2017; Obermann et

al., 2008). Some studies included patients with history of BoNT-A treatment, but currently off treatment for several years (Castrop et al., 2012), or did not provide any information on treatment schedule and timing (Ceballos-Baumann et al., 1997; de Vries et al., 2008). Hence, only interventional studies involving at least two measurements (before and after BoNT-A) are further discussed in detail, with a few exceptions where substantiated by relevant findings. Notably, prominent differences may be observed even among studies that evaluated BoNT-A effects using repeated examinations before and after treatment. These inconsistencies may arise from long-term effects of BoNT-A involving neuronal plasticity, which may differ from short-term effects of the first dose (Currà et al., 2004; Giladi, 1997; Kaňovský and Rosales, 2011; Weise et al., 2019). For this reason, the distinction between BoNT-A-naïve and pre-treated cohorts has been taken into consideration in the following paragraphs.

BoNT-A effect on somatosensory task-related activation

As discussed in previous sections and illustrated in many electrophysiological (Grünewald et al., 1997; Kaňovský et al., 2003, 1998; Rome and Grünewald, 1999; Rosenkranz et al., 2005) and imaging studies (Butterworth et al., 2003; Feiwell et al., 1999; Tempel and Perlmutter, 1990) involving peripheral stimulation, dystonia is rightfully considered a disorder of sensorimotor integration (Kaňovský and Rosales, 2011). Two studies have, therefore, evaluated the central effects of BoNT-A by comparing pre-treatment and post-treatment brain responses to external stimulation, using either affected or unaffected body parts (Dresel et al., 2011; Opavský et al., 2012).

A study in pre-treated patients with blepharospasm and Meige's syndrome compared somatosensory activations during tactile stimulation of the forehead, lips, and hand. Before BoNT-A, patients hypoactivated bilateral S1 and right S2 (regardless of the stimulated side). This hypoactivation, however, remained significant even after treatment, which in turn, reduced activation in the left mesial PMd/SMA in several stimulation paradigms, and in the bilateral thalami and contralateral putamen during forehead stimulation only (Dresel et al., 2011).

An fMRI study from our laboratory utilised electrical median nerve stimulation in patients with cervical dystonia who were regularly receiving BoNT-A. The study demonstrated that at baseline, i.e., after the expiration of the previous BoNT-A injection effect, patients with cervical dystonia also hypoactivated the contralateral S2 and insula compared to healthy controls. In this study, the hypoactivation was restored back to normal 4 weeks after the BoNT-A injection (Opavský et al., 2012).

Therefore, it seems that although abnormal (reduced) sensory processing in S2 is a common hallmark in several forms of focal dystonia, BoNT-A treatment exerts specific effects depending on the stimulation site and underlying disease.

BoNT-A effect on motor task-related activation

Patients with various forms of dystonia have been also shown to exhibit abnormal sensorimotor activations during voluntary movements, including pure activation increases (Ceballos-Baumann et al., 1995a; Obermann et al., 2008; Opavský et al., 2011), decreases (de Vries et al., 2008; Haslinger et al., 2005; Nevrlý et al., 2018), and both (Ali et al., 2006; Burciu et al., 2017; Ceballos-Baumann et al., 1997, 1995b; Dresel et al., 2006). Some recurring observations of baseline differences between patients and control subjects include overactivation of the basal ganglia (Ceballos-Baumann et al., 1995b; Obermann et al., 2008), cerebellum (Ali et al., 2006; Burciu et al., 2017; Ceballos-Baumann et al., 1997, 1995a; Dresel et al., 2006), anterior cingulate (Ali et al., 2006; Ceballos-Baumann et al., 1995a, 1995b), lateral premotor (Ali et al., 2006; Burciu et al., 2017; Ceballos-Baumann et al., 1997, 1995b, 1995a) and parietal cortices (Ali et al., 2006; Ceballos-Baumann et al., 1997, 1995a; Dresel et al., 2006; Opavský et al., 2011), but also hypoactivation of the parietal cortices (Burciu et al., 2017; Haslinger et al., 2005), basal ganglia (de Vries et al., 2008; Nevrlý et al., 2018), SMA (Ali et al., 2006; Ceballos-Baumann et al., 1997, 1995b; Haslinger et al., 2005; Nevrlý et al., 2018), PMC (Dresel et al., 2006; Haslinger et al., 2005), M1 (Ceballos-Baumann et al., 1997, 1995b; Dresel et al., 2006; Haslinger et al., 2005), anterior cingulate cortex (Ceballos-Baumann et al., 1997; Haslinger et al., 2005; Nevrlý et al., 2018). Further abnormalities in patients with dystonia were documented during passive movements (Obermann et al., 2010) and motor imagery (Castrop et al., 2012; de Vries et al., 2008), but a complete account of all differences is beyond the scope of this thesis. This list only illustrates that it is currently impossible to delineate a single activation pattern associated with dystonia in general, and it implicates that it will be equally difficult to identify a universal pattern of changes following BoNT-A injections. Nevertheless, the following text attempts to provide a comprehensive overview of treatment-related activation changes in a search for common features that might be identified in the future as specific effects of BoNT-A.

Among studies directly assessing BoNT-A effects, two utilised H₂¹⁵O PET. A study by Ceballos-Baumann et al. (1997) evaluated activation during writing in patients with writer's cramp receiving chronic BoNT-A treatment who were off medication for >3 months. It revealed reduced activation in the contralateral M1 and SMA with simultaneously enhanced rCBF in the ipsilateral frontal association cortices, bilateral

parietal cortices, and in the cerebellum. In a follow-up examination after BoNT-A injection, treatment did not affect the hypoactivation in M1, but instead, it further increased activation in the already hyperactivated contralateral S1, normalised activation in the SMA and reduced activation in the anterior cingulate and cerebellum. Compared to controls, patients after treatment showed even stronger hyperactivation of bilateral premotor and parietal cortices, expressed no differences in the cerebellum or SMA, but still hypoactivated the contralateral M1. It was suggested that increased activation in the parietal regions reflected cortical reorganisation following BoNT-A (Ceballos-Baumann et al., 1997).

The second H₂¹⁵O PET study (Ali et al., 2006) showed that speech-related activation was decreased in patients with spasmodic dysphonia in the left temporoparietal cortex, SMA, and brainstem, whereas it was increased in the cerebellum, left S2, right M1 and PMC, insula, primary auditory cortex and anterior cingulate before BoNT-A. Most of the patients were chronically treated (7 out of 9), but did not receive any BoNT-A injection within last 6 months. In a follow-up PET after treatment, activations increased in the left temporal and parietal cortices and brainstem originally attenuated in patients, and decreased in areas originally hyperactivated, including the cerebellum, right M1/PMC, anterior cingulate, right insula and auditory cortex. BoNT-A further lowered activation in right thalamus, left caudate and right putamen, and in pre-SMA, and enhanced activation in the left ventral M1/PMC, frontal operculum and insula. The activation decrease in the cerebellum, anterior cingulate and right thalamus, as well as increase in the left temporoparietal cortices, brainstem, left BA 44 were consistently correlated with clinical improvement (Ali et al., 2006).

An even larger body of neuroimaging research on central effects of BoNT-A on motor-related activations in dystonia was conducted using BOLD fMRI imaging. One study evaluated activation during passive forearm movements in patients with cervical dystonia chronically treated with BoNT-A. The activation was increased in the S1, S2, cingulate cortex and cerebellum in the middle of the 3-month treatment cycle. Although only one time point was evaluated, activation in the SMA was strongly negatively correlated with the applied dose of BoNT-A and the TWSTRS (Obermann et al., 2010).

In pre-treated patients with spasmodic dysphonia, vocalisation and whispering at baseline were associated with attenuated activation of the bilateral primary SMC, anterior cingulate, SMA, PMd, and sensory association cortices, however, subsequent BoNT-A treatment had no effect on these abnormalities (Haslinger et al., 2005). A study by the same group also evaluated activation during whistling in mostly pre-treated patients with

blepharospasm and Meige's syndrome. Both patient groups were associated with overactivation in the bilateral S1, SMA, and cerebellum. In the group of pure blepharospasm, baseline activation was additionally decreased in a different part of the cerebellum, whereas in Meige's syndrome, baseline activation was additionally reduced in the bilateral M1 and PMv. After treatment, activation decreased in the SMA and right parietal cortex (S1/IPL) in the Meige's syndrome group, but there was no change in the blepharospasm group (Dresel et al., 2006).

Two fMRI studies from our lab evaluated activation during sequential finger opposition (SFO) in patients with cervical dystonia (Nevrlý et al., 2018; Opavský et al., 2011). In the first study, Opavský et al. (2011) demonstrated that previously treated patients hyperactivated the contralateral S2 at the time of their next scheduled BoNT-A injection. Application of BoNT-A led to activation decrease in the SMA and PMd 4 weeks later. At that point, patients hypoactivated the bilateral pallidum compared to healthy subjects. A follow-up study by Nevrlý et al. (2018) in a cohort of previously untreated patients revealed that baseline performance of the same motor task was associated rather with hypoactivation of the bilateral SMA, cingulate and paracingulate cortices and the ipsilateral caudate, pallidum and thalamus. Application of BoNT-A resulted in a widespread activation increase throughout the sensorimotor cortices, including the bilateral PMd, SMA, anterior cingulate cortex, S1 and S2, insulae, posterior parietal cortices, and contralateral M1. Furthermore, activation increased in several mostly ipsilateral subcortical areas, including the thalamus, putamen, midbrain and ipsilateral cerebellar hemisphere and vermis (Nevrlý et al., 2018). The apparently opposite changes in SMA and PMd observed by Opavský et al. (Opavský et al., 2011) were speculated to reflect plastic changes in long-term treated patients (Nevrlý et al., 2018). These shifts in motor cortex responses to BoNT-A treatment may also explain some inconsistencies among studies. Whereas most of the studies evaluating BoNT-A intervention in task-related fMRI included patients already on regular treatment (Ceballos-Baumann et al., 1997; Dresel et al., 2011; Haslinger et al., 2005; Opavský et al., 2012, 2011), some actually involved mixed cohorts of treated and untreated patients (Ali et al., 2006; Dresel et al., 2006). The study from our group (Nevrlý et al., 2018) has thus provided so far the only evidence of BoNT-A effects in naïve patients with dystonia.

To summarise, in pre-treated patients with dystonia, BoNT-A led to task-related activation increase (Ceballos-Baumann et al., 1997), decrease (Dresel et al., 2006; Opavský et al., 2011), both (Ali et al., 2006), or none (Haslinger et al., 2005). The individual observations differ considerably, including increased activation in the parietal cortices (Ali et al., 2006;

Ceballos-Baumann et al., 1997), M1/PMC (Ali et al., 2006), SMA (Ceballos-Baumann et al., 1997), insula and brainstem (Ali et al., 2006), but also reduced activation in the parietal cortices (Dresel et al., 2006), M1/PMC (Ali et al., 2006; Opavský et al., 2011), SMA (Dresel et al., 2006; Opavský et al., 2011), anterior cingulate (Ali et al., 2006; Ceballos-Baumann et al., 1997), insula, thalamus and basal ganglia (Ali et al., 2006), and cerebellum (Ali et al., 2006; Ceballos-Baumann et al., 1997). In contrast, BoNT-A naïve patients expressed only large activation increases after treatment, including the parietal cortices, M1/PMC, SMA, anterior cingulate cortex, insulae, basal ganglia, brainstem, and cerebellum (Nevrlý et al., 2018). The data thus indicate that treatment induces global sensorimotor adaptations that manifest in different ways depending on imaging protocols and dystonic phenotypes. While some intersections among the results are apparent, they are far from being a basis for consensus. Therefore, current state of evidence requires further confirmation in better characterised and larger patient cohorts, as well as clear outcome measures that can be associated with activation changes.

BoNT-A effect on resting-state activation

More insight into central effects of BoNT-A may be gained by analysing data at rest, which are unaffected by specific stimulation or task. While several studies evaluated resting state brain function in dystonia at a single time point (Delnooz et al., 2012; Dresel et al., 2014; Haslinger et al., 2017; Jiang et al., 2019; Li et al., 2017; Sarasso et al., 2020), this section focuses on studies specifically evaluating BoNT-A intervention. An FDG PET study (Suzuki et al., 2007) evaluated resting state metabolism in patients with blepharospasm at a single time point following BoNT-A injections. Patients were divided into two groups, either showing complete or incomplete response. The results revealed that patients had increased resting metabolism in the bilateral thalami and pons. Uncorrected maps additionally showed that patients with incomplete improvement had increased glucose metabolism in the cerebellum (Suzuki et al., 2007). The same group evaluated later the effects of BoNT-A on resting FDG intake in non-dystonic abnormal movements, namely in hemifacial spasm. They again revealed bilateral glucose hypermetabolism in the thalamus that decreased after BoNT-A treatment, though it still remained higher than in controls. However, there was significant correlation with the score of neurovascular compression, confirming that this cohort of patients involved different underlying pathophysiological mechanisms than those previously demonstrated in focal dystonia forms (Shimizu et al., 2012).

Alteration of brain function in the resting state has also been evaluated in several fMRI studies. In contrast to PET, which provides a meaningful baseline data directly comparable

between groups of subjects, fMRI cannot provide information on absolute resting brain activity. Instead, fMRI data have been frequently utilised to evaluate correlations in spontaneous BOLD signal fluctuations among different brain areas, the so-called FC (see “III.3.2. Blood oxygenation level-dependent (BOLD) contrast” for more details). A study by Mohammadi et al. (2012) evaluated resting-state FC using ICA decomposition in 16 patients with writer’s cramp on chronic BoNT-A therapy in comparison to healthy subjects. They observed increased FC of the default mode network with the contralateral putamen, and decreased FC of the bilateral sensorimotor network with the contralateral S1. However, none of these differences were affected by the subsequent BoNT-A application.

A study in pre-treated cervical dystonia patients using ICA (Delnooz et al., 2013) revealed baseline abnormalities in three large-scale networks in comparison to healthy controls. The observed differences between groups involved decreased FC of the sensorimotor network (consisting of PMC, SMA, primary SMC, and S2) with prefrontal and premotor cortices and SPL, as well as decreased FC of the (primary) visual network with the prefrontal and premotor cortices, SPL, and middle temporal gyrus. On the other hand, connectivity was enhanced between the executive control networks (consisting of the anterior cingulate, prefrontal, and parietal cortices) and the M1, PMC, prefrontal and visual cortices. Application of BoNT-A led to partial normalisation of the abnormal connectivity within the sensorimotor and visual network. Namely, connectivity with the visual network increased in the M1 and within secondary visual cortices, whereas connectivity with the sensorimotor network increased in the PMv. Notably, FC between PMv and the rest of the sensorimotor network decreased again at the second follow-up before the next BoNT-A injection (Delnooz et al., 2013). In a follow-up study by the same group (Delnooz et al., 2015), authors examined voxel-wise connectivity of the basal ganglia in a similar cohort of pre-treated patients with cervical dystonia. They found that patients exhibited weaker FC between the left (associative) frontoparietal network and right putamen and right external pallidum. In contrast, the bilateral putamen showed trend towards increased FC with the sensorimotor network. However, treatment affected different connections as it led to increase in FC between the executive control network and the right ventral striatum and external pallidum (Delnooz et al., 2015).

More recently, resting state connectivity was studied in patients with blepharospasm and Meige’s syndrome (Jochim et al., 2018). In a cohort of regularly treated patients, baseline (off BoNT-A) connectivity was abnormally reduced between the caudate nucleus and primary SMC, parietal and visual cortices; between the putamen and parietal cortices;

between the cingulate cortex and primary SMC, PMC, and parietal cortices; between PMC and S1; and between S1 and S2, cingulate cortex and cerebellum. Cerebellum also showed decreased connectivity to visual cortices, which was the only connection augmented after BoNT-A. In contrast, several areas exhibited decreased connectivity. Connectivity strength was reduced between the pallidum and cerebellum, caudate nucleus, and putamen; between the cerebellum and posterior cingulate cortex, prefrontal, parietal, temporal, visual, premotor cortices, and SMA; and between the thalamus and SMA/cingulate cortex (Jochim et al., 2018). The study therefore supports the central role of the cerebellum in the manifestation of dystonia (Corp et al., 2019; Filip et al., 2013; Shakkottai et al., 2017), in line with previous reports of abnormal cerebellar resting-state connectivity (Dresel et al., 2014; Haslinger et al., 2017) and task-related activation (Filip et al., 2017).

Our recent efforts to elucidate the role of the cerebellum in mediating the effects of BoNT-A in a cohort of naïve patients (Nevrlý et al., in preparation) indicate that cortico-cerebellar connectivity is significantly affected by treatment in several areas: on average, treatment reduced FC between the vermis lobule VIIIa and the left dorsal mesial frontal cortex. Furthermore, reduction in FC between the nearby vermis lobule VIIIb and bilateral prefrontal cortices and right temporoparietal junction was positively correlated with reduction in clinical scores. The same was observed for the right crus II. Additionally, the similar positive correlations were observed for intracerebellar connectivity between the anterior (right VI) and posterior (right crus II) cerebellum, as well as between the right IX and left VI–VII (Nevrlý et al., in preparation).

To summarise, the changes in resting-state connectivity occurring after BoNT-A application are as manifold as the observations in task-related studies. Whereas resting-state PET studies indicated changes in thalamic activation (Shimizu et al., 2012; Suzuki et al., 2007), fMRI studies pointed to more wide-spread effects including changes in intracortical (Delnooz et al., 2013), cortico-subcortical (Delnooz et al., 2015; Jochim et al., 2018), cortico-cerebellar (Jochim et al., 2018; Nevrlý et al., in preparation), striato-cerebellar, pallido-cerebellar (Jochim et al., 2018), and intracerebellar connectivity (Nevrlý et al., in preparation). While such variety of results certainly indicates far-reaching effects of BoNT-A, it is challenging to identify a single key structure or network that would be responsible for all observed changes. In fact, these data rather support the notion that dystonia is a network-wide disorder in which a lesion of any single node could lead to a common manifestation (Gracien et al., 2019; Lehericy et al., 2013; Nevrlý et al., 2018). Likewise, the central effects of BoNT-A may hinge upon dynamic modulatory changes in multiple nodes of the sensorimotor network, which could be differently weighted in

various patient cohorts, reflecting the variability of clinical manifestations and individual responses to treatment.

2.2.2. Spasticity

As opposed to relatively scarce electrophysiological evidence, there has been an increasing number of imaging studies assessing central effect of BoNT-A in spasticity. Since spasticity is a common consequence of stroke (Dorňák et al., 2019), most of the research was dedicated to stroke patients, whereas studies in other patient cohorts are less frequent. For the same reason, effects of BoNT-A have been most frequently investigated in patients with upper limb spasticity. Importantly, comprehensive treatment in stroke patients requires also regular physiotherapy, therefore, the reported effects of BoNT-A are usually combined with effects of physiotherapy (Thibaut et al., 2013). As this is the recommended treatment approach, application of BoNT-A without physiotherapy would be unethical and, therefore, their effects have usually been studied together (Bergfeldt et al., 2015; Šenkárová et al., 2010; Tomášová et al., 2013; Veverka et al., 2019, 2016, 2014, 2012), but see (Chang et al., 2015; Manganotti et al., 2010). Despite a wide range of structural lesions that lead to spasticity, the following paragraphs illustrate that changes observed in spasticity seem to be much more uniform than observations in dystonia.

A study by Bergfeldt et al. (2015) in 6 chronic stroke patients used finger extension-flexion to investigate motor task-related activity before the BoNT-A injection and at a follow-up after 6 and 12 weeks. Using a region of interest (ROI)-based analysis of individual BOLD responses rather than group-wise statistics, authors demonstrated increased activation levels in patients in the contralesional M1/PMC with reduced lateralisation of activation as compared to controls. As spasticity improved after BoNT-A, activation levels decreased numerically in both ipsilesional and contralesional cortices after treatment, with larger change in the ipsilesional cortex, thus normalising partially the left-to-right lateralisation. At the second follow-up, activation increased nominally, but on overall, it remained lower than at baseline. However, the within-group differences were not formally statistically tested by the authors, casting some doubt on the statistical significance of the observed differences (Bergfeldt et al., 2015). However, the results are in line with those observed by Manganotti et al. (2010) who utilised combined EMG-fMRI imaging in 8 chronic stroke patients naïve to BoNT-A during an isotonic hand grip task. Before BoNT-A, patients activated a bilateral network of areas consisting of primary SMC, SMA, and the cerebellum. Using an ROI-based approach, study revealed that the extent of activation (number of active voxels) decreased bilaterally and the distribution of active voxels was

more lateralised than at baseline. Importantly, EMG recordings showed no muscle activity in the contralateral hand at any time point, instead, it illustrated a reduction of co-contractions in the paretic hand (Manganotti et al., 2010). Another small study of in 4 chronic stroke patients using similar task showed an overactivation in the cerebellum during gripping with the paretic hand, however, there were no significant changes 1 week after injection, possibly due to small sample size and too short follow-up (Chang et al., 2015).

The effects of BoNT-A on brain activations in patients with spasticity have also been extensively evaluated in a large series of fMRI studies from our lab (Hok et al., 2011; Šenkárová et al., 2010; Tomášová et al., 2013; Veverka et al., 2014, 2013, 2012). In several studies on upper limb spasticity, our lab has utilised complex SFO (Tomášová et al., 2013; Veverka et al., 2019, 2014) according to Roland et al. (1980). In patients with hand paralysis who were not able to perform active movements, we have utilised passive hand movements (Veverka et al., 2016) and kinaesthetic movement imagery (Šenkárová et al., 2010; Veverka et al., 2014, 2012). All patients included in the studies were naïve to the BoNT-A treatment and all received concomitant physiotherapy.

The feasibility of movement imagery as a substitute for real movements in assessment of central effects of BoNT-A was demonstrated by Šenkárová et al. (2010) in a preliminary study including 4 hemiplegic patients. The task involved performance of kinesthetic imagery of complex SFO using the plegic hand after training the same movement with the unaffected hand. Comparison of BOLD activations before and 4 weeks after BoNT-A showed significant decrease in activation in the posterior cingulate cortex. The average activation maps also indicated a global decrease of activation throughout the sensorimotor system (Šenkárová et al., 2010). These findings were further expanded by a follow-up study by Veverka et al. (2012) that utilised the same task in 14 patients following a longitudinal design with examination scheduled before BoNT-A and 4 and 11 weeks post-treatment. Group-wise maps again showed overall reduction of the activation extent, which continued throughout the follow-up. Direct contrasts confirmed decreased activation in the posterior parietal cortex (IPL and precuneus). At the final follow-up, activation further decreased in the bilateral prefrontal cortices and ipsilesional insular cortex. The differences were the most extensive when the first examination was contrasted with the final one when they could also be observed in the contralesional primary SMC (Veverka et al., 2012).

In patients with severe hand paresis, effect of BoNT-A was also assessed using passive wrist movements (Veverka et al., 2016). The study in 7 hemiplegic patients followed the

same longitudinal design with baseline exam before treatment and re-evaluation at 4 and 11 weeks post-treatment. In contrast to the active movement imagery, application of BoNT-A resulted in activation increase in the bilateral posterior cerebellum and occipital cortices. At the second follow-up, activation decreased in the anterior cerebellum and SMA/pre-SMA. The decrease in the SMA, along with the reduced activation in the ipsilesional primary SMC (foot area), was also significant when compared to the study baseline. While it may seem that BoNT-A effects in kinesthetic imagery (Šenkárová et al., 2010; Veverka et al., 2012) and passive movements (Veverka et al., 2016) are contradictory, it was argued that BoNT-A may have essentially distinct influence on internally driven and externally evoked activation. For instance, it was further suggested that reduced abnormal (noisy) afferentation evoked implicit motor visualisation (Veverka et al., 2016).

In patients with less severe hand paresis, use of overt active movements allowed for a more direct investigation of central influence of BoNT-A on motor control. In a group of 5 hemiparetic patients after stroke, Tomášová (formerly Šenkárová) et al. (2013) utilised SFO to assess longitudinal changes in brain activation following BoNT-A. The study showed that, 4 weeks after BoNT-A application, the extent of group-wise activation was apparently reduced, but it returned to the original state at week 11. Although direct comparison revealed no significant voxel-wise differences, a weighted contrast between session 2 and sessions 1 and 3 revealed treatment-related activation decrease in the ipsilesional inferior frontal gyrus, DLPFC, PMd, postcentral gyrus and IPL, representing the transient effect of BoNT-A controlled for the effect of concomitant physiotherapy (Tomášová et al., 2013).

In another study (Veverka et al., 2014), BoNT-A effects on real and imagined movements were more closely compared in two groups of patients matched for age (7 patients per group). In the plegic group performing kinaesthetic imagery, activation transiently decreased in the posterior cingulate and occipital cortices 4 weeks after BoNT-A and increased again at 11 weeks post-treatment. In the paretic group performing overt SFO, activation extensively decreased throughout the sensorimotor system, predominantly in the ipsilesional DLPFC, PMd, SMA, primary SMC (foot area) and posterior parietal cortex (SPL and IPL), but also in bilateral inferior frontal, orbitofrontal, and occipital cortices. At the final follow-up, activation increased again in a subset of these areas, namely in the anterior cingulate, ipsilesional posterior parietal (IPL, SPL) and inferior frontal cortices. In contrast, activation remained reduced in the bilateral occipital cortices (Veverka et al., 2014).

Our most recent and largest study so far evaluated 30 patients with post-stroke spasticity and mild paresis (Veverka et al., 2019). It again followed the same longitudinal design and analysis aimed at disentangling the effects of BoNT-A from the effects of concomitant physiotherapy using a weighted contrast. It demonstrated that the central cortical structure reflecting the transient improvement of spasticity was localised to the ipsilesional posterior parietal cortex (SPL and intraparietal sulcus, IPS) that decreased transiently after BoNT-A. No consistent effect of time (on physiotherapy) was observed. This result is in line with our previous reports, where decrease in posterior parietal activation was consistently observed (Tomášová et al., 2013; Veverka et al., 2014), including kinaesthetic motor imagery data (Veverka et al., 2012). While differences in other cortical areas are likely to accompany the changes in parietal cortices, modulation of the ipsilesional SPL/IPS seems to be the least variable change. However, further studies are required are warranted in order to establish whether activation decrease in SPL/IPS is simply a marker or has causal relationship to the clinical improvement.

Besides evidence from chronic stroke patients, our preliminary fMRI study assessed activation changes following BoNT-A in 4 multiple sclerosis patients with lower limb spasticity and 4 control subjects (Hok et al., 2011). In the study, patients received their first-time BoNT-A into spastic hip adductor muscles. During the fMRI acquisition, they performed extension-flexion of the knee. The examinations were scheduled immediately before BoNT-A as well as 4 and 12 weeks after injection. In general agreement with data on post-stroke spasticity, patients showed overactivation in the bilateral sensorimotor cortices (mostly PMd and SPL) at baseline, which was reduced to normal level after BoNT-A, but returned close to original state at week 12 when mostly parietal cortices were again hyperactivated by patients relative to controls. This illustrates that effects of BoNT-A on spasticity are likely to have more universal impact on brain activation, independent on injection site and underlying aetiology of spasticity.

2.2.3. Summary of central effects of BoNT-A

As illustrated in the previous paragraphs, muscle denervation using BoNT-A has a considerable impact on function of the CNS structures. Most consistent findings include imaging reports of decreased sensorimotor activation during voluntary movements and kinaesthetic imagery in post-stroke spasticity, with possibly central role of the contralateral SPL/IPS. Widespread activation changes were also observed in patients with dystonia, however, the individual patterns of changes seem to differ considerably among patient cohorts, potentially reflecting different underlying aetiologies, but also variety of imaging

protocols. Electrophysiological evidence for central effects of BoNT-A was also reported, but the amount of literature is scarce, especially in spasticity. For complete understanding of the central effects of BoNT-A, studies in healthy subjects are also desirable, although they are certainly more controversial to conduct. Moreover, to establish any causal relationship between clinical improvement and central effects of BoNT-A, specific interventions should be designed that would either mitigate or augment the clinical effects by interaction with the putative central targets of BoNT-A.

Finally, with respect to general theme of this thesis, BoNT-A is an example of peripheral intervention that, based on empirical observations, became gradually accepted as a tool to enact plastic changes affecting central sensorimotor control. While mechanical stimulation of peripheral receptors and invasive blockade of the neuromuscular junction may seem fundamentally different, the resulting imbalance of afferentation (or restoration of balance in case of disease) might be in fact the critical drive for plastic changes as the brain seems to rely in some cases more on relative contribution of afferents rather than on absolute signal (cf. Sittig et al., 1985). From this perspective, reduction of some peripheral input may be considered as an “inverted” stimulation with relative overflow of the otherwise normal remaining afferentation. Under such assumption, evidence from peripheral stimulation studies and research on deafferentation or BoNT-A is, in fact, complementary. Thus it could be speculated that proper combination of the two approaches could evoke even more profound plastic changes. However, thorough assessment of central effects of each individual method is a necessary prerequisite before studies of combined multimodal stimulation protocols can be commenced.

VI. PREMISES AND THEORETICAL BACKGROUND OF THE EXPERIMENTAL STUDIES

As outlined in the introduction, neuronal plasticity is a key component in restoration of human motor function. Plastic changes can be induced via transient peripheral afferent stimulation (Powell et al., 1999). Outlasting modulatory effects in the sensorimotor cortex have been observed following sustained electrical (Chipchase et al., 2011), magnetic (Gallasch et al., 2015), and vibratory (Rosenkranz and Rothwell, 2003) stimulation. Peripheral pressure stimulation has been studied as well, though less extensively (e.g., Chung et al., 2015; Kim et al., 2016a; Sanz-Esteban et al., 2018) despite the fact that it serves as a major component of clinical physiotherapeutic techniques, including RLT (Vojta, 1973b).

The technique, also known as Vojta method, uses sustained manual pressure stimulation of specific body surface areas to gradually evoke a stereotypic pattern of tonic muscle contractions in both sides of the neck, trunk, and limbs (Vojta, 1973b). It has been speculated that the motor response is controlled by a brainstem region (Laufens et al., 1991), possibly related to the so-called CPG that were discovered in vertebrate animals (Grillner and Wallén, 1985) and more recently became associated with human locomotion and postural control (Jahn et al., 2008; la Fougère et al., 2010; Takakusaki, 2013). However, direct evidence of involvement of supraspinal CPG during therapeutic stimulation has been until now missing.

Previous imaging studies of pressure stimulation recently provided valuable, yet still incomplete picture of the central somatosensory processing (Bodegård et al., 2003; Chung et al., 2015, 2014; Dehghan Nayyeri et al., 2019; Hao et al., 2013; Kim et al., 2016a; Miura et al., 2013; Sanz-Esteban et al., 2018; Wang et al., 2015). These studies reported predominantly somatosensory activations and remarkable though inconsistent involvement of motor cortices. However, wide-spread sensorimotor activations are non-specific as they are sensitive to modulation by higher-order processes, such as attention and cognitive task demands (Albanese et al., 2009; Goltz et al., 2015; Loayza et al., 2011). Only one study assessed specific cortical activation during manual stimulation according to Vojta applied to an active site at the anterior thorax in comparison to a sham stimulation (Sanz-Esteban et al., 2018). However, methodological issues, such as unbalanced group sizes, a control site in a distant body part, and statistical maps uncorrected for multiple comparisons, do not permit drawing strong conclusions (Sanz-Esteban et al., 2018). To our knowledge, no previous imaging study evaluated immediate central effects of pressure

stimulation of the foot according to reflex locomotion therapy (Vojta, 1973b, 1968) prior to initiation of this research, and in general physiology literature, there have been no fMRI data on responses to pressure foot stimulation delivered continuously over at least 30 s. More specifically, it is also unknown whether the sensorimotor system response is influenced by the choice of specific stimulation site, e.g., one used in RLT.

After the stimulation, changes in motor behaviour have been observed for at least 30 min (Vojta and Peters, 2007). Despite ongoing clinical use of the reflex locomotion therapy (e.g., Jung et al., 2017; Lim and Kim, 2013), there is limited knowledge of the neurobiological basis of these after-effects since the available evidence is mostly based on clinical observation studies (Vojta and Peters, 2007). Whereas prominent modulation of task-related activity in the sensorimotor cortex was repeatedly observed after transcutaneous electrical or magnetic stimulation (Gallasch et al., 2015; Golaszewski et al., 2004; Wu et al., 2005), no such data have been available for the sustained mechanical pressure stimulation.

Outlasting effects of extended peripheral electrical (Chipchase et al., 2011) or mechanical stimulation (Christova et al., 2011) were further demonstrated using motor evoked potentials and pTMS (Kujirai et al., 1993). In these studies, extended periods of sustained or repetitive stimulation (up to 2 hours) have led to longer lasting increase of motor cortical excitability, outlasting the stimulation period (on the order of several hours). The changes were accompanied by reduced SICI and/or increased ICF (Christova et al., 2011; Golaszewski et al., 2012, 2010; Ridding and Rothwell, 1999; Rosenkranz and Rothwell, 2006a). Decrease in intracortical inhibition facilitates plasticity (Ziemann et al., 2001) and has been associated with motor learning (Liepert et al., 1998; Perez et al., 2004; Smyth et al., 2010). SICI is therefore a possible candidate mechanism participating in motor improvement observed immediately after RLT (Vojta, 1973a; Vojta and Peters, 2007). Both the length of the experimentally tested sustained stimulation and the duration of effects are quite similar to the clinical applications of RLT (Jung et al., 2017; Vojta, 1973a; Vojta and Peters, 2007). Yet again, there are currently no data available on cortical excitability changes following sustained mechanical pressure.

An important consideration for assessment of motor effects of RLT and pressure stimulation in general are the associated autonomic nervous system (ANS) responses (Dimitrijević and Jakubi, 2005; Vojta and Peters, 2007). Though repeatedly observed, the effects of RLT and pressure stimulation in a broader sense on autonomic activity and autonomic control have not yet been systematically investigated in the published literature prior to commencement of this study. At the same time, changes in heart rate variability (HRV) reflecting the sympathovagal balance have been studied and reported for many

other types of surface or other somatosensory stimulation, including nociceptive (Baker and Shoemaker, 2013; Joseph et al., 2004; Koenig et al., 2014; S. L. Smith et al., 2013; Wijnen et al., 2006).

Considering the available indirect neurophysiological (Chipchase et al., 2011; Christova et al., 2011; Gallasch et al., 2015; Rosenkranz and Rothwell, 2003), imaging (e.g., Gallasch et al., 2015; Golaszewski et al., 2004; Wu et al., 2005) and direct clinical (Vojta, 1973b; Vojta and Peters, 2007) evidence, following hypotheses were formulated:

1. Hypothesis I

The first hypothesis states that different peripheral stimulation sites would differentially influence sensorimotor system during the stimulation. Furthermore, a site used in the RLT would specifically activate the putative brainstem nuclei participating in the involuntary motor responses.

To address the hypothesis, a block-design fMRI experiment was prepared involving sustained pressure stimulation applied at either an active (Vojta, 1968) or control site on the foot. This was expected to identify a general activation pattern involved in central processing of sustained pressure stimulation of the foot under conditions close to the clinical setting of RLT and the differences related to the stimulation site itself.

2. Hypothesis II

The second hypothesis proposes that extended peripheral pressure stimulation would cause modulation of the motor system outlasting the stimulation itself. Evidence from different stimulation modalities suggests such changes in the primary SMC (Gallasch et al., 2015). However, previous observations in RLT led researchers to postulate that the primary site of action resides in the brainstem CPGs (Laufens et al., 1991). Hence, it is speculated that the site used in RLT would alter specific motor areas as compared to a nearby silent control site on the foot.

To this end, a block-design fMRI experiment was proposed with a paced SFO task repeated before and after sustained pressure stimulation at either an active or control site. SFO robustly activates the motor system at both cortical and subcortical levels, providing an efficient probe into the motor control of fine finger movements (Solodkin et al., 2001).

3. Hypothesis III

The third hypothesis postulates that short-term changes after peripheral pressure stimulation involve increased cortical excitability of the M1 as shown following different modalities of peripheral stimulation (Christova et al., 2011; Golaszewski et al., 2012, 2010; Ridding and Rothwell, 1999; Rosenkranz and Rothwell, 2006a). More specifically, reduced SICI and/or increased ICF is expected to follow stimulation of the active site, but not control stimulation.

A pTMS protocol was designed to evaluate motor cortex excitability (including SICI and ICF; Kujirai et al., 1993) before and after sustained pressure stimulation applied either to an active site according Vojta (1968) or to a similar sham site.

4. Hypothesis IV

The fourth and the last hypothesis states that pressure stimulation would be associated with changes in autonomic control. Specifically, active stimulation site is expected to elicit greater changes than control stimulation (Dimitrijević and Jakubi, 2005; Vojta and Peters, 2007).

To test this hypothesis and probe the ANS, an experimental protocol was prepared using a modification of spectral analysis of HRV (SAHRV) with the imposed changes of orthoclinostatic load (Opavský, 2002; Opavský and Salinger, 1995; Salinger et al., 1998).

To avoid further confounds of various motor system disorders, all hypotheses were applied to and subsequently tested in healthy subject population.

VII. AIMS OF THE THESIS

The aim of this thesis was to evaluate central correlates of sustained manual pressure stimulation depending on the stimulation site: either a specific stimulation site according to reflex locomotion therapy associated with known motor behaviour after-effects or a non-specific control stimulation site with no associated motor consequences. To this end, four partial aims were formulated, each constituting a separate study:

1. Study I: Brain activation patterns associated with sustained manual pressure stimulation (fMRI during stimulation)

The aim of the study was to assess average brain activation patterns and the specific differences during the experimental interventions using functional magnetic resonance imaging in healthy subjects.

2. Study II: Brain activation changes following sustained manual pressure stimulation (fMRI of stimulation after-effects)

The aim of the study was to assess average brain activation patterns and the specific differences during a complex hand motor task following experimental interventions using functional magnetic resonance imaging in healthy subjects.

3. Study III: Cortical excitability changes following sustained manual pressure stimulation (TMS)

The aim of the study was to evaluate cortical excitability changes following the experimental interventions using transcranial magnetic stimulation.

4. Study IV: Changes in function of the autonomic nervous system following sustained manual pressure stimulation (HRV)

The aim of the study was to evaluate function of the autonomic nervous system following experimental interventions using spectral analysis of heart rate variability.

The research specified in aims of the thesis have been supported by the project *Central and autonomic nervous system correlates of prolonged peripheral stimulation in the human*, PI: prof. MUDr. Ing. Petr Hlušík, Ph.D., Czech Science Foundation (GACR) grant number GA14-22572S.

VIII. MATERIALS AND METHODS

1. Study design

All studies were conducted as randomised cross-over experimental studies in a cohort of healthy adults to determine the immediate or outlasting central and autonomous effects of the sustained manual pressure stimulation according to RLT (Vojta, 1973b; Vojta and Peters, 2007) versus a sham stimulation.

All studies were carried out in accordance with World Medical Association Declaration of Helsinki. The study protocol was approved by the Ethics Committee of the University Hospital Olomouc and the Faculty of Medicine and Dentistry of Palacký University Olomouc under a common approval number 9.4.2013 and all participants gave their written informed consent prior to their inclusion in the study.

2. Participants

The study participants were university students naïve to the technique of reflex locomotion, with no history of any neurological condition and no signs of motor disability. The samples were very similar across the four studies (for an overview, see **Table 1**):

2.1. Study I and II (fMRI)

Thirty healthy volunteers enrolled in Study I and II (16 women and 14 men, mean age 24.20, standard deviation [SD] 1.92). Twenty-seven subjects were right-handed and three were left-handed according to the Edinburgh handedness inventory (Oldfield, 1971).

2.2. Study III (TMS)

Twenty healthy volunteers enrolled in the third study (10 women and 10 men, mean age 23.87, SD 1.82). Data from one participant were lost due to technical error, final sample thus consisted of 19 participants (9 females, mean age 23.93, SD 1.85). According to the Edinburgh handedness inventory (Oldfield, 1971), 1 subject was left-handed (laterality index [LI] -0.2) and 18 subjects were right-handed, out of these 13 were strongly right-handed ($LI \geq 0.7$).

2.3. Study IV (HRV)

Thirty healthy participants were included in Study IV. Two participants were excluded after initial autonomic examination, one of them manifested extremely high and the other

extremely low values of HRV spectral parameters, which did not permit reliable assessment of changes during different phases of testing. The investigated group therefore included 28 participants (15 women and 13 men), mean age 23.3 years, range 20.4–25.7 years. All participants had to keep a recommended regime prior to the scheduled examination.

3. Tasks and procedures

Although the stimulation procedure was essentially almost identical in all studies, some details of the stimulation protocols had to be adjusted to address specific conditions of the used experimental methods. As a result, slight differences in stimulation parameters among the Studies I-IV could not be avoided. However, due to a considerable overlap, experimental tasks and procedures for Studies I-IV are still described together in this section to prevent unnecessary repetition, with the differences marked in text. For a better overview of the differences among the protocols, they have been also listed at the end of the section “VIII.3. Tasks and procedures” in **Table 1**.

3.1. Visit schedule

In each study, every participant underwent two stimulation sessions, each involving either heel stimulation (HS) or ankle stimulation (AS). The session order was randomised and counter-balanced, and the participants were not informed in advance that the stimulation would be performed in two different sites. The sessions were scheduled at least 7 days apart. Within each study, sessions were scheduled for the same part of day (for details, see **Table 1**).

3.2. Pressure stimulation

During the stimulation, participants were lying prone in the scanner bore (Studies I and II: fMRI) or on a comfortable examination table (Studies III and IV: TMS and HRV, respectively) with their arms positioned along the trunk. In Studies I and II, participants were positioned with their head prone and were asked to keep their eyes closed and not to think about anything in particular. In Studies III and IV, participants had their head rotated to the left and were asked to keep their eyes open and lie still. In Study III, they were additionally encouraged to report if the stimulation became painful.

The pressure was applied manually by an experienced therapist (MK or MŠ) using his/her thumb placed on one of two predefined sites located on the lateral side of the foot over bony structures and within the same dermatome (Foerster, 1933): either (1) the right lateral

heel zone (*processus lateralis tuberis calcanei*, HS) according to Vojta (1973b, 1968), or (2) a control site at the right lateral ankle (AS), see **Fig. 1**. Throughout the session, the stimulated limb was semi-flexed in the knee joint and supported above the table by the therapist who maintained constant tactile contact with the participant's foot to further simulate natural conditions of a therapeutic procedure.



Figure 1. Stimulation procedure and stimulation sites. The upper photograph shows the body position during the stimulation (Study III [TMS] and IV [HRV]). The lower right photograph shows the stimulation site (zone) at the right lateral heel according to Vojta (HS), whereas the lower left photograph shows the control stimulation site at the right lateral ankle (AS).

The therapists were instructed to apply manual pressure similar to that routinely used during physiotherapy according to Vojta. In Study III (TMS), they were encouraged to decrease the pressure if the stimulation was reported painful by the participant. The use of a single stimulation site, the specific body position and stimulation duration, were chosen to elicit only partial motor response (Vojta and Peters, 2007), avoiding gross body movements and/or head displacement in the scanner bore in Studies I and II.

The exact stimulation timecourse differed between the imaging and non-imaging studies due to methodological constraints of fMRI analysis. In Studies I and II (fMRI), stimulation

was delivered while inside the scanner bore during two consecutive 10-min functional imaging acquisitions. During each acquisition, stimulation was applied in twelve blocks (each 30 s long) alternating with jittered rest to permit modelling of the extended haemodynamic response (Dale, 1999). In total, this resulted in 6 min of stimulation and 4 min of rest per acquisition run.

In Studies III and IV (TMS and HRV), the stimulation was delivered in a single 20-min block in a quiet room lit with natural light dimmed with window blinds.

3.3. Pressure-related behavioural measures

After each session, participants reported discomfort/pain perceived during the stimulation using a visual analogue scale (VAS) for discomfort/pain, with 0 (no discomfort/pain) and 10 (the worst possible pain) marked as the extreme values.

In Studies I-III (fMRI and TMS), the force applied was continuously recorded during the stimulation using a custom-made (MRI-compatible) calibrated pressure/force monitor (based on a FlexiForce sensor, Tekscan, South Boston, MA, USA).

3.4. Motor task in Study II (fMRI of stimulation after-effects)

During fMRI acquisition, participants performed SFO with their right hand. They were asked to tap sequentially the right index, middle, ring and little finger against the thumb, and to repeat the sequence during 15-s blocks alternating with 15-s rest throughout a 6-min acquisition run. The performance was paced at 2 Hz by high-pitch (500 Hz) tones delivered using MR-compatible headphones. The rest was marked by low-pitch tones (300 Hz) of the same volume and pace. The motor task was trained briefly outside the scanner room before every session. Two SFO runs were separated by 20 min of intermittent manual pressure stimulation and by subsequent 8-min rest. In effect, the SFO was tested before (condition H1 or A1) and after the stimulation (condition H2 or A2).

Table 1. Differences among study samples and stimulation protocols

	Study I (fMRI during stimulation)	Study II (fMRI of stimu- lation after-effects)	Study III (TMS)	Study IV (HRV)
Total No. enrolled / excluded	30 / 2	30 / 5	20 / 1	30 / 2
Women / men	16 / 12*	14 / 11*	9 / 10*	15 / 13*
Right-handed	25*	22*	18*	26
Mean age (SD) [years]	24.2 (1.92)	24.2 (1.92)	23.9 (1.82)	23.3 (1.44)
Head position	prone	prone	rotated to the left	rotated to the left
Eyes	closed	closed	open	no instruction
Instruction	rest	rest	rest, report pain	rest
Session onset	1:00–4:00 p.m.	1:00–4:00 p.m.	12:30–1:30 p.m.	11:00 a.m.
Stimulation timecourse	intermittent	intermittent	continuous	continuous
Pressure duration [min]	12	12	20	20
Force monitor	Yes	Yes	Yes	No
Real-time pain feedback	No	No	Yes	No
Discomfort/pain rating	<i>post-hoc</i> VAS	<i>post-hoc</i> VAS	<i>post-hoc</i> VAS	<i>post-hoc</i> VAS
Median interval between sessions (range) [days]	70 (7–294)	70 (7–294)	28 (14–91)	14.5 (7–61)

Abbreviations: fMRI – functional magnetic resonance imaging; HRV – heart rate variability; IQR – interquartile range; SD – standard deviation; TMS – transcranial magnetic stimulation; VAS – visual analogue scale.

*) Only included participants.

4. Data acquisition

4.1. Study I and II (fMRI)

Data acquisition parameters were kept as similar as possible in Studies I and II, therefore they are described together, with differences between protocols highlighted in the text below.

MRI data were acquired using 1.5-Tesla scanners (Siemens Avanto and Symphony, Erlangen Germany) with standard head coils. The scanning schedule was counter-balanced to account for any possible differences due to the scanner used. The subject's head was immobilised with cushions to assure maximum comfort and minimise head

motion. The MRI protocol included functional T_2^* -weighted BOLD images during task performance, acquired with GE EPI sequence (30 axial slices parallel to the anterior commissure-posterior commissure line, 5 mm thick, TR/TE 2500/41 ms, flip angle $70^\circ/80^\circ$, field of view 220 mm, matrix 64×64) to provide $3.4 \times 3.4 \times 5.0$ mm resolution. GE phase and magnitude field map images were acquired to allow correction of the EPI distortions. Anatomical high-resolution three-dimensional MPRAGE scan was acquired to provide the anatomical reference. In-plane FLAIR images were used to screen for unsuspected brain lesions.

In Study I (fMRI during stimulation), each imaging session included 2 functional imaging acquisitions during 10 min of right foot stimulation as described above. In total, 240 images were acquired per each functional run.

In Study II (fMRI of stimulation-after effects), each imaging session included 2 functional imaging acquisitions during 6-min right hand SFO. In total, 144 images were acquired per each 6-min functional run.

4.2. Study III (TMS)

4.2.1. Motor evoked potentials (MEP)

MEPs were elicited using transcranial magnetic stimulator with a butterfly-shaped coil with outer diameter 97 mm and wing angle 150° (MagPro X100 including MagOption, MagVenture, Farum, Denmark). During the pTMS, participants were lying supine on a comfortable examination table and fully relaxed. The level of participants' attention was constantly monitored by the examiner and no subject fell asleep during the examination.

The pTMS was performed according to a previously published protocol (Bareš et al., 2007; Kaňovský et al., 2003). The coil was positioned with the handle oriented backwards and inclined to the sagittal plane at approximately 45° (Rosenkranz and Rothwell, 2003).

Surface electromyographic recordings were obtained from the fully relaxed FDI muscles in both hands using (Ag–AgCl) electrodes. The recorded signal was amplified, filtered using a bandpass filter in the range 2 Hz–10 kHz, digitised using the Keypoint software (Medtronic, Minneapolis, MN, USA), and exported using Cross Neuro Database software (Stefan Stålberg Software AB, Helsingborg, Sweden) for subsequent analysis.

First, the optimal stimulation site was established manually by moving the coil on the scalp around the expected hand area over the left/right motor cortex until a site consistently producing the largest MEPs in the target muscle at a slightly suprathreshold

stimulus intensity was detected. Throughout the session, the coil was fixated in a frame and the position on the scalp was marked with ink.

Next, we determined the motor threshold in the resting right/left FDI (Bareš et al., 2007). The motor threshold was defined as the minimum stimulus intensity that evoked an MEP between 300 and 450 μ V peak-to-peak size in at least three out of six consecutive trials. Threshold intensities were expressed as a percentage of maximum stimulator output.

4.2.2. Paired-pulse TMS protocol

Cortical excitability was evaluated using a paired conditioning-test stimulus paradigm with biphasic pulse shape (Kujirai et al., 1993) in the fully relaxed FDI. The subthreshold conditioning stimulus was delivered at 80% intensity of the motor threshold, whereas the test stimulus was set to 125%. The pairs of conditioning and test stimuli were applied with six different ISI pseudo-randomly mixed with single stimuli: 3, 5, 10, 15, and 20 ms. Single or paired pulses were applied every 3 s. In each session, 9 MEPs were recorded for each ISI and 9 MEPs were recorded using the test stimulus alone. In total, 63 MEPs were recorded for each side in each session.

The median MEP amplitude values were calculated from the single-trial peak-to-peak MEP amplitudes. The median conditioned MEP at a given ISI was expressed as a percentage of the size of the median single-trial MEP obtained in the same session (Bareš et al., 2007).

4.3. Study IV (HRV)

4.3.1. Spectral analysis of heart rate variability (SAHRV)

Cardiac autonomic control was studied on short-term electrocardiographic (ECG) recordings, evaluating so-called short-term heart rate variability (Task Force, 1996). We have used a modification evaluating the orthoclinostatic reaction in the supine-standing-supine test (Opavský, 2002; Opavský and Salinger, 1995; Salinger et al., 1998) to be able to register changes (shift) in cardiac autonomic control in situations with different orthostatic load. It was chosen due to the fact that vagal activity prevails in the supine body position, whereas in the standing position vagal influence on heart decreases and sympathetic activity increases. The acquired short-term ECG recordings were subjected to temporal and spectral analysis of HRV using the DiANS PF8 system (Dimea Group, Olomouc, Czechia). Spectral calculations were performed with fast Fourier transform using a partially modified algorithm of coarse-graining spectral analysis (CGSA; Yamamoto and Hughson, 1991), with suppression of noise components.

The duration of each of the three phases of the supine-standing-supine test depended on the heart rate of each investigated individual, about 5 min on average. The entire supine-standing-supine test thus lasted about 15 min (at a heart rate of 60 beats per minute). Details of the investigation and evaluation for SAHRV examination have been published elsewhere (Opavský, 2002).

The HRV analysis yielded the following parameters in the frequency domain related to cardiac autonomic control for short-time recordings: spectral power of the very low frequency band 0.02–0.05 Hz (VLF Power [ms^2]); spectral power of the low frequency band 0.05–0.15 Hz (LF Power [ms^2]); spectral power of the high frequency band 0.15–0.50 Hz (HF Power [ms^2]); ratio of spectral powers LF over HF (LF/HF ratio); relative representation of the VLF component in the entire frequency range (0.02–0.50 Hz), (Relative VLF [%]); relative representation of the LF component in the entire frequency range (Relative LF [%]); relative representation of the HF component in the entire frequency range (Relative HF [%]); total spectral power over the entire frequency range 0.02–0.50 Hz (Total Power [ms^2]). In the time domain: mean squared successive differences (MSSD) — indicator of HRV, and duration of the RR interval derived from ECG (RR interval [s]). See **Fig. 2** for graphical representation of the spectral analysis.

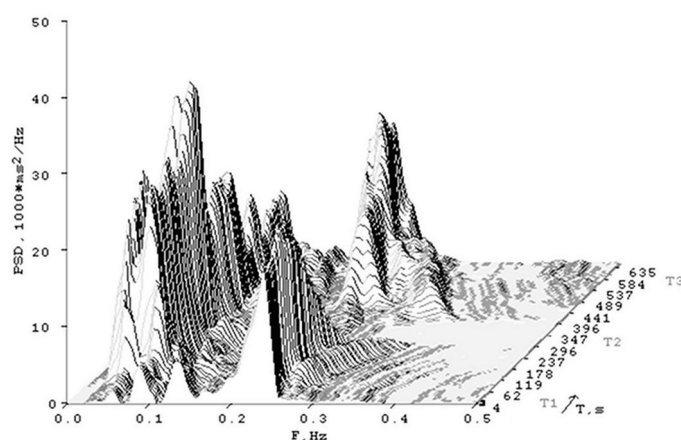


Figure 2. Spectral analysis of heart rate variability in a young healthy subject during the supine-standing-supine test. PSD — Power spectral density, F — frequency, T — time. T1 — first supine phase, T2 — standing phase, T3 — repeated supine phase. Frequency ranges: Low frequency (LF) — 0.05–0.15 Hz, high frequency (HF) 0.15–0.50 Hz. Note the clear decrease in the HF component in the standing position (T2), corresponding to decreased vagal activity, and its return to the previous level (or above that) in the repeated supine position (T3).

The whole supine-standing-supine test was performed twice within each examination: before and immediately after 20 min of peripheral pressure stimulation.

4.3.2. Respiratory rate assessment

Respiratory rate is another autonomic variable, which needs to be recorded and considered for an SAHRV study. Participants were breathing at their natural pace, respiration was recorded continuously with the DiANS PF8 system and simultaneously using adjustable chest belt with sensor. Respiration frequency was assessed in each of the three phases of the supine-standing supine test, together with SAHRV parameters in the same protocol.

5. Data analysis

5.1. Analysis of behavioural data

For all studies, the discomfort/pain scores for HS and AS were compared using Wilcoxon two-sample signed rank test, whereas mean pressure (where applicable) was compared using paired Student's *t*-test. Study-specific procedures are described below.

5.2. Study I (fMRI during stimulation)

5.2.1. Data pre-processing

The fMRI data were processed using FEAT Version 6.00, part of FSL (FMRIB's Software Library, www.fmrib.ox.ac.uk/fsl), version 5.0.9 (Jenkinson et al., 2012). The FEAT pre-processing pipeline included: correction of B_0 distortions using FUGUE (Jenkinson, 2003), motion correction using MCFLIRT (Jenkinson et al., 2002), non-brain removal using BET (Smith, 2002), and spatial smoothing using a Gaussian kernel with 8.0 mm full width at half maximum (FWHM). Functional data were registered to the individual's anatomical reference image, which was subsequently normalised non-linearly to the Montreal Neurological Institute (MNI) 152 standard space (Grabner et al., 2006). The fMRI data were then visually checked for susceptibility artefacts and two subjects were excluded due to an excessive signal loss in the brainstem. The final sample thus consisted of 28 subjects (16 women, 12 men, 25 right-handers).

Next, motion-related artefacts were removed from each time series using ICA-AROMA tool (Pruim et al., 2015b, 2015a), followed by high-pass temporal filtering with sigma 60.0 s. In a parallel preprocessing pipe-line, the ICA-AROMA noise components were removed from a dataset, which had no spatial smoothing applied. This dataset served for

extraction of nuisance signal from six sources in the supratentorial white matter and one source in the lateral ventricles. The masks were based on the MNI 152 Harvard-Oxford cortical atlas labels at 95 and 85% probabilistic threshold, respectively (Desikan et al., 2006). The white matter mask was split along the orthogonal planes into 6 areas roughly corresponding to the frontal ($Y \geq 0$ mm), parietal ($0 \text{ mm} > Y \geq -36$ mm, $Z \geq 18$ mm) and occipital white matter ($Y < -36$ mm), excluding the deep white matter around basal ganglia. From each source, the first eigenvariate was used to represent the non-neuronal signal.

5.2.2. Statistical analysis

The statistical analysis of the time-series was carried out in all remaining 28 subjects using FILM with local autocorrelation correction (Woolrich et al., 2001). The analysis of fMRI responses to sustained pressure stimulation had to address two physiological challenges: First, cortical response adapts rapidly within somatosensory areas, where it decreases exponentially over several seconds (Chung et al., 2015). Second, activation of the presumed generators of the gradually developing widespread tonic motor reflex response would be expected to follow the same slow timecourse supposedly resulting from temporal summation over tens of seconds (Bauer et al., 1988; Laufens et al., 1994; Vojta, 1973a; Vojta and Peters, 2007). Both phenomena preclude the use of common models convolving a rectangular stimulus function with the canonical HRF (Glover, 1999). Therefore, a more flexible modelling approach, such as a convolution with a set of finite impulse response (FIR) basis functions, was employed.

The GLM thus consisted of 9 delta functions (i.e., 9 temporally shifted unit spikes approximating Dirac delta function) that covered a 45-s time window (30 s on task and 15 s off task) aligned with the onset of each block with a 5-s (2 TR) steps to avoid noise over-fitting (Liu et al., 2017). To suppress residual physiological noise, the final model included also 6 nuisance signal regressors from the white matter and 1 from the ventricles.

The resulting beta parameters (in FSL terms, contrasts of parameter estimates or COPE) were carried over to a middle-level analysis in order to account for repeated measures in each subject. At this step, each time point (i.e., basis function) was still considered independent and analysed separately for each subject. Since only within-subject effects were modelled at this point, the middle-level analysis was carried out using the fixed effects mode in FEAT. To test the main hypotheses, three within-subject models were designed and evaluated in parallel pipelines: In the first one, the beta parameters from each session (involving either HS or AS) were averaged separately, resulting in Contrasts

I.1 (HS) and I.2 (AS). These contrasts represent the mean condition effects related either to HS or AS. In the second model, the functional series from both sessions were pooled together, providing Contrast I.3 (HS + AS). This contrast was necessary to obtain a mean activation map for HS and AS, which would provide common clusters for a *post-hoc* ROI analysis. Finally, the within-subject differences were assessed on a voxel-wise basis by subtracting the beta parameters from both sessions, yielding Contrast I.4 (HS – AS).

In the final third-level analysis, group-wise effects for all within-subject contrasts were evaluated. The group model consisted of one regressor for each basis function and an *F*-test collapsing all 9 basis functions to assess the overall effect over the entire stimulation block. In Contrast I.4 (HS – AS), additional linear covariates were included to account for the time difference between the two sessions and for individual differences in self-rated discomfort/pain intensity (condition HS – condition AS), with an additional *F*-test to evaluate the average discomfort/pain effect (Contrast I.5 [Pain]). The random effects analysis was performed using FLAME (FMRIB's Local Analysis of Mixed Effects) stage 1 (Woolrich et al., 2004). The whole-brain analysis was limited to the MNI standard brain mask (Grabner et al., 2006) minus a white-matter mask derived from the Harvard-Oxford probabilistic atlas (Desikan et al., 2006) using a conservative probability threshold of 95% as defined in the section "VIII.5.2.1. Data pre-processing". The masked *Z* (Gaussianised *t*) statistic images were thresholded using clusters determined by $Z > 5$ in case of Contrasts I.1 to I.3, or $Z > 3$ in case of Contrasts I.4 and I.5. The family-wise error (FWE) corrected cluster significance threshold was $p < 0.05$ (Worsley, 2001). Clusters in the thresholded maps were objectively labelled using the Harvard-Oxford Cortical and Subcortical Structural Atlases (Desikan et al., 2006), and the Probabilistic Cerebellar Atlas (Diedrichsen et al., 2011). Cytoarchitectonic labels were derived from the Jülich Histological Atlas (Eickhoff et al., 2007). The resulting statistical images were rendered in Mango v4.0 (Research Imaging Institute, UT Health Science Center at San Antonio, TX, United States, <http://ric.uthscsa.edu/mango/>).

5.2.3. *Post-hoc* ROI analysis: Mean condition effects

FIR model does not assume any specific shape of the haemodynamic response, which may differ slightly among different brain areas and even within one functional system (Glover, 1999; Lewis et al., 2018). Therefore, full comparison of two stimulation sites requires not only information where the differences are located, but also when they take place relative to the stimulation onset. Therefore, on top of the paired analysis of stimulus-related differences, a *post-hoc* analysis of the activations in the temporal domain (i.e., the shape of

HRF) is also needed.

The *post-hoc* ROI analysis was performed and visualised using custom scripts created in Matlab version R2017b and the Statistics Toolbox (MathWorks, Natick, MA, United States). Only clusters in Contrast I.3 (HS + AS) containing more than 5 voxels were considered.

First, average group-wise activations were investigated. Using the cluster mask from Contrast I.3 (HS + AS), group-wise beta parameters were extracted from the Contrasts I.1 (HS) and I.2 (AS) for each time point (i.e., basis function). The representative cluster-wise values were obtained using median of beta parameters in each cluster. Vectors of 9 consecutive median beta parameters in each cluster thus provided cluster-wise timecourses, each representing median response during a single stimulation block and the subsequent rest.

To assure that the extracted medians represented a homogeneous population of voxels, each median timecourse was correlated using Pearson's correlation coefficient with the first principal component (PC) obtained from the same cluster using singular value decomposition (Wall et al., 2003, pp. 91–109). In case of low correlation between the median of the whole cluster and the first PC ($r < 0.7$), the median was extracted only from a subset of voxels highly correlated with the first PC in both HS and AS ($r > 0.75$).

The resulting representative cluster-wise timecourses (i.e., vectors of the median beta parameters) were then correlated with each other using Pearson's correlation coefficient, providing one correlation matrix for HS and one for AS. Next, hierarchical clustering was applied to both correlation matrices in order to distinguish "subsystems" (sets of clusters) with similar haemodynamic responses. Agglomerative clustering trees were built using unweighted average distance algorithm and Euclidean distance as a dissimilarity measure (Rencher and Christensen, 2012). The optimal number of resulting subsystems was indicated using Caliński-Harabasz criterion (Caliński and Harabasz, 1974).

For visual comparison, the correlation matrix for AS was reordered according to the correlation matrix for HS. Finally, the original HRF in each cluster was reconstructed by multiplying the convolution matrix and the group-wise beta weights of each FIR regressor.

5.2.4. *Post-hoc* ROI analysis: Within-subject differences

Further *post-hoc* analysis was performed to determine the timing and directionality of differences detected in Contrast I.4 (HS – AS). This was done by extracting the median within-subject beta parameters from Contrasts I.1 (HS) and I.2 (AS) within the boundaries of the clusters from Contrast I.4 (HS – AS). To identify time points of significant

differences, corresponding beta parameters for HS and AS were compared using paired Wilcoxon signed-rank test at $p < 0.05$ (*post-hoc* confirmatory analysis without additional correction). Finally, the differences in activation levels in clusters from Contrast I.5 (Pain) were correlated with discomfort/pain rating difference using Spearman's correlation coefficient and marked significant at $p < 0.05$.

5.3. Study II (fMRI of stimulation after-effects)

5.3.1. Data pre-processing

Due to a considerable overlap of the acquisition parameters in Studies I and II, some pre-processing steps and settings could also remain identical. However, due to several significant differences and for clarity, a shortened description of the methods is still provided here.

The fMRI data were processed using FEAT Version 6.00 (Jenkinson et al., 2012). Standard pre-processing was applied (see Study I for more details), including high-pass temporal filtering with sigma 45.0 s. Time series statistical analysis included a temporal derivative of the main effect to account for slice timing shift and functional data were registered non-linearly to the MNI 152 standard space (Grabner et al., 2006). The fMRI data were then visually checked for susceptibility artefacts and two subjects were excluded due to an excessive signal loss in the brainstem. Three subjects were excluded due to a maximum frame-wise head displacement exceeding 3 mm in a single run as estimated during motion correction. The final sample thus consisted of 25 subjects (14 women, 22 right-handers).

For an additional analysis, motion-related artefacts were removed from each time series using ICA-AROMA tool and nuisance signal regressors of mean signal from cerebral ventricles and white matter were added to the model (Pruim et al., 2015b, 2015a). The following steps were performed for both original, and de-noised time series.

5.3.2. Statistical analysis

The group-level general linear model consisted of four conditions: SFO before and after the HS (conditions H1 and H2, respectively), and SFO before and after the AS (A1 and A2, respectively). Additionally, two subset conditions H1* and A1* were defined, including only datasets acquired at the first session. Using these conditions, five group *post-hoc* contrasts were constructed, including (II.1) a pooled group-wise activation image (H1 + H2 + A1 + A2), (II.2) differences between the baseline conditions at the first session (H1* vs. A1*), and (II.3) differences between the task repetitions regardless of stimulation type (H1 + A1 v. H2 + A2). The main research questions were assessed using (II.4) a two-

by-two interaction between the condition and the task repetition (H2 – H1 vs. A2 – A1). An additional linear covariate modelled individual differences in self-rated pain intensity (condition HS – condition AS), yielding statistical maps of (II.5) pain intensity effect on the interaction. All within-subject contrasts were first computed using a fixed effects analysis and the resulting parameter estimates (beta values) and variance were then carried over to the third-level analysis. The primary outcome measure was significant *F*-test in Contrasts II.4 and II.5, followed by *post-hoc* voxel-wise and cluster-wise analyses to assess directionality of the significant *F*-tests.

The random effects analysis was conducted using FLAME stage 1 (Woolrich et al., 2004). The whole-brain analysis was constrained to the MNI standard brain mask (Grabner et al., 2006) excluding white matter voxels according to the Harvard–Oxford probabilistic atlas (Desikan et al., 2006) using a conservative probability threshold of 95%. The masked *Z*(Gaussianised *t*) statistic images were thresholded using clusters determined by $Z > 2.3$ and a corrected cluster significance threshold of $p < 0.05$ (Worsley, 2001). The *post-hoc t*-tests in Contrast II.4 were carried out within the significant *F*-test clusters and thresholded voxel-wise at corrected significance level $p < 0.05$. The thresholded maps were objectively labelled based on Harvard–Oxford Cortical and Subcortical Structural Atlases (Desikan et al., 2006), and Probabilistic Cerebellar Atlas (Diedrichsen et al., 2011). Cytoarchitectonic labels were provided by Jülich Histological Atlas (Eickhoff et al., 2007).

A confirmatory third-level analysis was carried out for Contrast II.4 using non-parametric Conditional Monte Carlo permutation testing implemented in Randomise v2.9 (Winkler et al., 2014). An identical design with the pain intensity covariate was employed. Ten thousand permutations were performed using sign-flipping to estimate the null distribution of the maximum cluster mass under the cluster forming threshold of $t > 3.0$.

A *post-hoc* ROI analysis was performed to investigate the contribution of each condition to the overall interaction in Contrasts II.4 and II.5 and to assess the correlation with the self-reported pain intensity. First, significant voxels in each cluster were identified using a *post-hoc* voxel-wise *t*-test carried out within the *F*-test mask and the resulting mask was transformed back to the individual subject space. Next, average (mean) *Z* scores and %SC values across the ROI were extracted from each individual single-subject statistical map in the specified mask using the Featquery tool, part of FSL. The obtained values were plotted and compared group-wise using paired Wilcoxon signed-rank test and correlated with the pain intensity covariate using Spearman’s correlation coefficient.

5.4. Study III (TMS)

Ratios of normalised MEP responses (After/Before) were calculated to evaluate the effect of both interventions (Rosenkranz and Rothwell, 2006a). Differences between HS and AS were evaluated for SICI (ISI 3 ms) and ICF (ISI 15 ms) using linear regression analysis with difference between mean force for HS and AS as an independent variable.

5.5. Study IV (HRV)

As data from the “supine 1” phase may be influenced by interfering factors both somatic and psychological (e.g., pre-examination stress, new experimental situation, white-coat syndrome, etc.), heart rate, SAHRV and respiration rate obtained during the third phase of the test, “supine 2” (supine position following orthostatic load in the prior standing), were used for statistical analysis (see also Opavský, 2002; Opavský and Salinger, 1995; Salinger et al., 1998).

The acquired data were processed with the software Statistica 12 (StatSoft, Tulsa, OK, USA). For within-subject effects, the non-parametric paired Wilcoxon signed-rank test was used, whereas between-session effects for the respiratory rate and the degree of stimulation-related discomfort were tested with the Mann-Whitney *U* test.

IX. RESULTS

1. Study I and II (fMRI): Behavioural data

In all subjects, the therapist observed discrete irregular focal muscle contractions in the stimulated extremity during stimulation, but no gross limb or trunk movements.

For technical reasons, continuous pressure recordings were only obtained in 15 subjects. The mean force applied at the sensor during HS was 22.33 N (SD 11.64 N) and 26.45 N (SD 9.72 N) during AS. The difference was not significant ($p = 0.32$, two-sample t -test). A paired t -test was possible in 11 subjects with a non-significant difference ($p = 0.22$, mean difference HS – AS = -3.94 N, SD 9.96 N).

After HS, the median reported discomfort/pain intensity (VAS) was 1.85 (range 0–6.9), while it was 0.90 after AS (range 0–5.5). HS was thus associated with significantly higher discomfort/pain intensity than AS ($p < 0.01$, Wilcoxon signed-rank test), with median difference 1.25 (range -5.0 – 6.4). The difference in discomfort/pain rating has been therefore included as a covariate in the Study I (fMRI during stimulation) in Contrast I.4 (HS – AS). Likewise, Contrast II.4 (H2 – H1 vs. A2 – A1) in Study II (fMRI of stimulation after-effects) was evaluated with and without the discomfort/pain rating as a covariate.

2. Study I (fMRI during stimulation): Imaging results

The study results were published as an original paper: **Hok, P., Opavský, J., Labounek, R., Kutín, M., Šlachťová, M., Tüdös, Z., Kaňovský, P., Hlušík, P., 2019. Differential Effects of Sustained Manual Pressure Stimulation According to Site of Action. Front. Neurosci. 13, 722. <https://doi.org/10.3389/fnins.2019.00722> WoS 2018: IF 3.648, Rank: 92/267**

2.1. Heel and Ankle: Mean activation maps and their conjunction

Group Contrasts I.1 (HS) and I.2 (AS) yielded separate Z statistical maps depicting areas with significant response either to HS or to AS (**Fig. 3**). The areas involved in the somatosensory processing of the pressure stimulation of each site overlapped partially (spatial correlation between thresholded Z statistical maps for HS and AS was 0.56 using Pearson correlation coefficient). The overlapping areas (binary conjunction, see yellow overlay in **Fig. 3**, row C) included mainly the left dorsomedial primary somatosensory and motor cortex (S1 and M1, respectively) in the somatotopic representation of the stimulated lower limb and the bilateral parietal operculum cortices (S2). Less extensive overlap was observed in the more posterior right postcentral gyrus and SPL, i.e., ipsilateral to the

stimulated limb. Both stimulation sites were also associated with signal changes in bilateral dorsolateral sensorimotor cortex (primary SMC, i.e., S1 and M1) in the somatotopic representation of the upper limb and face (Long et al., 2014). These were later identified as transient deactivations, see below. Further similarities between the responses to stimulation at either site were found in the left prefrontal and bilateral parietooccipital cortices, bilateral lingual gyri and thalami, but the involved areas mostly did not overlap. Several qualitative differences were observed: AS was associated with more involvement of temporal and prefrontal areas in the left hemisphere, whereas HS elicited responses in the left insular and bilateral frontal operculum cortices and the brainstem in the contralateral (left) pons.

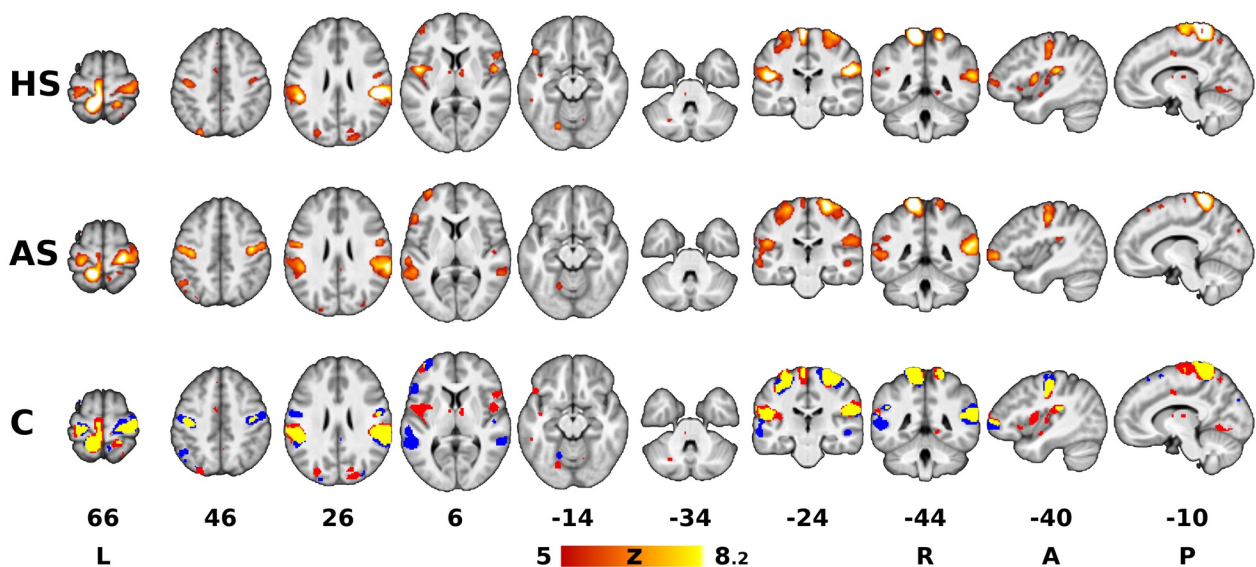


Figure 3. Areas associated with sustained pressure stimulation. The red-yellow Z statistical overlays in the top and middle rows represent significant F -tests of mean response to heel stimulation (**HS**, Contrast I.1) and ankle stimulation (**AS**, Contrast I.2). The bottom row shows the binary conjunction (**C**) of HS and AS (red = heel, blue = ankle, yellow = conjunction of both). The images were superimposed on top of a grey-scale mean T_1 -weighted background image. Clusters of activation were determined by $Z > 5$ and thresholded at corrected $p < 0.05$. The slices are numbered according to coordinates in the Montreal Neurological Institute (MNI) 152 standard space template. The right is right, according to neurological convention.

The analysis of pooled data (Contrast I.3 [HS + AS], sum of all colour overlays in Fig. 4A) yielded significant effects in all areas associated with either HS or AS alone. Therefore, a complete list of clusters with anatomical labels is only provided for Contrast I.3 (HS + AS; see Table 2).

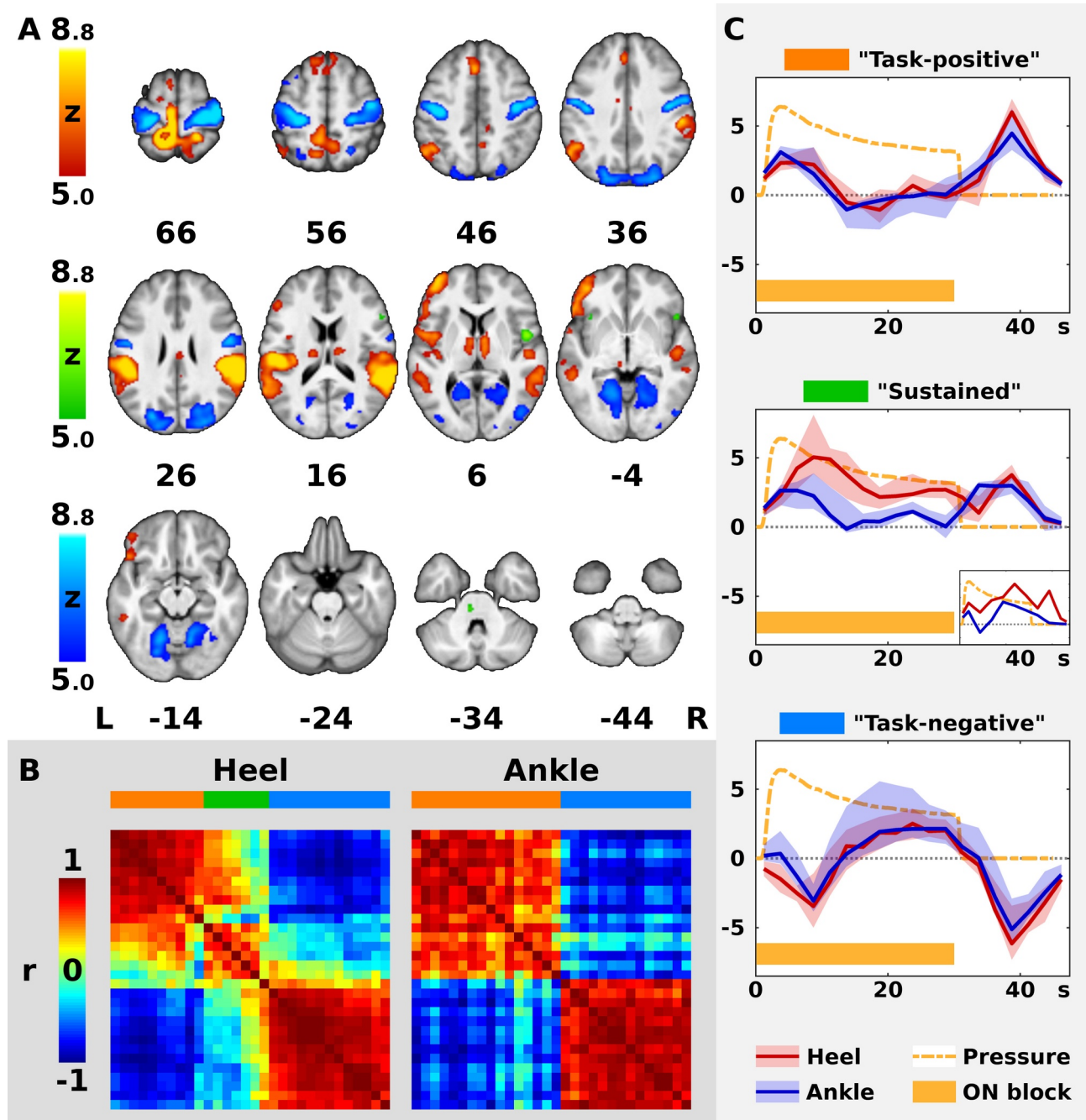


Figure 4. Timecourses of BOLD signal in the significant clusters. In panel (A), the colour Z statistical overlays represent together significant F -test of mean pooled response to both heel (HS) and ankle stimulation (AS). Significant clusters were separated into three colour-coded groups (red, green, and blue)

according to the shape of haemodynamic response function (HRF), as explained in panels (B,C). For remaining conventions in panel (A), see Fig. 3. In panel (B), the left matrix (Heel) represents cross-correlations of haemodynamic responses in 30 largest clusters from panel (A) as measured during HS, whereas the right matrix (Ankle) represents cross-correlations observed during AS. Both matrices are identically ordered according to the minimal Euclidean distance between neighbouring clusters in Heel condition (see section “VIII.5.2.3. Post-hoc ROI analysis: Mean condition effects”). Note the two well-formed anti-correlated subsystems in Ankle condition (right matrix), encoded in red and blue on the horizontal bar above the matrix. In Heel condition, another subsystem emerges in addition to the previous two. The three networks are encoded in red, green and blue. In panel (C), the plots display median (solid dark line) and inter-quartile range (semi-transparent fill) of HRF across all clusters in each network from panels (A,B) (from top to bottom: red, green, and blue). In the middle plot, a smaller plot represents a single cluster with a distinct timecourse during AS. Abscissa represents time since the block onset in s, whereas ordinate represents fitted blood oxygenation level-dependent response in arbitrary units. Dashed orange line shows the average applied pressure function (scaled to fit the plot), whereas the orange bar below indicates the duration of the stimulation block (ON).

2.2. Characterising temporal dynamics: *Post-hoc* ROI analysis

The ROI analysis of the clusters obtained from Contrast I.3 (HS + AS) was limited to the 30 biggest clusters with more than 5 voxels (see Table 2 for a complete list). The median group-wise beta parameters were highly correlated with the first principal component in all but one cluster, namely, Cluster 1. In this cluster, the first PC was dominant for both stimulation sites ($r > 0.75$) in 2,798 voxels (47.5% of the original cluster size), which were used to extract the representative response timecourse. The remaining voxels were not considered.

Table 2. Significant *F*-test clusters in Contrast I.3 (HS + AS): Overall stimulation effect

Cluster Response (HS/AS)	Anatomical atlas labels ^a	Cytoarchitectonic atlas labels ^a	Volume [cm ³]	Cluster <i>p</i>	<i>Z</i> _{max}	<i>Z</i> _{max} MNI coordinates (x,y,z [mm])
1 P/P	15.5% L Frontal Pole 11.4% L Parietal Operculum C 10.8% L Angular G 9.0% L Supramarginal G, p. d. 7.5% L Central Opercular C 5.9% L Inferior Frontal G, pars triangularis 5.8% L Supramarginal G, a. d.	14.6% L Broca's Area BA45 10.1% L Inferior Parietal Lobule PF 9.6% L Secondary Somatosensory C / Parietal Operculum OP1 8.8% L Inferior Parietal Lobule PFm 8.6% L Inferior Parietal Lobule PGa 6.3% L Inferior Parietal Lobule PFcm	47.10	<0.001	8.21	-50, 24, -10
2 N/N	23.2% R Lateral Occipital C, s. d. 21.2% R Lingual G 16.8% L Lateral Occipital C, s. d. 7.3% R Occipital Pole 5.9% R Cuneal C 5.5% L Cuneal C	19.9% R Visual C V2 BA18 6.9% R Visual C V1 BA17 6.1% L Superior Parietal Lobule 7A 6.1% L Visual C V2 BA18	39.51	<0.001	8.04	-16, -88, 32
3 P/P	20.8% L Postcentral G 16.6% L Superior Frontal G 14.8% L Precentral G 9.3% R Precuneus C 9.2% L Precuneus C 7.2% L Superior Parietal Lobule 5.7% R Superior Parietal Lobule	21.3% L Premotor C BA6 14.7% L Primary Motor C BA4a 11.2% L Superior Parietal Lobule 5L 10.1% R Superior Parietal Lobule 5L 9.0% L Superior Parietal Lobule 7A 6.1% L Superior Parietal Lobule 5M	33.38	<0.001	8.79	-14, -40, 70
4 P/P	20.9% R Supramarginal G, p. d. 16.3% R Parietal Operculum C 13.2% R Angular G 12.7% R Supramarginal G, a. d. 10.1% R Superior Temporal G, p. d. 9.4% R Middle Temporal G, temporooccipital part 7.9% R Planum Temporale	22.4% R Inferior Parietal Lobule PF 17.6% R Inferior Parietal Lobule PGa 13.2% R Secondary Somatosensory C / Parietal Operculum OP1 12.0% R Inferior Parietal Lobule PFm 10.8% R Inferior Parietal Lobule PFcm	28.24	<0.001	8.21	56, -50, 10
5 N/N	63.7% R Precentral G 36.0% R Postcentral G	34.3% R Premotor C BA6 14.3% R Primary Somatosensory C BA3b 12.7% R Primary Motor C BA4a 11.2% R Primary Somatosensory C BA1 8.9% R Primary Motor C BA4p 5.3% R Primary Somatosensory C BA3a	25.13	<0.001	8.21	42, -14, 36
6 N/N	54.8% L Precentral G 45.2% L Postcentral G	24.3% L Premotor C BA6 17.7% L Primary Somatosensory C BA1 14.3% L Primary Somatosensory C BA3b 12.8% L Primary Motor C BA4p 10.9% L Primary Motor C BA4a 7.9% L Primary Somatosensory C BA3a	19.50	<0.001	8.21	-50, -8, 34

Cluster Response (HS/AS)	Anatomical atlas labels ^a	Cytoarchitectonic atlas labels ^a	Volume [cm ³]	Cluster <i>p</i>	<i>Z</i> _{max}	<i>Z</i> _{max} MNI coordinates (x,y,z [mm])
7 N/N	62.0% L Lingual G 13.7% L Cerebellum V 11.0% L Precuneous C 10.4% L Occipital Fusiform G 9.7% L Cerebellum VI 5.4% L Temporal Occipital Fusiform C	26.2% L Visual C V2 BA18 20.9% L Visual C V4 11.1% L Visual C V1 BA17 9.5% L Visual C V3V	14.12	<0.001	8.04	-16, -58, -10
8 P/P	50.9% R Thalamus 43.8% L Thalamus	N/A	5.06	<0.001	7.84	8, -16, 12
9 N/N	95.1% R Lateral Occipital C, i. d.	54.7% R Visual C V5 14.2% R Visual C V4 12.8% R Inferior Parietal Lobule PGp	2.75	<0.001	6.72	44, -78, 6
10 P/P	54.2% R Cingulate G, p. d. 24.3% L Cingulate G, p. d. 15.0% R Cingulate G, a. d. 6.5% L Cingulate G, a. d.	N/A	0.86	<0.001	6.63	4, -16, 32
11 S/P	99.0% R Central Opercular C	75.0% R Secondary Somatosensory C / Parietal Operculum OP4 13.5% R Secondary Somatosensory C / Parietal Operculum OP3 7.3% R Broca's Area BA44	0.77	<0.001	7.17	50, 2, 6
12 S/P	33.3% R Frontal Orbital C 28.3% R Temporal Pole 21.7% R Inferior Frontal G, pars triangularis 11.7% R Frontal Operculum C	43.3% R Broca's Area BA45 33.3% R Primary Auditory C TE1.2	0.48	<0.001	7.00	50, 18, -8
13 N/N	89.7% L Lateral Occipital C, s. d. 10.3% L Superior Parietal Lobule	100.0% L Superior Parietal Lobule 7A	0.46	<0.001	5.73	-28, -64, 58
14 N/N	79.1% R Occipital Pole 20.9% R Lateral Occipital C, i. d.	86.0% R Visual C V3V 9.3% R Visual C V4	0.34	<0.001	5.70	32, -92, 0
15 N/N	81.4% L Middle Frontal G 18.6% L Superior Frontal G	32.6% L Premotor C BA6	0.34	<0.001	7.02	-30, 16, 60
16 P/P	79.5% L Cingulate G, a. d. 20.5% L SMA	64.1% L Premotor C BA6	0.31	<0.001	6.15	-10, -4, 40
17 P/P	54.8% R Cingulate G, p. d. 25.8% R Precuneous C 19.4% R Precentral G	96.8% R Superior Parietal Lobule 5Ci	0.25	<0.001	5.70	12, -30, 42
18 N/N	100.0% R Hippocampus 20.0% R Parahippocampal G, a. d.	80.0% R Hippocampus Cornu Ammonis 20.0% R Hippocampus Subiculum	0.24	<0.001	5.83	26, -16, -16

Cluster Response (HS/AS)	Anatomical atlas labels ^a	Cytoarchitectonic atlas labels ^a	Volume [cm ³]	Cluster <i>p</i>	<i>Z</i> _{max}	<i>Z</i> _{max} MNI coordinates (x,y,z [mm])
19 S/P	48.3% R Frontal Orbital C 41.4% R Insular C 10.3% R Frontal Operculum C	N/A	0.23	<0.001	5.42	32, 26, 0
20 P/P	92.6% Brain-Stem 7.4% L Thalamus	N/A	0.22	<0.001	6.04	-8, -28, -6
21 S/N	87.0% L Paracingulate G 13.0% R Paracingulate G	N/A	0.18	<0.001	5.72	-6, 44, 22
22 S/P	100.0% Brain-Stem	N/A	0.18	<0.001	5.93	-8, -30, -34
23 N/N	100.0% R Lingual G	85.7% R Visual C V2 BA18 14.3% R Visual C V1 BA17	0.17	<0.001	5.31	8, -82, -10
24 N/N	100.0% L Frontal Pole	N/A	0.16	<0.001	5.69	-18, 54, 30
25 N/N	100.0% L Frontal Pole	N/A	0.14	0.001	5.67	-18, 62, 22
26 S/P	100.0% R Inferior Frontal G, pars opercularis	64.7% R Broca's Area BA45 35.3% R Broca's Area BA44	0.14	0.001	5.47	54, 20, 16
27 N/N	100.0% L Middle Frontal G	18.8% L Premotor C BA6	0.13	0.001	5.45	-42, 12, 54
28 P/P	100.0% R Cingulate G, p. d.	N/A	0.12	0.001	5.63	6, -40, 24
29 P/P	100.0% R Cerebellum VIIIb 7.1% Brain-Stem	N/A	0.11	0.001	6.17	18, -46, -54
30 S/P	100.0% L Insular C	25.0% L Broca's area BA44	0.06	0.002	5.37	-36, 22, -2

Abbreviations: a. d. — anterior division; AS — ankle stimulation; C — cortex; BA — Brodmann area; G — gyrus; HS — heel stimulation; i. d. — inferior division; L — left; N — task-negative; N/A — not available; MNI — Montréal Neurological Institute; P — task-positive; p. d. — posterior division; R — right; S — sustained task-positive; s. d. — superior division; SMA — supplementary motor area (also juxtapositional lobule cortex); *Z*_{max} — maximum *Z* score.

^a) Anatomical and cytoarchitectonic labels are provided including the proportion of labelled voxels. Only labels consisting at least 5% of activated voxels are provided. Note that cerebellar labels may overlap with cortical labels and that cytoarchitectonic labels do not cover the whole brain.

In the 30 evaluated clusters, the modelled BOLD responses could be mostly separated into two distinct subsystems with anti-correlated timecourses (**Fig. 4B**). This was especially apparent in AS. Therefore, all clusters in AS condition and most clusters in HS condition were labelled either as “task-positive” or “task-negative” based on the sign of the immediate BOLD signal change. According to the timecourse plots, the median activation in the task-positive subsystem (“Task-positive” plot in **Fig. 4C**) increased immediately after the stimulation onset and peaked at 3.75 s, namely, at the centre of the second volume after onset. It decreased back to baseline as early as 10 s after onset. Following the stimulation offset, activation transiently increased again and remained positive 0 to 17.5 s after offset, peaking at 8.75 s. As opposed to the task-positive areas, the responses in the second subsystem (“Task-negative” plot in **Fig. 4C**) involved deactivations at the onset and at the offset of the stimulation. The median response remained negative 5 to 12.5 s after onset and 5 to 17.5 s after offset. Please note that the real time resolution of the plots is roughly 5 s, which is the approximate width of a single regressor spanning 2 TR.

Whereas there were only two subsystems with homogeneous responses in AS, a third type of response could be distinguished in HS (see dendrograms in **Fig. 5**). The 23 clusters with consistent task-positive or task-negative responses, which were similar in both conditions are represented by red and blue overlay, respectively, in **Fig. 4A**. The responses in the remaining 7 clusters in HS condition followed a distinct timecourse that deviated from the common task-positive or task-negative pattern (compare the matrices in **Fig. 4B**; see also **Fig. 5**, dendrogram “Heel”). Six out of these clusters were task-positive in AS and one was task-negative in AS, including the right frontal and central opercular cortex, inferior frontal gyrus, frontal orbital cortex, bilateral anterior insular cortex, left paracingulate gyrus and the left pons (see green overlay in **Fig. 4A**). In these clusters, the initial response in HS condition remained positive for the duration of the stimulation block (peak at 8.75 s after onset) instead of dropping immediately to baseline. After the offset, the second positive response could be observed at 8.75 s after offset. Therefore, the subsystem was labelled as “sustained task-positive” (compare the red solid line representing HS to the blue line representing AS in “Sustained” plot in **Fig. 4C**).

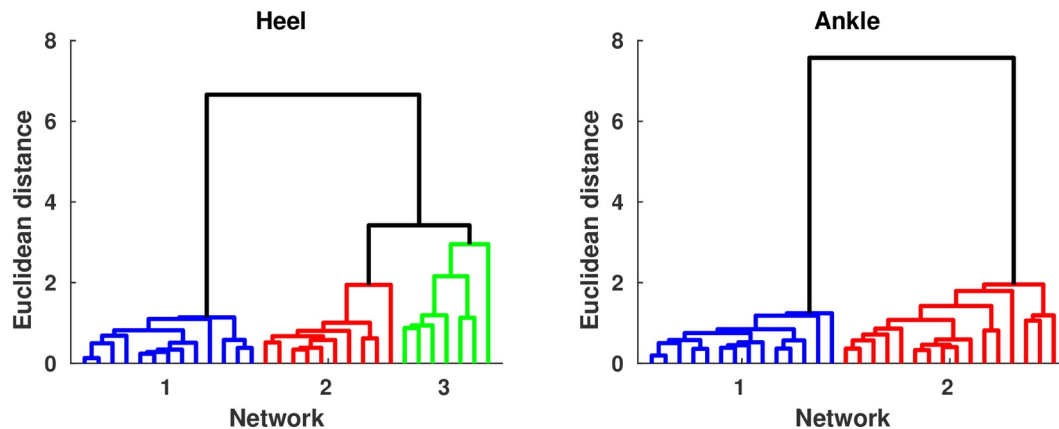


Figure 5. Hierarchical clustering of group-wise BOLD signal responses. Dendrograms illustrate agglomerative hierarchical clustering of correlation coefficients of BOLD signal responses in significant clusters obtained from Contrast I.3 (AS + HS, i.e., mean pooled response to both heel and ankle stimulation). On the left, clusters are grouped according to distance of correlation coefficients in Heel condition, whereas on the right, responses were clustered in Ankle condition. Abscissa represents the Euclidean distance between clusters, whereas ordinate represents correlation coefficient vectors, one per a significant cluster in Contrast I.3. Colours distinguish clusters as indicated by Caliński-Harabasz criterion (Caliński and Harabasz, 1974).

2.3. Heel versus Ankle: Within-subject differences between conditions

Contrast I.4 (HS – AS) yielded a map of average within-subject differences between HS and AS (**Fig. 6A**), as well as the interaction with the self-reported discomfort/pain intensity (**Fig. 6B**). The differences between HS and AS were observed in the IPL (area PGp; Cluster 1 in **Fig. 6A**) and in the left M1 and PMC in the somatotopic representation of the lower limb (BA 4a and 6; Cluster 2 in **Fig. 6A**). The discomfort/pain effect (Contrast I.5 [Pain]) was observed in the left SPL (BA 7A and 5L; Cluster 1 in **Fig. 6B**) posterior to the Cluster 2 in Contrast I.4 (HS – AS). A complete list of clusters with their anatomical labels is provided in **Table 3**.

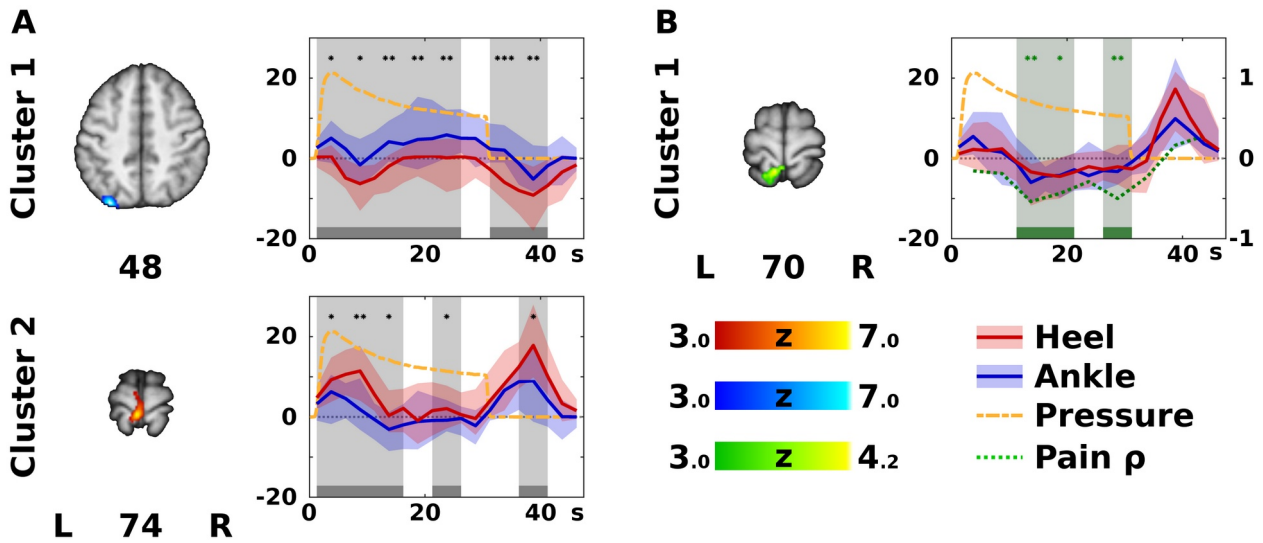


Figure 6. Significant differences according to stimulation site. In panel (A), the colour Z statistical overlays represent significant F -test of within-subject differences between the heel (HS) and ankle stimulation (AS), i.e., Contrast I.4 (HS – AS). The two clusters (labelled anatomically in **Table 3**) are coded either in red, if HS yielded higher activation than AS, or in blue, if the opposite was the case. The plots on the right side of each slice display median (solid dark line) and inter-quartile range (semi-transparent fill) of the modelled haemodynamic response function in the specified cluster across all subjects (HS in red, and AS in blue). Grey bars and background indicate epochs (each epoch represents one finite impulse response basis function) that significantly differed between HS and AS (Wilcoxon signed-rank test). Differences were significant at uncorrected $*p < 0.05$, $**p < 0.01$, or $***p < 0.001$ (post-hoc confirmatory analysis). For remaining conventions see **Fig. 4**. In panel (B), a cluster showing significant correlation between pain difference HS – AS and activation difference (HS – AS) is displayed in green (see Contrast I.5 [Pain] in the “VIII.5.2.2. Statistical analysis”). In the corresponding timecourse plot, green bars and background indicate significant correlation according to Spearman’s correlation coefficient (ρ), which is plotted as a green dotted line (the ordinate range is marked on the right). Note that correlations were significant in different areas and epochs than the significant differences between activation levels in HS and AS. For remaining conventions see panel (A).

Table 3. Significant clusters in Contrasts I.4 and I.5: Differences between stimulation sites and pain effect

Contrast	Cluster index	Anatomical atlas labels ^a	Cytoarchitectonic atlas labels ^a	Volume [cm ³]	Cluster <i>p</i>	Z_{\max}	Z_{\max} MNI coordinates (x,y,z [mm])
Contrast I.4: HS – AS	1	100.0% L Lateral Occipital C, s. d.	81.5% L Inferior Parietal Lobule PGp 7.1% L Inferior Parietal Lobule PGa 5.1% L Superior Parietal Lobule 7A	2.81	0.003	7.00	-30, -80, 48
	2	48.5% L Postcentral G 36.5% L Precentral G 8.8% R Precentral G 6.2% R Postcentral G	65.0% L Primary Motor C BA4a 18.1% L Premotor C BA6 8.5% R Primary Motor C BA4a	2.08	0.014	6.74	-4, -36, 74
Contrast I.5: Pain effect	1	53.0% L Superior Parietal Lobule 29.8% L Postcentral G 12.1% L Lateral Occipital C, s. d. 5.1% L Precuneous Cortex	46.0% L Superior Parietal Lobule 5L 45.5% L Superior Parietal Lobule 7A	1.58	0.043	4.16	-8, -48, 70

Abbreviations: AS – ankle stimulation; C – cortex; BA – Brodmann area; G – gyrus; HS – heel stimulation; L – left; MNI – Montréal Neurological Institute; R – right; s. d. – superior division; Z_{\max} – maximum Z score.

^a) Anatomical and cytoarchitectonic labels are provided including the proportion of labelled voxels. Only labels consisting at least 5% of activated voxels are provided. Note that cerebellar labels may overlap with cortical labels and that cytoarchitectonic labels do not cover the whole brain.

The ROI analysis of clusters in Contrast I.4 (HS – AS; see **Table 3**) revealed that the modelled BOLD response in the left M1 and PMC (Cluster 2 in **Fig. 6A**) was significantly higher in HS condition. This was observed mostly during short activation increases after stimulation onset and offset. In contrast, activation levels in the left IPL (Cluster 1 in **Fig. 6A**) were higher in AS condition than in HS condition. The differences in the IPL were spread almost over the entire stimulation block and the subsequent rest. The ROI analysis of the cluster obtained from Contrast I.5 (Pain) showed that the discomfort/pain difference (HS – AS) was negatively correlated with the difference in activation levels (HS – AS). The significant correlations were detected during the sustained phase of the stimulation (**Fig. 6B**).

3. Study II (fMRI of stimulation after-effects): Imaging results

The study results were published as an original paper: Hok, P., Opavský, J., Kutín, M., Tüdös, Z., Kaňovský, P., Hlušík, P., 2017. *Modulation of the sensorimotor system by sustained manual pressure stimulation*. *Neuroscience* 348, 11–22. <https://doi.org/10.1016/j.neuroscience.2017.02.005> WoS 2017: IF 3.382, Rank: 105/261

3.1. Mean fMRI activation during sequential finger opposition (SFO)

As illustrated in Fig. 7, the analysis of mean activation pooled across all conditions (H1, H2, A1, and A2) yielded a single significant cluster representing predominantly contralateral (left) frontoparietal and subcortical sensorimotor areas, as well as predominantly contralateral midbrain and pons, and ipsilateral (right) cerebellar hemisphere and vermis.

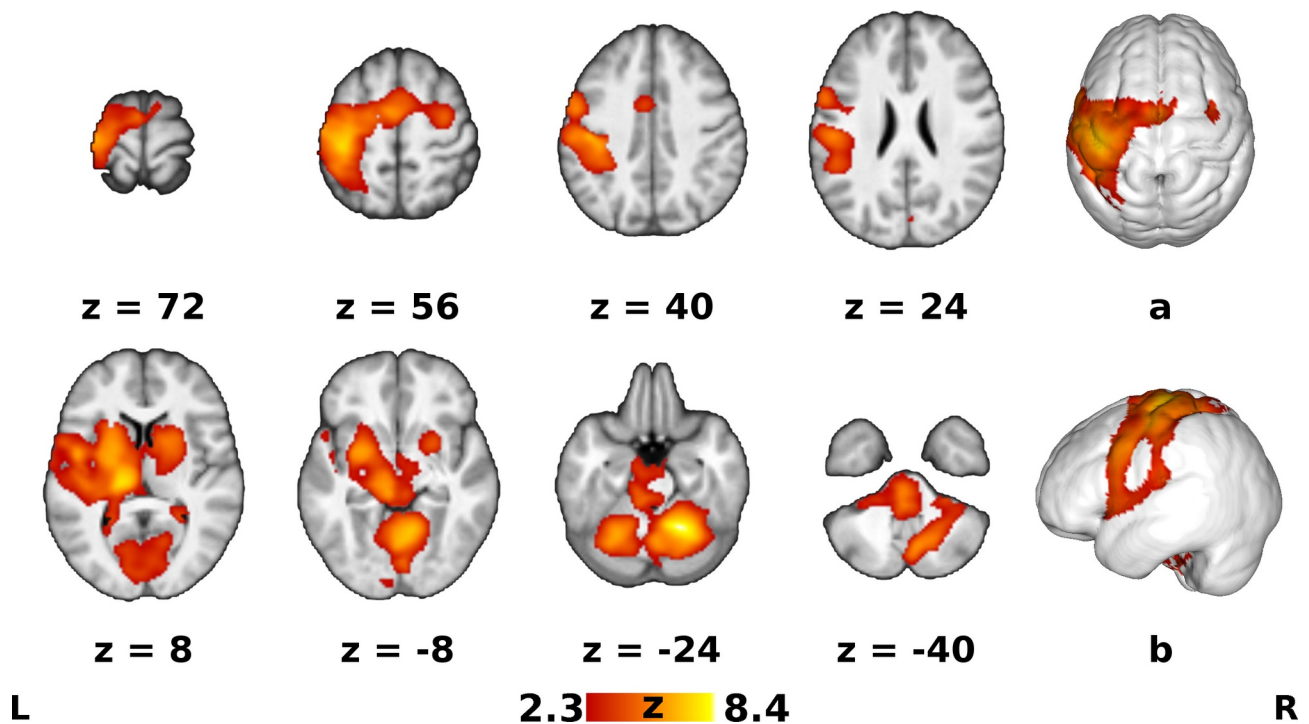


Figure 7. Mean activation during sequential finger opposition. The red-yellow Z statistical overlay represents mean activation during the right hand sequential finger opposition pooled across all runs and sessions. The image was superimposed on top of a grey-scale mean T_1 -weighted background image. Clusters of activation were determined by $Z > 2.3$ and thresholded at corrected $p < 0.05$. The axial slices are numbered over the z axis of the Montreal Neurological Institute (MNI) 152 standard space template. Panels (a) (top view) and (b) (left lateral view) show the statistical overlay on top of a three-dimensional reconstructed cortical surface. The right is right, according to neurological convention.

3.2. Differences between baseline conditions

The t -test comparing the condition H1* and condition A1* (i.e., the baseline at the first session) did not show any significant difference at the whole-brain level.

3.3. Repetition effects: Mean activation difference before and after the stimulation

The paired t -test before and after the stimulation averaged across both sessions showed that there was no significant mean activation increase after the stimulation. However, it revealed a decrease in activation in several areas, including the bilateral SMA and lateral PMC (lateral BA 6); SPL (mainly BA 7); S1 (mainly BA 2); intracalcarine (V1, V2) and ventral visual occipital cortex (V4); cerebellar hemispheres (mainly lobule VI) and vermis (blue in Fig. 8). Significant clusters are summarised in Table 4.

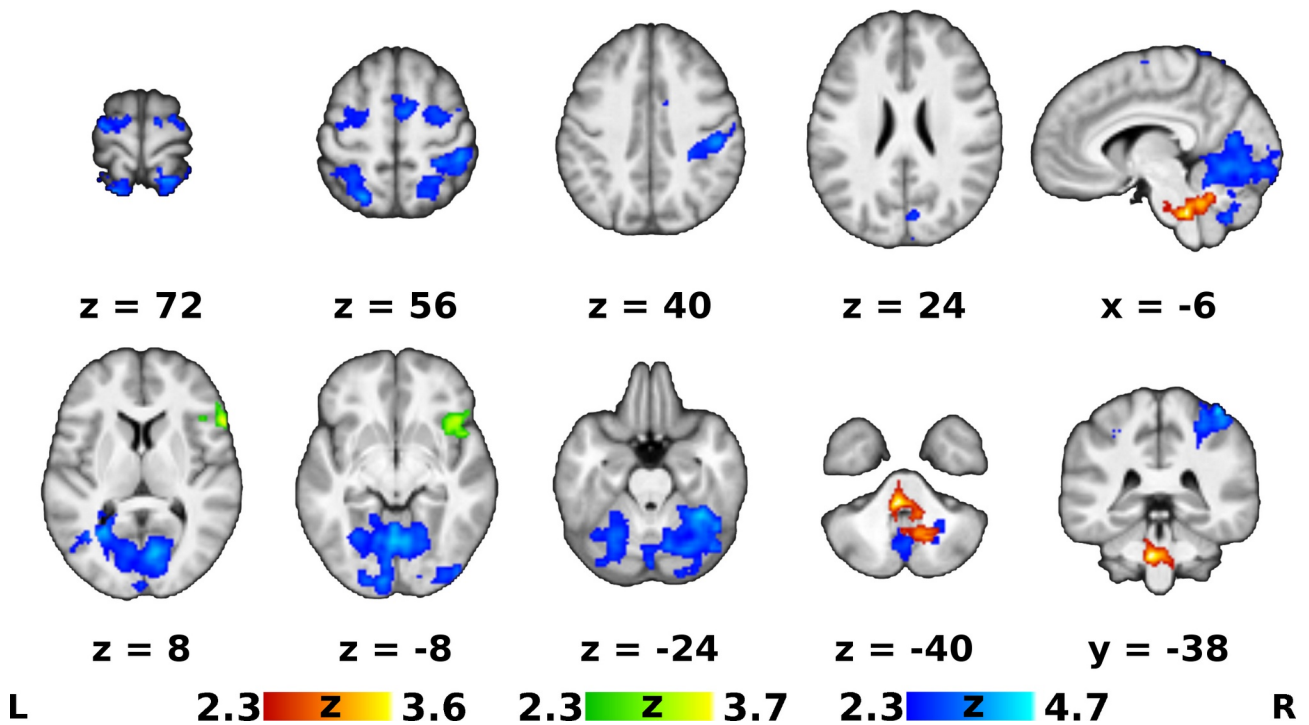


Figure 8. Mean activation decrease post-stimulation and interaction between condition and repetition. The blue Z statistical overlay represents a decrease in task-related activation after the stimulation common to both conditions, i.e., Contrast II.3: $(H1 + A1) - (H2 + A2)$. The red-yellow Z statistical overlay shows significant F -test of interaction between the condition and repetition (Contrast II.4: $H1 - H2$ v. $A1 - A2$) with the pain intensity covariate. The green Z statistical overlay shows the significant F -test of the pain covariate effect in the interaction (Contrast II.5). Remaining conventions, see Fig. 7.

Table 4. Significant clusters in Contrast II.3: Comparison before and after stimulation

Contrast	Anatomical atlas labels ^a	Cytoarchitectonic atlas labels ^a	Volume [cm ³]	Cluster <i>p</i>	<i>Z</i> _{max}	<i>Z</i> _{max} MNI coordinates (x,y,z [mm])
Contrast II.3: (H1 + A1) > (H2 + A2) <i>original data</i>	22.9% R cerebellar hemisphere (10.7% right VI)	8.0% L visual C V1 (BA17) 7.7% R visual C V1 (BA17)	98.9	<0.001	4.75	-26, -68, -18
	15.7% L cerebellar hemisphere (7.3% left VI)	7.4% L visual C V4 6.3% L visual C V2 (BA18)				
	14.3% L lingual G	5.6% R visual C V2 (BA18)				
	10.3% R lingual G					
	8.6% L occipital fusiform G 6.4% R occipital fusiform G 6.1% L intracalcarine C 6.0% R intracalcarine C 6.0% R temporooccipital fusiform C 5.0% cerebellar vermis					
	38.6% R superior parietal lobule 30.5% R postcentral G 16.3% R lateral occipital C 13.9% R supramarginal G	33.4% R superior parietal lobule (BA7) 25.9% R primary somatosensory C (BA2) 15.1% R inferior parietal lobule 8.3% R primary somatosensory C (BA1) 7.7% R superior parietal lobule (BA5)	17.6	<0.001	4.59	42, -40, 64
	38.6% R precentral G 31.3% R SMA 17.0% R superior frontal G	93.8% R premotor C (BA6) 5.5% L premotor C (BA6)	11.3	<0.001	3.58	16, -14, 68
	65.7% L superior parietal lobule 32.7% L lateral occipital C	78.5% L superior parietal lobule (BA7) 11.2% L primary somatosensory C (BA2)	10.3	<0.001	4.50	-30, -56, 64
	49.6% L precentral G 35.7% L superior frontal G 9.0% L middle frontal G 5.7% L SMA	97.4% L premotor C (BA6)	6.0	0.017	3.47	-42, 0, 60

Abbreviations: A1 — condition before AS; A2 — condition after AS; AS — ankle stimulation; BA — Brodmann area; C — cortex; G — gyrus; H1 — condition before HS; H2 — condition after HS; HS — heel stimulation; L — left; N/A — not available; MNI — Montréal Neurological Institute; R — right; SMA — supplementary motor area (also juxtapositional lobule cortex); *Z*_{max} — maximum *Z* score.

^a) Anatomical and cytoarchitectonic labels are provided including the proportion of labelled voxels. Only labels consisting of at least 5% of activated voxels are provided. Note that cerebellar labels may overlap with cortical labels and that cytoarchitectonic labels do not cover the whole brain.

3.4. Heel versus Ankle: Interaction between stimulation site and task repetition

The F -test of two-by-two interaction between the condition and repetition (H2 – H1 vs. A2 – A1) yielded a single significant cluster in the left ventral pons and bilateral pontomedullary junction at the base of the 4th ventricle. The cluster extended to the bilateral cerebellar hemispheres and vermis (mainly bilateral lobule IX and less right lobule VIII), bilateral interposed and the right dentate nucleus (red-yellow in **Fig. 8**), while there was no significant interaction in the cerebral cortex, thalamus or basal ganglia. The significance of the cluster in the brainstem was not affected by adding the pain intensity covariate and the same cluster was also observed in the confirmatory analysis using non-parametric thresholding (Randomise). Although additional data de-noising using ICA-AROMA (Pruim et al., 2015a, 2015b) led to decrease in the F -test cluster volume in each analysis, it remained significant in most analyses. These results are summarised in **Table 5**. To maintain clarity, only the results of original data analysis are further presented and discussed. The F -test cluster resulting from parametric analysis of interaction with pain intensity covariate is further referred to as the hindbrain cluster. The *post-hoc* voxel-wise t -test within the hindbrain cluster showed that only the contrast H2 – H1 > A2 – A1 was significant.

Table 5. Significant F -test clusters for Contrasts II.4 and II.5: Interaction and pain effect

Contrast	Anatomical atlas labels ^a	Cytoarchitectonic atlas labels ^a	Volume [cm ³]	Cluster p	Z_{\max}	Z_{\max} MNI coordinates (x,y,z [mm])
Contrast II.4: (H2 – H1 v. A2 – A1) without pain covariate (F -test in FEAT) <i>original data</i>	50.3% brainstem 25.7% R cerebellar hemisphere (15.3% right IX, 7.6% right VIII) 15.4% vermis (9.0% vermis IX) 9.2% R dentate nucleus 9.0% L cerebellar hemisphere (7.2% left IX)	N/A	8.17	0.004	3.68	-4, -36, -40
Contrast II.4: (H2 – H1 v. A2 – A1) without pain covariate (F -test in FEAT) <i>de-noised data</i>	42.0% brainstem 30.6% L cerebellar hemisphere (30.5% left IX) 27.4% vermis (16.9% vermis IX, 6.3% vermis X) 26.6% R cerebellar hemisphere (19.4% right IX, 7.1% right VIII)	N/A	4.94	0.034	3.40	-2, -54, -38
Contrast II.4: (H2 – H1 v. A2 – A1) with pain covariate (F -test in FEAT) <i>original data</i>	51.4% brainstem 25.2% R cerebellar hemisphere (16.0% right IX, 6.7% right VIII) 15.5% vermis (8.7% vermis IX) 9.1% R dentate nucleus 8.9% L cerebellar hemisphere (7.1% left IX)	N/A	7.98	0.004	3.64	-6, -38, -40

Contrast	Anatomical atlas labels ^a	Cytoarchitectonic atlas labels ^a	Volume [cm ³]	Cluster <i>p</i>	<i>Z</i> _{max}	<i>Z</i> _{max} MNI coordinates (x,y,z [mm])
Contrast II.4: (H2 – H1 v. A2 – A1) with pain covariate (<i>F</i> -test in FEAT) <i>de-noised data</i>	39.2% brainstem 32.8% R cerebellar hemisphere (18.7% right IX, 13.3% right VIII) 27.7% L cerebellar hemisphere (27.5% left IX) 25.6% vermis (16.6 vermis IX, 6.2% vermis X)	N/A	5.06	0.029	3.80	30, -54, -52
Contrast II.4: (H2 – H1 > A2 – A1) with pain covariate (<i>t</i> -test in Randomise) <i>original data</i>	58.8% brainstem 27.2% R cerebellar hemisphere (17.1% right IX, 7.9% right VIII) 14.2% vermis (7.4% vermis X, 5.1% vermis IX) 9.8% R dentate nucleus 8.4% L cerebellar hemisphere (7.9% left IX)	N/A	4.74	0.048	5.27 ^b	-4, -38, -42
Contrast II.4: (H2 – H1 > A2 – A1) with pain covariate (<i>t</i> -test in Randomise) <i>de-noised data</i>	45.3% brainstem 30.5% L cerebellar hemisphere (30.5% right IX) 30.3% R cerebellar hemisphere (30.3% right IX) 28.3% vermis (20.4% vermis IX, 6.9% vermis X)	N/A	3.25	0.081 ^c	4.49 ^b	-8, -50, -36
Contrast II.5: Correlation of (H2 – H1 v. A2 – A1) with pain intensity difference (H > A) <i>original data</i>	37.5% R inferior frontal G, pars triangularis 20.0% R frontal orbital C 17.9% R insular C 10.8% R frontal operculum C 7.6% R inferior frontal G, pars opercularis 5.8% R temporal pole	56.1% R Broca's area (BA45)	5.55	0.03	3.75	58, 22, 10

Abbreviations: A1 – condition before AS; A2 – condition after AS; AS – ankle stimulation; BA – Brodmann area; C – cortex; FEAT – FMRIB's Local Analysis of Mixed Effects; G – gyrus; H1 – condition before HS; H2 – condition after HS; HS – heel stimulation; L – left; N/A – not available; MNI – Montréal Neurological Institute; R – right; *Z*_{max} – maximum *Z* score.

^a) Anatomical and cytoarchitectonic labels, including the proportion of labelled voxels. Only labels consisting at least 5% of activated voxels are provided. Note that cerebellar labels may overlap with cortical labels and that cytoarchitectonic labels do not cover the whole brain.

^b) Maximum *t* score listed instead of *Z*_{max}.

^c) Cluster was listed despite non-significant *t*-test to allow comparison among performed analyses.

The effect of pain intensity yielded one cluster encompassing the right inferior frontal gyrus (BA 45), anterior insular cortex, frontal operculum, and frontal orbital cortex, as shown in green in **Fig. 8** and **Table 5**. This cluster is further referred to as insulo-opercular cluster.

3.5. Decomposing the interaction: *Post-hoc* ROI analysis

The ROI analysis of average Z scores derived from the hindbrain cluster (Contrast II.4) showed that the activation increased significantly after the HS (H2 – H1: median Z difference = 0.63, $p < 0.001$, uncorrected), and decreased significantly after the AS (A2 – A1: median Z difference = 1.1, $p < 0.001$, uncorrected), see **Fig. 9**. Likewise, the two effects differed significantly ($p < 0.001$, uncorrected).

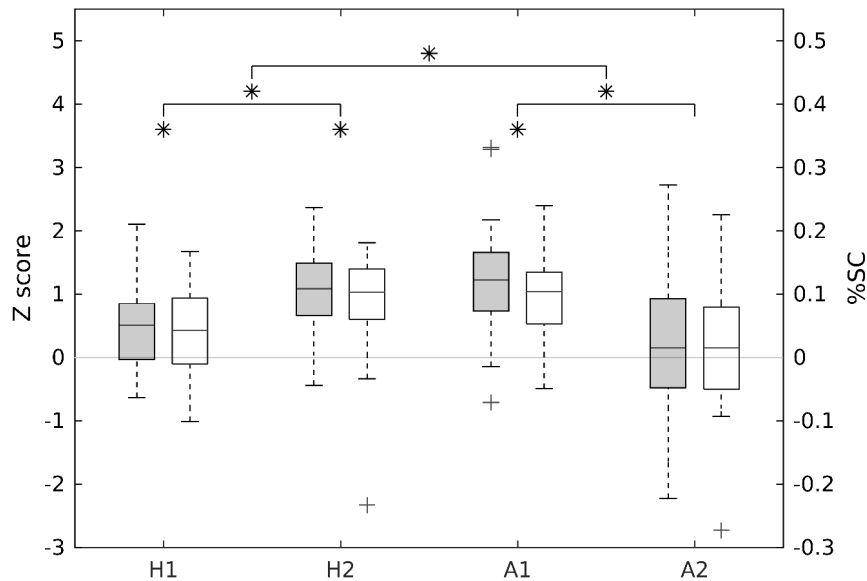


Figure 9. Post-hoc analysis of significant F -test. The box plots show average effects of main conditions in individual subjects extracted from the significant voxels in the hindbrain cluster (Contrast II.4). Gray boxes indicate average Z scores, whereas the white boxes indicate the average percent signal change (%SC) of the same conditions. The conditions are: H1 – before heel stimulation, H2 – after the heel stimulation, A1 – before the ankle stimulation, and A2 – after the ankle stimulation. Each box shows the interquartile range, median (inner horizontal line), extreme (whiskers) and outlier values (crosses). The asterisks above each box and above the horizontal lines indicate conditions and differences where Z scores were significantly different from zero at $p < 0.05$, using Wilcoxon signed-rank test.

In contrast, the insulo-opercular cluster representing the pain intensity effect did not show any significant difference in Z scores between the conditions or task repetitions ($p > 0.05$, uncorrected). The post-hoc ROI analysis confirmed that the interaction in Z scores (H2 – H1) > (A2 – A1) in the insulo-opercular cluster was negatively correlated with the pain intensity difference (HS – AS), see **Fig. 10**. The ρ was 0.54 ($p = 0.006$, uncorrected). In other words, the higher the perceived pain during the stimulation, the larger the decrease

in the BOLD response in the insulo-opercular cluster after the stimulation (i.e., in H2 or A2) relative to baseline (H1 or A1). However, the activation differences between the task repetitions (i.e., H2 – H1 and/or A2 – A1) were not significantly correlated with the average pain intensity in HS or AS condition ($p > 0.05$, uncorrected). Likewise, none of these correlations were significant in the hindbrain cluster ($p > 0.05$, uncorrected).

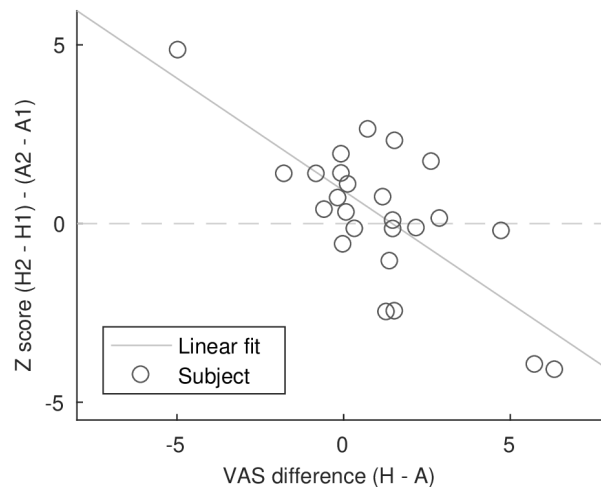


Figure 10. Correlation with pain intensity. The scatter plot shows negative correlation between the self-reported pain intensity difference heel stimulation – ankle stimulation (H – A) and the within-subject interaction (H2 – H1 > A2 – A1) represented by Z scores extracted from the pain effect cluster in the right frontal operculum and insula (Contrast II.5). Each circle represents a single subject, while the solid line represents the least-squares linear fit.

4. Study III (TMS)

The study is a part of a manuscript under preparation: **Hok, P.,** Nevrlý, M., Otruba, P., Valošek, J., Trnečková, M., Kutín, M., Opavský, J., Kaňovský, P., Hlušík, P. *Decreased intracortical inhibition after peripheral manual pressure stimulation*. In preparation.

4.1. Behavioural data

Due to hardware technical issues, complete continuous force measurements were only obtained in 14 subjects. The mean force applied during HS was 14.30 N (SD 3.79 N), and 20.75 N (SD 9.24 N) during AS. The difference was significant ($p = 0.03$, Student's paired t -test).

After HS, the median reported pain/discomfort intensity (VAS) was 4.40 (inter-quartile range [IQR] 3.25–5.55), while it was 4.10 (IQR 2.90–5.75) after AS. The difference was not significant ($p = 0.45$, Wilcoxon signed-rank test), with median difference 0.10 (IQR HS – AS: –0.70–1.65).

4.2. Electrophysiology

No participant reported any side effects of the pTMS. The mean size of the unconditioned MEP did not differ significantly before and after the stimulation in any condition (Student's paired t -test, **Fig. 11**).

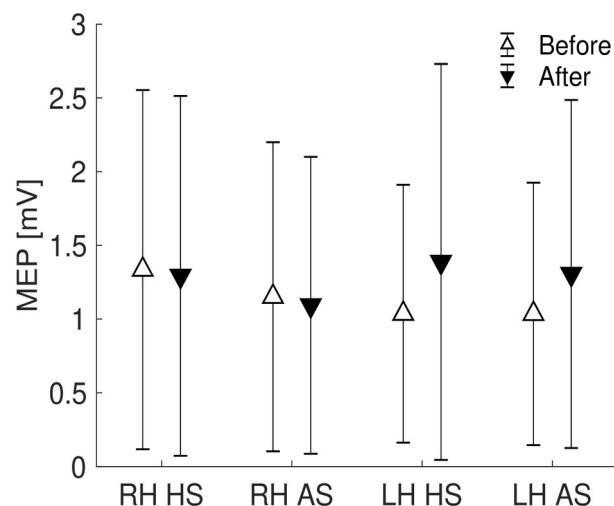


Figure 11. Unconditioned MEP sizes. Dot-and-whisker plots show (single-pulse) average unconditioned MEP sizes in mV for the right and the left hand (right hand [RH] and left hand [LH], respectively), either for the heel or ankle stimulation (HS and AS, respectively) session. Values before the stimulation are

shown with white downward pointing triangles, whereas values after the stimulation are shown with black upward pointing triangles. Whiskers indicate standard deviation (SD). There were no significant differences between any of the baseline and post-stimulation means ($N = 19$, $p_{RH-HS} = 0.83$, $p_{RH-AS} = 0.66$, $p_{LH-AS} = 0.11$, $p_{LH-AS} = 0.23$, paired Student's t -test).

4.2.1. Heel versus Ankle: pTMS results

Using linear regression analysis, we found a significant difference in the normalised MEP ratios (After/Before) for SICI (ISI 3 ms) in the right hand (RH, mean MEP ratio for HS was 2.38, SD 1.87, whereas for AS it was 1.09, SD 0.73; $p = 0.04$ for the intercept in linear regression, see **Fig. 12**), but not in the left hand (LH, mean MEP ratio for HS was 1.97, SD 2.94, whereas for AS it was 1.69, SD 1.50; $p = 0.46$ for the intercept). In RH, mean normalised MEP changed from 40.8% to 78.1% after HS, whereas in AS, the change was from 37.5% to 34.8% (**Fig. 13**). The individual differences in normalised MEP ratios were independent of the differences in mean pressure ($p = 0.44$, and $p = 0.41$, for interaction in RH and LH, respectively).

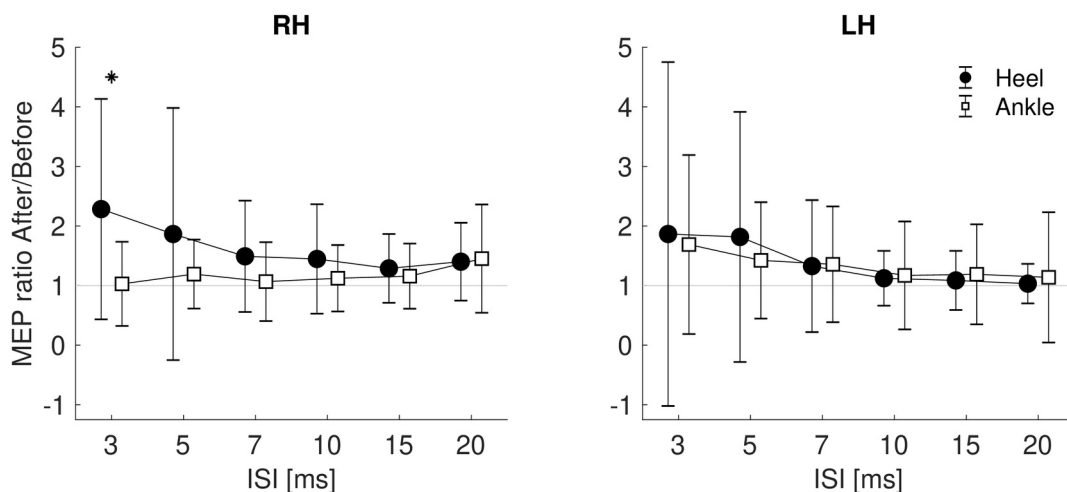


Figure 12. Normalised MEP ratio After/Before. Dot-and-whisker plots show average normalised MEP ratios (normalised MEP After/Before) for the right and the left hand (RH and LH, respectively), either for the heel or ankle stimulation (black circles and white squares, respectively) session. Whiskers indicate standard deviation (SD). Abscissa shows inter-stimulus interval (ISI) between the conditioning and test stimulus in ms. Significant difference controlled for the applied pressure using linear regression analysis is indicated with asterisk. Only the ISI 3 ms ($N = 14$, $p_{RH} = 0.04$, $p_{LH} = 0.46$) and 15 ms ($N = 14$, $p_{RH} = 0.37$, $p_{LH} = 0.54$) were formally tested.

There was neither a significant difference in the ICF (ISI 15 ms) between the two stimulation sites (RH, $p = 0.37$; LH, $p = 0.54$), nor a significant relationship with the pressure (RH, $p = 0.96$; LH, $p = 0.45$). The mean normalised MEP and standard errors for all ISI are shown in Fig. 13.

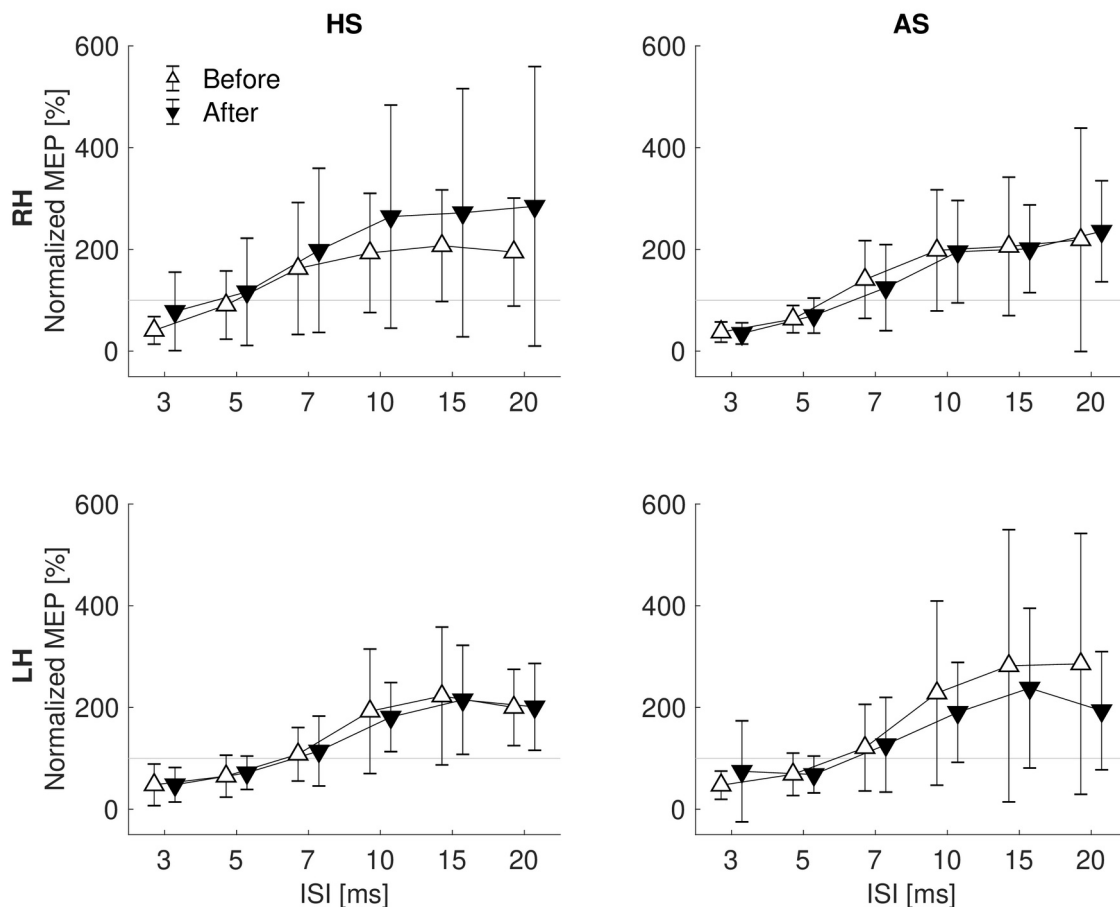


Figure 13. Normalised MEP sizes. Dot-and-whisker plots show average normalised MEP sizes (in %) before (white triangles) and after the stimulation (black triangles) for the right and the left hand (RH and LH, respectively), either for the heel or ankle stimulation (HS and AS, respectively) session. Whiskers indicate standard deviation. Abscissa shows inter-stimulus interval (ISI) between the conditioning and test stimulus in ms. There was no significant difference between any of the baseline and post-stimulation mean (*post-hoc* paired Student's *t*-test).

5. Study IV (HRV)

The study was published as an original paper: Opavský, J., Šlachťová, M., Kutín, M., Hok, P., Uhlíř, P., Opavská, H., Hluštík, P., 2018. *The effects of sustained manual pressure stimulation according to Vojta Therapy on heart rate variability*. Biomed Pap-Olomouc 162, 206–211. <https://doi.org/10.5507/bp.2018.028> WoS 2018: IF 1.141, Rank: 119/136

5.1. Heel versus Ankle: SAHRV

SAHRV of the first test phase, i.e., the first supine position (baseline), yielded in all participants spectral characteristics typical of healthy subjects of their age group (Opavský, 2002), with the possibility to distinguish individual spectral bands and with sufficiently high values of spectral power within individual frequency components to permit quantitative analysis, including assessment of the responses to changes in body position. The values of the calculated HRV parameters before and after active (heel) stimulation are provided in **Table 6**. Statistical significance refers to results of the Wilcoxon signed-rank test.

Table 6. Duration of RR intervals and heart rate variability: Heel stimulation

Parameter	Pre-stimulation median (Q1–Q3)	Post-stimulation median (Q1–Q3)	Statistical significance
RR interval [s]	1.00 (0.92–1.15)	1.08 (1.00–1.20)	$p < 0.001$
VLF Power [ms^2]	240.80 (164.69–344.74)	382.69 (199.19–641.88)	$p = 0.04$
LF Power [ms^2]	627.73 (398.88–849.29)	757.46 (462.45–1373.38)	$p = 0.01$
HF Power [ms^2]	1270.71 (462.45–1373.38)	2194.41 (934.12–4842.71)	$p = 0.02$
LF/HF ratio	0.419 (0.173–0.951)	0.409 (0.163–0.767)	n. s.
Relative VLF [%]	11.60 (6.29–15.66)	10.92 (6.33–14.79)	n. s.
Relative LF [%]	26.00 (13.74–39.65)	27.35 (12.80–36.01)	n. s.
Relative HF [%]	62.40 (45.74–77.24)	61.73 (45.23–78.62)	n. s.
Total Power [ms^2]	2246.04 (1486.41–5140.27)	4089.94 (2066.12–6912.44)	$p = 0.01$
MSSD [ms^2]	4681.60 (2735.95–14112.02)	8937.38 (4604.74–16404.76)	$p < 0.001$

Abbreviations: HF Power — spectral power of the high frequency band; LF Power — spectral power of the low frequency band; LF/HF ratio — ratio of the spectral powers LF over HF; MSSD — mean squared successive differences, indicator of heart rate variability in the time domain; n. s. — not significant; Q1, Q3 — 1st and 3rd quartile; Relative HF — relative representation of the HF component within the entire frequency range; Relative LF — relative representation of the LF component within the entire frequency range; Relative VLF — relative representation of the VLF component within the entire frequency range; RR interval — duration of the RR interval derived from ECG; Total Power — total spectral power over the entire frequency range 0.02–0.50 Hz; VLF Power — spectral power of the very low frequency band.

Values of the assessed ECG and SAHRV parameters before and after ankle stimulation (control site) are provided in **Table 7**.

Table 7. Duration of RR intervals and heart rate variability: Ankle stimulation

Parameter	Pre-stimulation median (Q1–Q3)	Post-stimulation median (Q1–Q3)	Statistical significance
RR interval [s]	0.99 (0.86–1.10)	1.07 (0.95–1.21)	$p < 0.001$
VLF Power [ms^2]	283.48 (163.63–478.29)	451.86 (203.26–797.65)	$p = 0.009$
LF Power [ms^2]	701.21 (306.40–975.36)	750.45 (287.81–1721.95)	n. s.
HF Power [ms^2]	1405.82 (720.84–3076.14)	2436.48 (835.47–3768.58)	$p = 0.03$
LF/HF ratio	0.476 (0.203–0.908)	0.534 (0.177–0.913)	n. s.
Relative VLF [%]	10.31 (7.82–14.95)	13.43 (5.16–19.08)	n. s.
Relative LF [%]	27.42 (15.93–36.10)	29.86 (12.09–41.26)	n. s.
Relative HF [%]	62.27 (38.55–75.95)	54.91 (42.28–76.30)	n. s.
Total Power [ms^2]	2617.85 (1689.78–4043.30)	3770.58 (1893.02–6456.51)	$p = 0.001$
MSSD [ms^2]	4814.96 (2388.49–8435.96)	8908.95 (3451.13–12689.16)	$p < 0.001$

For legend, see **Table 6**.

The results indicate that both stimulation types, i.e., stimulation in an “active” site according to Vojta (HS) and stimulation in a control “inactive” site (AS) were followed by statistically significant changes in MSSD values, duration of RR interval, and concurrently also in respiration rate. MSSD, which represents overall heart rate variability in the time domain, increased after both stimulation types. RR intervals lengthened (thus heart rate decreased) and respiration rate decreased after both active and control stimulations.

In the frequency domain, both stimulation types were associated with a statistically significant increase in VLF Power, HF Power and Total Power. LF Power increased significantly only after the active stimulation.

Neither the LF/HF ratio, nor the relative parameters of SAHRV, indicating the relative representation of individual frequency components, manifested any statistically significant changes after either stimulation type when compared to the pre-stimulation baseline.

5.2. Respiratory rate

Respiratory rate was assessed both before stimulation of each site (active versus control), and after stimulation. Before active stimulation (HS), the group mean respiratory rate was

12.3 breaths/min (SD 2.61), whereas before the control stimulation (AS), the rate was 12.9 breaths/min (SD 2.69); these values were not statistically significantly different.

After stimulation of the active zone (HS), respiratory rate decreased significantly to 10.9 breaths/min (SD 2.73), $p = 0.003$. Similarly, after control stimulation (AS), respiratory rate decreased significantly to 11.3 breaths/min (SD 2.88), $p = 0.003$. The respiratory rates after the two stimulation types were not significantly different (Mann-Whitney U test).

5.3. Stimulation discomfort

The VAS of pain indicated mean discomfort after active stimulation (HS) 3.01 (SD 1.94), range 0.2–7.4, whereas after control stimulation (AS) the mean VAS score was 1.62 (SD 1.48), range 0.2–6.2, this difference was statistically significant ($p = 0.003$). This reveals, even in young healthy participants, a certain unpleasantness associated with pressure at the active stimulation site. Nevertheless, despite this difference in perceived discomfort, no SAHRV parameters were apparently affected since the results were similar in both stimulation types.

5.4. Behavioural and motor responses to stimulation

During stimulation of the active site (HS), 9 out of the 28 participants (32%) manifested involuntary signs of muscle activation — fasciculations, finger movements, muscle twitches or the development of head rotation and/or deeper breathing. In contrast, three participants (10.7%) were falling asleep.

During stimulation of the control site (AS), slight head rotation appeared only in one participant (3.5% of the group), and another one manifested deeper breathing. Tendency to fall asleep appeared in 3 participants (10.7%), two of whom were also sleepy after the active stimulation.

X. DISCUSSION

In this section, the immediate central effects during the stimulation are first put into context of neuroimaging of somatosensory processing. Next, the evidence for stimulation after-effects is discussed, following by a synthesis of the results in an attempt to provide a bigger picture and integration of the findings. Finally, implications for physiotherapeutic techniques and summary of future directions conclude this work.

1. Patterns of activation associated with pressure stimulation

In this section, the main findings are discussed in the following order: brain structures associated with pressure stimulation of the foot, the dynamics of the BOLD responses, deactivations observed during the stimulation, and the site-specific differences, which are the main novel findings of the Study I (fMRI during stimulation).

Using a FIR model to deconvolve the haemodynamic response, we have confirmed that sustained peripheral pressure stimulation influences multiple elements of the sensorimotor system. The stimulus-related activation increases that we observed mainly in the contralateral S1 and bilateral S2 regardless of stimulation site (**Fig. 3**) are consistent with previous descriptions of the core somatosensory network activated during pressure stimulation applied either at the upper or the lower limb (Chung et al., 2015; Hao et al., 2013; Miura et al., 2013). Further consistent activations that we detected in the contralateral dorsomedial M1/PMC have only been observed in lower limb stimulation (Hao et al., 2013; Miura et al., 2013), whereas activations in the ipsilateral dorsomedial S1/SPL have been previously reported only in one study (Miura et al., 2013). Other brain structures activated either by HS or AS, or observed in the pooled analysis (Contrast I.3 [HS + AS]), such as frontal, insular or cingulate cortices and bilateral thalami, also agree with previous studies (Chung et al., 2015; Miura et al., 2013). Therefore, the described general activation pattern during sustained pressure stimulation of the foot may be considered rather independent of stimulation site and duration.

1.1. Temporal features of the BOLD responses

Apart from the localisation of signal changes, we also deconvolved the timecourse of the regional haemodynamic responses to natural manual pressure stimulation.

First, this allowed us to confirm that fast adaptation (Chung et al., 2015) occurs also during longer and repeated sustained stimulation. The sensation of static mechanical pressure is believed to be conducted via SA-I afferents (Johansson and Flanagan, 2009). These

afferents adapt exponentially to static stimuli (indentation or vibration) with a time constant of 8.4 s (Leung et al., 2005). Considering the time lag of the BOLD response, the activations in our data in the task-positive areas (coded in red in **Fig. 4A,C**) occurred and diminished within the expected time window (0 to 10 s after onset), which is in overall agreement with previous observations (Chung et al., 2015).

Second, we show that an equal response follows the release of pressure (**Fig. 4C**). Similar response has been observed after offset of sustained non-nociceptive vibratory (Marxen et al., 2012) or electrical stimulation (Hu et al., 2015), but it has not been reported so far in sustained pressure stimulation (Chung et al., 2015). Importantly, the offset responses have been shown to occur only after non-nociceptive stimulation (Hu et al., 2015), suggesting that the task-positive areas with offset responses in our data (red overlay in **Fig. 4A**) were not associated with processing of painful sensations and could potentially receive input mediated by FA afferents (Hu et al., 2015), but this has to be confirmed by future electrophysiological studies.

Regarding the magnitude of the offset responses, it should be noted that both positive and negative offset responses were apparently of higher amplitude and longer duration (0 to 17.5 s after offset) than the responses at the stimulation onset. We speculate that the reason might be to some extent related to our experimental design: the offset pressure decrease may have been on average more abrupt and less variable than the pressure increase at the block onset. As a result, onset responses might be slightly “blurred” in time.

1.2. Deactivations associated with pressure stimulation

In addition to areas activated during the stimulation, we also report a complementary set of brain areas, which were transiently suppressed by the stimulation and the pressure release. Similar inhibition in the bilateral S1 and M1 has been previously documented during vibrotactile finger or tactile foot stimulation (Hlushchuk and Hari, 2006; Tal et al., 2017). We extend this observation by showing that such suppression occurs also in response to sustained pressure stimulation of the lower limb. In line with Tal et al. (2017), we show that foot stimulation deactivates sensorimotor cortices in the bilateral somatotopic representations for upper limbs and face (blue overlay in **Fig. 4A**) as defined by Long et al. (2014). A new finding in the context of lower limb stimulation is the deactivation in areas outside the sensorimotor system, such as the temporal and occipital cortices. Similar cross-modal deactivations have been observed in humans only during somatosensory processing of tactile input from the upper limbs, and they have been speculated to enhance the somatosensory processing by suppressing unnecessary sensory

input (Ide et al., 2016; Kawashima et al., 1995; Merabet et al., 2007).

The observed deactivations are unlikely to be caused by local redistribution of blood flow (haemodynamic steal) as most of the areas showing differential responses are supplied by different main cerebral arteries (Tal et al., 2017). Electrophysiological evidence from direct intracortical recordings suggests that negative BOLD response is associated with suppressed neuronal activity in the deep cortical layers (Boorman et al., 2010; Yin et al., 2011). Simultaneous fMRI/electroencephalography (EEG) recordings in humans show considerable correlation between the EEG mu power and BOLD signal decrease, confirming its neuronal origin (Mullinger et al., 2014). Recent data show that inhibitory neurons may also contribute to the positive haemodynamic response, hence, deactivations could conversely reflect decreased neuronal activity of both excitatory and inhibitory cells (Vazquez et al., 2018). However, there is also evidence suggesting that the deactivated areas are not necessarily always “shut down.” Decrease in BOLD signal and cerebral blood flow may be at least in some cases accompanied by increased spiking (Hu and Huang, 2015) and/or glucose uptake (Devor et al., 2008). Since the underlying neuronal processes and functional role of negative haemodynamic responses are not yet clearly understood, they should be interpreted with caution (Tal et al., 2017).

1.3. Differences between the stimulation sites

1.3.1. Characterising temporal dynamics: Group-wise activation patterns

As outlined in the “VIII.5.2.3. *Post-hoc* ROI analysis: mean condition effects”, FIR model does not expect any specific shape of the haemodynamic response. As the BOLD signal is tightly coupled with the neuronal discharge at glutamate synapses (Logothetis, 2003), different HRF timecourses might reflect discharge patterns of distinct neuronal ensembles. Knowing that the motor response to stimulation according to RLT is rather gradual and results from temporal summation (Bauer et al., 1988; Laufens et al., 1994; Vojta, 1973a; Vojta and Peters, 2007), it can be expected that sets of brain structures (“networks”) with a distinguishable delayed or sustained haemodynamic response could play a specific role in generation of the motor or autonomic after-effects, apart from those structures related to fast somatosensory stimulus processing. The goal of the *post-hoc* hierarchical clustering analysis was therefore to identify the ensembles of brain regions with correlated HRF timecourse potentially implementing the same (or related) function, specifically looking for those with responses compatible with slow-onset motor activity.

During HS, average activation in several areas indeed followed a timecourse with more sustained positive BOLD response (red solid line in “Sustained” plot in **Fig. 4C**), whereas in AS, only transient onset/offset activations were detected (blue solid lines in **Fig. 4C**). Interestingly, some of these areas that were identified in the pooled analysis (Contrast I.3 [HS + AS]), including insular cortices and pons, were not observed in the group-wise map for AS condition (Contrast I.2), but they were still detected in HS (Contrast I.1; **Fig. 3**).

The involvement of the insular cortex in HS may in fact reflect increased discomfort/pain ratings during HS since the insular cortex is known to participate in emotional processing of pain (Apkarian et al., 2005; Hu et al., 2015; Kurth et al., 2010). However, other explanations remain possible as there was no significant correlation with discomfort/pain intensity difference in the insulo-opercular areas in Contrast I.5 (Pain). For further discussion on pain-related areas, see “X.6. Brain structures associated with discomfort/pain processing”.

Another structure associated with HS (but not significantly with AS, see **Fig. 3**, row C) was included in the sustained task-positive subsystem (green overlay in **Fig. 4A**) and located in the pontine tegmentum. The area most likely encompassed the pontine reticular formation (PRF) and pontine nuclei (Nieuwenhuys et al., 2008). These structures are adjacent to the pontomedullary reticular formation (PMRF) in which motor-related activation was modulated after pressure stimulation in Study II (fMRI of stimulation after-effects), see red-yellow overlay in **Fig. 8**. This area is further discussed in “X.2. After-effects of pressure stimulation on brain activation” and “X.5. Brain structures involved in site-specific pressure stimulation processing”. While the Study I (fMRI during stimulation) does not provide further direct evidence for a specific role of the PRF in physiotherapeutic effects of pressure stimulation, the sustained activation in the PRF during HS (see “Sustained” plot in **Fig. 4C**) indicates a potential for interaction between the PRF and the more caudal PMRF (**Fig. 8**).

1.3.2. Heel versus Ankle: Voxel-wise within-subject comparison

The hierarchical clustering analysis pointed towards several qualitatively different features of responses to AS and HS. However, quantitative differences in brain responses between the two stimulation sites may also occur beyond the areas identified in average activation maps. A pair-wise analysis was designed to test for such quantitative differences in voxel-wise responses. Furthermore, by including discomfort/pain covariate, pain-related brain activations could be controlled for. The voxel-wise analysis discussed in the following section (Contrast I.4 [HS – AS]) therefore represents a different view of the data, i.e.,

showing consistent differences between HS and AS across subjects regardless of the average activation patterns and after removing pain effect, which was evaluated in a separate contrast (Contrast I.5 [Pain]) and is discussed in “X.6. Brain structures associated with discomfort/pain processing”.

The voxel-wise analysis demonstrated that, compared to control stimulation, HS was associated with significantly increased activation in the left M1/PMC (somatotopically lower limb area; see Cluster 2 in **Fig. 6A**) and decreased activation in the left IPL.

Activations in the contralateral motor cortex have already been observed during pressure stimulation of the lower limb (Hao et al., 2013; Miura et al., 2013) as discussed in “X.1. Patterns of activation associated with pressure stimulation”. Although both AS and HS were associated with transient activations in the M1 representation for the stimulated limb, the results indicate higher synaptic activity during HS (**Fig. 6A**, Cluster 2). This may have several possible reasons: (1) Different locations of somatosensory representations. This is unlikely as the activations in the postcentral gyrus did not differ. (2) Local stimulation site properties. While this may also influence the activations, we believe that there were no sources of bias other than those which may be in fact important for RLT (see also “X.8. Limitations”). (3) The increased motor activation may also be a secondary phenomenon, for instance, reflecting pain-evoked movements (Apkarian et al., 2005). Since the Contrast 4 (HS – AS) was controlled for the difference in discomfort/pain rating, we consider the M1/PMC activation differences to be less likely pain-related (see also “X.8. Limitations”). Rather than that, (4) we propose that the increased motor activation during HS may represent a site-specific difference in sensorimotor integration. (5) Alternatively, the observed difference in the M1/PMC may result from an incipient involuntary muscle response to stimulation according to Vojta and may be mediated by a different, possibly subcortical or brainstem structure (e.g., Laufens et al., 1991; Vojta, 1973a), see also “X.2. After-effects of pressure stimulation on brain activation”. For further discussion on the role of the M1/PMC in sensorimotor integration, see “X.5. Brain structures involved in site-specific pressure stimulation processing” below.

In contrast to the task-positive motor activations, the differences in the IPL (**Fig. 6A**, Cluster 1) are more likely related to cross-modal deactivations (Ide et al., 2016; Kawashima et al., 1995; Merabet et al., 2007) as discussed in “X.1.2. Deactivations associated with pressure stimulation” above. The posterior IPL (cytoarchitectonically the area PGp) is considered a part of the default mode network, specifically its medial temporal lobe subsystem (Igelström and Graziano, 2017). Similar stimulus-related deactivations in parts of the default mode network have been previously observed during sustained electrical

stimulation (Hu et al., 2015). These deactivations varied over different phases of stimulation, left IPL being predominantly deactivated during the onset phase of periodic stimuli (Hu et al., 2015). Nevertheless, the role of those deactivations remains unclear. Since cognitive processes were not explicitly controlled in this study, we can only speculate that the higher amplitude of deactivations in the IPL-PGp could mean that the sensory input associated with HS was suppressing internally driven cognitive processes, possibly by drawing more externally oriented attention.

The quantitative differences evaluated in Contrast I.4 (HS – AS) using pair-wise (within-subject) comparison yielded areas in which hierarchical clustering identified similar responses during both HS and AS. Although it would be reasonable to expect that quantitative analysis should reflect the qualitative dissimilarities, this was not the case in Study I. There are several reasons why the two approaches might not necessarily be equal: (1) In the hierarchical clustering approach, group-wise responses were averaged within clusters, so only one representative timecourse per cluster was considered which reduced the inherent variability of data within the clusters (although clusters were first confirmed to contain highly correlated voxel-wise responses). (2) By using the group-wise data, the chosen clustering approach disregarded the inter-subject variability, whereas voxel-wise analysis accounted for inter-subject variability by subtracting the within-subject responses. (3) No formal statistical comparison of the hierarchical clustering between HS and AS was done. (4) The clustering approach using Pearson's correlation coefficient is not sensitive to the size of the BOLD signal relative to the background noise. In contrast, low BOLD signal change is detrimental for GLM analysis, which is especially pronounced in noisy regions, such as the brainstem. (5) The clustering approach considered the timecourse of a single block as a whole, whereas voxel-wise analysis tested for differences in each of the 9 FIR regressors separately (5 s per regressor) with a subsequent *F*-test. (6) Given the significant difference in discomfort/pain rating, pain difference covariate was added to the model of the voxel-wise analysis, further lowering the degrees of freedom and possibly filtering out pain-related brain areas. Therefore, the voxel-wise and the clustering analyses discussed in this section represent different perspectives on the same data, i.e., the former being more likely to emphasise high-amplitude and low-variability differences and miss differences in low-signal noisy areas, which is where the latter may add interesting information.

2. After-effects of pressure stimulation on brain activation

There are two main findings related to site-specific after-effects of stimulation: one using the SFO as a robust task to probe multiple levels of the sensorimotor system (Study II

[fMRI of stimulation after-effects]), the second, using a pTMS protocol to test corticospinal excitability (Study III [TMS]). Study II demonstrated that despite an extensive decrease in activation following both stimulation paradigms (blue in **Fig. 8**), the sustained pressure stimulation of the heel (HS) differentially modulated the task-related activation in the predominantly contralateral pons and ipsilateral cerebellum (red-yellow in **Fig. 8**), whereas Study III, thoroughly discussed in section “X.3. After-effects of pressure stimulation on cortical excitability”, showed that HS specifically modulated intracortical inhibitory circuits in the contralateral M1 (**Fig. 12**).

The following sections put the imaging findings into a broader context, providing an overview of the putative mechanisms underlying activation changes during a skilled hand motor task. Further considerations regarding the specific role of the brain structures identified in Study II in sensorimotor integration of pressure stimuli as well as clinical implications are discussed in “X.5. Brain structures involved in site-specific pressure stimulation processing” and “X.7. Implications for physiotherapeutic techniques”.

2.1. Average activation during SFO

The cortical, subcortical and cerebellar areas activated during SFO correspond well to previous reports of motor control of complex finger tasks (Solodkin et al., 2001). Despite the fact that the brainstem areas observed in this study (**Fig. 7**) are reported less frequently during skilled hand movement, midbrain/pons regions have been shown to engage during imagery of motor hand movement (Sauvage et al., 2011; Ueno et al., 2010). Moreover, PRF participates in motor control of the forelimbs in animal studies (Sharp and Ryan, 1984).

2.2. Repetition effects: Activation decrease post-stimulation

All the areas showing activation decrease post-stimulation (blue in **Fig. 8**) have been associated with control of complex finger movements (Solodkin et al., 2001) and their activation is known to decrease when repeating the same motor task, both over shorter (Kincses et al., 2008) and longer time scales (Steele and Penhune, 2010). These decreases have therefore been mostly interpreted as early stages of motor learning (Steele and Penhune, 2010) which is also the most likely explanation of the activation decrease upon repeating the same finger motor task in the present study. Without another control group with simple task repetition (i.e., no foot stimulation between the first and second finger movement task), we cannot exclude the possibility that at least some of the decreases were related to non-specific after-effects of peripheral stimulation (of a different body part), even though such effects have not been reported so far.

2.3. Heel versus Ankle: Site-specific effects on motor-related activation

An interaction between the stimulation site and task repetition was found in the brainstem and cerebellum, whereas no such effect was observed in the cerebral cortex. In contrast, previous functional imaging studies have shown that other modalities of peripheral stimulation, such as peripheral magnetic stimulation of the forearm between two repetitions of a finger movement task (Gallasch et al., 2015), resulted in increased activation of the contralateral sensorimotor cortex. We suggest that the absence of such an effect on the cortex in this study may result from the distance between the sensorimotor representations of the stimulated foot and of the fingers involved in the SFO.

The reported effect on hindbrain structures, on the other hand, may reflect less topographical and more diffuse arrangement of afferent or efferent pathways in the hindbrain, which are not necessarily related to motor control of a single extremity.

Here, the site-specific interaction was found mainly in the bilateral posterior cerebellar hemispheres and vermis, as well as in the left ventral and bilateral dorsocaudal pons, i.e., in areas likely corresponding to the left pontine nuclei and bilateral lateral PMRF according to a post-mortem brainstem atlas (Nieuwenhuys et al., 2008).

The *post-hoc* analysis of the interaction indicated that the activation decreased after the AS, likely matching the non-specific extensive BOLD response reduction in other sensorimotor areas due to early motor learning (Steele and Penhune, 2010). In contrast, the opposite effect represented by increased activation after the HS likely reflects specific effects of the peripheral stimulation site as the task execution pace was kept constant across all conditions. Similar activation increase post-stimulation was previously reported in the cerebral cortex (Gallasch et al., 2015). We argue that this effect was not due to the associated discomfort/pain perceived during the stimulation since the activation in the hindbrain areas did not correlate with the pain intensity and the effect remained significant after adding pain intensity covariate. In fact, Contrast 5 (green in **Fig. 8**) revealed that the task-related activation was modulated by pain intensity in the contralateral (left) anterior insula and frontal operculum, i.e., in areas overlapping with the pain network (Apkarian et al., 2005) as discussed below in section “X.6. Brain structures associated with discomfort/pain processing”. Last but not least, and as mentioned already, the discomfort/pain rating was rather small for both AS and HS.

For further discussion on the role of individual identified structures, see “X.5. Brain structures involved in site-specific pressure stimulation processing”.

3. After-effects of pressure stimulation on cortical excitability

The pTMS results of Study III demonstrate that sustained manual pressure stimulation elicits additional changes within the cortical circuits of the sensorimotor system associated with a specific site of action, namely, relative increases in conditioned MEP size, interpreted as decrease in intracortical inhibition, see **Fig. 12**.

Similar decrease in intracortical inhibition was observed after sustained stimulation in different modalities, such as vibrotactile (Christova et al., 2011, 2010), or electrical (Chipchase et al., 2011; Golaszewski et al., 2012, 2010). However, to our knowledge, the effects of sustained pressure stimulation on SICI or ICF have not been studied so far. Therefore, the results of Study III (TMS) are further discussed in the context of previous studies using different stimulation modalities.

3.1. Short-interval intracortical inhibition (SICI)

Models of modulation of intracortical inhibition through sustained or long-term stimulation have been based on evidence obtained mostly cutaneous electrical (Devanne et al., 2009; Kobayashi et al., 2003; McDonnell et al., 2007; Murakami et al., 2007; Ridding and Rothwell, 1999; Rocchi et al., 2017; Roy and Gorassini, 2008; Sailer et al., 2002), or muscle vibratory stimulation (Lapole et al., 2015; Marconi et al., 2008; Rosenkranz and Rothwell, 2006a, 2006b, 2004, 2003). It was shown that SICI reflects changes of the intracortical circuits independent of spinal motor neuron excitability (Rosenkranz and Rothwell, 2003; Ziemann et al., 1996b). There is further compelling evidence that SICI relies on activation of GABA_A receptors in the motor cortex (Hanajima et al., 1998; Ilić et al., 2002; Rosenkranz and Rothwell, 2003; Werhahn et al., 1999; Ziemann et al., 1996b, 1996a). However, previous studies have also established that the system of excitatory and inhibitory intracortical circuits is dynamically modulated in response to multiple exogenous and endogenous factors, which can all have a profound impact on the emergence and direction of the changes in SICI (Rosenkranz and Rothwell, 2006a, 2006b, 2004, 2003; Sailer et al., 2002).

One important consideration is that our paradigm involved a prolonged stimulation over 20 minutes, which might lead to potentially different effects from those observed when brief stimuli are delivered immediately before or during TMS (Ridding and Rothwell, 1999; Rosenkranz and Rothwell, 2003). In fact, the effects of prolonged electrical nerve stimulation reported so far have been inconsistent (Chipchase et al., 2011). Whereas some studies have reported changes in cortical excitability assessed by single-pulse TMS (Kaelin-Lang et al., 2002; Ridding et al., 2001), overall, there have been limited (Murakami et al., 2007; Rocchi et al., 2017) or no consistent changes in intracortical inhibition following

paired associative stimulation (Ridding and Taylor, 2001; Stefan et al., 2002) or electrical nerve stimulation alone (Fernandez-Del-Olmo et al., 2008; Kaelin-Lang et al., 2002; Pyndt and Ridding, 2004). Similarly, effects of prolonged muscle vibration also vary among different protocols, showing strong influence of attention (Rosenkranz and Rothwell, 2006b, 2004). More consistent effects require longer and repeated vibratory stimulation and simultaneous muscle contraction (Marconi et al., 2008). Outlasting changes in SICI were also observed when the stimulation was applied to the whole hand instead of a single muscle or nerve: 30 min of cutaneous electrical stimulation (Golaszewski et al., 2012, 2010) and 20 min of vibrotactile stimulation (Christova et al., 2011) caused reduction of SICI lasting up to one hour after the stimulation.

In general, sustained pressure stimulation in Study III (TMS) modulated motor cortex excitability in a way similar to previously published protocols that involved either long-term or less focal form of electrical, vibratory or vibrotactile stimulation (Christova et al., 2011; Golaszewski et al., 2012, 2010; Marconi et al., 2008). However, as there were no changes in unconditioned cortical excitability in Study III, the changes evoked by pressure stimulation were probably confined to the input side of motor cortex circuitry, potentially acting by unmasking latent horizontal connections as suggested for similar effects following muscle vibration (Jacobs and Donoghue, 1991; Rosenkranz and Rothwell, 2006a).

Further consideration is the local specificity of the stimulation effects. In other stimulation modalities, such as electric, tactile, or muscle vibration, changes in motor cortical excitability have been suggested to respect somatotopically organised cortico-cortical connections from the somatosensory cortex (Kaelin-Lang et al., 2002; Kaneko et al., 1994b, 1994a; Rosenkranz and Rothwell, 2006a; Terao et al., 1999). Although the effect observed in Study III was specific for one of two stimulation sites at the foot, it manifested in a somatotopically unrelated site in a hand representation, suggesting a more diffuse mechanism of action. Some less somatotopically organised effects have already been observed after or during electric stimulation (Ridding and Rothwell, 1999; Rosenkranz and Rothwell, 2003), but to our knowledge, there has been no evidence of peripheral foot stimulation affecting SICI in the hand muscles (Christova et al., 2011). Still, the change in SICI was only observed in the ipsilateral limb in this experiment, implying that the observed plastic changes are possibly mediated via a lateralised pathway. Both assumptions (diffuse, yet lateralised effects) are also in line with the simultaneous observation of a lateralised site-specific activation increase in the contralateral motor cortex during the stimulation (see "X.1.3.2. Heel versus Ankle: Voxel-wise within-subject

comparison”) and subsequent motor after-effects in the predominantly contralateral pontomedullary reticular formation and cerebellum (see “X.2.3. Heel versus Ankle: Site-specific effects on motor-related activation”). Based on this combined imaging and neurophysiological evidence, it can be assumed that sustained pressure stimulation may modulate sensorimotor structures at multiple brain levels when applied to a single specific body site. The putative structure involved in this modulation are discussed jointly in “X.5. Brain structures involved in site-specific pressure stimulation processing”.

3.2. Intracortical facilitation (ICF)

In Study III (TMS), we have observed no significant change in ICF. The circuits responsible for intracortical facilitation remain incompletely described and putatively involve NMDA excitatory interneurons (Golaszewski et al., 2010; Liepert et al., 1997; Nakamura et al., 1997). While ICF increased after 30-min whole-hand electrical (Golaszewski et al., 2012, 2010), or 20-min vibrotactile stimulation (Christova et al., 2011), and after 1 h of associative stimulation of two hand muscles (Pyndt and Ridding, 2004), multiple other studies of sustained peripheral stimulation showed no change in ICF (Fernandez-Del-Olmo et al., 2008; Kaelin-Lang et al., 2002; Marconi et al., 2008; Murakami et al., 2007; Rocchi et al., 2017), suggesting that ICF is affected by peripheral stimulation in a more variable and less reproducible way than SICI.

4. Autonomic after-effects of pressure stimulation

Besides motor manifestations (reflex locomotion), stimulation of trigger zones according to Vojta has been repeatedly shown to evoke responses of the autonomic nervous system (Dimitrijević and Jakubi, 2005; Kotnik, 2012; Vojta and Peters, 2007). Among them, the most significant are the cardiovascular responses, where vasomotor changes have been most frequently observed. However, these responses to stimulation according to RLT have not yet been systematically evaluated. At the same time, changes in HRV have been studied and reported for many other types of surface or other somatosensory stimulation, including nociceptive (Baker and Shoemaker, 2013; Joseph et al., 2004; Koenig et al., 2014; S. L. Smith et al., 2013; Wijnen et al., 2006).

Among the many established approaches to evaluation of HRV, some of which have clinical application (Ernst, 2014; Gang and Malik, 2003; Opavský, 2002; Task Force, 1996; Vlčková et al., 2010), Study IV employed the method of SAHRV in a modification with the imposed changes of orthoclinostatic load (Opavský, 2002; Opavský and Salinger, 1995; Salinger et al., 1998) that induce a shift in sympathovagal balance. The reason for choosing

this particular method was the possibility to record and assess the activity of vagal and sympathetic innervation, or their relative contribution, in different body positions (in the supine-standing-supine test) before and after specific active (RLT) stimulation as well as before and after a control stimulation outside the described trigger zone.

The results indicate that both active and control stimulations were followed by statistically significant lengthening of RR intervals and an increase in measures of overall variability, both in the frequency (Total Power) and time (MSSD) domain. Likewise, both stimulation types were associated with a statistically significant increase in the high-frequency (HF) spectral power, which reflects vagal activity (this also corresponds to lengthening of the average RR interval). Nevertheless, the relative representation of individual spectral components (VLF, LF and HF) has remained mostly unchanged after both stimulation types, which suggests that the ratio of sympathetic and vagal contribution to cardiac autonomic control remained unchanged as well.

Somewhat surprising was the finding of decreased respiration rate after both active and control stimulations, this usually occurs in a relaxed condition. Here, however, the subjective perception of the two stimulation types differed according to the VAS scores, which revealed a higher degree of stimulation discomfort (unpleasantness) during stimulation of an active trigger zone according to RLT. In both stimulation types, though, the VAS scores were low. The relationship between autonomic changes and discomfort/pain is further discussed in section "X.6. Brain structures associated with discomfort/pain processing".

Overall, the changes in SAHRV parameters may be interpreted as similar after both stimulation types, namely, that stimulation of the active zone on the heel has not evoked a clearly different response than stimulation outside the active zone (ankle). This stands in apparent contradiction to previous experience with autonomic reflex responses during application of RLT in the clinical practice (Vojta and Peters, 2007). This is further discussed in section "X.7. Implications for physiotherapeutic techniques".

5. Brain structures involved in site-specific pressure stimulation processing

In this section, brain structures showing differential responses to HS and AS are discussed. First, from the point of view of their general function, next, from the point of view of their putative role in sensorimotor integration of pressure stimuli.

5.1. Primary motor and premotor cortex (M1/PMC)

In Study I (fMRI during stimulation), HS was associated with increased activation of the M1/PMC within the somatotopic representation of the stimulated limb. The M1 is implicated in control of low-level dynamic characteristics of movement, especially in distal limb muscles (Chouinard and Paus, 2006; Omrani et al., 2017), whereas the dorsal PMC (i.e., PMd) participates in motor planning and movement generation (Picard and Strick, 2001), selection of movements based on arbitrary or spatial cues, and motor learning (Chouinard and Paus, 2006). Motor cortices have also been shown to assume sensory functions by transforming proprioceptive input into kinesthetic sensations in absence of overt movements or any intention to move (Naito et al., 2016). Although no kinesthetic sensations were reported by the subjects in Study I (fMRI during stimulation), it illustrates that motor cortices may be engaged in sensory processing not directly related to movement execution. On the other hand, motor cortex activation may be a substrate for subsequent plastic changes.

As various alternative explanations for the activation increase in M1/PMC have already been considered and mostly rejected in “X.1.3.2. Heel versus Ankle: Voxel-wise within-subject comparison”, it is therefore proposed that the increased motor activation during HS represents a site-specific difference in sensorimotor integration. In other words, HS may have more direct influence on the M1/PMC than the stimulation of the nearby ankle site, provided that all stimulation parameters are kept as similar as possible. It is possible that at least part of this effect would be related to (assumed) incipient involuntary muscle response to stimulation according to RLT with subcortical origin (Laufens et al., 1991; Vojta, 1973a). However, it remains to be established whether overactivation of the M1/PMC is its result, prerequisite, or simply a parallel phenomenon.

Notably, both AS and HS were associated with concomitant activation of the M1/PMC (**Fig. 3**). An outstanding question is at which level the pressure sensory input is redirected to the motor cortex. The M1 is known to receive cortical input from the PMd just rostral to the M1 (Picard and Strick, 2001), direct projections from the thalamus (Naito, 2004; Omrani et al., 2017), as well as indirect input, either from area 3a, 2, 1 (e.g., Ghosh et al., 1987), or 5 (Strick and Kim, 1978). Somatosensory cortices are also densely connected with SMA and PMd (Jones et al., 1978) and somatosensory influences are exerted via the cortico-subcortical loops involving the basal ganglia, cerebellum, and thalamus (Nachev et al., 2008; Omrani et al., 2017). Motor activations may therefore reflect a direct interaction between the adjacent somatosensory and motor cortices (Kaelin-Lang et al., 2002) or influence of a parallel bottom-up thalamocortical pathway (e.g., Asanuma et al., 1980;

Huffman and Krubitzer, 2001), although the direct dorsal column pathways ending in the M1 mostly serve muscle spindle afferentation (Naito, 2004; Omrani et al., 2017). An indirect influence from a more caudal structure, for example mediated by collaterals of the spinothalamic pathway and brainstem reticular formation (Kayalioglu, 2009), is also possible. As a result, multiple afferent pathways are most likely to converge in the motor cortex. It still remains to be established which of these channels is specifically strengthened by HS.

Further involvement of M1 was demonstrated in Study III (TMS), showing increased cortical excitability (decreased SICI) in the M1 after stimulation of the contralateral heel. As already outlined in “X.3.1. Short-interval intracortical inhibition (SICI)”, the effect was diffuse, though lateralised. Such a diffuse effect could result from a less somatotopically arranged afferent input, potentially the same affecting the M1/PMC during stimulation (see above), including but not limited to diffuse thalamocortical pathways to the M1 (Asanuma et al., 1980; Huffman and Krubitzer, 2001), indirect pathways via collateral branches of the spinothalamic tract relayed multiple brainstem areas (e.g., medullary reticular formation or parabrachial nuclei), (Hylden et al., 1989; Kayalioglu, 2009, p. 149; Kevetter and Willis, 1983), or spinoreticular and spinocerebellar tracts. Evidence from rodents suggest that the cerebellum may also play a key role in this process (Oulad Ben Taib et al., 2005). Indeed, repetitive TMS using theta burst stimulation of the cerebellum was shown to affect SICI even in human subjects (Koch et al., 2008). These candidate “relay structures” are discussed below in “X.5.2. Brainstem” and “X.5.3. Cerebellum” as the focus of the text shifts caudally.

5.2. Brainstem

Within the area of significant site-specific stimulation effect in Study II (fMRI of stimulation after-effects), the local maxima were identified in the PMRF. Stimulation of the reticulospinal pathway originating in the PMRF, especially in its lateral part (Takakusaki et al., 2016), elicits bilateral asymmetrical motor patterns in cats (Dyson et al., 2014) and monkeys (Hirschauer and Buford, 2015), which can be related to stereotypic tonic responses observed by Vojta (Vojta, 1973a; Vojta and Peters, 2007). In cats, the PMRF was also shown to contribute to postural control (Stapley and Drew, 2009) and locomotion (Dyson et al., 2014). In humans, the PMRF has been suggested to participate in locomotor control as well, being implicated in anticipatory postural control before gait initiation (Takakusaki, 2013). Neuroimaging studies during imagery of standing (Jahn et al., 2008) and walking (la Fougère et al., 2010) demonstrated activation in the lateral PMRF

corresponding to the area reported here. The PMRF is likely to support the locomotion by integrating descending cortical influences (Takakusaki, 2013) and ascending spinoreticular inputs (Kevetter et al., 1982; Sahara et al., 1990). Functions of the PMRF likely extend beyond locomotion control, since its neurons project also to the distal forelimb muscles in non-human primates (Riddle et al., 2009) and are modulated during voluntary reaching (Schepens and Drew, 2004) or finger movements (Hirschauer and Buford, 2015).

The presented results provide further evidence for such striking integration of seemingly heterogeneous functions by showing that BOLD response during skilled upper limb movements may be modulated by lower limb stimulation. Importantly, Study I (fMRI during stimulation) showed that HS elicited sustained activation in the nearby, though slightly more rostral PRF. We speculate that both regions might serve as input (PRF) or output areas (PMRF) of a more complex circuit involved in involuntary motor responses and motor after-effects of RLT.

Apart from PMRF, the brainstem cluster in Study II (fMRI of stimulation after-effects) included also pontine nuclei. In contrast to the PRMF, there is no anatomical evidence for bottom-up inputs to the pontine nuclei (Nagao, 2004), which have been suggested to serve merely as a relay station between the cerebral cortex of the same side and contralateral cerebellum (Nagao, 2004). The question remains whether pontine nuclei were activated along with the cerebellum or the activation in the PMRF was detected in the surrounding tissue due to spatial smoothing of the imaging data.

5.3. Cerebellum

In Study II (fMRI of stimulation after-effects), the peripheral stimulation modulated also cerebellar activation, mainly in the lobule VIII and IX. Both lobuli are known to receive spinal inputs (Brodal and Jansen, 1941), either via bilateral spinocerebellar tracts (Yaginuma and Matsushita, 1989) or via the lateral reticular nucleus, which has been suggested to integrate multimodal inputs from spinal afferents and spinal locomotor centres (Alstermark and Ekerot, 2013). In patients, lesions of the spinocerebellum lead to dyscoordination of upright posture and gait (Ilg et al., 2008). However, lobule IX is also implicated in oculomotor control and postural orientation in space and receives vestibulocerebellar fibres and cortical inputs via the contralateral pontine nuclei (Voogd et al., 2012).

The posterior cerebellum is also involved in sensorimotor circuits related to upper extremities, e.g., it is active during finger tapping task (Stoodley et al., 2012). Meta-analyses of functional imaging studies showed overlapping motor and somatosensory

activations in lobule VIII, suggesting a prominent role in the sensorimotor integration (Riedel et al., 2015).

By combining previous functional and anatomical evidence with observations presented here, we suggest that, first, the PRF/PMRF and posterior cerebellar areas interact during the motor performance within a common reticulocerebellar network, possibly integrating cortical and peripheral inputs. Second, this network may be transiently up-regulated in response to specific peripheral stimulation. In this circuit, the PRF/PMRF may serve both as the primary input and output node since it receives direct spinal inputs (Kevetter et al., 1982; Sahara et al., 1990) and can potentially elicit complex motor responses via the reticulospinal tract (Hirschauer and Buford, 2015). Finally, modulation of cerebellar activity may be a potential source of altered intracortical inhibition in the hand representation within the M1 (cf. Koch et al., 2008).

6. Brain structures associated with discomfort/pain processing

Both Study I (fMRI during stimulation) and II (fMRI of stimulation after-effects) revealed brain regions in which BOLD signal difference between HS and AS was correlated with the difference in discomfort/pain ratings. Peripheral stimulation according to RLT has previously been associated with concomitant pain (Müller, 1974), and indeed, HS was perceived more unpleasant/painful than AS in Studies I, II and IV, i.e., whenever participant was not allowed to provide an immediate feedback. In Study I, activation in SPL (areas 5 and 7) was negatively correlated with the discomfort/pain (Cluster 1 in **Fig. 6B** and **Table 3**), i.e., SPL was deactivating during more unpleasant stimuli. In contrast, no significant positive correlation was found. However, the average BOLD response map showed that at least some areas participating in pain processing, such as anterior insula, were engaged by pressure stimulation (**Fig. 3** and **Fig. 4A**). In HS, these areas exhibited a distinct HRF shape and were hierarchically clustered into the “sustained task-positive” subsystem.

In Study II (fMRI of stimulation after-effects), anterior insular cortex, frontal operculum, and frontal orbital cortex (insulo-opercular cluster), were significantly negatively correlated with discomfort/pain difference (green in **Fig. 8** and **Table 5**). A closer inspection revealed that the motor-related activation in the left anterior insula/frontal operculum decreased after a more painful stimulation (**Fig. 10**).

The insular cortex have been long associated with pain-related processing (Baliki and Apkarian, 2015). However, the contralateral anterior insula has also been shown to activate

during hand motor performance not associated with any pain (Sauvage et al., 2011) and has been mostly considered to host various cognitive and affective processes (Kurth et al., 2010; Uddin, 2015). The preceding unpleasant/painful stimulation may have therefore affected the background cognitive processes during the motor task, possibly lowering the subject's attention and engagement in the task.

Anterior insula also significantly contributes to the control of autonomic responses (Beissner et al., 2013). Nevertheless, despite some reports of various autonomic responses associated with RLT (Dimitrijević and Jakubi, 2005; Vojta and Peters, 2007), Study IV (HRV) did not indicate any site-specific effect of HS which would interfere with the current results, see "X.4. Autonomic after-effects of pressure stimulation".

7. Implications for physiotherapeutic techniques

The findings of Study I (fMRI during stimulation) indicate that sustained pressure stimulation affects the sensorimotor system on a global scale. While some areas (e.g., the primary SMC for the foot) respond with increased activation, other regions (such as the primary SMC for the hand and face) become transiently suppressed. This effect seems to be non-specific and independent of the stimulated site. However, specific effects during the HS were observed as well.

Pressure stimulation is an integral part of number of physiotherapeutic techniques, such as reflex locomotion (Vojta and Peters, 2007), clinical massage, acupressure (Wong et al., 2016), reflexology, or myofascial trigger point therapy (Smith et al., 2018). Whereas in reflex locomotion, the choice of exact stimulation site is pre-defined (Vojta and Peters, 2007), other techniques, such as myofascial trigger point therapy, do not rely on specific body sites (Smith et al., 2018). Our data show that even non-specific pressure stimulation may evoke far-reaching effects throughout the brain, including the motor system, which is relevant for physiotherapy. Whether the observed non-specific (common to HS and AS) cortical activations/deactivations in the Study I have any outlasting and clinically significant impact, cannot be established without further studies with comprehensive protocols employing imaging and repeated behavioural testing.

The choice of the active stimulation site (heel) was motivated by the stimulation employed in RLT, which is known to induce significant modulatory motor after-effects, e.g., facilitation of voluntary movements that outlast the stimulation (e.g., Laufens et al., 1995). While the present results provide new evidence that sustained pressure stimulation according to RLT may influence multiple sensorimotor areas (including representations of

distant extremities) without any evoked gross motor activity, the site-specific effects were local, i.e., confined to the motor cortex adjacent to the primary somatosensory representation of the stimulated limb. Although the co-activation in the primary motor and premotor cortex of the stimulated (lower) limb seems to be a relatively common phenomenon (e.g., Hao et al., 2013; Miura et al., 2013), Study I demonstrates that it can be augmented by the choice of a specific site, such as the lateral heel zone according to Vojta (1973a).

The need for targeted stimulation of empirically chosen sites in reflex locomotion resembles other therapeutic techniques, such as acupuncture. In (electro)acupuncture, a considerable number of fMRI studies compared brain activations in response to the “active” and sham sites, but results are often conflicting (Qiu et al., 2016). A specific activation increase in response to lower limb stimulation was observed in the contralateral primary motor cortex (Usichenko et al., 2015; Wu et al., 2002) in agreement with the results of Study I (fMRI during stimulation), suggesting that there might be a more universal mode of action common for both reflex locomotion and acupuncture. However, differences in many other brain areas not corresponding to our results, including frontal and temporal cortices and limbic structures, were also observed (Usichenko et al., 2015; Wu et al., 2002), therefore, other mechanisms might be involved as well. A head-to-head comparison of sites used in different techniques would be required to assess this.

The results of Study II (fMRI of stimulation after-effects) might suggest what structures are involved in the modulatory after-effects of the stimulation according to RLT, including facilitation of voluntary movements outlasting the stimulation (Laufens et al., 1995). These immediate effects have been observed to persist for at least 30 min (Vojta and Peters, 2007), which is well within the time span between the intervention and the second SFO acquisition in Study II. As thoroughly reviewed in “IV.2.2.1. Involuntary motor responses to pressure stimulation”, it has been originally speculated that the facilitation does not reflect the primary stimulation but rather a secondary effect resulting from the evoked global motor activation, contraction of numerous muscles associated with massive proprioceptive stimulation, which in turn promotes further facilitation of voluntary movements (Vojta, 1973a). Yet, muscle contractions and the associated proprioception were minimal in Study II, therefore, the observed differential modulation likely reflected other mechanisms.

Furthermore, the efferent pathways mediating the motor response to the stimulation according to Vojta have been speculated to be mediated by the non-pyramidal system (Vojta, 1973a), most likely involving a midbrain relay structure (Laufens et al., 1991; Vojta,

1973a). Although the midbrain is believed to contain a midbrain locomotor centre that plays a key role in human locomotion (Takakusaki et al., 2016), neither Study I (fMRI during stimulation) nor II (fMRI of stimulation after-effects) revealed any specific changes in that area. Instead, the site-specific modulation of task-related fMRI activity following pressure stimulation was revealed in the bilateral though predominantly contralateral (to stimulation) PMRF, a structure involved both in locomotion (Dyson et al., 2014; Jahn et al., 2008; la Fougère et al., 2010; Takakusaki, 2013) and postural control (Stapley and Drew, 2009; Takakusaki, 2013). The provided data are therefore highly suggestive that the PMRF could be directly associated with the effects of the RLT, especially on gait control (Laufens et al., 1995).

Moreover, as already discussed, the PMRF has already been shown to mediate various asymmetric reflex movement patterns, including the asymmetric tonic neck reflex (Dyson et al., 2014; Hirschauer and Buford, 2015; Takakusaki et al., 2016) that share some similarities with reflex locomotion (Vojta, 1973a). However, the fact that the stimulation in Study I-IV was deliberately adjusted in order to avoid any consistent gross involuntary motor responses limits the ability to connect present observations with the anatomical structures responsible for the generation of involuntary motor patterns associated with RLT (Vojta, 1973a). This, and possibly also the assumed gradual summation of afferent inputs in the central generator of reflex locomotion (Bauer et al., 1988; Laufens et al., 1994; Vojta, 1973a), might be the reasons why no quantitative differences were observed in the brainstem in Study I (fMRI during stimulation). The sustained activation of the nearby PRF during HS but not during AS (**Fig. 3**) still indicates that the brainstem reticular formation participates in sensory processing of pressure stimuli during RLT. As far as other subcortical areas are concerned, there was only one previous neuroimaging study of RLT besides this project, which reported the main effect of specific stimulation in the ipsilateral putamen as compared to non-specific sham stimulation (Sanz-Esteban et al., 2018), but it has already been pointed out in “IV.2.4. Neuroimaging evidence for central effects of pressure stimulation” that these conclusions should be considered at best as preliminary. Having no other direct imaging evidence, data from Studies I and II suggest that the involuntary response reflex locomotion involves a common set of pontomedullary structures that also mediate the after-effects of RLT.

Another consequence of the stimulation, specific for HS, was the effect on GABA_A-ergic intracortical circuits demonstrated in Study III (TMS). This finding, in addition to changes in PMRF and cerebellum, can be potentially associated with the observed motor after-effects of RLT on hand movements (Laufens et al., 1995). The decrease in SICI suggests

that pressure stimulation according to Vojta may facilitate practice-dependent plasticity (Ziemann et al., 2001) to improve motor performance as observed in clinical practice (Laufens et al., 1998). As no specific effect was observed in the hand motor cortex in Study I or II (fMRI), it can be speculated that the change in SICI was mediated by the cortico-subcortical circuits, possibly involving cerebellar influence on the M1 (Koch et al., 2008). However, longer-term motor behavioural studies in normal subjects and clinical trials in patients suffering from disorders of the motor system that would undergo the therapeutic stimulation under controlled conditions would be necessary to confirm the link between the behavioural and physiological changes induced by RLT.

Finally, another implication of this project inferred from Study IV (HRV) is that sustained pressure stimulation is associated with increased vagal and sympathetic activity, though the ratio of sympathetic and vagal contribution to cardiac autonomic control is not affected. Notably, this effect was non-specific and was observed to a similar degree after both HS and AS. However, this is in apparent contradiction to empirical observation of common autonomic responses during RLT (Vojta and Peters, 2007). There may be several reasons for this discrepancy. (1) The typical target group for RLT, neonates and infants, has autonomic responses different from those of adults, one of the underlying factors may be the immaturity of the central nervous system in children. (2) The other obvious difference is the absence of CNS lesions in the Study IV population, whereas in the clinical practice, the therapeutic stimulation is mostly applied to children with perinatal or prenatal brain damage. Taken together, the rather small and non-specific autonomic response to pressure stimulation of the foot in our young healthy adult participants (university students) may not be unexpected. (3) Finally, the therapeutic application in the clinical practice typically includes simultaneous stimulation in several trigger zones, whereas the protocol in Studies I-VI was simplified to using a single stimulation site.

8. Limitations

8.1. General limitations

The peripheral stimulation according to RLT is known to be associated with concomitant pain (Müller, 1974), and, in fact, heel stimulation was perceived slightly but statistically significantly more unpleasant or painful than ankle stimulation in Studies I, II (fMRI) and IV (HRV). Interestingly, this was not the case in Study III in which participants were allowed to immediately report if stimulation became painful. On the other hand, the therapist maintained similar pressure during both AS and HS in Study I and II, but applied significantly less force during HS in Study III. Although this might have

influenced some of the results, it is here argued that the main findings were unaffected by these differences.

First, the differences in discomfort/pain rating were overall small. The median VAS score in Study I and II (fMRI) was 1.85 for HS, while it was 0.90 after AS. In Study IV (HRV), the mean values were 3.01 and 1.62, respectively.

Still, it has to be acknowledged that average activation maps in Study I (fMRI during stimulation) might have reflected, at least to some degree, pain-related activity, which was not controlled for in the Contrasts I.1–I.3 (**Fig. 3 and Fig. 4A**). Previous studies employing painful cutaneous pressure stimulation have shown discomfort/pain-related activations in the primary motor cortex and brainstem that were not present during neutral stimulation (Rolls et al., 2003). The occasionally observed involvement of cortical motor areas during acute pain perception may be possibly associated with the withdrawal response to pain (Apkarian et al., 2005). While electromyographic recordings from the stimulated and non-stimulated limbs would be needed in future studies to completely exclude the possibility of pain-related movements, the site-specific differences (Contrast I.4) were controlled for differences in discomfort/pain using a linear covariate. Since the covariate significantly explained variance in the somatosensory cortex (areas 5 and 7, see **Fig. 6B**), i.e., parts of the pain perception network (Apkarian et al., 2005), it could be conceived that the individual variability of discomfort/pain levels was successfully captured by the model. Yet, activation in motor areas was not correlated with the discomfort/pain rating. Similar procedure was applied to the Study II (fMRI of stimulation after-effects), in which an even more complex interaction model successfully explained pain/discomfort-related variance in the contralateral anterior insula and opercular cortex, i.e., areas often associated with pain processing (Baliki and Apkarian, 2015). Again, the PMRF/cerebellar regions showing significant intervention effect were not correlated with discomfort/pain. Furthermore, Study IV (HRV) showed no apparent differences in autonomic responses following either HS or AS. This was somewhat surprising finding, as autonomic responses were often reported during RLT (Dimitrijević and Jakubi, 2005; Kotnik, 2012; Vojta and Peters, 2007). Likewise, in children, RLT is commonly accompanied by unpleasant feelings in children, often with pain resulting in withdrawal or reflex behaviour (Müller, 1974). It is therefore possible that autonomic responses in children are related to pain or the resulting withdrawal behaviour. Hence, the overall low levels of reported discomfort/pain might also explain why there were no gross differences in autonomic control in the sample of young healthy individuals.

Further potential bias may arise from differences in local characteristics between the two stimulation sites, such as density of sensory nerve endings, soft tissue properties or bony structures below the skin. As mentioned in “VIII.3.2. Pressure stimulation”, both sites were within the same dermatome (Foerster, 1933). Since the active site (heel) was defined by Vojta (1973a), the control site was carefully chosen to match as many properties as possible, i.e., neither site was located at the foot sole, but rather on the lateral aspect of the foot. Neither site is considered to contribute specifically to any motor or balance control function. Conversely, it is likely that some of the local site properties indeed play a role in the therapeutic effect of the RLT, but further studies testing multiple sites in different dermatomes over different types of tissues would be needed to elucidate this.

Notably, as all Studies used an “active” comparator (a different stimulation site), non-specific stimulation effects cannot be distinguished from effects of simple task repetition (Study II [fMRI of stimulation after-effects]) or rest (Studies III [TMS] and IV [HRV]). A third group with no stimulation would have been necessary to clarify test-retest variability and separate effects of stimulation from effects of motor learning and habituation.

Some further study-specific methodological limitations are further discussed below.

8.2. Study I and II (fMRI)

Because of the whole-brain fMRI acquisition, the spatial resolution of the T_2^* -weighted MR images may limit assignment of activation foci to a single anatomical area in a small structure such as the brainstem. Nevertheless, functional MR imaging of the brainstem was successfully performed in the past using spatial resolution and hardware comparable to ours (Jahn et al., 2008). Moreover, data acquisition using a 1.5-T scanner may be less prone to magnetic susceptibility artefacts that affect higher-field 3-T scanners more severely, despite their superior signal-to-noise ratio.

Another concern may arise regarding the influence of motion artefacts on the main results. In both Study I and II (fMRI), main interaction effect remained significant after advanced motion de-noising procedures using ICA-AROMA (Pruim et al., 2015a, 2015b). However, despite this highly sophisticated approach, there was a concern that the method may introduce another bias that may specifically affect brainstem regions. One of the image features exploited by the ICA-AROMA to detect a noisy signal component is the overlap of the independent component with a brain edge mask. Since the edge mask is defined as a 10-mm outer layer of the brain mask, it was expected that some neuronal signal sources might be erroneously removed from the data. Additionally, studies demonstrating the

effect of additional removal of suspected motion-related signals (Muschelli et al., 2014; Pruim et al., 2015b, 2015a) have shown its benefit for lower-level group contrasts. However, for higher-level contrasts such as group-by-time interaction used in Study II (fMRI of stimulation after-effects), the additional preprocessing pipelines, including ICA-based denoising, have yielded rather heterogeneous results and may introduce a substantial bias (Churchill et al., 2012). For these reasons, original (before denoising) results are primarily presented in Study II. In contrast, due to a more flexible modelling approach in Study I (fMRI during stimulation) inherently more prone to motion artefacts, and due to a less complex group contrast, the analysis was performed using denoised data only.

8.3. Study III (TMS)

It can be argued that changes in SICI are due to changes in testing pulse efficacy (Stefan et al., 2002). However, it is shown that amplitudes of unconditioned stimuli did not differ significantly before and after the intervention, effectively ruling out this possibility.

The changes in cortical excitability might have been affected by the non-equal pressure applied during HS and AS. However, the difference in SICI between the HS and AS remained significant even though the influence of the applied pressure has been controlled by linear regression analysis with difference between mean pressure for HS and AS as an independent variable.

Furthermore, it cannot be ruled out that certain cognitive processes affected the results, such as directed attention that is known to modulate cortical plasticity during peripheral stimulation (Rosenkranz and Rothwell, 2006b; Thomson et al., 2008). Since attention levels were not directly evaluated during and after the stimulation, the influence of attention remains to be evaluated in future studies. Only relatively young subjects were examined in this study. Since the capacity to modulate the SICI seems to be age-dependent (Smith et al., 2011), the results cannot be generalised to ageing subjects.

Furthermore, the history of specific repetitive motor activity or training was not assessed in the included participants, however, the cross-over design with paired statistical analysis was controlled for inter-individual differences among the subjects.

Finally, the stimulation coil was held at the optimal site in a mechanical frame using a previously published protocol without a neuronavigation system (Bareš et al., 2007; Kaňovský et al., 2003), which could have affected the accuracy of TMS (see also Rosenkranz and Rothwell, 2006a).

8.4. Study IV (HRV)

Participants were recruited from the most accessible study population, i.e., young healthy adults, whereas more pronounced autonomic changes might be observed in children and/or subjects with nervous system damage. The use of a single stimulation zone as opposed to stimulation of multiple sites at the same time has also been mentioned already. These issues may be addressed in future research.

9. Summary of effects of pressure stimulation and future directions

The Study I (fMRI during stimulation) confirmed that sustained manual pressure stimulation of the foot is associated with extensive activation throughout the sensorimotor system and, for the first time in the context of the pressure stimulation, that it is accompanied by equally prominent cross-modal deactivations, including the occipital cortices and sensorimotor representation of the upper limbs and face. The timecourse data confirm fast adaptation of the sensory processing system, but also reveal previously under-reported transient responses related to the stimulation offset. Furthermore, sustained pressure stimulation of the (active) site at the heel, which is used in RLT, elicited increased cortical activation in the primary motor representation of the stimulated limb and decreased activation in the posterior parietal cortex. Moreover, the stimulation of the active site was associated with a more sustained BOLD response in the insulo-opercular cortices and contralateral pons.

In Study II (fMRI of stimulation after-effects), it is shown that sustained pressure stimulation of the foot is associated with differential short-term changes in hand motor task-related activation and that these changes depend on the site of stimulation. These differential responses are located in the brainstem and cerebellum, namely in the bilateral, but predominantly contralateral PMRF and bilateral posterior cerebellar hemisphere and vermis. It is proposed that modulation of the PMRF, previously implicated in the postural control and generation of asymmetric motor patterns, might potentially mediate some therapeutic after-effects of RLT.

Based on Study III (TMS), it is further concluded that sustained pressure stimulation according to RLT specifically decreases the intracortical inhibition in the contralateral sensorimotor cortex. As in the case of the modulation of PMRF at the subcortical level, it is suggested that changes in intracortical inhibition may be related to the clinically observed motor after-effects of reflex locomotion therapy.

Finally, Study IV (HRV) demonstrated that heart rate variability parameters reflecting cardiac autonomic control changes were almost identical after both stimulation types. Whereas several markers indicated modest increase in parasympathetic activity, other measures suggested increased heart rate variability together with joint increase in activity of both vagal (parasympathetic) and sympathetic activity, without significant change in their relative contribution to cardiac autonomic control. Therefore, Study IV failed to demonstrate autonomic responses specific for the RLT.

As a secondary finding, presented studies demonstrated that, at comparable force levels, the stimulation at the skin area on the foot routinely used in RLT was perceived as more unpleasant than the stimulation of a nearby control site.

Overall, available data from behavioural, neurophysiological and neuroimaging studies, including this work, clearly demonstrate that the stimulation of peripheral afferents providing the sensation of sustained pressure may evoke complex involuntary responses, affect postural control, improve motor performance, locomotion, and facilitate neuroplastic changes of the motor cortical representations in the experimental setting. Despite the recent efforts to localise central structures potentially involved in these effects, just as many new questions arose as have been answered. The outstanding questions include the following:

1. What is the dynamic evolution of the cortico-subcortical activation patterns during continuous application of specific forms of pressure stimulation, such as RLT? Given the known slow development of responses (Bauer et al., 1988; Laufens et al., 1994; Vojta, 1968), a time-resolved analysis of the so-called dynamic connectivity (Calhoun et al., 2014) might prove useful for detection of slowly evolving states of brain function and their correlation with behaviour. To permit this, detailed behavioural and electrophysiological data (EMG) acquired simultaneously with fMRI are necessary prerequisites since the time-courses of individual responses may vary significantly across subjects. This might help us detect further brain structures which participate in these processes only transiently or whose activity gradually builds up. Such activations might be missed by classical approaches that effectively average the signal change across the whole imaging run (Calhoun et al., 2014).
2. Can we identify the brain structures that mediate the motor improvement? With current imaging data, unfortunately not. Follow-up studies with well-defined outcome measures of motor performance, both in healthy controls and patients

with motor system disorders, are warranted. Only then may improved performance or alleviated symptoms be directly linked to the involved brain structure. This is of paramount importance because such studies could finally draw clinically relevant conclusions, such as predictions of outcomes according to baseline fMRI data. Furthermore, by knowing the structures that are related to improvement, we may identify candidates for potential interventions that either enhance the effect of peripheral stimulation or interfere with it, such as repetitive TMS or transcranial direct current stimulation, eventually providing real-life causal data.

3. Knowing the cortical area or nuclei engaged by stimulation might not be enough to fully appreciate the brain network(s) underlying the motor after-effects and to understand interactions among the network nodes. Therefore, the next question is what are the pathways connecting the individual nodes, either those identified as potential sources of involuntary motor behaviour or those associated with motor after-effects (e.g., PMRF in RLT). By evaluating diffusion-weighted imaging data, one could identify the connecting pathways between these nodes to establish a task-specific connectome. With the knowledge of the network topology, modelling of causal relationships (i.e., effective connectivity) would be possible. Accurate network models might then serve as predictors of behavioural and clinical outcomes of various interventions.
4. Furthermore, knowing that muscle vibration research has demonstrated divergent results in different muscle groups (Rosenkranz and Rothwell, 2006a; Souron et al., 2017b) and study populations (Rosenkranz et al., 2005), the effects of pressure stimulation on corticomotor excitability should be studied using multiple stimulation sites and in patient cohorts with evidence of abnormal sensorimotor processing, such as dystonia (Rosenkranz et al., 2005). Likewise, patient populations, where RLT is routinely applied to alleviate neurological abnormalities (e.g., spasticity after stroke or in multiple sclerosis (Laufens et al., 2004)), would be candidates for studies correlating possible clinical improvement with cortical excitability changes.
5. Finally, the diverse effects of pressure stimulation should be further looked into. The postural responses to cutaneous stimulation of the foot sole (Kavounoudias et al., 2001; Roll et al., 2002), which are strikingly similar to the vibration-induced falling (Eklund, 1972), seem to be an especially interesting target for further evaluation. The documented manifold character of effects imposed by vibration, especially the manipulation of the internal body models and conscious percepts,

raises a fundamental question whether similar influence can be exerted via pressure stimulation. More well-controlled behavioural experiments tackling position sense and balance are needed in order to explore this area of interest.

To summarise, pressure stimulation is a feasible and widely used modality of peripheral stimulation in the clinical setting. Whereas other stimulation modalities, such as vibration, have already attracted a high amount of research interest and much evidence has been now gathered using state-of-the-art imaging techniques, allowing researchers to postulate fairly concrete hypotheses, similar research of pressure stimulation has barely entered the initial exploratory stage. This thesis highlights the recently published evidence for involvement of brainstem and cortical structures that potentially mediate some of the peculiar effects observed during sustained mechanical pressure stimulation. Inspired by the latest development, future directions are proposed to shed more light on these phenomena.

XI. REFERENCES

- Abraira, V.E., Ginty, D.D., 2013. The sensory neurons of touch. *Neuron* 79, 618–639. <https://doi.org/10.1016/j.neuron.2013.07.051>
- Adrian, E.D., 1940. Double representation of the feet in the sensory cortex of the cat. *J Physiol* 98, 16–18.
- Aimonetti, J.-M., Hospod, V., Roll, J.-P., Ribot-Ciscar, E., 2007. Cutaneous afferents provide a neuronal population vector that encodes the orientation of human ankle movements. *J. Physiol.* 580, 649–658. <https://doi.org/10.1113/jphysiol.2006.123075>
- Albanese, A., Abbruzzese, G., Dressler, D., Duzynski, W., Khatkova, S., Marti, M.J., Mir, P., Montecucco, C., Moro, E., Pinter, M., Relja, M., Roze, E., Skogseid, I.M., Timerbaeva, S., Tzoulis, C., 2015. Practical guidance for CD management involving treatment of botulinum toxin: a consensus statement. *J. Neurol.* 262, 2201–2213. <https://doi.org/10.1007/s00415-015-7703-x>
- Albanese, M.-C., Duerden, E.G., Bohotin, V., Rainville, P., Duncan, G.H., 2009. Differential effects of cognitive demand on human cortical activation associated with vibrotactile stimulation. *J. Neurophysiol.* 102, 1623–1631. <https://doi.org/10.1152/jn.91295.2008>
- Ali, S.O., Thomassen, M., Schulz, G.M., Hosey, L.A., Varga, M., Ludlow, C.L., Braun, A.R., 2006. Alterations in CNS activity induced by botulinum toxin treatment in spasmodic dysphonia: an H215O PET study. *J. Speech Lang. Hear. Res. JSLHR* 49, 1127–1146. [https://doi.org/10.1044/1092-4388\(2006/081\)](https://doi.org/10.1044/1092-4388(2006/081))
- Allam, N., Fonte-Boa, P.M. de O., Tomaz, C.A.B., Brasil-Neto, J.P., 2005. Lack of effect of botulinum toxin on cortical excitability in patients with cranial dystonia. *Clin. Neuropharmacol.* 28, 1–5. <https://doi.org/10.1097/01.wnf.0000152044.43822.42>
- Alstermark, B., Ekerot, C.-F., 2013. The lateral reticular nucleus: a precerebellar centre providing the cerebellum with overview and integration of motor functions at systems level. A new hypothesis. *J. Physiol.* 591, 5453–5458. <https://doi.org/10.1113/jphysiol.2013.256669>
- Amemiya, K., Naito, E., 2016. Importance of human right inferior frontoparietal network connected by inferior branch of superior longitudinal fasciculus tract in corporeal awareness of kinesthetic illusory movement. *Cortex J. Devoted Study Nerv. Syst. Behav.* 78, 15–30. <https://doi.org/10.1016/j.cortex.2016.01.017>
- Apkarian, A.V., Bushnell, M.C., Treede, R.-D., Zubieta, J.-K., 2005. Human brain mechanisms of pain perception and regulation in health and disease. *Eur. J. Pain Lond. Engl.* 9, 463–484. <https://doi.org/10.1016/j.ejpain.2004.11.001>
- Aprile, I., Di Sipio, E., Germanotta, M., Simbolotti, C., Padua, L., 2016. Muscle focal vibration in healthy subjects: evaluation of the effects on upper limb motor performance measured using a robotic device. *Eur. J. Appl. Physiol.* 116, 729–737. <https://doi.org/10.1007/s00421-016-3330-1>
- Asanuma, H., Larsen, K., Yumiya, H., 1980. Peripheral input pathways to the monkey motor cortex. *Exp. Brain Res.* 38, 349–355.

- Baker, J., Shoemaker, K.J., 2013. Effect of isometric handgrip exercise on heart rate variability with and without somatosensory stimulation. *FASEB J.* 27, lb833–lb833.
- Baliki, M.N., Apkarian, A.V., 2015. Nociception, Pain, Negative Moods, and Behavior Selection. *Neuron* 87, 474–491. <https://doi.org/10.1016/j.neuron.2015.06.005>
- Bandettini, P.A., 2001. Selection of the optimal pulse sequence for functional MRI, in: Jezzard, P., Matthews, P.M., Smith, S.M. (Eds.), *Functional MRI: An Introduction to Methods*. Oxford University Press, Oxford [England]; New York, pp. 123–143.
- Bard, C., Fleury, M., Teasdale, N., Paillard, J., Nougier, V., 1995. Contribution of proprioception for calibrating and updating the motor space. *Can. J. Physiol. Pharmacol.* 73, 246–254. <https://doi.org/10.1139/y95-035>
- Bareš, M., Kaňovský, P., Rektor, I., 2007. Disturbed intracortical excitability in early Parkinson's disease is l-DOPA dose related: a prospective 12-month paired TMS study. *Parkinsonism Relat. Disord.* 13, 489–494. <https://doi.org/10.1016/j.parkreldis.2007.02.008>
- Barthélémy, A., Gagnon, D.H., Duclos, C., 2016. Gait-like vibration training improves gait abilities: a case report of a 62-year-old person with a chronic incomplete spinal cord injury. *Spinal Cord Ser. Cases* 2, 16012. <https://doi.org/10.1038/scsandc.2016.12>
- Basaran, A., Emre, U., Karadavut, K.I., Bulmus, N., 2012. Somatosensory evoked potentials of hand muscles in stroke and their modification by botulinum toxin: a preliminary study. *J. Rehabil. Med.* 44, 541–546. <https://doi.org/10.2340/16501977-0978>
- Bauer, H., Appaji, G., Mundt, D., 1992. VOJTA neurophysiologic therapy. *Indian J. Pediatr.* 59, 37–51.
- Bauer, H., van de Lint, A., Soerjanto, R., Vojta, V., 1988. Kinesiologische EMG-Untersuchung bei Zerebralparese-Reflexlokomotion nach Vojta, in: Weinmann, H.-M. (Ed.), *Aktuelle Neuropädiatrie 1988*. Springer, Berlin, pp. 182–185.
- Bauer, H., Vojta, V., 1979. [Rehabilitation in meningomyelodysplasias]. *Monatsschrift Für Kinderheilkd.* 127, 351–353.
- Bauer, J., 1926. Das Kriechphänomen des Neugeborenen. *J. Mol. Med.* 5, 1468.
- Beckmann, C.F., DeLuca, M., Devlin, J.T., Smith, S.M., 2005. Investigations into resting-state connectivity using independent component analysis. *Philos. Trans. R. Soc. B Biol. Sci.* 360, 1001–1013. <https://doi.org/10.1098/rstb.2005.1634>
- Beckmann, C.F., Smith, S.M., 2004. Probabilistic independent component analysis for functional magnetic resonance imaging. *IEEE Trans. Med. Imaging* 23, 137–152. <https://doi.org/10.1109/TMI.2003.822821>
- Beissner, F., Meissner, K., Bär, K.-J., Napadow, V., 2013. The Autonomic Brain: An Activation Likelihood Estimation Meta-Analysis for Central Processing of Autonomic Function. *J. Neurosci.* 33, 10503–10511. <https://doi.org/10.1523/JNEUROSCI.1103-13.2013>
- Bergfeldt, U., Jonsson, T., Bergfeldt, L., Julin, P., 2015. Cortical activation changes and improved motor function in stroke patients after focal spasticity therapy--an interventional study applying repeated fMRI. *BMC Neurol.* 15, 52. <https://doi.org/10.1186/s12883-015-0306-4>
- Binkofski, F., Fink, G.R., Geyer, S., Buccino, G., Gruber, O., Shah, N.J., Taylor, J.G., Seitz,

- R.J., Zilles, K., Freund, H.-J., 2002. Neural activity in human primary motor cortex areas 4a and 4p is modulated differentially by attention to action. *J. Neurophysiol.* 88, 514–519. <https://doi.org/10.1152/jn.2002.88.1.514>
- Bliss, T.V., Lomo, T., 1973. Long-lasting potentiation of synaptic transmission in the dentate area of the anaesthetized rabbit following stimulation of the perforant path. *J. Physiol.* 232, 331–356. <https://doi.org/10.1113/jphysiol.1973.sp010273>
- Bobath, K., 1959. The effect of treatment by reflex-inhibition and facilitation of movement in cerebral palsy. *Folia Psychiatr. Neurol. Neurochir. Neerlandica* 62, 448–457.
- Bodegård, A., Geyer, S., Herath, P., Grefkes, C., Zilles, K., Roland, P.E., 2003. Somatosensory areas engaged during discrimination of steady pressure, spring strength, and kinesthesia. *Hum. Brain Mapp.* 20, 103–115. <https://doi.org/10.1002/hbm.10125>
- Boecker, H., Ceballos-Baumann, A., Bartenstein, P., Weindl, A., Siebner, H.R., Fassbender, T., Munz, F., Schwaiger, M., Conrad, B., 1999. Sensory processing in Parkinson's and Huntington's disease. *Brain* 122, 1651–1665. <https://doi.org/10.1093/brain/122.9.1651>
- Boendermaker, B., Meier, M.L., Luechinger, R., Humphreys, B.K., Hotz-Boendermaker, S., 2014. The cortical and cerebellar representation of the lumbar spine. *Hum. Brain Mapp.* 35, 3962–3971. <https://doi.org/10.1002/hbm.22451>
- Bongiovanni, L.G., Hagbarth, K.E., Stjernberg, L., 1990. Prolonged muscle vibration reducing motor output in maximal voluntary contractions in man. *J. Physiol.* 423, 15–26.
- Boorman, L., Kennerley, A.J., Johnston, D., Jones, M., Zheng, Y., Redgrave, P., Berwick, J., 2010. Negative blood oxygen level dependence in the rat: a model for investigating the role of suppression in neurovascular coupling. *J. Neurosci. Off. J. Soc. Neurosci.* 30, 4285–4294. <https://doi.org/10.1523/JNEUROSCI.6063-09.2010>
- Boroojerdi, B., Cohen, L.G., Hallett, M., 2003. Effects of botulinum toxin on motor system excitability in patients with writer's cramp. *Neurology* 61, 1546–1550. <https://doi.org/10.1212/01.wnl.0000095965.36574.0f>
- Bove, M., Diverio, M., Pozzo, T., Schieppati, M., 2001. Neck muscle vibration disrupts steering of locomotion. *J. Appl. Physiol. Bethesda Md* 91, 581–588. <https://doi.org/10.1152/jappl.2001.91.2.581>
- Brammer, M.J., 2001. Head motion and its correction, in: Jezzard, P., Matthews, P.M., Smith, S.M. (Eds.), *Functional MRI: An Introduction to Methods*. Oxford University Press, Oxford [England]; New York, pp. 243–250.
- Brasil-Neto, J.P., Cohen, L.G., Pascual-Leone, A., Jabir, F.K., Wall, R.T., Hallett, M., 1992. Rapid reversible modulation of human motor outputs after transient deafferentation of the forearm: a study with transcranial magnetic stimulation. *Neurology* 42, 1302–1306. <https://doi.org/10.1212/wnl.42.7.1302>
- Brasil-Neto, J.P., Valls-Solé, J., Pascual-Leone, A., Cammarota, A., Amassian, V.E., Cracco, R., Maccabee, P., Cracco, J., Hallett, M., Cohen, L.G., 1993. Rapid modulation of human cortical motor outputs following ischaemic nerve block. *Brain J. Neurol.* 116 (Pt 3), 511–525. <https://doi.org/10.1093/brain/116.3.511>
- Bretas, R.V., Taoka, M., Suzuki, H., Iriki, A., 2020. Secondary somatosensory cortex of

- primates: beyond body maps, toward conscious self-in-the-world maps. *Exp. Brain Res.* 238, 259–272. <https://doi.org/10.1007/s00221-020-05727-9>
- Brodal, A., Jansen, J., 1941. Beitrag zur Kenntnis der spino-cerebellaren Bahnen beim Menschen. *Anat Anz* 91, 185–195.
- Brouwer, G.J., Arnedo, V., Offen, S., Heeger, D.J., Grant, A.C., 2015. Normalization in human somatosensory cortex. *J. Neurophysiol.* 114, 2588–2599. <https://doi.org/10.1152/jn.00939.2014>
- Buonomano, D.V., Merzenich, M.M., 1998. Cortical plasticity: from synapses to maps. *Annu. Rev. Neurosci.* 21, 149–186. <https://doi.org/10.1146/annurev.neuro.21.1.149>
- Burciu, R.G., Hess, C.W., Coombes, S.A., Ofori, E., Shukla, P., Chung, J.W., McFarland, N.R., Wagle Shukla, A., Okun, M.S., Vaillancourt, D.E., 2017. Functional activity of the sensorimotor cortex and cerebellum relates to cervical dystonia symptoms. *Hum. Brain Mapp.* 38, 4563–4573. <https://doi.org/10.1002/hbm.23684>
- Burke, D., Hagbarth, K.E., Löfstedt, L., Wallin, B.G., 1976. The responses of human muscle spindle endings to vibration of non-contracting muscles. *J. Physiol.* 261, 673–693.
- Burton, H., Videen, T.O., Raichle, M.E., 1993. Tactile-Vibration-Activated Foci in Insular and Parietal-Opercular Cortex Studied with Positron Emission Tomography: Mapping the Second Somatosensory Area in Humans. *Somatosens. Mot. Res.* 10, 297–308. <https://doi.org/10.3109/08990229309028839>
- Bütefisch, C.M., 2006. Neurobiological bases of rehabilitation. *Neurol. Sci. Off. J. Ital. Neurol. Soc. Ital. Soc. Clin. Neurophysiol.* 27 Suppl 1, S18-23. <https://doi.org/10.1007/s10072-006-0540-z>
- Butterworth, S., Francis, S., Kelly, E., McGlone, F., Bowtell, R., Sawle, G.V., 2003. Abnormal cortical sensory activation in dystonia: an fMRI study. *Mov. Disord. Off. J. Mov. Disord. Soc.* 18, 673–682. <https://doi.org/10.1002/mds.10416>
- Byrnes, M.L., Mastaglia, F.L., Walters, S.E., Archer, S.-A.R., Thickbroom, G.W., 2005. Primary writing tremor: motor cortex reorganisation and disinhibition. *J. Clin. Neurosci. Off. J. Neurosurg. Soc. Australas.* 12, 102–104. <https://doi.org/10.1016/j.jocn.2004.08.004>
- Byrnes, M.L., Thickbroom, G.W., Wilson, S.A., Sacco, P., Shipman, J.M., Stell, R., Mastaglia, F.L., 1998. The corticomotor representation of upper limb muscles in writer's cramp and changes following botulinum toxin injection. *Brain J. Neurol.* 121 (Pt 5), 977–988. <https://doi.org/10.1093/brain/121.5.977>
- Caleo, M., Restani, L., 2018. Exploiting Botulinum Neurotoxins for the Study of Brain Physiology and Pathology. *Toxins* 10. <https://doi.org/10.3390/toxins10050175>
- Calhoun, V.D., Miller, R., Pearlson, G., Adalı, T., 2014. The chronnectome: time-varying connectivity networks as the next frontier in fMRI data discovery. *Neuron* 84, 262–274. <https://doi.org/10.1016/j.neuron.2014.10.015>
- Caliński, T., Harabasz, J., 1974. A dendrite method for cluster analysis. *Commun. Stat.-Theory Methods* 3, 1–27.
- Calvin-Figuère, S., Romaiguère, P., Gilhodes, J.-C., Roll, J.-P., 1999. Antagonist motor responses correlate with kinesthetic illusions induced by tendon vibration. *Exp. Brain Res.* 124, 342–350. <https://doi.org/10.1007/s002210050631>

- Capaday, C., Cooke, J.D., 1981. The effects of muscle vibration on the attainment of intended final position during voluntary human arm movements. *Exp. Brain Res.* 42, 228–230. <https://doi.org/10.1007/bf00236912>
- Castrop, F., Dresel, C., Hennenlotter, A., Zimmer, C., Haslinger, B., 2012. Basal ganglia-premotor dysfunction during movement imagination in writer's cramp. *Mov. Disord. Off. J. Mov. Disord. Soc.* 27, 1432–1439. <https://doi.org/10.1002/mds.24944>
- Ceballos-Baumann, A.O., Passingham, R.E., Marsden, C.D., Brooks, D.J., 1995a. Motor reorganization in acquired hemidystonia. *Ann. Neurol.* 37, 746–757. <https://doi.org/10.1002/ana.410370608>
- Ceballos-Baumann, A.O., Passingham, R.E., Warner, T., Playford, E.D., Marsden, C.D., Brooks, D.J., 1995b. Overactive prefrontal and underactive motor cortical areas in idiopathic dystonia. *Ann. Neurol.* 37, 363–372. <https://doi.org/10.1002/ana.410370313>
- Ceballos-Baumann, A.O., Sheean, G., Passingham, R.E., Marsden, C.D., Brooks, D.J., 1997. Botulinum toxin does not reverse the cortical dysfunction associated with writer's cramp. A PET study. *Brain J. Neurol.* 120 (Pt 4), 571–582. <https://doi.org/10.1093/brain/120.4.571>
- Čemusová, J., Pánek, D., Pavlů, D., 2011. Možnosti propojení aktivního a pasivního přístupu ve fyzioterapii. *Rehabil. Fyzikální Lékařství* 18, 161–166.
- Chang, C.-L., Weber, D.J., Munin, M.C., 2015. Changes in Cerebellar Activation After Onabotulinumtoxin A Injections for Spasticity After Chronic Stroke: A Pilot Functional Magnetic Resonance Imaging Study. *Arch. Phys. Med. Rehabil.* 96, 2007–2016. <https://doi.org/10.1016/j.apmr.2015.07.007>
- Charlton, C.S., Ridding, M.C., Thompson, P.D., Miles, T.S., 2003. Prolonged peripheral nerve stimulation induces persistent changes in excitability of human motor cortex. *J. Neurol. Sci.* 208, 79–85.
- Chen, J.J., 2019. Functional MRI of brain physiology in aging and neurodegenerative diseases. *NeuroImage* 187, 209–225. <https://doi.org/10.1016/j.neuroimage.2018.05.050>
- Chen, R., Corwell, B., Yaseen, Z., Hallett, M., Cohen, L.G., 1998. Mechanisms of cortical reorganization in lower-limb amputees. *J. Neurosci. Off. J. Soc. Neurosci.* 18, 3443–3450.
- Chen, R., Lozano, A.M., Ashby, P., 1999. Mechanism of the silent period following transcranial magnetic stimulation. Evidence from epidural recordings. *Exp. Brain Res.* 128, 539–542. <https://doi.org/10.1007/s002210050878>
- Chipchase, L.S., Schabrun, S.M., Hodges, P.W., 2011. Peripheral electrical stimulation to induce cortical plasticity: a systematic review of stimulus parameters. *Clin. Neurophysiol.* 122, 456–463. <https://doi.org/10.1016/j.clinph.2010.07.025>
- Chouinard, P.A., Paus, T., 2006. The primary motor and premotor areas of the human cerebral cortex. *Neurosci. Rev. J. Bringing Neurobiol. Neurol. Psychiatry* 12, 143–152. <https://doi.org/10.1177/1073858405284255>
- Christova, M., Rafolt, D., Golaszewski, S., Gallasch, E., 2011. Outlasting corticomotor excitability changes induced by 25 Hz whole-hand mechanical stimulation. *Eur. J. Appl. Physiol.* 111, 3051–3059. <https://doi.org/10.1007/s00421-011-1933-0>

- Christova, M., Rafolt, D., Mayr, W., Wilfling, B., Gallasch, E., 2010. Vibration stimulation during non-fatiguing tonic contraction induces outlasting neuroplastic effects. *J. Electromyogr. Kinesiol. Off. J. Int. Soc. Electrophysiol. Kinesiol.* 20, 627–635. <https://doi.org/10.1016/j.jelekin.2010.03.001>
- Chung, Y.G., Han, S.W., Kim, H.-S., Chung, S.-C., Park, J.-Y., Wallraven, C., Kim, S.-P., 2015. Adaptation of cortical activity to sustained pressure stimulation on the fingertip. *BMC Neurosci.* 16, 71. <https://doi.org/10.1186/s12868-015-0207-x>
- Chung, Y.G., Han, S.W., Kim, H.-S., Chung, S.-C., Park, J.-Y., Wallraven, C., Kim, S.-P., 2014. Intra- and inter-hemispheric effective connectivity in the human somatosensory cortex during pressure stimulation. *BMC Neurosci.* 15, 43. <https://doi.org/10.1186/1471-2202-15-43>
- Chung, Y.G., Kim, J., Han, S.W., Kim, H.-S., Choi, M.H., Chung, S.-C., Park, J.-Y., Kim, S.-P., 2013. Frequency-dependent patterns of somatosensory cortical responses to vibrotactile stimulation in humans: a fMRI study. *Brain Res.* 1504, 47–57. <https://doi.org/10.1016/j.brainres.2013.02.003>
- Churchill, N.W., Yourganov, G., Oder, A., Tam, F., Graham, S.J., Strother, S.C., 2012. Optimizing Preprocessing and Analysis Pipelines for Single-Subject fMRI: 2. Interactions with ICA, PCA, Task Contrast and Inter-Subject Heterogeneity. *PLOS ONE* 7, e31147. <https://doi.org/10.1371/journal.pone.0031147>
- Cicinelli, P., Traversa, R., Rossini, P.M., 1997. Post-stroke reorganization of brain motor output to the hand: a 2-4 month follow-up with focal magnetic transcranial stimulation. *Electroencephalogr. Clin. Neurophysiol.* 105, 438–450. [https://doi.org/10.1016/s0924-980x\(97\)00052-0](https://doi.org/10.1016/s0924-980x(97)00052-0)
- Cignetti, F., Vaugoyeau, M., Nazarian, B., Roth, M., Anton, J.-L., Assaiante, C., 2014. Boosted activation of right inferior frontoparietal network: A basis for illusory movement awareness. *Hum. Brain Mapp.* 35, 5166–5178. <https://doi.org/10.1002/hbm.22541>
- Classen, J., Liepert, J., Wise, S.P., Hallett, M., Cohen, L.G., 1998. Rapid Plasticity of Human Cortical Movement Representation Induced by Practice. *J. Neurophysiol.* 79, 1117–1123.
- Claus, D., Mills, K.R., Murray, N.M., 1988. Facilitation of muscle responses to magnetic brain stimulation by mechanical stimuli in man. *Exp. Brain Res.* 71, 273–278.
- Cochrane, D.J., 2011. The Potential Neural Mechanisms of Acute Indirect Vibration. *J. Sports Sci. Med.* 10, 19–30.
- Coghill, R.C., Talbot, J.D., Evans, A.C., Meyer, E., Gjedde, A., Bushnell, M.C., Duncan, G.H., 1994. Distributed processing of pain and vibration by the human brain. *J. Neurosci. Off. J. Soc. Neurosci.* 14, 4095–4108.
- Cohen, L.G., Bandinelli, S., Findley, T.W., Hallett, M., 1991. Motor reorganization after upper limb amputation in man. A study with focal magnetic stimulation. *Brain J. Neurol.* 114 (Pt 1B), 615–627. <https://doi.org/10.1093/brain/114.1.615>
- Colebatch, J.G., Sayer, R.J., Porter, R., White, O.B., 1990. Responses of monkey precentral neurones to passive movements and phasic muscle stretch: relevance to man. *Electroencephalogr. Clin. Neurophysiol.* 75, 44–55. <https://doi.org/10.1016/0013->

- Collins, D.F., Refshauge, K.M., Gandevia, S.C., 2000. Sensory integration in the perception of movements at the human metacarpophalangeal joint. *J. Physiol.* 529 Pt 2, 505–515. <https://doi.org/10.1111/j.1469-7793.2000.00505.x>
- Conforto, A.B., Kaelin-Lang, A., Cohen, L.G., 2002. Increase in hand muscle strength of stroke patients after somatosensory stimulation. *Ann. Neurol.* 51, 122–125.
- Conrad, M.O., Scheidt, R.A., Schmit, B.D., 2011. Effects of wrist tendon vibration on arm tracking in people poststroke. *J. Neurophysiol.* 106, 1480–1488. <https://doi.org/10.1152/jn.00404.2010>
- Contarino, M.F., Kruisdijk, J.J.M., Koster, L., Ongerboer de Visser, B.W., Speelman, J.D., Koelman, J.H.T.M., 2007. Sensory integration in writer's cramp: comparison with controls and evaluation of botulinum toxin effect. *Clin. Neurophysiol. Off. J. Int. Fed. Clin. Neurophysiol.* 118, 2195–2206. <https://doi.org/10.1016/j.clinph.2007.07.004>
- Cordo, P., Gandevia, S.C., Hales, J.P., Burke, D., Laird, G., 1993. Force and displacement-controlled tendon vibration in humans. *Electroencephalogr. Clin. Neurophysiol.* 89, 45–53. [https://doi.org/10.1016/0168-5597\(93\)90084-3](https://doi.org/10.1016/0168-5597(93)90084-3)
- Cordo, P., Gurfinkel, V.S., Bevan, L., Kerr, G.K., 1995. Proprioceptive consequences of tendon vibration during movement. *J. Neurophysiol.* 74, 1675–1688. <https://doi.org/10.1152/jn.1995.74.4.1675>
- Cordo, P.J., Gurfinkel, V.S., Brumagne, S., Flores-Vieira, C., 2005. Effect of slow, small movement on the vibration-evoked kinesthetic illusion. *Exp. Brain Res.* 167, 324–334. <https://doi.org/10.1007/s00221-005-0034-x>
- Corp, D.T., Joutsa, J., Darby, R.R., Delnooz, C.C.S., van de Warrenburg, B.P.C., Cooke, D., Prudente, C.N., Ren, J., Reich, M.M., Batla, A., Bhatia, K.P., Jinnah, H.A., Liu, H., Fox, M.D., 2019. Network localization of cervical dystonia based on causal brain lesions. *Brain J. Neurol.* 142, 1660–1674. <https://doi.org/10.1093/brain/awz112>
- Cotey, D., Hornby, T.G., Gordon, K.E., Schmit, B.D., 2009. Increases in muscle activity produced by vibration of the thigh muscles during locomotion in chronic human spinal cord injury. *Exp. Brain Res.* 196, 361–374. <https://doi.org/10.1007/s00221-009-1855-9>
- Craske, B., 1977. Perception of impossible limb positions induced by tendon vibration. *Science* 196, 71–73. <https://doi.org/10.1126/science.841342>
- Currà, A., Trompetto, C., Abbruzzese, G., Berardelli, A., 2004. Central effects of botulinum toxin type A: evidence and supposition. *Mov. Disord. Off. J. Mov. Disord. Soc.* 19 Suppl 8, S60-64. <https://doi.org/10.1002/mds.20011>
- Dale, A.M., 1999. Optimal experimental design for event-related fMRI. *Hum. Brain Mapp.* 8, 109–114.
- Darian-Smith, C., Darian-Smith, I., 1993. Thalamic projections to areas 3a, 3b, and 4 in the sensorimotor cortex of the mature and infant macaque monkey. *J. Comp. Neurol.* 335, 173–199. <https://doi.org/10.1002/cne.903350204>
- Darian-Smith, C., Darian-Smith, I., Burman, K., Ratcliffe, N., 1993. Ipsilateral cortical projections to areas 3a, 3b, and 4 in the macaque monkey. *J. Comp. Neurol.* 335, 200–213. <https://doi.org/10.1002/cne.903350205>

- D'Ascanio, P., Gahéry, Y., Pompeiano, O., Stampacchia, G., 1986. Effects of pressure stimulation of the body surface on posture and vestibulospinal reflexes. *Arch. Ital. Biol.* 124, 43–63.
- De Nunzio, A.M., Grasso, M., Nardone, A., Godi, M., Schieppati, M., 2010. Alternate rhythmic vibratory stimulation of trunk muscles affects walking cadence and velocity in Parkinson's disease. *Clin. Neurophysiol. Off. J. Int. Fed. Clin. Neurophysiol.* 121, 240–247. <https://doi.org/10.1016/j.clinph.2009.10.018>
- de Vries, P.M., Johnson, K.A., de Jong, B.M., Gieteling, E.W., Bohning, D.E., George, M.S., Leenders, K.L., 2008. Changed patterns of cerebral activation related to clinically normal hand movement in cervical dystonia. *Clin. Neurol. Neurosurg.* 110, 120–128. <https://doi.org/10.1016/j.clineuro.2007.09.020>
- Dehghan Nayyeri, M., Burgmer, M., Pfliegerer, B., 2019. Impact of pressure as a tactile stimulus on working memory in healthy participants. *PloS One* 14, e0213070. <https://doi.org/10.1371/journal.pone.0213070>
- Delhaye, B.P., Long, K.H., Bensmaia, S.J., 2018. Neural Basis of Touch and Proprioception in Primate Cortex. *Compr. Physiol.* 8, 1575–1602. <https://doi.org/10.1002/cphy.c170033>
- Delmas, P., Hao, J., Rodat-Despoix, L., 2011. Molecular mechanisms of mechanotransduction in mammalian sensory neurons. *Nat. Rev. Neurosci.* 12, 139–153. <https://doi.org/10.1038/nrn2993>
- Delnooz, C.C.S., Helmich, R.C., Toni, I., van de Warrenburg, B.P.C., 2012. Reduced parietal connectivity with a premotor writing area in writer's cramp. *Mov. Disord. Off. J. Mov. Disord. Soc.* 27, 1425–1431. <https://doi.org/10.1002/mds.25029>
- Delnooz, C.C.S., Pasman, J.W., Beckmann, C.F., van de Warrenburg, B.P.C., 2015. Altered striatal and pallidal connectivity in cervical dystonia. *Brain Struct. Funct.* 220, 513–523. <https://doi.org/10.1007/s00429-013-0671-y>
- Delnooz, C.C.S., Pasman, J.W., Beckmann, C.F., van de Warrenburg, B.P.C., 2013. Task-free functional MRI in cervical dystonia reveals multi-network changes that partially normalize with botulinum toxin. *PloS One* 8, e62877. <https://doi.org/10.1371/journal.pone.0062877>
- Demetriou, L., Kowalczyk, O.S., Tyson, G., Bello, T., Newbould, R.D., Wall, M.B., 2018. A comprehensive evaluation of increasing temporal resolution with multiband-accelerated protocols and effects on statistical outcome measures in fMRI. *NeuroImage* 176, 404–416. <https://doi.org/10.1016/j.neuroimage.2018.05.011>
- Desikan, R.S., Ségonne, F., Fischl, B., Quinn, B.T., Dickerson, B.C., Blacker, D., Buckner, R.L., Dale, A.M., Maguire, R.P., Hyman, B.T., Albert, M.S., Killiany, R.J., 2006. An automated labeling system for subdividing the human cerebral cortex on MRI scans into gyral based regions of interest. *NeuroImage* 31, 968–980. <https://doi.org/10.1016/j.neuroimage.2006.01.021>
- Devanne, H., Degardin, A., Tyvaert, L., Bocquillon, P., Houdayer, E., Manceaux, A., Derambure, P., Cassim, F., 2009. Afferent-induced facilitation of primary motor cortex excitability in the region controlling hand muscles in humans. *Eur. J. Neurosci.* 30, 439–448. <https://doi.org/10.1111/j.1460-9568.2009.06815.x>

- Devanne, H., Lavoie, B.A., Capaday, C., 1997. Input-output properties and gain changes in the human corticospinal pathway. *Exp. Brain Res.* 114, 329–338. <https://doi.org/10.1007/pl00005641>
- Devor, A., Hillman, E.M.C., Tian, P., Waeber, C., Teng, I.C., Ruvinskaya, L., Shalinsky, M.H., Zhu, H., Haslinger, R.H., Narayanan, S.N., Ulbert, I., Dunn, A.K., Lo, E.H., Rosen, B.R., Dale, A.M., Kleinfeld, D., Boas, D.A., 2008. Stimulus-induced changes in blood flow and 2-deoxyglucose uptake dissociate in ipsilateral somatosensory cortex. *J. Neurosci. Off. J. Soc. Neurosci.* 28, 14347–14357. <https://doi.org/10.1523/JNEUROSCI.4307-08.2008>
- di Pellegrino, G., Fadiga, L., Fogassi, L., Gallese, V., Rizzolatti, G., 1992. Understanding motor events: a neurophysiological study. *Exp. Brain Res.* 91, 176–180. <https://doi.org/10.1007/bf00230027>
- Di Pino, G., Pellegrino, G., Assenza, G., Capone, F., Ferreri, F., Formica, D., Ranieri, F., Tombini, M., Ziemann, U., Rothwell, J.C., Di Lazzaro, V., 2014. Modulation of brain plasticity in stroke: a novel model for neurorehabilitation. *Nat. Rev. Neurol.* 10, 597–608. <https://doi.org/10.1038/nrneurol.2014.162>
- Diedrichsen, J., Maderwald, S., Küper, M., Thürling, M., Rabe, K., Gizewski, E.R., Ladd, M.E., Timmann, D., 2011. Imaging the deep cerebellar nuclei: a probabilistic atlas and normalization procedure. *NeuroImage* 54, 1786–1794. <https://doi.org/10.1016/j.neuroimage.2010.10.035>
- Diener, H.C., Dichgans, J., Guschlbauer, B., Mau, H., 1984. The significance of proprioception on postural stabilization as assessed by ischemia. *Brain Res.* 296, 103–109. [https://doi.org/10.1016/0006-8993\(84\)90515-8](https://doi.org/10.1016/0006-8993(84)90515-8)
- Dilena, A., Todd, G., Berryman, C., Rio, E., Stanton, T.R., 2019. What is the effect of bodily illusions on corticomotoneuronal excitability? A systematic review. *PloS One* 14, e0219754. <https://doi.org/10.1371/journal.pone.0219754>
- Dimitrijević, L., Jakubi, B.J., 2005. The importance of early diagnosis and early physical treatment of cerebral palsy. *Facta Univ. Ser. Med. Biol.* 12, 119–122.
- Dincher, A., Schwarz, M., Wydra, G., 2019. Analysis of the Effects of Whole-Body Vibration in Parkinson Disease - Systematic Review and Meta-Analysis. *PM R* 11, 640–653. <https://doi.org/10.1002/pmrj.12094>
- Ding, Y.M., Kastin, A.J., Pan, W.H., 2005. Neural plasticity after spinal cord injury. *Curr. Pharm. Des.* 11, 1441–1450. <https://doi.org/10.2174/1381612053507855>
- Donaldson, D.I., Buckner, R.L., 2001. Effective paradigm design, in: Jezzard, P., Matthews, P.M., Smith, S.M. (Eds.), *Functional MRI: An Introduction to Methods*. Oxford University Press, Oxford [England]; New York, pp. 177–195.
- Donoghue, J.P., 1995. Plasticity of adult sensorimotor representations. *Curr. Opin. Neurobiol.* 5, 749–754. [https://doi.org/10.1016/0959-4388\(95\)80102-2](https://doi.org/10.1016/0959-4388(95)80102-2)
- Dorňák, T., Justanová, M., Konvalinková, R., Říha, M., Mužík, J., Hoskovicová, M., Srp, M., Navrátilová, D., Otruba, P., Gál, O., Svobodová, I., Dušek, L., Bareš, M., Kaňovský, P., Jech, R., 2019. Prevalence and evolution of spasticity in patients suffering from first-ever stroke with carotid origin: a prospective, longitudinal study. *Eur. J. Neurol.* 26, 880–886. <https://doi.org/10.1111/ene.13902>

- Drake, L.R., Hillmer, A.T., Cai, Z., 2020. Approaches to PET Imaging of Glioblastoma. *Mol. Basel Switz.* 25. <https://doi.org/10.3390/molecules25030568>
- Dresel, C., Bayer, F., Castrop, F., Rimpau, C., Zimmer, C., Haslinger, B., 2011. Botulinum toxin modulates basal ganglia but not deficient somatosensory activation in orofacial dystonia. *Mov. Disord. Off. J. Mov. Disord. Soc.* 26, 1496–1502. <https://doi.org/10.1002/mds.23497>
- Dresel, C., Haslinger, B., Castrop, F., Wohlschlaeger, A.M., Ceballos-Baumann, A.O., 2006. Silent event-related fMRI reveals deficient motor and enhanced somatosensory activation in orofacial dystonia. *Brain J. Neurol.* 129, 36–46. <https://doi.org/10.1093/brain/awh665>
- Dresel, C., Li, Y., Wilzeck, V., Castrop, F., Zimmer, C., Haslinger, B., 2014. Multiple changes of functional connectivity between sensorimotor areas in focal hand dystonia. *J. Neurol. Neurosurg. Psychiatry* 85, 1245–1252. <https://doi.org/10.1136/jnnp-2013-307127>
- Dressler, D., Bhidayasiri, R., Bohlega, S., Chahidi, A., Chung, T.M., Ebke, M., Jacinto, L.J., Kaji, R., Koçer, S., Kanovsky, P., Micheli, F., Orlova, O., Paus, S., Pirtosek, Z., Relja, M., Rosales, R.L., Sagástegui-Rodríguez, J.A., Schoenle, P.W., Shahidi, G.A., Timerbaeva, S., Walter, U., Saberi, F.A., 2017. Botulinum toxin therapy for treatment of spasticity in multiple sclerosis: review and recommendations of the IAB-Interdisciplinary Working Group for Movement Disorders task force. *J. Neurol.* 264, 112–120. <https://doi.org/10.1007/s00415-016-8304-z>
- Dyson, K.S., Miron, J.-P., Drew, T., 2014. Differential modulation of descending signals from the reticulospinal system during reaching and locomotion. *J. Neurophysiol.* 112, 2505–2528. <https://doi.org/10.1152/jn.00188.2014>
- Edin, B.B., 1992. Quantitative analysis of static strain sensitivity in human mechanoreceptors from hairy skin. *J. Neurophysiol.* 67, 1105–1113. <https://doi.org/10.1152/jn.1992.67.5.1105>
- Edin, B.B., Abbs, J.H., 1991. Finger movement responses of cutaneous mechanoreceptors in the dorsal skin of the human hand. *J. Neurophysiol.* 65, 657–670. <https://doi.org/10.1152/jn.1991.65.3.657>
- Ehrsson, H.H., Kito, T., Sadato, N., Passingham, R.E., Naito, E., 2005. Neural Substrate of Body Size: Illusory Feeling of Shrinking of the Waist. *PLOS Biol.* 3, e412. <https://doi.org/10.1371/journal.pbio.0030412>
- Eickhoff, S.B., Paus, T., Caspers, S., Grosbras, M.-H., Evans, A.C., Zilles, K., Amunts, K., 2007. Assignment of functional activations to probabilistic cytoarchitectonic areas revisited. *NeuroImage* 36, 511–521. <https://doi.org/10.1016/j.neuroimage.2007.03.060>
- Eickhoff, S.B., Schleicher, A., Zilles, K., Amunts, K., 2006. The human parietal operculum. I. Cytoarchitectonic mapping of subdivisions. *Cereb. Cortex N. Y. N* 1991 16, 254–267. <https://doi.org/10.1093/cercor/bhi105>
- Eklund, G., 1972. General features of vibration-induced effects on balance. *Ups. J. Med. Sci.* 77, 112–124. <https://doi.org/10.1517/03009734000000016>
- Ernst, G., 2014. Heart Rate Variability. Springer-Verlag, London.
- Fang, P.-C., Stepniewska, I., Kaas, J.H., 2006. The thalamic connections of motor, premotor,

- and prefrontal areas of cortex in a prosimian primate (*Otolemur garnetti*). *Neuroscience* 143, 987–1020. <https://doi.org/10.1016/j.neuroscience.2006.08.053>
- Farabet, A., Souron, R., Millet, G.Y., Lapole, T., 2016. Changes in tibialis anterior corticospinal properties after acute prolonged muscle vibration. *Eur. J. Appl. Physiol.* 116, 1197–1205. <https://doi.org/10.1007/s00421-016-3378-y>
- Fattorini, L., Ferraresi, A., Rodio, A., Azzena, G.B., Filippi, G.M., 2006. Motor performance changes induced by muscle vibration. *Eur. J. Appl. Physiol.* 98, 79–87. <https://doi.org/10.1007/s00421-006-0250-5>
- Fay, T., 1954a. Rehabilitation of patients with spastic paralysis. *J. Int. Coll. Surg.* 22, 200–203.
- Fay, T., 1954b. The use of pathological and unlocking reflexes in the rehabilitation of spastics. *Am. J. Phys. Med.* 33, 347–352.
- Feiwell, R.J., Black, K.J., McGee-Minnich, L.A., Snyder, A.Z., MacLeod, A.M., Perlmutter, J.S., 1999. Diminished regional cerebral blood flow response to vibration in patients with blepharospasm. *Neurology* 52, 291–297. <https://doi.org/10.1212/wnl.52.2.291>
- Feldman, D.E., 2009. Synaptic Mechanisms for Plasticity in Neocortex. *Annu. Rev. Neurosci.* 32, 33–55. <https://doi.org/10.1146/annurev.neuro.051508.135516>
- Feldman, D.E., 2000. Timing-based LTP and LTD at vertical inputs to layer II/III pyramidal cells in rat barrel cortex. *Neuron* 27, 45–56. [https://doi.org/10.1016/s0896-6273\(00\)00008-8](https://doi.org/10.1016/s0896-6273(00)00008-8)
- Fernandez-Del-Olmo, M., Alvarez-Sauco, M., Koch, G., Franca, M., Marquez, G., Sanchez, J.A., Acero, R.M., Rothwell, J.C., 2008. How repeatable are the physiological effects of TENS? *Clin. Neurophysiol. Off. J. Int. Fed. Clin. Neurophysiol.* 119, 1834–1839. <https://doi.org/10.1016/j.clinph.2008.04.002>
- Filip, P., Gallea, C., Lehericy, S., Bertasi, E., Popa, T., Mareček, R., Lungu, O.V., Kašpárek, T., Vaníček, J., Bareš, M., 2017. Disruption in cerebellar and basal ganglia networks during a visuospatial task in cervical dystonia. *Mov. Disord. Off. J. Mov. Disord. Soc.* <https://doi.org/10.1002/mds.26930>
- Filip, P., Lungu, O.V., Bareš, M., 2013. Dystonia and the cerebellum: a new field of interest in movement disorders? *Clin. Neurophysiol. Off. J. Int. Fed. Clin. Neurophysiol.* 124, 1269–1276. <https://doi.org/10.1016/j.clinph.2013.01.003>
- Floel, A., Nagorsen, U., Werhahn, K.J., Ravindran, S., Birbaumer, N., Knecht, S., Cohen, L.G., 2004. Influence of somatosensory input on motor function in patients with chronic stroke. *Ann. Neurol.* 56, 206–212. <https://doi.org/10.1002/ana.20170>
- Foerster, O., 1936. Sensible corticale Felder, in: *Handbuch Der Neurologie*. Springer-Verlag, Berlin, pp. 358–448.
- Foerster, O., 1933. The Dermatomes in Man. *Brain* 56, 1–39. <https://doi.org/10.1093/brain/56.1.1>
- Formby, C., Morgan, L.N., Forrest, T.G., Raney, J.J., 1992. The role of frequency selectivity in measures of auditory and vibrotactile temporal resolution. *J. Acoust. Soc. Am.* 91, 293–305. <https://doi.org/10.1121/1.402772>
- Fornier-Cordero, A., Steyvers, M., Levin, O., Alaerts, K., Swinnen, S.P., 2008. Changes in corticomotor excitability following prolonged muscle tendon vibration. *Behav.*

- Brain Res. 190, 41–49. <https://doi.org/10.1016/j.bbr.2008.02.019>
- Fourment, A., Chenneville, J.M., Belhaj-Saïf, A., Maton, B., 1996. Responses of motor cortical cells to short trains of vibration. *Exp. Brain Res.* 111, 208–214. <https://doi.org/10.1007/bf00227298>
- Fox, P.T., Burton, H., Raichle, M.E., 1987. Mapping human somatosensory cortex with positron emission tomography. *J. Neurosurg.* 67, 34–43. <https://doi.org/10.3171/jns.1987.67.1.0034>
- Fox, P.T., Perlmutter, J.S., Raichle, M.E., 1985. A stereotactic method of anatomical localization for positron emission tomography. *J. Comput. Assist. Tomogr.* 9, 141–153. <https://doi.org/10.1097/00004728-198501000-00025>
- Francis, S.T., Kelly, E.F., Bowtell, R., Dunseath, W.J.R., Folger, S.E., McGlone, F., 2000. fMRI of the Responses to Vibratory Stimulation of Digit Tips. *NeuroImage* 11, 188–202. <https://doi.org/10.1006/nimg.2000.0541>
- Frascarelli, F., Di Rosa, G., Bisozzi, E., Castelli, E., Santilli, V., 2011. Neurophysiological changes induced by the botulinum toxin type A injection in children with cerebral palsy. *Eur. J. Paediatr. Neurol. EJPN Off. J. Eur. Paediatr. Neurol. Soc.* 15, 59–64. <https://doi.org/10.1016/j.ejpn.2010.04.002>
- Fraser, C., Power, M., Hamdy, S., Rothwell, J., Hobday, D., Hollander, I., Tyrell, P., Hobson, A., Williams, S., Thompson, D., 2002. Driving plasticity in human adult motor cortex is associated with improved motor function after brain injury. *Neuron* 34, 831–840.
- Frima, N., Rome, S.M., Grünewald, R.A., 2003. The effect of fatigue on abnormal vibration induced illusion of movement in idiopathic focal dystonia. *J. Neurol. Neurosurg. Psychiatry* 74, 1154–1156. <https://doi.org/10.1136/jnnp.74.8.1154>
- Friston, K., 2011. What is optimal about motor control? *Neuron* 72, 488–498. <https://doi.org/10.1016/j.neuron.2011.10.018>
- Froemke, R.C., 2015. Plasticity of cortical excitatory-inhibitory balance. *Annu. Rev. Neurosci.* 38, 195–219. <https://doi.org/10.1146/annurev-neuro-071714-034002>
- Fuhr, P., Cohen, L.G., Dang, N., Findley, T.W., Haghghi, S., Oro, J., Hallett, M., 1992. Physiological analysis of motor reorganization following lower limb amputation. *Electroencephalogr. Clin. Neurophysiol.* 85, 53–60. [https://doi.org/10.1016/0168-5597\(92\)90102-h](https://doi.org/10.1016/0168-5597(92)90102-h)
- Fulton, J.F., 1949. *Physiology of the nervous system.* Oxford Univ. Press, New York.
- Gajewska, E., Huber, J., Kulczyk, A., Lipiec, J., Sobieska, M., 2018. An attempt to explain the Vojta therapy mechanism of action using the surface polyelectromyography in healthy subjects: A pilot study. *J. Bodyw. Mov. Ther.* 22, 287–292. <https://doi.org/10.1016/j.jbmt.2017.07.002>
- Gallasch, E., Christova, M., Kunz, A., Rafolt, D., Golaszewski, S., 2015. Modulation of sensorimotor cortex by repetitive peripheral magnetic stimulation. *Front. Hum. Neurosci.* 9. <https://doi.org/10.3389/fnhum.2015.00407>
- Gallese, V., Fadiga, L., Fogassi, L., Rizzolatti, G., 1996. Action recognition in the premotor cortex. *Brain J. Neurol.* 119 (Pt 2), 593–609. <https://doi.org/10.1093/brain/119.2.593>
- Gang, Y., Malik, M., 2003. Heart Rate Variability Analysis in General Medicine. *Indian*

- Pacing Electrophysiol. J. 3, 34–40.
- Gauthier, C.J., Fan, A.P., 2019. BOLD signal physiology: Models and applications. *NeuroImage* 187, 116–127. <https://doi.org/10.1016/j.neuroimage.2018.03.018>
- Gelnar, P.A., Krauss, B.R., Szeverenyi, N.M., Apkarian, A.V., 1998. Fingertip representation in the human somatosensory cortex: an fMRI study. *NeuroImage* 7, 261–283. <https://doi.org/10.1006/nimg.1998.0341>
- Geyer, S., Ledberg, A., Schleicher, A., Kinomura, S., Schormann, T., Bürgel, U., Klingberg, T., Larsson, J., Zilles, K., Roland, P.E., 1996. Two different areas within the primary motor cortex of man. *Nature* 382, 805–807. <https://doi.org/10.1038/382805a0>
- Ghez, C., Sainburg, R., 1995. Proprioceptive control of interjoint coordination. *Can. J. Physiol. Pharmacol.* 73, 273–284. <https://doi.org/10.1139/y95-038>
- Ghosh, S., Brinkman, C., Porter, R., 1987. A quantitative study of the distribution of neurons projecting to the precentral motor cortex in the monkey (*M. fascicularis*). *J. Comp. Neurol.* 259, 424–444. <https://doi.org/10.1002/cne.902590309>
- Giannantonio, C., Papacci, P., Ciarniello, R., Tesfagabir, M.G., Purcaro, V., Cota, F., Semeraro, C.M., Romagnoli, C., 2010. Chest physiotherapy in preterm infants with lung diseases. *Ital. J. Pediatr.* 36, 65. <https://doi.org/10.1186/1824-7288-36-65>
- Giladi, N., 1997. The mechanism of action of Botulinum toxin type A in focal dystonia is most probably through its dual effect on efferent (motor) and afferent pathways at the injected site. *J. Neurol. Sci.* 152, 132–135. [https://doi.org/10.1016/S0022-510X\(97\)00151-2](https://doi.org/10.1016/S0022-510X(97)00151-2)
- Gilhodes, J.C., Gurfinkel, V.S., Roll, J.P., 1992. Role of Ia muscle spindle afferents in post-contraction and post-vibration motor effect genesis. *Neurosci. Lett.* 135, 247–251. [https://doi.org/10.1016/0304-3940\(92\)90447-f](https://doi.org/10.1016/0304-3940(92)90447-f)
- Gilio, F., Currà, A., Lorenzano, C., Modugno, N., Manfredi, M., Berardelli, A., 2000. Effects of botulinum toxin type A on intracortical inhibition in patients with dystonia. *Ann. Neurol.* 48, 20–26.
- Gizewski, E.R., Koeze, O., Uffmann, K., de Greiff, A., Ladd, M.E., Forsting, M., 2005. Cerebral activation using a MR-compatible piezoelectric actuator with adjustable vibration frequencies and in vivo wave propagation control. *NeuroImage* 24, 723–730. <https://doi.org/10.1016/j.neuroimage.2004.09.015>
- Gjedde, A., 2001. Brain energy metabolism and the physiological basis of the haemodynamic response, in: Jezzard, P., Matthews, P.M., Smith, S.M. (Eds.), *Functional MRI: An Introduction to Methods*. Oxford University Press, Oxford [England]; New York, pp. 37–65.
- Glover, G.H., 1999. Deconvolution of impulse response in event-related BOLD fMRI. *NeuroImage* 9, 416–429.
- Goble, D.J., Coxon, J.P., Van Impe, A., Geurts, M., Doumas, M., Wenderoth, N., Swinnen, S.P., 2011. Brain activity during ankle proprioceptive stimulation predicts balance performance in young and older adults. *J. Neurosci. Off. J. Soc. Neurosci.* 31, 16344–16352. <https://doi.org/10.1523/JNEUROSCI.4159-11.2011>
- Goble, D.J., Coxon, J.P., Van Impe, A., Geurts, M., Van Hecke, W., Sunaert, S., Wenderoth, N., Swinnen, S.P., 2012. The neural basis of central proprioceptive processing in

- older versus younger adults: an important sensory role for right putamen. *Hum. Brain Mapp.* 33, 895–908. <https://doi.org/10.1002/hbm.21257>
- Golaszewski, S.M., Bergmann, J., Christova, M., Kunz, A.B., Kronbichler, M., Rafolt, D., Gallasch, E., Staffen, W., Trinka, E., Nardone, R., 2012. Modulation of motor cortex excitability by different levels of whole-hand afferent electrical stimulation. *Clin. Neurophysiol. Off. J. Int. Fed. Clin. Neurophysiol.* 123, 193–199. <https://doi.org/10.1016/j.clinph.2011.06.010>
- Golaszewski, S.M., Bergmann, J., Christova, M., Nardone, R., Kronbichler, M., Rafolt, D., Gallasch, E., Staffen, W., Ladurner, G., Beisteiner, R., 2010. Increased motor cortical excitability after whole-hand electrical stimulation: a TMS study. *Clin. Neurophysiol. Off. J. Int. Fed. Clin. Neurophysiol.* 121, 248–254. <https://doi.org/10.1016/j.clinph.2009.09.024>
- Golaszewski, S.M., Siedentopf, C.M., Baldauf, E., Koppelstaetter, F., Eisner, W., Unterrainer, J., Guendisch, G.M., Mottaghy, F.M., Felber, S.R., 2002a. Functional Magnetic Resonance Imaging of the Human Sensorimotor Cortex Using a Novel Vibrotactile Stimulator. *NeuroImage* 17, 421–430. <https://doi.org/10.1006/nimg.2002.1195>
- Golaszewski, S.M., Siedentopf, C.M., Koppelstaetter, F., Fend, M., Ischebeck, A., Gonzalez-Felipe, V., Haala, I., Struhal, W., Mottaghy, F.M., Gallasch, E., Felber, S.R., Gerstenbrand, F., 2006. Human brain structures related to plantar vibrotactile stimulation: a functional magnetic resonance imaging study. *NeuroImage* 29, 923–929. <https://doi.org/10.1016/j.neuroimage.2005.08.052>
- Golaszewski, S.M., Siedentopf, C.M., Koppelstaetter, F., Rhomberg, P., Guendisch, G.M., Schlager, A., Gallasch, E., Eisner, W., Felber, S.R., Mottaghy, F.M., 2004. Modulatory effects on human sensorimotor cortex by whole-hand afferent electrical stimulation. *Neurology* 62, 2262–2269. <https://doi.org/10.1212/WNL.62.12.2262>
- Golaszewski, S.M., Zschiegner, F., Siedentopf, C.M., Unterrainer, J., Sweeney, R.A., Eisner, W., Lechner-Steinleitner, S., Mottaghy, F.M., Felber, S., 2002b. A new pneumatic vibrator for functional magnetic resonance imaging of the human sensorimotor cortex. *Neurosci. Lett.* 324, 125–128.
- Goltz, D., Gundlach, C., Nierhaus, T., Villringer, A., Müller, M., Pleger, B., 2015. Connections between intraparietal sulcus and a sensorimotor network underpin sustained tactile attention. *J. Neurosci. Off. J. Soc. Neurosci.* 35, 7938–7949. <https://doi.org/10.1523/JNEUROSCI.3421-14.2015>
- Goodwin, G.M., McCloskey, D.I., Matthews, P.B., 1972. The contribution of muscle afferents to kinaesthesia shown by vibration induced illusions of movement and by the effects of paralysing joint afferents. *Brain J. Neurol.* 95, 705–748.
- Gordon, J., Ghilardi, M.F., Ghez, C., 1995. Impairments of reaching movements in patients without proprioception. I. Spatial errors. *J. Neurophysiol.* 73, 347–360. <https://doi.org/10.1152/jn.1995.73.1.347>
- Grabner, G., Janke, A.L., Budge, M.M., Smith, D., Pruessner, J., Collins, D.L., 2006. Symmetric atlasing and model based segmentation: an application to the hippocampus in older adults. *Med. Image Comput. Comput.-Assist. Interv.* 9, 58–

- Gracien, R.-M., Nürnberger, L., Hok, P., Hof, S.-M., Reitz, S.C., Rüb, U., Steinmetz, H., Hilker-Roggendorf, R., Klein, J.C., Deichmann, R., Baudrexel, S., 2017. Evaluation of brain ageing: a quantitative longitudinal MRI study over 7 years. *Eur. Radiol.* 27, 1568–1576. <https://doi.org/10.1007/s00330-016-4485-1>
- Gracien, R.-M., Petrov, F., Hok, P., van Wijnen, A., Maiworm, M., Seiler, A., Deichmann, R., Baudrexel, S., 2019. Multimodal Quantitative MRI Reveals No Evidence for Tissue Pathology in Idiopathic Cervical Dystonia. *Front. Neurol.* 10, 914. <https://doi.org/10.3389/fneur.2019.00914>
- Grillner, S., 1975. Locomotion in vertebrates: central mechanisms and reflex interaction. *Physiol. Rev.* 55, 247–304.
- Grillner, S., Wallén, P., 1985. Central pattern generators for locomotion, with special reference to vertebrates. *Annu. Rev. Neurosci.* 8, 233–261. <https://doi.org/10.1146/annurev.ne.08.030185.001313>
- Grünewald, R.A., Yoneda, Y., Shipman, J.M., Sagar, H.J., 1997. Idiopathic focal dystonia: a disorder of muscle spindle afferent processing? *Brain J. Neurol.* 120 (Pt 12), 2179–2185. <https://doi.org/10.1093/brain/120.12.2179>
- Gurfinkel, V.S., Levik, Yu.S., Kazennikov, O.V., Selionov, V.A., 1998. Locomotor-like movements evoked by leg muscle vibration in humans. *Eur. J. Neurosci.* 10, 1608–1612. <https://doi.org/10.1046/j.1460-9568.1998.00179.x>
- Hagbarth, K.E., Eklund, G., 1968. The effects of muscle vibration in spasticity, rigidity, and cerebellar disorders. *J. Neurol. Neurosurg. Psychiatry* 31, 207.
- Hagura, N., Oouchida, Y., Aramaki, Y., Okada, T., Matsumura, M., Sadato, N., Naito, E., 2009. Visuokinesthetic perception of hand movement is mediated by cerebro-cerebellar interaction between the left cerebellum and right parietal cortex. *Cereb. Cortex N. Y. N* 19, 176–186. <https://doi.org/10.1093/cercor/bhn068>
- Hamdy, S., Rothwell, J.C., Aziz, Q., Singh, K.D., Thompson, D.G., 1998. Long-term reorganization of human motor cortex driven by short-term sensory stimulation. *Nat. Neurosci.* 1, 64–68. <https://doi.org/10.1038/264>
- Hanajima, R., Ugawa, Y., Terao, Y., Sakai, K., Furubayashi, T., Machii, K., Kanazawa, I., 1998. Paired-pulse magnetic stimulation of the human motor cortex: differences among I waves. *J. Physiol.* 509 (Pt 2), 607–618.
- Hao, Y., Manor, B., Liu, J., Zhang, K., Chai, Y., Lipsitz, L., Peng, C.-K., Novak, V., Wang, X., Zhang, J., Fang, J., 2013. A Novel MRI-compatible Tactile Stimulator for Cortical Mapping of Foot Sole Pressure Stimuli with fMRI. *Magn. Reson. Med. Off. J. Soc. Magn. Reson. Med. Soc. Magn. Reson. Med.* 69, 1194–1199. <https://doi.org/10.1002/mrm.24330>
- Harmann, P.A., Carlton, S.M., Willis, W.D., 1988. Collaterals of spinothalamic tract cells to the periaqueductal gray: a fluorescent double-labeling study in the rat. *Brain Res.* 441, 87–97. [https://doi.org/10.1016/0006-8993\(88\)91386-8](https://doi.org/10.1016/0006-8993(88)91386-8)
- Harrington, G.S., Wright, C.T., Downs, J.H., 2000. A new vibrotactile stimulator for functional MRI. *Hum. Brain Mapp.* 10, 140–145.
- Haslinger, B., Erhard, P., Dresel, C., Castrop, F., Roettinger, M., Ceballos-Baumann, A.O.,

2005. "Silent event-related" fMRI reveals reduced sensorimotor activation in laryngeal dystonia. *Neurology* 65, 1562–1569. <https://doi.org/10.1212/01.wnl.0000184478.59063.db>
- Haslinger, B., Noé, J., Altenmüller, E., Riedl, V., Zimmer, C., Mantel, T., Dresel, C., 2017. Changes in resting-state connectivity in musicians with embouchure dystonia. *Mov. Disord. Off. J. Mov. Disord. Soc.* 32, 450–458. <https://doi.org/10.1002/mds.26893>
- Hellebrandt, F.A.M.D., Schade, M.M.S., Carns, M.L.M.D., 1962. Methods of evoking the tonic neck reflexes in normal human subjects. *J. Phys. Med.* 41, 90–139.
- Hess, G., Donoghue, J.P., 1996a. Long-term depression of horizontal connections in rat motor cortex. *Eur. J. Neurosci.* 8, 658–665. <https://doi.org/10.1111/j.1460-9568.1996.tb01251.x>
- Hess, G., Donoghue, J.P., 1996b. Long-term potentiation and long-term depression of horizontal connections in rat motor cortex. *Acta Neurobiol. Exp. (Warsz.)* 56, 397–405.
- Hirschauer, T.J., Buford, J.A., 2015. Bilateral force transients in the upper limbs evoked by single-pulse microstimulation in the pontomedullary reticular formation. *J. Neurophysiol.* 113, 2592–2604. <https://doi.org/10.1152/jn.00852.2014>
- Hlushchuk, Y., Hari, R., 2006. Transient Suppression of Ipsilateral Primary Somatosensory Cortex during Tactile Finger Stimulation. *J. Neurosci.* 26, 5819–5824. <https://doi.org/10.1523/JNEUROSCI.5536-05.2006>
- Hoffstaedter, F., Grefkes, C., Caspers, S., Roski, C., Palomero-Gallagher, N., Laird, A.R., Fox, P.T., Eickhoff, S.B., 2014. The role of anterior midcingulate cortex in cognitive motor control. *Hum. Brain Mapp.* 35, 2741–2753. <https://doi.org/10.1002/hbm.22363>
- Hoffstaedter, F., Grefkes, C., Zilles, K., Eickhoff, S.B., 2013. The "what" and "when" of self-initiated movements. *Cereb. Cortex N. Y. N 1991* 23, 520–530. <https://doi.org/10.1093/cercor/bhr391>
- Hok, P., Hlušík, P., Tüdös, Z., Frantis, P., Klosová, J., Sládková, V., Mareš, J., Otruba, P., Kaňovský, P., 2011. Changes in motor cortex activation after botulinum toxin treatment in MS patients with leg spasticity. *Aktual. Neurol.* 11, 251–256.
- Hongo, T., Kudo, N., Oguni, E., Yoshida, K., 1990. Spatial patterns of reflex evoked by pressure stimulation of the foot pads in cats. *J. Physiol.* 420, 471–487.
- Hooker, D., 1938. The Origin of the Grasping Movement in Man. *Proc. Am. Philos. Soc.* 597.
- Hooks, B.M., 2017. Sensorimotor Convergence in Circuitry of the Motor Cortex. *Neuroscientist* 23, 251–263. <https://doi.org/10.1177/1073858416645088>
- Hore, J., Preston, J.B., Cheney, P.D., 1976. Responses of cortical neurons (areas 3a and 4) to ramp stretch of hindlimb muscles in the baboon. *J. Neurophysiol.* 39, 484–500. <https://doi.org/10.1152/jn.1976.39.3.484>
- Hu, D., Huang, L., 2015. Negative hemodynamic response in the cortex: evidence opposing neuronal deactivation revealed via optical imaging and electrophysiological recording. *J. Neurophysiol.* 114, 2152–2161. <https://doi.org/10.1152/jn.00246.2015>
- Hu, L., Zhang, L., Chen, R., Yu, H., Li, H., Mouraux, A., 2015. The primary somatosensory

- cortex and the insula contribute differently to the processing of transient and sustained nociceptive and non-nociceptive somatosensory inputs. *Hum. Brain Mapp.* 36, 4346–4360. <https://doi.org/10.1002/hbm.22922>
- Huerta, M.F., Pons, T.P., 1990. Primary motor cortex receives input from area 3a in macaques. *Brain Res.* 537, 367–371. [https://doi.org/10.1016/0006-8993\(90\)90388-r](https://doi.org/10.1016/0006-8993(90)90388-r)
- Huffman, K.J., Krubitzer, L., 2001. Thalamo-cortical connections of areas 3a and M1 in marmoset monkeys. *J. Comp. Neurol.* 435, 291–310.
- Hund-Georgiadis, M., von Cramon, D.Y., 1999. Motor-learning-related changes in piano players and non-musicians revealed by functional magnetic-resonance signals. *Exp. Brain Res.* 125, 417–425. <https://doi.org/10.1007/s002210050698>
- Hylden, J.L., Anton, F., Nahin, R.L., 1989. Spinal lamina I projection neurons in the rat: collateral innervation of parabrachial area and thalamus. *Neuroscience* 28, 27–37.
- Ide, M., Hidaka, S., Ikeda, H., Wada, M., 2016. Neural mechanisms underlying touch-induced visual perceptual suppression: An fMRI study. *Sci. Rep.* 6. <https://doi.org/10.1038/srep37301>
- Igelström, K.M., Graziano, M.S.A., 2017. The inferior parietal lobule and temporoparietal junction: A network perspective. *Neuropsychologia* 105, 70–83. <https://doi.org/10.1016/j.neuropsychologia.2017.01.001>
- Ilg, W., Giese, M.A., Gizewski, E.R., Schoch, B., Timmann, D., 2008. The influence of focal cerebellar lesions on the control and adaptation of gait. *Brain* 131, 2913–2927. <https://doi.org/10.1093/brain/awn246>
- Ilić, T.V., Meintzschel, F., Cleff, U., Ruge, D., Kessler, K.R., Ziemann, U., 2002. Short-interval paired-pulse inhibition and facilitation of human motor cortex: the dimension of stimulus intensity. *J. Physiol.* 545, 153–167.
- Iriki, A., Pavlides, C., Keller, A., Asanuma, H., 1989. Long-term potentiation in the motor cortex. *Science* 245, 1385–1387. <https://doi.org/10.1126/science.2551038>
- Ismail, F.Y., Fatemi, A., Johnston, M.V., 2017. Cerebral plasticity: Windows of opportunity in the developing brain. *Eur. J. Paediatr. Neurol. EJPN Off. J. Eur. Paediatr. Neurol. Soc.* 21, 23–48. <https://doi.org/10.1016/j.ejpn.2016.07.007>
- Ivanenko, Y.P., Grasso, R., Lacquaniti, F., 2000. Influence of leg muscle vibration on human walking. *J. Neurophysiol.* 84, 1737–1747. <https://doi.org/10.1152/jn.2000.84.4.1737>
- Iwamura, Y., 2000. Bilateral receptive field neurons and callosal connections in the somatosensory cortex. *Philos. Trans. R. Soc. Lond. B. Biol. Sci.* 355, 267–273. <https://doi.org/10.1098/rstb.2000.0563>
- Iwamura, Y., Iriki, A., Tanaka, M., 1994. Bilateral hand representation in the postcentral somatosensory cortex. *Nature* 369, 554–556. <https://doi.org/10.1038/369554a0>
- Iwamura, Y., Tanaka, M., Sakamoto, M., Hikosaka, O., 1993. Rostrocaudal gradients in the neuronal receptive field complexity in the finger region of the alert monkey's postcentral gyrus. *Exp. Brain Res.* 92, 360–368. <https://doi.org/10.1007/bf00229023>
- Jacobs, K.M., Donoghue, J.P., 1991. Reshaping the cortical motor map by unmasking latent intracortical connections. *Science* 251, 944–947. <https://doi.org/10.1126/science.2000496>
- Jacobs, M., Premji, A., Nelson, A.J., 2012. Plasticity-inducing TMS protocols to investigate

- somatosensory control of hand function. *Neural Plast.* 2012, 350574. <https://doi.org/10.1155/2012/350574>
- Jahn, K., Deutschländer, A., Stephan, T., Kalla, R., Wiesmann, M., Strupp, M., Brandt, T., 2008. Imaging human supraspinal locomotor centers in brainstem and cerebellum. *NeuroImage* 39, 786–792. <https://doi.org/10.1006/j.neuroimage.2007.09.047>
- Jenkinson, M., 2003. Fast, automated, N-dimensional phase-unwrapping algorithm. *Magn. Reson. Med.* 49, 193–197. <https://doi.org/10.1002/mrm.10354>
- Jenkinson, M., Bannister, P., Brady, M., Smith, S., 2002. Improved Optimization for the Robust and Accurate Linear Registration and Motion Correction of Brain Images. *NeuroImage* 17, 825–841. <https://doi.org/10.1006/nimg.2002.1132>
- Jenkinson, M., Beckmann, C.F., Behrens, T.E.J., Woolrich, M.W., Smith, S.M., 2012. FSL. *NeuroImage* 62, 782–790. <https://doi.org/10.1016/j.neuroimage.2011.09.015>
- Jezzard, P., Clare, S., 2001. Principles of nuclear magnetic resonance and MRI, in: Jezzard, P., Matthews, P.M., Smith, S.M. (Eds.), *Functional MRI: An Introduction to Methods*. Oxford University Press, Oxford [England]; New York, pp. 67–92.
- Jiang, W., Lei, Y., Wei, J., Yang, L., Wei, S., Yin, Q., Luo, S., Guo, W., 2019. Alterations of Interhemispheric Functional Connectivity and Degree Centrality in Cervical Dystonia: A Resting-State fMRI Study. *Neural Plast.* 2019, 7349894. <https://doi.org/10.1155/2019/7349894>
- Jochim, A., Li, Y., Gora-Stahlberg, G., Mantel, T., Berndt, M., Castrop, F., Dresel, C., Haslinger, B., 2018. Altered functional connectivity in blepharospasm/orofacial dystonia. *Brain Behav.* 8, e00894. <https://doi.org/10.1002/brb3.894>
- Johansson, R.S., Flanagan, J.R., 2009. Coding and use of tactile signals from the fingertips in object manipulation tasks. *Nat. Rev. Neurosci.* 10, 345–359. <https://doi.org/10.1038/nrn2621>
- Johansson, R.S., Landström, U., Lundström, R., 1982. Responses of mechanoreceptive afferent units in the glabrous skin of the human hand to sinusoidal skin displacements. *Brain Res.* 244, 17–25. [https://doi.org/10.1016/0006-8993\(82\)90899-x](https://doi.org/10.1016/0006-8993(82)90899-x)
- Johansson, R.S., Vallbo, Å.B., 1983. Tactile sensory coding in the glabrous skin of the human hand. *Trends Neurosci.* 6, 27–32. [https://doi.org/10.1016/0166-2236\(83\)90011-5](https://doi.org/10.1016/0166-2236(83)90011-5)
- Jones, E.G., Coulter, J.D., Hendry, S.H., 1978. Intracortical connectivity of architectonic fields in the somatic sensory, motor and parietal cortex of monkeys. *J. Comp. Neurol.* 181, 291–347. <https://doi.org/10.1002/cne.901810206>
- Jones, E.G., Porter, R., 1980. What is area 3a? *Brain Res.* 203, 1–43. [https://doi.org/10.1016/0165-0173\(80\)90002-8](https://doi.org/10.1016/0165-0173(80)90002-8)
- Jones, R.A., Brookes, J.A., Moonen, C.T.W., 2001. Ultra-fast fMRI, in: Jezzard, P., Matthews, P.M., Smith, S.M. (Eds.), *Functional MRI: An Introduction to Methods*. Oxford University Press, Oxford [England]; New York, pp. 251–270.
- Joseph, P., Acharya, U.R., Poo, C.K., Chee, J., Min, L.C., Iyengar, S.S., Wei, H., 2004. Effect of reflexological stimulation on heart rate variability. *ITBM-RBM* 25, 40–45. <https://doi.org/10.1016/j.rbmret.2004.02.002>
- Juárez-Albuixech, M.L., Redondo-González, O., Tello, I., Collado-Vázquez, S., Jiménez-

- Antona, C., 2020. Vojta Therapy versus transcutaneous electrical nerve stimulation for lumbosciatica syndrome: A quasi-experimental pilot study. *J. Bodyw. Mov. Ther.* 24, 39–46. <https://doi.org/10.1016/j.jbmt.2019.05.015>
- Jung, M.W., Landenberger, M., Jung, T., Lindenthal, T., Philippi, H., 2017. Vojta therapy and neurodevelopmental treatment in children with infantile postural asymmetry: a randomised controlled trial. *J. Phys. Ther. Sci.* 29, 301–306. <https://doi.org/10.1589/jpts.29.301>
- Kaas, J.H., Nelson, R.J., Sur, M., Lin, C.S., Merzenich, M.M., 1979. Multiple representations of the body within the primary somatosensory cortex of primates. *Science* 204, 521–523. <https://doi.org/10.1126/science.107591>
- Kaas, J.H., Qi, H.-X., Stepniewska, I., 2018. The evolution of parietal cortex in primates. *Handb. Clin. Neurol.* 151, 31–52. <https://doi.org/10.1016/B978-0-444-63622-5.00002-4>
- Kabat, H., 1958. 12. Proprioceptive Facilitation, in: *Therapeutic Exercise*. Waverly Press, Baltimore.
- Kaelin-Lang, A., Luft, A.R., Sawaki, L., Burstein, A.H., Sohn, Y.H., Cohen, L.G., 2002. Modulation of human corticomotor excitability by somatosensory input. *J. Physiol.* 540, 623–633.
- Kaji, R., Rothwell, J.C., Katayama, M., Ikeda, T., Kubori, T., Kohara, N., Mezaki, T., Shibasaki, H., Kimura, J., 1995. Tonic vibration reflex and muscle afferent block in writer's cramp. *Ann. Neurol.* 38, 155–162. <https://doi.org/10.1002/ana.410380206>
- Kanda, T., Pidcock, F.S., Hayakawa, K., Yamori, Y., Shikata, Y., 2004. Motor outcome differences between two groups of children with spastic diplegia who received different intensities of early onset physiotherapy followed for 5 years. *Brain Dev.* 26, 118–126. [https://doi.org/10.1016/S0387-7604\(03\)00111-6](https://doi.org/10.1016/S0387-7604(03)00111-6)
- Kaneko, T., Caria, M.A., Asanuma, H., 1994a. Information processing within the motor cortex. II. Intracortical connections between neurons receiving somatosensory cortical input and motor output neurons of the cortex. *J. Comp. Neurol.* 345, 172–184. <https://doi.org/10.1002/cne.903450203>
- Kaneko, T., Caria, M.A., Asanuma, H., 1994b. Information processing within the motor cortex. I. Responses of morphologically identified motor cortical cells to stimulation of the somatosensory cortex. *J. Comp. Neurol.* 345, 161–171. <https://doi.org/10.1002/cne.903450202>
- Kaňovský, P., Bares, M., Streitova, H., Klajblova, H., Daniel, P., Rektor, I., 2004. The disorder of cortical excitability and cortical inhibition in focal dystonia is normalised following successful botulinum toxin treatment: An evidence from somatosensory evoked potentials and transcranial magnetic stimulation recordings. *Mov. Disord.* 19, S78–S79.
- Kaňovský, P., Bares, M., Streitová, H., Klajblová, H., Daniel, P., Rektor, I., 2003. Abnormalities of cortical excitability and cortical inhibition in cervical dystonia Evidence from somatosensory evoked potentials and paired transcranial magnetic stimulation recordings. *J. Neurol.* 250, 42–50. <https://doi.org/10.1007/s00415-003-0942-2>
- Kaňovský, P., Rosales, R.L., 2011. Debunking the pathophysiological puzzle of dystonia--

- with special reference to botulinum toxin therapy. *Parkinsonism Relat. Disord.* 17 Suppl 1, S11-14. <https://doi.org/10.1016/j.parkreldis.2011.06.018>
- Kaňovský, P., Streitová, H., Dufek, J., Rektor, I., 1997. Lateralization of the P22/N30 component of somatosensory evoked potentials of the median nerve in patients with cervical dystonia. *Mov. Disord. Off. J. Mov. Disord. Soc.* 12, 553–560. <https://doi.org/10.1002/mds.870120412>
- Kaňovský, P., Streitová, H., Dufek, J., Znojil, V., Daniel, P., Rektor, I., 1998. Change in lateralization of the P22/N30 cortical component of median nerve somatosensory evoked potentials in patients with cervical dystonia after successful treatment with botulinum toxin A. *Mov. Disord.* 13, 108–117. <https://doi.org/10.1002/mds.870130122>
- Karnath, H.O., Sievering, D., Fetter, M., 1994. The interactive contribution of neck muscle proprioception and vestibular stimulation to subjective “straight ahead” orientation in man. *Exp. Brain Res.* 101, 140–146. <https://doi.org/10.1007/bf00243223>
- Karni, A., Meyer, G., Jezzard, P., Adams, M.M., Turner, R., Ungerleider, L.G., 1995. Functional MRI evidence for adult motor cortex plasticity during motor skill learning. *Nature* 377, 155–158. <https://doi.org/10.1038/377155a0>
- Karni, A., Meyer, G., Rey-Hipolito, C., Jezzard, P., Adams, M.M., Turner, R., Ungerleider, L.G., 1998. The acquisition of skilled motor performance: fast and slow experience-driven changes in primary motor cortex. *Proc. Natl. Acad. Sci. U. S. A.* 95, 861–868.
- Kaut, O., Becker, B., Schneider, C., Zhou, F., Fliessbach, K., Hurlmann, R., Wüllner, U., 2016. Stochastic resonance therapy induces increased movement related caudate nucleus activity. *J. Rehabil. Med.* 48, 815–818. <https://doi.org/10.2340/16501977-2143>
- Kavounoudias, A., Roll, J.P., Anton, J.L., Nazarian, B., Roth, M., Roll, R., 2008. Proprio-tactile integration for kinesthetic perception: An fMRI study. *Neuropsychologia* 46, 567–575. <https://doi.org/10.1016/j.neuropsychologia.2007.10.002>
- Kavounoudias, A., Roll, R., Roll, J.-P., 2001. Foot sole and ankle muscle inputs contribute jointly to human erect posture regulation. *J. Physiol.* 532, 869–878. <https://doi.org/10.1111/j.1469-7793.2001.0869e.x>
- Kavounoudias, A., Roll, R., Roll, J.P., 1998. The plantar sole is a “dynamometric map” for human balance control. *Neuroreport* 9, 3247–3252.
- Kawashima, R., O’Sullivan, B.T., Roland, P.E., 1995. Positron-emission tomography studies of cross-modality inhibition in selective attentional tasks: closing the “mind’s eye”. *Proc. Natl. Acad. Sci. U. S. A.* 92, 5969–5972.
- Kayalioglu, G., 2009. Chapter 10 - Projections from the Spinal Cord to the Brain, in: Watson, C., Paxinos, G., Kayalioglu, G. (Eds.), *The Spinal Cord*. Academic Press, San Diego, pp. 148–167. <https://doi.org/10.1016/B978-0-12-374247-6.50014-6>
- Kayalioglu, G., Hariri, N.I., Govsa, F., Erdem, B., Peker, G., Maiskii, V.A., 1996. Laminar distribution of the cells of origin of the spinocerebral pathways involved in nociceptive transmission and pain modulation in the rat. *Neurophysiology* 28, 111–118. <https://doi.org/10.1007/BF02262771>
- Kevetter, G.A., Haber, L.H., Yeziarski, R.P., Chung, J.M., Martin, R.F., Willis, W.D., 1982. Cells of origin of the spinoreticular tract in the monkey. *J. Comp. Neurol.* 207, 61–74. <https://doi.org/10.1002/cne.902070106>

- Kevetter, G.A., Willis, W.D., 1983. Collaterals of spinothalamic cells in the rat. *J. Comp. Neurol.* 215, 453–464. <https://doi.org/10.1002/cne.902150409>
- Kiebzak, W., Kowalski, I.M., Domagalska, M., Szopa, A., Dwornik, M., Kujawa, J., Stępień, A., Śliwiński, Z., 2012. Assessment of visual perception in adolescents with a history of central coordination disorder in early life – 15-year follow-up study. *Arch. Med. Sci. AMS* 8, 879–885. <https://doi.org/10.5114/aoms.2012.28638>
- Kim, D.-Y., Oh, B.-M., Paik, N.-J., 2006. Central effect of botulinum toxin type A in humans. *Int. J. Neurosci.* 116, 667–680. <https://doi.org/10.1080/00207450600674525>
- Kim, J., Chung, Y.G., Chung, S.-C., Bühlhoff, H.H., Kim, S.-P., 2016a. Decoding pressure stimulation locations on the fingers from human neural activation patterns. *Neuroreport* 27, 1232–1236. <https://doi.org/10.1097/WNR.0000000000000683>
- Kim, J., Chung, Y.G., Chung, S.-C., Bulthoff, H.H., Kim, S.-P., 2016b. Neural Categorization of Vibrotactile Frequency in Flutter and Vibration Stimulations: An fMRI Study. *IEEE Trans. Haptics* 9, 455–464. <https://doi.org/10.1109/TOH.2016.2593727>
- Kim, J., Müller, K.-R., Chung, Y.G., Chung, S.-C., Park, J.-Y., Bühlhoff, H.H., Kim, S.-P., 2014. Distributed functions of detection and discrimination of vibrotactile stimuli in the hierarchical human somatosensory system. *Front. Hum. Neurosci.* 8, 1070. <https://doi.org/10.3389/fnhum.2014.01070>
- Kincses, Z.T., Johansen-Berg, H., Tomassini, V., Bosnell, R., Matthews, P.M., Beckmann, C.F., 2008. Model-free characterization of brain functional networks for motor sequence learning using fMRI. *NeuroImage* 39, 1950–1958. <https://doi.org/10.1016/j.neuroimage.2007.09.070>
- Kito, T., Hashimoto, T., Yoneda, T., Katamoto, S., Naito, E., 2006. Sensory processing during kinesthetic aftereffect following illusory hand movement elicited by tendon vibration. *Brain Res.* 1114, 75–84. <https://doi.org/10.1016/j.brainres.2006.07.062>
- Kobayashi, M., Ng, J., Théoret, H., Pascual-Leone, A., 2003. Modulation of intracortical neuronal circuits in human hand motor area by digit stimulation. *Exp. Brain Res.* 149, 1–8. <https://doi.org/10.1007/s00221-002-1329-9>
- Koch, G., Mori, F., Marconi, B., Codecà, C., Pecchioli, C., Salerno, S., Torriero, S., Lo Gerfo, E., Mir, P., Oliveri, M., Caltagirone, C., 2008. Changes in intracortical circuits of the human motor cortex following theta burst stimulation of the lateral cerebellum. *Clin. Neurophysiol. Off. J. Int. Fed. Clin. Neurophysiol.* 119, 2559–2569. <https://doi.org/10.1016/j.clinph.2008.08.008>
- Koch, S.C., Acton, D., Goulding, M., 2018. Spinal Circuits for Touch, Pain, and Itch, in: Julius, D. (Ed.), *Annual Review of Physiology*, Vol 80. Annual Reviews, Palo Alto, pp. 189–217. <https://doi.org/10.1146/annurev-physiol-022516-034303>
- Koenig, J., Jarczok, M.N., Ellis, R.J., Hillecke, T.K., Thayer, J.F., 2014. Heart rate variability and experimentally induced pain in healthy adults: a systematic review. *Eur. J. Pain Lond. Engl.* 18, 301–314. <https://doi.org/10.1002/j.1532-2149.2013.00379.x>
- Kojovic, M., Caronni, A., Bologna, M., Rothwell, J.C., Bhatia, K.P., Edwards, M.J., 2011. Botulinum toxin injections reduce associative plasticity in patients with primary dystonia. *Mov. Disord. Off. J. Mov. Disord. Soc.* 26, 1282–1289. <https://doi.org/10.1002/mds.23681>

- Kossev, A., Siggelkow, S., Kapels, H.-H., Dengler, R., Rollnik, J.D., 2001. Crossed effects of muscle vibration on motor-evoked potentials. *Clin. Neurophysiol.* 112, 453–456. [https://doi.org/10.1016/S1388-2457\(01\)00473-4](https://doi.org/10.1016/S1388-2457(01)00473-4)
- Kossev, A., Siggelkow, S., Schubert, M., Wohlfarth, K., Dengler, R., 1999. Muscle vibration: Different effects on transcranial magnetic and electrical stimulation. *Muscle Nerve* 22, 946–948. [https://doi.org/10.1002/\(SICI\)1097-4598\(199907\)22:7<946::AID-MUS22>3.0.CO;2-O](https://doi.org/10.1002/(SICI)1097-4598(199907)22:7<946::AID-MUS22>3.0.CO;2-O)
- Kotnik, S.S., 2012. Vojta in rehabilitation of children with neurodevelopmental disorders. *Paediatr. Croat.* 56, 227–231.
- Krägeloh-Mann, I., Lidzba, K., Pavlova, M.A., Wilke, M., Staudt, M., 2017. Plasticity during Early Brain Development Is Determined by Ontogenetic Potential. *Neuropediatrics* 48, 66–71. <https://doi.org/10.1055/s-0037-1599234>
- Kujirai, T., Caramia, M.D., Rothwell, J.C., Day, B.L., Thompson, P.D., Ferbert, A., Wroe, S., Asselman, P., Marsden, C.D., 1993. Corticocortical inhibition in human motor cortex. *J. Physiol.* 471, 501–519.
- Kurth, F., Zilles, K., Fox, P.T., Laird, A.R., Eickhoff, S.B., 2010. A link between the systems: functional differentiation and integration within the human insula revealed by meta-analysis. *Brain Struct. Funct.* 214, 519–534. <https://doi.org/10.1007/s00429-010-0255-z>
- la Fougère, C., Zwergal, A., Rominger, A., Förster, S., Fesl, G., Dieterich, M., Brandt, T., Strupp, M., Bartenstein, P., Jahn, K., 2010. Real versus imagined locomotion: A [18F]-FDG PET-fMRI comparison. *NeuroImage* 50, 1589–1598. <https://doi.org/10.1016/j.neuroimage.2009.12.060>
- Lackner, J.R., Levine, M.S., 1979. Changes in apparent body orientation and sensory localization induced by vibration of postural muscles: vibratory myesthetic illusions. *Aviat. Space Environ. Med.* 50, 346–354.
- Lapole, T., Deroussen, F., Pérot, C., Petitjean, M., 2012. Acute effects of Achilles tendon vibration on soleus and tibialis anterior spinal and cortical excitability. *Appl. Physiol. Nutr. Metab. Physiol. Appl. Nutr. Metab.* 37, 657–663. <https://doi.org/10.1139/h2012-032>
- Lapole, T., Temesi, J., Arnal, P.J., Gimenez, P., Petitjean, M., Millet, G.Y., 2015. Modulation of soleus corticospinal excitability during Achilles tendon vibration. *Exp. Brain Res.* 233, 2655–2662. <https://doi.org/10.1007/s00221-015-4336-3>
- Lapole, T., Tindel, J., 2015. Acute effects of muscle vibration on sensorimotor integration. *Neurosci. Lett.* 587, 46–50. <https://doi.org/10.1016/j.neulet.2014.12.025>
- Laufens, G., Poltz, W., Jugelt, E., Prinz, E., Reimann, G., Van Slobbe, T., 1995. Motor improvements in multiple-sclerosis patients by Vojta physiotherapy and the influence of treatment positions. *Phys. Med. Rehabil. Kurortmed.* 5, 115–119.
- Laufens, G., Poltz, W., Prinz, E., Reimann, G., Schmiegel, F., 2004. Alternating treadmill-Vojta-treadmill-therapy in patients with multiple sclerosis with severely affected gait. *Phys. Med. Rehabil. Kurortmed.* 14, 134–139. <https://doi.org/10.1055/s-2003-814921>
- Laufens, G., Poltz, W., Reimann, C., Schmiegel, F., Stempski, S., 1998. Treadmill training

- and Voita physiotherapy applied to selected MS- patients - A comparison of the immediate effects. *Phys. Med. Rehabil. Kurortmed.* 8, 174–177.
- Laufens, G., Poltz, W., Reimann, G., Seitz, S., 1994. Physiological mechanisms in Voita-physiotherapy for MS-patients. *Phys. Med. Rehabil. Kurortmed.* 4, 1–4.
- Laufens, G., Seitz, S., Staenicke, G., 1991. Vergleichend biologische Grundlagen zur angeborenen Lokomotion insbesondere zum “reflektorischen Kriechen” nach Voita. *Krankengymnast. Z. Für Physiother.* 43, 448–456.
- Layne, C.S., Malaya, C.A., Levine, J.T., 2019. The effects of muscle vibration on gait control: a review. *Somatosens. Mot. Res.* 36, 212–222.
<https://doi.org/10.1080/08990220.2019.1652585>
- Lehéricy, S., Tijssen, M.A.J., Vidailhet, M., Kaji, R., Meunier, S., 2013. The anatomical basis of dystonia: current view using neuroimaging. *Mov. Disord. Off. J. Mov. Disord. Soc.* 28, 944–957. <https://doi.org/10.1002/mds.25527>
- Leis, A.A., Dimitrijevic, M.R., Delapasse, J.S., Sharkey, P.C., 1992. Modification of cervical dystonia by selective sensory stimulation. *J. Neurol. Sci.* 110, 79–89.
- Lekhel, H., Popov, K., Anastasopoulos, D., Bronstein, A., Bhatia, K., Marsden, C.D., Gresty, M., 1997. Postural responses to vibration of neck muscles in patients with idiopathic torticollis. *Brain J. Neurol.* 120 (Pt 4), 583–591.
<https://doi.org/10.1093/brain/120.4.583>
- Lemon, R.N., van der Burg, J., 1979. Short-latency peripheral inputs to thalamic neurones projecting to the motor cortex in the monkey. *Exp. Brain Res.* 36, 445–462.
<https://doi.org/10.1007/bf00238515>
- Leung, Y.Y., Bensmaïa, S.J., Hsiao, S.S., Johnson, K.O., 2005. Time-course of vibratory adaptation and recovery in cutaneous mechanoreceptive afferents. *J. Neurophysiol.* 94, 3037–3045. <https://doi.org/10.1152/jn.00001.2005>
- Levy, W.J., Amassian, V.E., Traad, M., Cadwell, J., 1990. Focal magnetic coil stimulation reveals motor cortical system reorganized in humans after traumatic quadriplegia. *Brain Res.* 510, 130–134. [https://doi.org/10.1016/0006-8993\(90\)90738-w](https://doi.org/10.1016/0006-8993(90)90738-w)
- Lewis, L.D., Setsompop, K., Rosen, B.R., Polimeni, J.R., 2018. Stimulus-dependent hemodynamic response timing across the human subcortical-cortical visual pathway identified through high spatiotemporal resolution 7T fMRI. *NeuroImage* 181, 279–291. <https://doi.org/10.1016/j.neuroimage.2018.06.056>
- Li, Z., Prudente, C.N., Stilla, R., Sathian, K., Jinnah, H.A., Hu, X., 2017. Alterations of resting-state fMRI measurements in individuals with cervical dystonia. *Hum. Brain Mapp.* 38, 4098–4108. <https://doi.org/10.1002/hbm.23651>
- Liepert, J., Bauder, H., Wolfgang, H.R., Miltner, W.H., Taub, E., Weiller, C., 2000. Treatment-induced cortical reorganization after stroke in humans. *Stroke* 31, 1210–1216. <https://doi.org/10.1161/01.str.31.6.1210>
- Liepert, J., Classen, J., Cohen, L.G., Hallett, M., 1998. Task-dependent changes of intracortical inhibition. *Exp. Brain Res.* 118, 421–426.
- Liepert, J., Schwenkreis, P., Tegenthoff, M., Malin, J.P., 1997. The glutamate antagonist riluzole suppresses intracortical facilitation. *J. Neural Transm. Vienna Austria* 1996 104, 1207–1214. <https://doi.org/10.1007/BF01294721>

- Liepert, J., Tegenthoff, M., Malin, J.P., 1995. Changes of cortical motor area size during immobilization. *Electroencephalogr. Clin. Neurophysiol.* 97, 382–386. [https://doi.org/10.1016/0924-980x\(95\)00194-p](https://doi.org/10.1016/0924-980x(95)00194-p)
- Lim, H., Kim, T., 2013. Effects of vojta therapy on gait of children with spastic diplegia. *J. Phys. Ther. Sci.* 25, 1605–1608. <https://doi.org/10.1589/jpts.25.1605>
- Linden, D.J., 1994. Long-term synaptic depression in the mammalian brain. *Neuron* 12, 457–472. [https://doi.org/10.1016/0896-6273\(94\)90205-4](https://doi.org/10.1016/0896-6273(94)90205-4)
- Liu, J., Duffy, B.A., Bernal-Casas, D., Fang, Z., Lee, J.H., 2017. Comparison of fMRI analysis methods for heterogeneous BOLD responses in block design studies. *NeuroImage* 147, 390–408. <https://doi.org/10.1016/j.neuroimage.2016.12.045>
- Loayza, F.R., Fernández-Seara, M.A., Aznárez-Sanado, M., Pastor, M.A., 2011. Right parietal dominance in spatial egocentric discrimination. *NeuroImage* 55, 635–643. <https://doi.org/10.1016/j.neuroimage.2010.12.011>
- Logothetis, N.K., 2003. The underpinnings of the BOLD functional magnetic resonance imaging signal. *J. Neurosci. Off. J. Soc. Neurosci.* 23, 3963–3971.
- Long, X., Goltz, D., Margulies, D.S., Nierhaus, T., Villringer, A., 2014. Functional connectivity-based parcellation of the human sensorimotor cortex. *Eur. J. Neurosci.* 39, 1332–1342. <https://doi.org/10.1111/ejn.12473>
- Lotze, M., Kaethner, R.J., Erb, M., Cohen, L.G., Grodd, W., Topka, H., 2003. Comparison of representational maps using functional magnetic resonance imaging and transcranial magnetic stimulation. *Clin. Neurophysiol. Off. J. Int. Fed. Clin. Neurophysiol.* 114, 306–312. [https://doi.org/10.1016/s1388-2457\(02\)00380-2](https://doi.org/10.1016/s1388-2457(02)00380-2)
- Lucier, G.E., Rüegg, D.C., Wiesendanger, M., 1975. Responses of neurones in motor cortex and in area 3A to controlled stretches of forelimb muscles in cebus monkeys. *J. Physiol.* 251, 833–853. <https://doi.org/10.1113/jphysiol.1975.sp011125>
- Luft, A., Manto, M.-U., Oulad Ben Taib, N., 2005. Modulation of motor cortex excitability by sustained peripheral stimulation: The interaction between the motor cortex and the cerebellum. *The Cerebellum* 4, 90–96. <https://doi.org/10.1080/14734220410019084>
- Lund, S., 1980. Postural effects of neck muscle vibration in man. *Experientia* 36, 1398. <https://doi.org/10.1007/bf01960120>
- Macerollo, A., Palmer, C., Foltynie, T., Korlipara, P., Limousin, P., Edwards, M., Kilner, J.M., 2018. High-frequency peripheral vibration decreases completion time on a number of motor tasks. *Eur. J. Neurosci.* 48, 1789–1802. <https://doi.org/10.1111/ejn.14050>
- Mackel, R., Miyashita, E., 1993. Nucleus Z: a somatosensory relay to motor thalamus. *J. Neurophysiol.* 69, 1607–1620. <https://doi.org/10.1152/jn.1993.69.5.1607>
- Magnus, R., de Kleijn, A., 1912. Die Abhängigkeit des Tonus der Extremitätenmuskeln von der Kopfstellung. *Pflüg. Arch. Eur. J. Physiol.* 145, 455–548. <https://doi.org/10.1007/BF01681127>
- Maldjian, J.A., Gottschalk, A., Patel, R.S., Detre, J.A., Alsop, D.C., 1999. The sensory somatotopic map of the human hand demonstrated at 4 Tesla. *NeuroImage* 10, 55–62. <https://doi.org/10.1006/nimg.1999.0448>
- Malinow, R., Malenka, R.C., 2002. AMPA receptor trafficking and synaptic plasticity. *Annu.*

- Rev. Neurosci. 25, 103–126. <https://doi.org/10.1146/annurev.neuro.25.112701.142758>
- Mancheva, K., Rollnik, J.D., Wolf, W., Dengler, R., Kossev, A., 2017. Vibration-Induced Kinesthetic Illusions and Corticospinal Excitability Changes. *J. Mot. Behav.* 49, 299–305. <https://doi.org/10.1080/00222895.2016.1204263>
- Manganotti, P., Acler, M., Formaggio, E., Avesani, M., Milanese, F., Baraldo, A., Storti, S.F., Gasparini, A., Cerini, R., Mucelli, R.P., Fiaschi, A., 2010. Changes in cerebral activity after decreased upper-limb hypertonus: an EMG-fMRI study. *Magn. Reson. Imaging* 28, 646–652. <https://doi.org/10.1016/j.mri.2009.12.023>
- Manto, M., Oulad ben Taib, N., Luft, A.R., 2006. Modulation of excitability as an early change leading to structural adaptation in the motor cortex. *J. Neurosci. Res.* 83, 177–180. <https://doi.org/10.1002/jnr.20733>
- Marconi, B., Filippi, G.M., Koch, G., Giacobbe, V., Pecchioli, C., Versace, V., Camerota, F., Saraceni, V.M., Caltagirone, C., 2011. Long-term effects on cortical excitability and motor recovery induced by repeated muscle vibration in chronic stroke patients. *Neurorehabil. Neural Repair* 25, 48–60. <https://doi.org/10.1177/1545968310376757>
- Marconi, B., Filippi, G.M., Koch, G., Pecchioli, C., Salerno, S., Don, R., Camerota, F., Saraceni, V.M., Caltagirone, C., 2008. Long-term effects on motor cortical excitability induced by repeated muscle vibration during contraction in healthy subjects. *J. Neurol. Sci.* 275, 51–59. <https://doi.org/10.1016/j.jns.2008.07.025>
- Marxen, M., Cassidy, R.J., Dawson, T.L., Ross, B., Graham, S.J., 2012. Transient and sustained components of the sensorimotor BOLD response in fMRI. *Magn. Reson. Imaging* 30, 837–847. <https://doi.org/10.1016/j.mri.2012.02.007>
- Matthews, P.M., 2001. An introduction to functional magnetic resonance imaging of the brain, in: Jezzard, P., Matthews, P.M., Smith, S.M. (Eds.), *Functional MRI: An Introduction to Methods*. Oxford University Press, Oxford [England]; New York, pp. 3–34.
- McCloskey, D.I., 1973. Differences between the senses of movement and position shown by the effects of loading and vibration of muscles in man. *Brain Res.* 61, 119–131. [https://doi.org/10.1016/0006-8993\(73\)90521-0](https://doi.org/10.1016/0006-8993(73)90521-0)
- McDonnell, M.N., Thompson, P.D., Ridding, M.C., 2007. The effect of cutaneous input on intracortical inhibition in focal task-specific dystonia. *Mov. Disord. Off. J. Mov. Disord. Soc.* 22, 1286–1292. <https://doi.org/10.1002/mds.21508>
- McGlone, F., Kelly, E.F., Trulsson, M., Francis, S.T., Westling, G., Bowtell, R., 2002. Functional neuroimaging studies of human somatosensory cortex. *Behav. Brain Res.* 135, 147–158. [https://doi.org/10.1016/s0166-4328\(02\)00144-4](https://doi.org/10.1016/s0166-4328(02)00144-4)
- McGlone, F., Reilly, D., 2010. The cutaneous sensory system. *Neurosci. Biobehav. Rev., Touch, Temperature, Pain/Itch and Pleasure* 34, 148–159. <https://doi.org/10.1016/j.neubiorev.2009.08.004>
- McGlone, F., Wessberg, J., Olausson, H., 2014. Discriminative and Affective Touch: Sensing and Feeling. *Neuron* 82, 737–755. <https://doi.org/10.1016/j.neuron.2014.05.001>
- Meholjić-Fetahović, A., 2007. Treatment of the spasticity in children with cerebral palsy. *Bosn. J. Basic Med. Sci. Udruženje Basičnih Med. Znan. Assoc. Basic Med. Sci.* 7, 363–367.

- Meier, M.L., Hotz-Boendermaker, S., Boendermaker, B., Luechinger, R., Humphreys, B.K., 2014. Neural responses of posterior to anterior movement on lumbar vertebrae: a functional magnetic resonance imaging study. *J. Manipulative Physiol. Ther.* 37, 32–41. <https://doi.org/10.1016/j.jmpt.2013.09.004>
- Mendez-Balbuena, I., Manjarrez, E., Schulte-Mönting, J., Huethe, F., Tapia, J.A., Hepp-Reymond, M.-C., Kristeva, R., 2012. Improved sensorimotor performance via stochastic resonance. *J. Neurosci. Off. J. Soc. Neurosci.* 32, 12612–12618. <https://doi.org/10.1523/JNEUROSCI.0680-12.2012>
- Merabet, L.B., Swisher, J.D., McMains, S.A., Halko, M.A., Amedi, A., Pascual-Leone, A., Somers, D.C., 2007. Combined Activation and Deactivation of Visual Cortex During Tactile Sensory Processing. *J. Neurophysiol.* 97, 1633–1641. <https://doi.org/10.1152/jn.00806.2006>
- Meyer, E., Ferguson, S.S., Zatorre, R.J., Alivisatos, B., Marrett, S., Evans, A.C., Hakim, A.M., 1991. Attention modulates somatosensory cerebral blood flow response to vibrotactile stimulation as measured by positron emission tomography. *Ann. Neurol.* 29, 440–443. <https://doi.org/10.1002/ana.410290418>
- Mildren, R.L., Bent, L.R., 2016. Vibrotactile stimulation of fast-adapting cutaneous afferents from the foot modulates proprioception at the ankle joint. *J. Appl. Physiol.* 120, 855–864. <https://doi.org/10.1152/jappphysiol.00810.2015>
- Mileva, K.N., Bowtell, J.L., Kossev, A.R., 2009. Effects of low-frequency whole-body vibration on motor-evoked potentials in healthy men. *Exp. Physiol.* 94, 103–116. <https://doi.org/10.1113/expphysiol.2008.042689>
- Miura, N., Akitsuki, Y., Sekiguchi, A., Kawashima, R., 2013. Activity in the primary somatosensory cortex induced by reflexological stimulation is unaffected by pseudo-information: a functional magnetic resonance imaging study. *BMC Complement. Altern. Med.* 13, 114. <https://doi.org/10.1186/1472-6882-13-114>
- Mohammadi, B., Kollewe, K., Samii, A., Beckmann, C.F., Dengler, R., Münte, T.F., 2012. Changes in resting-state brain networks in writer's cramp. *Hum. Brain Mapp.* 33, 840–848. <https://doi.org/10.1002/hbm.21250>
- Mott, F.W., Sherrington, C.S., 1895. Experiments upon the influence of sensory nerves upon movement and nutrition of the limbs. Preliminary communication. *Proc. R. Soc. Lond.* 57, 481–488.
- Muellbacher, W., Richards, C., Ziemann, U., Wittenberg, G., Wetz, D., Boroojerdi, B., Cohen, L., Hallett, M., 2002. Improving hand function in chronic stroke. *Arch. Neurol.* 59, 1278–1282. <https://doi.org/10.1001/archneur.59.8.1278>
- Müller, H., 1974. [Comment on V.Vojta's: Early diagnosis and therapy of cerebral disturbances of motility in infancy (author's transl)]. *Z. Für Orthop. Ihre Grenzgeb.* 112, 361–364.
- Mullinger, K.J., Mayhew, S.D., Bagshaw, A.P., Bowtell, R., Francis, S.T., 2014. Evidence that the negative BOLD response is neuronal in origin: a simultaneous EEG-BOLD-CBF study in humans. *NeuroImage* 94, 263–274. <https://doi.org/10.1016/j.neuroimage.2014.02.029>
- Münte, T.F., Jöbges, E.M., Wieringa, B.M., Klein, S., Schubert, M., Johannes, S., Dengler, R.,

1996. Human evoked potentials to long duration vibratory stimuli: role of muscle afferents. *Neurosci. Lett.* 216, 163–166. [https://doi.org/10.1016/0304-3940\(96\)13036-6](https://doi.org/10.1016/0304-3940(96)13036-6)
- Murakami, T., Sakuma, K., Nomura, T., Nakashima, K., 2007. Short-interval intracortical inhibition is modulated by high-frequency peripheral mixed nerve stimulation. *Neurosci. Lett.* 420, 72–75. <https://doi.org/10.1016/j.neulet.2007.04.059>
- Murillo, N., Kumru, H., Vidal-Samsó, J., Benito, J., Medina, J., Navarro, X., Valls-Sole, J., 2011. Decrease of spasticity with muscle vibration in patients with spinal cord injury. *Clin. Neurophysiol. Off. J. Int. Fed. Clin. Neurophysiol.* 122, 1183–1189. <https://doi.org/10.1016/j.clinph.2010.11.012>
- Murillo, N., Valls-Sole, J., Vidal, J., Opisso, E., Medina, J., Kumru, H., 2014. Focal vibration in neurorehabilitation. *Eur. J. Phys. Rehabil. Med.* 50, 231–242.
- Muschelli, J., Nebel, M.B., Caffo, B.S., Barber, A.D., Pekar, J.J., Mostofsky, S.H., 2014. Reduction of motion-related artifacts in resting state fMRI using aCompCor. *NeuroImage* 96, 22–35. <https://doi.org/10.1016/j.neuroimage.2014.03.028>
- Nachev, P., Kennard, C., Husain, M., 2008. Functional role of the supplementary and pre-supplementary motor areas. *Nat. Rev. Neurosci.* 9, 856–869. <https://doi.org/10.1038/nrn2478>
- Nagao, S., 2004. Pontine nuclei-mediated cerebello-cerebral interactions and its functional role. *The Cerebellum* 3, 11–15. <https://doi.org/10.1080/14734220310012181>
- Naito, E., 2004. Sensing limb movements in the motor cortex: how humans sense limb movement. *Neurosci. Rev. J. Bringing Neurobiol. Neurol. Psychiatry* 10, 73–82. <https://doi.org/10.1177/1073858403259628>
- Naito, E., Ehrsson, H.H., 2006. Somatic sensation of hand-object interactive movement is associated with activity in the left inferior parietal cortex. *J. Neurosci. Off. J. Soc. Neurosci.* 26, 3783–3790. <https://doi.org/10.1523/JNEUROSCI.4835-05.2006>
- Naito, E., Ehrsson, H.H., Geyer, S., Zilles, K., Roland, P.E., 1999. Illusory Arm Movements Activate Cortical Motor Areas: A Positron Emission Tomography Study. *J. Neurosci.* 19, 6134–6144.
- Naito, E., Morita, T., Amemiya, K., 2016. Body representations in the human brain revealed by kinesthetic illusions and their essential contributions to motor control and corporeal awareness. *Neurosci. Res.* 104, 16–30. <https://doi.org/10.1016/j.neures.2015.10.013>
- Naito, E., Nakashima, T., Kito, T., Aramaki, Y., Okada, T., Sadato, N., 2007. Human limb-specific and non-limb-specific brain representations during kinesthetic illusory movements of the upper and lower extremities. *Eur. J. Neurosci.* 25, 3476–3487. <https://doi.org/10.1111/j.1460-9568.2007.05587.x>
- Naito, E., Roland, P.E., Ehrsson, H.H., 2002. I Feel My Hand Moving: A New Role of the Primary Motor Cortex in Somatic Perception of Limb Movement. *Neuron* 36, 979–988. [https://doi.org/10.1016/S0896-6273\(02\)00980-7](https://doi.org/10.1016/S0896-6273(02)00980-7)
- Naito, E., Roland, P.E., Grefkes, C., Choi, H.J., Eickhoff, S., Geyer, S., Zilles, K., Ehrsson, H.H., 2005. Dominance of the right hemisphere and role of area 2 in human kinesthesia. *J. Neurophysiol.* 93, 1020–1034. <https://doi.org/10.1152/jn.00637.2004>
- Naito, E., Scheperjans, F., Eickhoff, S.B., Amunts, K., Roland, P.E., Zilles, K., Ehrsson, H.H.,

2008. Human superior parietal lobule is involved in somatic perception of bimanual interaction with an external object. *J. Neurophysiol.* 99, 695–703.
<https://doi.org/10.1152/jn.00529.2007>
- Nakamura, H., Kitagawa, H., Kawaguchi, Y., Tsuji, H., 1997. Intracortical facilitation and inhibition after transcranial magnetic stimulation in conscious humans. *J. Physiol.* 498 (Pt 3), 817–823. <https://doi.org/10.1113/jphysiol.1997.sp021905>
- Nelson, A.J., Staines, W.R., Graham, S.J., McIlroy, W.E., 2004. Activation in SI and SII: the influence of vibrotactile amplitude during passive and task-relevant stimulation. *Brain Res. Cogn. Brain Res.* 19, 174–184.
<https://doi.org/10.1016/j.cogbrainres.2003.11.013>
- Nevrlý, M., Hlušík, P., Hok, P., Otruba, P., Tüdös, Z., Kaňovský, P., 2018. Changes in sensorimotor network activation after botulinum toxin type A injections in patients with cervical dystonia: a functional MRI study. *Exp. Brain Res.* 236, 2627–2637.
<https://doi.org/10.1007/s00221-018-5322-3>
- Nevrlý, M., Hok, P., Otruba, P., Kaiserová, M., Hvizdošová, L., Trnečková, M., Tüdös, Z., Hlušík, P., Kaňovský, P., in preparation. Botulinum toxin injection changes resting state cerebellar connectivity in cervical dystonia.
- Nicoll, R.A., 2017. A Brief History of Long-Term Potentiation. *Neuron* 93, 281–290.
<https://doi.org/10.1016/j.neuron.2016.12.015>
- Nieuwenhuys, R., Voogd, J., Huijzen, Chr. van, 2008. *The human central nervous system.* Springer, Berlin; New York.
- Nuriya, M., Hirase, H., 2016. Involvement of astrocytes in neurovascular communication. *Prog. Brain Res.* 225, 41–62. <https://doi.org/10.1016/bs.pbr.2016.02.001>
- Nürnberg, L., Gracien, R.-M., Hok, P., Hof, S.-M., Rüb, U., Steinmetz, H., Hilker, R., Klein, J.C., Deichmann, R., Baudrexel, S., 2017. Longitudinal changes of cortical microstructure in Parkinson's disease assessed with T1 relaxometry. *NeuroImage Clin.* 13, 405–414. <https://doi.org/10.1016/j.nicl.2016.12.025>
- Obermann, M., Vollrath, C., de Greiff, A., Gizewski, E.R., Diener, H.-C., Hallett, M., Maschke, M., 2010. Sensory disinhibition on passive movement in cervical dystonia. *Mov. Disord. Off. J. Mov. Disord. Soc.* 25, 2627–2633.
<https://doi.org/10.1002/mds.23321>
- Obermann, M., Yaldizli, O., de Greiff, A., Konczak, J., Lachenmayer, M.L., Tumczak, F., Buhl, A.R., Putzki, N., Vollmer-Haase, J., Gizewski, E.R., Diener, H.-C., Maschke, M., 2008. Increased basal-ganglia activation performing a non-dystonia-related task in focal dystonia. *Eur. J. Neurol.* 15, 831–838. <https://doi.org/10.1111/j.1468-1331.2008.02196.x>
- Ogawa, S., Lee, T.M., Kay, A.R., Tank, D.W., 1990. Brain magnetic resonance imaging with contrast dependent on blood oxygenation. *Proc. Natl. Acad. Sci. U. S. A.* 87, 9868–9872. <https://doi.org/10.1073/pnas.87.24.9868>
- Ogawa, S., Menon, R.S., Tank, D.W., Kim, S.G., Merkle, H., Ellermann, J.M., Ugurbil, K., 1993. Functional brain mapping by blood oxygenation level-dependent contrast magnetic resonance imaging. A comparison of signal characteristics with a biophysical model. *Biophys. J.* 64, 803–812.

- Oldfield, R.C., 1971. The assessment and analysis of handedness: the Edinburgh inventory. *Neuropsychologia* 9, 97–113.
- Omrani, M., Kaufman, M.T., Hatsopoulos, N.G., Cheney, P.D., 2017. Perspectives on classical controversies about the motor cortex. *J. Neurophysiol.* 118, 1828–1848. <https://doi.org/10.1152/jn.00795.2016>
- Opavský, J., 2002. Autonomní nervový systém a diabetická autonomní neuropatie. *Klinické aspekty a diagnostika*. Galén, Praha.
- Opavský, J., Salinger, J., 1995. Examinational methods of the autonomic system function – a review for the clinical practice [In Czech]. *Noninvasive Cardiol.* 139–153.
- Opavský, R., Hlušík, P., Otruba, P., Kaňovský, P., 2012. Somatosensory Cortical Activation in Cervical Dystonia and Its Modulation With Botulinum Toxin: An fMRI Study. *Int. J. Neurosci.* 122, 45–52. <https://doi.org/10.3109/00207454.2011.623807>
- Opavský, R., Hlušík, P., Otruba, P., Kaňovský, P., 2011. Sensorimotor network in cervical dystonia and the effect of botulinum toxin treatment: A functional MRI study. *J. Neurol. Sci., Special Section: ECF 2009 A New Treatment Era in Multiple Sclerosis: Options, Challenges, Risks European Charcot Foundation Symposium 2009* 306, 71–75. <https://doi.org/10.1016/j.jns.2011.03.040>
- Oulad Ben Taib, N., Manto, M., Laute, M.-A., Brotchi, J., 2005. The cerebellum modulates rodent cortical motor output after repetitive somatosensory stimulation. *Neurosurgery* 56, 811–820; discussion 811-820.
- Palomar, F.J., Mir, P., 2012. Neurophysiological changes after intramuscular injection of botulinum toxin. *Clin. Neurophysiol. Off. J. Int. Fed. Clin. Neurophysiol.* 123, 54–60. <https://doi.org/10.1016/j.clinph.2011.05.032>
- Paoloni, M., Mangone, M., Scettri, P., Procaccianti, R., Cometa, A., Santilli, V., 2010. Segmental muscle vibration improves walking in chronic stroke patients with foot drop: a randomized controlled trial. *Neurorehabil. Neural Repair* 24, 254–262. <https://doi.org/10.1177/1545968309349940>
- Park, E.S., Park, C.I., Kim, D.Y., Kim, Y.R., 2002. The effect of spasticity on cortical somatosensory-evoked potentials: changes of cortical somatosensory-evoked potentials after botulinum toxin type A injection. *Arch. Phys. Med. Rehabil.* 83, 1592–1596.
- Pascual-Leone, A., Cammarota, A., Wassermann, E.M., Brasil-Neto, J.P., Cohen, L.G., Hallett, M., 1993. Modulation of motor cortical outputs to the reading hand of braille readers. *Ann. Neurol.* 34, 33–37. <https://doi.org/10.1002/ana.410340108>
- Pascual-Leone, A., Grafman, J., Hallett, M., 1994. Modulation of cortical motor output maps during development of implicit and explicit knowledge. *Science* 263, 1287–1289. <https://doi.org/10.1126/science.8122113>
- Pauri, F., Boffa, L., Cassetta, E., Pasqualetti, P., Rossini, P.M., 2000. Botulinum toxin type-A treatment in spastic paraparesis: a neurophysiological study. *J. Neurol. Sci.* 181, 89–97. [https://doi.org/10.1016/s0022-510x\(00\)00439-1](https://doi.org/10.1016/s0022-510x(00)00439-1)
- Pavlidis, C., Miyashita, E., Asanuma, H., 1993. Projection from the sensory to the motor cortex is important in learning motor skills in the monkey. *J. Neurophysiol.* 70, 733–741.

- Pavlikova, M., Cattaneo, D., Jonsdottir, J., Gervasoni, E., Stetkarova, I., Angelova, G., Markova, M., Prochazkova, M., Prokopiusova, T., Hruskova, N., Reznickova, J., Zimova, D., Spanhelova, S., Rasova, K., 2020. The impact of balance specific physiotherapy, intensity of therapy and disability on static and dynamic balance in people with multiple sclerosis: A multi-center prospective study. *Mult. Scler. Relat. Disord.* 40, 101974. <https://doi.org/10.1016/j.msard.2020.101974>
- Pazzaglia, C., Camerota, F., Germanotta, M., Di Sipio, E., Celletti, C., Padua, L., 2016. Efficacy of focal mechanic vibration treatment on balance in Charcot-Marie-Tooth 1A disease: a pilot study. *J. Neurol.* 263, 1434–1441. <https://doi.org/10.1007/s00415-016-8157-5>
- Peiper, A., 1956. *Die Eigenart der kindlichen Hirntätigkeit*. Thieme, Leipzig.
- Penfield, W., Boldrey, E., 1937. Somatic Motor and Sensory Representation in the Cerebral Cortex of Man as Studied by Electrical Stimulation. *Brain* 60, 389–443. <https://doi.org/10.1093/brain/60.4.389>
- Perez, M.A., Lungholt, B.K.S., Nyborg, K., Nielsen, J.B., 2004. Motor skill training induces changes in the excitability of the leg cortical area in healthy humans. *Exp. Brain Res.* 159, 197–205. <https://doi.org/10.1007/s00221-004-1947-5>
- Petridou, N., Siero, J.C.W., 2019. Laminar fMRI: What can the time domain tell us? *NeuroImage* 197, 761–771. <https://doi.org/10.1016/j.neuroimage.2017.07.040>
- Phadke, C.P., Ismail, F., Boulias, C., 2012. Assessing the neurophysiological effects of botulinum toxin treatment for adults with focal limb spasticity: a systematic review. *Disabil. Rehabil.* 34, 91–100. <https://doi.org/10.3109/09638288.2011.591882>
- Picard, N., Strick, P.L., 2001. Imaging the premotor areas. *Curr. Opin. Neurobiol.* 11, 663–672.
- Picard, N., Strick, P.L., 1996. Motor areas of the medial wall: a review of their location and functional activation. *Cereb. Cortex N. Y. N* 1991 6, 342–353. <https://doi.org/10.1093/cercor/6.3.342>
- Powell, J., Pandyan, A.D., Granat, M., Cameron, M., Stott, D.J., 1999. Electrical stimulation of wrist extensors in poststroke hemiplegia. *Stroke* 30, 1384–1389.
- Priplata, A.A., Niemi, J.B., Harry, J.D., Lipsitz, L.A., Collins, J.J., 2003. Vibrating insoles and balance control in elderly people. *Lancet Lond. Engl.* 362, 1123–1124. [https://doi.org/10.1016/S0140-6736\(03\)14470-4](https://doi.org/10.1016/S0140-6736(03)14470-4)
- Priplata, A.A., Patriitti, B.L., Niemi, J.B., Hughes, R., Gravelle, D.C., Lipsitz, L.A., Veves, A., Stein, J., Bonato, P., Collins, J.J., 2006. Noise-enhanced balance control in patients with diabetes and patients with stroke. *Ann. Neurol.* 59, 4–12. <https://doi.org/10.1002/ana.20670>
- Proske, U., Gandevia, S.C., 2018. Kinesthetic Senses. *Compr. Physiol.* 8, 1157–1183. <https://doi.org/10.1002/cphy.c170036>
- Proske, U., Gandevia, S.C., 2012. The proprioceptive senses: their roles in signaling body shape, body position and movement, and muscle force. *Physiol. Rev.* 92, 1651–1697. <https://doi.org/10.1152/physrev.00048.2011>
- Pruim, R.H.R., Mennes, M., Buitelaar, J.K., Beckmann, C.F., 2015a. Evaluation of ICA-AROMA and alternative strategies for motion artifact removal in resting state fMRI.

- NeuroImage 112, 278–287. <https://doi.org/10.1016/j.neuroimage.2015.02.063>
- Pruim, R.H.R., Mennes, M., van Rooij, D., Llera, A., Buitelaar, J.K., Beckmann, C.F., 2015b. ICA-AROMA: A robust ICA-based strategy for removing motion artifacts from fMRI data. *NeuroImage* 112, 267–277. <https://doi.org/10.1016/j.neuroimage.2015.02.064>
- Puckett, A.M., Bollmann, S., Junday, K., Barth, M., Cunnington, R., 2020. Bayesian population receptive field modeling in human somatosensory cortex. *NeuroImage* 208, 116465. <https://doi.org/10.1016/j.neuroimage.2019.116465>
- Pyndt, H.S., Ridding, M.C., 2004. Modification of the human motor cortex by associative stimulation. *Exp. Brain Res.* 159, 123–128. <https://doi.org/10.1007/s00221-004-1943-9>
- Qiu, K., Jing, M., Sun, R., Yang, J., Liu, X., He, Z., Yin, S., Lan, Y., Cheng, S., Gao, F., Liang, F., Zeng, F., 2016. The Status of the Quality Control in Acupuncture-Neuroimaging Studies. *Evid.-Based Complement. Altern. Med. ECAM* 2016, 3685785. <https://doi.org/10.1155/2016/3685785>
- Raichle, M.E., 2011. Circulatory and Metabolic Correlates of Brain Function in Normal Humans, in: *Comprehensive Physiology*. American Cancer Society, pp. 643–674. <https://doi.org/10.1002/cphy.cp010516>
- Raichle, M.E., 1986. Neuroimaging. *Trends Neurosci.* 9, 525–529. [https://doi.org/10.1016/0166-2236\(86\)90166-9](https://doi.org/10.1016/0166-2236(86)90166-9)
- Rasman, B.G., Forbes, P.A., Tisserand, R., Blouin, J.-S., 2018. Sensorimotor Manipulations of the Balance Control Loop—Beyond Imposed External Perturbations. *Front. Neurol.* 9. <https://doi.org/10.3389/fneur.2018.00899>
- Redman, T.A., Gibson, N., Finn, J.C., Bremner, A.P., Valentine, J., Thickbroom, G.W., 2008. Upper limb corticomotor projections and physiological changes that occur with botulinum toxin-A therapy in children with hemiplegic cerebral palsy. *Eur. J. Neurol.* 15, 787–791. <https://doi.org/10.1111/j.1468-1331.2008.02194.x>
- Rencher, A.C., Christensen, W.F., 2012. Cluster Analysis, in: Rencher, A.C., Christensen, W.F. (Eds.), *Methods of Multivariate Analysis*. Wiley-Blackwell, Hoboken, New Jersey, pp. 501–554. <https://doi.org/10.1002/9781118391686.ch15>
- Ribot-Ciscar, E., Vedel, J.P., Roll, J.P., 1989. Vibration sensitivity of slowly and rapidly adapting cutaneous mechanoreceptors in the human foot and leg. *Neurosci. Lett.* 104, 130–135. [https://doi.org/10.1016/0304-3940\(89\)90342-X](https://doi.org/10.1016/0304-3940(89)90342-X)
- Ridding, M.C., Brouwer, B., Miles, T.S., Pitcher, J.B., Thompson, P.D., 2000. Changes in muscle responses to stimulation of the motor cortex induced by peripheral nerve stimulation in human subjects. *Exp. Brain Res.* 131, 135–143.
- Ridding, M.C., McKay, D.R., Thompson, P.D., Miles, T.S., 2001. Changes in corticomotor representations induced by prolonged peripheral nerve stimulation in humans. *Clin. Neurophysiol.* 112, 1461–9.
- Ridding, M.C., Rothwell, J.C., 1999. Afferent input and cortical organisation: a study with magnetic stimulation. *Exp. Brain Res.* 126, 536–544. <https://doi.org/10.1007/s002210050762>
- Ridding, M.C., Rothwell, J.C., 1997. Stimulus/response curves as a method of measuring motor cortical excitability in man. *Electroencephalogr. Clin. Neurophysiol.* 105, 340–

344. [https://doi.org/10.1016/s0924-980x\(97\)00041-6](https://doi.org/10.1016/s0924-980x(97)00041-6)
- Ridding, M.C., Sheean, G., Rothwell, J.C., Inzelberg, R., Kujirai, T., 1995. Changes in the balance between motor cortical excitation and inhibition in focal, task specific dystonia. *J. Neurol. Neurosurg. Psychiatry* 59, 493–498. <https://doi.org/10.1136/jnnp.59.5.493>
- Ridding, M.C., Taylor, J.L., 2001. Mechanisms of motor-evoked potential facilitation following prolonged dual peripheral and central stimulation in humans. *J. Physiol.* 537, 623–631.
- Riddle, C.N., Edgley, S.A., Baker, S.N., 2009. Direct and Indirect Connections with Upper Limb Motoneurons from the Primate Reticulospinal Tract. *J. Neurosci.* 29, 4993–4999. <https://doi.org/10.1523/JNEUROSCI.3720-08.2009>
- Riedel, M.C., Ray, K.L., Dick, A.S., Sutherland, M.T., Hernandez, Z., Fox, P.M., Eickhoff, S.B., Fox, P.T., Laird, A.R., 2015. Meta-analytic connectivity and behavioral parcellation of the human cerebellum. *NeuroImage* 117, 327–342. <https://doi.org/10.1016/j.neuroimage.2015.05.008>
- Rioult-Pedotti, M.S., Friedman, D., Donoghue, J.P., 2000. Learning-induced LTP in neocortex. *Science* 290, 533–536. <https://doi.org/10.1126/science.290.5491.533>
- Rocchi, L., Erro, R., Antelmi, E., Berardelli, A., Tinazzi, M., Liguori, R., Bhatia, K., Rothwell, J., 2017. High frequency somatosensory stimulation increases sensorimotor inhibition and leads to perceptual improvement in healthy subjects. *Clin. Neurophysiol. Off. J. Int. Fed. Clin. Neurophysiol.* 128, 1015–1025. <https://doi.org/10.1016/j.clinph.2017.03.046>
- Roelfsema, P.R., Holtmaat, A., 2018. Control of synaptic plasticity in deep cortical networks. *Nat. Rev. Neurosci.* 19, 166–180. <https://doi.org/10.1038/nrn.2018.6>
- Rogers, D.K., Bendrups, A.P., Lewis, M.M., 1985. Disturbed proprioception following a period of muscle vibration in humans. *Neurosci. Lett.* 57, 147–152. [https://doi.org/10.1016/0304-3940\(85\)90054-0](https://doi.org/10.1016/0304-3940(85)90054-0)
- Roland, P.E., Larsen, B., Lassen, N.A., Skinhøj, E., 1980. Supplementary motor area and other cortical areas in organization of voluntary movements in man. *J. Neurophysiol.* 43, 118–136.
- Roland, P.E., Zilles, K., 1996. Functions and structures of the motor cortices in humans. *Curr. Opin. Neurobiol.* 6, 773–781. [https://doi.org/10.1016/S0959-4388\(96\)80027-4](https://doi.org/10.1016/S0959-4388(96)80027-4)
- Roll, J.P., Gilhodes, J.C., Tardy-Gervet, M.F., 1980. [Perceptive and motor effects of muscular vibrations in the normal human: demonstration of a response by opposing muscles]. *Arch. Ital. Biol.* 118, 51–71.
- Roll, J.P., Vedel, J.P., 1982. Kinaesthetic role of muscle afferents in man, studied by tendon vibration and microneurography. *Exp. Brain Res.* 47, 177–190.
- Roll, J.P., Vedel, J.P., Ribot, E., 1989a. Alteration of proprioceptive messages induced by tendon vibration in man: a microneurographic study. *Exp. Brain Res.* 76, 213–222.
- Roll, J.P., Vedel, J.P., Roll, R., 1989b. Eye, head and skeletal muscle spindle feedback in the elaboration of body references. *Prog. Brain Res.* 80, 113–123; discussion 57–60. [https://doi.org/10.1016/s0079-6123\(08\)62204-9](https://doi.org/10.1016/s0079-6123(08)62204-9)
- Roll, R., Kavounoudias, A., Albert, F., Legré, R., Gay, A., Fabre, B., Roll, J.P., 2012. Illusory

- movements prevent cortical disruption caused by immobilization. *NeuroImage* 62, 510–519. <https://doi.org/10.1016/j.neuroimage.2012.05.016>
- Roll, R., Kavounoudias, A., Roll, J.-P., 2002. Cutaneous afferents from human plantar sole contribute to body posture awareness. *Neuroreport* 13, 1957–1961. <https://doi.org/10.1097/00001756-200210280-00025>
- Rollnik, J.D., Siggelkow, S., Schubert, M., Schneider, U., Dengler, R., 2001. Muscle vibration and prefrontal repetitive transcranial magnetic stimulation. *Muscle Nerve* 24, 112–115. [https://doi.org/10.1002/1097-4598\(200101\)24:1<112::aid-mus15>3.0.co;2-7](https://doi.org/10.1002/1097-4598(200101)24:1<112::aid-mus15>3.0.co;2-7)
- Rolls, E.T., O’Doherty, J., Kringelbach, M.L., Francis, S., Bowtell, R., McGlone, F., 2003. Representations of Pleasant and Painful Touch in the Human Orbitofrontal and Cingulate Cortices. *Cereb. Cortex* 13, 308–317. <https://doi.org/10.1093/cercor/13.3.308>
- Romaiguère, P., Anton, J.-L., Roth, M., Casini, L., Roll, J.-P., 2003. Motor and parietal cortical areas both underlie kinaesthesia. *Cogn. Brain Res.* 16, 74–82. [https://doi.org/10.1016/S0926-6410\(02\)00221-5](https://doi.org/10.1016/S0926-6410(02)00221-5)
- Romaiguère, P., Vedel, J.P., Azulay, J.P., Pagni, S., 1991. Differential activation of motor units in the wrist extensor muscles during the tonic vibration reflex in man. *J. Physiol.* 444, 645–667.
- Rome, S., Grünewald, R.A., 1999. Abnormal perception of vibration-induced illusion of movement in dystonia. *Neurology* 53, 1794–1800. <https://doi.org/10.1212/wnl.53.8.1794>
- Rosales, R.L., Dressler, D., 2010. On muscle spindles, dystonia and botulinum toxin. *Eur. J. Neurol. Off. J. Eur. Fed. Neurol. Soc.* 17 Suppl 1, 71–80. <https://doi.org/10.1111/j.1468-1331.2010.03056.x>
- Rosales, R.L., Kanovsky, P., Fernandez, H.H., 2011. What’s the “catch” in upper-limb post-stroke spasticity: expanding the role of botulinum toxin applications. *Parkinsonism Relat. Disord.* 17 Suppl 1, S3-10. <https://doi.org/10.1016/j.parkreldis.2011.06.019>
- Rosén, I., Asanuma, H., 1972. Peripheral afferent inputs to the forelimb area of the monkey motor cortex: input-output relations. *Exp. Brain Res.* 14, 257–273. <https://doi.org/10.1007/bf00816162>
- Rosenkranz, K., Altenmüller, E., Siggelkow, S., Dengler, R., 2000. Alteration of sensorimotor integration in musician’s cramp: impaired focusing of proprioception. *Clin. Neurophysiol.* 111, 2040–2045. [https://doi.org/10.1016/S1388-2457\(00\)00460-0](https://doi.org/10.1016/S1388-2457(00)00460-0)
- Rosenkranz, K., Butler, K., Williamon, A., Cordivari, C., Lees, A.J., Rothwell, J.C., 2008. Sensorimotor reorganization by proprioceptive training in musician’s dystonia and writer’s cramp. *Neurology* 70, 304–315. <https://doi.org/10.1212/01.wnl.0000296829.66406.14>
- Rosenkranz, K., Butler, K., Williamon, A., Rothwell, J.C., 2009. Regaining motor control in musician’s dystonia by restoring sensorimotor organization. *J. Neurosci. Off. J. Soc. Neurosci.* 29, 14627–14636. <https://doi.org/10.1523/JNEUROSCI.2094-09.2009>
- Rosenkranz, K., Pesenti, A., Paulus, W., Tergau, F., 2003. Focal reduction of intracortical inhibition in the motor cortex by selective proprioceptive stimulation. *Exp. Brain Res.* 149, 9–16. <https://doi.org/10.1007/s00221-002-1330-3>

- Rosenkranz, K., Rothwell, J.C., 2006a. Differences between the effects of three plasticity inducing protocols on the organization of the human motor cortex. *Eur. J. Neurosci.* 23, 822–829. <https://doi.org/10.1111/j.1460-9568.2006.04605.x>
- Rosenkranz, K., Rothwell, J.C., 2006b. Spatial attention affects sensorimotor reorganisation in human motor cortex. *Exp. Brain Res.* 170, 97–108. <https://doi.org/10.1007/s00221-005-0173-0>
- Rosenkranz, K., Rothwell, J.C., 2004. The effect of sensory input and attention on the sensorimotor organization of the hand area of the human motor cortex. *J. Physiol.* 561, 307–320. <https://doi.org/10.1113/jphysiol.2004.069328>
- Rosenkranz, K., Rothwell, J.C., 2003. Differential effect of muscle vibration on intracortical inhibitory circuits in humans. *J. Physiol.* 551, 649–660. <https://doi.org/10.1113/jphysiol.2003.043752>
- Rosenkranz, K., Williamon, A., Butler, K., Cordivari, C., Lees, A.J., Rothwell, J.C., 2005. Pathophysiological differences between musician's dystonia and writer's cramp. *Brain J. Neurol.* 128, 918–931. <https://doi.org/10.1093/brain/awh402>
- Rossini, P.M., Rossi, S., Tecchio, F., Pasqualetti, P., Finazzi-Agrò, A., Sabato, A., 1996. Focal brain stimulation in healthy humans: motor maps changes following partial hand sensory deprivation. *Neurosci. Lett.* 214, 191–195. [https://doi.org/10.1016/0304-3940\(96\)12940-2](https://doi.org/10.1016/0304-3940(96)12940-2)
- Roy, F.D., Gorassini, M.A., 2008. Peripheral sensory activation of cortical circuits in the leg motor cortex of man. *J. Physiol.* 586, 4091–4105. <https://doi.org/10.1113/jphysiol.2008.153726>
- Rushworth, G., 1959. The Nature of the Functional Disorder in the Hypertonic States. *Cereb. Palsy Bull.* 1, 3–7.
- Sahara, Y., Xie, Y.K., Bennett, G.J., 1990. Intracellular records of the effects of primary afferent input in lumbar spinoreticular tract neurons in the cat. *J. Neurophysiol.* 64, 1791–1800.
- Sailer, A., Molnar, G.F., Cunic, D.I., Chen, R., 2002. Effects of peripheral sensory input on cortical inhibition in humans. *J. Physiol.* 544, 617–629. <https://doi.org/10.1113/jphysiol.2002.028670>
- Sakamoto, T., Arissian, K., Asanuma, H., 1989. Functional role of the sensory cortex in learning motor skills in cats. *Brain Res.* 503, 258–264. [https://doi.org/10.1016/0006-8993\(89\)91672-7](https://doi.org/10.1016/0006-8993(89)91672-7)
- Sakamoto, T., Porter, L.L., Asanuma, H., 1987. Long-lasting potentiation of synaptic potentials in the motor cortex produced by stimulation of the sensory cortex in the cat: a basis of motor learning. *Brain Res.* 413, 360–364. [https://doi.org/10.1016/0006-8993\(87\)91029-8](https://doi.org/10.1016/0006-8993(87)91029-8)
- Salinger, J., Opavský, J., Stejskal, P., Vychodil, R., Olšák, S., Janura, M., 1998. The evaluation of heart rate variability in physical exercise by using the telemetric variapulse TF3 system. *Acta Univ. Palacki. Olomuc. Gymnica* 28, 13–23.
- Sammons, R.P., Keck, T., 2015. Adult plasticity and cortical reorganization after peripheral lesions. *Curr. Opin. Neurobiol.* 35, 136–141. <https://doi.org/10.1016/j.conb.2015.08.004>

- Sanchez-Panchuelo, R.M., Ackerley, R., Glover, P.M., Bowtell, R.W., Wessberg, J., Francis, S.T., McGlone, F., 2016. Mapping quantal touch using 7 Tesla functional magnetic resonance imaging and single-unit intraneural microstimulation. *eLife* 5. <https://doi.org/10.7554/eLife.12812>
- Sanchez-Panchuelo, R.M., Besle, J., Beckett, A., Bowtell, R., Schluppeck, D., Francis, S., 2012. Within-digit functional parcellation of Brodmann areas of the human primary somatosensory cortex using functional magnetic resonance imaging at 7 tesla. *J. Neurosci. Off. J. Soc. Neurosci.* 32, 15815–15822. <https://doi.org/10.1523/JNEUROSCI.2501-12.2012>
- Sanchez-Panchuelo, R.M., Besle, J., Schluppeck, D., Humberstone, M., Francis, S., 2018. Somatotopy in the Human Somatosensory System. *Front. Hum. Neurosci.* 12, 235. <https://doi.org/10.3389/fnhum.2018.00235>
- Sanz-Esteban, I., Calvo-Lobo, C., Ríos-Lago, M., Álvarez-Linera, J., Muñoz-García, D., Rodríguez-Sanz, D., 2018. Mapping the human brain during a specific Vojta's tactile input: the ipsilateral putamen's role. *Medicine (Baltimore)* 97, e0253. <https://doi.org/10.1097/MD.00000000000010253>
- Sarasso, E., Agosta, F., Piramide, N., Bianchi, F., Butera, C., Gatti, R., Amadio, S., Del Carro, U., Filippi, M., 2020. Sensory trick phenomenon in cervical dystonia: a functional MRI study. *J. Neurol.* <https://doi.org/10.1007/s00415-019-09683-5>
- Sauvage, C., Poirriez, S., Manto, M., Jissendi, P., Habas, C., 2011. Reevaluating brain networks activated during mental imagery of finger movements using probabilistic Tensorial Independent Component Analysis (TICA). *Brain Imaging Behav.* 5, 137–148. <https://doi.org/10.1007/s11682-011-9118-3>
- Schepens, B., Drew, T., 2004. Independent and convergent signals from the pontomedullary reticular formation contribute to the control of posture and movement during reaching in the cat. *J. Neurophysiol.* 92, 2217–2238. <https://doi.org/10.1152/jn.01189.2003>
- Schmidt, T.T., Wu, Y.-H., Blankenburg, F., 2017. Content-Specific Codes of Parametric Vibrotactile Working Memory in Humans. *J. Neurosci. Off. J. Soc. Neurosci.* 37, 9771–9777. <https://doi.org/10.1523/JNEUROSCI.1167-17.2017>
- Seitz, R.J., Roland, P.E., 1992. Vibratory stimulation increases and decreases the regional cerebral blood flow and oxidative metabolism: a positron emission tomography (PET) study. *Acta Neurol. Scand.* 86, 60–67.
- Seizova-Cajic, T., Smith, J.L., Taylor, J.L., Gandevia, S.C., 2007. Proprioceptive movement illusions due to prolonged stimulation: reversals and aftereffects. *PloS One* 2, e1037. <https://doi.org/10.1371/journal.pone.0001037>
- Šenkárová, Z., Hlustík, P., Otruba, P., Herzig, R., Kanovský, P., 2010. Modulation of cortical activity in patients suffering from upper arm spasticity following stroke and treated with botulinum toxin A: an fMRI study. *J. Neuroimaging Off. J. Am. Soc. Neuroimaging* 20, 9–15. <https://doi.org/10.1111/j.1552-6569.2009.00375.x>
- Seo, N.J., Lakshminarayanan, K., Lauer, A.W., Ramakrishnan, V., Schmit, B.D., Hanlon, C.A., George, M.S., Bonilha, L., Downey, R.J., DeVries, W., Nagy, T., 2019. Use of imperceptible wrist vibration to modulate sensorimotor cortical activity. *Exp. Brain*

- Res. 237, 805–816. <https://doi.org/10.1007/s00221-018-05465-z>
- Setsompop, K., Feinberg, D.A., Polimeni, J.R., 2016. Rapid brain MRI acquisition techniques at ultra-high fields. *NMR Biomed.* 29, 1198–1221. <https://doi.org/10.1002/nbm.3478>
- Shakkottai, V.G., Batla, A., Bhatia, K., Dauer, W.T., Dresel, C., Niethammer, M., Eidelberg, D., Raike, R.S., Smith, Y., Jinnah, H.A., Hess, E.J., Meunier, S., Hallett, M., Fremont, R., Khodakhah, K., LeDoux, M.S., Popa, T., Gallea, C., Lehericy, S., Bostan, A.C., Strick, P.L., 2017. Current Opinions and Areas of Consensus on the Role of the Cerebellum in Dystonia. *Cerebellum* 16, 577–594. <https://doi.org/10.1007/s12311-016-0825-6>
- Sharp, F.R., Ryan, A.F., 1984. Regional (14C) 2-deoxyglucose uptake during forelimb movements evoked by rat motor cortex stimulation: pons, cerebellum, medulla, spinal cord, muscle. *J. Comp. Neurol.* 224, 286–306.
- Sherrington, C.S., 1906. Lecture II: Co-ordination in the simple reflex (continued), in: *The Integrative Action of the Nervous System*, Yale University Mrs. Hepsa Ely Silliman Memorial Lectures. Yale University Press, New Haven, CT, US, pp. 36–69. <https://doi.org/10.1037/13798-002>
- Shimizu, M., Suzuki, Y., Kiyosawa, M., Wakakura, M., Ishii, K., Ishiwata, K., Mochizuki, M., 2012. Glucose hypermetabolism in the thalamus of patients with hemifacial spasm. *Mov. Disord. Off. J. Mov. Disord. Soc.* 27, 519–525. <https://doi.org/10.1002/mds.24925>
- Siedentopf, C.M., Heubach, K., Ischebeck, A., Gallasch, E., Fend, M., Mottaghy, F.M., Koppelstaetter, F., Haala, I.A., Krause, B.J., Felber, S., Gerstenbrand, F., Golaszewski, S.M., 2008. Variability of BOLD response evoked by foot vibrotactile stimulation: influence of vibration amplitude and stimulus waveform. *NeuroImage* 41, 504–510. <https://doi.org/10.1016/j.neuroimage.2008.02.049>
- Siggelkow, S., Kossev, A., Schubert, M., Kappels, H.-H., Wolf, W., Dengler, R., 1999. Modulation of motor evoked potentials by muscle vibration: The role of vibration frequency. *Muscle Nerve* 22, 1544–1548. [https://doi.org/10.1002/\(SICI\)1097-4598\(199911\)22:11<1544::AID-MUS9>3.0.CO;2-8](https://doi.org/10.1002/(SICI)1097-4598(199911)22:11<1544::AID-MUS9>3.0.CO;2-8)
- Simpson, D.M., Hallett, M., Ashman, E.J., Comella, C.L., Green, M.W., Gronseth, G.S., Armstrong, M.J., Gloss, D., Potrebic, S., Jankovic, J., Karp, B.P., Naumann, M., So, Y.T., Yablon, S.A., 2016. Practice guideline update summary: Botulinum neurotoxin for the treatment of blepharospasm, cervical dystonia, adult spasticity, and headache: Report of the Guideline Development Subcommittee of the American Academy of Neurology. *Neurology* 86, 1818–1826. <https://doi.org/10.1212/WNL.0000000000002560>
- Sittig, A.C., Denier van der Gon, J.J., Gielen, C.C., 1987. The contribution of afferent information on position and velocity to the control of slow and fast human forearm movements. *Exp. Brain Res.* 67, 33–40. <https://doi.org/10.1007/bf00269450>
- Sittig, A.C., Denier van der Gon, J.J., Gielen, C.C., 1985. Separate control of arm position and velocity demonstrated by vibration of muscle tendon in man. *Exp. Brain Res.* 60, 445–453. <https://doi.org/10.1007/bf00236930>

- Smetanin, B.N., Popov, K.Ye., Shlykov, V.Yu., 1993. Postural responses to vibrostimulation of the neck muscle proprioceptors in man. *Neurophysiology* 25, 86–92. <https://doi.org/10.1007/BF01054155>
- Smith, A.E., Ridding, M.C., Higgins, R.D., Wittert, G.A., Pitcher, J.B., 2011. Cutaneous afferent input does not modulate motor intracortical inhibition in ageing men. *Eur. J. Neurosci.* 34, 1461–1469. <https://doi.org/10.1111/j.1460-9568.2011.07869.x>
- Smith, C.A., Levett, K.M., Collins, C.T., Dahlen, H.G., Ee, C.C., Sukanuma, M., 2018. Massage, reflexology and other manual methods for pain management in labour. *Cochrane Database Syst. Rev.* 3, CD009290. <https://doi.org/10.1002/14651858.CD009290.pub3>
- Smith, L., Brouwer, B., 2005. Effectiveness of muscle vibration in modulating corticospinal excitability. *J. Rehabil. Res. Dev.* 42, 787–794.
- Smith, S.L., Lux, R., Haley, S., Slater, H., Beachy, J., Moyer-Mileur, L.J., 2013. The effect of massage on heart rate variability in preterm infants. *J. Perinatol.* 33, 59–64. <https://doi.org/10.1038/jp.2012.47>
- Smith, S.M., 2002. Fast robust automated brain extraction. *Hum. Brain Mapp.* 17, 143–155. <https://doi.org/10.1002/hbm.10062>
- Smith, S.M., 2001. Preparing fMRI data for statistical analysis, in: Jezzard, P., Matthews, P.M., Smith, S.M. (Eds.), *Functional MRI: An Introduction to Methods*. Oxford University Press, Oxford [England]; New York, pp. 229–241.
- Smith, S.M., Beckmann, C.F., Andersson, J., Auerbach, E.J., Bijsterbosch, J., Douaud, G., Duff, E., Feinberg, D.A., Griffanti, L., Harms, M.P., Kelly, M., Laumann, T., Miller, K.L., Moeller, S., Petersen, S., Power, J., Salimi-Khorshidi, G., Snyder, A.Z., Vu, A.T., Woolrich, M.W., Xu, J., Yacoub, E., Uğurbil, K., Van Essen, D.C., Glasser, M.F., WU-Minn HCP Consortium, 2013. Resting-state fMRI in the Human Connectome Project. *NeuroImage* 80, 144–168. <https://doi.org/10.1016/j.neuroimage.2013.05.039>
- Smyth, C., Summers, J.J., Garry, M.I., 2010. Differences in motor learning success are associated with differences in M1 excitability. *Hum. Mov. Sci.* 29, 618–630. <https://doi.org/10.1016/j.humov.2010.02.006>
- Solodkin, A., Hlušík, P., Noll, D.C., Small, S.L., 2001. Lateralization of motor circuits and handedness during finger movements. *Eur. J. Neurol.* 8, 425–434.
- Sörös, P., Marmurek, J., Tam, F., Baker, N., Staines, W.R., Graham, S.J., 2007. Functional MRI of working memory and selective attention in vibrotactile frequency discrimination. *BMC Neurosci.* 8, 48. <https://doi.org/10.1186/1471-2202-8-48>
- Souron, R., Besson, T., Lapole, T., Millet, G.Y., 2018. Neural adaptations in quadriceps muscle after 4 weeks of local vibration training in young versus older subjects. *Appl. Physiol. Nutr. Metab. Physiol. Appl. Nutr. Metab.* 43, 427–436. <https://doi.org/10.1139/apnm-2017-0612>
- Souron, R., Besson, T., McNeil, C.J., Lapole, T., Millet, G.Y., 2017a. An Acute Exposure to Muscle Vibration Decreases Knee Extensors Force Production and Modulates Associated Central Nervous System Excitability. *Front. Hum. Neurosci.* 11, 519. <https://doi.org/10.3389/fnhum.2017.00519>
- Souron, R., Besson, T., Millet, G.Y., Lapole, T., 2017b. Acute and chronic neuromuscular

- adaptations to local vibration training. *Eur. J. Appl. Physiol.* 117, 1939–1964. <https://doi.org/10.1007/s00421-017-3688-8>
- Souron, R., Farabet, A., Féasson, L., Belli, A., Millet, G.Y., Lapole, T., 2017c. Eight weeks of local vibration training increases dorsiflexor muscle cortical voluntary activation. *J. Appl. Physiol. Bethesda Md* 122, 1504–1515. <https://doi.org/10.1152/jappphysiol.00793.2016>
- Stapley, P.J., Drew, T., 2009. The Pontomedullary Reticular Formation Contributes to the Compensatory Postural Responses Observed Following Removal of the Support Surface in the Standing Cat. *J. Neurophysiol.* 101, 1334–1350. <https://doi.org/10.1152/jn.91013.2008>
- Stecina, K., Fedirchuk, B., Hultborn, H., 2013. Information to cerebellum on spinal motor networks mediated by the dorsal spinocerebellar tract. *J. Physiol.* 591, 5433–5443. <https://doi.org/10.1113/jphysiol.2012.249110>
- Steele, C.J., Penhune, V.B., 2010. Specific increases within global decreases: a functional magnetic resonance imaging investigation of five days of motor sequence learning. *J. Neurosci.* 30, 8332–8341. <https://doi.org/10.1523/JNEUROSCI.5569-09.2010>
- Stefan, K., Kunesch, E., Benecke, R., Cohen, L.G., Classen, J., 2002. Mechanisms of enhancement of human motor cortex excitability induced by interventional paired associative stimulation. *J. Physiol.* 543, 699–708. <https://doi.org/10.1113/jphysiol.2002.023317>
- Stefan, K., Kunesch, E., Cohen, L.G., Benecke, R., Classen, J., 2000. Induction of plasticity in the human motor cortex by paired associative stimulation. *Brain J. Neurol.* 123 Pt 3, 572–584. <https://doi.org/10.1093/brain/123.3.572>
- Stepniewska, I., Preuss, T.M., Kaas, J.H., 1993. Architectonics, somatotopic organization, and ipsilateral cortical connections of the primary motor area (M1) of owl monkeys. *J. Comp. Neurol.* 330, 238–271. <https://doi.org/10.1002/cne.903300207>
- Steyvers, M., Levin, O., Van Baelen, M., Swinnen, S.P., 2003a. Corticospinal excitability changes following prolonged muscle tendon vibration. *Neuroreport* 14, 1901–1905. <https://doi.org/10.1097/01.wnr.0000093296.63079.fa>
- Steyvers, M., Levin, O., Verschueren, S.M., Swinnen, S.P., 2003b. Frequency-dependent effects of muscle tendon vibration on corticospinal excitability: a TMS study. *Exp. Brain Res.* 151, 9–14. <https://doi.org/10.1007/s00221-003-1427-3>
- Stoodley, C.J., Valera, E.M., Schmahmann, J.D., 2012. Functional topography of the cerebellum for motor and cognitive tasks: an fMRI study. *NeuroImage* 59, 1560–1570. <https://doi.org/10.1016/j.neuroimage.2011.08.065>
- Strick, P.L., Kim, C.C., 1978. Input to primate motor cortex from posterior parietal cortex (area 5). I. Demonstration by retrograde transport. *Brain Res.* 157, 325–330. [https://doi.org/10.1016/0006-8993\(78\)90035-5](https://doi.org/10.1016/0006-8993(78)90035-5)
- Strzalkowski, N.D.J., Peters, R.M., Inglis, J.T., Bentz, L.R., 2018. Cutaneous afferent innervation of the human foot sole: what can we learn from single-unit recordings? *J. Neurophysiol.* 120, 1233–1246. <https://doi.org/10.1152/jn.00848.2017>
- Suzuki, T., Suzuki, M., Kanemura, N., Hamaguchi, T., 2019. Differential Effect of Visual and Proprioceptive Stimulation on Corticospinal Output for Reciprocal Muscles.

- Front. Integr. Neurosci. 13, 63. <https://doi.org/10.3389/fnint.2019.00063>
- Suzuki, Y., Mizoguchi, S., Kiyosawa, M., Mochizuki, M., Ishiwata, K., Wakakura, M., Ishii, K., 2007. Glucose hypermetabolism in the thalamus of patients with essential blepharospasm. *J. Neurol.* 254, 890–896. <https://doi.org/10.1007/s00415-006-0468-5>
- Swayne, O., Rothwell, J., Rosenkranz, K., 2006. Transcallosal sensorimotor integration: effects of sensory input on cortical projections to the contralateral hand. *Clin. Neurophysiol. Off. J. Int. Fed. Clin. Neurophysiol.* 117, 855–863. <https://doi.org/10.1016/j.clinph.2005.12.012>
- Swayne, O.B.C., Rothwell, J.C., Ward, N.S., Greenwood, R.J., 2008. Stages of motor output reorganization after hemispheric stroke suggested by longitudinal studies of cortical physiology. *Cereb. Cortex N. Y. N* 1991 18, 1909–1922. <https://doi.org/10.1093/cercor/bhm218>
- Takakusaki, K., 2013. Neurophysiology of gait: From the spinal cord to the frontal lobe. *Mov. Disord.* 28, 1483–1491. <https://doi.org/10.1002/mds.25669>
- Takakusaki, K., Chiba, R., Nozu, T., Okumura, T., 2016. Brainstem control of locomotion and muscle tone with special reference to the role of the mesopontine tegmentum and medullary reticulospinal systems. *J. Neural Transm. Vienna Austria* 1996 123, 695–729. <https://doi.org/10.1007/s00702-015-1475-4>
- Tal, Z., Geva, R., Amedi, A., 2017. Positive and Negative Somatotopic BOLD Responses in Contralateral Versus Ipsilateral Penfield Homunculus. *Cereb. Cortex N. Y. N* 1991 27, 962–980. <https://doi.org/10.1093/cercor/bhx024>
- Tan, H., Wade, C., Brown, P., 2016. Post-Movement Beta Activity in Sensorimotor Cortex Indexes Confidence in the Estimations from Internal Models. *J. Neurosci. Off. J. Soc. Neurosci.* 36, 1516–1528. <https://doi.org/10.1523/JNEUROSCI.3204-15.2016>
- Tanji, J., Shima, K., 1996. Supplementary motor cortex in organization of movement. *Eur. Neurol.* 36 Suppl 1, 13–19. <https://doi.org/10.1159/000118878>
- Task Force, 1996. Heart rate variability. Standards of measurement, physiological interpretation, and clinical use. Task Force of the European Society of Cardiology and the North American Society of Pacing and Electrophysiology. *Eur. Heart J.* 17, 354–381.
- Taub, E., Berman, A.J., 1968. Movement and learning in the absence of sensory feedback. *Neuropsychol. Spatially Oriented Behav.* 2, 173–192.
- Taylor, M.W., Taylor, J.L., Seizova-Cajic, T., 2017. Muscle Vibration-Induced Illusions: Review of Contributing Factors, Taxonomy of Illusions and User’s Guide. *Multisensory Res.* 30, 25–63. <https://doi.org/10.1163/22134808-00002544>
- Tempel, L.W., Perlmutter, J.S., 1990. Abnormal Vibration-Induced Cerebral Blood Flow Responses in Idiopathic Dystonia. *Brain* 113, 691–707. <https://doi.org/10.1093/brain/113.3.691>
- Terao, Y., Ugawa, Y., Hanajima, R., Furubayashi, T., Machii, K., Enomoto, H., Shiio, Y., Mochizuki, H., Uesugi, H., Uesaka, Y., Kanazawa, I., 1999. Air-puff-induced facilitation of motor cortical excitability studied in patients with discrete brain lesions. *Brain J. Neurol.* 122 (Pt 12), 2259–2277.
- Thibaut, A., Chatelle, C., Ziegler, E., Bruno, M.-A., Laureys, S., Gosseries, O., 2013.

- Spasticity after stroke: physiology, assessment and treatment. *Brain Inj.* 27, 1093–1105. <https://doi.org/10.3109/02699052.2013.804202>
- Thickbroom, G.W., Byrnes, M.L., Stell, R., Mastaglia, F.L., 2003. Reversible reorganisation of the motor cortical representation of the hand in cervical dystonia. *Mov. Disord. Off. J. Mov. Disord. Soc.* 18, 395–402. <https://doi.org/10.1002/mds.10383>
- Thomson, R.H.S., Garry, M.I., Summers, J.J., 2008. Attentional influences on short-interval intracortical inhibition. *Clin. Neurophysiol. Off. J. Int. Fed. Clin. Neurophysiol.* 119, 52–62. <https://doi.org/10.1016/j.clinph.2007.09.060>
- Tomášová, Z., Hlušík, P., Král, M., Otruba, P., Herzig, R., Krobot, A., Kaňovský, P., 2013. Cortical Activation Changes in Patients Suffering from Post-Stroke Arm Spasticity and Treated with Botulinum Toxin A. *J. Neuroimaging* 23, 337–344. <https://doi.org/10.1111/j.1552-6569.2011.00682.x>
- Tomi, M., 1985. Zur Früherkennung und Frühbehandlung bei Kindern mit cerebralen Bewegungsstörungen in Japan, in: *Entwicklungsrehabilitation Und Behindertenhilfe in Japan Und Der Bundesrepublik Deutschland*. Hansisches Verlagskontor, Lübeck, pp. 35–52.
- Topka, H., Cohen, L.G., Cole, R.A., Hallett, M., 1991. Reorganization of corticospinal pathways following spinal cord injury. *Neurology* 41, 1276–1283. <https://doi.org/10.1212/wnl.41.8.1276>
- Traversa, R., Cicinelli, P., Bassi, A., Rossini, P.M., Bernardi, G., 1997. Mapping of motor cortical reorganization after stroke. A brain stimulation study with focal magnetic pulses. *Stroke* 28, 110–117. <https://doi.org/10.1161/01.str.28.1.110>
- Trompetto, C., Bove, M., Avanzino, L., Francavilla, G., Berardelli, A., Abbruzzese, G., 2008. Intrafusal effects of botulinum toxin in post-stroke upper limb spasticity. *Eur. J. Neurol.* 15, 367–370. <https://doi.org/10.1111/j.1468-1331.2008.02076.x>
- Trompetto, C., Currà, A., Buccolieri, A., Suppa, A., Abbruzzese, G., Berardelli, A., 2006. Botulinum toxin changes intrafusal feedback in dystonia: A study with the tonic vibration reflex. *Mov. Disord.* 21, 777–782. <https://doi.org/10.1002/mds.20801>
- Tsay, A.J., Giummarra, M.J., Allen, T.J., Proske, U., 2016. The sensory origins of human position sense. *J. Physiol.* 594, 1037–1049. <https://doi.org/10.1113/JP271498>
- Uddin, L.Q., 2015. Salience processing and insular cortical function and dysfunction. *Nat. Rev. Neurosci.* 16, 55–61. <https://doi.org/10.1038/nrn3857>
- Ueno, T., Inoue, M., Matsuoka, T., Abe, T., Maeda, H., Morita, K., 2010. Comparison Between a Real Sequential Finger and Imagery Movements: An fMRI Study Revisited. *Brain Imaging Behav.* 4, 80–85. <https://doi.org/10.1007/s11682-009-9087-y>
- Urban, P.P., Rolke, R., 2004. Effects of botulinum toxin type A on vibration induced facilitation of motor evoked potentials in spasmodic torticollis. *J. Neurol. Neurosurg. Psychiatry* 75, 1541–1546. <https://doi.org/10.1136/jnnp.2003.029215>
- Usichenko, T.I., Wesolowski, T., Lotze, M., 2015. Verum and sham acupuncture exert distinct cerebral activation in pain processing areas: a crossover fMRI investigation in healthy volunteers. *Brain Imaging Behav.* 9, 236–244. <https://doi.org/10.1007/s11682-014-9301-4>
- Uzuegbunam, B.C., Librizzi, D., Hooshyar Yousefi, B., 2020. PET Radiopharmaceuticals for

- Alzheimer's Disease and Parkinson's Disease Diagnosis, the Current and Future Landscape. *Mol. Basel Switz.* 25. <https://doi.org/10.3390/molecules25040977>
- Vallbo, A.B., Johansson, R.S., 1984. Properties of cutaneous mechanoreceptors in the human hand related to touch sensation. *Hum. Neurobiol.* 3, 3–14.
- Vazquez, A.L., Fukuda, M., Kim, S.-G., 2018. Inhibitory Neuron Activity Contributions to Hemodynamic Responses and Metabolic Load Examined Using an Inhibitory Optogenetic Mouse Model. *Cereb. Cortex N. Y. N 1991* 28, 4105–4119. <https://doi.org/10.1093/cercor/bhy225>
- Vedel, J.P., Roll, J.P., 1982. Response to pressure and vibration of slowly adapting cutaneous mechanoreceptors in the human foot. *Neurosci. Lett.* 34, 289–294.
- Veverka, T., Hlušík, P., Hok, P., Otruba, P., Tüdös, Z., Zapletalová, J., Krobot, A., Kaňovský, P., 2014. Cortical activity modulation by botulinum toxin type A in patients with post-stroke arm spasticity: Real and imagined hand movement. *J. Neurol. Sci.* 346, 276–283. <https://doi.org/10.1016/j.jns.2014.09.009>
- Veverka, T., Hlušík, P., Hok, P., Otruba, P., Zapletalová, J., Tüdös, Z., Krobot, A., Kaňovský, P., 2016. Sensorimotor modulation by botulinum toxin A in post-stroke arm spasticity: Passive hand movement. *J. Neurol. Sci.* 362, 14–20. <https://doi.org/10.1016/j.jns.2015.12.049>
- Veverka, T., Hlušík, P., Hok, P., Tomášová, Z., Otruba, P., Král, M., Tüdös, Z., Krobot, A., Herzig, R., Kaňovský, P., 2013. Differences in the Modulation of Cortical Activity in Patients Suffering from Upper Arm Spasticity Following Stroke and Treated with Botulinum Toxin A. *Čes. Slov. Neurol. Neurochir.* 76, 175–182.
- Veverka, T., Hlušík, P., Tomášová, Z., Hok, P., Otruba, P., Král, M., Tüdös, Z., Zapletalová, J., Herzig, R., Krobot, A., Kaňovský, P., 2012. BoNT-A related changes of cortical activity in patients suffering from severe hand paralysis with arm spasticity following ischemic stroke. *J. Neurol. Sci.* 319, 89–95. <https://doi.org/10.1016/j.jns.2012.05.008>
- Veverka, T., Hok, P., Otruba, P., Zapletalová, J., Kukulová, B., Tüdös, Z., Krobot, A., Kaňovský, P., Hlušík, P., 2019. Botulinum Toxin Modulates Posterior Parietal Cortex Activation in Post-stroke Spasticity of the Upper Limb. *Front. Neurol.* 10, 495. <https://doi.org/10.3389/fneur.2019.00495>
- Veverka, T., Opavský, R., Hlušík, P., Otruba, P., Hok, P., Kaňovský, P., in submission. Cortical somatosensory processing after botulinum toxin therapy in post-stroke spasticity.
- Vidyasagar, R., Parkes, L.M., 2011. Reproducibility of functional MRI localization within the human somatosensory cortex. *J. Magn. Reson. Imaging JMRI* 34, 1439–1444. <https://doi.org/10.1002/jmri.22758>
- Vlčková, E., Bednařík, J., Buršová, Š., Šajgalíková, K., Mlčáková, L., 2010. Spectral Analysis of Heart Rate Variability – Normative Data [In Czech]. *Čes. Slov. Neurol. Neurochir.* 73/106, 663–672.
- Vojta, V., 1984. The basic elements of treatment according to Vojta, in: *Management of the Motor Disorders of Children with Cerebral Palsy*. Cambridge University Press, pp. 75–85.

- Vojta, V., 1973a. [Early diagnosis and therapy of cerebral movement disorders in childhood. C. Reflexogenous locomotion - reflex creeping and reflex turning. C1. The kinesiologic content and connection with the tonic neck reflexes]. *Z. Für Orthop. Ihre Grenzgeb.* 111, 268–291.
- Vojta, V., 1973b. [Early diagnosis and therapy of cerebral movement disorders in childhood. C. Reflexogenous locomotion - reflex creeping and reflex turning. C2. Its use in 207 risk children. Analysis of the final results]. *Z. Für Orthop. Ihre Grenzgeb.* 111, 292–309.
- Vojta, V., 1972a. [Early diagnosis and therapy of cerebral motor disorders in childhood. A. Postural reflexes in developmental kinesiology. 3. Pathological reflexes from the aspects of tonic neck reflexes and tonic labyrinthine reflexes]. *Z. Für Orthop. Ihre Grenzgeb.* 110, 467–476.
- Vojta, V., 1972b. [Early diagnosis and therapy of cerebral motor disorders in childhood. A. Postural reflexes in developmental kinesiology. 2. Pathologic reactions]. *Z. Für Orthop. Ihre Grenzgeb.* 110, 458–466.
- Vojta, V., 1970. [Reflex rotation as a pathway to human locomotion]. *Z. Für Orthop. Ihre Grenzgeb.* 108, 446–452.
- Vojta, V., 1968. [Reflex creeping as an early rehabilitation programme]. *Z. Für Kinderheilkd.* 104, 319–330. <https://doi.org/10.1007/BF00440004>
- Vojta, V., 1966. Plazení v rehabilitaci hybných poruch u dětí. *Českoslov. Neurol. Neurochir. Časopis Neurol. Spol.* 29, 234–239.
- Vojta, V., 1965. [Rehabilitation of the spastic infantile syndrome. Personal methodology]. *Beitr. Zur Orthop. Traumatol.* 12, 557–562.
- Vojta, V., 1964. [Reflex inhibition of spasticity in perinatal encephalopathy by means of voluntary movement using ontogenetically old structural movements]. *Ceskoslovenská Neurol.* 27, 329–340.
- Vojta, V., Peters, A., 2007. *Das Vojta-Prinzip: Muskelspiele in Reflexfortbewegung und motorischer Ontogenese, 3., vollst. überarb. Aufl.* ed. Springer, Berlin.
- Voogd, J., Schraa-Tam, C.K.L., van der Geest, J.N., De Zeeuw, C.I., 2012. Visuomotor Cerebellum in Human and Nonhuman Primates. *Cerebellum Lond. Engl.* 11, 392–410. <https://doi.org/10.1007/s12311-010-0204-7>
- Wall, M.E., Rechtsteiner, A., Rocha, L.M., 2003. Singular value decomposition and principal component analysis, in: Berrar, D.P., Dubitzky, W., Granzow, M. (Eds.), *A Practical Approach to Microarray Data Analysis*. Springer, pp. 91–109.
- Wang, Y., Hao, Y., Zhou, J., Fried, P.J., Wang, X., Zhang, J., Fang, J., Pascual-Leone, A., Manor, B., 2015. Direct current stimulation over the human sensorimotor cortex modulates the brain's hemodynamic response to tactile stimulation. *Eur. J. Neurosci.* 42, 1933–1940. <https://doi.org/10.1111/ejn.12953>
- Ward, N.S., Cohen, L.G., 2004. Mechanisms underlying recovery of motor function after stroke. *Arch. Neurol.* 61, 1844–1848. <https://doi.org/10.1001/archneur.61.12.1844>
- Weise, D., Schramm, A., Beck, M., Reiners, K., Classen, J., 2011. Loss of topographic specificity of LTD-like plasticity is a trait marker in focal dystonia. *Neurobiol. Dis.* 42, 171–176. <https://doi.org/10.1016/j.nbd.2010.11.009>

- Weise, D., Schramm, A., Stefan, K., Wolters, A., Reiners, K., Naumann, M., Classen, J., 2006. The two sides of associative plasticity in writer's cramp. *Brain J. Neurol.* 129, 2709–2721. <https://doi.org/10.1093/brain/awl221>
- Weise, D., Weise, C.M., Naumann, M., 2019. Central Effects of Botulinum Neurotoxin—Evidence from Human Studies. *Toxins* 11. <https://doi.org/10.3390/toxins11010021>
- Werhahn, K.J., Kunesch, E., Noachtar, S., Benecke, R., Classen, J., 1999. Differential effects on motorcortical inhibition induced by blockade of GABA uptake in humans. *J. Physiol.* 517 (Pt 2), 591–597.
- Werhahn, K.J., Mortensen, J., Kaelin-Lang, A., Boroojerdi, B., Cohen, L.G., 2002. Cortical excitability changes induced by deafferentation of the contralateral hemisphere. *Brain J. Neurol.* 125, 1402–1413. <https://doi.org/10.1093/brain/awf140>
- Wierzbicka, M.M., Gilhodes, J.C., Roll, J.P., 1998. Vibration-induced postural posteffects. *J. Neurophysiol.* 79, 143–150. <https://doi.org/10.1152/jn.1998.79.1.143>
- Wijnen, V.J.M., Heutink, M., van Boxtel, G.J.M., Eilander, H.J., de Gelder, B., 2006. Autonomic reactivity to sensory stimulation is related to consciousness level after severe traumatic brain injury. *Clin. Neurophysiol.* 117, 1794–1807. <https://doi.org/10.1016/j.clinph.2006.03.006>
- Windhorst, U., 2007. Muscle proprioceptive feedback and spinal networks. *Brain Res. Bull.* 73, 155–202. <https://doi.org/10.1016/j.brainresbull.2007.03.010>
- Windle, W.F., 1966. An experimental approach to prevention or reduction of the brain damage of birth asphyxia. *Dev. Med. Child Neurol.* 8, 129–140.
- Winkler, A.M., Ridgway, G.R., Webster, M.A., Smith, S.M., Nichols, T.E., 2014. Permutation inference for the general linear model. *NeuroImage* 92, 381–397. <https://doi.org/10.1016/j.neuroimage.2014.01.060>
- Wong, J.J., Shearer, H.M., Mior, S., Jacobs, C., Côté, P., Randhawa, K., Yu, H., Southerst, D., Varatharajan, S., Sutton, D., van der Velde, G., Carroll, L.J., Ameis, A., Ammendolia, C., Brison, R., Nordin, M., Stupar, M., Taylor-Vaisey, A., 2016. Are manual therapies, passive physical modalities, or acupuncture effective for the management of patients with whiplash-associated disorders or neck pain and associated disorders? An update of the Bone and Joint Decade Task Force on Neck Pain and Its Associated Disorders by the OPTIMa collaboration. *Spine J. Off. J. North Am. Spine Soc.* 16, 1598–1630. <https://doi.org/10.1016/j.spinee.2015.08.024>
- Wong, Y.C., Kwan, H.C., MacKay, W.A., Murphy, J.T., 1978. Spatial organization of precentral cortex in awake primates. I. Somatosensory inputs. *J. Neurophysiol.* 41, 1107–1119. <https://doi.org/10.1152/jn.1978.41.5.1107>
- Woolrich, M.W., Behrens, T.E.J., Beckmann, C.F., Jenkinson, M., Smith, S.M., 2004. Multilevel linear modelling for fMRI group analysis using Bayesian inference. *NeuroImage* 21, 1732–1747. <https://doi.org/10.1016/j.neuroimage.2003.12.023>
- Woolrich, M.W., Ripley, B.D., Brady, M., Smith, S.M., 2001. Temporal Autocorrelation in Univariate Linear Modeling of fMRI Data. *NeuroImage* 14, 1370–1386. <https://doi.org/10.1006/nimg.2001.0931>
- Worsley, K.J., 2001. Statistical analysis of activation images, in: Jezzard, P., Matthews, P.M., Smith, S.M. (Eds.), *Functional MRI: An Introduction to Methods*. Oxford University

- Press, Oxford [England]; New York, pp. 251–270.
- Wu, C.W.-H., van Gelderen, P., Hanakawa, T., Yaseen, Z., Cohen, L.G., 2005. Enduring representational plasticity after somatosensory stimulation. *NeuroImage* 27, 872–884. <https://doi.org/10.1016/j.neuroimage.2005.05.055>
- Wu, M.-T., Sheen, J.-M., Chuang, K.-H., Yang, P., Chin, S.-L., Tsai, C.-Y., Chen, C.-J., Liao, J.-R., Lai, P.-H., Chu, K.-A., Pan, H.-B., Yang, C.-F., 2002. Neuronal specificity of acupuncture response: a fMRI study with electroacupuncture. *NeuroImage* 16, 1028–1037.
- Wu, Y.-H., Uluç, I., Schmidt, T.T., Tertel, K., Kirilina, E., Blankenburg, F., 2018. Overlapping frontoparietal networks for tactile and visual parametric working memory representations. *NeuroImage* 166, 325–334. <https://doi.org/10.1016/j.neuroimage.2017.10.059>
- Yaginuma, H., Matsushita, M., 1989. Spinocerebellar projections from the upper lumbar segments in the cat, as studied by anterograde transport of wheat germ agglutinin-horseradish peroxidase. *J. Comp. Neurol.* 281, 298–319. <https://doi.org/10.1002/cne.902810211>
- Yamamoto, Y., Hughson, R.L., 1991. Coarse-graining spectral analysis: new method for studying heart rate variability. *J. Appl. Physiol.* Bethesda Md 1985 71, 1143–1150.
- Yin, H., Liu, Y., Li, M., Hu, D., 2011. Hemodynamic observation and spike recording explain the neuronal deactivation origin of negative response in rat. *Brain Res. Bull.* 84, 157–162. <https://doi.org/10.1016/j.brainresbull.2010.12.004>
- Zafeiriou, D.I., 2004. Primitive reflexes and postural reactions in the neurodevelopmental examination. *Pediatr. Neurol.* 31, 1–8. <https://doi.org/10.1016/j.pediatrneurol.2004.01.012>
- Zarzecki, P., Strick, P.L., Asanuma, H., 1978. Input to primate motor cortex from posterior parietal cortex (area 5). II. Identification by antidromic activation. *Brain Res.* 157, 331–335. [https://doi.org/10.1016/0006-8993\(78\)90036-7](https://doi.org/10.1016/0006-8993(78)90036-7)
- Ziemann, U., Corwell, B., Cohen, L.G., 1998a. Modulation of plasticity in human motor cortex after forearm ischemic nerve block. *J. Neurosci. Off. J. Soc. Neurosci.* 18, 1115–1123.
- Ziemann, U., Hallett, M., Cohen, L.G., 1998b. Mechanisms of deafferentation-induced plasticity in human motor cortex. *J. Neurosci. Off. J. Soc. Neurosci.* 18, 7000–7007.
- Ziemann, U., Lönnecker, S., Steinhoff, B.J., Paulus, W., 1996a. Effects of antiepileptic drugs on motor cortex excitability in humans: a transcranial magnetic stimulation study. *Ann. Neurol.* 40, 367–378. <https://doi.org/10.1002/ana.410400306>
- Ziemann, U., Muellbacher, W., Hallett, M., Cohen, L.G., 2001. Modulation of practice-dependent plasticity in human motor cortex. *Brain J. Neurol.* 124, 1171–1181.
- Ziemann, U., Rothwell, J.C., Ridding, M.C., 1996b. Interaction between intracortical inhibition and facilitation in human motor cortex. *J. Physiol.* 496 (Pt 3), 873–881.

XII. LIST OF ABBREVIATIONS

%SC	percent signal change	ECG	electrocardiography
A1	condition before AS	ECR	<i>extensor carpi radialis</i> (muscle)
A1*	condition before AS (baseline)	EDC	<i>extensor digitorum communis</i> (muscle)
A2	condition after AS	EEG	electroencephalography
AMPA	α -amino-3-hydroxy-5-methyl-4- isoxazolepropionic acid	EMG	electromyography
aMT	active motor threshold	EPI	echo-planar imaging
ANS	autonomic nervous system	FA	fast-adapting (afferents)
APB	<i>abductor pollicis brevis</i> (muscle)	FA-I	fast-adapting type I (afferents)
AS	ankle stimulation	FA-II	fast-adapting type II (afferents)
ASL	arterial spin labelling	FC	functional connectivity
AVR	antagonist vibratory response	FCR	<i>flexor carpi radialis</i> (muscle)
B₀	static magnetic field applied for MRI	FDG	fluoro-deoxy-glucose
B₁	oscillating RF magnetic field	FDI	first dorsal <i>interosseus</i> (muscle)
BA	Brodmann area	FEAT	(fMRI analysis tool, part of FSL)
BET	(fMRI analysis tool, part of FSL)	FIR	finite impulse response
BOLD	blood oxygenation level-dependent	FLAIR	fluid-attenuated inversion recovery
BoNT-A	botulinum neurotoxin type A	FLAME	(fMRI analysis tool, part of FEAT)
CGSA	coarse-graining spectral analysis	fMRI	functional magnetic resonance imaging
CMA	cingulate motor area	FSL	FMRIB's Software Library (fMRI analysis software)
CNS	central nervous system	FUGUE	(fMRI analysis tool, part of FEAT)
COPE	contrast of parameter estimates	FWE	family-wise error
CPG	central pattern generator	FWHM	full width at half maximum
CSP	cortical silent period		
DLPFC	dorsolateral prefrontal cortex		
DSCT	dorsal spinocerebellar tract		

GABA	γ -aminobutyric acid	LAI	long-latency afferent inhibition
GABA_A	GABA A (receptor)	LF	low frequency (power)
GABA_B	GABA B (receptor)	LH	left hand
GE	gradient echo	LI	laterality index
GLM	general linear model	LICI	long-interval intracortical inhibition
H1	condition before HS	LTP	long-term potentiation
H1*	condition before HS (baseline)	LTD	long-term depression
H2	condition after HS	LTMR	low-threshold mechanoreceptors
H₂¹⁵O	¹⁵ O-labelled water	M-wave	(early EMG component of motor nerve stimulation response)
HF	high frequency (power)	M1	primary motor cortex
HRF	haemodynamic response function	MCFLIRT	(fMRI analysis tool, part of FSL)
HRV	heart rate variability	MEG	magnetoencephalography
HS	heel stimulation	MEP	motor evoked potentials
HTMR	high-threshold mechanoreceptors	MNI	Montreal Neurological Institute
ICA	independent component analysis	MPRAGE	magnetisation-prepared rapid acquisition with gradient echo
ICA-AROMA	(fMRI analysis tool)	MRI	magnetic resonance imaging
ICF	intracortical facilitation	MSSD	mean squared successive differences
IF	Impact factor	MVC	maximal voluntary contraction
IHI	interhemispheric inhibition	NMDA	N-methyl-D-aspartate
INB	ischaemic nerve block	NMRI	nuclear magnetic resonance imaging
IPD	idiopathic Parkinson's disease	NO	nitric oxide
IPL	inferior parietal lobule	OP 1	(area) parietal operculum 1
IPS	intraparietal sulcus	OP 4	(area) parietal operculum 4
IQR	inter-quartile range		
ISI	interstimulus interval		

P22/N30	(component of median nerve SEP)	S2	secondary somatosensory cortex
PAS	paired associative stimulation	SA	slow-adapting (afferents)
PC	principal component	SA-I	slow-adapting type I (afferents)
PD	proton density	SA-II	slow-adapting type II (afferents)
PET	positron emission tomography	SAHRV	spectral analysis of heart rate variability
PGp	parietal area G posterior	SAI	short-latency afferent inhibition
PMC	premotor cortex	SCI	spinal cord injury
PMd	dorsal premotor cortex	SCM	sternocleidomastoid muscle
PMRF	pontomedullary reticular formation	SD	standard deviation
PMv	ventral premotor cortex	SE	spin echo
pre-SMA	pre-supplementary motor area	SEP	somatosensory evoked potentials
PRF	pontine reticular formation	SFO	sequential finger opposition
PV	parietal ventral (area)	SII	see S2
pTMS	paired-pulse TMS	SICI	short-interval intracortical inhibition
rCBF	regional cerebral blood flow	SMA	supplementary motor area
rCBV	regional cerebral blood volume	SMC	sensorimotor cortex
RF	radio-frequency	SMG	supramarginal gyrus
RH	right hand	SNARE	soluble <i>N</i> -ethylmaleimide-sensitive factor attachment protein receptor
RLT	reflex locomotion therapy	SPL	superior parietal lobule
rMT	resting motor threshold	SPM	Statistical Parametric Mapping (fMRI analysis software)
ROI	region of interest		
RR	(time between two QRS complexes)		
rTMS	repetitive TMS		
S1	primary somatosensory cortex		

T₁	longitudinal (spin-lattice) relaxation time constant	V2	secondary visual cortex
T₂	transverse (spin-spin) relaxation time constant	V4	visual association area V4
T₂[*]	transverse relaxation time constant including effect of B ₀ inhomogeneities	VAS	visual analogue scale
TE	echo time	VIF	vibration-induced falling
TMS	transcranial magnetic stimulation	VL	ventral lateral (thalamic nucleus)
TR	repetition time	VLF	very low frequency (power)
TVR	tonic vibration reflex	VPL	ventral posterolateral (thalamic nucleus)
V1	primary visual cortex	VPLo	oral part of VPL
		VPM	ventral posteromedial (thalamic nucleus)
		WoS	Web of Science

XIII. LIST OF FIGURES

Figure 1. Stimulation procedure and stimulation sites.....	83
Figure 2. Spectral analysis of heart rate variability in a young healthy subject during the supine–standing–supine test.....	88
Figure 3. Areas associated with sustained pressure stimulation.....	97
Figure 4. Timecourses of BOLD signal in the significant clusters.....	98
Figure 5. Hierarchical clustering of group-wise BOLD signal responses.....	104
Figure 6. Significant differences according to stimulation site.....	105
Figure 7. Mean activation during sequential finger opposition.....	107
Figure 8. Mean activation decrease post-stimulation and interaction between condition and repetition.....	108
Figure 9. <i>Post-hoc</i> analysis of significant <i>F</i> -test.....	112
Figure 10. Correlation with pain intensity.....	113
Figure 11. Unconditioned MEP sizes.....	114
Figure 12. Normalised MEP ratio After/Before.....	115
Figure 13. Normalised MEP sizes.....	116

XIV. LIST OF TABLES

Table 1. Differences among study samples and stimulation protocols.....	85
Table 2. Significant <i>F</i> -test clusters in Contrast I.3 (HS + AS): Overall stimulation effect....	100
Table 3. Significant clusters in Contrasts I.4 and I.5: Differences between stimulation sites and pain effect.....	106
Table 4. Significant clusters in Contrast II.3: Comparison before and after stimulation....	109
Table 5. Significant <i>F</i> -test clusters for Contrasts II.4 and II.5: Interaction and pain effect. .	110
Table 6. Duration of RR intervals and heart rate variability: Heel stimulation.....	117
Table 7. Duration of RR intervals and heart rate variability: Ankle stimulation.....	118

XV. LIST OF PUBLICATIONS

Works published during doctoral study (August 2013 – March 2020):

1. Published research papers directly related to the topic of the thesis

1. Hok, P.^{*}, Opavský, J., Kutín, M., Tüdös, Z., Kaňovský, P., Hluštík, P., 2017. *Modulation of the sensorimotor system by sustained manual pressure stimulation*. Neuroscience 348, 11–22. <https://doi.org/10.1016/j.neuroscience.2017.02.005>

WoS 2017: IF 3.382, Rank: 105/261, Times cited: 4

Author contributions: P. Hok has substantially contributed to the design of the work, data acquisition, analysis, and interpretation and drafted the manuscript. J. Opavský has substantially contributed to the conception, design and interpretation of the work and substantially revised the manuscript. M. Kutín has substantially contributed to the design of the work and data acquisition. Z. Tüdös has substantially contributed to the data acquisition and revised substantially the manuscript. P. Kaňovský has substantially contributed to the conception of the work. P. Hluštík has substantially contributed to the conception and design of the work, data acquisition and substantially revised the manuscript. All authors have read, revised critically and approved the final submitted manuscript, and agree to be accountable for the content of the work.

2. Opavský, J., Šlachtová, M., Kutín, M., Hok, P.^{*}, Uhlíř, P., Opavská, H., Hluštík, P., 2018. *The effects of sustained manual pressure stimulation according to Vojta Therapy on heart rate variability*. Biomed Pap-Olomouc 162, 206–211. <https://doi.org/10.5507/bp.2018.028>

WoS 2018: IF 1.141, Rank: 119/136, Times cited: 1

Author contributions: J. Opavský has substantially contributed to study design, data interpretation, manuscript writing and literature search, critical revision of the manuscript; M. Šlachtová has substantially contributed to data collection, figures; M. Kutín has substantially contributed to data collection; P. Hok has substantially contributed to study design, data interpretation, manuscript writing and literature search; P. Uhlíř has substantially contributed to data collection, statistical analysis; H. Opavská has substantially contributed to data collection, data analysis;

* Corresponding author

P. Hlušík has substantially contributed to study design, data interpretation; the final version was approved by all authors.

3. **Hok, P.***, Opavský, J., Labounek, R., Kutín, M., Šlachtová, M., Tüdös, Z., Kaňovský, P., Hlušík, P., 2019. *Differential Effects of Sustained Manual Pressure Stimulation According to Site of Action*. *Front. Neurosci.* 13, 722. <https://doi.org/10.3389/fnins.2019.00722>

WoS 2018: IF 3.648, Rank: 92/267, Times cited: 0

Author contributions: P. Hok has substantially contributed to the design of the work, data acquisition, analysis and interpretation, and drafted the manuscript. J. Opavský has substantially contributed to the conception, design, and interpretation of the work, and substantially revised the manuscript. R. Labounek has substantially contributed to the data analysis and drafted parts of the manuscript. M. Kutín has substantially contributed to the design of the work and data acquisition. M. Šlachtová has substantially contributed to the data acquisition. Z. Tüdös has substantially contributed to the data acquisition and substantially revised the manuscript. P. Kaňovský has substantially contributed to the conception of the work. P. Hlušík has substantially contributed to the conception and design of the work, data acquisition, and substantially revised the manuscript.

2. Research papers directly related to the topic of the thesis submitted and in preparation

1. **Hok, P.***, and Hlušík, P., in submission. *Modulation of the sensorimotor system by manipulation of afferent somatosensory input: evidence from mechanical pressure stimulation*. Biomed Pap-Olomouc

Author contributions: P. Hok has substantially contributed to the literature review and drafted and revised the manuscript. P. Hlušík has substantially contributed to the conception and design of the work, and substantially revised the manuscript.

2. **Hok, P.***, Nevrlý, M., Otruba, P., Valošek, J., Trnečková, M., Kutín, M., Opavský, J., Kaňovský, P., Hlušík, P., in preparation. *Decreased intracortical inhibition after peripheral manual pressure stimulation*.

Author contributions: P. Hok has substantially contributed to study design and conception, data acquisition, data analysis. Interpretation of the results, figure

* Corresponding author

preparation and drafted the manuscript. M. Nevrlý has substantially contributed to interpretation of the results and drafted the manuscript. P. Otruba has substantially contributed to data acquisition. J. Valošek has substantially contributed to data acquisition and data analysis. M. Trnečková has substantially contributed to data analysis. M. Kutín has substantially contributed to data acquisition. J. Opavský has substantially contributed to study design and conception and interpretation of the results. P. Kaňovský has substantially contributed to study design and conception and interpretation of the results. P. Hlušík has substantially contributed to study design and conception, interpretation of the results and drafted the manuscript. All authors critical reviewed and approval the final version of the manuscript.

3. Published research papers from broader area of sensorimotor plasticity research

1. Hrabálek, L., Hlušík, P., **Hok, P.**, Wanek, T., Otruba, P., Čecháková, E., Vaverka, M., Kaňovský, P., 2014. [*Effects of spinal cord decompression in patients with cervical spondylotic myelopathy on cortical brain activations*]. *Rozhl Chir* 93, 530–5. **WoS: N/A; Scopus 2014: CiteScore 0.14 Rank 1060/1510**
2. Veverka, T., Hlušík, P., **Hok, P.**, Otruba, P., Tüdös, Z., Zapletalová, J., Krobot, A., Kaňovský, P., 2014. *Cortical activity modulation by botulinum toxin type A in patients with post-stroke arm spasticity: Real and imagined hand movement*. *J Neurol Sci* 346, 276–283. <https://doi.org/10.1016/j.jns.2014.09.009> **WoS 2014: IF 2.474, Rank 82/192**
3. Hrabálek, L., Hlušík, P., **Hok, P.**, Čecháková, E., Wanek, T., Otruba, P., Vaverka, M., Kaňovský, P., 2015. [*Influence of Cervical Spondylotic Spinal Cord Compression on Cerebral Cortical Adaptation. Radiological Study*]. *Acta Chir Orthop Traumatol Cech* 82, 404–411. **WoS 2015: IF 0.552, Rank 64/74**
4. Vašík, M., **Hok, P.**, Hlušík, P., Otruba, P., Tüdös, Z., Kaňovský, P., 2016. *Botulinum toxin treatment of freezing of gait in Parkinson's disease patients as reflected in functional magnetic resonance imaging of leg movement*. *Neuro Endocrinol Lett* 37, 147–153. **WoS 2016: IF 0.918, Rank: 237/259**
5. Veverka, T., Hlušík, P., **Hok, P.**, Otruba, P., Zapletalová, J., Tüdös, Z., Krobot, A., Kaňovský, P., 2016. *Sensorimotor modulation by botulinum toxin A in post-stroke arm spasticity: Passive hand movement*. *J Neurol Sci* 362, 14–20. <https://doi.org/10.1016/j.jns.2015.12.049> **WoS 2016: IF 2.295, Rank: 106/194**

6. Hrabálek, L.[‡], Hok, P.^{*‡}, Hlušík, P., Čecháková, E., Wanek, T., Otruba, P., Vaverka, M., Kaňovský, P., 2018. *Longitudinal brain activation changes related to electrophysiological findings in patients with cervical spondylotic myelopathy before and after spinal cord decompression: an fMRI study*. *Acta Neurochir* 160, 923–932. <https://doi.org/10.1007/s00701-018-3520-1> **WoS 2018: IF 1.834, Rank: 106/203**
7. Nevrlý, M., Hlušík, P., Hok, P., Otruba, P., Tüdös, Z., Kaňovský, P., 2018. *Changes in sensorimotor network activation after botulinum toxin type A injections in patients with cervical dystonia: a functional MRI study*. *Exp Brain Res* 236, 2627–2637. <https://doi.org/10.1007/s00221-018-5322-3> **WoS 2018: IF 1.878, Rank: 216/267**
8. Veverka, T., Hok, P., Otruba, P., Zapletalová, J., Kukolová, B., Tüdös, Z., Krobot, A., Kaňovský, P., Hlušík, P., 2019. *Botulinum Toxin Modulates Posterior Parietal Cortex Activation in Post-stroke Spasticity of the Upper Limb*. *Front. Neurol.* 10, 495. <https://doi.org/10.3389/fneur.2019.00495> **WoS 2018: IF 2.635, Rank: 100/199**

4. Other published original research papers

1. Tüdös, Z., Hok, P., Hrdina, L., Hlušík, P., 2014. *Modality effects in paced serial addition task: Differential responses to auditory and visual stimuli*. *Neuroscience* 272, 10–20. <https://doi.org/10.1016/j.neuroscience.2014.04.057> **WoS 2014: IF 3.357, Rank 96/252**
2. Grambal, A., Tüdös, Z., Hok, P., Kamarádová, D., Divéky, T., Hlušík, P., Praško, J., 2015. *Predictors of poor treatment response to additional CBT in real panic disorder patients: The role of DLPF, orbitofrontal cortex, parietal lobule, frontal eye field and amygdala in PD*. *Neuro Endocrinol. Lett.* 36, 269–281. **WoS 2015: IF 0.946, Rank: 233/256**
3. Gracien, R.-M., Nürnberger, L., Hok, P., Hof, S.-M., Reitz, S.C., Rüb, U., Steinmetz, H., Hilker-Roggendorf, R., Klein, J.C., Deichmann, R., Baudrexel, S., 2017. *Evaluation of brain ageing: a quantitative longitudinal MRI study over 7 years*. *Eur Radiol* 27, 1568–1576. <https://doi.org/10.1007/s00330-016-4485-1> **WoS 2017: IF 4.027, Rank: 20/128**
4. Nürnberger, L., Gracien, R.-M., Hok, P., Hof, S.-M., Rüb, U., Steinmetz, H., Hilker, R., Klein, J.C., Deichmann, R., Baudrexel, S., 2017. *Longitudinal changes of cortical microstructure in Parkinson's disease assessed with T1 relaxometry*. *NeuroImage*

‡ Both author contributed equally to this work

* Corresponding author

- Clin 13, 405–414. <https://doi.org/10.1016/j.nicl.2016.12.025> **WoS 2017: IF 3.869, Rank: 3/14**
5. Vašítek, M., Hok, P., Valošek, J., Hlušík, P., Menšíkova, K., Kaňovský, P., 2017. *Freezing of gait is associated with cortical thinning in mesial frontal cortex*. Biomed Pap-Olomouc 161, 389–396. <https://doi.org/10.5507/bp.2017.035> **WoS 2017: IF 1.087, Rank: 115/133**
 6. Shrestha, M., Hok, P., Nöth, U., Lienerth, B., Deichmann, R., 2018. *Optimization of diffusion-weighted single-refocused spin-echo EPI by reducing eddy-current artifacts and shortening the echo time*. Magn Reson Mater Phy 31, 585–597. <https://doi.org/10.1007/s10334-018-0684-x> **WoS 2018: IF 2.836, Rank: 43/129**
 7. Tüdös, Z., Hok, P., Hlušík, P., Grambal, A., 2018. *Functional MRI study of gender effects in brain activations during verbal working memory task*. Physiol Res 67, 825–829. <https://doi.org/10.33549/physiolres.933742> **WoS 2018: IF 1.701, Rank: 64/81**
 8. Gehrig, J., Michalareas, G., Forster, M.-T., Lei, J., Hok, P., Laufs, H., Senft, C., Seifert, V., Schoffelen, J.-M., Hanslmayr, S., Kell, C.A., 2019. *Low-Frequency Oscillations Code Speech during Verbal Working Memory*. J. Neurosci. 39, 6498–6512. <https://doi.org/10.1523/JNEUROSCI.0018-19.2019> **WoS 2018: IF 6.074, Rank: 29/267**
 9. Gracien, R.-M., Petrov, F., Hok, P.*, van Wijnen, A., Maiworm, M., Seiler, A., Deichmann, R., Baudrexel, S., 2019. *Multimodal Quantitative MRI Reveals No Evidence for Tissue Pathology in Idiopathic Cervical Dystonia*. Front. Neurol. 10, 914. <https://doi.org/10.3389/fneur.2019.00914> **WoS 2018: IF 2.635, Rank: 100/199**

5. Author record

- **Number of publications (WoS):** 63
→ original research papers (WoS): 21
- **Sum of Times Cited (WoS):** 65
- **H-index (WoS):** 5
- **WoS ResearcherID:** K-8224-2017
- **ORCID iD:** 0000-0003-1010-384X

* Corresponding author

XVI. ABSTRACT

Peripheral afferent input provides critical drive for human motor control and motor learning. Stimulation of skin or deep muscle mechanoreceptors has been used to alter motor behaviour, both experimentally and therapeutically. While certain modalities, such as vibration, have attracted researchers for decades, central effects of mechanical pressure stimulation have been studied less frequently. This discrepancy is particularly striking given the limited understanding of physiological principles underlying common physiotherapeutic techniques that involve peripheral stimulation, such as reflex locomotion therapy (RLT). First, the thesis thoroughly reviews the current literature on central effects of pressure stimulation while contrasting it with some better understood examples of peripheral interventions, including vibration and muscle denervation using botulinum neurotoxin. Furthermore, results of four parallel investigations of central correlates of pressure stimulation are reported. Each study enrolled up to 30 young healthy individuals and was conducted according to single-blind randomised crossover design. The schedule consisted of two functional magnetic resonance imaging (fMRI), two paired-pulse transcranial magnetic stimulation (pTMS), or two heart rate variability (HRV) recording sessions. During each session, sustained manual pressure stimulation was delivered as an intervention, once at the right lateral heel according to RLT (active site), and once at the right lateral ankle (control site). fMRI data were acquired during the stimulation, as well as during performance of a sequential finger opposition motor task scheduled immediately before and after the intervention. Likewise, pTMS and HRV recordings were repeated before and after the stimulation. Statistical analyses evaluated differences between the active and control stimulation conditions. The fMRI results showed that stimulation at both sites evoked responses throughout the sensorimotor system that could be mostly separated into two anti-correlated networks of areas with transient positive or negative signal change and rapid adaptation. More sustained activation was only observed in the insulo-opercular cortices and pons during heel (active) stimulation. According to direct voxel-wise comparison, heel stimulation was also associated with significantly higher activation levels in the contralateral primary motor cortex and decreased activation in the posterior parietal cortex. In the second study, repeated motor performance was associated with extensive activation decreases regardless of stimulation site. However, stimulation of the heel specifically increased activation in the predominantly contralateral pontomedullary reticular formation and bilateral posterior cerebellum. On the other hand, heel stimulation reduced short-interval intracortical inhibition in the contralateral motor cortex in pTMS. Finally, spectral analysis of HRV

yielded modest increases in vagal and sympathetic activity, but revealed no differences between stimulation sites. In conclusion, this thesis reviews literature on sensorimotor plasticity induced by modulation of the afferent input, highlights the limited amount of research devoted to peripheral pressure stimulation, and presents recently published original research providing evidence for site-specific differences in brain function. These include increased activation of the motor cortex as an immediate response to stimulation, as well as modulation of task-related activation in the hindbrain and decreased intracortical inhibition representing outlasting effects after extended stimulation. Finally, these results are proposed to reflect the behavioural effects of physiotherapeutic interventions previously observed in the clinical setting.

XVII. LIST OF ANNEXES

1. Hok, P., et al., 2019. *Differential Effects of Sustained Manual Pressure Stimulation According to Site of Action*. Front. Neurosci. 13, 722.....205
2. Hok, P., et al., 2017. *Modulation of the sensorimotor system by sustained manual pressure stimulation*. Neuroscience 348, 11–22.....219
3. Hok, P. et al., in preparation. *Decreased intracortical inhibition after peripheral manual pressure stimulation*.....231
4. Opavský, J., et al., 2018. *The effects of sustained manual pressure stimulation according to Vojta Therapy on heart rate variability*. Biomed Pap-Olomouc 162, 206–211.....254
5. Hok, P., and Hlušík, P., in submission. *Modulation of the sensorimotor system by manipulation of afferent somatosensory input: evidence from mechanical pressure stimulation*. Biomed Pap-Olomouc.....260
6. Veverka, T. et al., 2014. *Cortical activity modulation by botulinum toxin type A in patients with post-stroke arm spasticity: Real and imagined hand movement*. J Neurol Sci 346, 276–283.....279
7. Veverka, T., et al., 2016. *Sensorimotor modulation by botulinum toxin A in post-stroke arm spasticity: Passive hand movement*. J Neurol Sci 362, 14–20.....287
8. Nevrlý, M., et al., 2018. *Changes in sensorimotor network activation after botulinum toxin type A injections in patients with cervical dystonia: a functional MRI study*. Exp Brain Res 236, 2627–2637.....294
9. Veverka, T., et al., 2019. *Botulinum Toxin Modulates Posterior Parietal Cortex Activation in Post-stroke Spasticity of the Upper Limb*. Front. Neurol. 10, 495.....305



Differential Effects of Sustained Manual Pressure Stimulation According to Site of Action

Pavel Hok^{1,2*}, Jaroslav Opavský³, René Labounek^{2,4}, Miroslav Kutín⁵, Martina Šlachtová³, Zbyněk Tüdös^{6,7}, Petr Kaňovský^{1,2} and Petr Hlušík^{1,2}

¹ Department of Neurology, University Hospital Olomouc, Olomouc, Czechia, ² Department of Neurology, Faculty of Medicine and Dentistry, Palacký University Olomouc, Olomouc, Czechia, ³ Department of Physiotherapy, Faculty of Physical Culture, Palacký University Olomouc, Olomouc, Czechia, ⁴ Department of Biomedical Engineering, University Hospital Olomouc, Olomouc, Czechia, ⁵ KM KINEPRO PLUS s.r.o., Olomouc, Czechia, ⁶ Department of Radiology, Faculty of Medicine and Dentistry, Palacký University Olomouc, Olomouc, Czechia, ⁷ Department of Radiology, University Hospital Olomouc, Olomouc, Czechia

OPEN ACCESS

Edited by:

Christian Wallraven,
Korea University, South Korea

Reviewed by:

Younbyoung Chae,
Kyung Hee University, South Korea
Christoph Braun,
University of Tübingen, Germany

*Correspondence:

Pavel Hok
pavel.hok@upol.cz

Specialty section:

This article was submitted to
Perception Science,
a section of the journal
Frontiers in Neuroscience

Received: 12 March 2019

Accepted: 27 June 2019

Published: 17 July 2019

Citation:

Hok P, Opavský J, Labounek R,
Kutín M, Šlachtová M, Tüdös Z,
Kaňovský P and Hlušík P (2019)
Differential Effects of Sustained
Manual Pressure Stimulation
According to Site of Action.
Front. Neurosci. 13:722.
doi: 10.3389/fnins.2019.00722

Sustained pressure stimulation of the body surface has been used in several physiotherapeutic techniques, such as reflex locomotion therapy. Clinical observations of global motor responses and subsequent motor behavioral changes after stimulation in certain sites suggest modulation of central sensorimotor control, however, the neuroanatomical correlates remain undescribed. We hypothesized that different body sites would specifically influence the sensorimotor system during the stimulation. We tested the hypothesis using functional magnetic resonance imaging (fMRI) in thirty healthy volunteers (mean age 24.2) scanned twice during intermittent manual pressure stimulation, once at the right lateral heel according to reflex locomotion therapy, and once at the right lateral ankle (control site). A flexible modeling approach with finite impulse response basis functions was employed since non-canonical hemodynamic response was expected. Subsequently, a clustering algorithm was used to separate areas with differential timecourses. Stimulation at both sites induced responses throughout the sensorimotor system that could be mostly separated into two anti-correlated subsystems with transient positive or negative signal change and rapid adaptation, although in heel stimulation, insulo-opercular cortices and pons showed sustained activation. In direct voxel-wise comparison, heel stimulation was associated with significantly higher activation levels in the contralateral primary motor cortex and decreased activation in the posterior parietal cortex. Thus, we demonstrate that the manual pressure stimulation affects multiple brain structures involved in motor control and the choice of stimulation site impacts the shape and amplitude of the blood oxygenation level-dependent response. We further discuss the relationship between the affected structures and behavioral changes after reflex locomotion therapy.

Keywords: magnetic resonance imaging, neurological rehabilitation, physical stimulation, sensorimotor cortex, brainstem

INTRODUCTION

Neuronal plasticity is a key component in restoration of human motor function. Plastic changes can be induced via transient peripheral afferent stimulation (Powell et al., 1999). Outlasting modulatory effects in the sensorimotor cortex have been observed following sustained electrical (Chipchase et al., 2011), magnetic (Gallasch et al., 2015), and vibratory (Rosenkranz and Rothwell, 2003) stimulation. Peripheral pressure stimulation has been studied less extensively (Miura et al., 2013; Chung et al., 2014, 2015; Sanz-Esteban et al., 2018) despite the fact that it serves as a major component of clinical physiotherapeutic techniques, such as the “reflex locomotion” (Vojta, 1973; Vojta and Peters, 2007; Hok et al., 2017; Jung et al., 2017).

The technique, also known as Vojta method, uses sustained manual pressure stimulation of specific body surface areas to gradually evoke a stereotypic pattern of tonic muscle contractions in both sides of the neck, trunk, and limbs (Vojta, 1973). It has been speculated that the motor response is controlled by a brainstem region (Laufens et al., 1991; Hok et al., 2017), possibly related to the so-called central pattern generators that were discovered in vertebrate animals (Grillner and Wallén, 1985) and more recently became associated with human locomotion and postural control (Jahn et al., 2008; la Fougère et al., 2010; Takakusaki, 2013). Indeed, we have previously shown that heel stimulation according to Vojta specifically modulates subsequent motor task-related activation in the dorsal pons, medulla (presumably in the pontomedullary reticular formation, PMRF), and cerebellum (Hok et al., 2017). Nevertheless, there is limited knowledge of the immediate neurobiological correlates of the therapeutic stimulation and the resulting interaction between the somatosensory and motor system.

Previous imaging studies of pressure stimulation recently provided valuable, yet still incomplete picture of the central somatosensory processing (Hao et al., 2013; Miura et al., 2013; Chung et al., 2014, 2015; Sanz-Esteban et al., 2018). Miura et al. (2013) observed bilateral activation in the primary and secondary somatosensory cortices during short manual foot sole stimulation applied at the base of the toes over 5 s. Similar pattern has been observed during 30 s of 1-Hz sinusoidal pressure applied to the foot sole (Hao et al., 2013). Chung et al. (2015) described patterns of somatosensory activations during static sustained pressure stimulation of the index finger tip, providing imaging evidence for gradual adaptation of the cortical areas to stimulation of moderate duration lasting up to 15 s. Only one study assessed cortical activation during manual stimulation

according to Vojta applied to an active site at the anterior thorax (Sanz-Esteban et al., 2018). However, methodological issues, such as unbalanced group sizes, a control site in a distant body part, and statistical maps uncorrected for multiple comparisons, do not permit drawing strong conclusions (Sanz-Esteban et al., 2018). To our knowledge, no previous imaging study evaluated immediate central effects of pressure stimulation of the foot according to reflex locomotion therapy (Vojta, 1973; Vojta and Peters, 2007), and in general, there are no fMRI data on responses to pressure foot stimulation delivered continuously over at least 30 s.

In summary, it is unknown whether the sensorimotor system response is influenced by a specific stimulation site, e.g., one used in reflex locomotion therapy. Furthermore, the link between the previously reported modulation of the motor task-evoked activation (Hok et al., 2017) and the stimulation-evoked responses remains to be established.

We hypothesized that, first, different body sites would differentially influence sensorimotor system during the stimulation, and second, that a site used in the reflex locomotion therapy would specifically activate the PMRF (Hok et al., 2017).

To address these hypotheses, we employed fMRI during block-designed sustained pressure stimulation at either an active (Vojta, 1973) or control site on the foot. We expected to identify the general activation pattern of cortical and subcortical areas involved in the central processing of sustained pressure stimulation of the foot while simulating clinical conditions of manual physiotherapy.

However, analysis of fMRI responses to sustained pressure stimulation has to address two physiological challenges: First, cortical response adapts rapidly within somatosensory areas, where it decreases exponentially over several seconds (Chung et al., 2015). Second, the activation of the presumed generators of the gradually developing widespread tonic motor reflex response would be expected to follow the same slow timecourse supposedly resulting from temporal summation over tens of seconds (Vojta, 1973). Both phenomena preclude the use of common models involving a rectangular stimulus function with the canonical HRF. Therefore, we utilized a more flexible modeling approach, namely, a convolution with a set of FIR basis functions. The main hypotheses were tested quantitatively on a voxel-wise basis, evaluating within-subject differences between the active and control stimulation. Nevertheless, the FIR model does not assume any specific shape of the hemodynamic response, which may differ slightly among different brain areas and even within one functional system (Glover, 1999; Lewis et al., 2018). Since there is no common reference for the BOLD signal throughout the brain, interpretation of significant differences critically relies on identification of brain areas that significantly respond to the stimulation and the timecourse of these evoked responses. Therefore, on top of the paired analysis of stimulus-related differences, we have employed a correlation-based clustering approach to characterize the shape of group-wise BOLD responses at different levels of the sensorimotor system and to delineate subsystems that differentially respond to the stimulation and may have different functions.

Abbreviations: AS, ankle stimulation; BA, Brodmann area; BOLD, blood oxygenation level-dependent; EEG, electroencephalography; EPI, echo-planar imaging; FIR, finite impulse response; fMRI, functional magnetic resonance imaging; FWE, family-wise error; FWHM, full width at half maximum; GLM, general linear model; HRF, hemodynamic response function; HS, heel stimulation; IPL, inferior parietal lobule; M1, primary motor cortex; MNI, Montreal Neurological Institute; MPRAGE, magnetization-prepared rapid acquisition with gradient echo; MRI, magnetic resonance imaging; PC, principal component; PMC, premotor cortex; PMRF, pontomedullary reticular formation; PRF, pontine reticular formation; ROI, region of interest; S1, primary somatosensory cortex; S2, secondary somatosensory cortex; SD, standard deviation; SMC, sensorimotor cortex; SPL, superior parietal lobule; VAS, visual analog scale.

MATERIALS AND METHODS

Study Design

This proof-of-concept study has been conducted as a randomized cross-over experimental study in a single cohort of healthy adults to determine the central effects of the sustained manual pressure stimulation according to Vojta reflex locomotion (Vojta, 1973; Vojta and Peters, 2007) versus a sham stimulation.

Participants

Thirty healthy volunteers enrolled in this study (16 females and 14 males, mean age 24.20, SD 1.92). The study participants were university students naïve to the technique of reflex locomotion, with no history of any neurological condition and no signs of motor disability. Twenty-seven subjects were right-handed and three were left-handed according to the Edinburgh handedness inventory (Oldfield, 1971). The study was carried out in accordance with World Medical Association Declaration of Helsinki. The study protocol was approved by the Ethics Committee of the University Hospital Olomouc and the Faculty of Medicine and Dentistry of Palacký University Olomouc under approval number 9.4.2013 and all participants gave their written informed consent prior to their inclusion in the study.

Task and Procedures

Each fMRI session included 2 functional imaging acquisitions during 10 min of right foot stimulation. Prior to the stimulation, participants performed a sequential motor task with their right hand as described elsewhere (Hok et al., 2017). During the stimulation, participants were lying prone in the scanner bore with their eyes closed and were asked not to think about anything in particular. The stimulation was delivered in twelve blocks (each 30 s long) alternating with jittered rest to permit modeling of the extended hemodynamic response (Dale, 1999). In total, this resulted in 6 min of stimulation and 4 min of rest per acquisition run. The pressure was applied manually by an experienced therapist (MK or MŠ) using his/her thumb placed on one of two predefined sites located on the lateral side of the foot over bony structures and within the same dermatome (Foerster, 1933): either (1) the right lateral heel zone (heel stimulation, HS) according to Vojta (1973), or (2) a control site at the right lateral ankle (ankle stimulation, AS). The therapists were instructed to apply manual pressure similar to that routinely used during physiotherapy according to Vojta. The force applied was continuously recorded during the stimulation runs using a custom-made MRI-compatible calibrated pressure/force monitor (based on a FlexiForce sensor, Tekscan, South Boston, MA, United States). Throughout the acquisition, the stimulated limb was semi-flexed in the knee joint and supported above the scanner table by the therapist who maintained constant tactile contact with the participant's foot to further simulate natural conditions of a therapeutic procedure. However, the use of a single stimulation site, the specific body position and stimulation duration, were chosen to elicit only partial motor response (Vojta and Peters, 2007), avoiding gross body movements and head displacement in the scanner bore.

After the session, participants reported discomfort/pain perceived during the stimulation using a VAS for discomfort/pain, with 0 (no discomfort/pain) and 10 (worst possible pain) marked as the extreme values. The discomfort/pain scores for HS and AS were compared using Wilcoxon two-sample signed rank test.

Every participant underwent two fMRI sessions, each involving either HS or AS. The session order was randomized and counter-balanced, and the participants were not informed in advance that the stimulation would be performed in one of two different sites. The sessions were scheduled at least 7 days apart (median interval was 70 days, range was 7–294 days).

Data Acquisition

MRI data were acquired using 1.5-Tesla scanners (Siemens Avanto and Symphony, Erlangen Germany) with standard head coils. The scanning schedule was counter-balanced to account for any possible differences due to the scanner used. The subject's head was immobilized with cushions to assure maximum comfort and minimize head motion. The MRI protocol included functional T_2^* -weighted BOLD images during task performance, acquired with gradient-echo EPI sequence (30 axial slices parallel to the anterior commissure-posterior commissure line, 5 mm thick, repetition time/echo time = 2500/41 ms, flip angle 70°, field of view = 220 mm, matrix 64 × 64) to provide 3.4 × 3.4 × 5.0 mm resolution. In total, 240 images were acquired per each functional run. Gradient-echo phase and magnitude field map images were acquired to allow correction of the echo planar imaging distortions. Anatomical high-resolution three-dimensional MPRAGE scan was acquired to provide the anatomical reference.

Data Pre-processing

The fMRI data were processed using FEAT Version 6.00, part of FSL (FMRIB's Software Library¹), version 5.0.9 (Jenkinson et al., 2012). The FEAT pre-processing pipeline included: correction of B_0 distortions using FUGUE (Jenkinson, 2003), motion correction using MCFLIRT (Jenkinson et al., 2002), non-brain removal using BET (Smith, 2002), and spatial smoothing using a Gaussian kernel with 8.0 mm FWHM. Functional data were registered to the individual's anatomical reference image, which was subsequently normalized non-linearly to the MNI 152 standard space (Grabner et al., 2006). The fMRI data were then visually checked for susceptibility artifacts and two subjects were excluded due to an excessive signal loss in the brainstem. The final sample thus consisted of 28 subjects (16 females, 12 males, 25 right-handers).

Next, motion-related artifacts were removed from each time series using ICA-AROMA tool (Pruim et al., 2015a,b), followed by high-pass temporal filtering with $\sigma = 60.0$ s. In a parallel preprocessing pipe-line, the ICA-AROMA noise components were removed from a dataset, which had no spatial smoothing applied. This dataset served for extraction of nuisance signal from six sources in the supratentorial white matter and one source in the lateral ventricles. The masks were based on the

¹www.fmrib.ox.ac.uk/fsl

MNI 152 Harvard-Oxford cortical atlas labels at 95 and 85% probabilistic threshold, respectively (Desikan et al., 2006). The white matter mask was split along the orthogonal planes into 6 areas roughly corresponding to the frontal ($Y \geq 0$ mm), parietal ($0 \text{ mm} > Y \geq -36$ mm, $Z \geq 18$ mm) and occipital white matter ($Y < -36$ mm), excluding the deep white matter around basal ganglia. From each source, the first eigenvariate was used to represent the non-neuronal signal.

Statistical Analysis of Imaging Data

The statistical analysis of the time-series was carried out in all remaining 28 subjects using FILM with local autocorrelation correction (Woolrich et al., 2001). To account for habituation with minimum assumptions, the onsets of stimulation blocks were convolved using a set of FIR basis functions instead of the canonical HRF. The GLM thus consisted of 9 delta functions (i.e., 9 temporally shifted unit spikes approximating Dirac delta function) that covered a 45 s time window (30 s on task and 15 s off task) aligned with the onset of each block with a 5 s (2 repetition times) steps to avoid noise over-fitting (Liu et al., 2017). To suppress residual physiological noise, the final model included also 6 nuisance signal regressors from the white matter and 1 from the ventricles.

The resulting beta parameters (in FSL terms, contrasts of parameter estimates or COPE) were carried over to a middle-level analysis in order to account for repeated measures in each subject. At this step, each time point (i.e., basis function) was still considered independent and analyzed separately for each subject. Since only within-subject effects were modeled at this point, the middle-level analysis was carried out using the fixed effects mode in FEAT. To test the main hypotheses, three within-subject models were designed and evaluated in parallel pipelines: In the first one, the beta parameters from each session (involving either HS or AS) were averaged separately, resulting in Contrasts 1 (HS) and 2 (AS). These contrasts represent the mean condition effects related either to HS or AS. In the second model, the functional series from both sessions were pooled together, providing Contrast 3 (HS + AS). This contrast was necessary to obtain a mean activation map for HS and AS, which would provide common clusters for a *post hoc* ROI analysis. Finally, the within-subject differences were assessed on a voxel-wise basis by subtracting the beta parameters from both sessions, yielding Contrast 4 (HS – AS).

In the final third-level analysis, group-wise effects for all within-subject contrasts were evaluated. The group model consisted of one regressor for each basis function and an *F*-test collapsing all 9 basis functions to assess the overall effect over the entire stimulation block. In Contrast 4 (HS – AS), additional linear covariates were included to account for the time difference between the two sessions and for individual differences in self-rated discomfort/pain intensity (condition H – condition A), with an additional *F*-test to evaluate the average discomfort/pain effect [Contrast 5 (Pain)]. The random effects analysis was performed using FLAME (FMRIB's Local Analysis of Mixed Effects) stage 1 (Woolrich et al., 2004). The whole-brain analysis was limited to the MNI standard brain mask

(Grabner et al., 2006) minus a white-matter mask derived from the Harvard-Oxford probabilistic atlas (Desikan et al., 2006) using a conservative probability threshold of 95% as defined in the Section “Data Pre-processing.” The masked Z (Gaussianised T) statistic images were thresholded using clusters determined by $Z > 5$ in case of Contrasts 1 to 3 (Figures 1, 2), or $Z > 3$ in case of Contrasts 4 and 5 (Figure 3). The FWE corrected cluster significance threshold was $p < 0.05$ (Worsley, 2001). Clusters in the thresholded maps were objectively labeled using the Harvard-Oxford Cortical and Subcortical Structural Atlases (Desikan et al., 2006), and the Probabilistic Cerebellar Atlas (Diedrichsen et al., 2011). Cytoarchitectonic labels were derived from the Jülich Histological Atlas (Eickhoff et al., 2007). The resulting statistical images were rendered in Mango v4.0 (Research Imaging Institute, UT Health Science Center at San Antonio, TX, United States²).

Post hoc ROI Analysis – Mean Condition Effects

To assess temporal features of the hemodynamic responses in the areas significantly activated or deactivated by either stimulation, a *post hoc* ROI analysis was performed and visualized using custom scripts created in Matlab version R2017b and the Statistics Toolbox (MathWorks, Natick, MA, United States). Only clusters in Contrast 3 (HS + AS) containing more than 5 voxels were considered.

First, average group-wise activations were investigated. Using the cluster mask from Contrast 3 (HS + AS), group-wise beta parameters were extracted from the Contrasts 1 (HS) and 2 (AS) for each time point (i.e., basis function). The representative cluster-wise values were obtained using median of beta parameters in each cluster. Vectors of 9 consecutive median beta parameters in each cluster thus provided cluster-wise timecourses, each representing median response during a single stimulation block and the subsequent rest.

To assure that the extracted medians represented a homogeneous population of voxels, each median timecourse was correlated using Pearson's correlation coefficient with the first PC obtained from the same cluster using singular value decomposition (Wall et al., 2003, 91–109). In case of low correlation between the median of the whole cluster and the first PC ($r < 0.7$), the median was extracted only from a subset of voxels highly correlated with the first PC in both HS and AS ($r > 0.75$).

The resulting representative cluster-wise timecourses (i.e., vectors of the median beta parameters) were then correlated with each other using Pearson's correlation coefficient, providing one correlation matrix for HS and one for AS. Next, hierarchical clustering was applied to both correlation matrices in order to distinguish “subsystems” (sets of clusters) with similar hemodynamic responses. Agglomerative clustering trees were built using unweighted average distance algorithm and Euclidean distance as a dissimilarity measure (Rencher and Christensen, 2012). The optimal number of resulting subsystems was indicated using Caliński-Harabasz criterion (Caliński and Harabasz, 1974).

²<http://ric.uthscsa.edu/mango/>

For visual comparison, the correlation matrix for AS was re-ordered according to the correlation matrix for HS (Figure 2B). Finally, the original HRF in each cluster was reconstructed by multiplying the convolution matrix and the group-wise beta weights of each FIR regressor (Figure 2C).

Post hoc ROI Analysis – Within-Subject Differences

Further *post hoc* analysis was performed to determine the timing and directionality of differences detected in Contrast 4 (HS – AS). This was done by extracting the median within-subject beta parameters from Contrasts 1 (HS) and 2 (AS) within the boundaries of the clusters from Contrast 4 (HS – AS). To identify time points of significant differences, corresponding beta parameters for HS and AS were compared using paired Wilcoxon signed rank test at $p < 0.05$ (*post hoc* confirmatory analysis without additional correction). Finally, the differences in activation levels in clusters from Contrast 5 (Pain) were correlated with discomfort/pain rating difference using Spearman's correlation coefficient and marked significant at $p < 0.05$. These results are presented in Figure 3.

RESULTS

Behavioral Data

In all subjects, the therapist observed discrete irregular focal muscle contractions in the stimulated extremity during stimulation, but no gross limb or trunk movements.

For technical reasons, continuous pressure recordings were only obtained in 15 subjects. The mean force applied at the sensor during HS was 22.33 N (SD = 11.64 N) and 26.45 N (SD = 9.72 N) during AS. The difference was not significant

($p = 0.32$, two-sample *t*-test). A paired *t*-test was possible in 11 subjects with a non-significant difference ($p = 0.22$, mean difference HS – AS = -3.94 N, SD = 9.96 N).

After HS, the median reported discomfort/pain intensity (VAS) was 1.85 (range 0–6.9), while it was 0.90 after AS (range 0–5.5). HS was thus associated with significantly higher discomfort/pain intensity than AS ($p < 0.01$, Wilcoxon signed rank test), with median difference 1.25 (range -5.0 –6.4). The difference in discomfort/pain rating has been therefore included as a covariate in the Contrast 4 (HS – AS).

Imaging Results

Spatial Maps of Mean Condition Effects

Group Contrasts 1 (HS) and 2 (AS) yielded separate Z statistical maps depicting areas with significant response either to HS or to AS (Figure 1). The areas involved in the somatosensory processing of the pressure stimulation of each site overlapped partially (spatial correlation between thresholded Z statistical maps for HS and AS was 0.56 using Pearson correlation coefficient). The overlapping areas (binary conjunction, see yellow overlay in Figure 1, row C) included mainly the left dorsomedial primary somatosensory and motor cortex (S1 and M1, respectively) in the somatotopic representation of the stimulated lower limb and the bilateral parietal operculum cortices (secondary somatosensory cortex, or S2). Less extensive overlap was observed in the more posterior right postcentral gyrus and SPL, i.e., ipsilateral to the stimulated limb. Both stimulation sites were also associated with signal changes in bilateral dorsolateral sensorimotor cortex (SMC, i.e., S1 and M1) in the somatotopic representation of the upper limb and face (Long et al., 2014). These were later identified as transient deactivations, see below. Further similarities between

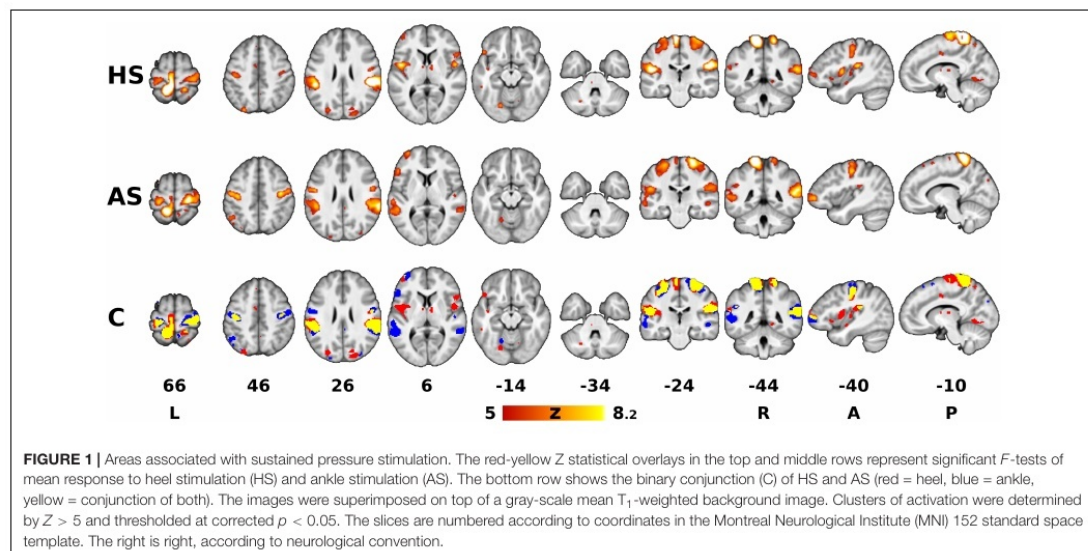
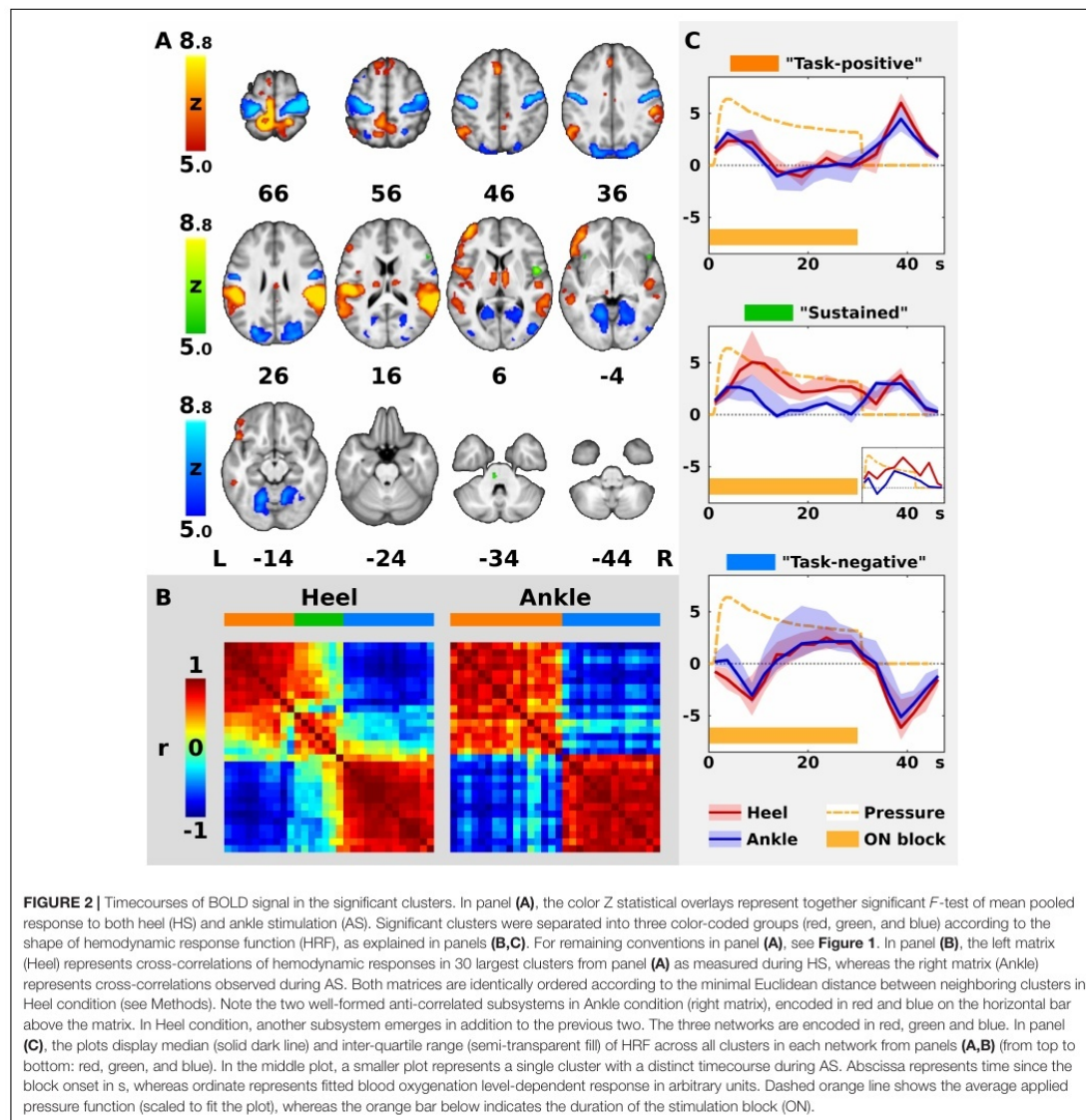


FIGURE 1 | Areas associated with sustained pressure stimulation. The red-yellow Z statistical overlays in the top and middle rows represent significant *F*-tests of mean response to heel stimulation (HS) and ankle stimulation (AS). The bottom row shows the binary conjunction (C) of HS and AS (red = heel, blue = ankle, yellow = conjunction of both). The images were superimposed on top of a gray-scale mean T₁-weighted background image. Clusters of activation were determined by $Z > 5$ and thresholded at corrected $p < 0.05$. The slices are numbered according to coordinates in the Montreal Neurological Institute (MNI) 152 standard space template. The right is right, according to neurological convention.



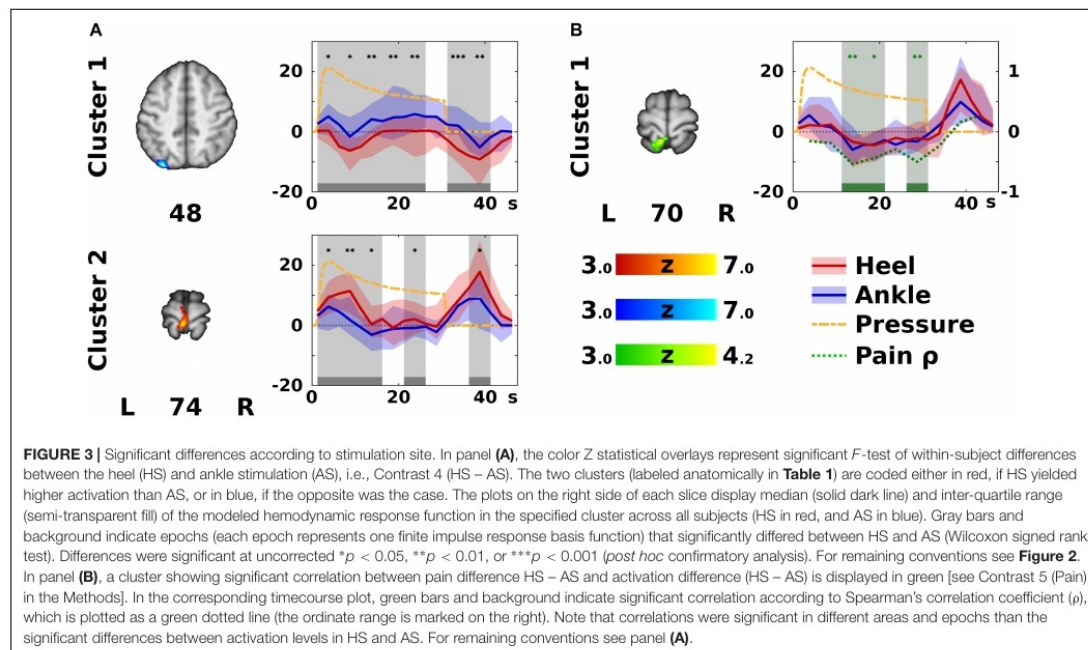
the responses to stimulation at either site were found in the left prefrontal and bilateral parieto-occipital cortices, bilateral lingual gyri and thalami, but the involved areas mostly did not overlap. Several qualitative differences were observed: AS was associated with more involvement of temporal and prefrontal areas in the left hemisphere, whereas HS elicited responses in the left insular and bilateral frontal operculum cortices and the brainstem in the contralateral (left) pons.

The analysis of pooled data (Contrast 3 [HS + AS], sum of all color overlays in Figure 2A) yielded significant effects in all areas

associated with either HS or AS alone. Therefore, a complete list of clusters with anatomical labels is only provided for Contrast 3 (HS + AS; see Supplementary Table S1).

Post hoc ROI Analysis

The ROI analysis of the clusters obtained from Contrast 3 (HS + AS) was limited to the 30 biggest clusters with more than 5 voxels (see Supplementary Table S1 for a complete list). The median group-wise beta parameters were highly correlated with the first principal component in all but one cluster, namely,



Cluster 1. In this cluster, the first PC was dominant for both stimulation sites ($r > 0.75$) in 2,798 voxels (47.5% of the original cluster size), which were used to extract representative response time-course. The remaining voxels were not considered.

In the 30 evaluated clusters, the modeled BOLD responses could be mostly separated into two distinct subsystems with anti-correlated timecourses (Figure 2B). This was especially apparent in AS. Therefore, all clusters in AS condition and most clusters in HS condition were labeled either as “task-positive” or “task-negative” based on the sign of the immediate BOLD signal change. According to the timecourse plots, the median activation in the task-positive subsystem (“Task-positive” plot in Figure 2C) increased immediately after the stimulation onset and peaked at 3.75 s, namely, at the center of the second volume after onset. It decreased back to baseline as early as 10 s after onset. Following the stimulation offset, activation transiently increased again and remained positive 0 to 17.5 s after offset, peaking at 8.75 s. As opposed to the task-positive areas, the responses in the second subsystem (“Task-negative” plot in Figure 2C) involved deactivations at the onset and at the offset of the stimulation. The median response remained negative 5 to 12.5 s after onset and 5 to 17.5 s after offset. Please note that the real time resolution of the plots is roughly 5 s, which is the approximate width of a single regressor spanning 2 TRs.

Whereas there were only two subsystems with homogeneous responses in AS, a third type of response could be distinguished in HS (see dendrograms in Supplementary Figure S1). The 23 clusters with consistent task-positive or task-negative responses, which were similar in both conditions are represented by red

and blue overlay, respectively, in Figure 2A. The responses in the remaining 7 clusters in HS condition followed a distinct timecourse that deviated from the common task-positive or task-negative pattern (compare the matrices in Figure 2B; see also Supplementary Figure S1, dendrogram “Heel”). Six out of these clusters were task-positive in AS and one was task-negative in AS, including the right frontal and central opercular cortex, inferior frontal gyrus, frontal orbital cortex, bilateral anterior insular cortex, left paracingulate gyrus and the left pons (see green overlay in Figure 2A). In these clusters, the initial response in HS condition remained positive for the duration of the stimulation block (peak at 8.75 s after onset) instead of dropping immediately to baseline. After the offset, the second positive response could be observed at 8.75 s after offset. Therefore, the subsystem was labeled as “sustained task-positive” (compare the red solid line representing HS to the blue line representing AS in “Sustained” plot in Figure 2C).

Within-Subject Differences Between Conditions

Contrast 4 (HS – AS) yielded a map of average within-subject differences between HS and AS (Figure 3A), as well as the interaction with the self-reported discomfort/pain intensity (Figure 3B). The differences between HS and AS were observed in the IPL (area PGp; Cluster 1 in Figure 3A) and in the left primary motor (M1) and PMC in the somatotopic representation of the lower limb (BA 4a and 6; Cluster 2 in Figure 3A). The discomfort/pain effect [Contrast 5 (Pain)] was observed in the left SPL (BA 7A and 5L; Cluster 1 in Figure 3B) posterior to the Cluster 2 in Contrast 4 (HS – AS). A complete

list of clusters with their anatomical labels is provided in **Table 1**.

The ROI analysis of clusters in Contrast 4 (HS – AS; see **Table 1**) revealed that the modeled BOLD response in the left M1 and PMC (Cluster 2 in **Figure 3A**) was significantly higher in HS condition. This was observed mostly during short activation increases after stimulation onset and offset. In contrast, activation levels in the left IPL (Cluster 1 in **Figure 3A**) were higher in AS condition than in HS condition. The differences in the IPL were spread almost over the entire stimulation block and the subsequent rest.

The ROI analysis of the cluster obtained from Contrast 5 (Pain) showed that the discomfort/pain difference (HS – AS) was negatively correlated with the difference in activation levels (HS – AS). The significant correlations were detected during the sustained phase of the stimulation (**Figure 3B**).

DISCUSSION

In this section, we discuss the main findings in the following order: brain structures associated with the pressure stimulation of the foot, the dynamics of the BOLD responses, deactivations observed during the stimulation, and the site-specific differences, which are the main novel findings of this study.

Patterns of Activation Associated With Pressure Stimulation

Using a FIR model to deconvolve the hemodynamic response, we have confirmed that sustained peripheral pressure stimulation influences multiple elements of the sensorimotor system. The

stimulus-related activation increases that we observed mainly in the contralateral S1 and bilateral S2 regardless of stimulation site (**Figure 1**) are consistent with previous descriptions of the core somatosensory network activated during pressure stimulation applied either at the upper or the lower limb (Hao et al., 2013; Miura et al., 2013; Chung et al., 2015). Further consistent activations that we detected in the contralateral dorsomedial M1/PMC have only been observed in lower limb stimulation (Hao et al., 2013; Miura et al., 2013), whereas activations in the ipsilateral dorsomedial S1/SPL have been previously reported only in one study (Miura et al., 2013). Other brain structures activated either by HS or AS, or observed in the pooled analysis [Contrast 3 (HS + AS)], such as frontal, insular or cingulate cortices and bilateral thalami, also agree with previous studies (Miura et al., 2013; Chung et al., 2015). Therefore, the described general activation pattern during sustained pressure stimulation of the foot may be considered rather independent of stimulation site and duration.

Temporal Features of the BOLD Responses

Apart from the localization of signal changes, we also deconvolved the timecourse of the regional hemodynamic responses to natural manual pressure stimulation.

First, this allowed us to confirm that fast adaptation (Chung et al., 2015) occurs also during longer and repeated sustained stimulation. The sensation of static mechanical pressure is believed to be conducted via slowly adapting I (SA-I) afferents (Johansson and Flanagan, 2009). These afferents adapt exponentially to static stimuli (indentation or vibration) with a time constant of 8.4 s (Leung et al., 2005). Considering the

TABLE 1 | List of clusters of significant differences according to stimulation site.

Contrast	Cluster index	Anatomical atlas labels	Cytoarchitectonic atlas labels	Volume (cm ³)	Cluster p	Z_{max}	Z_{max} MNI coordinates [x,y,z (mm)]
Contrast 4: HS – AS	1	100.0% L Lateral Occipital C, s. d.	81.5% L Inferior Parietal Lobule PGp 7.1% L Inferior Parietal Lobule PGa 5.1% L Superior Parietal Lobule 7A	2.81	0.003	7.00	–30, –80, 48
	2	48.5% L Postcentral G 36.5% L Precentral G 8.8% R Precentral G 6.2% R Postcentral G	65.0% L Primary Motor C BA4a 18.1% L Premotor C BA6 8.5% R Primary Motor C BA4a	2.08	0.014	6.74	–4, –36, 74
Contrast 5: Pain effect	1	53.0% L Superior Parietal Lobule 29.8% L Postcentral G 12.1% L Lateral Occipital C, s. d. 5.1% L Precuneous Cortex	46.0% L Superior Parietal Lobule 5L 45.5% L Superior Parietal Lobule 7A	1.58	0.043	4.16	–8, –48, 70

Table lists significant F -test clusters in Contrast 4 (HS – AS), i.e., the differences between heel and ankle stimulation, and in Contrast 5 (Pain), i.e., the pain effect. Anatomical and cytoarchitectonic labels are provided including the proportion of labeled voxels. Only labels consisting at least 5% of activated voxels are shown. Note that cerebellar labels may overlap with cortical labels and that cytoarchitectonic labels do not cover the whole brain. Abbreviations: C, cortex; BA, Brodmann area; G, gyrus; MNI, Montréal Neurological Institute; R, right; s. d., superior division; Z_{max} , maximum Z score.

time lag of the BOLD response, the activations in our data in the task-positive areas (coded in red in **Figures 2A,C**) occurred and diminished within the expected time window (0 to 10 s after onset), which is in overall agreement with previous observations (Chung et al., 2015).

Second, we show that an equal response follows the release of pressure (**Figure 2C**). Similar response has been observed after offset of sustained non-nociceptive vibratory (Marxen et al., 2012) or electrical stimulation (Hu et al., 2015), but it has not been reported so far in sustained pressure stimulation (Chung et al., 2015). Importantly, the offset responses have been shown to occur only after non-nociceptive stimulation (Hu et al., 2015), suggesting that the task-positive areas with offset responses in our data (red overlay in **Figure 2A**) were not associated with processing of painful sensations and could potentially receive input mediated by rapidly adapting (RA) afferents (Hu et al., 2015), but this has to be confirmed by future electrophysiological studies.

Regarding the magnitude of the offset responses, it should be noted that both positive and negative offset responses were apparently of higher amplitude and longer duration (0 to 17.5 s after offset) than the responses at the stimulation onset. We speculate that the reason might be to some extent related to our experimental design: the offset pressure decrease may have been on average more abrupt and less variable than the pressure increase at the block onset. As a result, onset responses might be slightly “blurred” in time.

Deactivations Associated With Pressure Stimulation

In addition to areas activated during the stimulation, we also report a complementary set of brain areas, which were transiently suppressed by the stimulation and the pressure release. Similar inhibition in the bilateral S1 and M1 has been previously documented during vibrotactile finger or tactile foot stimulation (Hlushchuk and Hari, 2006; Tal et al., 2017). We extend this observation by showing that such suppression occurs also in response to sustained pressure stimulation of the lower limb. In line with Tal et al. (2017), we show that foot stimulation deactivates sensorimotor cortices in the bilateral somatotopic representations for upper limbs and face (blue overlay in **Figure 2A**) as defined by Long et al. (2014). A new finding in the context of lower limb stimulation is the deactivation in areas outside the sensorimotor system, such as the temporal and occipital cortices. Similar cross-modal deactivations have been observed in humans only during somatosensory processing of tactile input from the upper limbs and they have been speculated to enhance the somatosensory processing by suppressing unnecessary sensory input (Kawashima et al., 1995; Merabet et al., 2007; Ide et al., 2016).

The observed deactivations are unlikely to be caused by local redistribution of the blood flow (hemodynamic steal) as most of the areas showing differential responses are supplied by different main cerebral arteries (Tal et al., 2017). Electrophysiological evidence from direct intracortical recordings suggests that negative BOLD response is associated with suppressed neuronal

activity in the deep cortical layers (Boorman et al., 2010; Yin et al., 2011). Simultaneous fMRI/EEG recordings in humans show considerable correlation between the EEG mu power and BOLD signal decrease, confirming its neuronal origin (Mullinger et al., 2014). Recent data show that inhibitory neurons may also contribute to the positive hemodynamic response, hence, deactivations could conversely reflect decreased neuronal activity of both excitatory and inhibitory cells (Vazquez et al., 2018). However, there is also evidence suggesting that the deactivated areas are not necessarily always “shut down.” Decrease in BOLD signal and cerebral blood flow may be at least in some cases accompanied by increased spiking (Hu and Huang, 2015) and/or glucose uptake (Devor et al., 2008). Since the underlying neuronal processes and functional role of negative hemodynamic responses are not yet clearly understood, they should be interpreted with caution (Tal et al., 2017).

Differences Between the Heel and Ankle Stimulation

Voxel-Wise Within-Subject Comparison

Compared to control stimulation, HS was associated with significantly increased activation in the left M1/PMC (somatotopically lower limb area; see Cluster 2 in **Figure 3A**) and decreased activation in the left IPL.

Activations in the contralateral motor cortex have already been observed during pressure stimulation of the lower limb (Hao et al., 2013; Miura et al., 2013) as discussed in the Section “Patterns of Activation Associated With Pressure Stimulation.” Although both AS and HS were associated with transient activations in the M1 representation for the stimulated limb, the results indicate higher neuronal activity during HS (**Figure 3A**, Cluster 2). This may have several possible reasons: A shift in somatosensory representation is unlikely as the activations in the postcentral gyrus did not differ. While the local stimulation site properties may also influence the activations, we believe that there were no sources of bias other than those, which may be in fact important for the reflex locomotion therapy (see also Limitations). The increased motor activation may also be a secondary phenomenon, for instance, reflecting pain-evoked movements (Apkarian et al., 2005). Since the Contrast 4 (HS – AS) was controlled for the difference in discomfort/pain rating, we consider the M1/PMC activation differences to be less likely pain-related (see also Limitations). Next, the observed difference in the M1/PMC may result from an incipient involuntary muscle response to stimulation according to Vojta and may be mediated by a different, possibly subcortical or brainstem structure (Vojta, 1973; Laufens et al., 1991; Hok et al., 2017). Finally, the increased motor activation during HS may also represent a site-specific difference in sensorimotor integration. It remains unknown at which level the sensory input is redirected to the motor cortex. It may either reflect a direct interaction between the adjacent somatosensory and motor cortices (Kaelin-Lang et al., 2002), or a parallel bottom-up thalamo-cortical pathway (Huffman and Krubitzer, 2001) or collaterals of the spinothalamic pathway (Kayalioglu, 2009). Such direct influence of sensory input on motor cortex function

is supported by electrophysiological evidence using sustained electrical (Golaszewski et al., 2012), vibratory (Marconi et al., 2008), or vibrotactile (Christova et al., 2011) stimulation, which shows outlasting effects on motor cortex excitability, possibly by affecting inhibitory GABA-ergic intracortical circuits (Ziemann et al., 1996).

In contrast to the task-positive motor activations, the differences in the IPL (**Figure 3A**, Cluster 1) are more likely related to cross-modal deactivations (Kawashima et al., 1995; Merabet et al., 2007; Ide et al., 2016) as discussed in the Section “Deactivations Associated With Pressure Stimulation.” The posterior IPL (cytoarchitectonically the area PGp) is considered a part of the default mode network, specifically its medial temporal lobe subsystem (Igelström and Graziano, 2017). Similar stimulus-related deactivations in parts of the default mode network have been previously observed during sustained electrical stimulation (Hu et al., 2015). These deactivations varied over different phases of stimulation, left IPL being predominantly deactivated during the onset phase of periodic stimuli (Hu et al., 2015). Nevertheless, the role of those deactivations remains unclear. Since cognitive processes were not explicitly controlled in this study, we can only speculate that the higher amplitude of deactivations in the IPL-PGp could mean that the sensory input associated with HS was suppressing internally driven cognitive processes, possibly by drawing more externally oriented attention.

Comparison of Group-Wise Activation Patterns

During HS, average activation in several areas followed a timecourse with more sustained positive BOLD response (red solid line in “Sustained” plot in **Figure 2C**), whereas in AS, only transient onset/offset activations were detected (blue solid lines in **Figure 2C**). Some of these areas, including insular cortices and pons, were not observed in the group-wise map for AS condition, but they were detected in HS (**Figure 1**).

The involvement of the insular cortex in HS may in fact reflect increased discomfort/pain ratings during HS since the insular cortex is known to participate in emotional processing of pain (Apkarian et al., 2005; Kurth et al., 2010; Hu et al., 2015). However, other explanations remain possible as there was no significant correlation with discomfort/pain intensity difference in the insulo-opercular areas in Contrast 5 (Pain). For instance, anterior insula also significantly contributes to the control of autonomic responses (Beissner et al., 2013) and various cognitive and affective processes (Kurth et al., 2010; Uddin, 2015). Indeed, stimulation according to Vojta has been associated with various autonomic responses (Vojta and Peters, 2007), but our parallel investigation of cardiac autonomic responses in a similar cohort of healthy subjects did not indicate any site-specific effect of HS which would interfere with our current results (Opavský et al., 2018).

Another structure associated with HS (but not significantly with AS, see **Figure 1**, row C) was included in the sustained task-positive subsystem (green overlay in **Figure 2A**) and located in the pontine tegmentum. The area most likely encompasses the PRF and pontine nuclei (Nieuwenhuys et al., 2008). These are adjacent to the PMRF in which we have previously observed modulation of motor-related activation after sustained pressure

stimulation (Hok et al., 2017). Based on that observation, we have previously speculated that the PMRF might play a role in the therapeutic stimulation according to Vojta (Hok et al., 2017). While the current study does not provide further direct evidence for the specific role of PRF or PMRF in the physiotherapeutic effects of pressure stimulation, the sustained activation in the PRF during HS (see “Sustained” plot in **Figure 2C**) provides a ground for potential interaction between the PRF and the more caudal PMRF.

In humans, the brainstem reticular formation, and more specifically the PMRF, is suggested to exert anticipatory postural control before gait initiation (Takakusaki, 2013). It also activates during the imagery of standing (Jahn et al., 2008) and walking (la Fougère et al., 2010). Most importantly, however, stimulation of the PMRF elicits bilateral asymmetrical motor patterns in cats (Dyson et al., 2014) and monkeys (Hirschauer and Buford, 2015), which can be related to stereotypic tonic responses observed by Vojta (1973) and Vojta and Peters (2007).

Implications for Physiotherapeutic Techniques

Our findings indicate that sustained pressure stimulation affects the sensorimotor system on a global scale. While some areas (e.g., the primary SMC for the foot) respond with increased activation, other regions (such as the primary SMC for the hand and face) became transiently suppressed. This effect seems to be non-specific and independent of the stimulated site. However, specific effects during the HS were observed as well.

Pressure stimulation is an integral part of number of physiotherapeutic techniques, such as reflex locomotion (Vojta and Peters, 2007), clinical massage, acupressure (Wong et al., 2016), reflexology, or myofascial trigger point therapy (Smith et al., 2018). Whereas in reflex locomotion, the choice of exact stimulation site is pre-defined (Vojta and Peters, 2007), other techniques, such as myofascial trigger point therapy, do not rely on specific body site (Smith et al., 2018). Our data show that even non-specific pressure stimulation may evoke far-reaching effects throughout the brain, including the motor system, which is relevant for physiotherapy. Whether the observed cortical activations/deactivations in the current study have any outlasting and clinically significant impact, cannot be established without further studies with comprehensive protocols employing imaging and repeated behavioral testing.

Our choice of the specific stimulation site was motivated by the stimulation according to Vojta, which is known to induce significant modulatory motor after-effects, e.g., facilitation of voluntary movements that outlast the stimulation (Laufens et al., 1995). Our current data provide further evidence that sustained pressure stimulation may influence multiple sensorimotor areas (including representations of distant extremities) without any evoked gross motor activity. The site-specific effects were local, i.e., confined to the motor cortex adjacent to the primary somatosensory representation of the stimulated limb. While the co-activation in the primary motor and premotor cortex of the stimulated (lower) limb seems to be relatively non-specific (Hao et al., 2013; Miura et al., 2013), we show that it can be augmented

by stimulation at certain sites, such as the lateral heel zone according to Vojta (1973).

However, the fact that we deliberately did not elicit any consistent gross involuntary motor responses limits our ability to connect our observations with the anatomical structures responsible for the control of the motor patterns observed during the reflex locomotion therapy (Vojta, 1973). Still, we expand our recent observation of the modulatory motor after-effects in the PMRF (Hok et al., 2017) by showing that HS is associated with sustained activation in the nearby PRF, which was not observed during control stimulation. We speculate that an interaction (possibly top-down) between these brainstem nuclei might be responsible for the global motor effects of the reflex locomotion therapy.

The need for targeted stimulation of empirically chosen sites in reflex locomotion resembles other therapeutic techniques, such as acupuncture. In (electro)acupuncture, a considerable number of fMRI studies compared brain activations in response to the “active” and sham sites, but results are often conflicting (Qiu et al., 2016). A specific activation increase in response to lower limb stimulation was observed in the contralateral primary motor cortex (Wu et al., 2002; Usichenko et al., 2015) in agreement with our results, suggesting that there might be a more universal mode of action common for both reflex locomotion and acupuncture. However, differences in many other brain areas not corresponding to our results, including frontal and temporal cortices and limbic structures, were also observed (Wu et al., 2002; Usichenko et al., 2015), therefore, other mechanisms might be involved as well. A head to head comparison would be required to assess this.

Limitations

Because of the whole-brain fMRI acquisition, the spatial resolution of the T_2^* -weighted MR images may limit assignment of activation foci to a single anatomical area in a small structure such as the brainstem. Nevertheless, functional MR imaging of the brainstem was successfully performed in the past using spatial resolution and hardware comparable to ours (Jahn et al., 2008). Moreover, data acquisition using a 1.5-T scanner may be less prone to magnetic susceptibility artifacts that affect higher-field 3-T scanners more severely, despite their superior signal to noise ratio.

Furthermore, the observed activation differences between HS and AS might be to some extent influenced by concomitant discomfort/pain. In this study, the HS was indeed rated more unpleasant/painful than the AS. This is in line with the reports that therapeutic stimulation according to Vojta is associated with concomitant pain (Müller, 1974). While electromyographic recordings from the stimulated and non-stimulated limbs would be needed in future studies to completely exclude the possibility of pain-related movements, the overall discomfort/pain intensity ratings in this study were quite low in both conditions (median VAS in HS 1.9, in AS 0.9). In the whole-brain analysis, the differences between HS and AS were controlled for the discomfort/pain effect. In fact, the interaction between discomfort/pain (self-rated discomfort/pain intensity difference) and stimulation modality (HS or AS) was observed in different

areas than the differences between stimulation modalities alone. The posterior parietal areas have been previously reported as parts of the pain perception network (Apkarian et al., 2005).

Further potential bias may arise from differences in local characteristics between the two stimulation sites, such as density of sensory nerve endings, soft tissue properties or bony structures below the skin. As mentioned in Methods, both sites were within the same dermatome (Foerster, 1933). Since the active site (heel) was defined by Vojta (1973), the control site was carefully chosen to match as many properties as possible, i.e., neither site was located at the foot sole, but rather on the lateral aspect of the foot. We do not consider either site to contribute specifically to any motor or balance control function. Conversely, it is likely that some of the local site properties indeed play a role in the therapeutic effect of the reflex locomotion therapy, but further studies testing multiple sites in different dermatomes over different types of tissues would be needed to elucidate this.

CONCLUSION

We have confirmed that sustained manual pressure stimulation of the foot is associated with extensive activation throughout the sensorimotor system and, for the first time in the context of the pressure stimulation, that it is accompanied by equally prominent cross-modal deactivations, including the occipital cortices and sensorimotor representation of the upper limbs and face. The timecourse data confirm fast adaptation of the sensory processing system, but also reveal previously underreported transient responses related to the stimulation offset. We further report that sustained pressure stimulation of the (active) site at the heel, which is used in the reflex locomotion therapy, elicited increased cortical activation in the primary motor representation of the stimulated limb and decreased activation in the posterior parietal cortex. Moreover, the stimulation of the active site was associated with a more sustained BOLD response in the insulo-opercular cortices and contralateral pons. We suggest that the increased motor activation and involvement of the pontine reticular formation could be associated with the previously observed motor after-effects of reflex locomotion therapy.

DATA AVAILABILITY

The raw data supporting the conclusions of this manuscript will be made available by the authors, without undue reservation, to any qualified researcher.

ETHICS STATEMENT

This study was carried out in accordance with the recommendations of Ethics Committee of the University Hospital Olomouc and the Faculty of Medicine and Dentistry of Palacký University Olomouc with written informed consent from all subjects. All subjects gave written informed consent in accordance with the Declaration of Helsinki. The protocol was approved by the Ethics Committee of the University Hospital

Olomouc and the Faculty of Medicine and Dentistry of Palacký University Olomouc.

All authors have read, revised critically and approved the final submitted manuscript, and agreed to be accountable for the content of the work.

AUTHOR CONTRIBUTIONS

PHo has substantially contributed to the design of the work, data acquisition, analysis and interpretation, and drafted the manuscript. JO has substantially contributed to the conception, design, and interpretation of the work, and substantially revised the manuscript. RL has substantially contributed to the data analysis and drafted parts of the manuscript. MK has substantially contributed to the design of the work and data acquisition. MŠ has substantially contributed to the data acquisition. ZT has substantially contributed to the data acquisition and substantially revised the manuscript. PK has substantially contributed to the conception of the work. PHl has substantially contributed to the conception and design of the work, data acquisition, and substantially revised the manuscript.

FUNDING

This work was supported by the Czech Science Foundation (GACR) (Grant No. 14-22572S) and Ministry of Health, Czechia – conceptual development of research organization (Grant No. FNOL, 00098892).

SUPPLEMENTARY MATERIAL

The Supplementary Material for this article can be found online at: <https://www.frontiersin.org/articles/10.3389/fnins.2019.00722/full#supplementary-material>

REFERENCES

- Apkarian, A. V., Bushnell, M. C., Treede, R.-D., and Zubieta, J.-K. (2005). Human brain mechanisms of pain perception and regulation in health and disease. *Eur. J. Pain* 9, 463–484. doi: 10.1016/j.ejpain.2004.11.001
- Beissner, F., Meissner, K., Bär, K.-J., and Napadow, V. (2013). The autonomic brain: an activation likelihood estimation meta-analysis for central processing of autonomic function. *J. Neurosci.* 33, 10503–10511. doi: 10.1523/JNEUROSCI.1103-13.2013
- Boorman, L., Kennerley, A. J., Johnston, D., Jones, M., Zheng, Y., Redgrave, P., et al. (2010). Negative blood oxygen level dependence in the rat: a model for investigating the role of suppression in neurovascular coupling. *J. Neurosci.* 30, 4285–4294. doi: 10.1523/JNEUROSCI.6063-09.2010
- Caliński, T., and Harabasz, J. (1974). A dendrite method for cluster analysis. *Commun. Stat. Theory Methods* 3, 1–27. doi: 10.1080/03610927408827101
- Chipchase, L. S., Schabrun, S. M., and Hodges, P. W. (2011). Peripheral electrical stimulation to induce cortical plasticity: a systematic review of stimulus parameters. *Clin. Neurophysiol.* 122, 456–463. doi: 10.1016/j.clinph.2010.07.025
- Christova, M., Rafolt, D., Golaszewski, S., and Gallasch, E. (2011). Outlasting corticomotor excitability changes induced by 25 Hz whole-hand mechanical stimulation. *Eur. J. Appl. Physiol.* 111, 3051–3059. doi: 10.1007/s00421-011-1933-0
- Chung, Y. G., Han, S. W., Kim, H.-S., Chung, S.-C., Park, J.-Y., Wallraven, C., et al. (2014). Intra- and inter-hemispheric effective connectivity in the human somatosensory cortex during pressure stimulation. *BMC Neurosci.* 15:43. doi: 10.1186/1471-2202-15-43
- Chung, Y. G., Han, S. W., Kim, H.-S., Chung, S.-C., Park, J.-Y., Wallraven, C., et al. (2015). Adaptation of cortical activity to sustained pressure stimulation on the fingertip. *BMC Neurosci.* 16:71. doi: 10.1186/s12868-015-0207-x
- Dale, A. M. (1999). Optimal experimental design for event-related fMRI. *Hum. Brain Mapp.* 8, 109–114.
- Desikan, R. S., Ségonne, F., Fischl, B., Quinn, B. T., Dickerson, B. C., Blacker, D., et al. (2006). An automated labeling system for subdividing the human cerebral cortex on MRI scans into gyral based regions of interest. *Neuroimage* 31, 968–980. doi: 10.1016/j.neuroimage.2006.01.021
- Devor, A., Hillman, E. M. C., Tian, P., Waeber, C., Teng, I. C., Ruvinskaya, L., et al. (2008). Stimulus-induced changes in blood flow and 2-deoxyglucose uptake dissociate in ipsilateral somatosensory cortex. *J. Neurosci.* 28, 14347–14357. doi: 10.1523/JNEUROSCI.4307-08.2008
- Diedrichsen, J., Maderwald, S., Küper, M., Thürling, M., Rabe, K., Gizewski, E. R., et al. (2011). Imaging the deep cerebellar nuclei: a probabilistic atlas and normalization procedure. *Neuroimage* 54, 1786–1794. doi: 10.1016/j.neuroimage.2010.10.035
- Dyson, K. S., Miron, J.-P., and Drew, T. (2014). Differential modulation of descending signals from the reticulospinal system during reaching and locomotion. *J. Neurophysiol.* 112, 2505–2528. doi: 10.1152/jn.00188.2014
- Eickhoff, S. B., Paus, T., Caspers, S., Grosbras, M.-H., Evans, A. C., Zilles, K., et al. (2007). Assignment of functional activations to probabilistic cytoarchitectonic areas revisited. *Neuroimage* 36, 511–521. doi: 10.1016/j.neuroimage.2007.03.060
- Foerster, O. (1933). The dermatomes in man. *Brain* 56, 1–39. doi: 10.1093/brain/56.1.1
- Gallasch, E., Christova, M., Kunz, A., Rafolt, D., and Golaszewski, S. (2015). Modulation of sensorimotor cortex by repetitive peripheral magnetic stimulation. *Front. Hum. Neurosci.* 9:407. doi: 10.3389/fnhum.2015.00407
- Glover, G. H. (1999). Deconvolution of impulse response in event-related BOLD fMRI. *Neuroimage* 9, 416–429. doi: 10.1006/nimg.1998.0419
- Golaszewski, S. M., Bergmann, J., Christova, M., Kunz, A. B., Kronbichler, M., Rafolt, D., et al. (2012). Modulation of motor cortex excitability by different levels of whole-hand afferent electrical stimulation. *Clin. Neurophysiol.* 123, 193–199. doi: 10.1016/j.clinph.2011.06.010
- Grabner, G., Janke, A. L., Budge, M. M., Smith, D., Pruessner, J., and Collins, D. L. (2006). Symmetric atlas and model based segmentation: an application to the hippocampus in older adults. *Med. Image Comput. Comput. Assist. Interv.* 9, 58–66. doi: 10.1007/11866763_8
- Grillner, S., and Wallén, P. (1985). Central pattern generators for locomotion, with special reference to vertebrates. *Annu. Rev. Neurosci.* 8, 233–261. doi: 10.1146/annurev.ne.08.030185.001313
- Hao, Y., Manor, B., Liu, J., Zhang, K., Chai, Y., Lipsitz, L., et al. (2013). A novel MRI-compatible tactile stimulator for cortical mapping of foot sole pressure stimuli with fMRI. *Magn. Reson. Med.* 69, 1194–1199. doi: 10.1002/mrm.24330
- Hirschauer, T. J., and Buford, J. A. (2015). Bilateral force transients in the upper limbs evoked by single-pulse microstimulation in the pontomedullary reticular formation. *J. Neurophysiol.* 113, 2592–2604. doi: 10.1152/jn.00852.2014
- Hlushchuk, Y., and Hari, R. (2006). Transient suppression of ipsilateral primary somatosensory cortex during tactile finger stimulation. *J. Neurosci.* 26, 5819–5824. doi: 10.1523/JNEUROSCI.5536-05.2006
- Hok, P., Opavský, J., Kutín, M., Tüdös, Z., Kaňovský, P., and Hlušík, P. (2017). Modulation of the sensorimotor system by sustained manual pressure stimulation. *Neuroscience* 348, 11–22. doi: 10.1016/j.neuroscience.2017.02.005
- Hu, D., and Huang, L. (2015). Negative hemodynamic response in the cortex: evidence opposing neuronal deactivation revealed via optical imaging and electrophysiological recording. *J. Neurophysiol.* 114, 2152–2161. doi: 10.1152/jn.00246.2015

- Hu, L., Zhang, L., Chen, R., Yu, H., Li, H., and Mouraux, A. (2015). The primary somatosensory cortex and the insula contribute differently to the processing of transient and sustained nociceptive and non-nociceptive somatosensory inputs. *Hum. Brain Mapp.* 36, 4346–4360. doi: 10.1002/hbm.22922
- Huffman, K. J., and Krubitzer, L. (2001). Thalamo-cortical connections of areas 3a and M1 in marmoset monkeys. *J. Comp. Neurol.* 435, 291–310. doi: 10.1002/cne.1031
- Ide, M., Hidaka, S., Ikeda, H., and Wada, M. (2016). Neural mechanisms underlying touch-induced visual perceptual suppression: an fMRI study. *Sci. Rep.* 6:37301. doi: 10.1038/srep37301
- Igelström, K. M., and Graziano, M. S. A. (2017). The inferior parietal lobule and temporoparietal junction: a network perspective. *Neuropsychologia* 105, 70–83. doi: 10.1016/j.neuropsychologia.2017.01.001
- Jahn, K., Deutschländer, A., Stephan, T., Kalla, R., Wiesmann, M., Strupp, M., et al. (2008). Imaging human supraspinal locomotor centers in brainstem and cerebellum. *Neuroimage* 39, 786–792. doi: 10.1016/j.neuroimage.2007.09.047
- Jenkinson, M. (2003). Fast, automated, N-dimensional phase-unwrapping algorithm. *Magn. Reson. Med.* 49, 193–197. doi: 10.1002/mrm.10354
- Jenkinson, M., Bannister, P., Brady, M., and Smith, S. (2002). Improved optimization for the robust and accurate linear registration and motion correction of brain images. *Neuroimage* 17, 825–841. doi: 10.1006/nimg.2002.1132
- Jenkinson, M., Beckmann, C. F., Behrens, T. E. J., Woolrich, M. W., and Smith, S. M. (2012). FSL. *Neuroimage* 62, 782–790. doi: 10.1016/j.neuroimage.2011.09.015
- Johansson, R. S., and Flanagan, J. R. (2009). Coding and use of tactile signals from the fingertips in object manipulation tasks. *Nat. Rev. Neurosci.* 10, 345–359. doi: 10.1038/nrn2621
- Jung, M. W., Landenberger, M., Jung, T., Lindenthal, T., and Philipp, H. (2017). Vojta therapy and neurodevelopmental treatment in children with infantile postural asymmetry: a randomised controlled trial. *J. Phys. Ther. Sci.* 29, 301–306. doi: 10.1589/jpts.29.301
- Kaelin-Lang, A., Luft, A. R., Sawaki, L., Burstein, A. H., Sohn, Y. H., and Cohen, L. G. (2002). Modulation of human corticomotor excitability by somatosensory input. *J. Physiol.* 540, 623–633. doi: 10.1113/jphysiol.2001.012801
- Kawashima, R., O'Sullivan, B. T., and Roland, P. E. (1995). Positron-emission tomography studies of cross-modality inhibition in selective attentional tasks: closing the “mind's eye”. *Proc. Natl. Acad. Sci. U.S.A.* 92, 5969–5972. doi: 10.1073/pnas.92.13.5969
- Kayalioglu, G. (2009). “Chapter 10 - Projections from the Spinal Cord to the Brain,” in *The Spinal Cord*, eds C. Watson, G. Paxinos, and G. Kayalioglu (San Diego, CA: Academic Press), 148–167. doi: 10.1016/B978-0-12-374247-6.50014-6
- Kurth, F., Zilles, K., Fox, P. T., Laird, A. R., and Eickhoff, S. B. (2010). A link between the systems: functional differentiation and integration within the human insula revealed by meta-analysis. *Brain Struct. Funct.* 214, 519–534. doi: 10.1007/s00429-010-0255-z
- la Fougère, C., Zwergal, A., Rominger, A., Förster, S., Fesl, G., Dieterich, M., et al. (2010). Real versus imagined locomotion: a [18F]-FDG PET-fMRI comparison. *Neuroimage* 50, 1589–1598. doi: 10.1016/j.neuroimage.2009.12.060
- Laufens, G., Poltz, W., Jugelt, E., Prinz, E., Reimann, G., and Van Slobbe, T. (1995). Motor improvements in multiple-sclerosis patients by Vojta physiotherapy and the influence of treatment positions. *Phys. Med. Rehab. Kuror* 5, 115–119.
- Laufens, G., Seitz, S., and Staenicke, G. (1991). Vergleichend biologische Grundlagen zur angeborenen Lokomotion insbesondere zum “reflektorischen Kriechen” nach Vojta. *Krankengymnastik* 43, 448–456.
- Leung, Y. Y., Bensmaïa, S. J., Hsiao, S. S., and Johnson, K. O. (2005). Time-course of vibratory adaptation and recovery in cutaneous mechanoreceptive afferents. *J. Neurophysiol.* 94, 3037–3045. doi: 10.1152/jn.00001.2005
- Lewis, L. D., Setsompop, K., Rosen, B. R., and Polimeni, J. R. (2018). Stimulus-dependent hemodynamic response timing across the human subcortical-cortical visual pathway identified through high spatiotemporal resolution 7T fMRI. *Neuroimage* 181, 279–291. doi: 10.1016/j.neuroimage.2018.06.056
- Liu, J., Duffy, B. A., Bernal-Casas, D., Fang, Z., and Lee, J. H. (2017). Comparison of fMRI analysis methods for heterogeneous BOLD responses in block design studies. *Neuroimage* 147, 390–408. doi: 10.1016/j.neuroimage.2016.12.045
- Long, X., Goltz, D., Margulies, D. S., Nierhaus, T., and Villringer, A. (2014). Functional connectivity-based parcellation of the human sensorimotor cortex. *Eur. J. Neurosci.* 39, 1332–1342. doi: 10.1111/ejn.12473
- Marconi, B., Filippi, G. M., Koch, G., Pecchioli, C., Salerno, S., Don, R., et al. (2008). Long-term effects on motor cortical excitability induced by repeated muscle vibration during contraction in healthy subjects. *J. Neurol. Sci.* 275, 51–59. doi: 10.1016/j.jns.2008.07.025
- Marxen, M., Cassidy, R. J., Dawson, T. L., Ross, B., and Graham, S. J. (2012). Transient and sustained components of the sensorimotor BOLD response in fMRI. *Magn. Reson. Imaging* 30, 837–847. doi: 10.1016/j.mri.2012.02.007
- Merabet, L. B., Swisher, J. D., McMains, S. A., Halko, M. A., Amadi, A., Pascual-Leone, A., et al. (2007). Combined activation and deactivation of visual cortex during tactile sensory processing. *J. Neurophysiol.* 97, 1633–1641. doi: 10.1152/jn.00806.2006
- Miura, N., Akitsuki, Y., Sekiguchi, A., and Kawashima, R. (2013). Activity in the primary somatosensory cortex induced by reflexological stimulation is unaffected by pseudo-information: a functional magnetic resonance imaging study. *BMC Compl. Altern. Med.* 13:114. doi: 10.1186/1472-6882-13-114
- Müller, H. (1974). Comment on V.Vojta's: early diagnosis and therapy of cerebral disturbances of motility in infancy (author's transl). *Z Orthop Ihre Grenzgeb* 112, 361–364.
- Mullinger, K. J., Mayhew, S. D., Bagshaw, A. P., Bowtell, R., and Francis, S. T. (2014). Evidence that the negative BOLD response is neuronal in origin: a simultaneous EEG-BOLD-CBF study in humans. *Neuroimage* 94, 263–274. doi: 10.1016/j.neuroimage.2014.02.029
- Nieuwenhuys, R., Voogd, J., and van Huijzen, C. (2008). *The Human Central Nervous System*. New York, NY: Springer.
- Oldfield, R. C. (1971). The assessment and analysis of handedness: the Edinburgh inventory. *Neuropsychologia* 9, 97–113. doi: 10.1016/0028-3932(71)90067-4
- Opavský, J., Šlachetová, M., Kutín, M., Hok, P., Uhlíř, P., Opavská, H., et al. (2018). The effects of sustained manual pressure stimulation according to Vojta Therapy on heart rate variability. *Biomed. Pap. Med. Fac. Univ. Palacký Olomouc Czech Repub* 162, 206–211. doi: 10.5507/bp.2018.028
- Powell, J., Pandyan, A. D., Granat, M., Cameron, M., and Stott, D. J. (1999). Electrical stimulation of wrist extensors in poststroke hemiplegia. *Stroke* 30, 1384–1389. doi: 10.1161/01.str.30.7.1384
- Pruim, R. H. R., Mennes, M., Buitelaar, J. K., and Beckmann, C. F. (2015a). Evaluation of ICA-AROMA and alternative strategies for motion artifact removal in resting state fMRI. *Neuroimage* 112, 278–287. doi: 10.1016/j.neuroimage.2015.02.063
- Pruim, R. H. R., Mennes, M., van Rooij, D., Llera, A., Buitelaar, J. K., and Beckmann, C. F. (2015b). ICA-AROMA: a robust ICA-based strategy for removing motion artifacts from fMRI data. *Neuroimage* 112, 267–277. doi: 10.1016/j.neuroimage.2015.02.064
- Qiu, K., Jing, M., Sun, R., Yang, J., Liu, X., He, Z., et al. (2016). The status of the quality control in acupuncture-neuroimaging studies. *Evid. Based Compl. Alternat. Med.* 2016:3685785. doi: 10.1155/2016/3685785
- Rencher, A. C., and Christensen, W. F. (2012). “Cluster Analysis,” in *Methods of Multivariate Analysis*, eds A. C. Rencher and W. F. Christensen (Hoboken, NJ: Wiley-Blackwell), 501–554. doi: 10.1002/9781118391686.ch15
- Rosenkranz, K., and Rothwell, J. C. (2003). Differential effect of muscle vibration on intracortical inhibitory circuits in humans. *J. Physiol.* 551, 649–660. doi: 10.1113/jphysiol.2003.043752
- Sanz-Esteban, I., Calvo-Lobo, C., Ríos-Lago, M., Álvarez-Linera, J., Muñoz-García, D., and Rodríguez-Sanz, D. (2018). Mapping the human brain during a specific Vojta's tactile input: the ipsilateral putamen's role. *Medicine* 97:e0253. doi: 10.1097/MD.00000000000010253
- Smith, C. A., Levett, K. M., Collins, C. T., Dahlen, H. G., Ee, C. C., and Sugauma, M. (2018). Massage, reflexology and other manual methods for pain management in labour. *Cochrane Database Syst. Rev.* 3:CD009290. doi: 10.1002/14651858.CD009290.pub3
- Smith, S. M. (2002). Fast robust automated brain extraction. *Hum. Brain Mapp.* 17, 143–155. doi: 10.1002/hbm.10062
- Takakusaki, K. (2013). Neurophysiology of gait: from the spinal cord to the frontal lobe. *Mov. Disord.* 28, 1483–1491. doi: 10.1002/mds.25669

- Tal, Z., Geva, R., and Amedi, A. (2017). Positive and negative somatotopic BOLD responses in contralateral versus ipsilateral penfield homunculus. *Cereb. Cortex* 27, 962–980. doi: 10.1093/cercor/bhx024
- Uddin, L. Q. (2015). Salience processing and insular cortical function and dysfunction. *Nat. Rev. Neurosci.* 16, 55–61. doi: 10.1038/nrn3857
- Usichenko, T. I., Wesolowski, T., and Lotze, M. (2015). Verum and sham acupuncture exert distinct cerebral activation in pain processing areas: a crossover fMRI investigation in healthy volunteers. *Brain Imaging Behav.* 9, 236–244. doi: 10.1007/s11682-014-9301-4
- Vazquez, A. L., Fukuda, M., and Kim, S.-G. (2018). Inhibitory neuron activity contributions to hemodynamic responses and metabolic load examined using an inhibitory optogenetic mouse model. *Cereb. Cortex* 28, 4105–4119. doi: 10.1093/cercor/bhy225
- Vojta, V. (1973). Early diagnosis and therapy of cerebral movement disorders in childhood. C. Reflexogenous locomotion - reflex creeping and reflex turning. C1. The kinesiologic content and connection with the tonic neck reflexes. *Z Orthop Ihre Grenzgeb* 111, 268–291.
- Vojta, V., and Peters, A. (2007). *Das Vojta-Prinzip: Muskelspiele in Reflexfortbewegung und motorischer Ontogenese. 3., vollst. überarb. Aufl.* Berlin: Springer.
- Wall, M. E., Rechtsteiner, A., and Rocha, L. M. (2003). "Singular value decomposition and principal component analysis," in *A Practical Approach to Microarray Data Analysis*, eds D. P. Berrar, W. Dubitzky, and M. Granzow (Berlin: Springer), 91–109. doi: 10.1007/0-306-47815-3_5
- Wong, J. J., Shearer, H. M., Mior, S., Jacobs, C., Côté, P., Randhawa, K., et al. (2016). Are manual therapies, passive physical modalities, or acupuncture effective for the management of patients with whiplash-associated disorders or neck pain and associated disorders? An update of the bone and joint decade task force on neck pain and its associated disorders by the OPTiMa collaboration. *Spine J.* 16, 1598–1630. doi: 10.1016/j.spinee.2015.08.024
- Woolrich, M. W., Behrens, T. E. J., Beckmann, C. F., Jenkinson, M., and Smith, S. M. (2004). Multilevel linear modelling for fMRI group analysis using Bayesian inference. *Neuroimage* 21, 1732–1747. doi: 10.1016/j.neuroimage.2003.12.023
- Woolrich, M. W., Ripley, B. D., Brady, M., and Smith, S. M. (2001). Temporal autocorrelation in univariate linear modeling of fMRI data. *Neuroimage* 14, 1370–1386. doi: 10.1006/nimg.2001.0931
- Worsley, K. J. (2001). "Statistical analysis of activation images," in *Functional MRI: an Introduction to Methods*, eds P. Jezzard, P. M. Matthews, and S. M. Smith (New York, NY: Oxford University Press).
- Wu, M.-T., Sheen, J.-M., Chuang, K.-H., Yang, P., Chin, S.-L., Tsai, C.-Y., et al. (2002). Neuronal specificity of acupuncture response: a fMRI study with electroacupuncture. *Neuroimage* 16, 1028–1037. doi: 10.1006/nimg.2002.1145
- Yin, H., Liu, Y., Li, M., and Hu, D. (2011). Hemodynamic observation and spike recording explain the neuronal deactivation origin of negative response in rat. *Brain Res. Bull.* 84, 157–162. doi: 10.1016/j.brainresbull.2010.12.004
- Ziemann, U., Lönnecker, S., Steinhoff, B. J., and Paulus, W. (1996). Effects of antiepileptic drugs on motor cortex excitability in humans: a transcranial magnetic stimulation study. *Ann. Neurol.* 40, 367–378. doi: 10.1002/ana.410400306

Conflict of Interest Statement: The authors declare that the research was conducted in the absence of any commercial or financial relationships that could be construed as a potential conflict of interest.

Copyright © 2019 Hok, Opavský, Labounek, Kutín, Šlachťová, Tűdős, Kaňovský and Hlušík. This is an open-access article distributed under the terms of the Creative Commons Attribution License (CC BY). The use, distribution or reproduction in other forums is permitted, provided the original author(s) and the copyright owner(s) are credited and that the original publication in this journal is cited, in accordance with accepted academic practice. No use, distribution or reproduction is permitted which does not comply with these terms.

2. Annex 2

Neuroscience 348 (2017) 11–22

MODULATION OF THE SENSORIMOTOR SYSTEM BY SUSTAINED MANUAL PRESSURE STIMULATION

PAVEL HOK^{a,b,*}, JAROSLAV OPAVSKÝ^c,
MIROSLAV KUTÍN^{d,e}, ZBYNĚK TŮDŮS^{f,g},
PETR KAŇOVSKÝ^{a,b} AND PETR HLUŠTÍK^{a,b}

^a Department of Neurology, Faculty of Medicine and Dentistry, Palacky University Olomouc, I. P. Pavlova 185/6, Olomouc CZ-77520, Czech Republic

^b Department of Neurology, University Hospital Olomouc, I. P. Pavlova 185/6, Olomouc CZ-77520, Czech Republic

^c Department of Physiotherapy, Faculty of Physical Culture, Palacky University Olomouc, tř. Miru 671/117, Olomouc CZ-77111, Czech Republic

^d KM KINEPRO PLUS s.r.o., Horní lán 1328/6, Olomouc CZ-77900, Czech Republic

^e Department of Physiotherapy, Faculty of Health Sciences, Palacky University Olomouc, Hněvotinská 976/3, Olomouc CZ-77515, Czech Republic

^f Department of Radiology, Faculty of Medicine and Dentistry, Palacky University Olomouc, I. P. Pavlova 185/6, Olomouc CZ-77520, Czech Republic

^g Department of Radiology, University Hospital Olomouc, I. P. Pavlova 185/6, Olomouc CZ-77520, Czech Republic

Abstract—In Vojta physiotherapy, also known as reflex locomotion therapy, prolonged peripheral pressure stimulation induces complex generalized involuntary motor responses and modifies subsequent behavior, but its neurobiological basis remains unknown. We hypothesized that the stimulation would induce sensorimotor activation changes in functional magnetic resonance imaging (fMRI) during sequential finger opposition. Thirty healthy volunteers (mean age 24.2) underwent two randomized fMRI sessions involving manual pressure stimulation applied either at the right lateral heel according to Vojta, or at the right lateral ankle (control site). Participants were scanned before and after the stimulation when performing auditory-paced sequential finger opposition with their right hand. Despite an extensive activation decrease following both stimulation paradigms, the stimulation of the heel specifically led to an increase in task-related

activation in the predominantly contralateral pontomedullary reticular formation and bilateral posterior cerebellar hemisphere and vermis. Our findings suggest that sustained pressure stimulation of the foot is associated with differential short-term changes in hand motor task-related activation depending on the stimulation. This is the first evidence for brainstem modulation after peripheral pressure stimulation, suggesting that the after-effects of reflex locomotion physiotherapy involve a modulation of the pontomedullary reticular formation. © 2017 IBRO. Published by Elsevier Ltd. All rights reserved.

Key words: functional magnetic resonance imaging, physical stimulation, neurophysiotherapy, movement, brainstem, cerebellum.

INTRODUCTION

Peripheral afferent stimulation has been used to induce experimental plasticity of the motor system and has become an important component of techniques to improve or restore human motor function (Powell et al., 1999). Most widely studied types of peripheral stimulation include nerve stimulation by electrical current, which is easy to control and administer (Chipchase et al., 2011). A prominent modulation of task-related activity in the sensorimotor cortex was repeatedly observed after transcutaneous electrical or magnetic stimulation (Golaszewski et al., 2004; Wu et al., 2005; Gallasch et al., 2015). Natural modalities of peripheral stimulation, such as tactile, pressure or proprioceptive, have been investigated less extensively (Rosenkranz and Rothwell, 2003), even though they represent essential elements of clinical rehabilitation techniques and procedures, such as the “reflex locomotion” (Vojta, 1973; Vojta and Peters, 2007).

The reflex locomotion technique, also known as Vojta method, utilizes sustained manual pressure stimulation of specific points on the skin surface to gradually evoke a stereotypic widespread motor response, i.e., an asymmetrical pattern of tonic muscle contractions in both sides of the neck, trunk and limbs (Vojta, 1973). After the stimulation, changes in motor behavior have been observed for at least 30 min (Vojta and Peters, 2007). Despite ongoing clinical use of the reflex locomotion therapy (Lim and Kim, 2013), there is limited knowledge of its neurobiological basis since the available evidence is mostly based on clinical observation studies (Vojta and Peters, 2007). Based on comparisons with other human

*Correspondence to: P. Hok, Department of Neurology, Faculty of Medicine and Dentistry, Palacky University Olomouc, I. P. Pavlova 185/6, Olomouc CZ-77520, Czech Republic. Fax: +420-585-413-841.

E-mail addresses: pavel.hok@upol.cz (P. Hok), jaroslav.opavsky@upol.cz (J. Opavský), mirek.kutin@kinepro.cz (M. Kutin), zbynek.tudos@fnol.cz (Z. Tűdűs), petr.kanovsky@fnol.cz (P. Kaňovský), phlustik@upol.cz (P. Hluštík).

Abbreviations: AS, stimulation of the ankle; BA, Brodmann's area; BOLD, blood oxygenation level-dependent; CPG, central pattern generators; fMRI, functional magnetic resonance imaging; HS, stimulation of the heel; MNI, Montreal Neurological Institute; MRI, magnetic resonance imaging; PMRF, pontomedullary reticular formation; SD, standard deviation; SFO, sequential finger opposition; VAS, visual analog scale.

<http://dx.doi.org/10.1016/j.neuroscience.2017.02.005>
0306-4522/© 2017 IBRO. Published by Elsevier Ltd. All rights reserved.

involuntary motor responses, such as tonic neck reflex (Magnus and de Kleijn, 1912), and responses elicited due to engagement of the central pattern generators (CPG) in vertebrate animals (Grillner and Wallén, 1985), the motor response to stimulation according to Vojta has been suggested to originate from the midbrain or neighboring structures (Vojta, 1973; Laufens et al., 1991). The concept of the CPG in the human sensorimotor system has recently gained support as the brainstem structures have been increasingly associated with human locomotion and postural control (Jahn et al., 2008; la Fougère et al., 2010; Takakusaki, 2013). Although there is no direct evidence that peripheral pressure stimulation according to Vojta (1973) involves the brainstem CPG, pressure stimulation applied at analogous sites in cats, i.e., at foot pads or chest, leads to similar complex tonic reflexes (Hongo et al., 1990) or modulation of posture-dependent muscle activity (D'Ascanio et al., 1986), respectively. In humans, cutaneous pressure input via slowly adapting afferents from the foot soles participates in postural control as well (Kavounoudias et al., 2001).

Considering the available neurophysiological (Gallasch et al., 2015), imaging (Golaszewski et al., 2004; Wu et al., 2005; Gallasch et al., 2015) and clinical (Vojta, 1973; Lim and Kim, 2013) evidence, we propose that extended peripheral pressure stimulation would cause modulation of the motor system that outlasts the stimulation itself. Presumably, one possible modulation site could be expected in the sensorimotor cortex (Gallasch et al., 2015). However, we hypothesize that stimulation according to Vojta primarily modulates the brainstem structures where the generator of the motor response to the stimulation has been suggested (Laufens et al., 1991). Lastly, we hypothesize that motor control will be differentially modulated by stimulating the empirical foot zone according to Vojta when compared to stimulation of a nearby silent control site on the foot.

We have employed functional magnetic resonance imaging (fMRI) with a paced sequential finger opposition (SFO) task repeated before and after sustained pressure stimulation at either an active or control site on the foot to test our hypotheses. The presented findings suggest that sustained pressure stimulation of the foot is associated with differential short-term changes in hand motor task-related activation in the brainstem and cerebellum that depend on the stimulation site. The pontomedullary reticular formation is speculated to play a key role in reflex locomotion physiotherapy.

EXPERIMENTAL PROCEDURES

Participants

Thirty healthy volunteers enrolled in this study (16 females and 14 males, mean age 24.20, standard deviation [SD] 1.92). The subjects were university students who were naïve to Vojta therapy (Vojta and Peters, 2007), had no history of any neurological condition, and had no signs of motor disability upon enrollment. Three participants were left-handed and 27 were right-handed as assessed by the Edinburgh handedness inventory (Oldfield, 1971). The study was carried out in

accordance with World Medical Association Declaration of Helsinki. Written informed consent was obtained from all participants prior to their inclusion in the study and the study was approved by the Ethics Committee of the University Hospital and the Faculty Medicine Palacky University in Olomouc, approval number 9.4.2013.

Task and procedures

Each fMRI session included 2 functional imaging acquisitions during 6-min right hand SFO. The task was performed in 15-s blocks alternating with 15-s rest. Participants were asked to tap sequentially the right index, middle, ring and little finger against the thumb, and to repeat the sequence throughout the block. The performance was paced at 2 Hz by high-pitch (500 Hz) tones delivered using MR-compatible headphones. The rest was marked by low-pitch tones (300 Hz) of the same volume and pace. The motor task was trained briefly outside the scanner room before every session.

The two SFO runs were separated by 20 min of intermittent manual pressure stimulation delivered by an experienced therapist (M.K.) and by subsequent 8-min rest. The pressure stimulation was applied with the therapist's thumb either at the right lateral heel zone (heel stimulation, HS) according to Vojta (1973), or at the control site at the right lateral ankle (ankle stimulation, AS), both sites within the same dermatome (Foerster, 1933) on the skin covering bony structures. In effect, the SFO was tested before (condition H1 or A1) and after the stimulation (condition H2 or A2). The therapist was instructed to use the same pressure routinely used during physiotherapy according to Vojta, while the participants were lying prone in the scanner bore throughout the session. The applied pressure was recorded during the stimulation using a custom-made MR-compatible calibrated pressure monitor (incorporating a FlexiForce pressure sensor, Tekscan, South Boston, MA, USA). The body position and stimulation duration, as well as usage of a single stimulation site, were chosen to elicit only partial motor response (Vojta and Peters, 2007), avoiding gross movements in the scanner bore and head displacement.

After each session, participants completed a visual analog scale for pain (VAS) form with 0 (no pain) and 10 (worst possible pain) marked as the extreme values to assess whether the stimulation evoked painful sensations (Joyce et al., 1975). The pain scores for HS and AS were compared using Wilcoxon's two-sample signed rank test.

Each participant underwent two fMRI sessions, each involving either HS or AS. The order of the sessions was randomized and counter-balanced, and the participants were not informed in advance that the stimulation would be performed in one of two different sites. The sessions were scheduled at least 1 week apart, the median time interval between sessions was 70 days (range 7–294 days).

Data acquisition

Magnetic resonance imaging (MRI) data were acquired using 1.5-Tesla scanners (Siemens Avanto and

Siemens Symphony, Erlangen Germany) with standard 12-channel head coils. The scanning schedule was counter-balanced to account for any possible differences due to the scanner used. The subject's head was immobilized with cushions to assure maximum comfort and minimize head motion. The MRI protocol included functional T_2^* -weighted blood oxygenation level-dependent (BOLD) images during task performance and control state. BOLD images were acquired with gradient-echo echo-planar imaging (EPI; 30 axial slices parallel to the anterior commissure-posterior commissure [AC-PC] line, 5 mm thick, repetition time/echo time = 2500/41 ms, flip angle 80° , field of view = 220 mm, matrix 64×64) to provide $3.4 \times 3.4 \times 5.0$ mm resolution. In total, 144 images were acquired per each 6-min functional run. Gradient-echo phase and magnitude fieldmap images were acquired to allow correction of the echo planar imaging distortions. Anatomical high-resolution three-dimensional magnetization-prepared rapid acquisition with gradient echo (MPRAGE) scan was acquired to provide the anatomical reference. In-plane fluid-attenuated inversion recovery (FLAIR) images were used to screen for unsuspected brain lesions.

Data analysis

The fMRI data were processed using FEAT (FMRI Expert Analysis Tool) Version 6.00, part of FSL (FMRIB's Software Library, www.fmrib.ox.ac.uk/fsl) (Jenkinson et al., 2012). Standard pre-processing was applied, including spatial smoothing using a Gaussian kernel with 8.0-mm full width at half maximum (FWHM) and high-pass temporal filtering with $\sigma = 45.0$ s. Time series statistical analysis included a temporal derivative of the main effect to account for slice timing shift and functional data were registered non-linearly to the Montreal Neurological Institute (MNI) 152 standard space (Grabner et al., 2006). The fMRI data were then visually checked for susceptibility artifacts and two subjects were excluded due to an excessive signal loss in the brainstem. Three subjects were excluded due to a maximum frame-wise head displacement exceeding 3 mm in a single run as estimated during motion correction. The final sample thus consisted of 25 subjects (14 females, 11 males, 22 right-handers).

For an additional analysis, motion-related artifacts were removed from each time series using ICA-AROMA tool and nuisance signal regressors of mean signal from cerebral ventricles and white matter were added to the model (Pruim et al., 2015a, 2015b). The following steps were performed for both original, and de-noised time series.

The group-level general linear model consisted of four conditions: SFO before and after the HS (conditions H1 and H2, respectively), and SFO before and after the AS (A1 and A2, respectively). Additionally, two subset conditions H1* and A1* were defined, including only datasets acquired at the first session. Using these conditions, five group post hoc contrasts were constructed, including (1) a pooled group-wise activation

image (H1 + H2 + A1 + A2), (2) differences between the baseline conditions at the first session (H1* v. A1*), and (3) differences between the task repetitions regardless of stimulation type (H1 + A1 v. H2 + A2). The main research questions were assessed using (4) a two-by-two interaction between the condition and the task repetition (H2 – H1 v. A2 – A1). An additional linear covariate modeled individual differences in self-rated pain intensity (condition H–condition A), yielding statistical maps of (5) pain intensity effect on the interaction. All within-subject contrasts were first computed using a fixed effects analysis, and the resulting parameter estimates (beta values) and variance were then carried over to the third-level analysis. The primary outcome measure was significant *F*-test in contrasts 4 and 5, followed by post hoc voxel-wise and cluster-wise analyses to assess the directionality of the significant *F*-test effects.

The random effects analysis was conducted using FLAME (FMRIB's Local Analysis of Mixed Effects) stage 1 (Woolrich et al., 2004). The whole-brain analysis was constrained to the MNI standard brain mask (Grabner et al., 2006) excluding white matter voxels according to the Harvard–Oxford probabilistic atlas (Desikan et al., 2006) using a conservative probability threshold of 95%. The masked *Z* (Gaussianized *T*) statistic images were thresholded using clusters determined by $Z > 2.3$ and a corrected cluster significance threshold of $p < 0.05$ (Worsley, 2001). The post hoc *t*-tests in contrast 4 were carried out within the significant *F*-test clusters and thresholded voxel-wise at corrected significance level $p < 0.05$. The thresholded maps were objectively labeled based on Harvard–Oxford Cortical and Subcortical Structural Atlases (Desikan et al., 2006), and Probabilistic Cerebellar Atlas (Diedrichsen et al., 2011). Cytoarchitectonic labels were provided by Jülich Histological Atlas (Eickhoff et al., 2007).

A confirmatory third-level analysis was carried out for contrast 4 using non-parametric Conditional Monte Carlo permutation testing implemented in Randomise v2.9 (Winkler et al., 2014). An identical design with the pain intensity covariate was employed. Ten thousand permutations were performed using sign-flipping to estimate the null distribution of the maximum cluster mass under the cluster forming threshold of $t > 3.0$.

A post hoc region of interest (ROI) analysis was performed to investigate the contribution of each condition to the overall interaction in contrasts 4 and 5 and to assess the correlation with the self-reported pain intensity. First, significant voxels in each cluster were identified using a post hoc voxel-wise *t*-test carried out within the *F*-test mask and the resulting mask was transformed back to the individual subject space. Next, average (mean) *Z* scores and percent signal change (% SC) values across the ROI were extracted from each individual single-subject statistical map in the specified mask using the Featquery tool, part of FSL. The obtained values were plotted and compared group-wise using paired Wilcoxon's signed rank test and correlated with the pain intensity covariate using Spearman's correlation coefficient.

RESULTS

Behavioral data

In all subjects, the therapist reported discrete irregular muscle contractions in the stimulated extremity during stimulation, but no gross limb or trunk movements were observed.

For technical reasons, pressure recordings were only obtained in 15 subjects. The mean pressure during the HS was 22.33 N (SD = 11.64 N), and it was 26.45 N (SD = 9.72 N) during the AS. The difference was not significant ($p = 0.32$, two-sample t test). A paired t -test was possible in 11 subjects, yielding an insignificant difference ($p = 0.22$, mean difference HS–AS = -3.94 N, SD = 9.96 N).

During the HS, the median reported pain intensity (VAS) was 1.85 (range 0–6.9), while it was 0.90 (range 0–5.5) during the AS. The HS was thus associated with significantly higher pain intensity than the AS ($p < 0.01$, Wilcoxon's signed rank test). The median difference was 1.25 (range -5.0 –6.4).

Imaging results

Mean fMRI activation during sequential finger opposition (SFO). As illustrated in Fig. 1, the analysis of mean activation pooled across all conditions (H1, H2, A1 and A2) yielded a single significant cluster representing predominantly contralateral (left) frontoparietal and subcortical sensorimotor areas, as well as predominantly contralateral midbrain and pons, and ipsilateral (right) cerebellar hemisphere and vermis.

Difference between baseline conditions. The t -test comparing the condition H1* and condition A1* (i.e., the

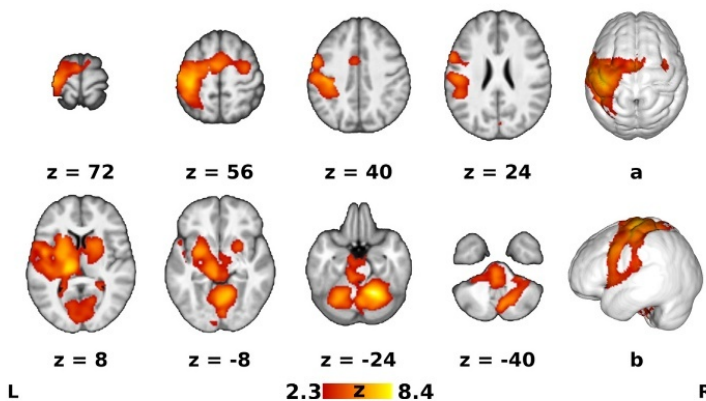


Fig. 1. Mean activation during sequential finger opposition. *Black-and-white figure in print.* The red-yellow Z statistical overlay represents mean activation during the right hand sequential finger opposition pooled across all runs and sessions. The image was superimposed on top of a grayscale mean T1-weighted background image. Clusters of activation were determined by $Z > 2.3$ and thresholded at corrected $p < 0.05$. The axial slices are numbered over the Z axis of the Montreal Neurological Institute (MNI) 152 standard space template. Panels a (top view) and b (left lateral view) show the statistical overlay on top of a three-dimensional reconstructed cortical surface. The right is right, according to neurological convention.

baseline at the first session) did not show any significant difference at the whole-brain level.

Mean activation difference before and after the stimulation. The paired t -test before and after the stimulation averaged across both sessions showed that there was no significant mean activation increase after the stimulation. However, it revealed a decrease in activation in several areas, including the bilateral supplementary motor area (SMA) and lateral premotor cortex (lateral BA 6); superior parietal lobule (mainly BA 7); primary somatosensory cortex (mainly BA 2); intracalcarine (V1, V2) and ventral visual occipital cortex (V4); cerebellar hemispheres (mainly lobule VI) and vermis (blue in Fig. 2). Significant clusters are summarized in Table 1.

Two-by-two interaction between condition and task repetition. The F -test of two-by-two interaction between the condition and repetition (H2–H1 v. A2–A1) yielded a single significant cluster in the left ventral pons and bilateral pontomedullary junction at the base of the 4th ventricle. The cluster extended to the bilateral cerebellar hemispheres and vermis (mainly bilateral lobule IX and less right lobule VIII), bilateral interposed and the right dentate nucleus (red-yellow in Fig. 2), while there was no significant interaction in the cerebral cortex, thalamus or basal ganglia. The significance of the cluster in the brainstem was not affected by adding the pain intensity covariate and the same cluster was also observed in the confirmatory analysis using non-parametric thresholding (Randomise). Although the data de-noising using ICA-AROMA (Pruim et al., 2015a,b) led to decrease in the F -test cluster volume in each analysis, it remained significant in most analyses. These results are summarized in Table 2. To maintain clarity, only the results of original data analysis are further presented and discussed. The

F -test cluster resulting from parametric analysis of interaction with pain intensity covariate is further referred to as the hindbrain cluster. The post hoc voxel-wise t -test within the hindbrain cluster showed that only the contrast H2–H1 > A2–A1 was significant.

The effect of pain intensity yielded one cluster encompassing the right inferior frontal gyrus (BA 45), anterior insular cortex, frontal operculum, and frontal orbital cortex, as shown in green in Fig. 2 and Table 2. This cluster is further referred to as insulo-opercular cluster.

Post-hoc ROI analysis. The ROI analysis of average Z scores derived from the hindbrain cluster (contrast 4) showed that the activation increased significantly after the HS (H2–H1: median Z difference = 0.63, $p < 0.001$, uncorrected), and decreased significantly after the AS (A2–A1: median Z difference = -1.1 ,

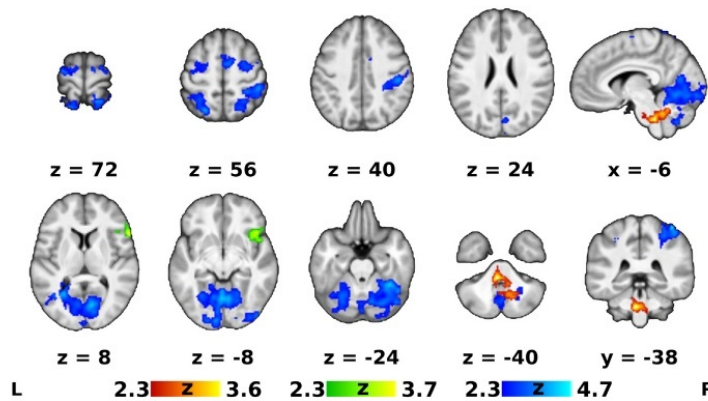


Fig. 2. Mean activation decrease post-stimulation and interaction between condition and repetition. *Black-and-white figure in print.* The blue Z statistical overlay represents a decrease in task-related activation after the stimulation common to both conditions, i.e., contrast 3: (H1 + A1)–(H2 + A2). The red-yellow Z statistical overlay shows significant *F*-test of interaction between the condition and repetition (contrast 4: H1–H2 v. A1–A2) with the pain intensity covariate. The green Z statistical overlay shows the significant *F*-test of the pain covariate effect in the interaction (contrast 5). Remaining conventions see Fig. 1.

$p < 0.001$, uncorrected), see Fig. 3. Likewise, the two effects differed significantly ($p < 0.001$, uncorrected).

In contrast, the insulo-opercular cluster representing the pain intensity effect did not show any significant difference in Z scores between the conditions or task repetitions ($p > 0.05$, uncorrected). The post hoc ROI analysis confirmed that the interaction in Z scores (H2–H1) > (A2–A1) in the insulo-opercular cluster was negatively correlated with the pain intensity difference (H–A), see Fig. 4. The ρ was -0.54 ($p = 0.006$, uncorrected). In other words, the higher the perceived pain during the stimulation, the larger the decrease in the BOLD response in the insulo-opercular cluster after the stimulation (i.e., in H2 or A2) relative to baseline (H1 or A1). However, the activation differences between the task repetitions (i.e., H2–H1 and/or A2–A1) were not significantly correlated with the average pain intensity in H or A condition ($p > 0.05$, uncorrected). Likewise, none of these correlations were significant in the hindbrain cluster ($p > 0.05$, uncorrected).

DISCUSSION

Using the SFO as a robust task activating multiple levels of the sensorimotor system (red-yellow in Fig. 1), we have demonstrated that despite an extensive decrease in activation following both stimulation paradigms (blue in Fig. 2), the sustained pressure stimulation of the heel (HS) differentially modulated the task-related activation in the predominantly contralateral pons and ipsilateral cerebellum (red-yellow in Fig. 2). The following sections discuss putative underlying mechanisms and the implications of these results.

Average activation during SFO

The cortical, subcortical and cerebellar areas activated during SFO correspond well to previous reports of motor

control of complex finger tasks (Solodkin et al., 2001). Despite the fact that the brainstem areas observed in this study (Fig. 1) are reported less frequently during skilled hand movement, midbrain/pons regions have been shown to engage during imagery of motor hand movement (Ueno et al., 2010; Sauvage et al., 2011). Moreover, pontine reticular formation participates in motor control of the forelimbs in animal studies (Sharp and Ryan, 1984).

Activation decrease post-stimulation

All of the areas showing activation decrease post-stimulation (blue in Fig. 2) have been associated with control of complex finger movements (Solodkin et al., 2001) and their activation is known to decrease when repeating the same motor task, both over shorter (Kincses et al., 2008) and longer time scales (Steele and Penhune, 2010). These decreases have therefore been mostly interpreted as early stages of motor learning (Steele and Penhune, 2010) which is also the most likely explanation of the activation decrease upon repeating the same finger motor task in the present study. With the present design lacking another control group with simple task repetition (i.e., no foot stimulation between the first and second finger movement task), we cannot exclude the possibility that at least some of the decreases were related to nonspecific after-effects of peripheral stimulation (of a different body part), even though such effects have not been reported so far.

Site-specific effects of stimulation

An interaction between the stimulation site and the task repetition was found in the brainstem and cerebellum, whereas no such effect was observed in the cerebral cortex. In contrast, previous functional imaging studies have shown that other modalities of peripheral stimulation, such as peripheral magnetic stimulation of the forearm between two repetitions of a finger movement task (Gallasch et al., 2015), resulted in increased activation of the contralateral sensorimotor cortex. We suggest that the absence of such an effect on the cortex in this study may result from the distance between the sensorimotor representations of the stimulated foot and of the fingers involved in the SFO.

The reported effect on hindbrain structures, on the other hand, may reflect less topographical and more diffuse arrangement of afferent or efferent pathways in the hindbrain, which are not necessarily related to the motor control of a single extremity.

Here, the site-specific interaction was found mainly in the bilateral posterior cerebellar hemispheres and vermis, as well as in the left ventral and bilateral dorso-caudal pons, i.e., in areas likely corresponding to the left

Table 1. List of significant clusters in comparison before and after the stimulation (contrast 3)

Contrast	Anatomical atlas labels ^a	Cytoarchitectonic atlas labels ^a	Volume [cm ³]	Cluster p	Z_{max}	Z_{max} MNI coordinates [x, y, z (mm)]
Contrast 3: (H1 + A1) > (H2 + A2) – original data			98.9	<0.001	4.75	-26, -68, -18
	22.9% R cerebellar hemisphere (10.7% right V1)	8.0% L visual cortex V1 (BA17)				
	15.7% L cerebellar hemisphere (7.3% left V1)	7.7% R visual cortex V1 (BA17)				
	14.3% L lingual gyrus	7.4% L visual cortex V4				
	10.3% R lingual gyrus	6.3% L visual cortex V2 (BA18)				
	8.6% L occipital fusiform gyrus	5.6% R visual cortex V2 (BA18)				
	6.4% R occipital fusiform gyrus					
	6.1% L intracalcarine cortex					
	6.0% R intracalcarine cortex					
	6.0% R temporo-occipital fusiform cortex					
	5.0% cerebellar vermis					
	38.6% R superior parietal lobule	33.4% R superior parietal lobule (BA7)	17.6	<0.001	4.59	42, -40, 64
	30.5% R postcentral gyrus	25.9% R primary somatosensory cortex (BA2)				
	16.3% R lateral occipital cortex	15.1% R inferior parietal lobule				
	13.9% R supramarginal gyrus	8.3% R primary somatosensory cortex (BA1)				
		7.7% R superior parietal lobule (BA5)				
	38.6% R precentral gyrus	93.8% R premotor cortex (BA6)	11.3	<0.001	3.58	16, -14, 68
	31.3% R SMA	5.5% L premotor cortex (BA6)				
	17.0% R superior frontal gyrus					
	65.7% L superior parietal lobule	78.5% L superior parietal lobule (BA7)	10.3	<0.001	4.50	-30, -56, 64
	32.7% L lateral occipital cortex	11.2% L primary somatosensory cortex (BA2)				
	49.6% L precentral gyrus	97.4% L premotor cortex (BA6)	6.0	0.017	3.47	-42, 0, 60
	35.7% L superior frontal gyrus					
	9.0% L middle frontal gyrus					
	5.7% L SMA					

Abbreviations: BA – Brodmann area; L – left; N/A – not available; MNI – Montreal Neurological Institute; R – right; SMA – supplementary motor area (also juxtapositional lobule cortex); Z_{max} – maximum Z score.
^a Anatomical and cytoarchitectonic labels are provided including the proportion of labeled voxels. Only labels containing at least 5% of activated voxels are provided. Note that cerebellar labels may overlap with whole-brain labels and that cytoarchitectonic labels do not cover the whole brain.

Table 2. List of significant *F*-test clusters in the interaction between condition and repetition (contrast 4) and the pain-related effect (contrast 5)

Contrast	Anatomical atlas labels ^a	Cytoarchitectonic atlas labels ^a	Volume [cm ³]	Cluster <i>p</i>	Z _{max}	Z _{max} MNI coordinates [x, y, z (mm)]
Contrast 4: (H2–H1 v. A2–A1) without pain covariate (F test) – original data	50.3% brainstem 25.7% R cerebellar hemisphere (15.3% right IX, 7.6% right VIII) 15.4% cerebellar vermis (9.0% vermis IX) 9.2% R dentate nucleus 9.0% L cerebellar hemisphere (7.2% left IX)	N/A	8.17	0.004	3.68	–4, –36, –40
Contrast 4: (H2–H1 v. A2–A1) without pain covariate (F test) – de-noised data	42.0% brainstem 30.6% L cerebellar hemisphere (30.5% left IX) 27.4% cerebellar vermis (16.9% vermis IX, 6.3% vermis X) 26.6% R cerebellar hemisphere (19.4% right IX, 7.1% right VIII)	N/A	4.94	0.034	3.40	–2, –54, –38
Contrast 4: (H2–H1 v. A2–A1) with pain covariate (F test) – original data	51.4% brainstem 25.2% R cerebellar hemisphere (16.0% right IX, 6.7% right VIII) 15.5% cerebellar vermis (8.7% vermis IX) 9.1% R dentate nucleus 8.9% L cerebellar hemisphere (7.1% left IX)	N/A	7.98	0.004	3.64	–6, –38, –40
Contrast 4: (H2–H1 v. A2–A1) with pain covariate (F test) – de-noised data	39.2% brainstem 32.8% R cerebellar hemisphere (18.7% right IX, 13.3% right VIII) 27.7% L cerebellar hemisphere (27.5% left IX) 25.6% cerebellar vermis (16.6% vermis IX, 6.2% vermis X)	N/A	5.06	0.029	3.80	30, –54, –52
Contrast 4: (H2–H1 > A2–A1) with pain covariate (t-test in Randomise) – original data	58.8% brainstem 27.2% R cerebellar hemisphere (17.1% right IX, 7.9% right VIII) 14.2% cerebellar vermis (7.4% vermis X, 5.1% vermis IX) 9.8% R dentate nucleus 8.4% L cerebellar hemisphere (7.9% left IX)	N/A	4.74	0.048	5.27 ^b	–4, –38, –42
Contrast 4: (H2–H1 > A2–A1) with pain covariate (t-test in Randomise) – de-noised data	45.3% brainstem 30.5% L cerebellar hemisphere (30.5% right IX) 30.3% R cerebellar hemisphere (30.3% right IX) 28.3% cerebellar vermis (20.4% vermis IX, 6.9% vermis X)	N/A	3.25	0.081 ^c	4.49 ^b	–8, –50, –36
Contrast 5: Correlation of (H2–H1 v. A2–A1) with pain intensity difference (H > A) – original data	37.5% R inferior frontal gyrus, pars triangularis 20.0% R frontal orbital cortex	56.1% R Broca's area (BA45)	5.55	0.03	3.75	58, 22, 10

(continued on next page)

Table 2 (continued)

Contrast	Anatomical atlas labels ^a	Cytoarchitectonic atlas labels ^a	Volume [cm ³]	Cluster p	Z _{max}	Z _{max} MNI coordinates [x, y, z (mm)]
	17.9% R insular cortex 10.8% R frontal operculum cortex 7.6% R inferior frontal gyrus, pars opercularis 5.8% R temporal pole					

Abbreviations: BA – Brodmann area; L – left; N/A – not available; MNI – Montréal Neurological Institute; R – right; SMA – supplementary motor area (also juxtapositional lobule cortex); Z_{max} – maximum Z score.

^a Anatomical and cytoarchitectonic labels, including the proportion of labeled voxels. Only labels containing at least 5% of activated voxels are provided. Note that cerebellar labels may overlap with whole-brain labels and that cytoarchitectonic labels do not cover the whole brain.

^b Maximum t score listed instead of Z_{max}.

^c Cluster was listed despite non-significant. t -Test to allow comparison among performed analyses.

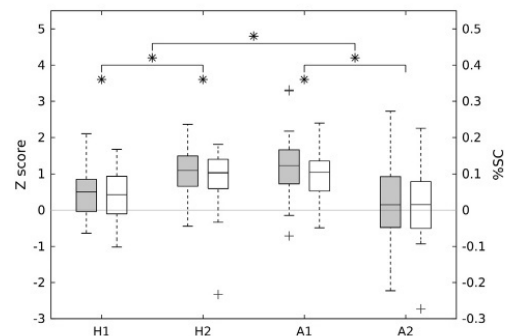


Fig. 3. Post-hoc analysis of significant F -test. *Black-and-white figure in print.* The box plots show average effects of main conditions in individual subjects extracted from the significant voxels in the hindbrain cluster (contrast 4). Gray boxes indicate average Z scores, whereas the white boxes indicate the average percent signal change (%sC) of the same conditions. The conditions are: H1 – before heel stimulation, H2 – after the heels stimulation, A1 – before the ankle stimulation, and A2 – after the ankle stimulation. Each box shows the interquartile range, median (inner horizontal line), extreme (whiskers) and outlier values (crosses). The asterisks above each box and above the horizontal lines indicate conditions and differences where Z scores were significantly different from zero at $p < 0.05$, using Wilcoxon's signed rank test.

pontine nuclei and bilateral lateral pontomedullary reticular formation (PMRF) according to a post-mortem brainstem atlas (Nieuwenhuys et al., 2008).

The post hoc analysis of the interaction indicated that the activation decreased after the AS, likely matching the non-specific extensive BOLD response reduction in other sensorimotor areas due to early motor learning (Steele and Penhune, 2010). In contrast, the opposite effect represented by increased activation after the HS likely reflects specific effects of the peripheral stimulation site as the task execution pace was kept constant across all conditions. Similar activation increase post-stimulation was previously reported in the cerebral cortex (Gallasch et al., 2015). We argue that this effect was not due to the associated pain perceived during the stimulation since

the activation in the hindbrain areas did not correlate with the pain intensity and the effect remained significant after adding pain intensity covariate. In fact, contrast 5 (green in Fig. 2) revealed that the task-related activation was modulated by pain intensity in the contralateral (left) anterior insula and frontal operculum, i.e., in areas overlapping with the pain network (Apkarian et al., 2005) as discussed below.

Brainstem

Within the area of significant site-specific stimulation effect, the local maxima were found in the PMRF, which is known to be involved in sensorimotor control. Stimulation of the reticulospinal pathway originating in the PMRF, especially in its lateral part (Takakusaki and Nozu, 2016), elicits bilateral asymmetrical motor patterns in cats (Dyson et al., 2014) and monkeys (Hirschauer and Buford, 2015). In cats, the PMRF has been also shown to contribute to postural control (Stapley and Drew, 2009) and locomotion (Dyson et al., 2014). In humans, the PMRF is suggested to participate in locomotor control as well, as it is implicated in anticipatory postural control before gait initiation (Takakusaki, 2013). In neuroimaging studies, the imagery of standing (Jahn et al., 2008) and walking (la Fougère et al., 2010) engaged lateral PMRF corresponding to the area reported here. The PMRF is likely to support the locomotion by integrating descending cortical influences (Takakusaki, 2013) and ascending spinoreticular inputs (Kevetter et al., 1982; Sahara et al., 1990). The functions of the PMRF likely extend beyond locomotion control as its neurons project also to the distal forelimb muscles in non-human primates (Riddle et al., 2009) and are modulated during voluntary reaching (Schepens and Drew, 2004) or finger movements (Hirschauer and Buford, 2015). Our results thus provide further evidence for such convergence of sensory afferent and motor efferent pathways by showing that BOLD response during upper limb movements may be modulated by the lower limb stimulation.

In contrast to the PRMF, there is no anatomical evidence for bottom-up inputs to the pontine nuclei (Nagao, 2004), which have been suggested to serve

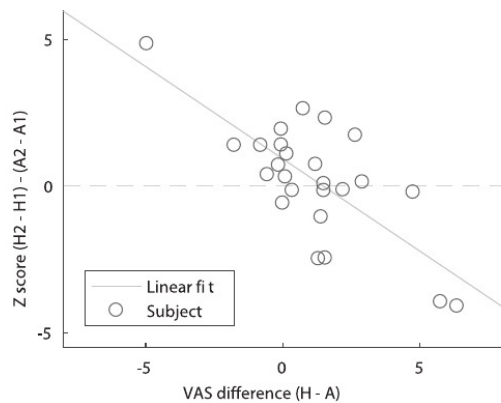


Fig. 4. Correlation with pain intensity. *Black-and-white figure in print.* The scatter plot shows negative correlation between the self-reported pain intensity difference (H–A) and the within-subject interaction (H1–H2 > A1–A2) represented by Z scores extracted from the pain effect cluster in the right frontal operculum and insula (contrast 5). Each circle represents a single subject, while the solid line represents the least-squares linear fit.

merely as a relay station between the cerebral cortex of the same side and contralateral cerebellum (Nagao, 2004).

Cerebellum

The peripheral stimulation modulated activation mainly in the lobule VIII and IX. Both lobuli are known to receive spinal inputs (Brodal and Jansen, 1941), either via bilateral spinocerebellar tracts (Yaginuma and Matsushita, 1989) or via the lateral reticular nucleus, which has been suggested to integrate multimodal inputs from spinal afferents and spinal locomotor centers (Alstermark and Ekerot, 2013). In patients, lesions of the spinocerebellum lead to dyscoordination of upright posture and gait (Ilg et al., 2008). However, lobule IX is also implicated in oculomotor control and postural orientation in space and receives vestibulocerebellar fibers and cortical inputs via the contralateral pontine nuclei (Voogd et al., 2012).

The posterior cerebellum is also involved in sensorimotor circuits related to upper extremities, e.g., during finger tapping task (Stoodley et al., 2012). Meta-analyses of functional imaging studies showed overlapping motor and somatosensory activations in the lobule VIII, suggesting a prominent role in the sensorimotor integration (Riedel et al., 2015).

By combining the previous functional and anatomical evidence with our observations, we suggest that, first, the PMRF and posterior cerebellar areas interact during the motor performance within a common reticulo-cerebellar network, possibly integrating cortical and peripheral inputs. Second, this network may be transiently up-regulated in response to specific peripheral stimulation. In this circuit, the PMRF may serve both as the primary input and output node since it receives direct spinal inputs (Kevetter et al., 1982;

Sahara et al., 1990) and can potentially elicit complex motor responses via the reticulospinal tract (Hirschauer and Buford, 2015).

Correlation with the pain intensity difference

The peripheral stimulation according to Vojta is known to be associated with concomitant pain (Müller, 1974), and indeed, the heel stimulation was perceived more painful than the ankle stimulation in our study. Previous studies employing painful cutaneous pressure stimulation have shown pain-related activations in the primary motor cortex and brainstem that were not present during neutral stimulation (Rolls et al., 2003). The occasionally observed involvement of cortical motor areas during acute pain perception may be possibly associated with the withdrawal response to pain (Apkarian et al., 2005). In contrast, our data reveal a correlation between the complex interaction in task-related activation and the difference in post hoc self-rated pain intensity (VAS). A closer inspection reveals that the motor-related activation in the left anterior insula/frontal operculum decreased after a more painful stimulation (Fig. 4). The contralateral anterior insula has been shown to activate during hand motor performance (Sauvage et al., 2011) and has been mostly considered as a multimodal associative area (Kurth et al., 2010). The preceding painful stimulation may therefore affect the background cognitive processes during the motor task, possibly lowering the subject's attention and engagement in the task.

Implications for the reflex locomotion physiotherapy

Our findings might indicate what structures are involved in the modulatory after-effects of the stimulation according to Vojta (1973), such as facilitation of voluntary movements outlasting the stimulation (Laufens et al., 1995). These immediate effects have been observed to persist for at least 30 min (Vojta and Peters, 2007). It has been speculated that the facilitation does not reflect the primary stimulation but rather a secondary effect resulting from the evoked global motor activation, contraction of numerous muscles associated with massive proprioceptive stimulation, which in turn promotes further facilitation of voluntary movements (Vojta, 1973). In our paradigm, muscle contractions and the associated proprioception were minimal and the observed differential modulation likely reflected other mechanisms.

The efferent pathways mediating the motor response to the stimulation according to Vojta have been speculated to involve the non-pyramidal system (Vojta, 1973). Due to the complex nature of the evoked postural changes, a common coordination supraspinal center has been suggested, most likely midbrain (Vojta, 1973; Laufens et al., 1991). Although the midbrain is believed to contain a midbrain locomotor center (MLR) that plays a key role in human locomotion (Takakusaki and Nozu, 2016), we did not observe any specific changes in that area. Instead, the site-specific modulation of task-related fMRI activity was revealed in the bilateral PMRF, a structure involved both in locomotion (Jahn et al., 2008; la Fougère et al., 2010; Takakusaki, 2013; Dyson

et al., 2014) and postural control (Stapley and Drew, 2009; Takakusaki, 2013). Moreover, the PMRF has already been shown to mediate various asymmetric reflex movement patterns, including the asymmetric tonic neck reflex (Dyson et al., 2014; Hirschauer and Buford, 2015; Takakusaki and Nozu, 2016) that can also be observed in healthy humans and patients with brain lesions (Magnus and de Kleijn, 1912) and shares some similarities with the motor responses observed during stimulation according to Vojta (1973). The provided data are therefore highly suggestive that the PMRF could be directly associated with the effects of the therapeutic stimulation according to Vojta (1973).

Limitations

The spatial resolution of the BOLD data may limit any detailed assignment of activation foci to a single anatomical region in a small structure such as the brainstem. However, brainstem imaging was successfully performed in the past using hardware specifications and spatial resolution similar to ours (Jahn et al., 2008). Additionally, even though higher field 3T scanners might provide better signal-to-noise ratio, data acquisition using a 1.5T scanner may be less prone to magnetic susceptibility artifacts.

Another concern may arise regarding the influence of motion artifacts on the main results. We have demonstrated that the main interaction effect remained significant after advanced de-noising procedures (Pruim et al., 2015b). Whereas removal of residual motion artifact has been strongly recommended for resting-state connectivity analyses (Muschelli et al., 2014), block design analysis may suffer from a decrease in sensitivity to true activations (Johnstone et al., 2006).

Despite a highly sophisticated approach implemented in the ICA-AROMA (Pruim et al., 2015b), we are concerned that the method may introduce another bias that may specifically affect brainstem regions. One of the image features exploited by the ICA-AROMA to detect a noisy signal component is the overlap of the independent component with a brain edge mask. Since the edge mask is defined as a 10-mm outer layer of the brain mask, we would expect that some neuronal signal sources might be erroneously removed from the data.

Finally, studies demonstrating the effect of additional removal of suspected motion-related signals (Muschelli et al., 2014; Pruum et al., 2015a) have shown the benefit for lower level group contrasts. However, for higher level contrasts such as group-by-time interaction used in our analysis, the additional preprocessing pipelines, including ICA-based denoising, have yielded rather heterogeneous results and may introduce a substantial bias (Churchill et al., 2012). For these reasons, we decided to primarily present the original data analysis.

CONCLUSIONS

We have shown that sustained pressure stimulation of the foot was associated with differential short-term changes in hand motor task-related activation that depended on the site of stimulation. These differential responses were

located in the brainstem and cerebellum, namely in the bilateral, but predominantly contralateral pontomedullary reticular formation and bilateral posterior cerebellar hemisphere and vermis. We propose that the pontomedullary reticular formation, previously implicated in the postural control and generation of asymmetric motor patterns, might be specifically modulated by the pressure stimulation according to Vojta.

GLOSSARY

Vojta physiotherapy (reflex locomotion physiotherapy) – a therapeutic procedure used in several world countries that involves involuntary tonic motor responses elicited by manual pressure applied at certain body surface areas and is known to facilitate voluntary movements and improve motor deficits post-stimulation.

Acknowledgments—The authors thank Dr. Ana Solodkin for valuable comments on an earlier version of this manuscript.

Funding: This work was supported by grant of the Czech Science Foundation (GACR) [grant number 14–22572S].

REFERENCES

- Alstermark B, Ekerot C-F (2013) The lateral reticular nucleus: a precerebellar centre providing the cerebellum with overview and integration of motor functions at systems level. A new hypothesis. *J Physiol* 591:5453–5458.
- Apkarian AV, Bushnell MC, Treede R-D, Zubieta J-K (2005) Human brain mechanisms of pain perception and regulation in health and disease. *Eur J Pain* 9:463–484.
- Brodal A, Jansen J (1941) [Beitrag zur Kenntnis der spino-cerebellaren Bahnen beim Menschen]. *Anat Anz* 91:185–195.
- Chipchase LS, Schabrun SM, Hodges PW (2011) Peripheral electrical stimulation to induce cortical plasticity: a systematic review of stimulus parameters. *Clin Neurophysiol* 122:456–463.
- Churchill NW, Yourganov G, Oder A, Tam F, Graham SJ, Strother SC (2012) Optimizing preprocessing and analysis pipelines for single-subject fMRI: 2. Interactions with ICA, PCA, task contrast and inter-subject heterogeneity. *PLoS One* 7:e31147.
- D'Ascanio P, Gahéry Y, Pompeiano O, Stampacchia G (1986) Effects of pressure stimulation of the body surface on posture and vestibulospinal reflexes. *Arch Ital Biol* 124:43–63.
- Desikan RS, Ségonne F, Fischl B, Quinn BT, Dickerson BC, Blacker D, Buckner RL, Dale AM, Maguire RP, Hyman BT, Albert MS, Killiany RJ (2006) An automated labeling system for subdividing the human cerebral cortex on MRI scans into gyral based regions of interest. *Neuroimage* 31:968–980.
- Diedrichsen J, Maderwald S, Küper M, Thürling M, Rabe K, Gizewski ER, Ladd ME, Timmann D (2011) Imaging the deep cerebellar nuclei: a probabilistic atlas and normalization procedure. *Neuroimage* 54:1786–1794.
- Dyson KS, Miron J-P, Drew T (2014) Differential modulation of descending signals from the reticulospinal system during reaching and locomotion. *J Neurophysiol* 112:2505–2528.
- Eickhoff SB, Paus T, Caspers S, Grosbras M-H, Evans AC, Zilles K, Amunts K (2007) Assignment of functional activations to probabilistic cytoarchitectonic areas revisited. *Neuroimage* 36:511–521.
- Foerster O (1933) The dermatomes in man. *Brain* 56:1–39.
- Gallasch E, Christova M, Kunz A, Rafolt D, Golaszewski S (2015) Modulation of sensorimotor cortex by repetitive peripheral magnetic stimulation. *Front Hum Neurosci* 9.
- Golaszewski SM, Siedentopf CM, Koppelstaetter F, Rhomberg P, Guendisch GM, Schlagler A, Gallasch E, Eisner W, Felber SR, Mottaghy FM (2004) Modulatory effects on human sensorimotor

- cortex by whole-hand afferent electrical stimulation. *Neurology* 62:2262–2269.
- Grabner G, Janke AL, Budge MM, Smith D, Pruessner J, Collins DL (2006) Symmetric atlas and model based segmentation: an application to the hippocampus in older adults. *Med Image Comput Assist Interv* 9:58–66.
- Grillner S, Wallén P (1985) Central pattern generators for locomotion, with special reference to vertebrates. *Annu Rev Neurosci* 8:233–261.
- Hirschauer TJ, Buford JA (2015) Bilateral force transients in the upper limbs evoked by single-pulse microstimulation in the pontomedullary reticular formation. *J Neurophysiol* 113:2592–2604.
- Hongo T, Kudo N, Oguni E, Yoshida K (1990) Spatial patterns of reflex evoked by pressure stimulation of the foot pads in cats. *J Physiol* 420:471–487.
- Ilg W, Giese MA, Gizewski ER, Schoch B, Timmann D (2008) The influence of focal cerebellar lesions on the control and adaptation of gait. *Brain* 131:2913–2927.
- Jahn K, Deutschländer A, Stephan T, Kalla R, Wiesmann M, Strupp M, Brandt T (2008) Imaging human supraspinal locomotor centers in brainstem and cerebellum. *Neuroimage* 39:786–792.
- Jenkinson M, Beckmann CF, Behrens TEJ, Woolrich MW, Smith SM (2012) FSL. *Neuroimage* 62:782–790.
- Johnstone T, Ores Walsh KS, Greischar LL, Alexander AL, Fox AS, Davidson RJ, Oakes TR (2006) Motion correction and the use of motion covariates in multiple-subject fMRI analysis. *Hum Brain Mapp* 27:779–788.
- Joyce CR, Zutshi DW, Hrubec V, Mason RM (1975) Comparison of fixed interval and visual analogue scales for rating chronic pain. *Eur J Clin Pharmacol* 8:415–420.
- Kavounoudias A, Roll R, Roll J-P (2001) Foot sole and ankle muscle inputs contribute jointly to human erect posture regulation. *J Physiol* 532:869–878.
- Kevetter GA, Haber LH, Yezierski RP, Chung JM, Martin RF, Willis WD (1982) Cells of origin of the spinothalamic tract in the monkey. *J Comp Neurol* 207:61–74.
- Kincses ZT, Johansen-Berg H, Tomassini V, Bosnell R, Matthews PM, Beckmann CF (2008) Model-free characterization of brain functional networks for motor sequence learning using fMRI. *Neuroimage* 39:1950–1958.
- Kurth F, Zilles K, Fox PT, Laird AR, Eickhoff SB (2010) A link between the systems: functional differentiation and integration within the human insula revealed by meta-analysis. *Brain Struct Funct* 214:519–534.
- la Fougère C, Zwergal A, Rominger A, Förster S, Fesl G, Dieterich M, Brandt T, Strupp M, Bartenstein P, Jahn K (2010) Real versus imagined locomotion: A [¹⁸F]-FDG PET-fMRI comparison. *Neuroimage* 50:1589–1598.
- Laufens G, Seitz S, Staenicke G (1991) Vergleichend biologische Grundlagen zur angeborenen Lokomotion insbesondere zum "reflektorischen Kriechen" nach Vojta. *Z Physiother* 43:448–456.
- Laufens G, Poltz W, Jugelt E, Prinz E, Reimann G, Van Slobbe T (1995) Motor improvements in multiple-sclerosis patients by Vojta physiotherapy and the influence of treatment positions. *Phys Med Rehabil Kurortmed* 5:115–119.
- Lim H, Kim T (2013) Effects of vojta therapy on gait of children with spastic diplegia. *J Phys Ther Sci* 25:1605–1608.
- Magnus R, de Kleijn A (1912) [Die Abhängigkeit des Tonus der Extremitätenmuskeln von der Kopfstellung]. *Pflügers Archiv Eur J Physiol* 145:455–548.
- Müller H (1974) Comment on V. Vojta's: early diagnosis and therapy of cerebral disturbances of motility in infancy (author's transl). *Z Orthop Ihre Grenzgeb* 112:361–364.
- Muschelli J, Nebel MB, Caffo BS, Barber AD, Pekar JJ, Mostofsky SH (2014) Reduction of motion-related artifacts in resting state fMRI using aCompCor. *Neuroimage* 96:22–35.
- Nagao S (2004) Pontine nuclei-mediated cerebello-cerebral interactions and its functional role. *Cerebellum* 3:11–15.
- Nieuwenhuys R, Voogd J, Huijzen C van (2008) *The human central nervous system*. Berlin; New York: Springer.
- Oldfield RC (1971) The assessment and analysis of handedness: the Edinburgh inventory. *Neuropsychologia* 9:97–113.
- Powell J, Pandyan AD, Granat M, Cameron M, Stott DJ (1999) Electrical stimulation of wrist extensors in poststroke hemiplegia. *Stroke* 30:1384–1389.
- Pruim RHR, Mennes M, Buitelaar JK, Beckmann CF (2015a) Evaluation of ICA-AROMA and alternative strategies for motion artifact removal in resting state fMRI. *Neuroimage* 112:278–287.
- Pruim RHR, Mennes M, van Rooij D, Llera A, Buitelaar JK, Beckmann CF (2015b) ICA-AROMA: a robust ICA-based strategy for removing motion artifacts from fMRI data. *Neuroimage* 112:267–277.
- Riddle CN, Edgley SA, Baker SN (2009) Direct and indirect connections with upper limb motoneurons from the primate reticulospinal tract. *J Neurosci* 29:4993–4999.
- Riedel MC, Ray KL, Dick AS, Sutherland MT, Hernandez Z, Fox PM, Eickhoff SB, Fox PT, Laird AR (2015) Meta-analytic connectivity and behavioral parcellation of the human cerebellum. *Neuroimage* 117:327–342.
- Rolls ET, O'Doherty J, Kringelbach ML, Francis S, Bowtell R, McGlone F (2003) Representations of pleasant and painful touch in the human orbitofrontal and cingulate cortices. *Cereb Cortex* 13:308–317.
- Rosenkranz K, Rothwell JC (2003) Differential effect of muscle vibration on intracortical inhibitory circuits in humans. *J Physiol* 551:649–660.
- Sahara Y, Xie YK, Bennett GJ (1990) Intracellular records of the effects of primary afferent input in lumbar spinothalamic tract neurons in the cat. *J Neurophysiol* 64:1791–1800.
- Sauvage C, Poirriez S, Manto M, Jissendi P, Habas C (2011) Reevaluating brain networks activated during mental imagery of finger movements using probabilistic Tensorial Independent Component Analysis (TICA). *Brain Imag Behav* 5:137–148.
- Schepens B, Drew T (2004) Independent and convergent signals from the pontomedullary reticular formation contribute to the control of posture and movement during reaching in the cat. *J Neurophysiol* 92:2217–2238.
- Sharp FR, Ryan AF (1984) Regional (¹⁴C) 2-deoxyglucose uptake during forelimb movements evoked by rat motor cortex stimulation: pons, cerebellum, medulla, spinal cord, muscle. *J Comp Neurol* 224:286–306.
- Solodkin A, Hluštík P, Noll DC, Small SL (2001) Lateralization of motor circuits and handedness during finger movements. *Eur J Neurol* 8:425–434.
- Stapley PJ, Drew T (2009) The pontomedullary reticular formation contributes to the compensatory postural responses observed following removal of the support surface in the standing cat. *J Neurophysiol* 101:1334–1350.
- Steele CJ, Penhune VB (2010) Specific increases within global decreases: a functional magnetic resonance imaging investigation of five days of motor sequence learning. *J Neurosci* 30:8332–8341.
- Stoodley CJ, Valera EM, Schmahmann JD (2012) Functional topography of the cerebellum for motor and cognitive tasks: an fMRI study. *Neuroimage* 59:1560–1570.
- Takakusaki K, Chiba R, Nozu T, Okumura T (2016) Brainstem control of locomotion and muscle tone with special reference to the role of the mesopontine tegmentum and medullary reticulospinal systems. *J Neural Transm* 123:695–729.
- Takakusaki K (2013) Neurophysiology of gait: From the spinal cord to the frontal lobe. *Mov Disord* 28:1483–1491.
- Ueno T, Inoue M, Matsuoka T, Abe T, Maeda H, Morita K (2010) Comparison between a real sequential finger and imagery movements: an fMRI study revisited. *Brain Imag Behav* 4:80–85.
- Vojta V, Peters A (2007) [Das Vojta-Prinzip: Muskelspiele in Reflexfortbewegung und motorischer Ontogenese]. 3. vollst. überarb. Aufl. Berlin: Springer.
- Vojta V (1973) Early diagnosis and therapy of cerebral movement disorders in childhood. C. Reflexogenous locomotion-reflex creeping and reflex turning. C1. The kinesiologic content and

- connection with the tonic neck reflexes. *Z Orthop Ihre Grenzgeb* 111:268–291.
- Voogd J, Schraa-Tam CKL, van der Geest JN, De Zeeuw CI (2012) Visuomotor cerebellum in human and nonhuman primates. *Cerebellum* 11:392–410.
- Winkler AM, Ridgway GR, Webster MA, Smith SM, Nichols TE (2014) Permutation inference for the general linear model. *Neuroimage* 92:381–397.
- Woolrich MW, Behrens TEJ, Beckmann CF, Jenkinson M, Smith SM (2004) Multilevel linear modelling for fMRI group analysis using Bayesian inference. *Neuroimage* 21:1732–1747.
- Worsley KJ (2001) Statistical analysis of activation images. In: Jezzard P, Matthews PM, Smith SM, editors. *Functional MRI: An Introduction to Methods*. Oxford [England]; New York: Oxford University Press.
- Wu CW-H, van Gelderen P, Hanakawa T, Yaseen Z, Cohen LG (2005) Enduring representational plasticity after somatosensory stimulation. *Neuroimage* 27:872–884.
- Yaginuma H, Matsushita M (1989) Spinocerebellar projections from the upper lumbar segments in the cat, as studied by anterograde transport of wheat germ agglutinin-horseradish peroxidase. *J Comp Neurol* 281:298–319.

(Received 5 October 2016, Accepted 5 February 2017)
(Available online 14 February 2017)

Intracortical inhibition decrease after pressure stimulation

Abstract

31 Central effects of sustained pressure stimulation remain poorly understood despite its use in several
32 physiotherapeutic techniques, such as reflex locomotion therapy (RLT). We sought to determine
33 whether stimulation according to RLT affects motor cortex excitability by evaluating short-interval
34 intracortical inhibition (SICI) and intracortical facilitation (ICF) using paired transcranial magnetic
35 stimulation (pTMS). We assessed pTMS in nineteen healthy volunteers (mean age 23.9) before and
36 after 20-minute sustained manual pressure stimulation applied in a cross-over design either at the
37 right lateral heel according to RLT or at the right lateral ankle (control site). SICI and ICF were
38 assessed in both upper extremities using pTMS with 3 ms and 15 ms inter-stimulus intervals,
39 respectively. Differences between sites were evaluated using linear regression analysis with
40 pressure as an independent variable. Compared to control stimulation, SICI in the ipsilateral upper
41 limb was significantly reduced after stimulation according to RLT, whereas there was no significant
42 difference in the contralateral limb or in ICF. We conclude that sustained pressure stimulation
43 according to RLT specifically decreases intracortical inhibition within the same hemisphere,
44 suggesting increased potential for cortical plasticity.

Keywords

45 motor evoked potentials; paired transcranial magnetic stimulation; physical stimulation;
46 neurological rehabilitation; sensorimotor cortex.

Intracortical inhibition decrease after pressure stimulation

New & Noteworthy

47 Sustained mechanical pressure stimulation is being used in physiotherapy, however, it is unknown
48 whether it modulates intracortical inhibition as other modes of afferent stimulation do. Effects of
49 sustained pressure stimulation at two sites on the foot were studied with paired transcranial
50 magnetic stimulation and motor evoked potentials. We report that pressure stimulation of an
51 empirical site reduces intracortical inhibition in the hand motor cortical representation compared to
52 stimulation of a nearby control site.

Intracortical inhibition decrease after pressure stimulation

1. Introduction

53 The restoration of human motor function depends on neuronal plasticity, which can be triggered by
54 peripheral afferent stimulation (41). Inspired by decades of clinical and experimental observations
55 that afferent stimulation can facilitate movement in a variety of conditions (8), researchers have
56 studied different paradigms of extended peripheral electrical stimulation (3) and mechanical
57 stimulation (4) and their effects on corticomotor excitability assessed with paired-pulse transcranial
58 magnetic stimulation and motor evoked potentials (29). In these studies, longer periods of sustained
59 or repetitive stimulation (up to 2 hours) have lead to longer lasting increase of motor cortical
60 excitability, outlasting the stimulation period (on the order of several hours). Brain structures other
61 than cortex have also been suggested to mediate the observed increase of motor output after
62 peripheral nerve stimulation, e.g., the cerebellum (39).

63 Both the length of the experimentally tested sustained stimulation and the duration of effects are
64 quite similar to the clinical applications of sustained tactile pressure stimulation according to Vojta
65 reflex locomotion therapy (20, 58, 59). In this physiotherapeutic technique, sustained manual
66 pressure stimulation applied to specific body surface areas is used to evoke a gradually developing
67 stereotypic pattern of bilateral involuntary tonic muscle contractions in the neck, trunk and limbs
68 (58). Following the stimulation, outlasting facilitation of voluntary movements has been observed
69 (59), but the underlying central mechanisms remained mostly unclear. In recent functional magnetic
70 resonance imaging (fMRI) studies, sustained pressure stimulation has been shown to engage a
71 variety of sensorimotor cortical and subcortical areas (6, 7). We have recently demonstrated that the
72 pressure stimulation modulates the motor task-related brain activation during subsequent complex
73 upper limb movements and that this modulatory effect is also specific for the stimulation according
74 to Vojta, involving increased activation in the pontomedullary reticular formation and cerebellum
75 (15). These imaging results suggest that sustained pressure stimulation according to Vojta could

Intracortical inhibition decrease after pressure stimulation

76 modulate the function of cortical motor circuits, possibly as a consequence of interaction with
77 cortico-subcortical loops. We expected the short-term changes to involve increased cortical
78 excitability of the primary motor cortex (M1) by reduced short-interval intracortical inhibition
79 (SICI) and/or increased intracortical facilitation (ICF) as shown previously following different
80 modalities of peripheral stimulation (4, 12, 13, 44, 49). Decrease in intracortical inhibition
81 facilitates plasticity (62) and has been associated with motor learning (32, 40, 54). SICI is therefore
82 a possible candidate mechanism responsible for motor improvement observed immediately after
83 Vojta reflex locomotion therapy (20, 58, 59). Yet, to our knowledge, motor cortical excitability
84 changes due to stimulation according to Vojta, or sustained tactile pressure stimulation in general,
85 have not been studied so far. In this study, we have addressed this by evaluating motor cortex
86 excitability, including SICI and ICF, in young healthy adults before and after sustained pressure
87 stimulation applied either to an active site according Vojta or to a similar sham site.

2. Materials and Methods

2.1. Participants

88 Nineteen healthy volunteers enrolled in this study (9 females and 10 males, mean age 23.93,
89 standard deviation [SD] 1.85). The study participants were university students naïve to the
90 technique of reflex locomotion therapy (59), with no history of any neurological condition and no
91 signs of motor disability, and no history of use of central nervous system active medication.
92 According to the Edinburgh handedness inventory (38), 1 subject was left-handed (laterality index
93 [LI] -0.2) and 18 subjects were right-handed, out of these 13 were strongly right-handed (LI \geq 0.7).
94 The study was carried out in accordance with World Medical Association Declaration of Helsinki.
95 The study protocol was approved by the Ethics Committee of the University Hospital and the
96 Faculty of Medicine and Dentistry of Palacký University Olomouc under approval number 9.4.2013
97 and all participants gave their written informed consent prior to their inclusion in the study.

Intracortical inhibition decrease after pressure stimulation

99 **2.2. Study protocol**

100 Participants underwent two paired transcranial magnetic stimulation (pTMS) sessions, each
101 involving one measurement before and one after manual pressure stimulation of the foot applied
102 under two different conditions. The sessions were scheduled at least 7 days apart (median interval
103 was 28 days, interquartile range [IQR] 24.5–35 days). The order of sessions was randomized and
104 counter-balanced. Participants were not informed in advance that the stimulation would be
105 delivered under two different conditions.

106 **2.3. Intervention: Pressure stimulation**

107 During the stimulation, participants were lying prone on a comfortable examination table, with their
108 head rotated to the left and arms positioned along the trunk. Participants were asked to keep their
109 eyes open, lie still and report if the stimulation became painful. The room was kept quiet and lit
110 with natural light dimmed with window blinds. Each session was scheduled between 12:30 p.m. and
111 1:30 p.m.

112 The stimulation was delivered manually by an experienced therapist (MK) in a single 20-minute
113 block. The pressure was applied using a thumb placed on one of two predefined sites over bony
114 structures in the same dermatome (Foerster 1933): (1) an active site at the right lateral heel zone
115 according to Vojta (1973) (heel stimulation, HS), and (2) a control site at the right lateral ankle
116 (ankle stimulation, AS). The therapist was instructed to use the same pressure as routinely applied
117 during physiotherapy according to Vojta and to decrease the pressure if the stimulation was reported
118 painful by the participant. During the stimulation, the applied force was continuously recorded
119 using a custom-made calibrated monitor based on a FlexiForce sensor (Tekscan, South Boston,
120 MA, USA). The stimulated limb was kept semi-flexed in the knee joint and supported above the
121 examination table by the therapist who maintained constant tactile contact with the participant's
122 foot, thus further simulating natural conditions of a physiotherapeutic session.

Intracortical inhibition decrease after pressure stimulation

123 Immediately after the stimulation, participants rated overall degree of pain/discomfort perceived
124 during the stimulation using a visual analogue scale for pain/discomfort (VAS), with 0 (no
125 pain/discomfort) and 10 (worst possible pain/discomfort) indicating the minimum and maximum
126 values.

127 2.4. Transcranial magnetic stimulation

128 Motor evoked potentials (MEP) were elicited using transcranial magnetic stimulator with a
129 butterfly-shaped coil with outer diameter 97 mm and wing angle 150° (MagPro X100 including
130 MagOption, MagVenture, Farum, Denmark). During the pTMS, participants were lying supine on a
131 comfortable examination table and fully relaxed. The level of participants' attention was constantly
132 monitored by the examiner and no subject fell asleep during the examination.

133 The pTMS was performed according to a previously published protocol (2, 24). The coil was
134 positioned with the handle oriented backwards and inclined to the sagittal plane at approximately
135 45° (Rosenkranz and Rothwell 2003).

136 Surface electromyographic recordings were obtained from the fully relaxed first dorsal interosseus
137 (FDI) muscles in both hands using (Ag–AgCl) electrodes. The recorded signal was amplified,
138 filtered using a bandpass filter in the range 2 Hz–10 kHz, digitised using the Keypoint software
139 (Medtronic, Minneapolis, MN, USA), and exported using Cross Neuro Database software (Stefan
140 Stålberg Software AB, Helsingborg, Sweden) for subsequent analysis.

141 First, the optimal stimulation site was established manually by moving the coil on the scalp around
142 the expected hand area over the left/right motor cortex until a site consistently producing the largest
143 MEPs in the target muscle at a slightly suprathreshold stimulus intensity was detected. Throughout
144 the session, the coil was fixated in a frame and the position on the scalp was marked with ink.

145 Next, we determined the motor threshold in the resting right/left FDI (2). The motor threshold was

Intracortical inhibition decrease after pressure stimulation

146 defined as the minimum stimulus intensity that evoked an MEP between 300 and 450 μ V peak-to-
147 peak size in at least three out of six consecutive trials. Threshold intensities were expressed as a
148 percentage of maximum stimulator output.

149 2.5. Paired TMS protocol

150 Cortical excitability was evaluated using a paired conditioning-test stimulus paradigm with biphasic
151 pulse shape (29) in the fully relaxed FDI. The subthreshold conditioning stimulus was delivered at
152 80% intensity of the motor threshold, whereas the test stimulus was set to 125%. The pairs of
153 conditioning and test stimuli were applied with six different interstimulus intervals (ISI) pseudo-
154 randomly mixed with single stimuli: 3, 5, 10, 15, and 20 ms. Single or paired pulses were applied
155 every 3 s. In each session, 9 MEPs were recorded for each ISI and 9 MEPs were recorded using the
156 test stimulus alone. In total, 63 MEPs were recorded for each side in each session.

157 The median MEP amplitude values were calculated from the single-trial peak-to-peak MEP
158 amplitudes. The median conditioned MEP at a given ISI was expressed as a percentage of the size
159 of the median single-trial MEP obtained in the same session (Bares et al. 2007).

160 2.6. Statistical analysis

161 The pain/discomfort scores for HS and AS were compared using Wilcoxon signed rank test,
162 whereas mean pressure was compared using paired Student's t-test.

163 Ratios of normalized MEP responses (After / Before) were calculated to evaluate the effect of both
164 interventions (49). Differences between HS and AS were evaluated for SICI (ISI 3 ms) and ICF (ISI
165 15 ms) using linear regression analysis with difference between mean force for HS and AS as an
166 independent variable.

Intracortical inhibition decrease after pressure stimulation

3. Results

167 3.1. Pressure stimulation

168 Due to hardware technical issues, complete continuous force measurements were only obtained in
169 14 subjects. The mean force applied during HS was 14.30 N (SD 3.79 N), and 20.75 N (SD 9.24 N)
170 during AS. The difference was significant ($P = 0.03$, Student's paired t-test).

171 After HS, the median reported pain/discomfort intensity (VAS) was 4.40 (IQR 3.25–5.55), while it
172 was 4.10 (IQR 2.90–5.75) after AS. The difference was not significant ($P = 0.45$, Wilcoxon signed
173 rank test), with median difference 0.10 (IQR HS – AS: -0.70–1.65).

174 3.2. Electrophysiology

175 No participant reported any side-effects of the pTMS. The mean size of the unconditioned MEP did
176 not differ significantly before and after the stimulation in any condition (Student's paired t-test, Fig.
177 1).

178 3.2.1. pTMS results

179 Using linear regression analysis, we found a significant difference in the normalized MEP ratios
180 (After / Before) for SICI (ISI 3 ms) in the right hand (RH, mean MEP ratio for HS was 2.38, SD
181 1.87, whereas for AS it was 1.09, SD 0.73; $P = 0.04$ for the intercept in linear regression, see Fig.
182 2), but not in the left hand (LH, mean MEP ratio for HS was 1.97, SD 2.94, whereas for AS it was
183 1.69, SD 1.50; $P = 0.46$ for the intercept). The individual differences in normalized MEP ratios
184 were independent of the differences in mean pressure ($P = 0.44$, and $P = 0.41$, for interaction in RH
185 and LH, respectively). In RH, SICI tended to decrease after HS (mean normalized MEP changed
186 from 40.8% to 78.1%, $P = 0.09$, post-hoc t-test), but not after the AS (change from 37.5% to 34.8%,
187 $P = 0.64$, post-hoc t-test, Fig. 3).

188 There was neither a significant difference in the ICF (ISI 15 ms) between the two stimulation sites
189 (RH, $P = 0.37$; LH, $P = 0.54$), nor a significant relationship with the pressure (RH, $P = 0.96$; LH, P

Intracortical inhibition decrease after pressure stimulation

190 = 0.45).

191 The mean normalized MEP and standard errors for all ISI are shown in Fig. 3.

4. Discussion

192 The present results demonstrate that sustained manual pressure stimulation elicits changes within
193 the cortical circuits of the sensorimotor system and that the effects are associated with a specific site
194 of action.

195 Similar decrease in intracortical inhibition was observed after sustained stimulation in different
196 modalities, such as vibrotactile (4, 5), or electrical (for review, see 3, 12, 13). Although our
197 observed effect was specific for one of two stimulation sites at the foot, it manifested in a
198 somatotopically unrelated site in a hand representation, suggesting a more diffuse mechanism of
199 action. However, the change in SICI was only observed in the ipsilateral limb in our experiment,
200 implying that the observed plastic changes are possibly mediated via a lateralised pathway. Both
201 assumptions are in line with our previous observation of a site-specific activation increase in the
202 contralateral motor cortex during the stimulation (16) and subsequent motor after-effects in the
203 contralateral pontomedullary reticular formation (15). Based on this combined imaging and
204 neurophysiological evidence, it can be assumed that sustained pressure stimulation may modulate
205 sensorimotor structures at multiple brain levels when applied to a specific body site. From the
206 clinical perspective, the underlying mechanisms are likely related to the behavioural after-effects of
207 the reflex locomotion therapy (58), providing ground for future clinical research.

4.1. Mechanisms of cortical excitability modulation

208 To our knowledge, the effects of sustained pressure stimulation on SICI or ICF have not been
209 studied so far. Models of modulation of intracortical inhibition through sustained or long-term
210 stimulation have been based on evidence obtained using different modalities of peripheral
211 stimulation have been based on evidence obtained using different modalities of peripheral

Intracortical inhibition decrease after pressure stimulation

212 stimulation, such as cutaneous electrical stimulation (9, 12, 13, 27, 35, 36, 44, 46, 51, 52), muscle
213 vibratory (30, 34, 47–50), or vibrotactile stimulation (4), which suggests that the complex system of
214 excitatory and inhibitory intracortical circuits can be dynamically modulated in response to multiple
215 exogenous and intrinsic factors (47–50, 52).

216 An important consideration is that our paradigm involved a prolonged stimulation over 20 minutes,
217 which might lead to potentially different effects from those observed when brief stimuli are
218 delivered immediately before or during TMS (44, 47). Indeed, the effects of prolonged electrical
219 nerve stimulation reported so far have been inconsistent (3). Whereas some studies report changes
220 in cortical excitability assessed by single-pulse TMS (21, 43), overall, there were limited (36, 46) or
221 no consistent changes in intracortical inhibition following paired associative stimulation (45, 55) or
222 electrical nerve stimulation alone (10, 21, 42). Similarly, effects of prolonged muscle vibration also
223 vary among different protocols. Whereas SICI did not change after 15-min single hand muscle
224 vibration alone (48, 50), a protocol of 30-min repetitive muscle vibration during voluntary
225 contraction applied for 3 consecutive days resulted in increased SICI in the vibrated and decreased
226 SICI in the non-vibrated muscle lasting for 2 weeks (34). More consistent effects were also
227 observed when the stimulation was applied to the whole hand instead of a single muscle or nerve:
228 30 minutes of cutaneous electrical stimulation (12, 13) and 20 minutes of vibrotactile stimulation
229 (4) caused reduction of SICI lasting up to one hour after the stimulation. In general, sustained
230 pressure stimulation in our study modulated the motor cortex excitability in a way similar to
231 previously published protocols that involved either long-term or less focal form of electrical,
232 vibratory or vibrotactile stimulation (4, 12, 13, 34). In the following section, we briefly discuss the
233 most prominent differences between pressure stimulation and other stimulation modalities, as well
234 as the structures and circuits that likely participate in modulation of cortical excitability.

235 In vibratory stimulation, changes in motor cortical excitability have been suggested to be mediated

Intracortical inhibition decrease after pressure stimulation

236 via somatotopically organised cortico-cortical connections from the somatosensory cortex (21–23,
237 56). However, in the present work, we show that sustained pressure foot stimulation affected the
238 primary motor representation of the ipsilateral hand. Although less somatotopically organised
239 effects have already been observed after or during electric stimulation (44, 47), to our knowledge,
240 there has been no evidence of peripheral foot stimulation affecting SICI in the hand muscles (4).
241 Such a diffuse effect could be due to less somatotopically arranged afferent input, possibly
242 involving more diffuse direct thalamo-cortical pathways to the motor cortex (1, 17), collateral
243 branches of the spinothalamic tract to multiple brainstem areas (e.g., medullary reticular formation
244 or parabrachial nuclei), (18, 25, 26), or spinoreticular and spinocerebellar tracts. Evidence from
245 rodents suggest that the cerebellum may also play a key role in this process (39). Indeed, repetitive
246 TMS using theta burst stimulation of the cerebellum may influence the SICI in the primary motor
247 cortex in human subjects (28).

248 Irrespective of the afferent pathway, SICI reflect changes that finally involve the intracortical
249 circuits (47, 63). There is compelling evidence that SICI relies on activation of γ -aminobutyric acid
250 A (GABA_A) receptors in the motor cortex (14, 19, 47, 60, 61, 63).

251 4.2. Intracortical facilitation (ICF)

252 In our study, we have observed no significant change in ICF. The circuits responsible for
253 intracortical facilitation remain incompletely described and putatively involve *N*-methyl-D-aspartate
254 (NMDA) excitatory interneurons (13, 33, 37). While ICF increased after 30-min whole-hand
255 electrical (12, 13), or 20-min vibrotactile stimulation (4), and after 1 h of associative stimulation of
256 two hand muscles (42), multiple studies of sustained peripheral stimulation showed no change in
257 ICF (10, 21, 34, 36, 46), suggesting that ICF is affected by peripheral stimulation in a more variable
258 and less reproducible way than SICI.

Intracortical inhibition decrease after pressure stimulation

259 ***4.3. Implications for the reflex locomotion therapy***

260 The effect of pressure stimulation on GABA_A-ergic intracortical circuits demonstrated in this study
261 can be associated with the observed motor after-effects of the reflex locomotion therapy that utilises
262 manual stimulation of several body surface areas including the heel (59). The decrease in SICI
263 suggests that pressure stimulation according to Vojta may facilitate practice-dependent plasticity
264 (62) to improve motor performance as observed in clinical practice (31). The therapy effect may be
265 mediated by the brainstem (e.g., ponto-medullary reticular formation, PMRF) and cerebellum (15),
266 but the putative mechanisms may also involve more direct modulation of motor cortex function due
267 to peripheral pressure stimulation (16). However, longer-term motor behavioural studies in normal
268 subjects and clinical studies in patients suffering from disorders of the motor system that would
269 undergo the therapeutic stimulation under controlled conditions would be necessary to find the link
270 between the behavioural and functional changes induced by reflex locomotion therapy.

271 ***4.4. Limitations***

272 It can be argued that changes in SICI are due to changes in testing pulse efficacy (55). However, we
273 show that amplitudes of unconditioned stimuli did not differ significantly before and after the
274 intervention, effectively ruling out this possibility.

275 The changes in cortical excitability might have been affected by the non-equal pressure applied
276 during HS and AS. However, the difference in SICI between the HS and AS remained significant
277 even though the influence of the applied pressure has been controlled by linear regression analysis
278 with difference between mean pressure for HS and AS as an independent variable.

279 Furthermore, we cannot rule out possible effects of directed attention, which is known to modulate
280 cortical plasticity during peripheral stimulation (50, 57).

281 Only relatively young subjects were examined in this study. Since the capacity to modulate the SICI
282 seems to be age-dependent (53), the results cannot be generalised to ageing subjects.

Intracortical inhibition decrease after pressure stimulation

283 We have not assessed the history of specific repetitive motor activity or training, however, our
284 cross-over design with paired statistical analysis was controlled for individual differences among
285 the subjects.

286 Finally, in this study, we have held the stimulation coil at the optimal site in a mechanical frame
287 using a previously published protocol (2, 24), without a neuronavigation system (see also 49).

288 4.5. Conclusions

289 We conclude that sustained pressure stimulation according to reflex locomotion therapy specifically
290 decreases the intracortical inhibition in the ipsilateral sensorimotor cortex. We suggest that the
291 effect may be related to the clinically observed motor after-effects of reflex locomotion therapy.

Conflict of Interest Statement

292 None of the authors have potential conflicts of interest to be disclosed.

Acknowledgment

293 We acknowledge the assistance of Dr. Martina Šlachtová in recruitment and preliminary data
294 acquisition and Dr. Michaela Kaiserová in data acquisition. We also thank Stefan Stålberg (Stefan
295 Stålberg Software AB, Helsingborg, Sweden) for providing support and custom software
296 modifications.

Grants

297 This work was supported by grant of the Czech Science Foundation (GACR) [grant number
298 14-22572S] and by Ministry of Health, Czech Republic – conceptual development of research
299 organization (University Hospital Olomouc - FNOL, 00098892).

Disclosures

300 None of the authors have potential conflicts of interest to be disclosed.

Intracortical inhibition decrease after pressure stimulation

301 **References**

1. **Asanuma H, Larsen K, Yumiya H.** Peripheral input pathways to the monkey motor cortex. *Exp Brain Res* 38: 349–355, 1980.
2. **Bares M, Kanovský P, Rektor I.** Disturbed intracortical excitability in early Parkinson's disease is L-DOPA dose related: a prospective 12-month paired TMS study. *Parkinsonism Relat Disord* 13: 489–494, 2007.
3. **Chipchase LS, Schabrun SM, Hodges PW.** Peripheral electrical stimulation to induce cortical plasticity: a systematic review of stimulus parameters. *Clin Neurophysiol* 122: 456–463, 2011.
4. **Christova M, Rafolt D, Golaszewski S, Gallasch E.** Outlasting corticomotor excitability changes induced by 25 Hz whole-hand mechanical stimulation. *Eur J Appl Physiol* 111: 3051–3059, 2011.
5. **Christova M, Rafolt D, Mayr W, Wilfling B, Gallasch E.** Vibration stimulation during non-fatiguing tonic contraction induces outlasting neuroplastic effects. *J Electromyogr Kinesiol* 20: 627–635, 2010.
6. **Chung YG, Han SW, Kim H-S, Chung S-C, Park J-Y, Wallraven C, Kim S-P.** Intra- and inter-hemispheric effective connectivity in the human somatosensory cortex during pressure stimulation. *BMC Neurosci* 15: 43, 2014.
7. **Chung YG, Han SW, Kim H-S, Chung S-C, Park J-Y, Wallraven C, Kim S-P.** Adaptation of cortical activity to sustained pressure stimulation on the fingertip. *BMC Neurosci* 16: 71, 2015.
8. **Conforto AB, Kaelin-Lang A, Cohen LG.** Increase in hand muscle strength of stroke patients after somatosensory stimulation. *Ann Neurol* 51: 122–125, 2002.
9. **Devanne H, Degardin A, Tyvaert L, Bocquillon P, Houdayer E, Manceaux A, Derambure P, Cassim F.** Afferent-induced facilitation of primary motor cortex excitability in the region controlling hand muscles in humans. *Eur J Neurosci* 30: 439–448, 2009.
10. **Fernandez-Del-Olmo M, Alvarez-Sauco M, Koch G, Franca M, Marquez G, Sanchez JA, Acero RM, Rothwell JC.** How repeatable are the physiological effects of TENS? *Clin Neurophysiol* 119: 1834–1839, 2008.
11. **Foerster O.** The Dermatomes in Man. *Brain* 56: 1–39, 1933.
12. **Golaszewski SM, Bergmann J, Christova M, Kunz AB, Kronbichler M, Rafolt D, Gallasch E, Staffen W, Trinka E, Nardone R.** Modulation of motor cortex excitability by different levels of whole-hand afferent electrical stimulation. *Clin Neurophysiol* 123: 193–199, 2012.
13. **Golaszewski SM, Bergmann J, Christova M, Nardone R, Kronbichler M, Rafolt D, Gallasch E, Staffen W, Ladurner G, Beisteiner R.** Increased motor cortical excitability after whole-hand electrical stimulation: a TMS study. *Clin Neurophysiol* 121: 248–254, 2010.

Intracortical inhibition decrease after pressure stimulation

14. **Hanajima R, Ugawa Y, Terao Y, Sakai K, Furubayashi T, Machii K, Kanazawa I.** Paired-pulse magnetic stimulation of the human motor cortex: differences among I waves. *J Physiol (Lond)* 509 (Pt 2): 607–618, 1998.
15. **Hok P, Opavský J, Kutín M, Tüdös Z, Kaňovský P, Hlušík P.** Modulation of the sensorimotor system by sustained manual pressure stimulation. *Neuroscience* 348: 11–22, 2017.
16. **Hok P, Opavský J, Labounek R, Kutín M, Šlachťová M, Tüdös Z, Kaňovský P, Hlušík P.** Differential effects of sustained manual pressure stimulation according to site of action. .
17. **Huffman KJ, Krubitzer L.** Thalamo-cortical connections of areas 3a and M1 in marmoset monkeys. *J Comp Neurol* 435: 291–310, 2001.
18. **Hylden JL, Anton F, Nahin RL.** Spinal lamina I projection neurons in the rat: collateral innervation of parabrachial area and thalamus. *Neuroscience* 28: 27–37, 1989.
19. **Ilić TV, Meintzschel F, Cleff U, Ruge D, Kessler KR, Ziemann U.** Short-interval paired-pulse inhibition and facilitation of human motor cortex: the dimension of stimulus intensity. *J Physiol (Lond)* 545: 153–167, 2002.
20. **Jung MW, Landenberger M, Jung T, Lindenthal T, Philippi H.** Vojta therapy and neurodevelopmental treatment in children with infantile postural asymmetry: a randomised controlled trial. *J Phys Ther Sci* 29: 301–306, 2017.
21. **Kaelin-Lang A, Luft AR, Sawaki L, Burstein AH, Sohn YH, Cohen LG.** Modulation of human corticomotor excitability by somatosensory input. *J Physiol (Lond)* 540: 623–633, 2002.
22. **Kaneko T, Caria MA, Asanuma H.** Information processing within the motor cortex. I. Responses of morphologically identified motor cortical cells to stimulation of the somatosensory cortex. *J Comp Neurol* 345: 161–171, 1994.
23. **Kaneko T, Caria MA, Asanuma H.** Information processing within the motor cortex. II. Intracortical connections between neurons receiving somatosensory cortical input and motor output neurons of the cortex. *J Comp Neurol* 345: 172–184, 1994.
24. **Kaňovský P, Bares M, Streitová H, Klajblová H, Daniel P, Rektor I.** Abnormalities of cortical excitability and cortical inhibition in cervical dystonia Evidence from somatosensory evoked potentials and paired transcranial magnetic stimulation recordings. *J Neurol* 250: 42–50, 2003.
25. **Kayalioglu G.** Chapter 10 - Projections from the Spinal Cord to the Brain. In: *The Spinal Cord*, edited by Watson C, Paxinos G, Kayalioglu G. Academic Press, p. 148–167.
26. **Kevetter GA, Willis WD.** Collaterals of spinothalamic cells in the rat. *J Comp Neurol* 215: 453–464, 1983.
27. **Kobayashi M, Ng J, Théoret H, Pascual-Leone A.** Modulation of intracortical neuronal circuits in human hand motor area by digit stimulation. *Exp Brain Res* 149: 1–8, 2003.

Intracortical inhibition decrease after pressure stimulation

28. **Koch G, Mori F, Marconi B, Codecà C, Pecchioli C, Salerno S, Torriero S, Lo Gerfo E, Mir P, Oliveri M, Caltagirone C.** Changes in intracortical circuits of the human motor cortex following theta burst stimulation of the lateral cerebellum. *Clin Neurophysiol* 119: 2559–2569, 2008.
29. **Kujirai T, Caramia MD, Rothwell JC, Day BL, Thompson PD, Ferbert A, Wroe S, Asselman P, Marsden CD.** Corticocortical inhibition in human motor cortex. *J Physiol* 471: 501–519, 1993.
30. **Lapole T, Temesi J, Arnal PJ, Gimenez P, Petitjean M, Millet GY.** Modulation of soleus corticospinal excitability during Achilles tendon vibration. *Exp Brain Res* 233: 2655–2662, 2015.
31. **Laufens G, Poltz W, Reimann C, Schmiegel F, Stempki S.** Treadmill training and Vojta physiotherapy applied to selected MS- patients - A comparison of the immediate effects. *Physikalische Medizin Rehabilitationsmedizin Kurortmedizin* 8: 174–177, 1998.
32. **Liepert J, Classen J, Cohen LG, Hallett M.** Task-dependent changes of intracortical inhibition. *Exp Brain Res* 118: 421–426, 1998.
33. **Liepert J, Schwenkreis P, Tegenthoff M, Malin JP.** The glutamate antagonist riluzole suppresses intracortical facilitation. *J Neural Transm (Vienna)* 104: 1207–1214, 1997.
34. **Marconi B, Filippi GM, Koch G, Pecchioli C, Salerno S, Don R, Camerota F, Saraceni VM, Caltagirone C.** Long-term effects on motor cortical excitability induced by repeated muscle vibration during contraction in healthy subjects. *J Neurol Sci* 275: 51–59, 2008.
35. **McDonnell MN, Thompson PD, Ridding MC.** The effect of cutaneous input on intracortical inhibition in focal task-specific dystonia. *Mov Disord* 22: 1286–1292, 2007.
36. **Murakami T, Sakuma K, Nomura T, Nakashima K.** Short-interval intracortical inhibition is modulated by high-frequency peripheral mixed nerve stimulation. *Neurosci Lett* 420: 72–75, 2007.
37. **Nakamura H, Kitagawa H, Kawaguchi Y, Tsuji H.** Intracortical facilitation and inhibition after transcranial magnetic stimulation in conscious humans. *J Physiol (Lond)* 498 (Pt 3): 817–823, 1997.
38. **Oldfield RC.** The assessment and analysis of handedness: the Edinburgh inventory. *Neuropsychologia* 9: 97–113, 1971.
39. **Oulad Ben Taib N, Manto M, Laute M-A, Brotchi J.** The cerebellum modulates rodent cortical motor output after repetitive somatosensory stimulation. *Neurosurgery* 56: 811–820; discussion 811–820, 2005.
40. **Perez MA, Lugholt BKS, Nyborg K, Nielsen JB.** Motor skill training induces changes in the excitability of the leg cortical area in healthy humans. *Exp Brain Res* 159: 197–205, 2004.
41. **Powell J, Pandyan AD, Granat M, Cameron M, Stott DJ.** Electrical stimulation of wrist extensors in poststroke hemiplegia. *Stroke* 30: 1384–1389, 1999.

Intracortical inhibition decrease after pressure stimulation

42. **Pyndt HS, Ridding MC.** Modification of the human motor cortex by associative stimulation. *Exp Brain Res* 159: 123–128, 2004.
43. **Ridding MC, McKay DR, Thompson PD, Miles TS.** Changes in corticomotor representations induced by prolonged peripheral nerve stimulation in humans. *Clinical Neurophysiology* 112: 1461–9., 2001.
44. **Ridding MC, Rothwell JC.** Afferent input and cortical organisation: a study with magnetic stimulation. *Exp Brain Res* 126: 536–544, 1999.
45. **Ridding MC, Taylor JL.** Mechanisms of motor-evoked potential facilitation following prolonged dual peripheral and central stimulation in humans. *J Physiol (Lond)* 537: 623–631, 2001.
46. **Rocchi L, Erro R, Antelmi E, Berardelli A, Tinazzi M, Liguori R, Bhatia K, Rothwell J.** High frequency somatosensory stimulation increases sensori-motor inhibition and leads to perceptual improvement in healthy subjects. *Clin Neurophysiol* 128: 1015–1025, 2017.
47. **Rosenkranz K, Rothwell JC.** Differential effect of muscle vibration on intracortical inhibitory circuits in humans. *J Physiol* 551: 649–660, 2003.
48. **Rosenkranz K, Rothwell JC.** The effect of sensory input and attention on the sensorimotor organization of the hand area of the human motor cortex. *J Physiol (Lond)* 561: 307–320, 2004.
49. **Rosenkranz K, Rothwell JC.** Differences between the effects of three plasticity inducing protocols on the organization of the human motor cortex. *Eur J Neurosci* 23: 822–829, 2006.
50. **Rosenkranz K, Rothwell JC.** Spatial attention affects sensorimotor reorganisation in human motor cortex. *Exp Brain Res* 170: 97–108, 2006.
51. **Roy FD, Gorassini MA.** Peripheral sensory activation of cortical circuits in the leg motor cortex of man. *J Physiol (Lond)* 586: 4091–4105, 2008.
52. **Sailer A, Molnar GF, Cunic DI, Chen R.** Effects of peripheral sensory input on cortical inhibition in humans. *J Physiol* 544: 617–629, 2002.
53. **Smith AE, Ridding MC, Higgins RD, Wittert GA, Pitcher JB.** Cutaneous afferent input does not modulate motor intracortical inhibition in ageing men. *Eur J Neurosci* 34: 1461–1469, 2011.
54. **Smyth C, Summers JJ, Garry MI.** Differences in motor learning success are associated with differences in M1 excitability. *Hum Mov Sci* 29: 618–630, 2010.
55. **Stefan K, Kunesch E, Benecke R, Cohen LG, Classen J.** Mechanisms of enhancement of human motor cortex excitability induced by interventional paired associative stimulation. *J Physiol* 543: 699–708, 2002.
56. **Terao Y, Ugawa Y, Hanajima R, Furubayashi T, Machii K, Enomoto H, Shiio Y, Mochizuki H, Uesugi H, Uesaka Y, Kanazawa I.** Air-puff-induced facilitation of motor

Intracortical inhibition decrease after pressure stimulation

cortical excitability studied in patients with discrete brain lesions. *Brain* 122 (Pt 12): 2259–2277, 1999.

57. **Thomson RHS, Garry MI, Summers JJ.** Attentional influences on short-interval intracortical inhibition. *Clin Neurophysiol* 119: 52–62, 2008.
58. **Vojta V.** [Early diagnosis and therapy of cerebral movement disorders in childhood. C. Reflexogenous locomotion - reflex creeping and reflex turning. C1. The kinesiological content and connection with the tonic neck reflexes]. *Z Orthop Ihre Grenzgeb* 111: 268–291, 1973.
59. **Vojta V, Peters A.** *Das Vojta-Prinzip: Muskelspiele in Reflexfortbewegung und motorischer Ontogenese.* 3., vollst. überarb. Aufl. Berlin: Springer, 2007.
60. **Werhahn KJ, Kunesch E, Noachtar S, Benecke R, Classen J.** Differential effects on motorcortical inhibition induced by blockade of GABA uptake in humans. *J Physiol (Lond)* 517 (Pt 2): 591–597, 1999.
61. **Ziemann U, Lönnecker S, Steinhoff BJ, Paulus W.** Effects of antiepileptic drugs on motor cortex excitability in humans: a transcranial magnetic stimulation study. *Ann Neurol* 40: 367–378, 1996.
62. **Ziemann U, Muellbacher W, Hallett M, Cohen LG.** Modulation of practice-dependent plasticity in human motor cortex. *Brain* 124: 1171–1181, 2001.
63. **Ziemann U, Rothwell JC, Ridding MC.** Interaction between intracortical inhibition and facilitation in human motor cortex. *J Physiol (Lond)* 496 (Pt 3): 873–881, 1996.

Intracortical inhibition decrease after pressure stimulation

302 **Figure Captions**

303 **Fig. 1 Unconditioned MEP sizes** (*Black-and-white figure in print*)

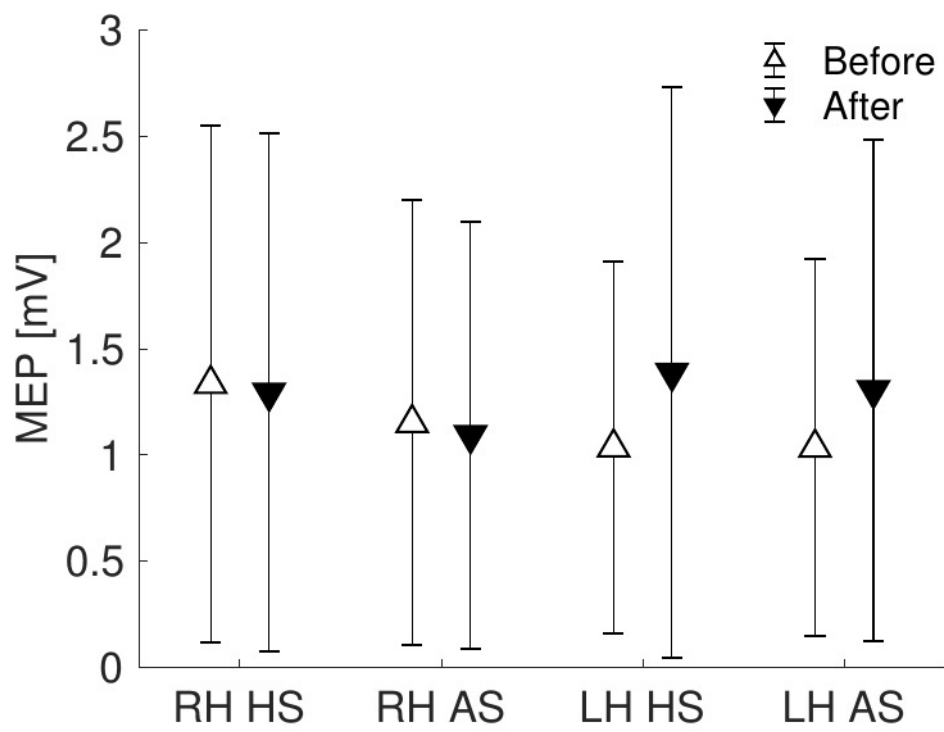
304 Dot-and-whisker plots show (single-pulse) average unconditioned MEP sizes in mV for the right
305 and the left hand (RH and LH, respectively), either for the heel or ankle stimulation (HS and AS,
306 respectively) session. Values before the stimulation are shown with white downward pointing
307 triangles, whereas values after the stimulation are shown with black upward pointing triangles.
308 Whiskers indicate standard deviation (SD). There were no significant differences between any of
309 the baseline and post-stimulation means ($N = 19$, $P_{RH-HS} = 0.83$, $P_{RH-AS} = 0.66$, $P_{LH-AS} = 0.11$, P_{LH-AS}
310 $= 0.23$, paired Student's t-test).

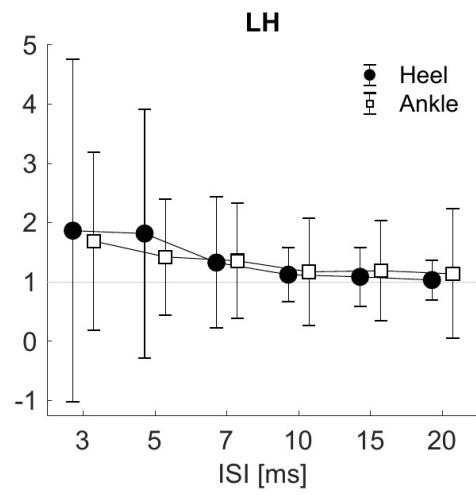
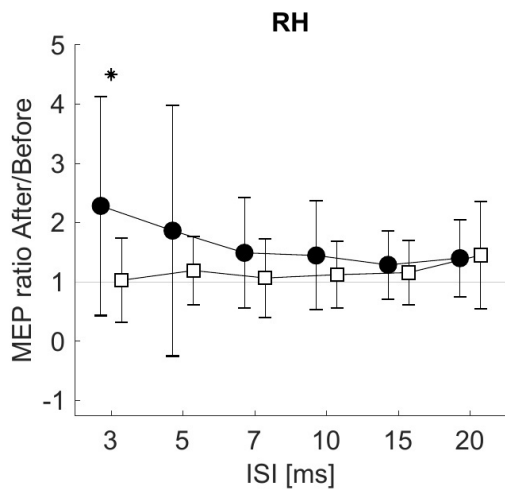
311 **Fig. 2 Normalized MEP ratio After/Before** (*Black-and-white figure in print*)

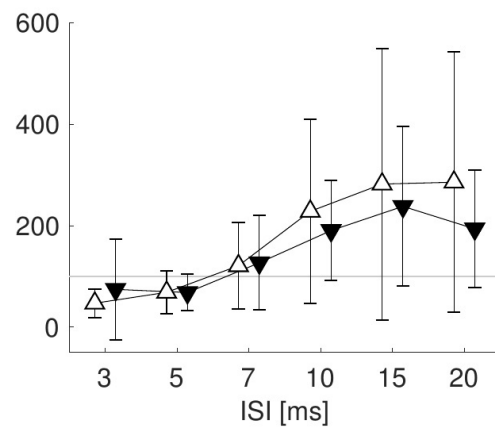
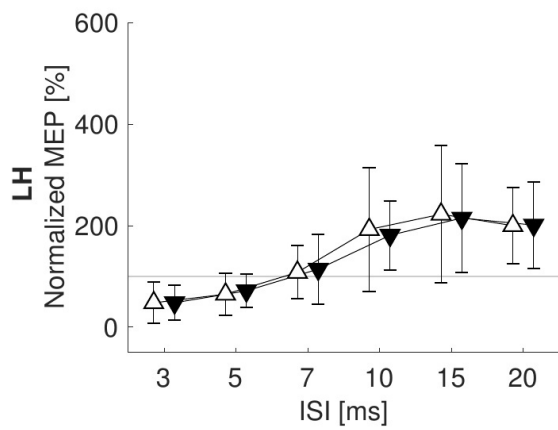
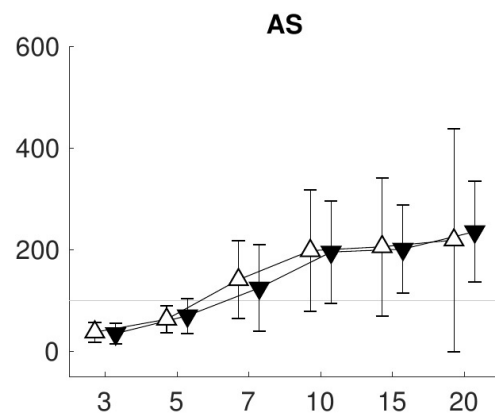
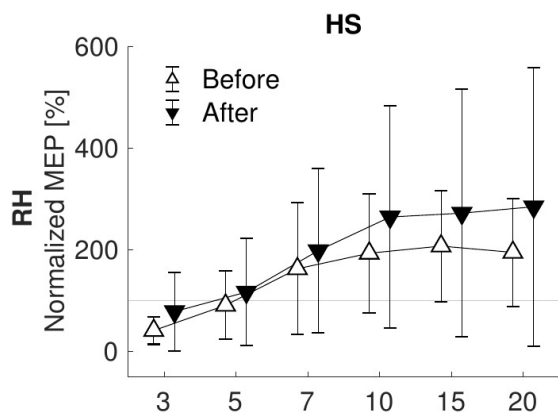
312 Dot-and-whisker plots show average normalized MEP ratios (normalized MEP After/Before) for
313 the right and the left hand (RH and LH, respectively), either for the heel or ankle stimulation (black
314 circles and white squares, respectively) session. Whiskers indicate standard deviation (SD).
315 Abscissa shows inter-stimulus interval (ISI) between the conditioning and test stimulus in ms.
316 Significant difference controlled for the applied pressure using linear regression analysis is
317 indicated with asterisk. Only the ISI 3 ms ($N = 14$, $P_{RH} = 0.04$, $P_{LH} = 0.46$) and 15 ms ($N = 14$, P_{RH}
318 $= 0.37$, $P_{LH} = 0.54$) were formally tested.

319 **Fig. 3 Normalized MEP sizes** (*Black-and-white figure in print*)

320 Dot-and-whisker plots show average normalized MEP sizes (in %) before (white triangles) and after
321 the stimulation (black triangles) for the right and the left hand (RH and LH, respectively), either for
322 the heel or ankle stimulation (HS and AS, respectively) session. Whiskers indicate standard
323 deviation. Abscissa shows inter-stimulus interval (ISI) between the conditioning and test stimulus in
324 ms. There was no significant difference between any of the baseline and post-stimulation mean
325 (post-hoc paired Student's t-test).







The effects of sustained manual pressure stimulation according to Vojta Therapy on heart rate variability

Jaroslav Opavsky^a, Martina Slachtova^a, Miroslav Kutin^{b,c}, Pavel Hok^d, Petr Uhlir^a, Hana Opavska^a, Petr Hlustik^d

Background. The physiotherapeutic technique of Vojta reflex locomotion is often accompanied by various autonomic activity changes and unpleasant sensations. It is unknown whether these effects are specific to Vojta Therapy. Therefore, the aim of this study was to compare changes in cardiac autonomic control after Vojta reflex locomotion stimulation and after an appropriate sham stimulation.

Methods. A total of 28 young healthy adults (20.4 – 25.7 years) were enrolled in this single-blind randomized cross-over study. Participants underwent two modes of 20-minute sustained manual pressure stimulation on the surface of the foot on two separate visits. One mode used manual pressure on the lateral heel, i.e., in a zone employed in the Vojta Therapy (active stimulation). The other mode used pressure on the lateral ankle (control), in an area not included among the active zones used by Vojta Therapy and whose activation does not evoke manifestations of reflex locomotion. Autonomic nervous system activity was evaluated using spectral analysis of heart rate variability before and after the intervention.

Results. The active stimulation was perceived as more unpleasant than the control stimulation. Heart rate variability parameters demonstrated almost identical autonomic responses after both stimulation types, showing either modest increase in parasympathetic activity, or increased heart rate variability with similar contribution of parasympathetic and sympathetic activity.

Conclusion. The results demonstrate changes of cardiac autonomic control in both active and control stimulation, without evidence for a significant difference between the two.

Key words: heart rate variability, spectral analysis, pressure stimulation, reflex locomotion, Vojta Therapy

Received: September 26, 2017; Accepted with revision: May 16, 2018; Available online: May 23, 2018
<https://doi.org/10.5507/bp.2018.028>

^aDepartment of Physiotherapy, Faculty of Physical Culture, Palacky University Olomouc, Czech Republic

^bDepartment of Physiotherapy, Faculty of Health Sciences, Palacky University Olomouc, Czech Republic

^cKM KINEPRO PLUS s.r.o., Olomouc, Czech Republic

^dDepartment of Neurology, Faculty of Medicine and Dentistry, Palacky University Olomouc and University Hospital Olomouc, Czech Republic
 Corresponding author: Pavel Hok, e-mail: pavel.hok@upol.cz

INTRODUCTION

The technique of reflex locomotion according to Václav Vojta¹ belongs to neurophysiological physiotherapeutic methods, currently used in many disorders and injuries affecting the central and/or peripheral nervous or musculoskeletal systems. Application of the technique is associated not only with motor manifestations but also with autonomic nervous system (ANS) responses. Whereas the influence on human motor activity has been repeatedly studied²⁻⁵, we have not found any reports of the effect of Vojta Therapy on autonomic activity and autonomic control in the published literature. Our previous study using functional MRI of the brain demonstrated specific modulation of hand motor control in the pontomedullary reticular formation (PMRF) following the stimulation according to Vojta⁵. Besides motor control, the PMRF is also implicated in various aspects of autonomic control⁶. Therefore, we decided to study the effect of Vojta Therapy on cardiac autonomic control using spectral analysis of heart rate variability (SAHRV). Stimulation in an active (trigger) zone on the lateral heel

according to Vojta was compared to stimulation outside the known active zones (control or sham stimulation) within the same young healthy participants.

MATERIALS AND METHODS

Subjects

Study participants were recruited among students of health care professions at Palacky University in Olomouc. Participants were enrolled following informed consent and after keeping a recommended regime prior to the scheduled examination. Study protocol has been approved by Ethics Committee of the University Hospital and the Faculty of Medicine and Dentistry, Palacky University Olomouc, approval number 9.4.2013.

Thirty students with no history of neurologic or psychiatric disease were included. Two participants were excluded after initial autonomic examination, one of them manifested extremely high and the other extremely low values of heart rate variability (HRV) spectral parameters, which did not permit reliable assessment of

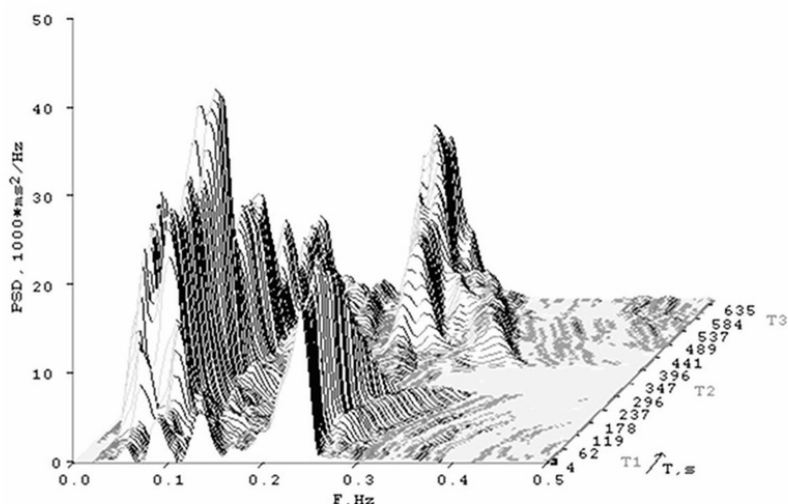


Fig. 1. Spectral analysis of heart rate variability in a young healthy subject during the supine-standing-supine test.

PSD – Power spectral density, F – frequency, T – time. T1 – first supine phase, T2 – standing phase, T3 – repeated supine phase. Frequency ranges: Low frequency (LF) – 0.05-0.15 Hz, high frequency (HF) 0.15-0.50 Hz. Note the clear decrease in the HF component in the standing position (T2), corresponding to decreased vagal activity, and its return to the previous level (or above that) in the repeated supine position (T3).

changes during different phases of testing. The investigated group therefore included 28 participants (15 women and 13 men), mean age 23.3 years, range 20.4–25.7 years.

Assessment of cardiac autonomic control – spectral analysis of heart rate variability

Cardiac autonomic control was studied on short-term ECG recordings, evaluating so-called short-term heart rate variability⁷. We have used a modification evaluating the orthoclinostatic reaction in the supine-standing-supine test⁸⁻¹⁰ to be able to register the changes (shift) in cardiac autonomic control in situations with different orthostatic load. It was chosen due to the fact that vagal activity prevails in the supine body position, whereas in the standing position vagal influence on heart decreases and sympathetic activity increases. The acquired short-term ECG recordings were subjected to temporal and spectral analysis of HRV using the DiANS PF8 system (Dimeia Group, Olomouc, Czech Republic). Spectral calculations were performed with fast Fourier transform using a partially modified algorithm CGSA (coarse-graining spectral analysis) (ref.¹¹), with suppression of noise components.

The duration of each of the three phases of the supine-standing-supine test depended on the heart rate of each investigated individual, about 5 min on average. The entire supine-standing-supine test thus lasted about 15 minutes (at a heart rate of 60 beats per minute). Details of the investigation and evaluation for SAHRV examination have been published elsewhere⁹.

The HRV analysis yielded the following parameters in the frequency domain related to cardiac autonomic control for short-time recordings: VLF Power (ms^2) = spectral

power of the very low frequency band 0.02 Hz – 0.05 Hz, LF Power (ms^2) = spectral power of the low frequency band 0.05 Hz – 0.15 Hz, HF Power (ms^2) = spectral power of the high frequency band 0.15 Hz – 0.50 Hz, LF/HF ratio = ratio of spectral powers LF over HF, Relative VLF (%) = relative representation of the VLF component in the entire frequency range (0.02 – 0.50 Hz), Relative LF (%) = relative representation of the LF component in the entire frequency range, Relative HF (%) = relative representation of the HF component in the entire frequency range, Total Power (ms^2) = total spectral power over the entire frequency range 0.02 – 0.50 Hz. In the time domain: MSSD = mean squared successive differences – indicator of HRV, RR interval (s) = duration of the RR interval derived from ECG. See Fig. 1 for graphical representation of the spectral analysis.

Respiratory rate assessment

Respiratory rate is another autonomic variable, which needs to be recorded and considered for an SAHRV study. Participants were breathing at their natural pace, respiration was recorded continuously with the DiANS PF8 system and simultaneously using adjustable chest belt with sensor. Respiration frequency was assessed in each of the three phases of the supine-standing supine test, together with SAHRV parameters in the same protocol.

Assessment of the degree of stimulation discomfort (unpleasantness of the stimulation)

Stimulation, which evokes unpleasant feelings, including pain, will influence and modify ANS activity. We have therefore used a visual analogue scale (VAS) to capture



Fig. 2. Stimulation procedure and stimulation sites. The upper photograph shows the body position during the stimulation. The lower right photograph shows the stimulation site (zone) at the right lateral heel according to Vojta, whereas the lower left photograph shows the control stimulation site at the right lateral ankle.

the degree of stimulation discomfort, that is the degree of unpleasantness of the stimulation, so that we might account for the possible influence of negatively perceived stimulation or frank nociception on the SAHRV parameters, which might prevail over the effect of the two different types of manual stimulation. VAS was assessed on a scale 0 to 10 (minimum and maximum discomfort sensation, respectively), the perceived value was recorded immediately after stimulation end.

Procedures

Each participant underwent two autonomic nervous system examinations (SAHRV), at least a week apart (maximum 5 weeks). Each session was scheduled at 11 a.m. and used one or the other of two stimulation sites (see below), the order of examinations was randomized. Stimulation sites at the right leg were either 1) the foot zone according to prof. Vojta: processus lateralis tuberis calcanei (active stimulation) or 2) lateral ankle (sham stimulation), see Fig. 2. During both stimulation types, the participant lay prone, in an initial position for the so called reflex crawling¹ and each stimulation involved 20 min of manual pressure applied by a trained and experienced physiotherapist.

To allow subsequent HRV analysis, the ECG recording was performed twice within each examination: before and immediately after 20 min of peripheral pressure stimulation.

As data from the “supine 1” phase may be influenced

by interfering factors both somatic and psychological (e.g., pre-examination stress, new experimental situation, white-coat syndrome, etc.), heart rate, SAHRV and respiration rate obtained during the third phase of the test, “supine 2” (supine position following orthostatic load in the prior standing), were used for statistical analysis (see also ref.⁸⁻¹⁰).

Statistical analysis

The acquired data were processed with the software Statistica 12 (StatSoft, Tulsa, OK, USA). For within-subject effects, the non-parametric Wilcoxon paired test was used, whereas between-session effects for the respiratory rate and the degree of stimulation-related discomfort were tested with the Mann-Whitney test.

RESULTS

Spectral analysis of heart rate variability

SAHRV of the first test phase, i.e., the first supine position (baseline), yielded in all participants spectral characteristics typical of healthy subjects of their age group⁹, with the possibility to distinguish individual spectral bands and with sufficiently high values of spectral power within individual frequency components to permit quantitative analysis, including assessment of the responses to changes in body position.

The values of the calculated HRV parameters before and after active (heel) stimulation are provided in Table 1. Statistical significance refers to results of the Wilcoxon paired test. Values of the assessed ECG and SAHRV parameters before and after ankle stimulation (control site) are provided in Table 2.

The results indicate that both stimulation types, i.e., stimulation in an “active” site according to prof. Vojta (heel) and stimulation in a control “inactive” site were followed by statistically significant changes in MSSD values, duration of RR interval, and concurrently also in respiration rate. MSSD, which represents overall heart rate variability in the time domain, increased after both stimulation types. RR intervals lengthened (thus heart rate decreased) and respiration rate decreased after both active and control stimulations.

In the frequency domain, both stimulation types were associated with a statistically significant increase in VLF Power, HF Power and Total Power. LF Power increased significantly only after the active stimulation.

Neither the LF/HF ratio, nor the relative parameters of SAHRV, indicating the relative representation of individual frequency components, manifested any statistically significant changes after either stimulation type when compared to the pre-stimulation baseline.

Respiratory rate

Respiratory rate was assessed both before stimulation of each site (active versus control), as well as after stimulation. Before active (heel) stimulation, the group mean respiratory rate was 12.3 breaths/min (SD=2.61), whereas before the control (ankle) stimulation, the rate

Table 1. Duration of RR intervals and parameters of heart rate variability: heel (active) stimulation site.

Parameter	Pre-stimulation Median (Q1-Q3)	Post-stimulation Median (Q1-Q3)	Statistical Significance
RR interval (s)	1.00 (0.92-1.15)	1.08 (1.00-1.20)	$P < 0.001$
VLF Power (ms ²)	240.80 (164.69-344.74)	382.69 (199.19-641.88)	$P = 0.04$
LF Power (ms ²)	627.73 (398.88-849.29)	757.46 (462.45-1373.38)	$P = 0.01$
HF Power (ms ²)	1270.71 (462.45-1373.38)	2194.41 (934.12-4842.71)	$P = 0.02$
LF/HF ratio	0.419 (0.173-0.951)	0.409 (0.163-0.767)	N.S.
Relative VLF (%)	11.60 (6.29-15.66)	10.92 (6.33-14.79)	N.S.
Relative LF (%)	26.00 (13.74-39.65)	27.35 (12.80-36.01)	N.S.
Relative HF (%)	62.40 (45.74-77.24)	61.73 (45.23-78.62)	N.S.
Total Power (ms ²)	2246.04 (1486.41-5140.27)	4089.94 (2066.12-6912.44)	$P = 0.01$
MSSD (ms ²)	4681.60 (2735.95-14112.02)	8937.38 (4604.74-16404.76)	$P < 0.001$

Legend: RR interval (s) = duration of the RR interval derived from ECG, VLF Power (ms²) = spectral power of the very low frequency band, LF Power (ms²) = spectral power of the low frequency band, HF Power (ms²) = spectral power of the high frequency band, LF/HF ratio = ratio of the spectral powers LF over HF, Relative VLF (%) = relative representation of the VLF component within the entire frequency range, Relative LF (%) = relative representation of the LF component within the entire frequency range, Relative HF (%) = relative representation of the HF component within the entire frequency range, Total Power (ms²) = total spectral power over the entire frequency range 0.02 - 0.50 Hz, MSSD = mean squared successive differences - indicator of heart rate variability in the time domain, Q1, Q3 = 1st and 3rd quartile.

Table 2. Duration of RR intervals and parameters of heart rate variability: ankle (control) stimulation.

Parameter	Pre-stimulation Median (Q1-Q3)	Post-stimulation Median (Q1-Q3)	Statistical Significance
RR interval (s)	0.99 (0.86-1.10)	1.07 (0.95-1.21)	$P < 0.001$
VLF Power (ms ²)	283.48 (163.63-478.29)	451.86 (203.26-797.65)	$P = 0.009$
LF Power (ms ²)	701.21 (306.40-975.36)	750.45 (287.81-1721.95)	N.S.
HF Power (ms ²)	1405.82 (720.84-3076.14)	2436.48 (835.47-3768.58)	$P = 0.03$
LF/HF ratio	0.476 (0.203-0.908)	0.534 (0.177-0.913)	N.S.
Relat. VLF (%)	10.31 (7.82-14.95)	13.43 (5.16-19.08)	N.S.
Relat. LF (%)	27.42 (15.93-36.10)	29.86 (12.09-41.26)	N.S.
Relat. HF (%)	62.27 (38.55-75.95)	54.91 (42.28-76.30)	N.S.
Total Power (ms ²)	2617.85 (1689.78-4043.30)	3770.58 (1893.02-6456.51)	$P = 0.001$
MSSD (ms ²)	4814.96 (2388.49-8435.96)	8908.95 (3451.13-12689.16)	$P < 0.001$

Legend: See Legend for Table 1.

was 12.9 breaths/min (SD=2.69); these values were not statistically significantly different.

After stimulation of the active zone (heel), respiratory rate decreased significantly to 10.9 breaths/min (SD=2.73), $P = 0.003$. Similarly, after control (ankle) stimulation, respiratory rate decreased significantly to 11.3 breaths/min (SD=2.88), $P = 0.003$. The respiratory rates after the two stimulation types were not significantly different (Mann-Whitney test).

Stimulation discomfort

The VAS of pain indicated mean discomfort after active (heel) stimulation 3.01 (SD 1.94), range 0.2-7.4, whereas after ankle (control) stimulation the mean VAS score was 1.62 (SD 1.48), range 0.2-6.2, this difference was statistically significant ($P = 0.003$). This reveals, even in young healthy participants, a certain unpleasantness associated with pressure at the active stimulation site. Nevertheless, despite this difference in perceived discomfort, no SAHRV parameters were apparently affected since the results were similar in both stimulation types.

Behavioral and motor responses to stimulation

During stimulation of the active site (heel), 9 out of the 28 participants (32%) manifested involuntary signs of muscle activation - fasciculations, finger movements, muscle twitches or the development of head rotation and/or deeper breathing. In contrast, three participants (10.7%) were falling asleep.

During stimulation of the control site (ankle), slight head rotation appeared only in one participant (3.5% of the group), and another one manifested deeper breathing. Tendency to fall asleep appeared in 3 participants (10.7%), two of whom were also sleepy after the active stimulation.

DISCUSSION

Reflex locomotion, introduced by Václav Vojta, is based upon stimulation of so-called trigger zones on the surface of human body and has become one of rehabilitation methods preferably used in central nervous system disorders of childhood, especially cerebral palsy and cen-

tral coordination disorder^{1,12}. Later, it was also applied to disorders of the peripheral nervous system and to selected structural and functional disorders and injuries of the musculoskeletal system. Clinical studies of the Vojta Therapy focused on motor activity^{2,4,13-15}.

Stimulation of the empirically discovered trigger zones according to Vojta, which evokes motor manifestations – reflex locomotion, concurrently evokes responses of the autonomic nervous system as described in the method's characteristics^{1,16,17}. Among them, the most significant are the cardiovascular responses, where vasomotor changes have been most frequently observed.

Surprisingly, our search of the medical and scientific literature did not discover any reports on observed influences on the autonomic nervous system in general, and neither on the heart rate (and specifically its variability) during application of the reflex stimulation according to Vojta. At the same time, changes in HRV have been studied and reported for many other types of surface or other somatosensory stimulation, including nociceptive¹⁸⁻²².

Among the many established approaches to evaluation of HRV, some of which have clinical application^{7,9,23-25}, we have chosen the method of spectral analysis of HRV (SAHRV) in a modification with the changes of orthoclinostatic load⁸⁻¹⁰, which induce a shift in sympathovagal balance.

The reason for choosing this particular method was the possibility to record and assess the activity of vagal and sympathetic innervation, or their relative contribution, in different body positions (in the supine-standing-supine test) before and after specific active (Vojta) stimulation as well as before and after a control stimulation outside the described trigger zone(s).

The results indicate that both active and control stimulations were followed by statistically significant lengthening of RR intervals and an increase in measures of overall variability, both in the frequency (Total Power) and time (MSSD) domain. Likewise, both stimulation types were associated with a statistically significant increase in the high-frequency (HF) spectral power, which reflects vagal activity (this also corresponds to lengthening of the average RR interval). Nevertheless, the relative representation of individual spectral components (VLF, LF and HF) has remained mostly unchanged after both stimulation types, which suggests that the degree of sympathetic and vagal contribution to cardiac autonomic control remained unchanged as well. Smith et al. (ref.²¹) reported the results of another stimulation modality, repeated massage, in neonates, where assessment of HRV indicated increase in parasympathetic activity.

Somewhat surprising was our finding of decreased respiration rate after both active and control stimulations, this usually occurs in a relaxed condition. Here, however, the subjective perception of the two stimulation types differed according to the VAS scores, which revealed a higher degree of stimulation discomfort (unpleasantness) during stimulation of an active trigger zone of the Vojta Therapy. In both stimulation types, though, the VAS scores were low.

Overall, the changes in SAHRV parameters may be interpreted as similar after both stimulation types, namely, that stimulation of the active zone on the heel has not evoked a clearly different response than stimulation outside the active zone (ankle). This stands in apparent contradiction to previous experience with autonomic reflex responses during application of the Vojta Therapy in the clinical practice¹.

There may be several reasons for this discrepancy. The typical target group for the Vojta technique, neonates and infants, has autonomic responses different from those of adults, one of the underlying factors may be the immaturity of the central nervous system in the children. The other obvious difference is the absence of CNS lesions in our research population, whereas in the clinical practice, the therapeutic stimulation is mostly applied to children with perinatal or prenatal brain damage. Taken together, the rather small and non-specific autonomic response to pressure stimulation of the foot in our young healthy adult participants (university students) may not be unexpected when the more prominent responses have been observed in children with CNS damage in the first months and years of life.

Furthermore, the therapeutic application in the clinical practice typically includes simultaneous stimulation in several trigger zones, whereas our protocol was simplified to using a single stimulation site (either active or control).

Another possible explanation for the similarity of autonomic responses after both stimulation types is the fact that our participants did not manifest obvious emotional reactions, whereas in children, Vojta Therapy is commonly accompanied by unpleasant feelings, often with pain, and concomitant autonomic responses. Last but not least, children manifest the tendency to escape and withdraw from unpleasant stimulation and the withdrawal or reflex motor behavior may be closely associated with the observed autonomic responses.

As mentioned above, the study involved several limitations: We have used the most accessible study population, young healthy adults, whereas more pronounced autonomic changes might be observed in children and/or subjects with nervous system damage. The use of a single stimulation zone has also been mentioned already. A third group with no stimulation might have been useful to clarify test-retest variability. These issues may be addressed in future research.

CONCLUSION

Sustained manual pressure stimulation in an active (empirically discovered and clinically used) skin area on the foot was perceived as more unpleasant than stimulation of a nearby control site. Heart rate variability parameters reflecting cardiac autonomic control changes demonstrated almost identical autonomic responses after both stimulation types. Whereas several markers indicated modest increase in parasympathetic activity, other measures suggested increased heart rate variabil-

ity together with joint increase in activity of both vagal (parasympathetic) and sympathetic activity, without significant change in their relative contribution to cardiac autonomic control. Therefore, in the present study, we were unable to demonstrate autonomic responses specific for the Vojta Therapy.

ABBREVIATIONS

ANS, Autonomic nervous system; CGSA, Coarse-graining spectral analysis; ECG, Electrocardiography; HF, High frequency; HRV, heart rate variability; LF, Low frequency; MSSD, Mean squared successive differences; PMRF, Pontomedullary reticular formation; SAHRV, Spectral analysis of heart rate variability; SD, Standard deviation; VAS, Visual analog scale; VLF, Very low frequency.

Acknowledgement: This work was supported by grant of the Czech Science Foundation (GACR) (grant number 14-22572S).

Author contributions: JO: study design, data interpretation, manuscript writing and literature search, critical revision of the manuscript; MS: data collection, Figures; MK: data collection; PH: study design, data interpretation, manuscript writing and literature search; PU: data collection, statistical analysis; HO: data collection, data analysis; PH: study design, data interpretation; the final version was approved by all authors.

Conflict of interest statement: The authors state that there are no conflicts of interest regarding the publication of this article.

REFERENCES

- Vojta V, Peters A. *Das Vojta-Prinzip: Muskelspiele in Reflexfortbewegung und motorischer Ontogenese*. 3rd ed. Berlin: Springer; 2007.
- Bäckström B, Dahlgren L. Vojta Self-training: Experiences of six neurologically impaired people: A qualitative study. *Physiotherapy* 2000;86(11):567-74.
- Imamura S, Sakuma K, Takahashi T. Follow-up study of children with cerebral coordination disturbance (CCD, Vojta). *Brain Dev* 1983;5(3):311-4.
- Kanda T, Pidcock FS, Hayakawa K, Yamori Y, Shikata Y. Motor outcome differences between two groups of children with spastic diplegia who received different intensities of early onset physiotherapy followed for 5 years. *Brain Dev* 2004;26(2):118-26.
- Hok P, Opavský J, Kutín M, Tüdös Z, Kaňovský P, Hlušík P. Modulation of the sensorimotor system by sustained manual pressure stimulation. *Neuroscience* 2017;348:11-22.
- Stremel RW, Waldrop TG, Richard CA, Iwamoto GA. Cardiorespiratory responses to stimulation of the nucleus reticularis gigantocellularis. *Brain Res Bull* 1990;24(1):1-6.
- Task Force. Heart rate variability. Standards of measurement, physiological interpretation, and clinical use. Task Force of the European Society of Cardiology and the North American Society of Pacing and Electrophysiology. *Eur Heart J* 1996;17(3):354-81.
- Opavský J, Salinger J. Examination methods of the autonomic system function – a review for the clinical practice. *Noninvasive Cardiol* 1995;4(4):139-53.
- Opavský J. *Autonomní nervový systém a diabetická autonomní neuropatie: Klinické aspekty a diagnostika*. Praha: Galén; 2002.
- Salinger J, Opavský J, Stejskal P, Vychodil R, Olšák S, Janura M. The evaluation of heart rate variability in physical exercise by using the telemetric variapulse TF3 system. *Acta Univ Palacki Olomuc Gymnica* 1998;28:13-23.
- Yamamoto Y, Hughson RL. Coarse-graining spectral analysis: new method for studying heart rate variability. *J Appl Physiol Bethesda Md* 1985 1991;71(3):1143-50.
- Vojta V. Early diagnosis and therapy of cerebral movement disorders in childhood. C. Reflexogenous locomotion - reflex creeping and reflex turning. C1. The kinesiological content and connection with the tonic neck reflexes. *Z Für Orthop Ihre Grenzgeb* 1973;111(3):268-91.
- Bauer H, Appaji G, Mundt D. VOJTA neurophysiologic therapy. *Indian J Pediatr* 1992;59(1):37-51.
- Kanda T, Yuge M, Yamori Y, Suzuki J, Fukase H. Early physiotherapy in the treatment of spastic diplegia. *Dev Med Child Neurol* 1984;26(4):438-44.
- Senthilkumar S, Swarnakumari P. A study on Vojta therapy approach to improve the motor development of cerebral palsy children. *Int J Med Sci* 2011;4(1&2):39-45.
- Dimitrijević L, Jakubi BJ. The importance of early diagnosis and early physical treatment of cerebral palsy. *Facta Univ Ser Med Biol* 2005;12(3):119-22.
- Kotnik SS. Vojta in rehabilitation of children with neurodevelopmental disorders. *Paediatr Croat* 2012;56(Supplement 1):227-31.
- Baker J, Shoemaker KJ. Effect of isometric handgrip exercise on heart rate variability with and without somatosensory stimulation. *FASEB J* 2013;27(1 Supplement):1b833-1b833.
- Joseph P, Acharya UR, Poo CK, Chee J, Min LC, Iyengar SS, Wei H. Effect of reflexological stimulation on heart rate variability. *ITBM-RBM* 2004;25(1):40-5.
- Koenig J, Jarczok MN, Ellis RJ, Hillecke TK, Thayer JF. Heart rate variability and experimentally induced pain in healthy adults: a systematic review. *Eur J Pain Lond Engl* 2014;18(3):301-14.
- Smith SL, Lux R, Haley S, Slater H, Beachy J, Moyer-Mileur LJ. The effect of massage on heart rate variability in preterm infants. *J Perinatol* 2013;33(1):59-64.
- Wijnen VJM, Heutink M, van Boxtel GJM, Eilander HJ, de Gelder B. Autonomic reactivity to sensory stimulation is related to consciousness level after severe traumatic brain injury. *Clin Neurophysiol* 2006;117(8):1794-807.
- Ernst G. *Heart Rate Variability*. London: Springer-Verlag; 2014.
- Gang Y, Malik M. Heart Rate Variability Analysis in General Medicine. *Indian Pacing Electrophysiol J* 2003;3(1):34-40.
- Vlčková E, Bednařík J, Buršová Š, Šajgalíková K, Mlčáková L. Spectral Analysis of Heart Rate Variability – Normative Data. *Čes Slov Neurol Neurochir* 2010;73/106(6):663-72.

5. Annex 5

Modulation of the sensorimotor system by manipulation of afferent somatosensory input: evidence from mechanical pressure stimulation

Pavel Hok^{a,b}, Petr Hlustik^{a,b}

1 **Background**

2 Peripheral afferent input is critical for human motor control and motor learning. Both skin and deep
3 muscle mechanoreceptors can affect motor behaviour when stimulated. Whereas some modalities
4 such as vibration have been employed for decades to alter cutaneous and proprioceptive input, both
5 experimentally and therapeutically, central effects of mechanical pressure stimulation have been
6 studied less frequently. This discrepancy is especially striking when considering the limited
7 knowledge of neurobiological principles of commonly used physiotherapeutic techniques that
8 utilise peripheral stimulation, such as reflex locomotion therapy.

9 **Methods and results**

10 Our review of the available literature pertaining pressure stimulation focused on transcranial
11 magnetic stimulation (TMS) and neuroimaging studies, including both experimental studies in
12 healthy subjects and clinical trials. Our search revealed limited number of neuroimaging papers
13 related to peripheral pressure stimulation and no evidence of effects on cortical excitability. In
14 general, majority of imaging studies agreed on significant involvement of cortical motor areas
15 during processing of pressure stimulation. Recent data also point to a specific role of subcortical
16 structures, such as putamen or brainstem reticular formation. However, a thorough comparison of
17 the published results often showed major inconsistencies which are proposed to be due to variable
18 stimulation protocols and statistical power.

19 **Conclusions**

20 Localised peripheral sustained pressure is a potent stimulus inducing changes in motor behaviour
21 and cortical activation. We highlight the limited amount of research devoted to this stimulus
22 modality, emphasise current knowledge gaps, present recent development in the field and
23 accentuate evidence awaiting replication or confirmation in future neuroimaging and
24 electrophysiological studies.

25 **KEY WORDS**

26 somatosensory system, motor system, sensorimotor integration, pressure stimulation,
27 neurorehabilitation, Vojta reflex locomotion therapy

28 **AFFILIATIONS**

a)Department of Neurology, Faculty of Medicine and Dentistry, Palacký University Olomouc, Czechia;

b)Department of Neurology, University Hospital Olomouc, Czechia.

29 **CORRESPONDING AUTHOR**

30 MUDr. Pavel Hok

31 E-Mail: pavel.hok@upol.cz

32 **BRIEF SUMMARY**

33 In this review, we assemble literature on motor sequelae of mechanical pressure stimulation with
34 special emphasis on clinical applications, including reflex locomotion therapy. We highlight the
35 limited amount of research devoted to this stimulus modality, emphasise current knowledge gaps,
36 present recent development in the field and accentuate evidence awaiting replication or
37 confirmation in future neuroimaging studies.

38

39 **INTRODUCTION**

40 Peripheral afferent input provides a critical drive for primate motor control and its complete
41 removal (deafferentation) leads to paralysis¹. Deafferentation in the absence of specific intervention
42 also suppresses motor plasticity and learning². Conversely, long term potentiation-like (LTP-like)
43 facilitation of primary motor cortex (M1) neuronal discharge can be demonstrated following direct
44 stimulation of the primary somatosensory cortex (S1) in the mammalian brain³. Peripheral afferent
45 stimulation has therefore been used to induce experimental plasticity of the human motor system⁴
46 and has become an important component of techniques to improve or restore motor function⁵.
47 Beyond short-term facilitation of motor responses known since Sherrington⁶, longer duration of
48 peripheral stimulation can induce facilitatory changes that persist for minutes and hours⁷. Most
49 commonly studied peripheral stimulation modalities include electrical nerve stimulation or
50 vibration, which are easy to control and administer⁷⁻¹¹. Natural modalities of peripheral stimulation,
51 such as tactile, pressure or proprioceptive, have been studied less extensively^{12,13}, even though they
52 represent essential elements of clinical some rehabilitation techniques and procedures¹⁴⁻¹⁶. Whereas
53 noxious mechanical pressure stimulation has been employed in research of central pain
54 processing¹⁷, effects of sustained innocuous pressure have been explored to a lower degree and even
55 less attention has been paid to its interaction with the “classical” motor systems, but see ref.^{12,13,18}.

56 In this review, we provide an overview of how the sensorimotor system is affected by pressure
57 stimulation with emphasis on its current clinical applications. Since a full overview would be
58 beyond the scope of a single review article, we focus on the central effects of prolonged
59 manipulation. For the same reasons, primarily the evidence from studies using transcranial magnetic
60 stimulation (TMS), functional magnetic resonance imaging (fMRI), and positron emission
61 tomography (PET) is considered, although other selected approaches are discussed where required
62 to provide a sufficient background. Finally, we attempt to delineate where the future research
63 interests may lie and suggest directions for follow-up studies.

64 **SENSORY STRUCTURES RESPONDING TO INNOCUOUS PRESSURE**

65 The perception of innocuous mechanical skin stimulation, on which we focus in this review, is
66 mediated by the so called low-threshold mechanoreceptors (LTMR) (ref.¹⁹). These include four
67 types of afferents defined based on their receptive fields and discharge pattern: slow-adapting
68 type I afferents (SA-I, Merkel endings or disks) for static stimuli; slow-adapting type II (SA-II) for
69 skin stretching; fast-adapting type I (FA-I, Meissner endings) detecting flutter up to 40-50 Hz; and
70 fast-adapting type II (FA-II, Pacinian corpuscles) responding to high-frequency (vibratory) stimuli
71 up to 400 Hz. Mechanical pressure stimulation excites mainly SA-I afferents which, in addition to
72 static pressure, respond to low frequency mechanical stimulation (usually below 5 Hz) and skin
73 deformation²⁰. In microneurographic studies, SA-I endings were also shown to participate in coding
74 joint positions^{21,22}, which illustrates their ability to transmit proprioceptive information about
75 relative limb positions⁹. Before reaching the cortex, information from cutaneous afferents is already
76 combined with motor efferent signals at multiple levels of the central nervous system (CNS),
77 including the spinal cord grey matter, brainstem nuclei and thalamus. For detailed reviews of central
78 projecting pathways and physiological background of sensorimotor integration at the cortical level,
79 see ref.^{9,11,19,23,24}.

80 **BEHAVIOURAL EFFECTS OF PERIPHERAL PRESSURE STIMULATION**

81 Central effects of peripheral pressure stimulation on motor control are best demonstrated by taking
82 a closer look at the phenomena that alter motor behaviour and performance. A rather thorough
83 physiological background is introduced here, as it is crucial for describing the observed behavioural
84 effects as well as understanding the rationale and correct interpretation of the electrophysiology and
85 imaging studies.

86 Peripheral mechanical stimulation modalities, such as vibration, have been long known to elicit
87 muscle contraction, overt involuntary tonic and phasic movements, postural sways, and

88 modification of voluntary motor actions during and after the stimulation^{9–11}. Similar modulation of
89 motor behaviour, including involuntary motor responses and outlasting motor after-effects, has also
90 been demonstrated after mechanical pressure stimulation^{25–27}. It is therefore no surprise that
91 pressure stimulation has been incorporated into a number of physiotherapeutic techniques, such as
92 clinical massage, acupressure¹⁴, reflexology, or myofascial trigger point therapy¹⁵. Another example
93 of mechanical pressure stimulation in clinical use is stimulation according to Vojta, i.e., a
94 component of physiotherapeutic technique also known as reflex locomotion therapy (RLT) or Vojta
95 method^{16,26–31} which is clinically employed in several European^{32–39} and Asian countries^{40,41}. Given
96 the lack of comprehensive literature on RLT and its relevance to some published imaging research,
97 we provide here a broader historical perspective on this topic.

98 **Involuntary motor responses to pressure stimulation**

99 Inspired by the published neurophysiological and clinical studies^{25,42–47} and his own clinical
100 observations^{27,48}, Vojta noted that, in several body configurations, sustained manual pressure
101 stimulation of specific points on the skin surface (“stimulus points” or “stimulation/reflex/trigger
102 zones”) gradually evokes a widespread motor response (asymmetrical muscle contraction in both
103 sides of the neck, trunk, and limbs) which has been called “reflex locomotion” and involves two
104 basic patterns, “reflex creeping” (also called crawling) – first observed by Bauer^{25,27} – and “reflex
105 turning” (also called rotation or rolling) (ref.^{26,27,30,31}). These tonic motor responses share some
106 similarities with other automatisms described in neonates, pre-term infants, human foetuses, and
107 under certain conditions in healthy adults^{30,31,49–52}. Reflex locomotion is likewise easiest to observe
108 in healthy newborns up to 6 weeks of age³⁰, but can also be elicited in children with cerebral palsy,
109 adults with nervous system injury, as well as in healthy humans upon longer sustained peripheral
110 stimulation of multiple trigger zones (temporal and spatial summation) (ref.^{16,30,53}).

111 Besides evoked (involuntary) muscle contraction, further effects of reflex locomotion have been
112 described as well: voluntary movement facilitation, improvement of neurological abnormalities, and
113 autonomic changes^{16,30,34,35,51,54–57}. The effects have been observed to persist for at least 30
114 minutes¹⁶. It has been originally speculated that these sequelae of stimulation are mediated by
115 massive, mainly proprioceptive afferentation which accompanies the reflex locomotion^{16,30,51}.
116 Supported by the published works^{58–60} and his own observations^{48,61}, Vojta emphasized the central
117 role of proprioception also in the development of spasticity, as opposed to a mere loss of inhibitory
118 control from higher-order motor centres^{31,48,51}.

119 Despite the decades of clinical use of RLT, there has been limited knowledge of its neurobiological
120 basis, as the available evidence mostly consisted of kinesiology and observation studies¹⁶.

121 Originally, proprioception has been suggested to dominate the sensory afferentation triggering the
122 motor response^{16,30}. Indeed, pressure sensation from the foot soles contributes to maintenance of
123 upright stance^{62,63}. It was further emphasized that, in certain cases, the initial body configuration is
124 essential to elicit the complete motor response³⁰. Such posture-dependent involuntary responses
125 were also demonstrated using cutaneous and muscle vibration^{64,65}. The efferent pathways mediating
126 reflex locomotion have been speculated to involve extrapyramidal or parapyramidal system (i.e.,
127 bypassing the corticospinal tract), since reflex locomotion is best observed in neonates whose motor
128 cortex is not yet mature³⁰. Due to its complex nature involving all extremities and truncal muscles at
129 the same time, a common coordination centre has been suggested³⁰. The horizontal gaze deviation
130 observed during the motor response indicates that its neural substrate involves supraspinal, at least
131 upper brainstem structure, including the midbrain reticular formation^{16,27,30,48,66}. In fact, the
132 evidence for central pattern generators (CPG) from animal experimental research suggests an
133 existence of similar structures also in humans, possibly located to the midbrain or neighbouring
134 structures⁶⁷⁻⁶⁹. However, a frequent observation of partial motor responses limited to one or more
135 extremities additionally suggests an existence of multiple lower-level independent sources of the
136 motor responses¹⁶. This is again in line with the animal research evidence showing that lower-order
137 generators of simple locomotion patterns independent for each extremity reside on the spinal level
138 and are under top-down control of higher-order areas⁶⁹. Reflex locomotion has been also contrasted
139 with other primitive reflexes, e.g., “tonic neck reflexes” (TNR) (ref.^{26,27,30,46}), which have could be
140 suppressed by reflex locomotion³⁰. The structures responsible for the TNR have been therefore
141 suggested to lie hierarchically lower than those implicated in reflex locomotion, namely in the
142 lower brainstem³⁰. However, at the time of methodological development of RLT, there were no non-
143 invasive human methods available to test these hypotheses.

144 **EVIDENCE FROM ELECTROPHYSIOLOGY STUDIES**

145 Several studies using electromyographic (EMG) recordings in both animals and humans evaluated
146 the reflex muscle activity during pressure stimulation. In cats, complex tonic reflexes were elicited
147 by short as well as longer maintained pressure applied at the pads⁷⁰, whereas pressure stimulation of
148 the chest modulated posture-dependent muscle activity⁷¹. In humans, EMG studies demonstrated
149 gradual and rhythmical motor response during RLT (ref.⁵³) and confirmed the spatial and temporal
150 summation of these responses⁷². Despite slight inter-individual differences, the order of muscle
151 engagement seems to be relatively constant across subjects^{32,73}. Gajewska et al. (ref.³²) suggested
152 that the stereotypic and crossed nature of the observed muscle activations reflected excitation via
153 long propriospinal pathways, but an influence of supraspinal motor centres could not be ruled out.

154 Currently, there are no non-invasive methods available to directly investigate electrophysiological
155 activity in the brainstem sensorimotor nuclei. However, non-invasive assessment of cortical
156 excitability may still provide some indications of changes occurring in cortico-subcortical loops,
157 beyond the cortex itself. Studies employing paired-pulse TMS (ref.⁷⁴) have evaluated corticomotor
158 excitability changes due to extended peripheral electrical⁷ and mechanical stimulation⁷⁵ and
159 revealed that longer periods of sustained or repetitive stimulation (up to 2 hours) lead to an increase
160 of motor cortical excitability outlasting the stimulation period (on the order of several hours). It is
161 likely that sustained pressure stimulation involving the same cutaneous afferents would evoke
162 similar changes of cortical excitability. The underlying mechanisms within intracortical circuits
163 potentially involve changes in intracortical inhibition (SICI) and/or intracortical facilitation (ICF) as
164 seen in a number of studies using different modalities of peripheral stimulation⁷⁵⁻⁷⁹. However, to
165 our knowledge, there are currently no published studies regarding such changes following
166 mechanical pressure.

167 Our own unpublished paired-pulse TMS data in healthy subjects⁸⁰ indicate that sustained manual
168 pressure applied over 20 min to the foot produces differential effects according to the stimulation
169 site. Whereas a site at the right lateral heel routinely used in RLT (ref.^{16,27}) was associated with
170 decreased SICI in the first dorsal interosseus muscle of the ipsilateral upper limb, there was no such
171 change following control stimulation at a nearby site at the lateral ankle. No change in cortical
172 excitability was observed either for the limb contralateral to stimulation site. We speculate that
173 decreased SICI reflects altered function of the GABA_A-ergic inhibitory intracortical circuits⁸¹,
174 possibly indicating facilitation of neuroplasticity by unmasking of latent horizontal intracortical
175 projections^{79,82}. Although this effect is similar to the after-effects of focal muscle vibration^{79,83}, it is
176 much less localized since it could be observed in the ipsilateral limb³². In general, our data suggest
177 that the common mechanisms governing cortical plasticity evoked by afferent input can also take
178 place in response to sustained mechanical pressure stimulation.

179 **EVIDENCE FROM FMRI AND PET STUDIES**

180 The lack of neurophysiological evidence for the central motor effects of peripheral pressure
181 stimulation has been compensated for by an increasing body of neuroimaging research. However, in
182 most of these studies, the relationship between sensory stimulation and motor control has not been
183 purposefully investigated. In this section, we therefore present mostly indirect evidence for
184 sensorimotor integration based on the reported motor cortex co-activations.

185 A pioneering PET study assessed activation during discrimination task of slow onset, yet short

186 pressure stimuli applied to the distal phalanx of the right index finger⁸⁴. Compared to a rest
187 condition, subjects activated the contralateral S1 (Brodmann area [BA] 3b, 1 and 2), M1 (BA 4a),
188 dorsal premotor cortex (PMd), posterior insula and S2, and ipsilateral supramarginal gyrus (SMG).
189 The study thus demonstrated immediate involvement of motor cortices during steady pressure
190 stimulation.

191 Two fMRI studies evaluated static pressure stimulation applied over the right index fingertip using
192 an air-cuff^{85,86}. Stimulation evoked an extensive activation pattern including bilateral postcentral
193 gyrus (S1), S2, paracentral lobuli, insulae, ipsilateral dorsolateral precentral gyrus (M1), and
194 contralateral midcingulate gyrus⁸⁶. Subsequent dynamic connectivity modelling (DCM) revealed
195 that the intrahemispheric processing of the pressure stimuli employed both serial (from S1 to S2)
196 and parallel processing in the S1 and S2 (ref.⁸⁶). In the follow-up study, Chung et al. (ref.⁸⁵)
197 evaluated temporal evolution of the cortical activation during static sustained pressure stimulation
198 of the index fingertip applied over 3 to 15 s. On overall, they found most consistent activations in
199 the contralateral postcentral gyrus (S1), ipsilateral precentral gyrus (M1), bilateral S2, insulae,
200 cingulate cortices, thalami and cerebellum. Notably, they observed that activations differed
201 substantially depending on duration of stimulus and the time-window chosen and provided evidence
202 for gradual adaptation of the activated areas to stimulation.

203 However, several studies of sustained pressure finger stimulation reported much less extensive
204 activations restricted to somatosensory areas. Contralateral S1 and SMG activations were observed
205 in a small group of 8 subjects in response to air-cuff sustained 30-s pressure applied to one of the
206 four fingers: index, middle, ring, and little finger. A multivariate analysis found that activation in the
207 contralateral SMG encoded the stimulated finger locations (proximal vs. distal) (ref.⁸⁷). Another
208 study evaluated the effect of sustained pressure applied via a plastic piston to a thumb in 24 subjects
209 during a working memory n-back task. No effect on task performance was observed and imaging
210 data revealed pressure-related activation (contrast n-back with pressure vs. n-back without pressure)
211 again only in the contralateral S1 and S2, but motor activations could be masked by the required
212 button responses (ref.⁸⁸).

213 Several studies also evaluated pressure stimulation applied to lower limbs. In the first yet still
214 preliminary fMRI study, only limited activation in the primary sensorimotor cortex and bilateral S2
215 was observed during sustained 1 Hz sinusoidal pressure stimulation applied for 30 s to the foot
216 sole⁸⁹. In a follow-up fMRI study with twice as many participants (16), sustained right foot sole
217 stimulation evoked more widespread activations in the bilateral precentral, postcentral, middle and
218 superior frontal cortices, cingulate gyrus (CMA), and inferior parietal lobule (IPL) as well as in the

219 contralateral insula, temporal cortex, superior parietal lobule (SPL) (ref.⁹⁰). In an even bigger
220 sample (30 subjects), Miura et al. (ref.⁹¹) reported more circumscribed activation in the contralateral
221 S1, S2, M1, supplementary motor area (SMA), and ipsilateral cerebellum in response to
222 considerably shorter 5-s manual pressure stimuli applied over the base of the toes of either foot.

223 Further fMRI studies^{92,93} investigated central correlates of manual pressure applied over the lumbar
224 vertebrae in the prone position. Besides bilateral activation in the medial S1 and S2, insular and
225 cingulate cortices as well as cerebellum were significantly activated⁹³. Nevertheless, the roles of
226 cutaneous afferents from the limbs and trunk in motor control may be essentially different.

227 To summarise, non-therapeutic pressure stimulation of the fingers, foot sole, or lower back were
228 mostly associated with somatosensory cortical activity in the S1 and S2, and in sufficiently powered
229 studies, also with widespread sensorimotor activations including M1, SMA, posterior parietal
230 cortices, insulae and cerebellum. The differences among studies may be related not only to various
231 sample sizes, but also to different stimulus intensities, duration, tactile stimulus properties, attention
232 level, or differences in statistical analysis. The analytic approach seems to be especially important
233 since Chung et al. (ref.⁸⁵) demonstrated that canonical haemodynamic response function may be
234 insensitive to adapting cortical activations. An intriguing picture emerges when we contrast these
235 results with different stimulation modalities, such as mechanical vibration. The widespread
236 activation pattern observed in sufficiently powered focal pressure stimulation studies is consistent
237 with studies using rather broad-area vibrotactile stimulation^{94,95} or muscle stimulation^{96,97} and far
238 exceeds cortical maps of relatively circumscribed finger vibrotactile stimulation in other studies^{98–}
239 ¹⁰⁰. Though qualitatively different stimuli are not directly comparable, this illustrates that pressure
240 stimulation can be associated with robust motor activations that provide the neuroanatomical
241 substrate for sensorimotor interactions and motor after-effects of mechanical pressure stimulation.

242 However, as shown in vibration studies, sensorimotor activations are sensitive to modulation by
243 higher-order processes, such as attention and cognitive task demands¹⁰¹. This necessitates an
244 adequate control condition, e.g., a comparison between similar kinds of stimulation with or without
245 known motor consequences. Therefore, several functional imaging studies contrasted effects of
246 therapeutic stimulation according to Vojta^{26,27} with a sham stimulation^{12,13,18}. Sanz-Esteban et al.
247 (ref.¹⁸) applied pressure stimulus to an active site at the anterior thorax²⁶ and reported the main
248 effect of stimulation site (active versus control) in the ipsilateral putamen¹⁸. However, due to
249 unbalanced group sizes, a control stimulation site in a distant body part, and uncorrected statistical
250 thresholds, the conclusions that can be drawn are substantially limited.

251 In our fMRI study of sustained manual pressure stimulation¹³, we have compared an active lateral
252 heel site at the right foot²⁷ to a nearby control lateral ankle site in 30 healthy volunteers who
253 underwent two fMRI sessions according to a cross-over single-blinded randomised study design. To
254 more closely match the characteristic postural conditions and prolonged manual stimulation during
255 RLT (ref.^{26,27}), pressure was applied manually by an experienced therapist while the subjects were
256 lying in prone position. As we expected considerable adaptation of the blood oxygenation level-
257 dependent (BOLD) response⁸⁵, we have delivered the stimulation in irregularly spaced (jittered)
258 30-s blocks and utilized a flexible modelling approach using finite impulse response basis functions
259 to capture the dynamics of the BOLD signal during a 45-s time window. Subsequently, a clustering
260 algorithm was employed to classify individual clusters of significant signal change based on the
261 shape of the BOLD response and to identify both activations and deactivations associated with
262 stimulation. Our results showed that stimulation at both sites evoked widespread responses
263 throughout the sensorimotor system. Despite sustained though gradually somewhat decreasing
264 pressure, most of the clusters were characterized only by transient onset and offset responses that
265 could be classified into two anti-correlated sets of areas. Task-positive areas were found in the
266 bilateral S1, S2, contralateral M1, PMd (dorsomedial part), bilateral thalami, and left prefrontal
267 cortex. Task-negative areas were detected in the bilateral sensorimotor cortices and PMd
268 (dorsolateral part), medial occipital cortex (visual cortex), and SPL. In fact, some of the transient
269 deactivations in motor representations of non-stimulated limbs could explain apparent motor
270 activations observed in previous studies^{85,86}. If stimulated for sufficiently long time, BOLD
271 response rises again even above the baseline producing a “false” net activation increase. The
272 mechanisms behind deactivations are not yet completely understood. Even so, they should still be
273 considered when interpreting data involving prolonged stimulation¹³.

274 Our study also demonstrated some specific effects of stimulation according to RLT (ref.¹³). The
275 “active” stimulation site was additionally associated with a more sustained task-positive activation
276 in another set of brain areas. These included the bilateral insulo-opercular cortices and contralateral
277 pons. Quantitative differences between the two stimulation types (sites) were also assessed and
278 detected in the contralateral (left) IPL and M1.

279 Importantly, these differences were independent of pain/unpleasantness, which in turn, correlated
280 with activation difference in the contralateral SPL. Besides, our parallel study established that the
281 autonomic nervous system responses do not differ between the two stimulation types¹⁰². Our
282 imaging data thus demonstrated that manual pressure stimulation affects multiple brain structures
283 involved in motor control and that the choice of stimulation site impacts the shape (insulo-opercular

284 cortices and pons) and amplitude (contralateral M1 and IPL) of the blood oxygenation level-
285 dependent (BOLD) response in sensory and proper motor areas¹³.

286 In our second study¹², we have evaluated the motor sequelae of sustained manual pressure
287 stimulation. Using the same cross-over design, we investigated the changes in brain activation
288 during a complex hand motor task sequential finger opposition (SFO). Subjects performed auditory-
289 paced SFO with their right hand before and after 20 min of intermittent manual pressure (in total
290 12 min on stimulation) applied either to the heel (active site) or ankle (control site). A simple
291 repetition of the motor task regardless of the intervention site resulted in a widespread sensorimotor
292 and cross-modal activation decrease, possibly due to motor learning. An analysis of two-way
293 interaction between stimulation site and repetition revealed an effect in the contralateral
294 pontomedullary reticular formation (PMRF) and bilateral posterior cerebellum. Whereas after the
295 heel stimulation, activation in the PMRF/cerebellum increased, it decreased following sham
296 stimulation at the ankle¹². PMRF is known to modulate postural control¹⁰³, locomotion¹⁰⁴, possibly
297 by exerting anticipatory postural control¹⁰⁵, and even targeted limb movements¹⁰⁶ or finger
298 movements¹⁰⁷. Moreover, it has been shown to mediate complex asymmetrical motor patterns in
299 mammalian preparations^{104,107}, bearing some resemblance to involuntary motor behaviour elicited
300 during RLT (ref.^{26,27}). As we have seen involvement of nearby pontine areas also during the heel
301 (active) stimulation¹³, we have speculated that the PMRF may play a role in mediating (some of)
302 the therapeutic effects of RLT (ref.^{12,13}).

303 **SUMMARY AND FUTURE DIRECTIONS**

304 Though the research on central effects of peripheral pressure stimulation is not as rich and elaborate
305 as, for example, in the case of vibratory stimulation, available data from behavioural,
306 neurophysiological and neuroimaging studies, including our own works, clearly demonstrate that
307 the stimulation of peripheral afferents providing the sensation of sustained pressure may evoke
308 equally complex involuntary responses, affect postural control, improve motor performance,
309 locomotion, and facilitate neuroplastic changes of the motor cortical representations in the
310 experimental setting. Despite our recent successful efforts to localise some of the central structures
311 potentially involved in these effects, just as many new questions arose as have been answered. The
312 outstanding questions include the following:

- 313 1. What is the dynamic evolution of the cortico-subcortical activation patterns during
314 continuous application of specific forms of pressure stimulation, such as RLT? Given the
315 known slow development of responses^{27,53,72}, a time-resolved analysis of the so-called

316 dynamic connectivity¹⁰⁸ might prove useful for detection of slowly evolving states of brain
317 function and their correlation with behaviour. To permit this, detailed behavioural and
318 electrophysiological data (EMG) acquired simultaneously with fMRI are necessary
319 prerequisites since the time-courses of individual responses may vary significantly across
320 subjects. This might help us detect further brain structures which participate in these
321 processes only transiently or whose activity gradually builds up. Such activations might be
322 missed by classical approaches that effectively average the signal change across the whole
323 imaging run¹⁰⁸.

324 2. Can we identify the brain structures that mediate the motor improvement? With current
325 imaging data, unfortunately no. Follow-up studies with well-defined outcome measures of
326 motor performance, both in healthy controls and patients with motor system disorders, are
327 warranted. Only then may improved performance or alleviated symptoms be directly linked
328 to the involved brain structure. This is of paramount importance because such studies could
329 finally draw clinically relevant conclusions, such as predictions of outcomes according to
330 baseline fMRI data. Furthermore, by knowing the structures that are related to improvement,
331 we may identify candidates for potential interventions that either enhance the effect of
332 peripheral stimulation or interfere with it, such as repetitive TMS or transcranial direct
333 current stimulation (tDCS), eventually providing real-life causal data.

334 3. Knowing the cortical area or nuclei engaged by stimulation might not be enough to fully
335 appreciate the brain network(s) underlying the motor after-effects and to understand
336 interactions among the network nodes. Therefore, the next question is what are the pathways
337 connecting the individual nodes, either those identified as potential sources of involuntary
338 motor behaviour or those associated with motor after-effects (e.g., PMRF in RLT)? By
339 evaluating diffusion-weighted imaging (DWI) data, one could identify the connecting
340 pathways between these nodes to establish a task-specific connectome. With the knowledge
341 of the network topology, modelling of causal relationships (i.e., effective connectivity)
342 would be possible. Accurate network models might then serve as predictors of behavioural
343 and clinical outcomes of various interventions.

344 4. Finally, knowing that muscle vibration research has demonstrated divergent results in
345 different muscle groups^{10,79} and study populations⁸³, the effects of pressure stimulation on
346 corticomotor excitability should be studied using multiple stimulation sites and in patient
347 cohorts with evidence of abnormal sensorimotor processing, such as dystonia⁸³. Likewise,
348 patient populations, where RLT is routinely applied to alleviate neurological abnormalities

349 (e.g., spasticity after stroke or in multiple sclerosis³⁷), would be candidates for studies
350 correlating possible clinical improvement with cortical excitability changes.

351 To summarize, pressure stimulation is a viable and widely used modality of peripheral stimulation
352 in the clinical setting. Whereas other stimulation modalities, such as vibration, have already
353 attracted a high amount of research interest and much evidence has been now gathered using state-
354 of-the-art imaging techniques, allowing researchers to postulate fairly concrete hypotheses, similar
355 research of pressure stimulation has barely entered the initial exploratory stage. We have
356 highlighted recent evidence showing involvement of brainstem and cortical structures that
357 potentially mediate some of the peculiar effects observed during sustained mechanical pressure
358 stimulation. Inspired by the latest development, we propose future directions to shed more light on
359 these phenomena.

360 **SEARCH STRATEGY AND SELECTION CRITERIA**

361 Our review of the available literature pertaining innocuous pressure stimulation focused on
362 transcranial magnetic stimulation (TMS) and neuroimaging studies including both human
363 experimental studies in healthy subjects and clinical trials as well as secondary sources. Scientific
364 articles from 1950 to 2020 were searched using the PubMed and Web of Science databases, results
365 were up to date as of March 2020. The main search terms used included '(PET OR fMRI) AND
366 (skin OR cutaneous OR peripheral OR manual OR tactile) AND ("pressure stimulation" OR
367 ("tactile stimulation" AND pressure))'; 'TMS AND (skin OR cutaneous OR peripheral OR manual
368 OR tactile) AND ("pressure stimulation" OR ("tactile stimulation" AND pressure))'; ("Vojta
369 therapy" OR "Vojta physiotherapy" OR "reflex locomotion" OR "Vojta method" OR "Vojta") AND
370 (PET OR fMRI)); and ("Vojta therapy" OR "Vojta physiotherapy" OR "reflex locomotion" OR
371 "Vojta method" OR "Vojta") AND TMS'. Studies investigating only noxious pressure stimulation
372 were discarded. To provide historical perspective, non-English literature on reflex locomotion
373 therapy was included, whereas the database search only considered English language original
374 research papers and reviews. Relevant secondary cited sources were included as well.

375 **AUTHOR CONTRIBUTIONS**

376 P. Hok: literature search, manuscript writing and revision; P. Hlustik: conception and design of the
377 work, manuscript writing and revision. Both authors have read and approved the final version of the
378 manuscript.

379 **CONFLICT OF INTEREST STATEMENT**

380 The authors state that there are no conflicts of interest regarding the publication of this article.

381 **ACKNOWLEDGEMENTS**

382 This work was supported by the Czech Science Foundation (GACR) (Grant No. 14-22572S) and
383 Ministry of Health, Czechia – conceptual development of research organization (Grant No. FNOI,
384 00098892).

REFERENCES

1. Mott FW, Sherrington CS. Experiments upon the influence of sensory nerves upon movement and nutrition of the limbs. Preliminary communication. *Proc R Soc Lond* 1895;57(340–346):481–8.
2. Pavlides C, Miyashita E, Asanuma H. Projection from the sensory to the motor cortex is important in learning motor skills in the monkey. *J Neurophysiol* 1993;70(2):733–41.
3. Sakamoto T, Porter LL, Asanuma H. Long-lasting potentiation of synaptic potentials in the motor cortex produced by stimulation of the sensory cortex in the cat: a basis of motor learning. *Brain Res* 1987;413(2):360–4. [https://doi.org/10.1016/0006-8993\(87\)91029-8](https://doi.org/10.1016/0006-8993(87)91029-8).
4. Ridding MC, McKay DR, Thompson PD, Miles TS. Changes in corticomotor representations induced by prolonged peripheral nerve stimulation in humans. *Clin Neurophysiol* 2001;112(8):1461–9.
5. Powell J, Pandyan AD, Granat M, Cameron M, Stott DJ. Electrical stimulation of wrist extensors in poststroke hemiplegia. *Stroke* 1999;30(7):1384–9.
6. Sherrington CS. Lecture II: Co-ordination in the simple reflex (continued). In: *Integr. Action Nerv. Syst.* New Haven, CT, US: Yale University Press; 1906;36–69. <https://doi.org/10.1037/13798-002>.
7. Chipchase LS, Schabrun SM, Hodges PW. Peripheral electrical stimulation to induce cortical plasticity: a systematic review of stimulus parameters. *Clin Neurophysiol* 2011;122(3):456–63. <https://doi.org/10.1016/j.clinph.2010.07.025>.
8. Proke U, Gandevia SC. Kinesthetic Senses. *Compr Physiol* 2018;8(3):1157–83. <https://doi.org/10.1002/cphy.c170036>.
9. Proke U, Gandevia SC. The proprioceptive senses: their roles in signaling body shape, body position and movement, and muscle force. *Physiol Rev* 2012;92(4):1651–97. <https://doi.org/10.1152/physrev.00048.2011>.
10. Souron R, Besson T, Millet GY, Lapole T. Acute and chronic neuromuscular adaptations to local vibration training. *Eur J Appl Physiol* 2017;117(10):1939–64. <https://doi.org/10.1007/s00421-017-3688-8>.
11. Hok P. Modulation and plasticity of the sensorimotor brain networks during afferent stimulation. Dissertation thesis. Palacký University Olomouc, in preparation.
12. Hok P, Opavský J, Kutín M, Tüdös Z, Kaňovský P, Hluštík P. Modulation of the sensorimotor system by sustained manual pressure stimulation. *Neuroscience* 2017;348:11–22. <https://doi.org/10.1016/j.neuroscience.2017.02.005>.
13. Hok P, Opavský J, Labounek R, Kutín M, Šlachtová M, Tüdös Z, Kaňovský P, Hluštík P. Differential Effects of Sustained Manual Pressure Stimulation According to Site of Action. *Front Neurosci* 2019;13:722. <https://doi.org/10.3389/fnins.2019.00722>.
14. Wong JJ, Shearer HM, Mior S, Jacobs C, Côté P, Randhawa K, Yu H, Southerst D, Varatharajan S, Sutton D, van der Velde G, Carroll LJ, Ameis A, Ammendolia C, Brisson R, Nordin M, Stupar M, Taylor-Vaisey A. Are manual therapies, passive physical modalities, or acupuncture effective for the management of patients with whiplash-associated disorders or neck pain and associated disorders? An update of the Bone and Joint Decade Task Force on Neck Pain and Its Associated Disorders by the OPTIMA collaboration. *Spine J Off J North Am Spine Soc* 2016;16(12):1598–630. <https://doi.org/10.1016/j.spinee.2015.08.024>.

15. Smith CA, Levett KM, Collins CT, Dahlen HG, Ee CC, Sukanuma M. Massage, reflexology and other manual methods for pain management in labour. *Cochrane Database Syst Rev* 2018;3:CD009290. <https://doi.org/10.1002/14651858.CD009290.pub3>.
16. Vojta V, Peters A. *Das Vojta-Prinzip: Muskelspiele in Reflexfortbewegung und motorischer Ontogenese*. 3., vollst. überarb. Aufl. Berlin: Springer; 2007.
17. Baliki MN, Apkarian AV. Nociception, Pain, Negative Moods, and Behavior Selection. *Neuron* 2015;87(3):474–91. <https://doi.org/10.1016/j.neuron.2015.06.005>.
18. Sanz-Esteban I, Calvo-Lobo C, Ríos-Lago M, Álvarez-Linera J, Muñoz-García D, Rodríguez-Sanz D. Mapping the human brain during a specific Vojta's tactile input: the ipsilateral putamen's role. *Medicine (Baltimore)* 2018;97(13):e0253. <https://doi.org/10.1097/MD.00000000000010253>.
19. Abraira VE, Ginty DD. The sensory neurons of touch. *Neuron* 2013;79(4):618–39. <https://doi.org/10.1016/j.neuron.2013.07.051>.
20. Johansson RS, Flanagan JR. Coding and use of tactile signals from the fingertips in object manipulation tasks. *Nat Rev Neurosci* 2009;10(5):345–59. <https://doi.org/10.1038/nrn2621>.
21. Aimonetti J-M, Hospod V, Roll J-P, Ribot-Ciscar E. Cutaneous afferents provide a neuronal population vector that encodes the orientation of human ankle movements. *J Physiol* 2007;580(Pt 2):649–58. <https://doi.org/10.1113/jphysiol.2006.123075>.
22. Edin BB, Abbs JH. Finger movement responses of cutaneous mechanoreceptors in the dorsal skin of the human hand. *J Neurophysiol* 1991;65(3):657–70. <https://doi.org/10.1152/jn.1991.65.3.657>.
23. McGlone F, Reilly D. The cutaneous sensory system. *Neurosci Biobehav Rev* 2010;34(2):148–59. <https://doi.org/10.1016/j.neubiorev.2009.08.004>.
24. Omrani M, Kaufman MT, Hatsopoulos NG, Cheney PD. Perspectives on classical controversies about the motor cortex. *J Neurophysiol* 2017;118(3):1828–48. <https://doi.org/10.1152/jn.00795.2016>.
25. Bauer J. Das Kriechphänomen des Neugeborenen. *J Mol Med* 1926;5(32):1468.
26. Vojta V. [Reflex rotation as a pathway to human locomotion]. *Z Für Orthop Ihre Grenzgeb* 1970;108(3):446–52.
27. Vojta V. [Reflex creeping as an early rehabilitation programme]. *Z Für Kinderheilkd* 1968;104(4):319–30. <https://doi.org/10.1007/BF00440004>.
28. Bauer H, Appaji G, Mundt D. VOJTA neurophysiologic therapy. *Indian J Pediatr* 1992;59(1):37–51.
29. Vojta V. The basic elements of treatment according to Vojta. In: *Manag. Mot. Disord. Child. Cereb. Palsy*. Cambridge University Press; 1984;75–85.
30. Vojta V. [Early diagnosis and therapy of cerebral movement disorders in childhood. C. Reflexogenous locomotion - reflex creeping and reflex turning. C1. The kinesiological content and connection with the tonic neck reflexes]. *Z Für Orthop Ihre Grenzgeb* 1973;111(3):268–91.
31. Vojta V. Plazení v rehabilitaci hybných poruch u dětí. *Českoslov Neurol Neurochir Časopis Neurol Spol* 1966;29(4):234–9.
32. Gajewska E, Huber J, Kulczyk A, Lipiec J, Sobieska M. An attempt to explain the Vojta therapy mechanism of action using the surface polyelectromyography in healthy subjects: A pilot study. *J Bodyw Mov Ther* 2018;22(2):287–92. <https://doi.org/10.1016/j.jbmt.2017.07.002>.
33. Giannantonio C, Papacci P, Ciarniello R, Tesfagabir MG, Purcaro V, Cota F, Semeraro CM, Romagnoli C. Chest physiotherapy in preterm infants with lung diseases. *Ital J Pediatr* 2010;36:65. <https://doi.org/10.1186/1824-7288-36-65>.
34. Juárez-Albuijch ML, Redondo-González O, Tello I, Collado-Vázquez S, Jiménez-Antona C. Vojta Therapy versus transcutaneous electrical nerve stimulation for lumbosciatica syndrome:

- A quasi-experimental pilot study. *J Bodyw Mov Ther* 2020;24(1):39–46. <https://doi.org/10.1016/j.jbmt.2019.05.015>.
35. Jung MW, Landenberger M, Jung T, Lindenthal T, Philippi H. Vojta therapy and neurodevelopmental treatment in children with infantile postural asymmetry: a randomised controlled trial. *J Phys Ther Sci* 2017;29(2):301–6. <https://doi.org/10.1589/jpts.29.301>.
 36. Kiebzak W, Kowalski IM, Domagalska M, Szopa A, Dwornik M, Kujawa J, Stępień A, Śliwiński Z. Assessment of visual perception in adolescents with a history of central coordination disorder in early life – 15-year follow-up study. *Arch Med Sci AMS* 2012;8(5):879–85. <https://doi.org/10.5114/aoms.2012.28638>.
 37. Laufens G, Poltz W, Prinz E, Reimann G, Schmiegelt F. Alternating treadmill-Vojta-treadmill-therapy in patients with multiple sclerosis with severely affected gait. *Phys Med Rehabil Kurortmed* 2004;14(3):134–9. <https://doi.org/10.1055/s-2003-814921>.
 38. Meholjić-Fetahović A. Treatment of the spasticity in children with cerebral palsy. *Bosn J Basic Med Sci Udruženje Basičnih Med Znan Assoc Basic Med Sci* 2007;7(4):363–7.
 39. Pavlikova M, Cattaneo D, Jonsdottir J, Gervasoni E, Stetkarova I, Angelova G, Markova M, Prochazkova M, Prokopiusova T, Hruskova N, Reznickova J, Zimova D, Spanhelova S, Rasova K. The impact of balance specific physiotherapy, intensity of therapy and disability on static and dynamic balance in people with multiple sclerosis: A multi-center prospective study. *Mult Scler Relat Disord* 2020;40:101974. <https://doi.org/10.1016/j.msard.2020.101974>.
 40. Kanda T, Pidcock FS, Hayakawa K, Yamori Y, Shikata Y. Motor outcome differences between two groups of children with spastic diplegia who received different intensities of early onset physiotherapy followed for 5 years. *Brain Dev* 2004;26(2):118–26. [https://doi.org/10.1016/S0387-7604\(03\)00111-6](https://doi.org/10.1016/S0387-7604(03)00111-6).
 41. Lim H, Kim T. Effects of vojta therapy on gait of children with spastic diplegia. *J Phys Ther Sci* 2013;25(12):1605–8. <https://doi.org/10.1589/jpts.25.1605>.
 42. Bobath K. The effect of treatment by reflex-inhibition and facilitation of movement in cerebral palsy. *Folia Psychiatr Neurol Neurochir Neerlandica* 1959;62:448–57.
 43. Fay T. Rehabilitation of patients with spastic paralysis. *J Int Coll Surg* 1954;22(2:1):200–3.
 44. Fay T. The use of pathological and unlocking reflexes in the rehabilitation of spastics. *Am J Phys Med* 1954;33(6):347–52.
 45. Kabat H. 12. Proprioceptive Facilitation. In: *Ther. Exerc.* Baltimore: Waverly Press; 1958;
 46. Magnus R, de Kleijn A. Die Abhängigkeit des Tonus der Extremitätenmuskeln von der Kopfstellung. *Pflüg Arch Eur J Physiol* 1912;145(10):455–548. <https://doi.org/10.1007/BF01681127>.
 47. Peiper A. *Die Eigenart der kindlichen Hirntätigkeit.* Leipzig: Thieme; 1956.
 48. Vojta V. [Reflex inhibition of spasticity in perinatal encephalopathy by means of voluntary movement using ontogenetically old structural movements]. *Ceskoslovenská Neurol* 1964;27:329–40.
 49. Hellebrandt FAM, Schade MMS, Carns MLMD. Methods of evoking the tonic neck reflexes in normal human subjects. *J Phys Med* 1962;41(3):90–139.
 50. Hooker D. The Origin of the Grasping Movement in Man. *Proc Am Philos Soc* 1938;(4):597.
 51. Vojta V. [Early diagnosis and therapy of cerebral motor disorders in childhood. A. Postural reflexes in developmental kinesiology. 3. Pathological reflexes from the aspects of tonic neck reflexes and tonic labyrinthine reflexes]. *Z Für Orthop Ihre Grenzgeb* 1972;110(4):467–76.
 52. Zafeiriou DI. Primitive reflexes and postural reactions in the neurodevelopmental examination. *Pediatr Neurol* 2004;31(1):1–8. <https://doi.org/10.1016/j.pediatrneurol.2004.01.012>.
 53. Bauer H, van de Lint A, Soerjanto R, Vojta V. Kinesiologische EMG-Untersuchung bei Zerebralparese-Reflexlokomotion nach Vojta. In: Weinmann H-M, ed. *Aktuelle Neuropädiatr.* 1988. 1st ed. Berlin: Springer; 1988;182–5.
 54. Bauer H, Vojta V. [Rehabilitation in meningomyelodysplasias]. *Monatsschrift Für*

- Kinderheilkd 1979;127(5):351–3.
55. Laufens G, Poltz W, Jugelt E, Prinz E, Reimann G, Van Slobbe T. Motor improvements in multiple-sclerosis patients by Vojta physiotherapy and the influence of treatment positions. *Phys Med Rehabil Kurortmed* 1995;5(4):115–9.
 56. Tomi M. Zur Früherkennung und Frühbehandlung bei Kindern mit cerebralen Bewegungsstörungen in Japan. In: *Entwicklungsrehabilitation Behindertenhilfe Jpn. Bundesrepub. Dtschl. Lübeck: Hansisches Verlagskontor; 1985;35–52.*
 57. Vojta V. [Early diagnosis and therapy of cerebral movement disorders in childhood. C. Reflexogenous locomotion - reflex creeping and reflex turning. C2. Its use in 207 risk children. Analysis of the final results]. *Z Für Orthop Ihre Grenzgeb* 1973;111(3):292–309.
 58. Fulton JF. *Physiology of the nervous system.* New York: Oxford Univ. Press; 1949.
 59. Rushworth G. The Nature of the Functional Disorder in the Hypertonic States. *Cereb Palsy Bull* 1959;1(7):3–7.
 60. Windle WF. An experimental approach to prevention or reduction of the brain damage of birth asphyxia. *Dev Med Child Neurol* 1966;8(2):129–40.
 61. Vojta V. [Rehabilitation of the spastic infantile syndrome. Personal methodology]. *Beitr Zur Orthop Traumatol* 1965;12(9):557–62.
 62. Kavounoudias A, Roll R, Roll J-P. Foot sole and ankle muscle inputs contribute jointly to human erect posture regulation. *J Physiol* 2001;532(Pt 3):869–78.
<https://doi.org/10.1111/j.1469-7793.2001.0869e.x>.
 63. Rasman BG, Forbes PA, Tisserand R, Blouin J-S. Sensorimotor Manipulations of the Balance Control Loop—Beyond Imposed External Perturbations. *Front Neurol* 2018;9.
<https://doi.org/10.3389/fneur.2018.00899>.
 64. Gurfinkel VS, Levik YuS, Kazennikov OV, Selionov VA. Locomotor-like movements evoked by leg muscle vibration in humans. *Eur J Neurosci* 1998;10(5):1608–12.
<https://doi.org/10.1046/j.1460-9568.1998.00179.x>.
 65. Smetanin BN, Popov KYe, Shlykov VYu. Postural responses to vibrostimulation of the neck muscle proprioceptors in man. *Neurophysiology* 1993;25(2):86–92.
<https://doi.org/10.1007/BF01054155>.
 66. Vojta V. [Early diagnosis and therapy of cerebral motor disorders in childhood. A. Postural reflexes in developmental kinesiology. 2. Pathologic reactions]. *Z Für Orthop Ihre Grenzgeb* 1972;110(4):458–66.
 67. Grillner S. Locomotion in vertebrates: central mechanisms and reflex interaction. *Physiol Rev* 1975;55(2):247–304.
 68. Grillner S, Wallén P. Central pattern generators for locomotion, with special reference to vertebrates. *Annu Rev Neurosci* 1985;8:233–61.
<https://doi.org/10.1146/annurev.ne.08.030185.001313>.
 69. Laufens G, Seitz S, Staenicke G. Vergleichend biologische Grundlagen zur angeborenen Lokomotion insbesondere zum “reflektorischen Kriechen” nach Vojta. *Krankengymnast Z Für Physiother* 1991;43(5):448–56.
 70. Hongo T, Kudo N, Oguni E, Yoshida K. Spatial patterns of reflex evoked by pressure stimulation of the foot pads in cats. *J Physiol* 1990;420:471–87.
 71. D’Ascanio P, Gahéry Y, Pompeiano O, Stampacchia G. Effects of pressure stimulation of the body surface on posture and vestibulospinal reflexes. *Arch Ital Biol* 1986;124(1):43–63.
 72. Laufens G, Poltz W, Reimann G, Seitz S. Physiological mechanisms in Vojta-physiotherapy for MS-patients. *Phys Med Rehabil Kurortmed* 1994;4(1):1–4.
 73. Čemusová J, Pánek D, Pavlů D. Možnosti propojení aktivního a pasivního přístupu ve fyzioterapii. *Rehabil Fyzikální Lékařství* 2011;18(4):161–6.
 74. Kujirai T, Caramia MD, Rothwell JC, Day BL, Thompson PD, Ferbert A, Wroe S, Asselman P, Marsden CD. Corticocortical inhibition in human motor cortex. *J Physiol* 1993;471:501–19.

75. Christova M, Rafolt D, Golaszewski S, Gallasch E. Outlasting corticomotor excitability changes induced by 25 Hz whole-hand mechanical stimulation. *Eur J Appl Physiol* 2011;111(12):3051–9. <https://doi.org/10.1007/s00421-011-1933-0>.
76. Golaszewski SM, Bergmann J, Christova M, Kunz AB, Kronbichler M, Rafolt D, Gallasch E, Staffen W, Trinka E, Nardone R. Modulation of motor cortex excitability by different levels of whole-hand afferent electrical stimulation. *Clin Neurophysiol Off J Int Fed Clin Neurophysiol* 2012;123(1):193–9. <https://doi.org/10.1016/j.clinph.2011.06.010>.
77. Golaszewski SM, Bergmann J, Christova M, Nardone R, Kronbichler M, Rafolt D, Gallasch E, Staffen W, Ladurner G, Beisteiner R. Increased motor cortical excitability after whole-hand electrical stimulation: a TMS study. *Clin Neurophysiol Off J Int Fed Clin Neurophysiol* 2010;121(2):248–54. <https://doi.org/10.1016/j.clinph.2009.09.024>.
78. Ridding MC, Rothwell JC. Afferent input and cortical organisation: a study with magnetic stimulation. *Exp Brain Res* 1999;126(4):536–44. <https://doi.org/10.1007/s002210050762>.
79. Rosenkranz K, Rothwell JC. Differences between the effects of three plasticity inducing protocols on the organization of the human motor cortex. *Eur J Neurosci* 2006;23(3):822–9. <https://doi.org/10.1111/j.1460-9568.2006.04605.x>.
80. Hok P, Nevrlý M, Otruba P, Valošek J, Trnečková M, Kutín M, Opavský J, Kaňovský P, Hlušík P. Decreased intracortical inhibition after peripheral manual pressure stimulation in preparation.
81. Ziemann U, Lönnecker S, Steinhoff BJ, Paulus W. Effects of antiepileptic drugs on motor cortex excitability in humans: a transcranial magnetic stimulation study. *Ann Neurol* 1996;40(3):367–78. <https://doi.org/10.1002/ana.410400306>.
82. Jacobs KM, Donoghue JP. Reshaping the cortical motor map by unmasking latent intracortical connections. *Science* 1991;251(4996):944–7. <https://doi.org/10.1126/science.2000496>.
83. Rosenkranz K, Williamon A, Butler K, Cordivari C, Lees AJ, Rothwell JC. Pathophysiological differences between musician's dystonia and writer's cramp. *Brain J Neurol* 2005;128(Pt 4):918–31. <https://doi.org/10.1093/brain/awh402>.
84. Bodegård A, Geyer S, Herath P, Grefkes C, Zilles K, Roland PE. Somatosensory areas engaged during discrimination of steady pressure, spring strength, and kinesthesia. *Hum Brain Mapp* 2003;20(2):103–15. <https://doi.org/10.1002/hbm.10125>.
85. Chung YG, Han SW, Kim H-S, Chung S-C, Park J-Y, Wallraven C, Kim S-P. Adaptation of cortical activity to sustained pressure stimulation on the fingertip. *BMC Neurosci* 2015;16:71. <https://doi.org/10.1186/s12868-015-0207-x>.
86. Chung YG, Han SW, Kim H-S, Chung S-C, Park J-Y, Wallraven C, Kim S-P. Intra- and inter-hemispheric effective connectivity in the human somatosensory cortex during pressure stimulation. *BMC Neurosci* 2014;15:43. <https://doi.org/10.1186/1471-2202-15-43>.
87. Kim J, Chung YG, Chung S-C, Bühlhoff HH, Kim S-P. Decoding pressure stimulation locations on the fingers from human neural activation patterns. *Neuroreport* 2016;27(16):1232–6. <https://doi.org/10.1097/WNR.0000000000000683>.
88. Dehghan Nayyeri M, Burgmer M, Pfeleiderer B. Impact of pressure as a tactile stimulus on working memory in healthy participants. *PLoS One* 2019;14(3):e0213070. <https://doi.org/10.1371/journal.pone.0213070>.
89. Hao Y, Manor B, Liu J, Zhang K, Chai Y, Lipsitz L, Peng C-K, Novak V, Wang X, Zhang J, Fang J. A Novel MRI-compatible Tactile Stimulator for Cortical Mapping of Foot Sole Pressure Stimuli with fMRI. *Magn Reson Med Off J Soc Magn Reson Med Soc Magn Reson Med* 2013;69(4):1194–9. <https://doi.org/10.1002/mrm.24330>.
90. Wang Y, Hao Y, Zhou J, Fried PJ, Wang X, Zhang J, Fang J, Pascual-Leone A, Manor B. Direct current stimulation over the human sensorimotor cortex modulates the brain's hemodynamic response to tactile stimulation. *Eur J Neurosci* 2015;42(3):1933–40. <https://doi.org/10.1111/ejn.12953>.

91. Miura N, Akitsuki Y, Sekiguchi A, Kawashima R. Activity in the primary somatosensory cortex induced by reflexological stimulation is unaffected by pseudo-information: a functional magnetic resonance imaging study. *BMC Complement Altern Med* 2013;13:114. <https://doi.org/10.1186/1472-6882-13-114>.
92. Boendermaker B, Meier ML, Luechinger R, Humphreys BK, Hotz-Boendermaker S. The cortical and cerebellar representation of the lumbar spine. *Hum Brain Mapp* 2014;35(8):3962–71. <https://doi.org/10.1002/hbm.22451>.
93. Meier ML, Hotz-Boendermaker S, Boendermaker B, Luechinger R, Humphreys BK. Neural responses of posterior to anterior movement on lumbar vertebrae: a functional magnetic resonance imaging study. *J Manipulative Physiol Ther* 2014;37(1):32–41. <https://doi.org/10.1016/j.jmpt.2013.09.004>.
94. Golaszewski SM, Siedentopf CM, Koppelstaetter F, Fend M, Ischebeck A, Gonzalez-Felipe V, Haala I, Struhal W, Mottaghy FM, Gallasch E, Felber SR, Gerstenbrand F. Human brain structures related to plantar vibrotactile stimulation: a functional magnetic resonance imaging study. *NeuroImage* 2006;29(3):923–9. <https://doi.org/10.1016/j.neuroimage.2005.08.052>.
95. Siedentopf CM, Heubach K, Ischebeck A, Gallasch E, Fend M, Mottaghy FM, Koppelstaetter F, Haala IA, Krause BJ, Felber S, Gerstenbrand F, Golaszewski SM. Variability of BOLD response evoked by foot vibrotactile stimulation: influence of vibration amplitude and stimulus waveform. *NeuroImage* 2008;41(2):504–10. <https://doi.org/10.1016/j.neuroimage.2008.02.049>.
96. Naito E, Nakashima T, Kito T, Aramaki Y, Okada T, Sadato N. Human limb-specific and non-limb-specific brain representations during kinesthetic illusory movements of the upper and lower extremities. *Eur J Neurosci* 2007;25(11):3476–87. <https://doi.org/10.1111/j.1460-9568.2007.05587.x>.
97. Naito E, Roland PE, Grefkes C, Choi HJ, Eickhoff S, Geyer S, Zilles K, Ehrsson HH. Dominance of the right hemisphere and role of area 2 in human kinesthesia. *J Neurophysiol* 2005;93(2):1020–34. <https://doi.org/10.1152/jn.00637.2004>.
98. Francis ST, Kelly EF, Bowtell R, Dunseath WJR, Folger SE, McGlone F. fMRI of the Responses to Vibratory Stimulation of Digit Tips. *NeuroImage* 2000;11(3):188–202. <https://doi.org/10.1006/nimg.2000.0541>.
99. Gelnar PA, Krauss BR, Szeverenyi NM, Apkarian AV. Fingertip representation in the human somatosensory cortex: an fMRI study. *NeuroImage* 1998;7(4 Pt 1):261–83. <https://doi.org/10.1006/nimg.1998.0341>.
100. Kim J, Chung YG, Chung S-C, Bulthoff HH, Kim S-P. Neural Categorization of Vibrotactile Frequency in Flutter and Vibration Stimulations: An fMRI Study. *IEEE Trans Haptics* 2016;9(4):455–64. <https://doi.org/10.1109/TOH.2016.2593727>.
101. Albanese M-C, Duerden EG, Bohotin V, Rainville P, Duncan GH. Differential effects of cognitive demand on human cortical activation associated with vibrotactile stimulation. *J Neurophysiol* 2009;102(3):1623–31. <https://doi.org/10.1152/jn.91295.2008>.
102. Opavský J, Šlachtová M, Kutín M, Hok P, Uhlíř P, Opavská H, Hlušík P. The effects of sustained manual pressure stimulation according to Vojta Therapy on heart rate variability. *Biomed Pap Med Fac Univ Palacky Olomouc Czechoslov* 2018;162(3):206–11. <https://doi.org/10.5507/bp.2018.028>.
103. Stapley PJ, Drew T. The Pontomedullary Reticular Formation Contributes to the Compensatory Postural Responses Observed Following Removal of the Support Surface in the Standing Cat. *J Neurophysiol* 2009;101(3):1334–50. <https://doi.org/10.1152/jn.91013.2008>.
104. Dyson KS, Miron J-P, Drew T. Differential modulation of descending signals from the reticulospinal system during reaching and locomotion. *J Neurophysiol* 2014;112(10):2505–28. <https://doi.org/10.1152/jn.00188.2014>.
105. Takakusaki K. Neurophysiology of gait: From the spinal cord to the frontal lobe. *Mov Disord*

- 2013;28(11):1483–91. <https://doi.org/10.1002/mds.25669>.
106. Schepens B, Drew T. Independent and convergent signals from the pontomedullary reticular formation contribute to the control of posture and movement during reaching in the cat. *J Neurophysiol* 2004;92(4):2217–38. <https://doi.org/10.1152/jn.01189.2003>.
 107. Hirschauer TJ, Buford JA. Bilateral force transients in the upper limbs evoked by single-pulse microstimulation in the pontomedullary reticular formation. *J Neurophysiol* 2015;113(7):2592–604. <https://doi.org/10.1152/jn.00852.2014>.
 108. Calhoun VD, Miller R, Pearlson G, Adalı T. The chronnectome: time-varying connectivity networks as the next frontier in fMRI data discovery. *Neuron* 2014;84(2):262–74. <https://doi.org/10.1016/j.neuron.2014.10.015>.

6. Annex 6

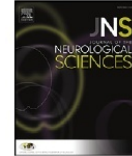
Journal of the Neurological Sciences 346 (2014) 276–283



Contents lists available at ScienceDirect

Journal of the Neurological Sciences

journal homepage: www.elsevier.com/locate/jns



Cortical activity modulation by botulinum toxin type A in patients with post-stroke arm spasticity: Real and imagined hand movement



Tomáš Veverka^{a,*}, Petr Hlušík^{a,c}, Pavel Hok^a, Pavel Otruba^a, Zbyněk Tüdös^c, Jana Zapletalová^d, Alois Krobot^b, Petr Kaňovský^a

^a Department of Neurology, Faculty of Medicine and Dentistry, Palacký University and University Hospital, Olomouc, Czech Republic

^b Department of Physiotherapy, Faculty of Medicine and Dentistry, Palacký University and University Hospital, Olomouc, Czech Republic

^c Department of Radiology, Faculty of Medicine and Dentistry, Palacký University and University Hospital, Olomouc, Czech Republic

^d Department of Biophysics, Biometry and Statistics, Faculty of Medicine and Dentistry, Palacký University and University Hospital, Olomouc, Czech Republic

ARTICLE INFO

Article history:

Received 8 July 2014

Received in revised form 4 September 2014

Accepted 8 September 2014

Available online 16 September 2014

Keywords:

Stroke

Hand weakness

Spasticity

Botulinum toxin

Functional magnetic resonance imaging

Neuronal plasticity

ABSTRACT

Background: Our aim was to use functional magnetic resonance imaging (fMRI) to compare brain activation changes due to botulinum toxin A (BoNT) application between two chronic stroke patient groups with different degree of weakness treated for upper limb spasticity.

Methods: Fourteen ischemic stroke patients with hand weakness and spasticity were studied. Spasticity was scored by modified Ashworth scale (MAS). fMRI was performed 3 times: before (W0) and 4 (W4) and 11 weeks (W11) after BoNT application. Group A: 7 patients (2 males, 5 females; mean age 59.14 years) with hand plegia, who imagined moving fingers. Group B: 7 age-matched patients (6 males, 1 female; mean age 59.57 years) able to perform sequential finger movement.

Results: BoNT transiently lowered MAS in W4 in both groups. In group A, activation of the frontal premotor cortex dominated and persisted for all three fMRI sessions whereas the ipsilesional cerebellum and cortex bordering bilateral intraparietal sulcus activation changed over time. Between-session contrasts showed treatment-related activation decreases in the mesial occipitoparietal and lateral occipital cortex. In group B, brain activation was markedly reduced after BoNT (W4). Whereas some of these areas manifested only transient reduction and expanded again at W11, in others the reduction persisted.

Conclusion: Study of two age-matched groups with mild and severe weakness demonstrated different effects of BoNT-lowered spasticity on sensorimotor networks. Group A performing movement imagery manifested BoNT-induced reduction of activation in structures associated with visual imagery. Group B performing movement manifested reduced activation extent and reduced activation of structures outside classical motor system, suggestive of motor network normalization.

© 2014 Elsevier B.V. All rights reserved.

1. Introduction

Stroke is the leading cause of disability worldwide and one of the most common causes of death [27]. Despite the progress in the stroke management, a majority of stroke survivors experience motor deficit with impaired function of upper extremity [21]. Ischemic lesion of pyramidal and parapyramidal tracts cause upper motoneuron syndrome (UMS) [38]. Negative signs (weakness, loss of dexterity) of UMS are crucial in determining the degree of movement deficit [22]. Nevertheless positive signs of UMS (especially spasticity) may play an important role. By Lance's historical definition, spasticity is a motor disorder characterized by a velocity-dependent increase in tonic stretch reflexes with exaggerated tendon jerks resulting from hyperexcitability of the

stretch reflex [26]. Spasticity prevalence estimates range from 19% to 42.6% in stroke survivors [43,46]. It is generally recognized that poststroke spasticity (PSS) may interfere with voluntary movement [31]. Disability associated with PSS may undoubtedly affect patient's quality of life, increase caregiver and socioeconomic burden [57]. Current multidisciplinary approach to relieve focal spasticity combines physiotherapy with botulinum toxin A (BoNT-A) application. Numerous clinical trials have shown that BoNT-A is safe and effective way to reduce upper limb PSS [44,52]. Although BoNT-A acts primarily on muscle spindles there is growing evidence that BoNT-A also exerts central (remote) effects. BoNT-A affects intrafusal fibers as well as extrafusal ones and thus alters abnormal sensory input to the CNS via Ia afferents [36]. This is probably the mechanism how BoNT-A injected in the periphery can induce cortical reorganization [7]. This hypothesis has been supported by studies in focal dystonia [6,12,23,24]. We have consistently studied the neuroanatomical correlate of BoNT-related post-stroke spasticity relief using functional MRI (fMRI). In our previous

* Corresponding author at: Department of Neurology, University Hospital, I. P. Pavlova 6, 77520 Olomouc, Czech Republic. Tel.: +420 588 443 419; fax: +420 585 428 201.

E-mail address: veverka.tomas@seznam.cz (T. Veverka).

studies we have provided evidence that effective treatment of upper limb spasticity is associated with dynamic changes at the level of the cerebral cortex [47,48]. The aim of the present study was to localize and analyze BoNT-related pattern of cerebral cortex activation during motor or mental tasks in patients with PSS.

2. Material and methods

Patients were studied using a previously published protocol [45]. The following text summarizes the methodology and highlights differences particular for the present study.

2.1. Patients

The patients were recruited in the Comprehensive Stroke Centre at Department of Neurology, University Hospital, Olomouc, Czech Republic. The study was conducted in accordance with the Declaration of Helsinki 1964 (in the latest revision in 2013) and it was approved by the institutional ethics committee.

Fourteen ischemic stroke patients with hand weakness and spasticity were studied. Group A consisted of 7 patients (2 males, 5 females; mean age 59.14 years, range 33–78 years, SD 16.94) with hand plegia, who imagined moving fingers. Group B consisted of 7 age-matched patients (6 males, 1 female; mean age 59.57 years, range 34–80 years, SD 16.93) able to perform sequential finger movement. All subjects were in the chronic stage of the ischemic stroke; the time from stroke onset to the study entry ranged from 3 to 83 months, the median was 10.5 months. Localization of the ischemic lesions were subcortical or corticosubcortical within the middle cerebral artery territory. Hand spasticity was clinically relevant and exceeded 1 on modified Ashworth scale (MAS) [4]. Exclusion criteria were: time after stroke onset less than 3 months; history of BoNT application or drugs affecting muscle hypertonus intake; severe cognitive deficit and severe depression, assessed using the MMSE [10] and Zung Self-rating Depression Scale [58], which could affect cooperation during the study protocol; and finally the magnetic resonance imaging exclusion criteria. The patients' characteristics are listed in Tables 1 and 2.

2.2. Clinical evaluation

Patients were clinically examined (after previous screening) at Week 0, when they were enrolled into the study and injected with BoNT, then at Week 4, four weeks following the injection of BoNT, when BoNT effect is assumed to be maximal, and at Week 11, three months after the BoNT injection, when peripheral BoNT effect was expected to wane.

Evaluation of spasticity using the modified Ashworth scale (MAS) was performed at each visit. The MAS was assessed separately for

fingers and wrist and the values were averaged together (mean MAS). Further clinical investigations included following standardized scales were performed at study enrollment: the modified Medical Research Council (mMRC) [33] scale to test upper extremity strength; the National Institutes of Health (NIH) [5] stroke scale to assess neurological impairment, the Barthel index (BI) [28] and the modified Rankin Scale (mRS) [34] to assess disability.

2.3. Treatment

Enrolled patients were treated with BoNT injections into the muscles of the affected arm at Week 0 and then they underwent a dedicated physiotherapy protocol.

The injections were performed using the EMG guidance (Medtronic Keypoint, Alpine Biomed ApS, Denmark), preferably with electrical stimulation for localization of the muscle intended to be treated. The following muscles were always injected: flexor carpi ulnaris (FCU), flexor carpi radialis (FCR), flexor digitorum superficialis (FDS), and flexor digitorum profundus (FDP). The dose of BoNT (BOTOX®; Allergan, Inc., Irvine, CA, USA) per muscle was 50 U. Such dose reflects current recommendation [52]. The BoNT was given consistently in a fixed dose per muscle basis in both groups.

The rehabilitation treatment started several days after the BoNT injection (W0). Initial inpatient physiotherapy (2–4 weeks) was followed by outpatient therapy until the third clinical and fMRI evaluation (total of 11 weeks). The patients underwent daily physiotherapy sessions, for a total of 1 h, using various techniques such as Bobath concept, proprioceptive neuromuscular facilitation (PNF), passive and active stretching and occupational therapy. Proper adherence to the physiotherapy protocol has been repeatedly checked every session within the whole study [25].

2.4. Tasks

Patients were scanned while performing imaginary or real finger movement with the impaired hand. Subjects with preserved finger movements (group B) performed sequential finger movements (Roland's paradigm) [35] at the rate of approximately 1 movement per second. Subjects with hand paralysis (group A) first trained the sequential finger movement with the non-paretic hand and then were asked to imagine performing the same movement with the impaired fingers in association with kinesthetic feeling [42]. Inside the bore of the scanner, the task was performed with eyes closed, instructions to start and stop task performance were signaled verbally (start/stop) in MR-compatible headphones. In a block paradigm, imagery or real finger movement alternated with rest (15 s). Each experimental run consisted of 12 repetitions of the same task-rest block pairs, for a total of 6 min. Each participant had two experimental runs with the impaired hand.

Table 1
Group A - demographic and clinical characteristics.

Patient	Sex	Age	Stroke onset to W0 (months)	Lesion	Affected hand	mRS	BI	Initial NIHSS	MMSE	Zung (SDS index)	mMRC (WF/WE)	mMRC (FF/FE)	Mean MAS (W0)	Mean MAS (W4)	Mean MAS (W11)
1	F	76	6	Thalamus, IC, insula	Left	4	45	7	24	65	1/0	1/0	3	1.75	2.5
2	F	78	5	Thalamus, IC	Right	4	60	10	N/A	49	0/0	0/0	3	2	3
3	F	44	83	FP lobe, insula	Right	2	95	4	29	39	2/1	2/1	2	1	2
4	F	64	6	Insula, BG, FT lobe	Right	3	70	8	N/A	63	0/0	0/0	2	1.25	1.75
5	M	68	9	Thalamus, BG, FT lobe, insula	Left	3	75	7	29	34	0/0	0/0	3	1.75	3
6	M	33	32	BG, IC	Left	3	70	5	28	59	2/1	2+/1	2	1	2
7	F	51	23	BG, insula, FT lobe	Right	3	65	9	N/A	43	0/0	0/0	3	2	2

Note: L = left; R = right; BG = basal ganglia; IC = internal capsule; F = frontal; T = temporal; P = parietal; NIHSS = NIH stroke scale; mMRC = modified MRC scale; BI = Barthel index; WE = wrist extensors; WF = wrist flexors; FE = finger extensors; FF = finger flexors; MAS = Modified Ashworth scale; and N/A = not applicable – the MMSE score could not be interpreted because of the presence of expressive aphasia.

2.5. Data acquisition

Similar to the behavioral (clinical) assessments, the functional MRI examinations were done at Week 0, Week 4 and Week 11. The three-session design aimed to allow separation of the expected transient effect of BoNT from the progressive effects of time and/or rehabilitation.

Magnetic resonance imaging data were acquired on 1.5 Tesla scanners (Avanto and Symphony, Siemens, Erlangen, Germany) with a standard head coil. The MR imaging protocol covered the whole brain with 30 axial slices 5 mm thick, including anatomical T1-weighted images to provide an immediate overlay with functional data, fluid-attenuated inversion recovery (FLAIR) images to visualize brain lesions, functional T2*-weighted (BOLD) images during task performance and rest, and a high-resolution 3D anatomical scan (MPRAGE). BOLD images were acquired with gradient-echo echo-planar imaging sequence (EPI), TR/TE = 2500/40 ms, FOV 220 mm, to provide 3.4 × 3.4 × 5 mm resolution. In total, 144 volumes were acquired per each 6-minute functional run. Subject's head was immobilized with cushions to assure maximum comfort and minimize head motion. Task performance and the presence of mirror movements were monitored visually.

2.6. Analysis

Prior to fMRI analysis, the imaging data of 7 patients with right-hemispheric lesions were flipped in the left–right direction to allow group analysis of activation task with the impaired hand [20,50].

fMRI data processing was carried out using FEAT (fMRI Expert Analysis Tool) Version 6.00, part of FSL [18,41,55] Version 5.0 (FMRIB's Software Library, www.fmrib.ox.ac.uk/fsl). The following pre-statistics processing was applied: motion correction using MCFLIRT [17]; slice-timing correction using Fourier-space time-series phase-shifting; non-brain removal using BET [40]; spatial smoothing using a Gaussian kernel of full width at half-maximum (FWHM) 10 mm; grand-mean intensity normalization of the entire 4D dataset by a single multiplicative factor; high-pass temporal filtering (Gaussian-weighted least-squares straight line fitting, with sigma = 15 s). Time-series statistical analysis was carried out using FILM with local autocorrelation correction [56]. The model included 6 motion estimate vectors to remove residual signal changes due to head motion; a confound matrix representing volumes with excessive motion detected by the FSL Motion Outliers tool to account for non-linear motion effects; and 2 nuisance signal vectors extracted from the individual functional images to reduce physiological noise: white matter signal, and signal from the cerebrospinal fluid. The latter two time-series were extracted using transformed standard brain anatomical masks, as provided by the Harvard–Oxford anatomical atlases [8,9,11,13,14,29]. Registration to high resolution structural and/or standard space images was carried out using FLIRT and FNIRT [17,19].

Higher-level analysis was carried out using FLAME (FMRIB's Local Analysis of Mixed Effects) stages 1 and 2 [1,53]. Z (Gaussianized T/F) statistic images were thresholded using a corrected cluster significance threshold of $p = 0.05$ [56]. Group mean activation maps were generated for each session, furthermore, post-hoc linear contrasts yielded maps of

significant pairwise differences between sessions. The design using three sessions permitted decomposition of the treatment effect at 4 weeks into the progressive time and/or rehabilitation component and the transient botulinum toxin effect.

3. Results

3.1. Clinical

BoNT transiently lowered arm spasticity at Week 4 in both groups, but the alleviation of spasticity was statistically significant only in group A. The mean MAS changes from baseline were: in group A 1.03 ($p = 0.032$, Wilcoxon Signed Ranks Test with Bonferroni correction), in group B 0.72 ($p = 0.053$, Wilcoxon Signed Ranks Test with Bonferroni correction).

The mean MAS score at Week 11 did not significantly differ from Week 0 in both groups (mean MAS change in group A was 0.25, $p = 0.218$; mean MAS change in group B was 0.25, $p = 0.433$, Wilcoxon Signed Ranks Test with Bonferroni correction).

The mean MAS scores in group A were: at Week 0: 2.57 (SD 0.53), at Week 4: 1.54 (SD 0.44), and at Week 11: 2.32 (SD 0.51). The mean MAS scores in group B were: at Week 0: 2.11 (SD 0.64), at Week 4: 1.39 (SD 0.56), and at Week 11: 1.86 (SD 0.80). The mean MAS scores of each subject are listed in Tables 1 and 2.

3.2. Imaging – group average

In group A, activation of frontal premotor cortex dominated at all three fMRI sessions. Prior to the BoNT application (W0), a cluster of activation was observed at the contralesional intraparietal sulcus but was absent at following examinations. After BoNT treatment (W4) ipsilesional cerebellum engaged and persisted at W11. Additionally, the premotor cortex activation was spread more ventrally at the ipsilesional hemisphere towards the central opercular cortex, which diminished at W11. Third fMRI session (W11) revealed an additional activation cluster in the cortex surrounding the ipsilesional intraparietal sulcus. Group A mean activation maps for each session are shown in Fig. 1.

In group B, the contralesional primary and secondary sensorimotor cortices, SMA, and bilateral cerebellum remain active at all three fMRI sessions. At W0, the subjects additionally activated the motor cingulate cortex, dorsal and ventral ipsilesional premotor cortex, bilateral lateral occipital cortex, bilateral thalamus, contralesional basal ganglia and contralesional insular cortex and inferior frontal gyrus (pars opercularis). A substantial decrease of activation extent was observed at W4 in comparison to W0, however an increase of activation was detected in the ipsilesional dorsal premotor cortex. At W11, a similar pattern to W4 was observed, with additional activation in contralesional ventral primary sensorimotor cortex. Besides the activation in SMA, no further activation was detected in the ipsilesional cortex. Group B mean activation maps for each session are shown in Fig. 2.

Table 2

Group B – demographic and clinical characteristics.

Patient	Sex	Age	Stroke onset to W0 (months)	Lesion	Affected hand	mRS	BI	Initial NIHSS	MMSE	Zung (SDS index)	mMRC (WF/WE)	mMRC (FF/FE)	Mean MAS (W0)	Mean MAS (W4)	Mean MAS (W11)
1	M	54	15	Thalamus, IC, BG	Right	2	85	9	24	31	4/3	4/3	1.5	2	2
2	M	77	18	Thalamus, IC, BG	Right	2	70	5	24	40	4/3	4/3	3	1.75	3
3	M	60	9	BG, IC	Left	2	90	3	28	41	4+/4	4+/4	3	2	2.5
4	M	80	12	Thalamus, IC	Right	3	60	5	N/A	49	4/3+	4/3+	2	1.25	1.5
5	M	68	7	BG, IC, FT lobe	Left	2	90	4	26	50	4/4	4/4	2	1.25	2
6	F	34	14	BG, IC	Left	2	100	3	27	44	5/4	4/4	1.75	1	1.5
7	M	44	3	BG, IC	Left	2	100	4	30	48	4/3	4/3	1.5	0.5	0.5

Note: L = left; R = right; BG = basal ganglia; IC = internal capsule; F = frontal; T = temporal; P = parietal; NIHSS = NIH stroke scale; mMRC = modified MRC scale; BI = Barthel index; WE = wrist extensors; WF = wrist flexors; FE = finger extensors; FF = finger flexors; MAS = Modified Ashworth scale; and N/A = not applicable – the MMSE score could not be interpreted because of the presence of expressive aphasia.

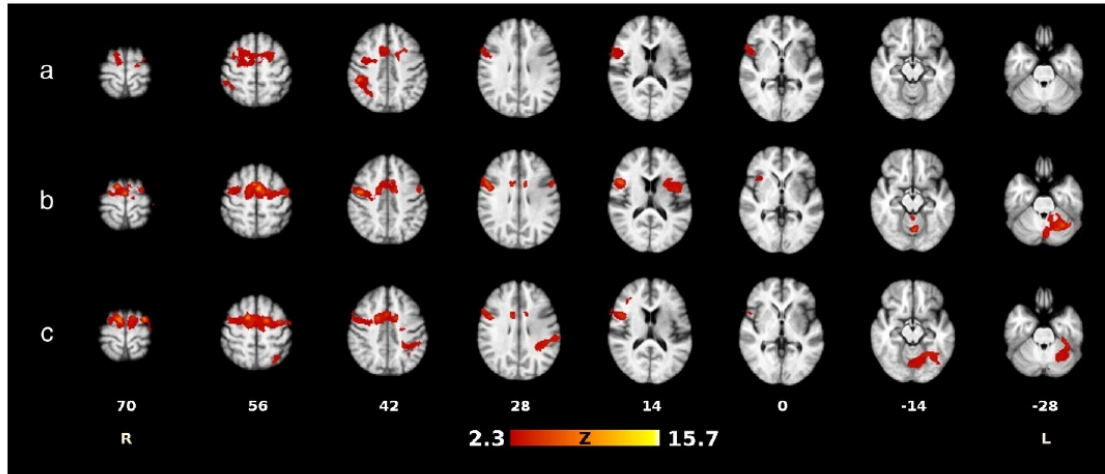


Fig. 1. Functional MRI activation during imagery of finger movement in group A (plegic): before BoNT treatment (a), 4 (b) and 11 weeks after BoNT application (c). (The Z-statistical images (were) thresholded using a corrected cluster significance threshold of $P = 0.05$ (and) overlaid on the top of averaged high resolution T1-weighted images.

3.3. Between-session contrasts

In group A, paired contrast $W0 > W4$ showed activation decrease in the bilateral occipital cortex (ipsilesional occipital fusiform gyrus, lingual gyrus, occipitoparietal cortex on the mesial interhemispheric surface, contralesional lateral occipital cortex, inferior temporal gyrus, occipital pole) (Fig. 3a). $W11 > W4$ contrast revealed decrease of activation in the ipsilesional lateral occipital cortex, occipital pole and occipitoparietal cortex on the mesial interhemispheric surface (Fig. 3b). Summary of the active areas' coordinates and statistical parameters for individual contrasts in group A are provided in Table 3.

In group B, paired contrast $W0 > W4$ showed activation decrease in the bilateral occipital cortex (ipsilesional lateral occipital cortex, bilateral occipital pole), bilateral inferior frontal gyrus (pars opercularis,

Broca's area), bilateral orbitofrontal cortex, ipsilesional dorsolateral prefrontal cortex (DLPFC) and contralesional cerebellum (Fig. 4a). $W0 > W11$ contrast revealed the decrease of activation which was limited to the bilateral occipital cortex (namely bilateral lingual gyrus, cortex bordering the contralesional calcarine sulcus and ipsilesional occipital pole) (Fig. 4b). $W11 > W4$ contrast showed activation increase over time in the ipsilesional lateral occipital cortex, ipsilesional angular and supramarginal gyrus, ipsilesional superior frontal gyrus (pre-supplementary motor area), ipsilesional anterior cingulate gyrus, cortex on lateral surface of ipsilesional temporal lobe and contralesional cerebellum (Fig. 4c). Summary of the active areas' coordinates and statistical parameters for individual contrasts in group B are provided in Table 4.

The remaining between-session contrasts in both groups did not reveal any areas of significant change in the local BOLD effect magnitude.

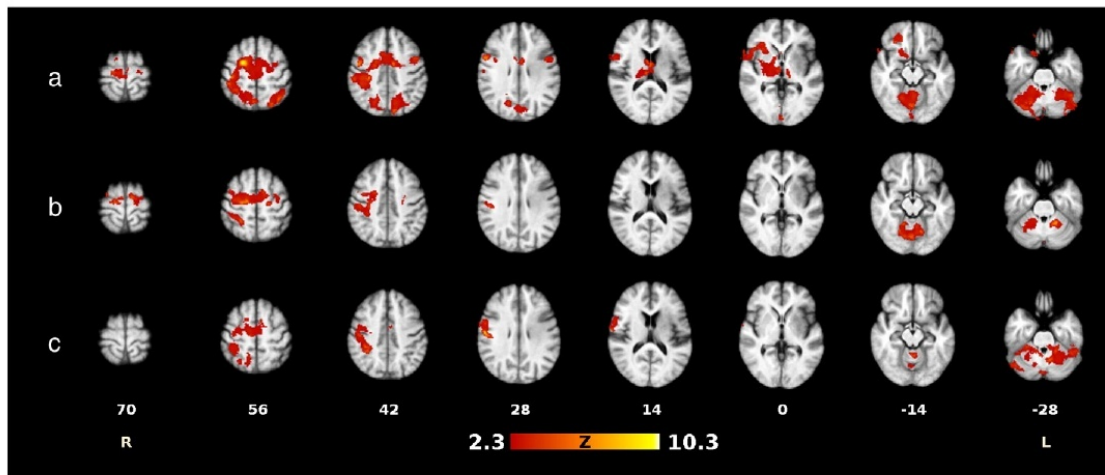


Fig. 2. Functional MRI activation during sequential finger movement in group B (paretic): before BoNT treatment (a), 4 (b) and 11 weeks after BoNT application (c). (The Z-statistical images (were) thresholded using a corrected cluster significance threshold of $P = 0.05$ (and) overlaid on the top of averaged high resolution T1-weighted images.

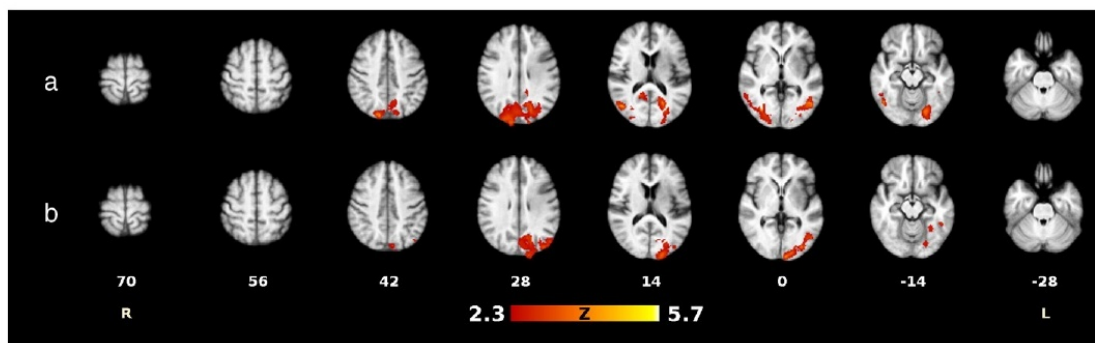


Fig. 3. Between-session fMRI contrasts in group A (plegic): a = W0 > W4, and b = W11 > W4.

4. Discussion

Stroke triggers a number of processes at various levels of motor system that can cause spontaneous recovery or motor improvement (adaptive plasticity). Plastic changes within the sensorimotor system not only are beneficial but also may even worsen residual function. From this point of view, the appearance of post-stroke upper limb spasticity that interferes with motor performance could be attributed to so-called maladaptive plasticity. BoNT injection is a well established component of multimodal treatment of PSS. The growing evidence of BoNT-related central (remote) effects makes BoNT a promising tool to favorably affect maladaptive changes even at the cortical level.

In the present study extending our previous work, we have focused on functional neuroimaging findings (plasticity) in cortical and subcortical areas attributable to changes of spasticity following BoNT application.

As expected, BoNT application temporarily relieved spasticity expressed in MAS. In group A, the change of mean MAS score was statistically significant. In group B, the values did not reach statistical significance most likely due to less prominent clinical effect in less severely affected patients and concurrently relatively small size of studied group. Mean MAS score at Week 11, when pharmacological peripheral effect of BoNT is expected to be minimized, did not significantly differ from the score at Week 0, despite ongoing physiotherapy. This trend should not be interpreted as a failure of physiotherapy. The primary goal of physiotherapy protocol in PSS is functional improvement. However our study protocol did not include testing of such functional gains.

In the plegic group, comparing group-averaged statistical maps of all three fMRI session, no prominent changes in the extent of participating brain networks emerged. As expected and consistent with earlier neuroimaging studies in healthy subjects, mental task with kinesthetic imagery was associated with the activation of frontal premotor cortex (SMA, pre-SMA, bilateral premotor cortex) [2,42]. This cluster of fMRI signal remained stable within the whole study. Group-averaged statistical maps further revealed other clusters in which fMRI signal changed

over time. First, pre-BoNT (W0) activation of cortex bordering the contralesional intraparietal sulcus disappeared after BoNT application (W4), whereas another cluster surrounding the ipsilesional intraparietal sulcus emerged at W11, when BoNT effect is expected to wane. The intraparietal sulcus (IPS) belongs to frontoparietal circuits controlling more complex and goal-directed movement. In normal subjects performing imagery of sequential finger movements, IPS areas participate bilaterally with contralateral predominance [15,42]. Therefore, predominantly ipsilateral (contralesional) activation reflects abnormal motor control, which then reverts to a more physiological pattern by W11. A second cluster that emerged following BoNT application (W4) and persisted at W11 was located in the ipsilesional cerebellum. Whereas contralesional cerebellar engagement was reported during the process of successful motor recovery and rehabilitation after stroke [20,39], transient ipsilesional cerebellar activation was associated with poorer motor recovery after stroke [39]. In our previous study of PSS with a similar design but including several very young stroke patients, activation of the ipsilesional cerebellum remained unchanged over time, whereas the contralesional cerebellum revealed transient BoNT-related activation at W4 [48]. Despite using age as covariate in the fMRI analysis of that study, it is possible that the inclusion of several young stroke patients (below the age of 30), with considerably higher potential for brain plasticity, contributed to the transient normalization of motor networks, which was not observed in the present study of more typical older stroke patients.

Complementary between-session contrasts revealed significant changes in activation located in occipital lobe. On direct statistical pairwise comparison, W0 > W4 and W11 > W4 demonstrated significant activation decreases related to BoNT treatment in the occipitoparietal cortex on the mesial interhemispheric surface and in the lateral occipital cortex. The abovementioned areas have been previously shown to be recruited when subjects visualize hand movements [15,16,42]. Present findings suggest that BoNT application, which substantially relieved spasticity, also temporarily diminished activation in structures tightly associated with visual imagery. Regarding the occipitoparietal changes,

Table 3

Local maxima of between-session contrasts – group A (plegic).

	Area description	Voxels	Maximum Z-score	x mm	y mm	z mm
W0 > W4	Cluster 1:	7676				
	40% left occipital fusiform gyrus, 16% left lingual gyrus		5.7	–22	–78	–8
	38% right lateral occipital cortex, inferior division, 26% right inferior temporal gyrus		4.89	48	–62	–14
	29% left cuneal cortex		4.75	–20	–74	22
	50% right lateral occipital cortex, superior division		4.67	16	–84	44
W11 > W4	Cluster 1:	4314				
	68% left occipital pole		5.23	–8	–98	–2
	33% left intracalcarine cortex		4.35	–10	–74	16
	39% left lateral occipital cortex, inferior division		4.17	–32	–86	–2

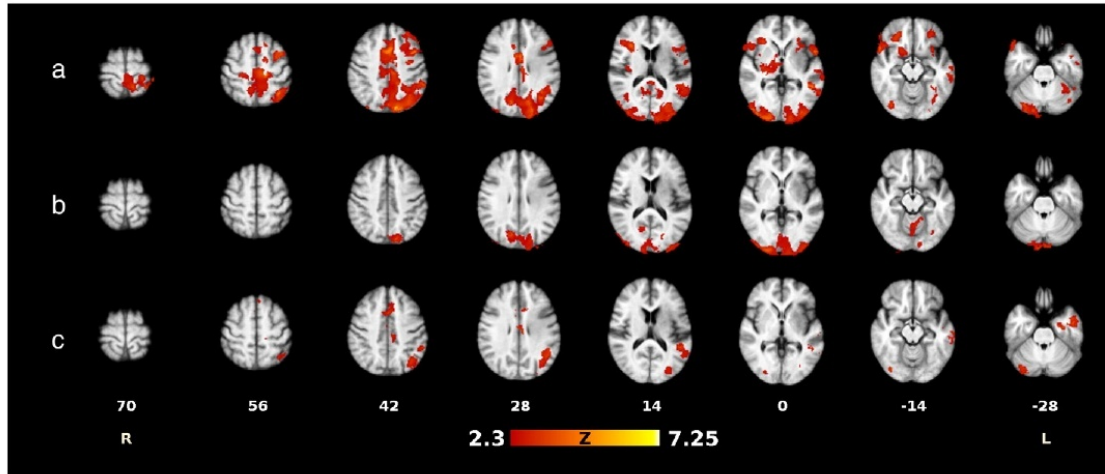


Fig. 4. Between-session fMRI contrasts in group B (paretic): a = W0 > W4, b = W0 > W11, and c = W11 > W4.

we assume that BoNT treatment in plegic subjects might switch their neural processing from visual to kinesthetic imagery pattern.

In the paretic group, the group-averaged statistical maps showed extensive activation of bilateral cortical and subcortical regions before BoNT application (W0). As we suggested in our previous work, this pre-treatment widespread activation might represent a general response of

the affected brain to the increased proprioceptive afferentation (via Ia fibers) from spastic muscles [37,48]. BoNT application significantly relieved spasticity across paretic patients and this beneficial effect was associated with substantial reduction of activation in the most of previously active areas at W4. This BoNT-related reduction in the extent of the active sensorimotor networks is consistent with results of our

Table 4
Local maxima of between-session contrasts – group B (paretic).

	Area description	Voxels	Maximum Z-score	x mm	y mm	z mm
W0 > W4	Cluster 1:	23083				
	54% left lateral occipital cortex, superior division		7.25	-14	-82	44
	69% left occipital pole		6.66	-26	-100	-4
	13% left precentral gyrus	5.51	-12	-28	52	
	Cluster 2:	3740				
	99% right crus II		4.53	18	-88	-32
	56% right occipital pole		4.49	30	-94	-4
	55% right crus I	4.44	28	-78	-20	
	Cluster 3:	3651				
	60% right frontal orbital cortex		4.79	34	28	-6
	55% right frontal pole		4.34	24	42	-20
	36% right frontal operculum cortex		4.32	36	20	12
	70% right temporal pole	4.31	56	14	-12	
Cluster 4:	1358					
63% left inferior frontal gyrus, pars opercularis		5.14	-52	16	12	
49% left frontal orbital cortex, 21% left frontal operculum cortex		4.54	-44	22	-6	
57% left frontal pole	4.09	-28	42	-10		
W0 > W11	Cluster 1:	6940				
	44% right lingual gyrus, 22% right intracalcarine cortex, 14% left lingual gyrus		5.11	2	-76	2
60% left occipital pole	5.04	-6	-102	2		
W11 > W4	Cluster 1:	2360				
	53% left angular gyrus		5.38	-46	-56	24
	14% left supramarginal gyrus, posterior division		4.32	-50	-46	18
	50% left lateral occipital cortex, superior division, 11% left angular gyrus		3.91	-44	-64	30
	59% left middle temporal gyrus, temporooccipital part		3.9	-58	-54	6
	Cluster 2:	1301				
	69% right crus I		4.3	36	-78	-22
	96% right crus II	4.11	24	-82	-40	
	Cluster 3:	1006				
	24% left superior frontal gyrus		3.79	-8	22	50
	37% left cingulate gyrus, anterior division		3.75	-4	-10	30
	23% left paracingulate gyrus, 20% Left Superior Frontal Gyrus	3.65	-8	18	48	
	Cluster 4:	982				
	39% left middle temporal gyrus, posterior division		4.55	-58	-18	-20
	26% left temporal pole, 20% left middle temporal gyrus, anterior division		4.1	-48	2	-32
	60% left superior temporal gyrus, posterior division, 25% left middle temporal gyrus, posterior division		4.05	-66	-24	-2
27% left middle temporal gyrus, anterior division	3.93	-48	-2	-28		

pilot study reported by Tomášová et al. [45] and a similar effect was reported by Manganotti et al. [30]. We have previously hypothesized about the similarity of this phenomenon with motor recovery after stroke. Motor recovery is associated with task-related activation in a number of secondary motor areas early after stroke and subsequent decrease in their extent with increasing laterality with successful recovery, whereas patients with poorer outcome reveal persisting overactivation in bilateral sensorimotor areas. [49,50]. Our BoNT-off data (W11) yielded a pattern nearly similar to W4. This particular trend differs from Tomášová et al. [45] where BoNT-off data (W11) again resembled the pre-BoNT examination (W0). Synergic effect of BoNT application and physiotherapy in less severely affected patients may play a crucial role in this phenomenon. Absence of physiological activation in ipsilesional primary sensorimotor cortex during execution of motor task with contralateral hand can be attributed to the size and location of infarction affecting the corticospinal tract in most of the studied patients.

Significant differences in local BOLD responses were then shown in the post-hoc linear contrasts comparing pairs of individual sessions. In the paretic group as well as in the previously cited study of paretic patients [45], post-hoc contrasts W0 > W4 yielded significant BoNT-related changes in the ipsilesional DLPFC and Broca's area. Both areas have been reported to participate in motor learning, rather than volitional motor performance and control [3]. In the present study, further activation decreases were observed in the bilateral occipital cortex and bilateral orbitofrontal cortex, areas not related to motor function. Several of the areas with decreased task-related BOLD response after BoNT-induced spasticity relief subsequently increased their activation again as BoNT effect waned (post-hoc contrast W11 > W4). These included the ipsilesional lateral occipital cortex, ipsilesional cortex bordering the intraparietal sulcus and contralesional cerebellum. It is well known that under pathological conditions, such as stroke damaging the sensorimotor network, motor control involves structures outside the classical motor system [51]. We have previously shown that bilateral brain areas may be recruited in the presence of PSS [37,45,48]. This overactivation in such areas then diminished after effective BoNT treatment that reduces spastic muscle contraction and thus alters inappropriate sensory inputs to the CNS. Activation decreases over the whole three-month study period (W0 > W11) were located in the bilateral occipital cortex, which may reflect the decreased need to engage visualization in order to perform movement with the paretic hand.

Future fMRI studies might be complemented by electrophysiology using transcranial magnetic stimulation (TMS), as an alternative method to study cortical plasticity in the sensorimotor system [32].

5. Conclusion

The presented results of our study provided a novel functional imaging evidence of the remote central effects of BoNT. This fact might suggest that successful treatment of PSS with BoNT modulates cortical reorganization, and that this modulation is probably the primary mechanism underlying the clinical improvement of this debilitating motor disorder.

Conflict of interest

There are no conflicts of interest associated with this manuscript, financial or otherwise. The manuscript has been read and approved by all authors.

Acknowledgments

This work was supported by the IGA Ministry of Health of the Czech Republic grant number NT13575.

References

- [1] Beckmann CF, Jenkinson M, Smith SM. General multilevel linear modeling for group analysis in FMRI. *Neuroimage* Oct 2003;20(2):1052–63.
- [2] Binkofski F, Amunts K, Stephan KM, Posse S, Schormann T, Freund HJ, et al. Broca's region subserves imagery of motion: a combined cytoarchitectonic and fMRI study. *Hum Brain Mapp* Dec 2000;11(4):273–85.
- [3] Binkofski F, Buccino G. Motor functions of the Broca's region. *Brain Lang* May 2004; 89(2):362–9.
- [4] Bohannon RW, Smith MB. Interrater reliability of a modified Ashworth scale of muscle spasticity. *Phys Ther* Feb 1987;67(2):206–7.
- [5] Brott T, Adams Jr HP, Olinger CP, Marler JR, Barsan WG, Biller J, et al. Measurements of acute cerebral infarction: a clinical examination scale. *Stroke* Jul 1989;20(7): 864–70.
- [6] Byrnes ML, Thickbroom GW, Wilson SA, Sacco P, Shipman JM, Stell R, et al. The corticomotor representation of upper limb muscles in writer's cramp and changes following botulinum toxin injection. *Brain* May 1998;121(5):977–88.
- [7] Currà A, Trompetto C, Abbruzzese G, Berardelli A. Central effects of botulinum toxin type A: evidence and supposition. *Mov Disord* Mar 2004;19(Suppl. 8):S60–4.
- [8] Desikan RS, Ségonne F, Fischl B, Quinn BT, Dickerson BC, Blacker D, et al. An automated labeling system for subdividing the human cerebral cortex on MRI scans into gyral based regions of interest. *Neuroimage* Jul 1 2006;31(3):968–80.
- [9] Diedrichsen J, Balsters JH, Flavell J, Cussans E, Ramnani N. A probabilistic MR atlas of the human cerebellum. *Neuroimage* May 15 2009;46(1):39–46.
- [10] Folstein MF, Folstein SE, McHugh PR. Mini-mental state. A practical method for grading the cognitive state of patients for the clinician. *J Psychiatr Res* Nov 1975; 12(3):189–98.
- [11] Frazier JA, Chiu S, Breeze JL, Makris N, Lange N, Kennedy DN, et al. Structural brain magnetic resonance imaging of limbic and thalamic volumes in pediatric bipolar disorder. *Am J Psychiatry* 2005;162(7):1256–65 [eview].
- [12] Gilio F, Currà A, Lorenzano C, Modugno N, Manfredi M, Berardelli A. Effects of botulinum toxin type A on intracortical inhibition in patients with dystonia. *Ann Neurol* Jul 2000;48(1):20–6.
- [13] Goldstein JM, Seidman LJ, Makris N, Ahern T, O'Brien LM, Caviness Jr VS, et al. Hypothalamic abnormalities in schizophrenia: sex effects and genetic vulnerability. *Biol Psychiatry* Apr 15 2007;61(8):935–45.
- [14] Grabner G, Janke AL, Budge MM, Smith D, Pruessner J, Collins DL. Symmetric atlas and model based segmentation: an application to the hippocampus in older adults. *Med Image Comput Assist Interv* 2006;9(Pt 2):58–66.
- [15] Guillot A, Collet C, Nguyen VA, Malouin F, Richards C, Doyon J. Brain activity during visual versus kinesthetic imagery: an fMRI study. *Hum Brain Mapp* Jul 2009;30(7): 2157–72.
- [16] Jackson PL, Meltzoff AN, Decety J. Neural circuits involved in imitation and perspective-taking. *Neuroimage* May 15 2006;31(1):429–39.
- [17] Jenkinson M, Bannister P, Brady M, Smith S. Improved optimization for the robust and accurate linear registration and motion correction of brain images. *Neuroimage* Oct 2002;17(2):825–41.
- [18] Jenkinson M, Beckmann CF, Behrens TEJ, Woolrich MW, Smith SM. FSL neuroimage Aug 15 2012;62(2):782–90.
- [19] Jenkinson M, Smith S. A global optimisation method for robust affine registration of brain images. *Med Image Anal* Jun 2001;5(2):143–56.
- [20] Johansen-Berg H, Dawes H, Guy C, Smith SM, Wade DT, Matthews PM. Correlation between motor improvements and altered fMRI activity after rehabilitative therapy. *Brain* Dec 2002;125(Pt 12):2731–42.
- [21] Jørgensen HS, Nakayama H, Raaschou HO, Vive-Larsen J, Støier M, Olsen TS. Outcome and time course of recovery in stroke. Part I: outcome. The Copenhagen Stroke Study. *Arch Phys Med Rehabil* May 1995;76(5):399–405.
- [22] Kamper DG, Fischer HC, Cruz EG, Rymer WZ. Weakness is the primary contributor to finger impairment in chronic stroke. *Arch Phys Med Rehabil* Sep 2006;87(9):1262–9.
- [23] Kanovsky P, Bares M, Streitová H, Klajblová H, Daniel P, Rektor I. Abnormalities of cortical excitability and cortical inhibition in cervical dystonia. Evidence from somatosensory evoked potentials and paired transcranial magnetic stimulation recordings. *J Neurol* Jan 2003;250(1):42–50.
- [24] Kanovsky P, Streitová H, Dufek J, Znojil V, Daniel P, Rektor I. Change in lateralization of the P22/N30 cortical component of median nerve somatosensory evoked potentials in patients with cervical dystonia after successful treatment with botulinum toxin A. *Mov Disord* Jan 1998;13(1):108–17.
- [25] Krobot A, Schusterová B, Tomsová J, Kristková V, Konečný P. Specific protocol of physiotherapy in stroke patients. *Cesk Slov Neurol N* 2008;71(104):V74.
- [26] Lance JW. Symposium synopsis. Spasticity: disordered motor control. Chicago: Yearbook Medical Publishers; 1980.
- [27] Lopez AD, Mathers CD, Ezzati M, Jamison DT, Murray CJL. Global and regional burden of disease and risk factors, 2001: systematic analysis of population health data. *Lancet* May 27 2006;367(9524):1747–57.
- [28] Mahoney FI, Barthel DW. Functional evaluation: the Barthel index. *Md State Med J* Feb 1965;14:61–5.
- [29] Makris N, Goldstein JM, Kennedy D, Hodge SM, Caviness VS, Faraone SV, et al. Decreased volume of left and total anterior insular lobule in schizophrenia. *Schizophr Res* 2006;83(2–3):155–71 [Duben].
- [30] Manganotti P, Acler M, Formaggio E, Avesani M, Milanese F, Baraldo A, et al. Changes in cerebral activity after decreased upper-limb hypertonus: an EMG-fMRI study. *Magn Reson Imaging* Jun 2010;28(5):646–52.
- [31] Mayer NH, Esquenazi A, Childers MK. Common patterns of clinical motor dysfunction. *Muscle Nerve Suppl* 1997;6:S21–35.
- [32] Palomar FJ, Mir P. Neurophysiological changes after intramuscular injection of botulinum toxin. *Clin Neurophysiol* Jan 2012;123(1):54–60.

- [33] Paternostro-Sluga T, Grim-Stieger M, Posch M, Schuhfried O, Vacariu G, Mittermaier C, et al. Reliability and validity of the Medical Research Council (MRC) scale and a modified scale for testing muscle strength in patients with radial palsy. *J Rehabil Med* 2008;40(8):665–71.
- [34] Quinn TJ, Dawson J, Walters MR, Lees KR. Variability in modified Rankin scoring across a large cohort of international observers. *Stroke* Nov 2008;39(11):2975–9.
- [35] Roland PE, Larsen B, Lassen NA, Skinhaj E. Supplementary motor area and other cortical areas in organization of voluntary movements in man. *J Neurophysiol* Jan 1980;43(1):118–36.
- [36] Rosales RL, Dressler D. On muscle spindles, dystonia and botulinum toxin. *Eur J Neurol* Jul 2010;17(Suppl. 1):71–80.
- [37] Senkárová Z, Hlustik P, Otruba P, Herzig R, Kanovský P. Modulation of cortical activity in patients suffering from upper arm spasticity following stroke and treated with botulinum toxin A: an fMRI study. *J Neuroimaging* Jan 2010;20(1):9–15.
- [38] Sheean G. The pathophysiology of spasticity. *Eur J Neurol* May 2002;9(Suppl. 1):3–9 [discussion 53–61].
- [39] Small SL, Hlustik P, Noll DC, Genovese C, Solodkin A. Cerebellar hemispheric activation ipsilateral to the paretic hand correlates with functional recovery after stroke. *Brain* Jul 2002;125(Pt 7):1544–57.
- [40] Smith SM. Fast robust automated brain extraction. *Hum Brain Mapp* Nov 2002;17(3):143–55.
- [41] Smith SM, Jenkinson M, Woolrich MW, Beckmann CF, Behrens TEJ, Johansen-Berg H, et al. Advances in functional and structural MR image analysis and implementation as FSL. *Neuroimage* 2004;23(Suppl. 1):S208–19.
- [42] Solodkin A, Hlustik P, Chen EE, Small SL. Fine modulation in network activation during motor execution and motor imagery. *Cereb Cortex* Nov 2004;14(11):1246–55.
- [43] Sommerfeld DK, Eek EU-B, Svensson A-K, Holmqvist LW, Von Arbin MH. Spasticity after stroke: its occurrence and association with motor impairments and activity limitations. *Stroke* Jan 2004;35(1):134–9.
- [44] Sunnerhagen KS, Olver J, Francisco GE. Assessing and treating functional impairment in poststroke spasticity. *Neurology* Jan 15 2013;80(3 Suppl. 2):S35–44.
- [45] Tomášová Z, Hluštík P, Král M, Otruba P, Herzig R, Krobot A, et al. Cortical activation changes in patients suffering from post-stroke arm spasticity and treated with botulinum toxin a. *J Neuroimaging* Jul 2013;23(3):337–44.
- [46] Urban PP, Wolf T, Uebele M, Marx JJ, Vogt T, Stoeter P, et al. Occurrence and clinical predictors of spasticity after ischemic stroke. *Stroke* Sep 2010;41(9):2016–20.
- [47] Veverka T, Hlustik P, Hok P, Tomášová Z, Otruba P, Král M, et al. Differences in the modulation of cortical activity in patients suffering from upper arm spasticity following stroke and treated with botulinum toxin A. *Cesk Slov Neurol N* 2013;76/109(2):175–82.
- [48] Veverka T, Hluštík P, Tomášová Z, Hok P, Otruba P, Král M, et al. BoNT-A related changes of cortical activity in patients suffering from severe hand paralysis with arm spasticity following ischemic stroke. *J Neurol Sci* Aug 15 2012;319(1–2):89–95.
- [49] Ward NS, Brown MM, Thompson AJ, Frackowiak RSJ. Neural correlates of motor recovery after stroke: a longitudinal fMRI study. *Brain* Nov 2003;126(Pt 11):2476–96.
- [50] Ward NS, Brown MM, Thompson AJ, Frackowiak RSJ. Neural correlates of outcome after stroke: a cross-sectional fMRI study. *Brain* Jun 2003;126(Pt 6):1430–48.
- [51] Weiller C, Chollet F, Friston KJ, Wise RJ, Frackowiak RS. Functional reorganization of the brain in recovery from striatocapsular infarction in man. *Ann Neurol* May 1992;31(5):463–72.
- [52] Wissel J, Ward AB, Erztgaard P, Bensmail D, Hecht MJ, Lejeune TM, et al. European consensus table on the use of botulinum toxin type A in adult spasticity. *J Rehabil Med* Jan 2009;41(1):13–25.
- [53] Woolrich MW, Behrens TEJ, Beckmann CF, Jenkinson M, Smith SM. Multilevel linear modelling for fMRI group analysis using Bayesian inference. *Neuroimage* Apr 2004;21(4):1732–47.
- [54] Woolrich MW, Jbabdi S, Patenaude B, Chappell M, Makni S, Behrens T, et al. Bayesian analysis of neuroimaging data in FSL. *Neuroimage* Mar 2009;45(1 Suppl):S173–86.
- [55] Woolrich MW, Ripley BD, Brady M, Smith SM. Temporal autocorrelation in univariate linear modeling of fMRI data. *Neuroimage* Dec 2001;14(6):1370–86.
- [56] Worsley KJ. Statistical analysis of activation images. *Functional MRI: an introduction to methods*. Oxford: Oxford University Press; 2001 251–70.
- [57] Zorowitz RD, Gillard PJ, Brainin M. Poststroke spasticity: sequelae and burden on stroke survivors and caregivers. *Neurology* Jan 15 2013;80(3 Suppl. 2):S45–52.
- [58] Zung WW. A self-rating depression scale. *Arch Gen Psychiatry* Jan 1965;12:63–70.

7. Annex 7

Journal of the Neurological Sciences 362 (2016) 14–20



Contents lists available at ScienceDirect

Journal of the Neurological Sciences

journal homepage: www.elsevier.com/locate/jns



Sensorimotor modulation by botulinum toxin A in post-stroke arm spasticity: Passive hand movement



Tomáš Veverka^{a,*}, Petr Hlušík^{a,b}, Pavel Hok^a, Pavel Otruba^a, Jana Zapletalová^d, Zbyněk Tüdös^b, Alois Krobot^c, Petr Kaňovský^a

^a Department of Neurology, Faculty of Medicine and Dentistry, Palacký University and University Hospital, Olomouc, Czech Republic

^b Department of Radiology, Faculty of Medicine and Dentistry, Palacký University and University Hospital, Olomouc, Czech Republic

^c Department of Physiotherapy, Faculty of Medicine and Dentistry, Palacký University and University Hospital, Olomouc, Czech Republic

^d Department of Biophysics, Biometry and Statistics, Faculty of Medicine and Dentistry, Palacký University and University Hospital, Olomouc, Czech Republic

ARTICLE INFO

Article history:

Received 25 October 2015

Received in revised form 8 December 2015

Accepted 31 December 2015

Available online 11 January 2016

Keywords:

Stroke

Hand weakness

Spasticity

Botulinum toxin

Functional magnetic resonance imaging

Neuronal plasticity

ABSTRACT

Introduction: In post-stroke spasticity, functional imaging may uncover modulation in the central sensorimotor networks associated with botulinum toxin type A (BoNT) therapy. Investigations were performed to localize brain activation changes in stroke patients treated with BoNT for upper limb spasticity using functional magnetic resonance imaging (fMRI).

Methods: Seven ischemic stroke patients (4 females; mean age 58.86) with severe hand paralysis and notable spasticity were studied. Spasticity was scored according to the modified Ashworth scale (MAS). fMRI examination was performed 3 times: before (W0) and 4 (W4) and 11 weeks (W11) after BoNT. The whole-brain fMRI data were acquired during paced repetitive passive movements of the plegic hand (flexion/extension at the wrist) alternating with rest. Voxel-by-voxel statistical analysis using the General Linear Model (GLM) implemented in FSL (v6.00)/FEAT yielded group session-wise statistical maps and paired between-session contrasts, thresholded at the corrected cluster-wise significance level of $p < 0.05$.

Results: As expected, BoNT transiently lowered MAS scores at W4. Across all the sessions, fMRI activation of the ipsilesional sensorimotor cortex (M1, S1, and SMA) dominated. At W4, additional clusters transiently emerged bilaterally in the cerebellum, in the contralesional sensorimotor cortex, and in the contralesional occipital cortex. Paired contrasts demonstrated significant differences $W4 > W0$ (bilateral cerebellum and contralesional occipital cortex) and $W4 > W11$ (ipsilesional cerebellum and SMA). The remaining paired contrast ($W0 > W11$) showed activation decreases mainly in the ipsilesional sensorimotor cortex (M1, S1, and SMA).

Conclusions: The present study confirms the feasibility of using passive hand movements to map the cerebral sensorimotor networks in patients with post-stroke arm spasticity and demonstrates that BoNT-induced spasticity relief is associated with changes in task-induced central sensorimotor activation, likely mediated by an altered afferent drive from the spasticity-affected muscles.

© 2016 Elsevier B.V. All rights reserved.

1. Introduction

Post-stroke spasticity (PSS) is one of the major sequelae following ischemic stroke [62]. Ischemic lesions of descending tracts result in upper motor neuron syndrome (UMNS) comprising both negative signs (weakness and loss of dexterity) and positive signs (especially spasticity) [39]. Spasticity, defined by Lance as “a motor disorder characterized by a velocity-dependent increase in tonic stretch reflex (muscle tone) with exaggerated tendon jerks, resulting from hyperexcitability of the stretch reflex,” is a component of UMNS [27]. It is generally recognized that post-stroke spasticity (PSS) may interfere with voluntary movement [31]. Disabling PSS affects patient quality of life; significant

reductions in manual dexterity, mobility, walking/falling, and performance of activities of daily living (ADL) have been reported among patients with PSS [44]. The disabilities associated with PSS place a significant burden on stroke survivors and subsequently on caregivers [62]. Prevalence data for PSS are limited by a lack of population-based studies; however, current estimates range from 19% to 42.6% [44,48]. Numerous clinical trials have shown that botulinum toxin type A (BoNT) is a safe and effective therapeutic tool to relieve upper limb PSS and improve function of the affected limb [40,45,57]. The current treatment strategy to relieve focal spasticity combines BoNT application and physiotherapy. BoNT blocks acetylcholine release at neuromuscular junctions [15]. In addition to this peripheral site of BoNT-action, there is growing evidence that indirect (remote) effects on the spinal cord and brain may also occur. BoNT-A affects intrafusal fibers as well as extrafusal ones, and thus alters abnormal sensory input to the CNS via

* Corresponding author.

la afferents [36]. This is probably the mechanism by which BoNT injected in the periphery can induce cortical reorganization [9]. This hypothesis has been supported by studies of focal dystonia [7,13,24,25]. We have consistently studied changes in the sensorimotor cortex elicited by BoNT application in chronic stroke patients with arm spasticity associated with either severe [38,49,52] or moderate [47,49] hand weakness. Effects on task-related cerebral activation have been assessed using functional magnetic resonance imaging (fMRI). In our previous fMRI studies of severely affected patients, kinesthetic imagery of finger movements was used as an experimental task. Motor imagery evokes activation in the cortical areas associated with performed movements [37]; however, such a mental task is difficult to monitor. Unlike motor imagery, passive movement is easy to perform and monitor; on the other hand, it induces sensorimotor cortex activation in another way, with particular emphasis on afferent inputs to the CNS [56]. The aim of the present study was to localize and analyze BoNT-related patterns of cerebral cortex activation during passive flexion–extension movements of the affected hand at the wrist.

2. Material and methods

Patients were studied using a previously published protocol [47]. The following text summarizes the methodology and highlights the specific differences in the present study.

2.1. Patients

The patients were recruited from the Comprehensive Stroke Center at the Department of Neurology, University Hospital, Olomouc, Czech Republic. The study was conducted in accordance with the Declaration of Helsinki 1964 (2013 revision) and it was approved by the institution's ethics committee.

Seven ischemic stroke patients (4 females; mean age 58.86; range 48–75; SD 10.85) with severe hand paralysis and notable spasticity were studied.

All subjects were in the chronic stage of first-ever ischemic stroke; the time from stroke onset to the study entry ranged from 7 to 28 months, the median was 10 months. The ischemic lesions were subcortical or corticosubcortical within the middle cerebral artery territory. Hand spasticity was clinically relevant and exceeded 1 on the modified Ashworth scale (MAS) [5]. Exclusion criteria were: time after stroke onset less than 3 months; history of BoNT application or drugs affecting muscle hypertonus intake; severe cognitive deficit or severe depression, as assessed using the MMSE [12] and Zung Self-rating Depression Scale [63], which could affect cooperation during the study protocol; and MRI exclusion criteria. The patient characteristics are listed in Table 1.

2.2. Clinical evaluation

Patients were clinically examined (after previous screening) at Week 0, when they were enrolled in the study and injected with

BoNT, then at Week 4, 4 weeks following the injection of BoNT, when BoNT effect is assumed to be maximal, and at Week 11, 3 months after the BoNT injection, when peripheral BoNT effect was expected to wane.

Spasticity was evaluated using MAS at each visit. The MAS was assessed separately for fingers and wrist and the values were averaged together (mean MAS). Further clinical investigations included the following standardized scales were performed at study enrollment: the modified Medical Research Council (mMRC) scale [32] to test upper extremity strength; the National Institutes of Health (NIH) stroke scale [6] to assess neurological impairment, and the Barthel Index (BI) [29] and the modified Rankin Scale (mRS) [34] to assess disability.

2.3. Treatment

Enrolled patients were treated with BoNT injections into the muscles of the affected arm at Week 0, followed by a dedicated physiotherapy protocol.

The injections were performed using EMG guidance (Medtronic Keypoint, Alpine Biomed ApS, Denmark), preferably with electrical stimulation to localize the muscles to be treated. The following muscles were always injected: flexor carpi ulnaris (FCU), flexor carpi radialis (FCR), flexor digitorum superficialis (FDS), flexor digitorum profundus (FDP). The dose of BoNT (BOTOX®; Allergan, Inc., Irvine, CA, USA) per muscle was 50 U. This dosage reflects current recommendations [57]. The BoNT was given consistently in a fixed dose per muscle basis.

The rehabilitation treatment started several days after the BoNT injection (W0). Initial inpatient physiotherapy (2–4 weeks) was followed by outpatient therapy until the third clinical and fMRI evaluation (total of 11 weeks). The patients underwent daily physiotherapy sessions on workdays, i.e., five times a week, for a total session duration of 1 h.

Individual kinesiotherapy included posture-locomotion training towards restitution of bipedal posture and gait, motor recovery of the girdles and trunk using elements of Bobath concept and proprioceptive neuromuscular facilitation, respiratory physiotherapy, reflex and myofascial techniques, antispastic positioning, occupational therapy and training of independence in activities of daily living. Proper adherence to the physiotherapy protocol was checked at each examination throughout the whole study [26].

2.4. Task

fMRI data were acquired during passive flexion–extension movement of the affected hand at the wrist. In a block paradigm, passive movements (15 s) alternated with rest (15 s). Each experimental run consisted of 12 repetitions of the movement–rest block pairs, for a total of 6 min. The repetitive flexion–extension of the wrist were executed by a physician at the rate of one flexion or extension per second each. Subjects were examined in a supine position and were secured with the forearm pronated. The range of movement was determined as the largest that was permitted by the resistance of spastic

Table 1
Demographic and clinical characteristics.

Patient	Sex	Age	Stroke onset to W0 (months)	Lesion	Affected hand	mRS	BI	Initial NIHSS	MMSE	Zung (SDS index)	mMRC (WF/WE)	mMRC (FF/FE)	Mean MAS (W0)	Mean MAS (W4)	Mean MAS (W11)
1	F	75	10	Thalamus, IC, insula	Right	3	85	5	29	39/49	1/1	2/1	2	1	2
2	F	51	19	Thalamus, IC	Left	3	75	7	30	42/53	0/0	0/0	3	1.75	2
3	M	69	22	FP lobe, insula	Right	3	85	11	N/A	37/46	0/0	0/0	2	1.75	1.75
4	M	53	28	Insula, BG, FT lobe	Left	4	60	11	20	27/34	0/0	0/0	2.5	1.25	1.75
5	M	50	9	Thalamus, BG, FT lobe, insula	Right	3	90	10	N/A	35/44	0/0	0/0	1.75	1	2
6	F	48	7	BG, IC	Left	3	90	6	30	56/70	1/0	1/0	2	0.5	2
7	F	66	9	BG, insula, FT lobe	Left	4	65	5	28	52/65	0/0	0/0	2	1.5	2

Note: BG = basal ganglia; IC = internal capsule; F = frontal; T = temporal; P = parietal; NIHSS = NIH stroke scale; mMRC = modified MRC scale; BI = Barthel index; WE = wrist extensors; WF = wrist flexors; FE = finger extensors; FF = finger flexors; MAS = modified Ashworth scale; N/A = not applicable – the MMSE score could not be interpreted because of the presence of expressive aphasia.

muscles and could be tolerated by each patient. Timing of the alternating movements during active blocks was given by acoustic signals in MR-compatible headphones.

2.5. Data acquisition

The behavioral (clinical) assessments and fMRI examinations were done at Week 0, Week 4, and Week 11. The three-session design enabled the separation of the expected transient effect of BoNT from the progressive effects of time and/or rehabilitation.

Magnetic resonance imaging data were acquired on 1.5 T scanners (Avanto and Symphony, Siemens, Erlangen, Germany) with a standard head coil. The MRI protocol covered the whole brain with 30 axial slices 5 mm thick, including a gradient echo field map for spatial distortion correction of BOLD images, anatomical T1-weighted images to provide an immediate overlay with functional data, fluid-attenuated inversion recovery (FLAIR) images to visualize brain lesions, functional T2*-weighted (BOLD) images during task performance and rest, and a high-resolution 3D anatomical scan (MPRAGE). BOLD images were acquired with a gradient-echo echo-planar imaging sequence (EPI), TR/TE = 2500/40 ms, FOV 220 mm, to provide $3.4 \times 3.4 \times 5$ mm resolution. In total, 144 volumes were acquired per each 6-min functional run. The subject's head was immobilized with cushions to assure maximum comfort and to minimize head motion.

2.6. Analysis

Prior to fMRI analysis, the imaging data of four patients with right-hemispheric lesions were flipped in the left–right direction to allow group analysis of activation task with the impaired hand [21,54].

Voxel-by-voxel statistical analysis was performed using the General Linear Model (GLM) implemented in FEAT v6.00, part of FSL (FMRIB's Software Library, www.fmrib.ox.ac.uk/fsl) [19]. A standard pre-processing pipeline was applied, including motion correction using MCFLIRT [18], slice-timing correction, non-brain removal using BET [42], spatial smoothing with Gaussian kernel of FWHM 10 mm, grand-mean intensity normalization of the entire dataset, and highpass temporal filtering with $\sigma = 15$ s. Time-series statistical analysis was carried out using FILM with local autocorrelation correction [60]. To account for the subject motion and physiological noise, the volumes with severe motion were de-weighted and several nuisance signal regressors were added to the GLM: 6 motion parameters, 6 regressors from the white matter, and 1 regressor from the ventricles [2]. Registration to high resolution structural and/or standard space images was carried out using FLIRT and FNIRT [18,20].

Higher-level analysis was carried out using FLAME (FMRIB's Local Analysis of Mixed Effects) stages 1 and 2 [1,59] and automatic outlier de-weighting [58]. Post-hoc linear contrasts yielded Z (Gaussianized T/F) statistic images thresholded using a corrected cluster significance threshold of $p = 0.05$ at a cluster-forming threshold of $Z > 2$ [61]. The group average was computed for each timepoint (W0, W4, and W11), and the between-session contrasts were obtained using paired t-tests (W0 > W4, W0 > W11, W4 > W0, W4 > W11, W11 > W0, and W11 > W4) employing a "Tripled t-test", i.e., repeated measures analysis of variance (ANOVA) with a 3-level fixed time factor. The between-session contrasts were masked with the corresponding group average maps after thresholding (e.g. W0 > W4 with W0), since only the effects within the areas significantly activated by the task were of interest. Whereas the two pairwise comparisons between W0 and W4 (first) and W11 and W4 (second) reflect the transient changes associated with BoNT administration, the comparison between W0 and W11 reflects the longitudinal effect of physiotherapy.

3. Results

3.1. Clinical

BoNT significantly lowered arm spasticity at W4. The mean MAS change from baseline was 0.93 ($p = 0.018$, Wilcoxon Signed Ranks Test). The mean MAS score at W11 did not significantly differ from W0 (mean MAS change was 0.25, $p = 0.197$, Wilcoxon Signed Ranks Test). The mean MAS scores were: 2.18 at W0 (SD 0.43), 1.25 at W4 (SD 0.46), and 1.93 at W11 (SD 0.12). The MAS scores for each subject are listed in Table 1.

3.2. Imaging-group average

Across all the sessions, fMRI activation of the ipsilesional sensorimotor cortex (M1, S1, and SMA contralateral to the hand being moved) dominated in the group average statistical maps reflecting activation during the passive movement task. At W4, at the time of the maximal pharmacological effect of BoNT, three additional activation clusters transiently emerged: bilaterally in the cerebellum, in the contralesional sensorimotor cortex (M1, S1, and SMA ipsilateral to the hand being moved), and in the contralesional occipital cortex. Mean activation maps for each session are shown in Fig. 1.

3.3. Between-session contrasts

Paired contrast W4 > W0 demonstrated a post-treatment increase in activation in the bilateral cerebellum and contralesional occipital cortex. Paired contrast W4 > W11 revealed a decrease in activation in the ipsilesional cerebellum and supplementary motor cortex while the clinical effect of BoNT waned. The remaining paired contrast comparing the initial and final examination (W0 > W11) showed activation decreases mainly in the ipsilesional sensorimotor cortex (M1, S1, and SMA). The between-session contrasts are shown in Fig. 2. A summary of the active area coordinates along with their standard space coordinates is provided in Table 2. The remaining between-session contrasts did not reveal any areas of significant change in the local BOLD effect magnitude.

4. Discussion

Current research is gradually expanding our knowledge of the central and remote effects of BoNT. The research suggests that successful treatment of focal spasticity modulates cortical and subcortical sensorimotor circuits. In our previous work, we concluded that effective treatment of spasticity led to a reduction of bilateral overactivation in cortical and subcortical areas during actively performed or imagined finger movement [38,47,49,50,52]. We assumed that the expanded pretreatment activation might represent a general response of the lesioned brain. This pattern probably contains both adaptive changes (neuroplasticity–substitution) and maladaptive changes due to pathologically increased proprioceptive afferentation, associated with spasticity. BoNT-related reduction of afferent firing from the spastic muscles then modulates such maladaptive plasticity and might restore the "physiological" spatial distribution of cortical activity with clear lateralization [51].

In the present study, extending our previous research, we provide further functional imaging evidence of the dynamic changes in the sensorimotor network following BoNT-application and physiotherapy.

As expected, the combination of BoNT-A treatment and physiotherapy significantly relieved spasticity.

Unlike our previous studies using a similar study protocol, the present study used passive movement as the activation task. Passive movement predominantly generates a proprioceptive afferent drive to the somatosensory cortex, which is exactly the presumed mechanism of indirect BoNT effect upon central sensorimotor networks. Passive

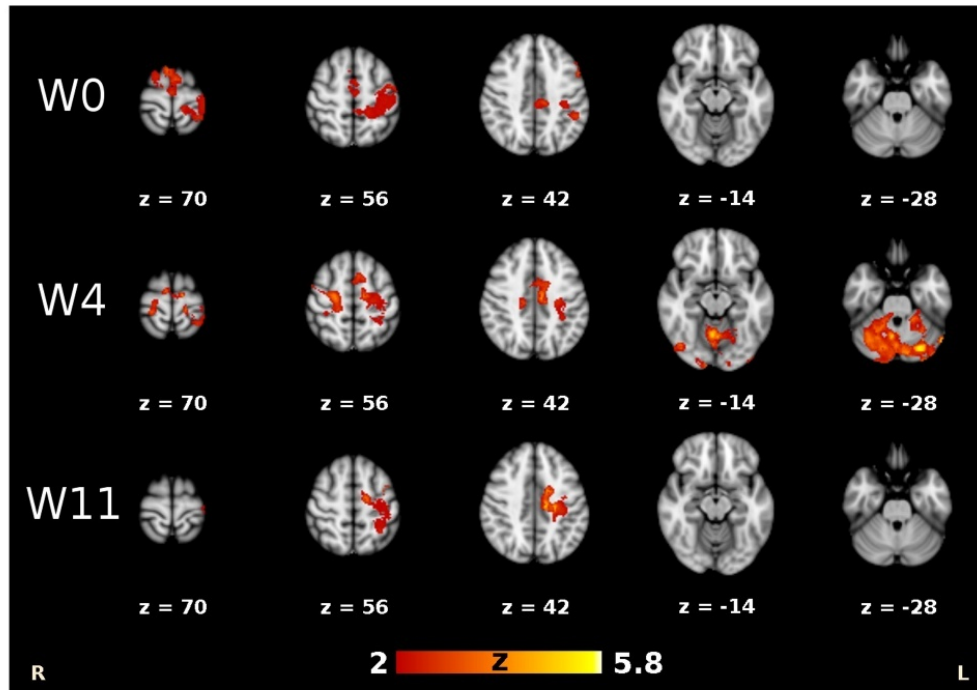


Fig. 1. fMRI activation during passive hand movement (group mean statistical maps overlaid in color on the MNI anatomical template). (For interpretation of the references to color in this figure legend, the reader is referred to the web version of this article.)

movement has been shown to extensively activate not only sensory but also motor cortical areas [4,46,56]. Passive movements have also been used in imaging post-stroke motor recovery [17,23,35,55] and studying the relief of spasticity [10,28].

In agreement with these studies, passive movement performed with the affected hand elicited activation in the ipsilesional sensorimotor cortex (M1, S1 and SMA). This “physiological” activation pattern persisted through all the sessions. Between-session contrast $W0 > W11$ showed a decrease in task-related activation in the precentral gyrus (medial part), postcentral gyrus, and SMA. The temporal reduction of activation within the sensorimotor cortex throughout the study might represent long-term changes due to BoNT and physiotherapy. An overall reduction in the extent of active sensorimotor networks throughout the duration of a study, similar to that shown in successful post-stroke recovery, was reported previously [30,49,52].

At W4, at the time of the maximal pharmacological effect of BoNT, three additional clusters of activation transiently emerged: bilaterally in the cerebellum, in the contralesional sensorimotor cortex, and in the contralesional occipital cortex.

First, transient bilateral cerebellum engagement was shown in group activation maps at W4. Pairwise comparisons $W4 > W0$ and $W4 > W11$ revealed a significant increase in activation in the bilateral cerebellum after BoNT therapy, followed by a decrease in the ipsilesional cerebellum when the clinical BoNT effect diminished. Cerebellar activity (ipsilateral to the hand being moved) has been reported in elderly healthy subjects during the passive movement of their wrist [55]. The cerebellum undoubtedly plays an important role in post-stroke recovery. Whereas contralesional cerebellar engagement was reported during the process of successful motor recovery and post-stroke physiotherapy [21,41], transient ipsilesional cerebellar activation indicated poorer motor recovery after stroke [41]. In our previous studies of PSS using real or

imagined finger movement as the experimental task, we have also reported transient cerebellar activation after BoNT application [47,52]. We have hypothesized that such cerebellar activation associated with alleviation of spasticity might represent a “normalization” of sensorimotor circuits similar to that in successful post-stroke recovery [41] or intensive physiotherapy [21].

The contralesional sensorimotor cortex was the second regional cluster that transiently emerged at W4. Contralesional sensorimotor cortex engagement early after stroke was reported in most poststroke-recovery studies [53]. In patients with a higher degree of motor recovery, the activation of contralesional sensorimotor areas diminished in association with motor improvement [8,11]. On the other hand, in severely affected patients with poor outcome, the contralesional sensorimotor cortex activation persisted [22,54]. Lindberg et al., studying cortical correlates of spasticity in adults with chronic PSS, reported a correlation between resistance to passive movement and BOLD activity in the contralesional primary sensorimotor cortex [28]. In a recent study using a study protocol similar to ours, Bergfeldt et al. reported an increase in brain activation in response to an active motor task in the motor and pre-motor cortex (predominantly contralesional) at the baseline and an overall decrease in activation with contralesional predominance following comprehensive focal spasticity therapy [3]. In our previous study of PSS using motor imagery, the contralesional primary somatosensory cortex revealed reduced BOLD activity when comparing $W0$ and $W11$ [52]. In the present study, the contralesional sensorimotor cortex was among the areas showing changes in BOLD activity but in the opposite direction; there was a post-BoNT increase in activity. To our knowledge, few studies have reported that mitigation of spasticity following rehabilitation was correlated with increased task-related activation in the contralesional sensorimotor cortex [10,33]. The above-mentioned studies and our results support the important role of

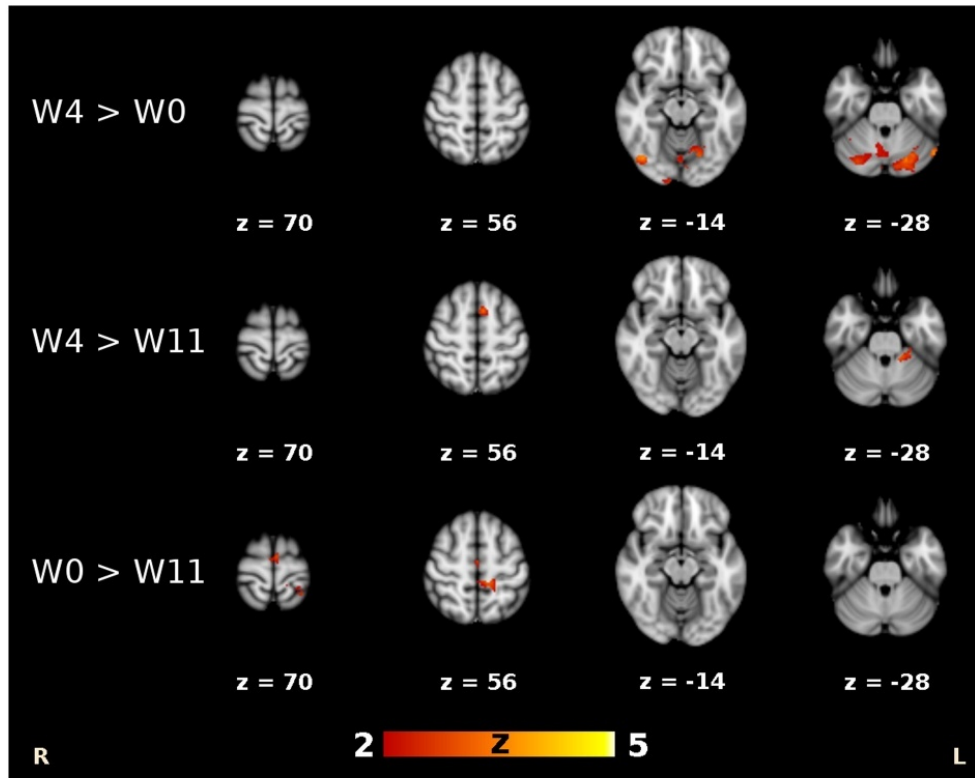


Fig. 2. Between-session fMRI contrasts (group post-hoc contrast overlaid on the MNI anatomical template).

afferent somatosensory input from spastic muscles in modulating the bilateral sensorimotor network.

The third region that became transiently active at W4 was the contralesional occipital cortex. On direct statistical pairwise comparison, W4 > W0 showed a significant activation increase in the lateral occipital cortex and occipital pole post-BoNT. These structures have been shown to be recruited when healthy subjects visualize hand movements [14, 16,43]. In our previous study using motor imagery or real finger movement as an experimental task, BoNT-application temporarily diminished activity in structures closely associated with visual imagery [49], therefore we concluded that BoNT treatment might switch neural processing from a visual to a kinesthetic imagery pattern. In contrast to our previous results, in the present study we found a significant increase in activation

in the contralesional occipital cortex at W4. We assume that the opposite pattern of activation is due to the different activation task. On one hand, the passive movement activates similar sensorimotor areas to the active one [56]; on the other hand, cortical processing of the afferent proprioceptive and somatosensory drive generated by passive movement undoubtedly also includes distinct neural circuits comprising areas outside of the sensorimotor cortex. Engagement of the occipital cortex during passive movement at the time of the maximal effect of BoNT might represent the evoked motor visualization. We assume that the BoNT-related decrease in pathological afferent input from spastic muscles enables the motor (visual) imagery associated with passive movement. Such motor imagery, when combined with physiotherapy, can offer functional benefits after stroke [64,65].

Table 2

Local maxima of clusters resulting from between-session contrasts.

	Area description	Maximum Z-score	x mm	y mm	z mm
W4 > W0	61% right occipital pole	4.31	10	-102	6
	29% right lateral occipital cortex, inferior division, 22% right occipital fusiform gyrus	3.90	40	-72	-12
	78% cerebellum, left crus I	3.89	-30	-76	-32
	100% cerebellum, right crus I	3.65	32	-76	-24
W4 > W11	82% cerebellum, left I-IV, 14% cerebellum, left V	3.25	-14	-38	-22
	32% left superior frontal gyrus, 18% left supplementary motor cortex), 11% left paracingulate gyrus	3.32	-6	10	56
W0 > W11	28% left postcentral gyrus, 19% left precentral gyrus, 16% left precuneous cortex	4.08	-12	-38	50
	36% left supplementary motor cortex, 13% right supplementary motor cortex	3.20	0	-10	60
	36% left superior parietal lobule, 11% left postcentral gyrus	3.15	-28	-46	72
	42% left precentral gyrus, 34% left supplementary motor cortex	2.74	-2	-14	64

Our results should be interpreted with caution. The relatively small size of our patient group reduces the overall statistical power to detect smaller effects. Together with heterogeneity in stroke location and the degree of cortical involvement this limits the possibility of generalizing the results to the whole population of patients with upper limb PSS.

5. Conclusion

The present study confirms the feasibility of using passive hand movements to map the cerebral sensorimotor networks in patients with post-stroke arm spasticity and demonstrates that BoNT-induced spasticity relief is associated with changes in task-induced central sensorimotor activation, likely mediated by an altered afferent drive from the spasticity-affected muscles.

Acknowledgments

This study was supported by the grant of the Internal Grant Agency of Ministry of Health of the Czech Republic NT13575, by the grant of the Agency for Healthcare Research of Ministry of Health of the Czech Republic 15-31921 A, and by the Institutional Support RVO FNOL 00098892.

References

- [1] C.F. Beckmann, M. Jenkinson, S.M. Smith, General multilevel linear modeling for group analysis in fMRI, *NeuroImage* 20 (2) (Oct 2003) 1052–1063.
- [2] Y. Behzadi, K. Restom, J. Liu, T.T. Liu, A component based noise correction method (CompCor) for BOLD and perfusion based fMRI, *NeuroImage* 37 (1) (Aug 1 2007) 90–101.
- [3] U. Bergfeldt, T. Jonsson, L. Bergfeldt, P. Julin, Cortical activation changes and improved motor function in stroke patients after focal spasticity therapy—an interventional study applying repeated fMRI, *BMC Neurol.* 15 (2015) 52.
- [4] R.A. Bernard, D.A. Goran, S.T. Sakai, T.H. Carr, D. McFarlane, B. Nordell, et al., Cortical activation during rhythmic hand movements performed under three types of control: an fMRI study, *Cogn. Affect. Behav. Neurosci.* 2 (3) (Sep 2002) 271–281.
- [5] R.W. Bohannon, M.B. Smith, Interrater reliability of a modified Ashworth scale of muscle spasticity, *Phys. Ther.* 67 (2) (Feb 1987) 206–207.
- [6] T. Brott, H.P. Adams Jr., C.P. Olinger, J.R. Marler, W.G. Barsan, J. Biller, et al., Measurements of acute cerebral infarction: a clinical examination scale, *Stroke* 20 (7) (Jul 1989) 864–870.
- [7] M.L. Byrnes, G.W. Thickbroom, S.A. Wilson, P. Sacco, J.M. Shipman, R. Stell, et al., The corticomotor representation of upper limb muscles in writer's cramp and changes following botulinum toxin injection, *Brain* 121 (5) (May 1 1998) 977–988.
- [8] C. Calautti, F. Leroy, J.Y. Guineestre, R.M. Marié, J.C. Baron, Sequential activation brain mapping after subcortical stroke: changes in hemispheric balance and recovery, *Neuroreport* 12 (18) (Dec 21 2001) 3883–3886.
- [9] A. Currà, C. Trompetto, G. Abbuzzese, A. Berardelli, Central effects of botulinum toxin type A: evidence and supposition, *Mov. Disord.* 19 (Suppl. 8) (Mar 2004) S60–S64.
- [10] K. Diserens, D. Ruegg, R. Kleiser, S. Hyde, N. Perret, P. Vuadens, et al., Effect of repetitive arm cycling following botulinum toxin injection for poststroke spasticity: evidence from fMRI, *Neurorehabil. Neural Repair* 24 (8) (Oct 2010) 753–762.
- [11] A. Feydy, R. Carlier, A. Roby-Brami, B. Bussel, F. Cazalis, L. Pierot, et al., Longitudinal study of motor recovery after stroke: recruitment and focusing of brain activation, *Stroke* 33 (6) (Jun 2002) 1610–1617.
- [12] M.F. Folstein, S.E. Folstein, P.R. McHugh, "Mini-mental state". A practical method for grading the cognitive state of patients for the clinician, *J. Psychiatr. Res.* 12 (3) (Nov 1975) 189–198.
- [13] F. Gilio, A. Currà, C. Lorenzano, N. Modugno, M. Manfredi, A. Berardelli, Effects of botulinum toxin type A on intracortical inhibition in patients with dystonia, *Ann. Neurol.* 48 (1) (Jul 2000) 20–26.
- [14] A. Guillot, C. Collet, V.A. Nguyen, F. Malouin, C. Richards, J. Doyon, Brain activity during visual versus kinesthetic imagery: an fMRI study, *Hum. Brain Mapp.* 30 (7) (Jul 2009) 2157–2172.
- [15] M. Hallett, F.X. Glocker, G. Deuschl, Mechanism of action of botulinum toxin, *Ann. Neurol.* 36 (3) (Sep 1994) 449–450.
- [16] P.L. Jackson, A.N. Meltzoff, J. Decety, Neural circuits involved in imitation and perspective-taking, *NeuroImage* 31 (1) (May 15 2006) 429–439.
- [17] S.H. Jang, Contra-lesional somatosensory cortex activity and somatosensory recovery in two stroke patients, *J. Rehabil. Med.* 43 (3) (Feb 2011) 268–270.
- [18] M. Jenkinson, P. Bannister, M. Brady, S. Smith, Improved optimization for the robust and accurate linear registration and motion correction of brain images, *NeuroImage* 17 (2) (Oct 2002) 825–841.
- [19] M. Jenkinson, C.F. Beckmann, T.E.J. Behrens, M.W. Woolrich, S.M. Smith, FSL, *NeuroImage* 62 (2) (Aug 15 2012) 782–790.
- [20] M. Jenkinson, S. Smith, A global optimisation method for robust affine registration of brain images, *Med. Image Anal.* 5 (2) (Jun 2001) 143–156.
- [21] H. Johansen-Berg, H. Dawes, C. Guy, S.M. Smith, D.T. Wade, P.M. Matthews, Correlation between motor improvements and altered fMRI activity after rehabilitative therapy, *Brain* 125 (Pt 12) (Dec 2002) 2731–2742.
- [22] H. Johansen-Berg, M.F.S. Rushworth, M.D. Bogdanovic, U. Kischka, S. Wimalaratna, P.M. Matthews, The role of ipsilateral premotor cortex in hand movement after stroke, *Proc. Natl. Acad. Sci. U. S. A.* 99 (22) (Oct 29 2002) 14518–14523.
- [23] T.-D. Jung, J.-Y. Kim, J.-H. Seo, S.-U. Jin, H.J. Lee, S.-H. Lee, et al., Combined information from resting-state functional connectivity and passive movements with functional magnetic resonance imaging differentiates fast late-onset motor recovery from progressive recovery in hemiplegic stroke patients: a pilot study, *J. Rehabil. Med.* 45 (6) (Jun 2013) 546–552.
- [24] P. Kaňovský, M. Bares, H. Streitová, H. Klajblová, P. Daniel, I. Rektor, Abnormalities of cortical excitability and cortical inhibition in cervical dystonia evidence from somatosensory evoked potentials and paired transcranial magnetic stimulation recordings, *J. Neurol.* 250 (1) (Jan 2003) 42–50.
- [25] P. Kaňovský, H. Streitová, J. Dufek, V. Znojil, P. Daniel, I. Rektor, Change in lateralization of the P22/N30 cortical component of median nerve somatosensory evoked potentials in patients with cervical dystonia after successful treatment with botulinum toxin A, *Mov. Disord.* 13 (1) (Jan 1998) 108–117.
- [26] A. Krobot, B. Schusterová, J. Tomšová, V. Kristková, P. Konečný, Specific protocol of physiotherapy in stroke patients, *Cesk. Slov. Neurol. N.* 71/104 (2008) V74.
- [27] J. Lance, Symposium Synopsis, Spasticity: Disordered Motor Control, Yearbook Medical Publishers, Chicago, 1980.
- [28] P.G. Lindberg, J. Gäverth, A. Fagergren, P. Fransson, H. Forssberg, J. Borg, Cortical activity in relation to velocity dependent movement resistance in the flexor muscles of the hand after stroke, *Neurorehabil. Neural Repair* 23 (8) (Oct 2009) 800–810.
- [29] F.I. Mahoney, D.W. Barthel, Functional evaluation: the Barthel index, *Md. State Med. J.* 14 (Feb 1965) 61–65.
- [30] P. Manganotti, M. Accler, E. Formaggio, M. Avesani, F. Milanese, A. Baraldo, et al., Changes in cerebral activity after decreased upper-limb hypertonus: an EMG-fMRI study, *Magn. Reson. Imaging* 28 (5) (Jun 2010) 646–652.
- [31] N.H. Mayer, A. Esquenazi, M.K. Childers, Common patterns of clinical motor dysfunction, *Muscle Nerve Suppl.* 6 (1997) S21–S35.
- [32] T. Paternostro-Sluga, M. Grim-Stieger, M. Posch, O. Schuhfried, G. Vacariu, C. Mittermaier, et al., Reliability and validity of the Medical Research Council (MRC) scale and a modified scale for testing muscle strength in patients with radial palsy, *J. Rehabil. Med.* 40 (8) (Aug 2008) 665–671.
- [33] S. Pundik, A.D. Falchook, J. McCabe, K. Litinas, J.J. Daly, Functional brain correlates of upper limb spasticity and its mitigation following rehabilitation in chronic stroke survivors, *Stroke Res. Treat.* 2014 (2014) 306325.
- [34] T.J. Quinn, J. Dawson, M.R. Walters, K.R. Lees, Variability in modified Rankin scoring across a large cohort of international observers, *Stroke* 39 (11) (Nov 2008) 2975–2979.
- [35] A.K. Rehme, S.B. Eickhoff, C. Rottschy, G.R. Fink, C. Grefkes, Activation likelihood estimation meta-analysis of motor-related neural activity after stroke, *NeuroImage* 59 (3) (Feb 1 2012) 2771–2782.
- [36] R.L. Rosales, D. Dressler, On muscle spindles, dystonia and botulinum toxin, *Eur. J. Neurol.* 17 (Suppl. 1) (Jul 2010) 71–80.
- [37] M. Roth, J. Decety, M. Raybaudi, R. Massarelli, C. Delon-Martin, C. Segebarth, et al., Possible involvement of primary motor cortex in mentally simulated movement: a functional magnetic resonance imaging study, *Neuroreport* 7 (7) (May 17 1996) 1280–1284.
- [38] Z. Senkárová, P. Hluštík, P. Otruba, R. Herzig, P. Kanovský, Modulation of cortical activity in patients suffering from upper arm spasticity following stroke and treated with botulinum toxin A: an fMRI study, *J. Neuroimaging* 20 (1) (Jan 2010) 9–15.
- [39] G. Sheean, The pathophysiology of spasticity, *Eur. J. Neurol.* 9 (Suppl. 1) (May 2002) 3–9 (discussion 53–61).
- [40] G. Sheean, N.A. Lannin, L. Turner-Stokes, B. Rawicki, B.J. Snow, Botulinum toxin assessment, intervention and after-care for upper limb hypertonicity in adults: international consensus statement, *Eur. J. Neurol.* 17 (Suppl. 2) (Aug 2010) 74–93.
- [41] S.L. Small, P. Hluštík, D.C. Noll, C. Genovese, A. Solodkin, Cerebellar hemispheric activation ipsilateral to the paretic hand correlates with functional recovery after stroke, *Brain* 125 (Pt 7) (Jul 2002) 1544–1557.
- [42] S.M. Smith, Fast robust automated brain extraction, *Hum. Brain Mapp.* 17 (3) (Nov 2002) 143–155.
- [43] A. Solodkin, P. Hluštík, E.E. Chen, S.L. Small, Fine modulation in network activation during motor execution and motor imagery, *Cereb. Cortex* 14 (11) (Nov 2004) 1246–1255.
- [44] D.K. Sommerfeld, E.U.-B. Eek, A.-K. Svensson, L.W. Holmqvist, M.H. Von Arbin, Spasticity after stroke: its occurrence and association with motor impairments and activity limitations, *Stroke* 35 (1) (Jan 2004) 134–139.
- [45] K.S. Sunnerhagen, J. Olver, G.E. Francisco, Assessing and treating functional impairment in poststroke spasticity, *Neurology* 80 (3 Suppl. 2) (Jan 15 2013) S35–S44.
- [46] A.J. Szameitat, S. Shen, A. Conforto, A. Sterr, Cortical activation during executed, imagined, observed, and passive wrist movements in healthy volunteers and stroke patients, *NeuroImage* 62 (1) (Aug 1 2012) 266–280.
- [47] Z. Tomášová, P. Hluštík, M. Král, P. Otruba, R. Herzig, A. Krobot, et al., Cortical activation changes in patients suffering from post-stroke arm spasticity and treated with botulinum toxin A, *J. Neuroimaging* 23 (3) (Jul 2013) 337–344.
- [48] P.P. Urban, T. Wolf, M. Uebele, J.J. Marx, T. Vogt, P. Stoeter, et al., Occurrence and clinical predictors of spasticity after ischemic stroke, *Stroke* 41 (9) (Sep 2010) 2016–2020.
- [49] T. Veverka, P. Hluštík, P. Hok, P. Otruba, Z. Tüds, J. Zapletalová, et al., Cortical activity modulation by botulinum toxin type A in patients with post-stroke arm spasticity: real and imagined hand movement, *J. Neurol. Sci.* 346 (1–2) (Nov 15 2014) 276–283.

- [50] T. Veverka, P. Hlušík, P. Hok, Z. Tomášová, P. Otruba, M. Král, et al., Differences in the modulation of cortical activity in patients suffering from upper arm spasticity following stroke and treated with botulinum toxin A, *Cesk. Slov. Neurol. N.* 76/109 (2) (2013) 175–182.
- [51] T. Veverka, P. Hlušík, P. Kaňovský, Post-stroke spasticity as a manifestation of maladaptive plasticity and its modulation by botulinum toxin treatment, *Cesk. Slov. Neurol. N.* 77 (3) (2014) 295–301.
- [52] T. Veverka, P. Hlušík, Z. Tomášová, P. Hok, P. Otruba, M. Král, et al., BoNT-A related changes of cortical activity in patients suffering from severe hand paralysis with arm spasticity following ischemic stroke, *J. Neurol. Sci.* 319 (1–2) (Aug 15 2012) 89–95.
- [53] N.S. Ward, M.M. Brown, A.J. Thompson, R.S.J. Frackowiak, Neural correlates of motor recovery after stroke: a longitudinal fMRI study, *Brain* 126 (Pt 11) (Nov 2003) 2476–2496.
- [54] N.S. Ward, M.M. Brown, A.J. Thompson, R.S.J. Frackowiak, Neural correlates of outcome after stroke: a cross-sectional fMRI study, *Brain* 126 (Pt 6) (Jun 2003) 1430–1448.
- [55] N.S. Ward, M.M. Brown, A.J. Thompson, R.S.J. Frackowiak, Longitudinal changes in cerebral response to proprioceptive input in individual patients after stroke: an fMRI study, *Neurorehabil. Neural Repair* 20 (3) (Sep 2006) 398–405.
- [56] C. Weiller, M. Jüptner, S. Fellows, M. Rijntjes, G. Leonhardt, S. Kiebel, et al., Brain representation of active and passive movements, *NeuroImage* 4 (2) (Oct 1996) 105–110.
- [57] J. Wissel, A.B. Ward, P. Ertzgaard, D. Bensmail, M.J. Hecht, T.M. Lejeune, et al., European consensus table on the use of botulinum toxin type A in adult spasticity, *J. Rehabil. Med.* 41 (1) (Jan 2009) 13–25.
- [58] M. Woolrich, Robust group analysis using outlier inference, *NeuroImage* 41 (2) (Jun 2008) 286–301.
- [59] M.W. Woolrich, T.E.J. Behrens, C.F. Beckmann, M. Jenkinson, S.M. Smith, Multilevel linear modelling for fMRI group analysis using Bayesian inference, *NeuroImage* 21 (4) (Apr 2004) 1732–1747.
- [60] M.W. Woolrich, B.D. Ripley, M. Brady, S.M. Smith, Temporal autocorrelation in univariate linear modeling of fMRI data, *NeuroImage* 14 (6) (Dec 2001) 1370–1386.
- [61] K.J. Worsley, *Statistical Analysis of Activation Images. Functional MRI: An Introduction to Methods*, Oxford University Press, Oxford, 2001 251–270.
- [62] R.D. Zorowitz, P.J. Gillard, M. Brainin, Poststroke spasticity: sequelae and burden on stroke survivors and caregivers, *Neurology* 80 (3 Suppl. 2) (Jan 15 2013) S45–S52.
- [63] W.W. Zung, A self-rating depression scale, *Arch. Gen. Psychiatry* 12 (Jan 1965) 63–70.
- [64] R. Dickstein, J.E. Deutsch, Motor imagery in physical therapist practice, *Phys. Ther.* 87 (7) (Jul 2007) 942–953.
- [65] C. Schuster, J. Butler, B. Andrews, U. Kischka, T. Ettlin, Comparison of embedded and added motor imagery training in patients after stroke: results of a randomised controlled pilot trial, *Trials* 13 (Jan 23 2012) 11.

8. Annex 8

Experimental Brain Research (2018) 236:2627–2637
https://doi.org/10.1007/s00221-018-5322-3

RESEARCH ARTICLE



Changes in sensorimotor network activation after botulinum toxin type A injections in patients with cervical dystonia: a functional MRI study

Martin Nevrlý¹ · Petr Hlušík^{1,2} · Pavel Hok¹ · Pavel Otruba¹ · Zbyněk Tüdös² · Petr Kaňovský¹

Received: 7 November 2017 / Accepted: 28 June 2018 / Published online: 3 July 2018
© The Author(s) 2018

Abstract

Botulinum toxin type A (BoNT) is considered an effective therapeutic option in cervical dystonia (CD). The pathophysiology of CD and other focal dystonias has not yet been fully explained. Results from neurophysiological and imaging studies suggest a significant involvement of the basal ganglia and thalamus, and functional abnormalities in premotor and primary sensorimotor cortical areas are considered a crucial factor in the development of focal dystonias. Twelve BoNT-naïve patients with CD were examined with functional MRI during a skilled hand motor task; the examination was repeated 4 weeks after the first BoNT injection to the dystonic neck muscles. Twelve age- and gender-matched healthy controls were examined using the same functional MRI paradigm without BoNT injection. In BoNT-naïve patients with CD, BoNT treatment was associated with a significant increase of activation in finger movement-induced fMRI activation of several brain areas, especially in the bilateral primary and secondary somatosensory cortex, bilateral superior and inferior parietal lobule, bilateral SMA and premotor cortex, predominantly contralateral primary motor cortex, bilateral anterior cingulate cortex, ipsilateral thalamus, insula, putamen, and in the central part of cerebellum, close to the vermis. The results of the study support observations that the BoNT effect may have a correlate in the central nervous system level, and this effect may not be limited to cortical and subcortical representations of the treated muscles. The results show that abnormalities in sensorimotor activation extend beyond circuits controlling the affected body parts in CD even the first BoNT injection is associated with changes in sensorimotor activation. The differences in activation between patients with CD after treatment and healthy controls at baseline were no longer present.

Keywords Functional MRI · Cervical dystonia · Botulinum toxin · Brain plasticity

Background

Cervical dystonia (CD) is the most common form of focal dystonia, characterized by involuntary sustained contractions of neck muscles resulting in an abnormal rotation or tilt of the head in specific directions (Stacy 2000). The pathophysiology of CD and other focal dystonias has not yet been fully elucidated. Results from neurophysiological

and imaging studies suggest a significant contribution of the basal ganglia and thalamus in the development of focal dystonias (Peterson et al. 2010). Recently, it has become clear that the role of the basal ganglia extends beyond motor control into cognitive and sensory functions as well as into sensorimotor integration (Tinazzi et al. 2009a, b). In the last few years, an increasing number of studies have also presented the cerebellum as another important subcortical brain structure in patients with dystonia (Filip et al. 2013a, b, 2017). Finally, other functional imaging and electrophysiological experiments suggest functional abnormalities in the premotor and primary sensorimotor cortical areas together with aberrant sensorimotor integration, which is considered to be a crucial factor in the development of focal dystonia (Tinazzi et al. 2009a, b; Hinkley et al. 2009; Opavský et al. 2011, 2012). However, the published studies differ in terms of observed hypo- and hyperactivation in these cortical

✉ Martin Nevrlý
martin.nevrlý@fnol.cz

¹ Department of Neurology, University Hospital and Faculty of Medicine and Dentistry of Palacký University, I. P. Pavlova 6, 775 20 Olomouc, Czech Republic

² Department of Radiology, University Hospital and Faculty of Medicine and Dentistry of Palacký University, Olomouc, Czech Republic

areas. Differences among task conditions, including testing of dystonia-affected and unaffected body parts, can partly explain this variance.

Further important insights into the pathophysiology of focal dystonias have come from studies investigating the effects of botulinum toxin (BoNT) treatment. BoNT is currently considered to be one of the most effective therapeutic options in the management of focal dystonias (Jankovic 2004). Undoubtedly, the introduction of the first-generation BoNT products not only led to a breakthrough in dystonia treatment but also to advances in dystonia research. We now know that the dystonic hyperactive and cholinergically sensitive extrafusal fibers as well as the intrafusal muscle fibers are the prime targets of BoNT therapy (Rosales and Dressler 2010). It is the effect of BoNT in muscle spindles that would eventually modify proprioceptive spindle afferents, as these are partly dependent on the intrafusal muscle fiber tensions. A modification of the central programs with BoNT may eventually occur at the spinal and supraspinal levels (Rosales and Dressler 2010). The clinical effect of BoNT on dystonia is, therefore, assumed to be mediated by dynamic changes at multiple levels of the sensorimotor system, from the neuromuscular junction up to the cerebral cortex, as documented by the previous behavioral and electrophysiological studies (Kaňovský et al. 1998; Abbruzzese and Berardelli 2006). The previous functional magnetic resonance imaging (fMRI) studies from our center showed significant treatment-related changes in the sensorimotor network in patients receiving long-term treatment with BoNT type A (Opavský et al. 2011, 2012).

Nevertheless, specialists in movement disorders clinics soon realized that dystonia may behave differently over the course of BoNT treatment. The first reports described the changes of the muscular pattern (Gelb et al. 1991; Deuschl et al. 1992; Marin et al. 1992, 1995; Kaňovský et al. 1997) that may have also implied a central mechanism of dystonia.

We assume that the changing clinical behavior and evolving clinical response to BoNT treatment will also be reflected in changes of task-related functional MRI activation after therapy. The aim of the presented work is to study changes in the sensorimotor network in patients after the very first BoNT injection, using the same task as in our previous work (Opavský et al. 2011).

Subject and methods

Patients enrolled in the project underwent a comprehensive neurological examination by a movement disorders specialist. All subjects had typical clinical symptoms for at least 12 months and underwent polyelectromyographic examination of neck muscles. To be eligible for the study each patient had to have magnetic resonance (MR) imaging of the brain

with no structure abnormality. Each patient was informed in detail about the goal and the course of investigation, and signed an informed consent form. The study protocol was approved by the local ethics committee, in accordance with the principles and recommendations of the Declaration of Helsinki, 1975 and later revisions.

Twelve BoNT-naïve patients (1 male and 11 females; aged 48.8 ± 11.7 years, range 31–70 years) with CD were examined with fMRI during a skilled hand movement with their eyes closed. The examination was repeated 4 weeks after the first BoNT injection to the dystonic neck muscles. Twelve age- and gender-matched healthy controls (2 males and 10 females; aged 49.7 ± 13.9 years, range 25–64 years) were examined using the same functional MRI paradigm without BoNT injection.

The severity of CD was evaluated using the Toronto Western Spasmodic Torticollis Rating Scale (TWSTRS) (Consky and Lang 1994) at two sessions: at week 0, on the day of screening, of the first fMRI examination before the BoNT injection, and at week 4, on the day of the second fMRI examination. In all patients, the injected muscles were determined on the basis of a polyelectromyographic examination, provided by 4-channel Keypoint workstation, Medtronic®, Minneapolis, MN, USA. The details of the electromyographic examination and BoNT injection were described in our previous work (Kaňovský et al. 1998). All patients were treated with onabotulinum toxin type A (Botox®; Allergan, Inc, Irvine, CA, USA) in concentrations of 25 IU/ml. The demographic and clinical data of the patients are presented in Table 1.

Prior to the imaging session, participants were trained in the laboratory in the active task to be performed in the scanner. The task was a complex sequential opposition of individual fingers to thumb with the following order of movements: index finger 1×, ring finger 2×, middle finger 3×, and little finger 4×. During fMRI scanning, patients had their eyes closed, and instructions to start and stop movement were given verbally in MR-compatible headphones. In a block paradigm, movement (7.5 s) was alternated with rest (7.5 s). Each experimental run consisted of 16 movement-rest block pairs, for a total of 4 min. Experimental conditions were repeated twice with the same hand. Performance was visually monitored, recording the number of finger sequences completed per block.

MR imaging data were acquired on 1.5 T scanners (Avanto and Symphony, Siemens, Erlangen, Germany) with a standard head coil. The MR imaging protocol covered the whole brain and included anatomical T₁-weighted images to provide an immediate overlay with functional data, fluid-attenuated inversion recovery (FLAIR) images to visualize brain lesions, functional T₂*-weighted (BOLD) images during task performance and rest, and a high-resolution 3D anatomical scan (MPRAGE). BOLD images were

Table 1 Demographic data of the patients (both CD and control group) and results of TWSTRS before and after BoNT-A injection

Control group		Study group				
Sex	Age (years)	Sex	Age (years)	Total BoNT-A dose (Botox U)	TWSTRS at week 0	TWSTRS at week 4
F	52	F	45	200	19	10
M	59	F	45	200	15	8
F	34	M	60	150	10	4
F	25	F	42	150	24	19
F	26	F	56	150	18	9
F	55	F	40	200	17	7
F	64	F	64	100	16	6
F	61	F	33	200	19	12
F	62	F	55	100	13	7
M	57	F	44	200	15	8
F	46	F	70	100	13	7
F	55	F	31	200	12	7
Mean	49.7	Mean	48.8	162.5	15.9	8.7

acquired using gradient-echo echo-planar imaging (EPI) sequence, with repetition/echo time (TR/TE) = 2500/40 ms, field of view (FOV) 220 mm, and 30 axial slices, to provide $3.4 \times 3.4 \times 5$ mm resolution. A total of 96 images were acquired per each 4-min functional run. The subject's head was immobilized with cushions to assure maximum comfort and minimize head motion.

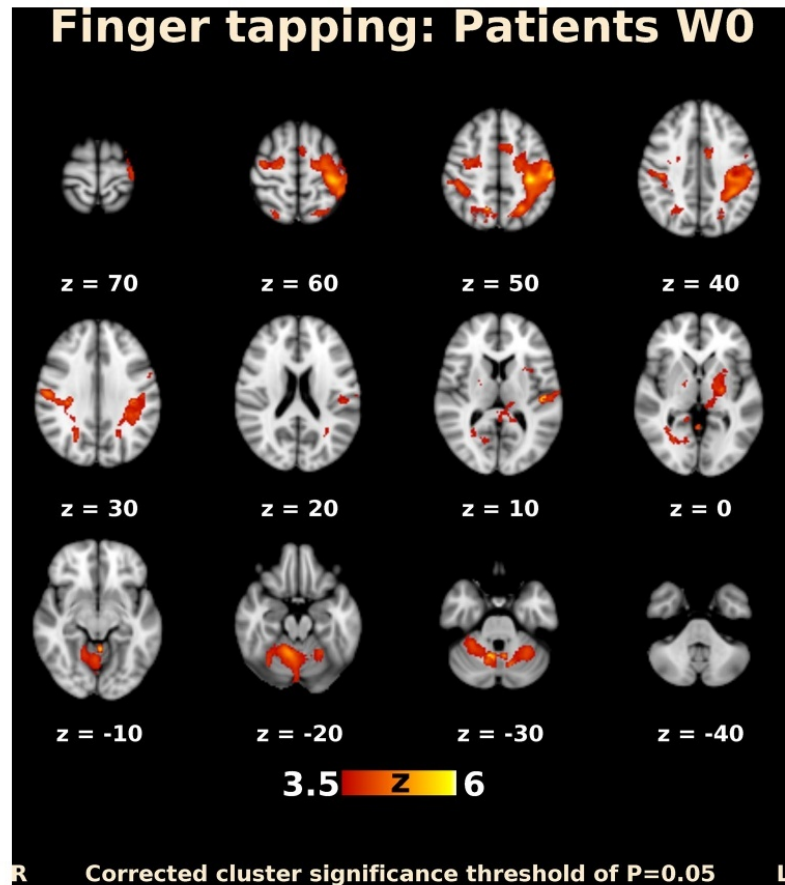
Prior to fMRI analysis, the imaging data of patients with the left-sided dystonia leading muscle were flipped in the left–right direction (Johansen-Berg et al. 2002). fMRI data processing was carried out using the FSL version 5.0 (FMRIB's Software Library, <http://www.fmrib.ox.ac.uk/fsl>) (Smith et al. 2004; Jenkinson et al. 2012). The following pre-statistics processing was applied: motion correction; slice-timing correction using Fourier-space time-series phase-shifting; non-brain removal; spatial smoothing using a Gaussian kernel of full-width at half-maximum (FWHM) 8 mm; grand-mean intensity normalization; high-pass temporal filtering with sigma 7.5 s; and spatial normalization/registration to the standard-space MNI template. Time-series statistical analysis was carried out using a generalized linear model, implemented in FMRIB's improved linear model (FILM) with local autocorrelation correction. Group analysis was performed using FMRIB's Local Analysis of Mixed Effects (FLAME) stages 1 and stage 2 with automatic outlier detection. Statistical maps were thresholded using clusters corrected $P = 0.05$. The voxelwise Z (Gaussianized T) threshold was adjusted to reflect the expected effect size. We evaluated (1) mean activation thresholded at $Z > 3.5$; (2) within-group differences in patients at $Z > 2$; and (3) between-group differences at each timepoint and within-group changes over time at $Z > 1.7$. The differences were evaluated within the respective significant clusters of mean activation.

Results

All patients were injected into the muscles identified by polyelectromyography. The dose for each cervical muscle was 50 IU, and the mean total dose for a patient was 162.5 ± 43.3 IU. The significant clinical effect of BoNT injections was evaluated using the TWSTRS at week 4. The mean value of TWSTRS at week 0 was 15.9 ± 3.8 , and at week 4, it was 8.7 ± 3.8 ($P = 0.00002$, one-sided paired t test). Details are provided in Table 1. All patients and controls were right-handed, and conventional brain MRI was completely normal in all subjects. For the hand motor task, patients used the hand ipsilateral to the dystonic leading muscle. In 7/12 patients, it was the dominant hand, and in the remaining 5/12 cases, the non-dominant one. Subjects in the control group used hand randomly. The proportion of dominant vs. non-dominant hands was the same in both groups.

Before BoNT injection, patients performing finger movements activated multiple brain areas, predominantly within the sensorimotor system, including the contralateral primary motor and somatosensory cortex, contralateral secondary somatosensory cortex, bilateral premotor cortex, contralateral supplementary motor area (SMA), bilateral superior and inferior parietal lobule, bilateral cerebellum, contralateral thalamus, bilateral pallidum, and putamen (Fig. 1). The activation map at week 4 after BoNT injection showed a more extended but similar distributed brain network (Fig. 2). A direct comparison of both timepoints (paired contrast) revealed that the activation increased after treatment in most of the brain areas activated before BoNT injection, especially in the bilateral primary and secondary somatosensory cortex, bilateral superior and inferior parietal lobule, bilateral SMA and premotor cortex, predominantly contralateral

Fig. 1 Functional MRI activation map in patients with CD before BoNT-A injection. Slices are labeled with Z/Y coordinate in standard MNI152 space

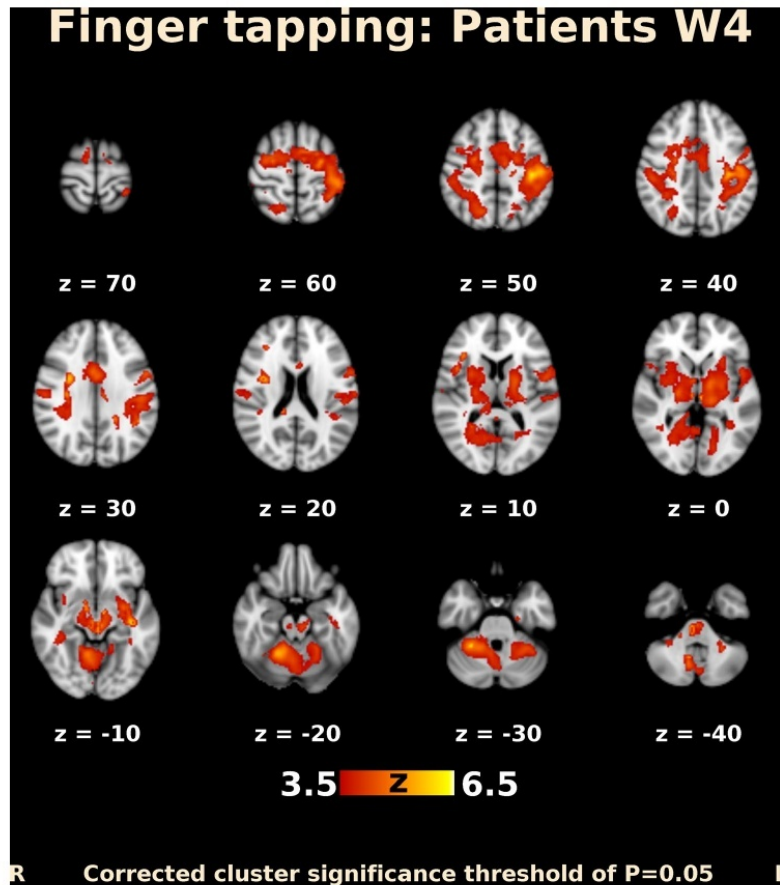


primary motor cortex, bilateral anterior cingulate cortex, as well as in the predominantly ipsilateral thalamus, insula, and putamen. A significant increase in activation was also apparent in the central part of cerebellum, close to the vermis (Figs. 3, 4); however, there was no significant activation decrease after BoNT injection. When compared to the control group, patients before treatment showed significantly lower activation mainly in the bilateral SMA, ipsilateral cingulate and paracingulate cortex, as well as in the ipsilateral caudate, pallidum, and thalamus (Fig. 5), whereas there was no significant difference between the control group and the patient group after BoNT injection. No significant movement artifacts (maximal framewise movement head displacement was 2.28 mm in one subject; in the rest, it was smaller than 2 mm) were found in any of the MRI images.

The possible influence of faster movements was correlated with the expected task-related hemodynamic response function, which could potentially negatively

affect presented results. Evaluating the amount and influencing of task-correlated motion were extracted six original motion parameters (three rotations and three translations) and two derived motion parameters (the absolute voxel displacement from a reference volume and the relative voxel displacement between two consecutive volumes), which were estimated in each subject during the preprocessing. Next, Spearman correlation coefficient was used to correlate each motion vector with the task vector convolved with the hemodynamic response function. The absolute values of the correlation coefficients were compared between the sessions using pairwise sign rank Wilcoxon test. As a result, none of the tested coefficients differed significantly between the sessions ($p=0.2$ or greater). The overall correlation coefficients were rather low (ranging from $\rho=0.08$ to $\rho=0.19$). Thus, we consider any potential effect of task-correlated motion to be negligible.

Fig. 2 Functional MRI activation map in patients with CD 4 weeks after BoNT-A injection. Slices are labeled with Z/Y coordinate in standard MNI152 space



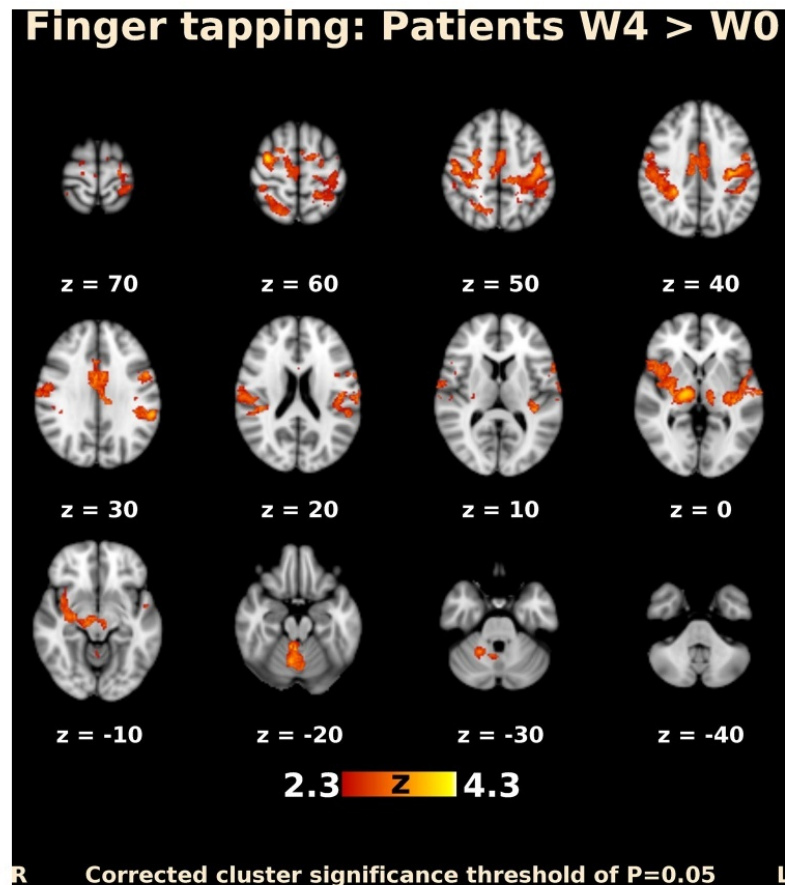
Discussion

In this work, we have studied changes in fMRI activation after the first BoNT injection. We consider this trait of the study population as one of the significant contributions of our study, since most of the previous papers reported either changes in long-term-treated patients with CD (Carbon et al. 2008; Obermann et al. 2008, 2010; Opavský et al. 2011, 2012; Burciu et al. 2017) or focused on differences between treated patients and controls, rather than on effects of therapy (de Vries et al. 2008). In BoNT-naïve patients with CD, BoNT treatment was associated with a significant increase of activation in finger movement-induced fMRI activation of several brain areas, especially in the bilateral primary and secondary somatosensory cortex, bilateral superior and inferior parietal lobule, bilateral SMA and premotor cortex, predominantly contralateral primary motor cortex, bilateral anterior cingulate cortex, ipsilateral thalamus, insula, and

putamen, and the central part of cerebellum, close to the vermis. These results support the previous observations that the BoNT effect has a correlate at the central nervous system level (e.g., Kaňovský et al. 1998; Šenkárová et al. 2010; Palomar and Mir 2012). The abnormal cortical activation detected during skilled motor tasks performed with a non-dystonic body part also confirms the previous electrophysiological and functional imaging observations that sensorimotor abnormalities in the dystonic brain extend beyond the directly clinically affected sensorimotor representations (Kaňovský et al. 2003; Thickbroom et al. 2003; Opavský et al. 2011, 2012).

In cervical dystonia, earlier fMRI studies by Opavský et al. (2011, 2012) showed significant changes in the sensorimotor network in patients receiving long-term treatment with BoNT. The results of the present study in patients after the first BoNT injection show certain similarities, especially with respect to the localization of the

Fig. 3 Functional MRI activation map (transversal slices) in patients with CD. Differences in activation after and before BoNT-A injection. Slices are labeled with *Z/Y* coordinate in standard MNI152 space

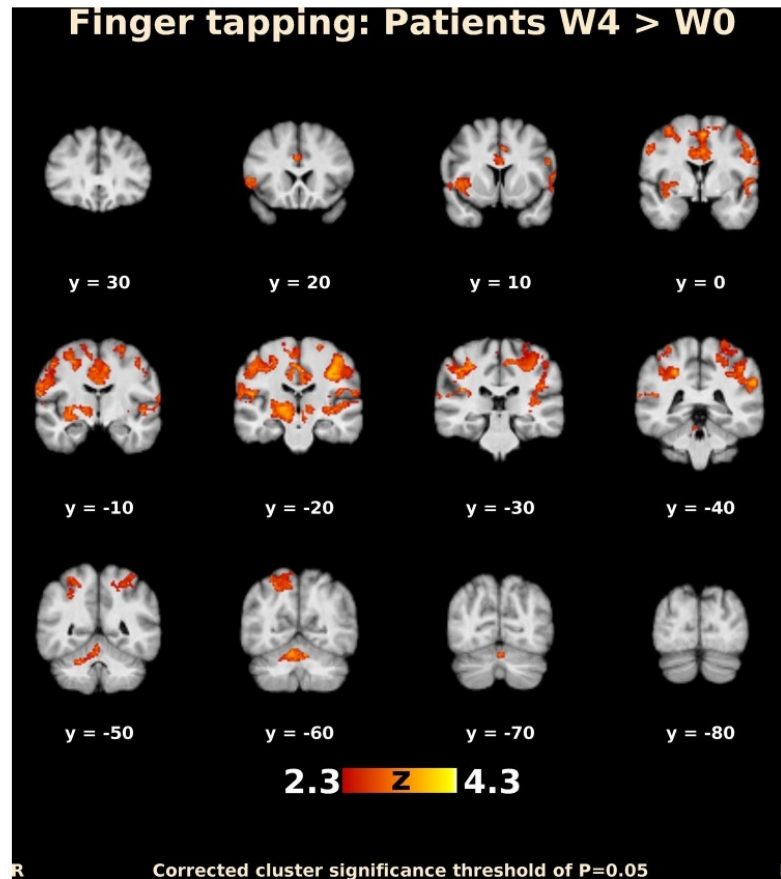


activation changes. However, in contrast to the decrease of activation in long-term-treated patients reported by Opavský et al. (2011, 2012), the present results demonstrate an increase of activation in patients with CD after the very first BoNT injection. Although the limitation of a small patient cohort has to be acknowledged, the opposite direction of activation changes occurring in almost the same brain areas in a single type of focal dystonia in response to either initial or long-term BoNT therapy could provide evidence for long-term brain plasticity and more complex changes induced by BoNT, which involve not only the neuromuscular junction, but also the central nervous system.

The significant treatment-induced changes in our study were detected in areas involved in sensorimotor control and motor learning. In the following section, we will review the function of these regions and discuss their role in the pathophysiology of CD and in the response to BoNT treatment.

The SMA, which was hypoactivated in CD and showed activation increase after BoNT treatment, is considered to be involved in many processes such as posture regulation, internal generation of movement, bimanual coordination, and movement sequencing (Tanji 1996; Chouinard and Paus 2010). In primates, dystonia models demonstrated SMA hyperexcitability, an abnormal increase of proprioceptive inputs to the SMA, and wider sensory receptive fields and a mismatch between sensory inputs and motor outputs (Cuny et al. 2008). These observations may suggest that abnormal sensory inputs coming to SMA neurons participate in the development of dystonia. Hyperexcitability may then decrease the demand for recruitment of SMA neurons to control voluntary movement, which would manifest as reduced task-related activation in functional MRI. BoNT treatment supposedly reduces the abnormal afferent input, thereby reducing the baseline hyperexcitability of the SMA. After treatment, voluntary movement may, therefore,

Fig. 4 Functional MRI activation map (coronal slices) in patients with CD. Differences in activation after and before BoNT-A injection. Slices are labeled with Z/Y coordinate in standard MNI152 space



require increased engagement of SMA neurons. Such adaptive increase in activation of the medial premotor cortex has been demonstrated in response to many pathological processes, such as stroke, injury, etc. (e.g., Katak et al. 2012).

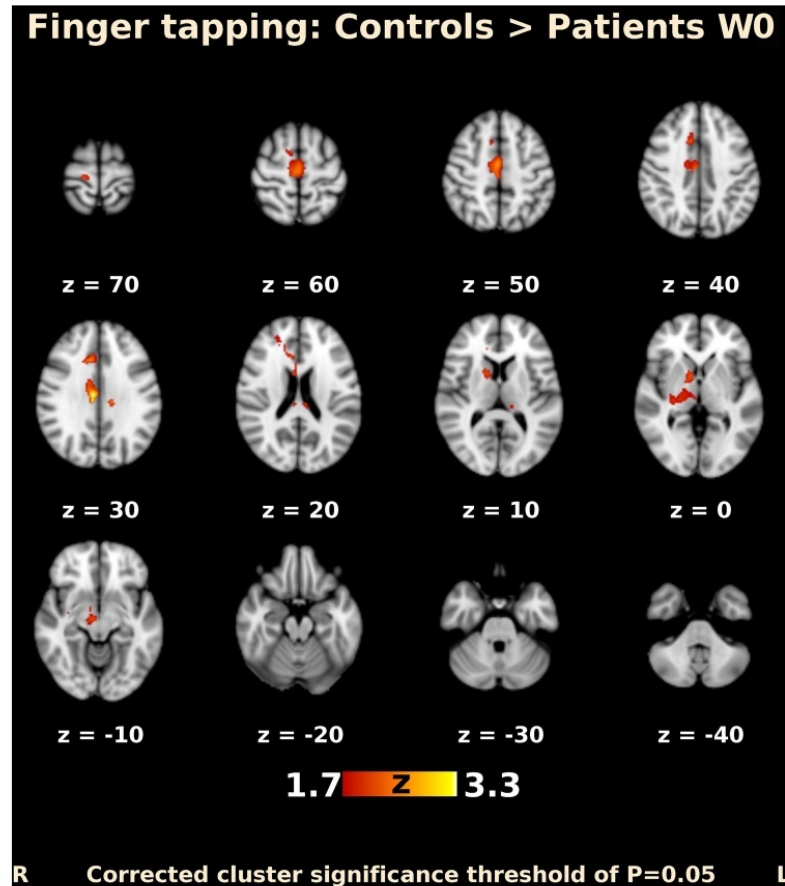
The cingulate cortex is another structure that showed significant hypoactivation in patients with CD and treatment-related activation increase. It is a structurally heterogeneous brain region involved in emotional, cognitive, and motor tasks (Torta and Cauda 2011). The dorsal cingulate sulcus has several motor regions that are active during movement. The cingulate cortex has rich anatomical connections with SMA and both structures are implicated in integration of emotional and motor processing (Oliveri et al. 2003). Therefore, the presented changes in the cingulate cortex probably reflect a similar mechanism as the changes in SMA.

Further intriguing treatment-related activation changes were detected in the central and pericentral parts of the cerebellum. Although the cerebellum is not traditionally noted among the major substrates for development of dystonia,

interest in this neuronal structure has increased recently (Avanzino and Abbruzzese 2017; Sadnicka et al. 2012; Filip et al. 2013a, b) as its role in the pathophysiology of dystonia has been suggested by animal models (Jin et al. 2005; Raïke et al. 2005; Vidailhet et al. 2009), imaging studies (Carbon et al. 2008; Obermann et al. 2010; Opavský et al. 2011, 2012; Prudente et al. 2016; Burciu et al. 2017), neurophysiological studies (Liepert et al. 2004), and even analyses of secondary CD (LeDoux and Brand 2003; Extremera et al. 2008). Neurological disorders originating from the cerebellum (e.g., ataxia) are usually associated with a loss of function. However, different syndromes can arise from the same pathway as different defects alter the output in different ways. In dystonia, it is still disputable whether the cerebellum is the source of the disease or just a node in a complex network trying to compensate for dysfunction of other parts of the brain.

The activation increases post-treatment and was also observed in the secondary somatosensory cortex, which is

Fig. 5 Functional MRI activation map (transversal slices). Differences in activation between CD patients group before BoNT-A injection and control group. Slices are labeled with Z/Y coordinate in standard MNI152 space



located in the parietal operculum. It is implicated in higher order functions in somatosensory processing, but it is also believed to integrate information from the two sides of the body, and to participate in visuospatial attention, learning, and memory. According to the previous electrophysiological and imaging evidence, CD seems to be associated with disorders of not only motor but also sensory cortical processing, perhaps at the level of sensorimotor integration (Siggelkow et al. 2002; Abbruzzese et al. 2001; Fransson et al. 2001; Rosales and Dressler 2010). Abbruzzese and Berardelli (2003) consider the aberrant sensorimotor processing to be a key factor for the development of focal dystonias. In a broader sense, the sensorimotor integration involves all parts of the motor and sensory system, including the motor circuits, in which the basal ganglia and the premotor and motor cortex are the principal components.

Finally, the hypoactivations and treatment-related activation increases were also detected in the ipsilateral striatum,

pallidum, and thalamus. The involvement of subcortical structures is not unexpected as some previous studies in CD-reported abnormal bilateral activation of the basal ganglia and thalamus during non-dystonia-associated tasks (Obermann et al. 2008; Opavský et al. 2011). Moreover, the internal pallidum serves as a target for effective modulation of CD and other forms of primary dystonias using deep brain stimulation, with an imprecisely characterized mode of action. Whereas higher field MR scanners have certainly provided better spatial and temporal resolution, our spatial resolution of $3.5 \times 3.5 \times 5$ mm appears sufficient to reliably detect basal ganglia activation in normal subjects and neurological patients (Obermann et al. 2008; Hok et al. 2017; Marchal-Crespo et al. 2017).

With respect to overall pattern and direction of activation changes, the previous studies in long-term-treated patients with CD reported that CD was associated with hyperactivations before the BoNT injection (Obermann et al. 2008;

Opavský et al. 2011), whereas our study in untreated patients demonstrates widespread hypoactivations. Similar activation decrease was documented previously in a heterogeneous group of eight patients with CD, where five of them were BoNT-naïve (de Vries et al. 2008) and also in another focal dystonia, writer's cramp (Castrop et al. 2012). However, the global picture seems to be even more complex, since a recent study utilizing fMRI in CD during a force production task reported both distributed activation increases and decreases in comparison with healthy controls (Burciu et al. 2017). Although the provided evidence is difficult to reconcile, the differing direction of functional changes (increased vs. decreased activity compared to healthy controls) may be explained by differences in patient populations, especially the differences in treatment [e.g., naïve vs. long-term-treated patients (Obermann et al. 2008; Opavský et al. 2011)], and functional MRI activation tasks [sequential finger opposition (Opavský et al. 2011) vs. forearm contraction (Obermann et al. 2008) vs. wrist flexion/extension and fist clenching (de Vries et al. 2008)].

Both in neurophysiology and functional imaging, cortical differences between baseline HC and patients with dystonia diminish following a successful treatment with BoNT. The implication is that a peripheral blockade of effectors may influence the central motor programs in dystonia. As we await more data on the probable 'direct' retrograde effects of BoNT (e.g., Antonucci et al. 2008), the 'indirect' effects remain tenable to date, the latter being hinged upon the normalization of abnormal muscle-spindle functioning in dystonia (Rosales and Dressler 2010). The consequent and apparent normalization of the cortical disorder following BoNT injections in dystonia as observed in neurophysiological studies may indicate that the manipulation of proprioceptive afferent input has a substantial impact on the disorder directly at the central level (Kaňovský et al. 1998; Gilio et al. 2000; Kaňovský and Rosales 2011). It is important to emphasize that treatment with BoNT leads to changes in the central nervous system not only in dystonia, but also in spasticity, as shown in the previous fMRI (Šenkárová et al. 2010; Veverka et al. 2012; Tomášová et al. 2013) and transcranial magnetic stimulation (Huynh et al. 2013) studies. We are aware that there are similarities as well as differences in the two BoNT indications. Dystonia reflects maladaptive plasticity, whereas patients with stroke manifest both adaptive changes related to recovery of function and maladaptive changes likely underlying spasticity. BoNT aims to specifically target the maladaptive process in both conditions. The results of these studies showed a much more complex effect of the long term and regular BoNT injections, although the pathophysiology of spasticity differs from pathophysiological processes in dystonia (Veverka et al. 2016).

We acknowledge that the mechanism how BoNT could affect the central activity is not fully elucidated.

Marchand-Pauvert et al. (2013) summarize the recent evidence of blockade of the gamma motor endings, of plastic changes following blockade of the neuromuscular transmission and of retrograde transport and transcytosis. Presently, it is not clear, which of these mechanisms contributes to the changes observed in functional imaging studies.

We acknowledge several limitations of the study which temper our conclusions and should be addressed in future research: recording the number of finger sequences completed per block does not capture all aspects of motor performance. The results should be replicated in a larger patient cohort, possibly using several different motor tasks, so that effects of a specific, carefully controlled and/or monitored motor task and a specific patient cohort might be separated. More timepoints post-treatment from baseline would permit better insight as to whether the changes in fMRI occurred before, after or at the same time as the improvements in clinical parameters—this may help explain whether the central changes are in fact primary driving the improvement or secondary effects. We acknowledge that the controls were scanned only once, whereas a balanced design would be more powerful to rule out effects of repeated motor testing. Nevertheless, single repetition of a motor task typically leads to a decrease, rather than increase, in sensorimotor activation (Hok et al. 2017 + další mimoOI citace). MRI-compatible electromyographic recording from the cervical musculature would permit modeling the influences of possible changes in dystonic activity after BoNT treatment. Finally, combining multiple examination methods in the same protocol, e.g., functional MRI and TMS, would provide richer data to help describe the complex pathophysiological processes (de Vries et al. 2012).

In conclusion, the results of the present study demonstrate that in treatment of CD, the first BoNT injection is associated with changes in widespread sensorimotor networks, which diminish the observed baseline differences between the patients and healthy controls. This study also confirms that abnormalities in sensorimotor activation extend beyond circuits controlling the affected body parts in CD.

Acknowledgements Research supported by Grant AZV MH CR 16-30210A from the Czech Health Research Council and by the Institutional support of the Research Organisation—Ministry of Health, Czech Republic, RVO—FNOL 2017. Thanks to Anne Johnson for grammatical assistance.

Open Access This article is distributed under the terms of the Creative Commons Attribution 4.0 International License (<http://creativecommons.org/licenses/by/4.0/>), which permits unrestricted use, distribution, and reproduction in any medium, provided you give appropriate credit to the original author(s) and the source, provide a link to the Creative Commons license, and indicate if changes were made.

References

- Abbruzzese G, Berardelli A (2003) Sensorimotor integration in movement disorders. *Mov Disord* 3:231–240
- Abbruzzese G, Berardelli A (2006) Neurophysiological effects of botulinum toxin type A. *Neurotox Res* 9:109–114
- Abbruzzese G, Marchese R, Buccolieri A, Gasparetto B, Trompetto C (2001) Abnormalities of sensorimotor integration in focal dystonia: a transcranial magnetic stimulation study. *Brain* 124(Pt 3):537–545
- Antonucci F, Rossi C, Gianfranceschi L, Rossetto O, Caleo M (2008) Long-distance retrograde effects of botulinum neurotoxin A. *J Neurosci* 28(14):3689–3696
- Avanzino L, Abbruzzese G (2012) How does the cerebellum contribute to the pathophysiology of dystonia? *Basal Ganglia* 2(4):231–235
- Burciu RG, Hess CW, Coombes SA, Ofori E, Shukla P, Chung JW, McFarland NR, Wagle Shukla A, Okun MS, Vaillancourt DE (2017) Functional activity of the sensorimotor cortex and cerebellum relates to cervical dystonia symptoms. *Hum Brain Mapp* 38(9):4563–4573
- Carbon M, Ghilardi MF, Argyelan M, Dhawan V, Bressman SB, Eidelberg D (2008) Increased cerebellar activation during sequence learning in DYT1 carriers: an equiperformance study. *Brain* 131(1):146–154
- Castrop F, Dresel C, Hennenlotter A, Zimmer C, Haslinger B (2012) Basal ganglia-premotor dysfunction during movement imagination in writer's cramp. *Mov Disord* 27(11):1432–1439
- Chouinard PA, Paus T (2010) What have we learned from “perturbing” the human cortical motor system with transcranial magnetic stimulation? *Front Hum Neurosci* 19(4):173
- Consky E, Lang A (1994) Clinical assessments of patients with cervical dystonia. In: Jankovic JHM (ed) *Therapy with Botulinum Toxin*. Marcel Dekker Inc., New York
- Cuny E, Ghorayeb I, Guehl D, Escola L, Bioulac B, Burbaud P (2008) Sensory motor mismatch within the supplementary motor area in the dystonic monkey. *Neurobiol Dis* 2:151–161
- de Vries PM, Johnson KA, de Jong BM, Gieteling EW, Bohning DE, George MS, Leenders KL (2008) Changed patterns of cerebral activation related to clinically normal hand movement in cervical dystonia. *Clin Neurol Neurosurg* 110(2):120–128
- de Vries PM, de Jong BM, Bohning DE, Hinson VK, George MS, Leenders KL (2012) Reduced parietal activation in cervical dystonia after parietal TMS interleaved with fMRI. *Clin Neurol Neurosurg* 114(7):914–921
- Deuschl G, Heinen F, Kleedorfer B, Wagner M, Lücking CH, Poewe W (1992) Clinical and polymyographic investigation of spasmodic torticollis. *J Neurol* 239(1):9–15
- Extremiera VC, Alvarez-Coca J, Rodriguez GA, Perez JM, de Villanueva JLR, Diaz CP (2008) Torticollis is a usual symptom in posterior fossa tumors. *Eur J Pediatr* 167(2):249–250
- Filip P, Lungu OV, Bares M (2013a) Dystonia and the cerebellum: a new field of interest in movement disorders? *Clin Neurophysiol* 124(7):1269–1276
- Filip P, Lungu OV, Shaw DJ, Kasperek T, Bareš M (2013b) The mechanisms of movement control and time estimation in cervical dystonia patients. *Neural Plast* 2013:908741
- Filip P, Gallea C, Lehericy S, Bertasi E, Popa T, Mareček R, Lungu OV, Kašpárek T, Vaníček J, Bareš M (2017) Disruption in cerebellar and basal ganglia networks during a visuospatial task in cervical dystonia. *Mov Disord* 32(5):757–768
- Frasson E, Priori A, Bertolasi L, Mauguière F, Fiaschi A, Tinazzi M (2001) Somatosensory disinhibition in dystonia. *Mov Disord* 16(4):674–682
- Gelb DJ, Yoshimura DM, Olney RK, Lowenstein DH, Aminoff MJ (1991) Change in pattern of muscle activity following botulinum toxin injections for torticollis. *Ann Neurol* 29(4):370–376
- Gilio F, Currà A, Lorenzano C, Modugno N, Manfredi M, Berardelli A (2000) Effects of botulinum toxin type A on intracortical inhibition in patients with dystonia. *Ann Neurol* 48(1):20–26
- Hinkley LB, Webster RL, Byl NN, Nagarajan SS (2009) Neuroimaging characteristics of patients with focal hand dystonia. *J Hand Ther* 2:125–134
- Hok P, Opavský J, Kutín M, Tüdös Z, Kaňovský P, Hlušík P (2017) Modulation of the sensorimotor system by sustained manual pressure stimulation. *Neuroscience* 21:348:11–22
- Huynh W, Krishnan AV, Lin CS, Vucic S, Katrak P, Hornberger M, Kiernan MC (2013) Botulinum toxin modulates cortical maladaptation in poststroke spasticity. *Muscle Nerve* 48(1):93–99
- Jankovic J (2004) Treatment of cervical dystonia with botulinum toxin. *Mov Disord (Suppl 8)*:S109–S115
- Jenkinson M, Beckmann CF, Behrens TEJ, Woolrich MW, Smith SM (2012) FSL. *Neuroimage* 62:782–790
- Jinnah HA, Hess EJ, LeDoux MS, Sharma N, Baxter MG, DeLong MR (2005) Rodent models for dystonia research: characteristics, evaluation, and utility. *Mov Disord* 20(3):283–292
- Johansen-Berg H, Dawes H, Guy C, Smith SM, Wade DT, Matthews PM (2002) Correlation between motor improvements and altered fMRI activity after rehabilitative therapy. *Brain* 125:2731–2742
- Kaňovský P, Rosales RL (2011) Debunking the pathophysiological puzzle of dystonia with special reference to botulinum toxin therapy. *Parkinsonism Relat Disord* 17(Suppl 1):S11–S14
- Kaňovský P, Dufek J, Halačková H, Rektor I (1997) Change in the pattern of cervical dystonia might be the cause of benefit loss during botulinum toxin treatment. *Eur J Neurol* 4(1):79–84
- Kaňovský P, Streitová H, Dufek J, Znojil V, Daniel P, Rektor I (1998) Change in lateralization of the P22/N30 cortical component of median nerve somatosensory evoked potentials in patients with cervical dystonia after successful treatment with botulinum toxin A. *Mov Disord* 1:108–117
- Kaňovský P, Bareš M, Streitová H, Klajblová H, Daniel P, Rektor I (2003) Abnormalities of cortical excitability and cortical inhibition in cervical dystonia. Evidence from somatosensory evoked potentials and paired transcranial magnetic stimulation recordings. *J Neurol* 250:42–50
- Kantak SS, Stinear JW, Buch ER, Cohen LG (2012) Rewiring the brain: potential role of the premotor cortex in motor control, learning, and recovery of function following brain injury. *Neurorehabil Neural Repair* 26(3):282–292
- LeDoux MS, Brand KA (2003) Secondary cervical dystonia associated with structural lesions of the central nervous system. *Mov Disord* 18(1):60–69
- Liepert J, Kucinski T, Tuschler O, Pawlas F, Baumer T, Weiller C (2004) Motor cortex excitability after cerebellar infarction. *Stroke* 35(11):2484–2488
- Marchal-Crespo L, Michels L, Jaeger L, López-Olóriz J, Riener R (2017) Effect of error augmentation on brain activation and motor learning of a complex locomotor task. *Front Neurosci* 11:526
- Marchand-Pauvert V, Aymard C, Giboin LS, Dominici F, Rossi A, Mazzocchio R (2013) Beyond muscular effects: depression of spinal recurrent inhibition after botulinum neurotoxin A. *J Physiol* 591(4):1017–1029
- Marin C, Martí MJ, Tolosa E, Alvarez R, Montserrat LL, Santamaria J (1992) Modification of muscle activity after BOTOX injections in spasmodic torticollis. *Ann Neurol* 32(3):411–412
- Marin C, Martí MJ, Tolosa E, Alvarez R, Montserrat L, Santamaria J (1995) Muscle activity changes in spasmodic torticollis after botulinum toxin treatment. *Eur J Neurol* 1(3):243–247

- Obermann M, Yaldizli O, de Greiff A, Konczak J, Lachenmayer ML, Tumczak F et al (2008) Increased basal-ganglia activation performing a non-dystonia-related task in focal dystonia. *Eur J Neurol* 8:831–838
- Obermann M, Vollrath C, de Greiff A, Gizewski ER, Diener HC, Hallett M, Maschke M (2010) Sensory disinhibition on passive movement in cervical dystonia. *Mov Disord* 25(15):2627–2633
- Oliveri M, Babiloni C, Filippi MM, Caltagirone C, Babiloni F, Cicinelli P, Traversa R, Palmieri MG, Rossini PM (2003) Influence of the supplementary motor area on primary motor cortex excitability during movements triggered by neutral or emotionally unpleasant visual cues. *Exp Brain Res* 149(2):214–221
- Opavský R, Hlušík P, Otruba P, Kaňovský P (2011) Sensorimotor network in cervical dystonia and the effect of botulinum toxin treatment: a functional MRI study. *J Neur Sci* 306(1–2):71–75
- Opavský R, Hlušík P, Otruba P, Kaňovský P (2012) Somatosensory cortical activation in cervical dystonia and its modulation with botulinum toxin: an fMRI study. *Int J Neurosci* 122(1):45–52
- Palomar FJ, Mir P (2012) Neurophysiological changes after intramuscular injection of botulinum toxin. *Clin Neurophysiol* 123(1):54–60
- Peterson DA, Sejnowski TJ, Poizner H (2010) Convergent evidence for abnormal striatal synaptic plasticity in dystonia. *Neurobiol Dis* 3:558–573
- Prudente CN, Stilla R, Singh S, Bueteftisch C, Evatt M, Factor SA, Freeman A, Hu XP, Hess EJ, Sathian K, Jinnah HA (2016) A functional magnetic resonance imaging study of head movements in cervical dystonia. *Front Neurol* 7:201
- Raika RS, Jinnah HA, Hess EJ (2005) Animal models of generalized dystonia. *NeuroRx* 2(3):504–512
- Rosales RL, Dressler D (2010) On muscle spindles, dystonia and botulinum toxin. *Eur J Neurol* 17(Suppl 1):71–80
- Sadnicka A, Hoffland BS, Bhatia KP, van de Warrenburg BP, Edwards MJ (2012) The cerebellum in dystonia help or hindrance? *Clin Neurophysiol* 123(1):65–70
- Šenkárová Z, Hlušík P, Otruba P, Herzig R, Kaňovský P (2010) Modulation of cortical activity in patients suffering from upper arm spasticity following stroke and treated with botulinum toxin A: an fMRI study. *J Neuroimaging* 20(1):9–15
- Siggelkow S, Kossev A, Moll C, Däuper J, Dengler R, Rollnik JD (2002) Impaired sensorimotor integration in cervical dystonia: a study using transcranial magnetic stimulation and muscle vibration. *J Clin Neurophysiol* 3:232–239
- Smith SM, Jenkinson M, Woolrich MW, Beckmann CF, Behrens TEJ, Johansen-Berg H, Bannister PR, De Luca M, Drobnjak I, Flitney DE, Niazzy RK, Saunders J, Vickers J, Zhang Y, De Stefano N, Brady JM, Matthews PM (2004) Advances in functional and structural MR image analysis and implementation as FSL. *Neuroimage* 23(Suppl 1):208–219
- Stacy M (2000) Idiopathic cervical dystonia: an overview. *Neurology* 12(Suppl 5):2–8
- Tanji J (1996) New concepts of the supplementary motor area. *Curr Opin Neurobiol* 6:782–787
- Thickbroom GW, Byrnes ML, Stell R, Mastaglia FL (2003) Reversible reorganisation of the motor cortical representation of the hand in cervical dystonia. *Mov Disord* 18(4):395–402
- Tinazzi M, Fiorio M, Fiaschi A, Rothwell JC, Bhatia KP (2009a) Sensory functions in dystonia: insights from behavioral studies. *Mov Disord* 10:1427–1436
- Tinazzi M, Squintani G, Berardelli A (2009b) Does neurophysiological testing provide the information we need to improve the clinical management of primary dystonia? *Clin Neurophysiol* 8:1424–1432
- Tomášová Z, Hlušík P, Král M, Otruba P, Herzig R, Krobot A, Kaňovský P (2013) Cortical activation changes in patients suffering from post-stroke arm spasticity and treated with botulinum toxin a. *J Neuroimaging* 23(3):337–344
- Torta DM, Cauda F (2011) Different functions in the cingulate cortex, a meta-analytic connectivity modeling study. *Neuroimage* 56(4):2157–2172
- Veverka T, Hlušík P, Tomášová Z, Hok P, Otruba P, Král M, Tüdös Z, Zapletalová J, Herzig R, Krobot A, Kaňovský P (2012) BoNT-A related changes of cortical activity in patients suffering from severe hand paralysis with arm spasticity following ischemic stroke. *J Neurol Sci* 319(1–2):89–95
- Veverka T, Nevrlý M, Otruba P, Hlušík P, Kaňovský P (2016) How much evidence do we have on the central effects of botulinum toxin in spasticity and dystonia? In: Rosales R et al (ed) Botulinum toxin therapy manual for dystonia and spasticity. InTech, Rijeka, Croatia, pp 13–23
- Vidailhet M, Grabli D, Roze E (2009) Pathophysiology of dystonia. *Curr Opin Neurol* 22(4):406–413



Botulinum Toxin Modulates Posterior Parietal Cortex Activation in Post-stroke Spasticity of the Upper Limb

Tomáš Veverka^{1*}, Pavel Hok¹, Pavel Otruba¹, Jana Zapletalová², Barbora Kukolová³, Zbyněk Tüdös⁴, Alois Krobot⁵, Petr Kaňovský¹ and Petr Hlušík^{1,4}

¹ Department of Neurology, Palacký University and University Hospital, Olomouc, Czechia, ² Department of Biophysics, Biometry and Statistics, Palacký University and University Hospital, Olomouc, Czechia, ³ Rehabilitation Centre, Hrabyně, Czechia, ⁴ Department of Radiology, Palacký University and University Hospital, Olomouc, Czechia, ⁵ Department of Physiotherapy, Palacký University and University Hospital, Olomouc, Czechia

OPEN ACCESS

Edited by:

Martin Lotze,
University of Greifswald, Germany

Reviewed by:

Sergiu Groppa,
Johannes Gutenberg University
Mainz, Germany
Raymond Lotilla Rosales,
University of Santo Tomas, Philippines

*Correspondence:

Tomáš Veverka
tomas.veverka@fnol.cz

Specialty section:

This article was submitted to
Stroke,
a section of the journal
Frontiers in Neurology

Received: 04 February 2019

Accepted: 23 April 2019

Published: 09 May 2019

Citation:

Veverka T, Hok P, Otruba P, Zapletalová J, Kukolová B, Tüdös Z, Krobot A, Kaňovský P and Hlušík P (2019) Botulinum Toxin Modulates Posterior Parietal Cortex Activation in Post-stroke Spasticity of the Upper Limb. *Front. Neurol.* 10:495. doi: 10.3389/fneur.2019.00495

Post-stroke spasticity (PSS) is effectively treated with intramuscular botulinum toxin type A (BoNT-A), although the clinical improvement is likely mediated by changes at the central nervous system level. Using functional magnetic resonance imaging (fMRI) of the brain, this study aims to confirm and locate BoNT-A-related changes during motor imagery with the impaired hand in severe PSS. Temporary alterations in primary and secondary sensorimotor representation of the impaired upper limb were expected. Thirty chronic stroke patients with upper limb PSS undergoing comprehensive treatment including physiotherapy and indicated for BoNT treatment were investigated. A change in PSS of the upper limb was assessed with the modified Ashworth scale (MAS). fMRI and clinical assessments were performed before (W0) and 4 weeks (W4) and 11 weeks (W11) after BoNT-A application. fMRI data were acquired using 1.5-Tesla scanners during imagery of finger-thumb opposition sequences with the impaired hand. At the group level, we separately modeled (1) average activation at each time point with the MAS score and age at W0 as covariates; and (2) within-subject effect of BoNT-A and the effect of time since W0 as independent variables. Comprehensive treatment of PSS with BoNT-A significantly decreased PSS of the upper limb with a maximal effect at W4. Task-related fMRI prior to treatment (W0) showed extensive activation of bilateral frontoparietal sensorimotor cortical areas, bilateral cerebellum, and contralesional basal ganglia and thalamus. After BoNT-A application (W4), the activation extent decreased globally, mostly in the bilateral parietal cortices and cerebellum, but returned close to baseline at W11. The intra-subject contrast revealed a significant BoNT-A effect, manifesting as a transient decrease in the activation of the ipsilesional intraparietal sulcus and superior parietal lobule. We demonstrate that BoNT-A treatment of PSS of the upper limb is associated with transient changes in the ipsilesional posterior parietal cortex, possibly resulting from temporarily altered sensorimotor upper limb representations.

Keywords: stroke, spasticity, botulinum toxin, functional magnetic resonance imaging, neuronal plasticity, motor imagery

INTRODUCTION

Post-stroke spasticity (PSS) is a major sequelae among stroke survivors (1) with an estimated prevalence of 19–42.6% (2, 3). Clinically relevant PSS may interfere with voluntary movement and frequently causes deterioration in manual dexterity, mobility, walking, and hygiene (2). PSS of the upper limbs is currently treated with botulinum toxin type A (BoNT-A), which is an effective and safe therapeutic agent to improve function of the affected limb (4–6). BoNT-A treatment has been shown to relieve pain, enhance the effects of physiotherapy, improve performance in activities of daily living, and decrease the burden of caregivers (2). Over the last decade, there has been growing evidence that besides the well-known neuromuscular junction site of action, BoNT-A acts centrally. Whereas, direct effect on distant central circuits via retrograde transport and transcytosis in humans is still under debate (7), the central effects have been mostly ascribed to indirect changes due to plastic rearrangement subsequent to modulation of sensory input (8). BoNT-A likely relieves focal PSS by promoting dynamic changes at multiple levels of the sensorimotor system, presumably including the cerebral cortex. It has been suggested that BoNT-A acts on intrafusal as well as well as extrafusal fibers, thereby altering abnormal sensory input to the central nervous system via Ia afferent fibers (8, 9), which is likely the mechanism by which intramuscular BoNT-A injection induces cortical reorganization. The theory of central (remote) BoNT-A effects was first reported in electrophysiological studies of focal dystonia (10, 11). In dystonic disorders, one application of BoNT has been reported to be associated with even more pronounced microstructural gray matter changes in the frontal cortex, namely, primary motor cortex and pre-supplementary motor area (12). There have been several reports of the neuroanatomical correlates of BoNT-A-related relief of PSS using functional magnetic resonance imaging (fMRI) (13–16). However, the studies were conducted with small sample sizes; they differ in their activation tasks, and other methodological aspects. This makes direct comparison between the studies difficult. Patients with prominent upper limb spasticity indicated for BoNT-A treatment often have severe hand weakness, precluding the use of real hand movement. Motor imagery is feasible for severely affected patients and the sensorimotor representations may be preserved even in chronic paralysis (17). Motor imagery has been used widely in post-stroke paralysis, both as a functional neuroimaging probe sensitive to motor network abnormalities during stroke recovery (18) and as a motor training strategy (19). To our knowledge, our pilot study is the only one employing motor imagery to investigate cortical activation changes associated with PSS relief due to BoNT-A treatment (20). Using a longitudinal design, we expected that BoNT-A-induced change in afferent drive (8, 9) will be reflected in modulation of somatosensory cortical processing in the parietal areas (20). Even though our results showed several areas of change in the sensorimotor network over time, no regions showed transient effects following the course of dynamic changes in clinical spasticity. Therefore, the aim of the present longitudinal study was to identify BoNT-A-related patterns of cerebral cortex activation during motor imagery in a more

representative cohort of patients with moderate to severe PSS of the upper limbs.

METHODS

The study protocol is described in our previous report (20). The following text summarizes the methodology and highlights differences particular for the present study.

Patients

The study protocol was approved by the local Institutional Ethics Committee and conducted in accordance with the tenets of the Declaration of Helsinki. All subjects submitted written consent before participation in this study. The study cohort was limited to 30 right-handed chronic stroke patients (15 males and 15 females; median age, 65 years) with clinically relevant PSS of the upper limbs. Ischemic lesions were subcortical and corticosubcortical within the territory of the middle cerebral artery. The median time from stroke onset to study entry was 9 (range, 3–139) months. Exclusion criteria were: time after stroke of <3 months; PSS not exceeding a score of 1 on the modified Ashworth scale (MAS) (21); history of BoNT-A application or drug affecting muscle hypertonus intake; severe cognitive deficit or depression, as assessed with the Mini Mental State Exam (22) and Zung Self-Rating Depression Scale (23), respectively, which could affect cooperation during the study protocol; and general MRI exclusions and contraindications. The patients' characteristics are listed in **Table 1**.

Clinical Evaluation

All subjects were clinically evaluated just before BoNT-A injection (week 0, W0), then 4 weeks (W4) and 11 weeks (W11) later. Longitudinal within-subject design of the study partially overcomes the lack of a control group. Here, each patient serves as his/her internal control. PSS was evaluated with the MAS at each visit. The MAS was used to score the fingers and wrists separately, and the values were averaged (global MAS score). The MAS rater was blinded to the therapy and the recruitment to the present study. For statistical analysis, a MAS score of 1+ was recorded as 1.5. Further clinical investigations performed at study entry included the modified Medical Research Council scale (24) to test upper extremity strength, the National Institutes of Health stroke scale (25) to assess neurological impairment, and the Barthel Index (26) and the modified Rankin Scale (27) to assess disability.

Treatment

Enrolled patients received BoNT-A injections into the muscles of the affected upper limb at W0, which was followed by a dedicated physiotherapy protocol. The injections were performed under electromyographic guidance (Medtronic Keypoint; Alpine Biomed ApS, Skovlunde, Denmark), preferably with electrical stimulation to localize the muscles to be treated. The following muscles were always injected: flexor carpi ulnaris, flexor carpi radialis, flexor digitorum superficialis, and flexor digitorum profundus. Each muscle was consistently injected with a fixed dose of 50 U of BoNT-A (BOTOX®; Allergan, Inc., Irvine,

TABLE 1 | Demographic and clinical characteristics.

Patient	Stroke onset to WO (months)	Lesion	Affected hand	mRS	BI	NIHSS	MMSE	Zung (SDS index)	mMRC (WF/WE)	mMRC (FF/FE)	Global MAS WO	Global MAS W4	Global MAS W1
1	7	Thalamus, IC, BG	L	3	90	5	30	34	1+/0	1+/+	3	1.5	2.5
2	3	BG, IC	R	3	85	8	29	30	0/0	0/0	3	1	2.5
3	3	BG, insula, thalamus, FT	L	4	40	9	19	45	0/0	0/0	3	2	3
4	6	Thalamus, IC, insula	L	4	45	7	23	65	1/0	1/0	3	1.75	2.5
5	5	Thalamus, IC	R	4	60	10	22	49	0/0	0/0	3	2	3
6	83	Insula, FP	R	2	95	4	29	39	2/1	2/1	2	1	2
7	6	Insula, BG, FT	R	3	70	8	N/A	63	0/0	0/0	2	1.25	1.75
8	11	thalamus, IC, BG	L	3	80	5	29	64	1/0	0/0	2.5	1.5	2.5
9	9	thalamus, BG, FT, insula	L	3	75	7	29	34	0/0	0/0	3	1.75	3
10	4	BG, insula, thalamus	R	3	80	6	27	48	0/0	0/0	2	1	2
11	32	BG, IC	L	3	70	5	28	59	2/1	3/1	2	1	2
12	64	Insula, FT	R	2	95	6	18	50	2/2	2/1+	2	1.25	2
13	23	BG, insula, FT	R	3	65	9	N/A	43	0/0	0/0	3	2	2
14	7	IC, F	R	2	100	3	25	40	3/3	3/2+	1.5	1.25	1.25
15	10	Thalamus, IC, insula	R	3	85	5	29	49	1/1	2/1	2	1	2
16	4	Thalamus, BG, insula	R	4	50	9	N/A	54	0/0	0/0	1.75	1.75	2
17	19	Thalamus, IC	L	3	75	7	30	53	0/0	0/0	3	1.25	2
18	28	Insula, BG, FT	L	4	60	11	20	34	0/0	0/0	2.5	1.25	1.75
19	9	Thalamus, BG, FT, insula	R	3	90	10	N/A	44	0/0	0/0	1.75	1	2
20	7	BG, IC	L	3	90	6	30	70	1/0	1/0	2	0.5	2
21	9	BG, insula, FT	L	4	65	5	28	65	0/0	0/0	2	1.5	2
22	139	FTP, BG	L	3	90	4	27	44	0/0	0/0	2.5	1.5	2.25
23	9	IC, BG	R	3	85	8	N/A	60	0/0	0/0	2.5	1.5	2
24	9	F, insula	R	3	90	9	30	50	0/0	0/0	2.5	2	2.5
25	4	FTP	L	3	80	5	30	44	3/2	3/2	3	1.75	2.5
26	76	BG, IC, F	R	3	95	4	26	59	3/2	3/2	2.5	1.75	2.5
27	10	BG, FT	R	3	85	6	30	54	2/0	2/0	2.5	2	1.75
28	14	BG, IC, F	R	3	85	7	30	51	2/1	2/1	2	2	2
29	43	F, insula	L	2	100	1	29	73	4/3	3/3	2	0.5	0.5
30	38	BG, IC, FT	L	4	65	9	29	53	1/0	1/0	3	3	3

L, left; R, right; BG, basal ganglia; IC, internal capsule; F, frontal lobe; P, parietal lobe; T, temporal lobe; NIHSS, NIH stroke scale; mRS, modified Rankin Scale; mMRC, modified MRC scale; BI, Barthel index; WE, wrist extensors; WF, wrist flexors; FE, finger extensors; FF, finger flexors; MAS, Modified Ashworth scale; N/A, not applicable (MMSE score could not be interpreted because of the presence of expressive aphasia).

CA, USA) in accordance with current recommendations (4). Rehabilitation was started several days after the BoNT-A injection (W0). Initial inpatient physiotherapy for 2–4 weeks was followed by outpatient therapy until the third clinical and fMRI evaluation (total of 11 weeks). Patients underwent daily physiotherapy sessions for 1 h on workdays, i.e., five times per week. Individual kinesiotherapy included posture-locomotion training toward restitution of bipedal posture and gait, motor recovery of the girdles and trunk using elements of the Bobath concept, proprioceptive neuromuscular facilitation, respiratory physiotherapy, reflex and myofascial techniques, anti-spastic positioning, occupational therapy, and training of independence in activities of daily living. Proper adherence to the physiotherapy protocol was checked at each examination throughout the study period (28).

fMRI Data Acquisition

fMRI examinations were performed during the clinical evaluations at W0, W4, and W11 using a 1.5-Tesla scanner (Avanto or Symphony; Siemens Healthineers, Erlangen, Germany) equipped with a standard head coil. Whole-brain blood oxygenation level-dependent (BOLD) fMRI data (T_2^* -weighted echo-planar imaging; 30 slices, 5 mm thick; repetition time, 2,500 ms; 144 volumes; repeated twice) were acquired during imagery of finger movements with the impaired hand. A high resolution T_1 -weighted structural image was acquired using Magnetization-Prepared Rapid Gradient-Echo (MP-RAGE) sequence for anatomical reference. Before the first fMRI examination, each subject practiced the sequential finger-thumb opposition task with the non-paretic hand at the rate of approximately 1 movement per second over several repetitions and then was asked to imagine performing the same movement with the impaired fingers together with kinesthetic feeling. Before the follow-up fMRI examinations, we checked the correct performance of the task with the unimpaired hand. The only purpose of pre-imaging practice was to allow stable performance across the study. Inside the bore of the scanner, the task was performed with eyes closed, instructions to start and stop task performance were signaled verbally (start/stop) in MR-compatible headphones. In a block paradigm, imagery of finger movement alternated with rest (15 s). Each experimental run consisted of 12 repetitions of the same imagery-rest block pairs, for a total of 6 min. Each participant had two experimental runs with the impaired hand. The experimental paradigm has been already used and published in Veverka et al. (20).

Analysis

fMRI data of patients with right-sided lesions were swapped to match the left-sided lesions (29, 30). Next, a previously published preprocessing pipeline was applied (16). Functional images were registered to high resolution structural images and normalized to the standard space template using linear and non-linear algorithms, respectively (31). At the final pre-processing stage, residual motion-related signals were automatically removed using independent component analysis-based automatic removal of motion artifacts (32).

Statistical analysis of the functional time-series was conducted using general linear modeling with local autocorrelation correction (33). The boxcar function of the block design was convolved with a canonical hemodynamic response function (34) and a temporal derivative to account for the relative slice-dependent time shift rather than slice-wise time-course interpolation (35). Furthermore, several nuisance regressors were obtained from the functional data of each subject and added to the general linear model: six motion parameters, one signal from the white matter, and one from the cerebrospinal fluid.

After first-level processing, repeated measures from the same session were averaged for each subject using a middle-level analysis. Group statistical analyses were performed using stage 1 of the improved linear model for fMRI of the brain (36, 37). At the group level, (1) the average activation was separately modeled at each time-point with the MAS and age at W0 as linear covariates; and (2) the within-subject effect of BoNT-A $[(W0 + W11)/2 - W4]$ and linear effect of time from W0 were assigned as independent variables. The model was designed to separate the transient effect of BoNT from the presumed linear effect of physiotherapy. The resulting statistical maps were thresholded using clusters at $p < 0.05$ (family-wise error-corrected) formed at (1) $Z > 3.0$ for average activation and (2) $Z > 2.3$ for within-subject effects (family-wise error-corrected using Gaussian random field theory) (38). Within-subject effects were additionally Bonferroni-corrected for the number of contrasts.

Clinical data were analyzed using IBM SPSS Statistics for Windows, version 22.0 (IBM Corp., Armonk, NY, USA). The Wilcoxon signed-rank test with Bonferroni correction was used to compare global MAS scores from W0, W4, and W11. A probability (p) value of < 0.05 was considered statistically significant.

Additionally, a map of stroke lesions was created to visualize the overall volume of the affected tissue. First, T_1 -hypointense stroke lesions were delineated semi-automatically on the high-resolution structural images using interactive intensity-based volume segmentation in each individual. The resulting binary masks were manually corrected for errors by PaH. Next, masks with right-sided lesions were swapped to match the left-sided lesions and all masks were transformed into 1-mm MNI 152 standard space using a non-linear transformation (31). Finally, sum of all masks was created to provide a group-wise lesion map (Figure 1).

RESULTS

Clinical

Comprehensive treatment with BoNT-A and subsequent physiotherapy significantly decreased PSS of the upper limb with the maximal effect at W4 ($p < 0.0001$, Wilcoxon signed-rank test). There were significant differences in global MAS between W0 and W11 ($p = 0.006$) and between W4 and W11 ($p < 0.0001$, Wilcoxon signed-rank test). The median global MAS scores were 2.50 at W0 (interquartile range (IQR) = 2.0–3.0), 1.50 at W4 (IQR = 1.0–1.75), and 2.00 at W11 (IQR = 2.0–2.5). The data are presented in a box plot in Figure 2. The MAS scores for each

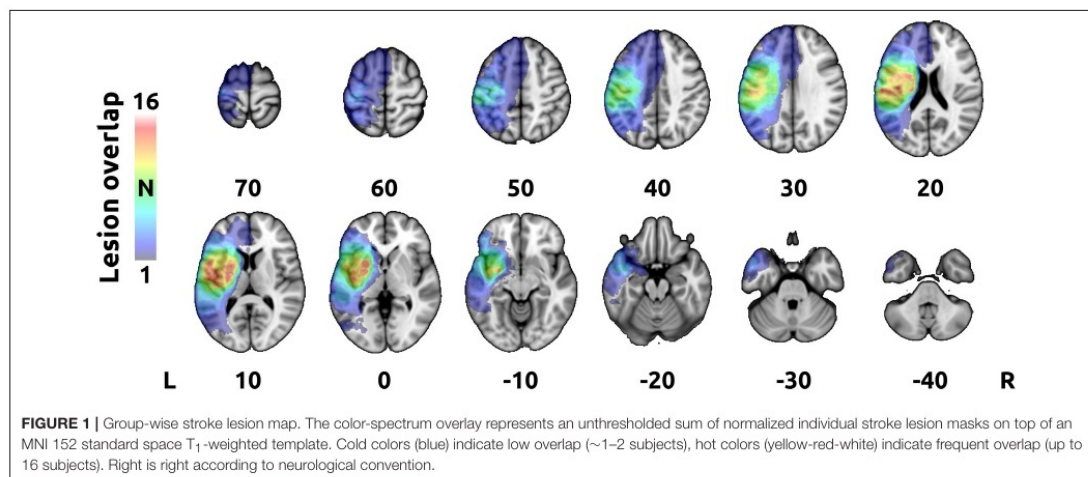


FIGURE 1 | Group-wise stroke lesion map. The color-spectrum overlay represents an unthresholded sum of normalized individual stroke lesion masks on top of an MNI 152 standard space T₁-weighted template. Cold colors (blue) indicate low overlap (~1–2 subjects), hot colors (yellow-red-white) indicate frequent overlap (up to 16 subjects). Right is right according to neurological convention.

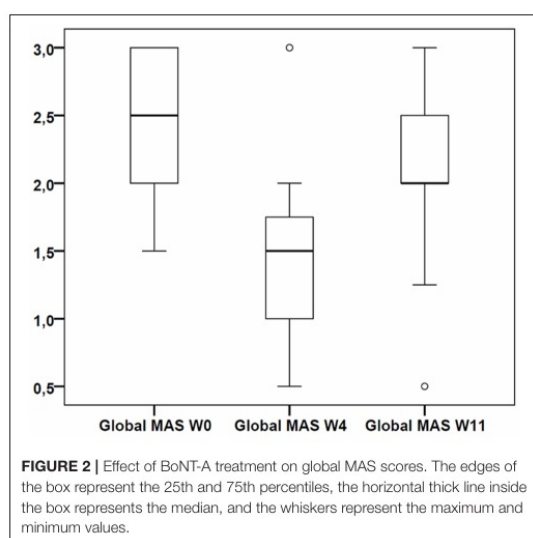


FIGURE 2 | Effect of BoNT-A treatment on global MAS scores. The edges of the box represent the 25th and 75th percentiles, the horizontal thick line inside the box represents the median, and the whiskers represent the maximum and minimum values.

subject are listed in **Table 1**. The overlap of stroke lesions in all participants is provided in **Figure 1**.

Functional Imaging

Task-related fMRI prior to treatment (W0) showed extensive activation of the bilateral frontoparietal sensorimotor cortical areas, bilateral cerebellum, and contralesional basal ganglia and thalamus, with peak activation in the supplementary motor area (SMA), bilateral intraparietal sulci (IPS), contralesional ventrolateral premotor cortex, and ipsilesional anterior and posterior cerebellar hemispheres. After BoNT-A application

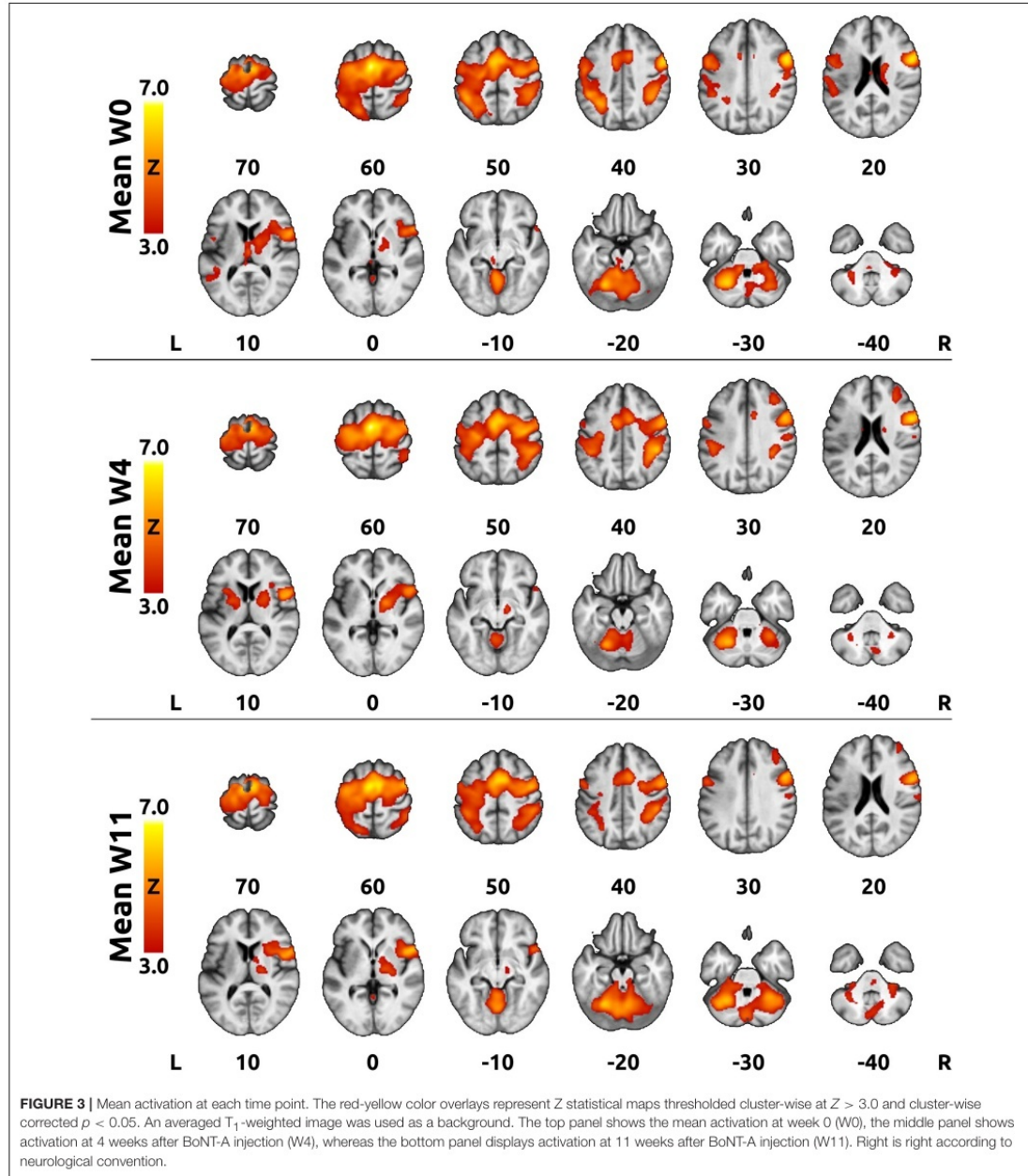
(W4), the activation extent decreased globally, mostly in the bilateral parietal cortices and cerebellum, but returned close to baseline at W11 (see average activation maps in **Figure 3**).

The intra-subject contrast revealed a significant BoNT-A effect, which manifested as transient decreases in activation of the ipsilesional superior parietal lobule (SPL) and IPS (**Figure 4** and **Table 2**). No consistent activation changes related to time since W0 were observed.

DISCUSSION

The brain is continually reorganizing (39). Stroke triggers processes in the central nervous system aimed to promote post-stroke recovery (adaptive plasticity). Some of these processes may not be beneficial or can even worsen primary neurological impairment (maladaptive plasticity), such as the substantially negative impact of PSS on manual dexterity, mobility, and ultimately harmful effects on the patient’s health-related quality of life (1, 2). From this point of view, effective treatment of PSS might not only diminish muscle hyperactivity, but could also replace maladaptive with adaptive plasticity.

The present study is an extension of our previous study of a smaller sample size (20) and provides new evidence supporting the theory of cortical reorganization after BoNT-A treatment. Imagery of sequential finger movement was used as an activation task in an fMRI experiment. Kinesthetic imagery activates highly similar cortical areas as actual movements (40, 41). A meta-analysis conducted by Héту et al. (42) showed that motor imagery consistently recruits the large frontoparietal network besides the subcortical and cerebellar regions, and identified the following areas as involved in motor imagery: the inferior parietal lobule, SPL, dorsal premotor cortex, SMA, cerebellum, and Broca’s area. It has been demonstrated that motor imagery is a feasible task for severely affected patients unable to perform an active motor task, although motor imagery is difficult to monitor



(17, 20). However, pre-scan practice in our patients before the first fMRI was intensive and sufficiently long to ensure reliable performance, and correct memory of the task was checked before the follow-up fMRIs, to overcome this limitation. Additionally,

each fMRI acquisition was checked separately for corresponding BOLD activations.

As expected, the combination of BoNT-A treatment and physiotherapy effectively alleviated PSS of the upper limb

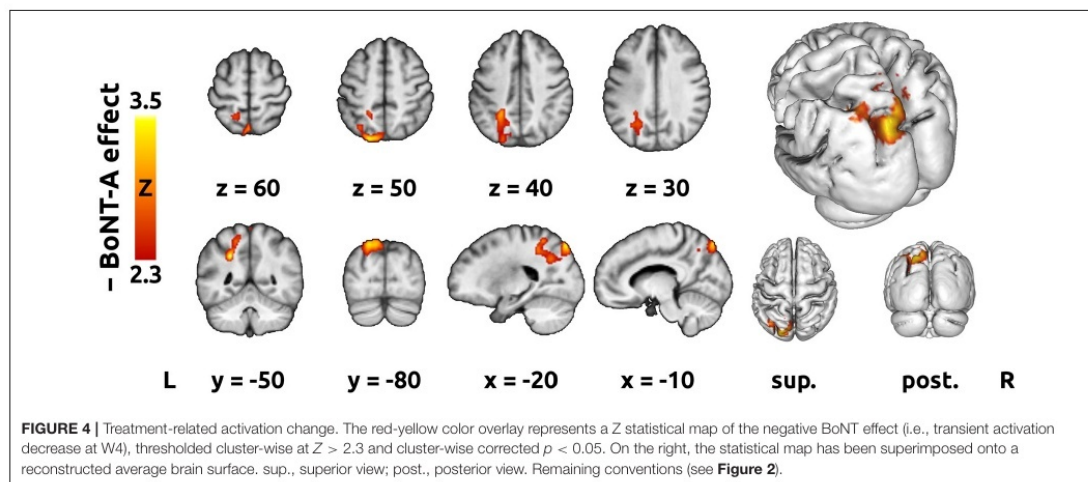


FIGURE 4 | Treatment-related activation change. The red-yellow color overlay represents a Z statistical map of the negative BoNT effect (i.e., transient activation decrease at W4), thresholded cluster-wise at $Z > 2.3$ and cluster-wise corrected $p < 0.05$. On the right, the statistical map has been superimposed onto a reconstructed average brain surface. sup., superior view; post., posterior view. Remaining conventions (see **Figure 2**).

TABLE 2 | Treatment-related activation differences—list of local maxima.

Contrast	Anatomical atlas labels ^a	Cytoarchitectonic atlas labels ^a	Volume [cm ³]	Cluster p (corrected for multiple comparisons)	Z_{max}	MNI coordinates of local maxima ^b [x,y,z (mm)]
Negative BoNT-A effect: Cluster 1	51.5% L Lateral Occipital Cortex, superior division 21.7% L Precuneus Cortex 20.2% L Superior Parietal Lobule	29.2% L Superior Parietal Lobule 7A 20.2% L Superior Parietal Lobule 7P 14.1% L Anterior intra-parietal sulcus hIP3 13.8% L Anterior intra-parietal sulcus hIP1	13.76	0.032	3.49	-24, -50, 36 -18, -82, 50 -12, -82, 52 -4, -74, 56 0, -70, 58

BoNT-A, botulinum toxin type A; L, left; MNI, Montréal Neurological Institute; Z_{max} , maximum Z score.

^aAnatomical and cytoarchitectonic labels are provided including the proportion of labeled voxels. Only labels consisting at least 5% of activated voxels are provided. Note that cytoarchitectonic labels do not cover the whole brain.

^bTop five local maxima with the highest Z score are provided.

as reflected by the MAS score. There was a significant transient decrease in the global MAS score at W4, when the pharmacological peripheral effect of BoNT-A is assumed to be maximal, and a subsequent increase in the global MAS score at further follow-up (W11). In contrast to our previous BoNT-A-studies (15, 16, 20), there was a significant change in the global MAS score from baseline to W11, when BoNT-A is expected to wane from the neuromuscular junctions (43). Namely, some improvement of spasticity persisted by the end of the study, even though local BoNT-A effect should have disappeared. Although this novel finding might support the theory of persistent central reorganization after BoNT-A application, the effect of ongoing physiotherapy should also be considered.

Task-related fMRI prior to treatment showed extensive activation of the bilateral frontoparietal sensorimotor cortical areas, bilateral cerebellum, and contralesional basal ganglia and thalamus, with peak activation in the SMA, IPS, contralesional ventrolateral premotor cortex, and ipsilesional anterior and posterior cerebellar hemispheres. The prominent involvement of the premotor cortical areas and relatively

minor activation of the primary motor cortices during motor imagery is consistent with previous observations both in healthy controls (41, 44–47) and stroke patients with motor deficits (18, 48).

Alleviation of PSS at W4 was associated with an apparent reduction in the extent of activation, mostly of the bilateral parietal cortices and cerebellum, but returned close to the original extent at W11. This finding is in agreement with our previous studies and other previously published fMRI studies uncovering cerebral correlations with PSS treatment (14–16, 20, 49–52). Extended task-related cortical activation probably represents a general response of the lesioned brain to increased proprioceptive afferent input associated with PSS (13, 14). The overall reduction in the extent of activation after treatment might reflect transient changes due to BoNT-A administration and/or physiotherapy.

A similar trend has been observed in the evolution of the extent of activation during stroke recovery (53–57). A vast motor task-related activation of the bilateral frontoparietal cortex early after stroke is followed by a decrease in the extent of activation and increase in laterality in recovering

patients (29, 30). We assume that this phenomenon did not bias our results for several reasons. First, all enrolled subjects were severely affected and their capacity for motor improvement was strongly limited. Second, only chronic stroke patients were included, thus the time from stroke onset to study entry was sufficiently long (median 9 months) to assure the stability of clinical features and a hemodynamic response (29, 58).

To address the main aim of the study, an intra-subject contrast design was used to separate the specific BoNT-A effect from the longitudinal effects of time and/or ongoing physiotherapy. The transient effect associated with BoNT-A observed in our study manifested as a significant decrease in activation of the ipsilesional posterior parietal cortex (PPC), namely the SPL and the cortex surrounding IPS.

The PPC, that is, the entire parietal cortex behind the primary and secondary somatosensory cortices, is part of a broad anatomical network of frontoparietal association (multisensory) cortical areas, which encode the more abstract aspects of sensorimotor control processes (59–61). Several functional domains have been attributed to this network, for instance, the dorsal attention network that directs visual attention and short-term memory (60). The dorsal attention network partially overlaps with another functional network, namely the motor imagery network (42). Finally, the PPC is involved in the visual system, particularly in its dorsal stream (occipito-parietal cortex) (62, 63).

In general, the PPC is therefore involved in perception and processing of action-related information. More specifically, the PPC is recruited by sensory control of visuomotor actions, such as reaching, pointing, grasping, and eye movement (59, 63). In our previous work with a similar design, but a smaller sample size, IPS and SPL were among the areas showing significant reductions of the spatial extent of activation after BoNT-A treatment, but the contrast assigned to the specific BoNT-A effect did not reveal any areas of significant change in the magnitude of the local BOLD effect (20). The absence of BoNT-A-related effects in our pilot study might be attributed to the relatively small sample size, which reduced the overall statistical power to detect smaller treatment effects.

As suggested by the findings of the present study, decreased activation of the IPS and SPL after treatment reflects a change in internal representation of the subject's hand resulting from decreased inflow of proprioceptive information from the spastic limb. It has been previously demonstrated that brain activation during motor imagery is strongly influenced by the proprioceptive information related to the pre-existing configuration of the limbs (64). After successful treatment of PSS, the internal models (predictions) of the upper limb are likely to adapt to the newly reduced flow of afferent information, which could, in turn, reduce the occurrence of unnecessary fMRI activation during motor imagery, as was observed with actual movement (15). Similar effects on overt and imagined upper limb movement were observed in Parkinson disease patients before and after treatment with L-DOPA (65, 66). A theory of internal model utilization

in motor imagery has been supported by a recent study conducted by Kiltner et al. (67), which concluded that motor imagery recruits the internal forward model to predict sensory consequences similarly to overt execution. Another study using magnetoencephalography suggested that kinesthetic feeling is subserved by an internal forward model located in the parietal cortex, particularly the cortex surrounding the IPS, highlighting its role in motor imagery (68). Moreover, a motor imagery study conducted by de Lange et al. (64) found that the PPC appears to incorporate afferent proprioceptive information into the motor plan.

Alternatively, we might speculate that in our group of severely affected poststroke patients, visual imagery may have prevailed over kinesthetic imagery at baseline, although the participants were asked to imagine the action with kinesthetic feeling. Studies of motor imagery in post-stroke patients suggest that for these subjects, it is very difficult to use either visual or kinesthetic imagery selectively (19, 69). Therefore, we assume that the severely affected subjects enrolled in the present study employed a combination of both imagery strategies. Moreover, we did not design the experiment to discriminate between different aspects of motor imagery, because the Movement Imagery Questionnaire and similar alternative tests were beyond the abilities of the patients (70, 71). Due to the prominent role of the SPL and occipital regions in visual input processing (41, 72), the BoNT-A-related reduction of PPC activation at W4 might be interpreted as a lower engagement of the cortical areas attributed to visual imagery. From this perspective, it is possible that alleviation of PSS renders the contribution of visual strategy in motor imagery less prominent.

There were some limitations to this study that should be mentioned. First, we did not include a control group without BoNT-A treatment, which would have been optimal to separate transient effect of BoNT-A from more longitudinal effect of concurrent physiotherapy. For several years, BoNT-A treatment has been a recommended component of the complex therapy regimen for PSS (4, 5). Therefore, non-treatment would have been unethical. Although functional cortical changes observed in the present study could have been induced by both the BoNT-A treatment and the physiotherapy, we argue that the within-subject longitudinal design, with three successive assessments over 3 months, captures both the transient changes due to BoNT-A and the more slowly evolving changes in sensorimotor control due to ongoing physiotherapy and symptomatic therapy. This approach has been considered sufficient to address the main goal of the study—to uncover specific effect of BoNT-A in the studied population of chronic stroke patients. Finally, the heterogeneity in stroke location and the degree of cortical involvement limit the possibility of generalizing the results to the whole population of patients with upper limb PSS.

CONCLUSIONS

Whole brain fMRI activation patterns during motor imagery in the course of BoNT-A treatment of upper limb

PSS and further follow-up documented mostly transient changes in the ipsilesional PPC. Our results indicated that BoNT-A therapy modulated posterior parietal cortical activation in PSS even in chronic patients with severe hand weakness.

ETHICS STATEMENT

The study protocol was approved by the local Institutional Ethics Committee and conducted in accordance with the tenets of the Declaration of Helsinki. All subjects submitted written consent before participation in this study.

REFERENCES

- Zorowitz RD, Gillard PJ, Brainin M. Poststroke spasticity: sequelae and burden on stroke survivors and caregivers. *Neurology*. (2013) 80:S45–52. doi: 10.1212/WNL.0b013e3182764c86
- Sommerfeld DK, Eek EU-B, Svensson A-K, Holmqvist LW, von Arbin MH. Spasticity after stroke: its occurrence and association with motor impairments and activity limitations. *Stroke*. (2004) 35:134–9. doi: 10.1161/01.STR.0000105386.05173.5E
- Urban PP, Wolf T, Uebele M, Marx JJ, Vogt T, Stoeter P, et al. Occurrence and clinical predictors of spasticity after ischemic stroke. *Stroke*. (2010) 41:2016–20. doi: 10.1161/STROKEAHA.110.581991
- Wissel J, Ward AB, Erztgaard P, Bensmail D, Hecht MJ, Lejeune TM, et al. European consensus table on the use of botulinum toxin type A in adult spasticity. *J Rehabil Med*. (2009) 41:13–25. doi: 10.2340/16501977-0303
- Sheean G, Lannin NA, Turner-Stokes L, Rawicki B, Snow BJ. Botulinum toxin assessment, intervention and after-care for upper limb hypertonicity in adults: international consensus statement. *Eur J Neurol*. (2010) 17 (Suppl. 2):74–93. doi: 10.1111/j.1468-1331.2010.03129.x
- Sunnerhagen KS, Olver J, Francisco GE. Assessing and treating functional impairment in poststroke spasticity. *Neurology*. (2013) 80:S35–44. doi: 10.1212/WNL.0b013e3182764aa2
- Curra A, Berardelli A. Do the unintended actions of botulinum toxin at distant sites have clinical implications? *Neurology*. (2009) 72:1095–9. doi: 10.1212/01.wnl.0000345010.98495.fc
- Rosales RL, Dressler D. On muscle spindles, dystonia and botulinum toxin. *Eur J Neurol*. (2010) 17 (Suppl. 1):71–80. doi: 10.1111/j.1468-1331.2010.03056.x
- Trompetto C, Bove M, Avanzino L, Francavilla G, Berardelli A, Abbruzzese G. Intrafusal effects of botulinum toxin in post-stroke upper limb spasticity. *Eur J Neurol*. (2008) 15:367–70. doi: 10.1111/j.1468-1331.2008.02076.x
- Kanovský P, Streitová H, Dufek J, Znojil V, Daniel P, Rektor I. Change in lateralization of the P22/N30 cortical component of median nerve somatosensory evoked potentials in patients with cervical dystonia after successful treatment with botulinum toxin A. *Mov Disord*. (1998) 13:108–17. doi: 10.1002/mds.870130122
- Gilio F, Currà A, Lorenzano C, Modugno N, Manfredi M, Berardelli A. Effects of botulinum toxin type A on intracortical inhibition in patients with dystonia. *Ann Neurol*. (2000) 48:20–6. doi: 10.1002/1531-8249(200007)48:1<20::AID-ANA5>3.0.CO;2-U
- Hanganu A, Muthuraman M, Chirumamilla VC, Koirala N, Paktas B, Deuschl G, et al. Grey matter microstructural integrity alterations in blepharospasm are partially reversed by botulinum neurotoxin therapy (vol 11, e0168652, 2016). *PLoS ONE*. (2017) 12:e0172374. doi: 10.1371/journal.pone.0172374
- Šenkárová Z, Hluštík P, Otruba P, Herzig R, Kanovský P. Modulation of cortical activity in patients suffering from upper arm spasticity following

AUTHOR CONTRIBUTIONS

TV and PeH: conceived and designed the experiments. TV, PeH, ZT, BK, and PO: performed the experiments. PaH and JZ: analyzed the data. TV, PaH, and PeH: interpretation of results. TV and PaH: wrote the paper. PK and AK: supervision.

FUNDING

This study was supported by the Ministry of Health of the Czech Republic—by the grant NV17-29452A and by the conceptual development of research organization grant (FNOL, 00098892).

- stroke and treated with botulinum toxin A: an fMRI study. *J Neuroimaging*. (2010) 20:9–15. doi: 10.1111/j.1552-6569.2009.00375.x
- Tomášová Z, Hluštík P, Král M, Otruba P, Herzig R, Krobot A, et al. Cortical activation changes in patients suffering from post-stroke arm spasticity and treated with botulinum toxin a. *J Neuroimaging*. (2013) 23:337–44. doi: 10.1111/j.1552-6569.2011.00682.x
 - Veverka T, Hluštík P, Hok P, Otruba P, Tüdös Z, Zapletalová J, et al. Cortical activity modulation by botulinum toxin type A in patients with post-stroke arm spasticity: real and imagined hand movement. *J Neurol Sci*. (2014) 346:276–83. doi: 10.1016/j.jns.2014.09.009
 - Veverka T, Hluštík P, Hok P, Otruba P, Zapletalová J, Tüdös Z, et al. Sensorimotor modulation by botulinum toxin A in post-stroke arm spasticity: passive hand movement. *J Neurol Sci*. (2016) 362:14–20. doi: 10.1016/j.jns.2015.12.049
 - Szameitat AJ, Shen S, Conforto A, Sterr A. Cortical activation during executed, imagined, observed, and passive wrist movements in healthy volunteers and stroke patients. *Neuroimage*. (2012) 62:266–80. doi: 10.1016/j.neuroimage.2012.05.009
 - Sharma N, Baron J-C, Rowe JB. Motor imagery after stroke: relating outcome to motor network connectivity. *Ann Neurol*. (2009) 66:604–16. doi: 10.1002/ana.21810
 - Sharma N, Pomeroy VM, Baron J-C. Motor imagery—A backdoor to the motor system after stroke? *Stroke*. (2006) 37:1941–52. doi: 10.1161/01.STR.0000226902.43357.fc
 - Veverka T, Hluštík P, Tomášová Z, Hok P, Otruba P, Král M, et al. BoNT-A related changes of cortical activity in patients suffering from severe hand paralysis with arm spasticity following ischemic stroke. *J Neurol Sci*. (2012) 319:89–95. doi: 10.1016/j.jns.2012.05.008
 - Bohannon RW, Smith MB. Interrater reliability of a modified Ashworth scale of muscle spasticity. *Phys Ther*. (1987) 67:206–7.
 - Folstein MF, Folstein SE, McHugh PR. “Mini-mental state”. A practical method for grading the cognitive state of patients for the clinician. *J Psychiatr Res*. (1975) 12:189–98.
 - Zung WW. A self-rating depression scale. *Arch Gen Psychiatry*. (1965) 12:63–70.
 - Paternostro-Sluga T, Grim-Stieger M, Posch M, Schuhfried O, Vacariu G, Mittermaier C, et al. Reliability and validity of the Medical Research Council (MRC) scale and a modified scale for testing muscle strength in patients with radial palsy. *J Rehabil Med*. (2008) 40:665–71. doi: 10.2340/16501977-0235
 - Brott T, Adams HP Jr, Olinger CP, Marler JR, Barsan WG, Biller J, et al. Measurements of acute cerebral infarction: a clinical examination scale. *Stroke*. (1989) 20:864–70.
 - Mahoney FI, Barthel DW. Functional evaluation: the Barthel index. *Md State Med J*. (1965) 14:61–5.
 - Quinn TJ, Dawson J, Walters MR, Lees KR. Variability in modified Rankin scoring across a large cohort of international observers. *Stroke*. (2008) 39:2975–9. doi: 10.1161/STROKEAHA.108.515262

28. Krobot A, Schusterová B, Tomšová J, Kristková V, Konečný P. Specific protocol of physiotherapy in stroke patients. *Cesk Slov Neurol N.* (2008) 71/104(Suppl):70.
29. Johansen-Berg H, Dawes H, Guy C, Smith SM, Wade DT, Matthews PM. Correlation between motor improvements and altered fMRI activity after rehabilitative therapy. *Brain.* (2002) 125:2731–42. doi: 10.1093/brain/aw282
30. Ward NS, Brown MM, Thompson AJ, Frackowiak RSJ. Neural correlates of outcome after stroke: a cross-sectional fMRI study. *Brain.* (2003) 126:1430–48. doi: 10.1093/brain/awg145
31. Jenkinson M, Smith S. A global optimisation method for robust affine registration of brain images. *Med Image Anal.* (2001) 5:143–56. doi: 10.1016/s1361-8415(01)00036-6
32. Pruim RHR, Mennes M, van Rooij D, Llera A, Buitelaar JK, Beckmann CF. ICA-AROMA: A robust ICA-based strategy for removing motion artifacts from fMRI data. *Neuroimage.* (2015) 112:267–77. doi: 10.1016/j.neuroimage.2015.02.064
33. Woolrich MW, Ripley BD, Brady M, Smith SM. Temporal autocorrelation in univariate linear modeling of FMRI data. *Neuroimage.* (2001) 14:1370–86. doi: 10.1006/nimg.2001.0931
34. Glover GH. Deconvolution of impulse response in event-related BOLD fMRI. *Neuroimage.* (1999) 9:416–29.
35. Calhoun VD, Stevens MC, Pearlson GD, Kiehl KA. fMRI analysis with the general linear model: removal of latency-induced amplitude bias by incorporation of hemodynamic derivative terms. *Neuroimage.* (2004) 22:252–7. doi: 10.1016/j.neuroimage.2003.12.029
36. Beckmann CF, Jenkinson M, Smith SM. General multilevel linear modeling for group analysis in FMRI. *Neuroimage.* (2003) 20:1052–63. doi: 10.1016/S1053-8119(03)00435-X
37. Woolrich MW, Behrens TEJ, Beckmann CF, Jenkinson M, Smith SM. Multilevel linear modelling for FMRI group analysis using Bayesian inference. *Neuroimage.* (2004) 21:1732–47. doi: 10.1016/j.neuroimage.2003.12.023
38. Worsley KJ. *Statistical Analysis of Activation Images. Functional MRI: An Introduction to Methods.* Oxford: Oxford University Press (2001), p. 251–70.
39. Pascual-Leone A, Amedi A, Fregni F, Merabet LB. The plastic human brain cortex. *Annu Rev Neurosci.* (2005) 28:377–401. doi: 10.1146/annurev.neuro.27.070203.144216
40. Grezes J, Decety J. Functional anatomy of execution, mental simulation, observation, and verb generation of actions: a meta-analysis. *Hum Brain Mapp.* (2001) 12:1–19. doi: 10.1002/1097-0193(200101)12:1<1::AID-HBM10>3.0.CO;2-V
41. Solodkin A, Hluštík P, Chen EE, Small SL. Fine modulation in network activation during motor execution and motor imagery. *Cereb Cortex.* (2004) 14:1246–55. doi: 10.1093/cercor/bhh086
42. Hetu S, Gregoire M, Saimpont A, Coll M-P, Eugene F, Michon P-E, et al. The neural network of motor imagery: an ALE meta-analysis. *Neurosci Biobehav Rev.* (2013) 37:930–49. doi: 10.1016/j.neubiorev.2013.03.017
43. Dressler D, Saberi FA, Barbosa ER. Botulinum toxin: mechanisms of action. *Arq Neuropsiquiatr.* (2005) 63:180–5. doi: 10.1590/s0004-282x2005000100035
44. Gerardin E, Sirigu A, Lehericy S, Poline JB, Gaymard B, Marsault C, et al. Partially overlapping neural networks for real and imagined hand movements. *Cereb Cortex.* (2000) 10:1093–104. doi: 10.1093/cercor/10.11.1093
45. Hanakawa T, Immisch I, Toma K, Dimyan MA, Van Gelderen P, Hallett M. Functional properties of brain areas associated with motor execution and imagery. *J Neurophysiol.* (2003) 89:989–1002. doi: 10.1152/jn.00132.2002
46. Dechent P, Merboldt KD, Frahm J. Is the human primary motor cortex involved in motor imagery? (vol 19, pg 138, 2004). *Cogn Brain Res.* (2004) 20:533–3. doi: 10.1016/j.cogbrainres.2004.05.001
47. Hanakawa T, Dimyan MA, Hallett M. Motor planning, imagery, and execution in the distributed motor network: a time-course study with functional MRI. *Cereb Cortex.* (2008) 18:2775–88. doi: 10.1093/cercor/bhn036
48. Sharma N, Simmons LH, Jones PS, Day DJ, Carpenter TA, Pomeroy VM, et al. Motor imagery after subcortical stroke: a functional magnetic resonance imaging study. *Stroke.* (2009) 40:1315–24. doi: 10.1161/STROKEAHA.108.525766
49. Manganotti P, Acler M, Formaggio E, Avesani M, Milanese F, Baraldo A, et al. Changes in cerebral activity after decreased upper-limb hypertonus: an EMG-fMRI study. *Magn Reson Imaging.* (2010) 28:646–52. doi: 10.1016/j.mri.2009.12.023
50. Diserens K, Ruegg D, Kleiser R, Hyde S, Perret N, Vuadens P, et al. Effect of repetitive arm cycling following botulinum toxin injection for poststroke spasticity: evidence from FMRI. *Neurorehabil Neural Repair.* (2010) 24:753–62. doi: 10.1177/1545968310372138
51. Bergfeldt U, Jonsson T, Bergfeldt L, Julin P. Cortical activation changes and improved motor function in stroke patients after focal spasticity therapy—an interventional study applying repeated fMRI. *BMC Neurol.* (2015) 15:52. doi: 10.1186/s12883-015-0306-4
52. Pundik S, Falchook AD, McCabe J, Litinas K, Daly JJ. Functional brain correlates of upper limb spasticity and its mitigation following rehabilitation in chronic stroke survivors. *Stroke Res Treat.* (2014) 2014:306325. doi: 10.1155/2014/306325
53. Ward NS, Brown MM, Thompson AJ, Frackowiak RSJ. Neural correlates of motor recovery after stroke: a longitudinal fMRI study. *Brain.* (2003) 126:2476–96. doi: 10.1093/brain/awg245
54. Small SL, Hluštík P, Noll DC, Genovese C, Solodkin A. Cerebellar hemispheric activation ipsilateral to the paretic hand correlates with functional recovery after stroke. *Brain.* (2002) 125:1544–57. doi: 10.1093/brain/awf148
55. Feydy A, Carlier R, Roby-Brami A, Bussel B, Cazalis F, Pierot L, et al. Longitudinal study of motor recovery after stroke: recruitment and focusing of brain activation. *Stroke.* (2002) 33:1610–7. doi: 10.1161/01.str.0000017100.68294.52
56. Calautti C, Baron J-C. Functional neuroimaging studies of motor recovery after stroke in adults: a review. *Stroke.* (2003) 34:1553–66. doi: 10.1161/01.STR.0000071761.36075.A6
57. Marshall RS, Perera GM, Lazar RM, Krakauer JW, Constantine RC, DeLaPaz RL. Evolution of cortical activation during recovery from corticospinal tract infarction. *Stroke.* (2000) 31:656–61. doi: 10.1161/01.str.31.3.656
58. Traversa R, Cicinelli P, Oliveri M, Giuseppina Palmieri M, Filippi MM, Pasqualetti P, et al. Neurophysiological follow-up of motor cortical output in stroke patients. *Clin Neurophysiol.* (2000) 111:1695–703. doi: 10.1016/S1388-2457(00)00373-4
59. Konen CS, Mruczek REB, Montoya JL, Kastner S. Functional organization of human posterior parietal cortex: grasping- and reaching-related activations relative to topographically organized cortex. *J Neurophysiol.* (2013) 109:2897–908. doi: 10.1152/jn.00657.2012
60. Brissenden JA, Levin EJ, Osher DE, Halko MA, Somers DC. Functional evidence for a cerebellar node of the dorsal attention network. *J Neurosci.* (2016) 36:6083–96. doi: 10.1523/JNEUROSCI.0344-16.2016
61. Sereno MI, Huang R-S. Multisensory maps in parietal cortex. *Curr Opin Neurobiol.* (2014) 24:39–46. doi: 10.1016/j.conb.2013.08.014
62. Goodale M, Milner A. Separate visual pathways for perception and action. *Trends Neurosci.* (1992) 15:20–5. doi: 10.1016/0166-2236(92)90344-8
63. Culham JC, Valyear KF. Human parietal cortex in action. *Curr Opin Neurobiol.* (2006) 16:205–12. doi: 10.1016/j.conb.2006.03.005
64. de Lange FP, Helmich RC, Toni I. Posture influences motor imagery: an fMRI study. *Neuroimage.* (2006) 33:609–17. doi: 10.1016/j.neuroimage.2006.07.017
65. Mailet A, Krainik A, Debu B, Tropres I, Lagrange C, Thobois S, et al. Levodopa effects on hand and speech movements in patients with Parkinson's disease: a fMRI study. *PLoS ONE.* (2012) 7:e46541. doi: 10.1371/journal.pone.0046541
66. Haslinger B, Erhard P, Kämpfe N, Boecker H, Rummery E, Schwaiger M, et al. Event-related functional magnetic resonance imaging in Parkinson's disease before and after levodopa. *Brain.* (2001) 124:558–70. doi: 10.1093/brain/124.3.558
67. Kiltner K, Andersson BJ, Houborg C, Ehrsson HH. Motor imagery involves predicting the sensory consequences of the imagined movement. *Nat Commun.* (2018) 9:1617. doi: 10.1038/s41467-018-03989-0
68. Tian X, Poeppel D. Mental imagery of speech and movement implicates the dynamics of internal forward models. *Front Psychol.* (2010) 1:166. doi: 10.3389/fpsyg.2010.00166

69. Milton J, Solodkin A, Hlustik P, Small SL. The mind of expert motor performance is cool and focused. *Neuroimage*. (2007) 35:804–13. doi: 10.1016/j.neuroimage.2007.01.003
70. Hall C, Pongrac J, Buckholz E. The measurement of imagery ability. *Hum Mov Sci*. (1985) 4:107–18. doi: 10.1016/0167-9457(85)90006-5
71. Naito E. Controllability of motor imagery and transformation of visual-imagery. *Percept Mot Skills*. (1994) 78:479–87. doi: 10.2466/pms.1994.78.2.479
72. Guillot A, Collet C, Nguyen VA, Malouin F, Richards C, Doyon J. Brain activity during visual versus kinesthetic imagery: an fMRI study. *Hum Brain Mapp*. (2009) 30:2157–72. doi: 10.1002/hbm.20658

Conflict of Interest Statement: The authors declare that the research was conducted in the absence of any commercial or financial relationships that could be construed as a potential conflict of interest.

Copyright © 2019 Veverka, Hok, Otruba, Zapletalová, Kukolová, Tüdös, Krobot, Kaňovský and Hluštík. This is an open-access article distributed under the terms of the Creative Commons Attribution License (CC BY). The use, distribution or reproduction in other forums is permitted, provided the original author(s) and the copyright owner(s) are credited and that the original publication in this journal is cited, in accordance with accepted academic practice. No use, distribution or reproduction is permitted which does not comply with these terms.